JUN 17 1982

208-C-7

C55.622: 981/v3

Environmental Assessment of the Alaskan Continental Shelf

ORIGINAL

COMPLETED
685

Final Reports of Principal Investigators
Volume 3. Physical Science Studies

U.S. DEPARTMENT OF COMMERCE
National Oceanic & Atmospheric Administration
Office of Marine Pollution Assessment

U.S. DEPARTMENT OF INTERIOR
Bureau of Land Management

October 1981

Environmental Assessment of the Alaskan Continental Shelf

Final Reports of Principal Investigators
Volume 3. Physical Science Studies

U.S. DEPARTMENT OF COMMERCE
National Oceanic & Atmospheric Administration
Office of Marine Pollution Assessment

U.S. DEPARTMENT OF INTERIOR
Bureau of Land Management

October 1981

I BEST DOCUMENT AVAILABLE

The facts, conclusions and issues appearing in these reports are based on interim results of an Alaskan environmental studies program managed by the Outer Continental Shelf Environmental Assessment Program (OCSEAP) of the National Oceanic and Atmospheric Administration (NOAA), U.S. Department of Commerce, and primarily funded by the Bureau of Land Management (BLM), U.S. Department of Interior, through interagency agreement.

DISCLAIMER

Mention of a commercial company or product does not constitute an endorsement by National Oceanic and Atmospheric Administration. Use for publicity or advertising purposes of information from this publication concerning proprietary products or the tests of such products is not authorized.

TABLE OF CONTENTS
Volume 3 - Physical Science Studies

RU	PI/Agency	Title	Page
016	Aagaard, K. -University of Washington Seattle, WA	Current Measurements in Possible Dispersal Regions of the Beaufort Sea	001
138	Muench, R.D. *et al.* -Pacific Marine Env. Lab Seattle, WA	Physical Oceanographic and Meteorological Conditions in the Northwest Gulf of Alaska	075
436	Schleuter, R.S. and C.I. Rauw	Oil Spill Trajectory Simulation Lower Cook Inlet - Shelikof Strait, Alaska	231
436	Schleuter, R.S. and M.W. Miller -Dames and Moore Los Angeles, CA	Wind Field Transition Matrix Analysis Lower Cook Inlet--Shelikof Strait, Alaska	347
436	Schleuter, R.S. and C.I. Rauw -Dames and Moore Los Angeles, CA	Evaluation of CODAR Data Lower Cook Inlet, Alaska	381
568	Cox, J.C. *et al.* -ARTEC, Incorporated Columbia, MD	The Transport and Behavior of Oil Spilled In and Under Sea Ice	427

FINAL NARRATIVE REPORT

Contract No.: 03-5-022-67, T.O. 3
Research Unit No.: 91
Reporting Period: 1 October 1979-31 December 1980
Number of Pages: 74

Current Measurements in Possible Dispersal Regions of the Beaufort Sea

Knut Aagaard

Department of Oceanography
University of Washington
Seattle, Washington 98195

21 January 1981

Knut Aagaard
Knut Aagaard, Research Professor
Principal Investigator

G. C. Anderson
George C. Anderson, Associate Chairman
for Research, Dept. of Oceanography

Ref: A81-02

Introduction

The Alaskan Beaufort Sea shelf extends some 600 km along the entire north coast of Alaska, from 156°30' - 141°W. The shelf is relatively narrow, with the shelf break typically 80-90 km offshore. Much of the coast is marked by numerous shallow embayments and by lagoons and barrier islands.

An important oceanographic factor is the sea ice, which essentially covers the entire area for all but 2-3 months of the year. Its physical effects include the following. (1) It provides thermostatic control, buffering the nearby temperature field in such a way as to keep it at the freezing point. (2) During its formation the ice serves as surface salt source (and hence a density source) by virtue of brine rejection. This drives gravitational convection. (3) During melting, the ice serves as a fresh water source (and hence a buoyancy source), stabilizing the surface layers. This has consequences for solar heat retention, for example. (4) The wind stress acts through the medium of the ice. This is most important nearshore, where the ice is landfast, so that the water is to some extent insulated from the local wind stress.

As to fresh water runoff from land, good estimates are lacking, since only three of the rivers have been gauged. However, on an annual basis, the fresh water discharge is not large. For example, Walker (1973) has estimated the annual discharge of the Colville, which is the largest of the rivers, as about $10^{10}m^3$, or only one-twentieth that of the Yukon. The runoff is highly seasonal, with the majority occurring during a short period in early summer.

The wind field is known primarily from surface wind observations at coastal stations, which show predominantly ENE winds in the western portion, but a bimodal ENE-WSW distribution in the eastern portion (compare Searby and Hunter, 1971, and Hufford, Lissauer and Welsh, 1976). Winds are moderately strong, with monthly mean speeds in excess of 6 m sec^{-1}.

Sea level variations are caused by both meteorological and astronomical tides. The largest sea level variations in the Beaufort Sea are due to storm surges, with measured sea level departures ranging from +3.0 m to -0.9 m (Schaeffer, 1966; Matthews, unpublished data). The largest setup appears to occur in the fall, when relatively long stretches of open water provide maximum fetch. Negative surges apparently are most common in winter (Henry, 1975).

The astronomic tides in the Beaufort Sea, which are mixed semidiurnal, are small, with mean ranges from 10-30 cm, i.e., only one-tenth the largest meteorological tides. For example, Matthews (1971) has estimated the amplitude of the principal lunar tide (M_2) at Pt. Barrow as 4.7 cm. The tide wave appears to approach the shelf from the north, showing little phase change from Barrow to Demarcation Point.

It is against this background that we shall discuss our work in the Beaufort Sea, the primary goal of which was a description and understanding of the shelf circulation, including its relationship to adjacent regions. The work involved both hydrographic sections (R.U. 151) and moored current measurements (R.U. 91).

The measurements

The hydrography consisted of about 110 CTD stations. The first year of field work, three CTD sections were run across the shelf by helicopter during each of the periods October-November 1975, February 1976 and May 1976, which were taken to respectively represent the fall, winter and spring. The following field season, four sections were run, again by helicopter, in each of the periods

October-November 1976 and March 1977. The approximate location of all of these sections is shown schematically in Figure 1, where PP (Pitt Point), NI (Narwhal Island), and HB (Humphrey Bay) denote the 1975-76 sections, and LW and LE (Lonely West and East) and OW and OE (Oliktok West and East) denote the 1976-77 sections. The temporal coverage is indicated in Figure 2. These data have been discussed earlier in RU 151 reports, including the Final Report of 21 June 1978, but we shall have frequent occasion to further use the results in the present discussion of the shelf circulation.

The current measurements were made with bottom-moored instruments, using the techniques for ice-covered waters described by Aagaard, Darnall and Karig (1978). Exceptions are the two records offshore from Narwhal Island (NAR-1 and -2), which are from instruments suspended from fast ice. All measurements are therefore in a true Eulerian reference frame, except for the last few days of the NAR-2 record, when the ice from which the instrument was suspended began to move. However, radar tracking of the site allowed this motion to be subtracted from the current record. The current meters also recorded time series of temperature. The sampling interval for the various instruments ranged from 15-60 minutes, depending upon the intended deployment time. A total of about 2335 days of usable records were obtained. The temporal distribution of the measurements is again shown in Figure 2, while Figure 3 shows the spatial coverage. A listing of mooring particulars is given in Table 1.

Implications of the hydrography

The principal features of the temperature and salinity distributions form a useful starting point for a discussion of the shelf circulation.

BEST DOCUMENT AVAILABLE

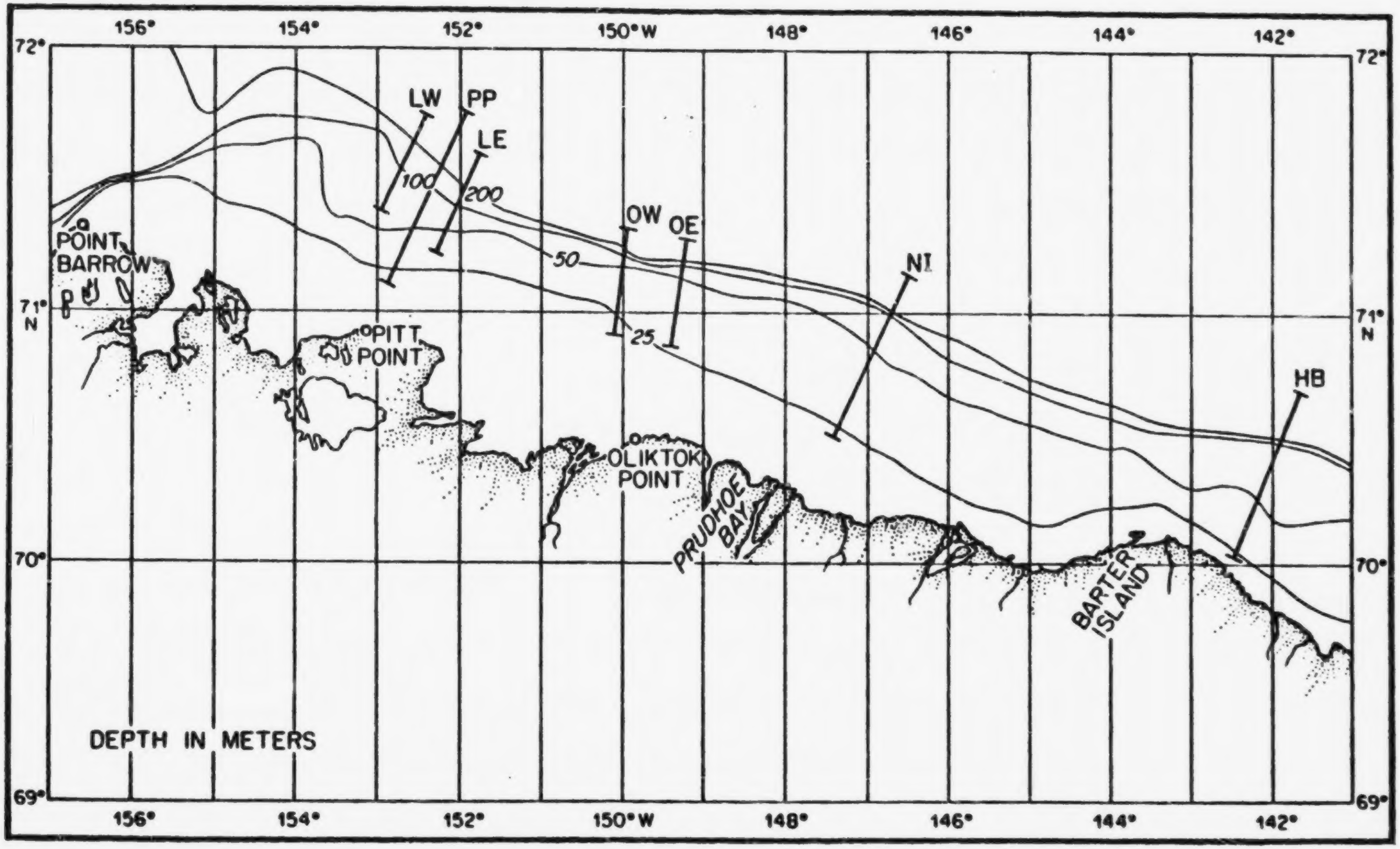
156°
154°
152°
150°W
148°
146°
144°
142°
72°
71° N
70°
69°
LW
PP
LE
100
200
50
25
OW
OE
NI
HB
POINT BARROW
PITT POINT
OLIKTOK POINT
PRUDHOE BAY
BARTER ISLAND
DEPTH IN METERS

Figure 1. Location of CTD sections, 1975-1977.

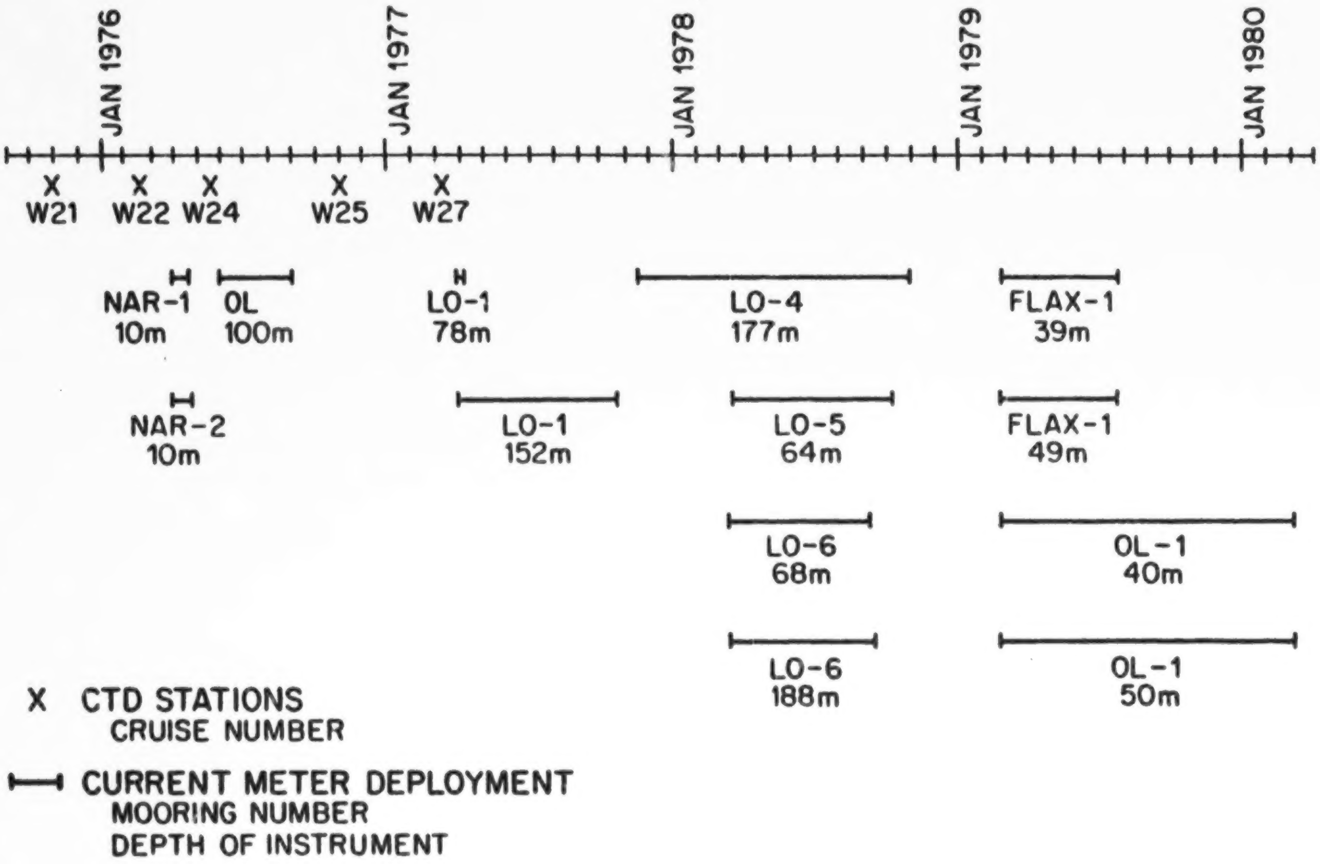

Figure 2. Distribution in time of CTD and current measurements.

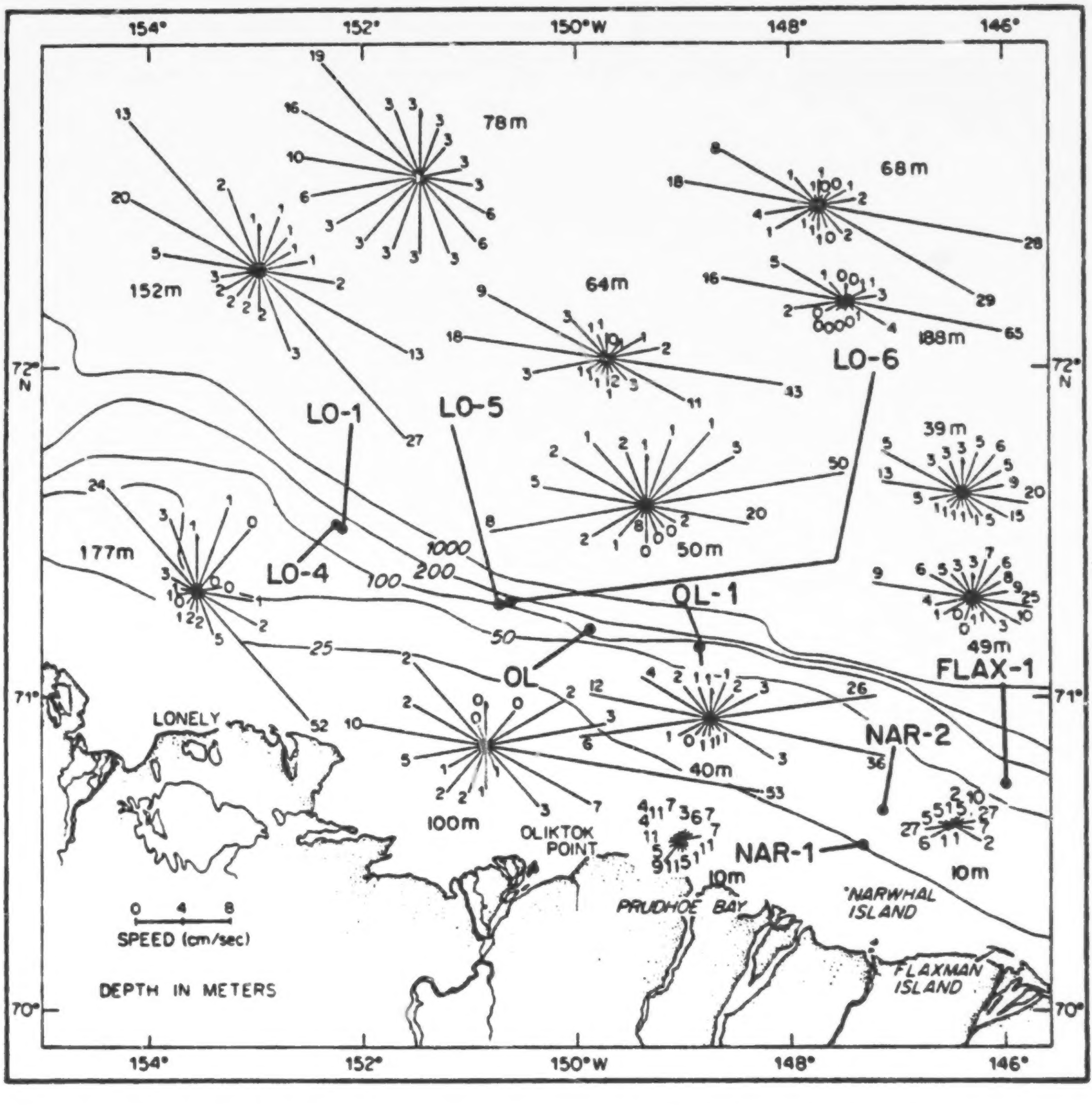
154°
152°
150°W
148°
146°
72° N
71°
70°
78m
68m
64m
188m
152m
LO-1
LO-5
LO-6
39m
50m
177m
LO-4
1000
200
100
OL-1
50
25
49m
FLAX-1
OL
LONELY
40m
NAR-2
100m
OLIKTOK POINT
NAR-1
10m
10m
PRUDHOE BAY
NARWHAL ISLAND
FLAXMAN ISLAND
0 4 8
SPEED (cm/sec)
DEPTH IN METERS

Figure 3. Current roses at all mooring sites. Each vector represents the mean current in a sector of 20°. The number at the end of each vector is the frequency of occurrence of a current within that sector. Depth of measurement shown adjacent to each rose. Heavy dots show mooring locations.

TABLE 1

RU 91 Current Records

Mooring	Latitude	Longitude	Sounding	Instrument Depth	Valid Record (GMT) Begins	Valid Record (GMT) Ends
NAR-1	70°38.7'N	147°09.0'W	27 m	10 m	28 March 1976	19 April 1976
NAR-2	70°32.2'N	147°20.0'W	38 m	10 m	"	22 April 1976
OL	71°12.6'N	149°53.0'W	225 m	100 m	27 May 1976	1 Sept. 1976
LO-1	71°31.1'N	152°11.3'W	192 m	78 m	29 March 1977	6 April 1977
LO-1	"	"	192 m	152 m	"	20 October 1977
LO-4	71°31.8'N	152°15.3'W	192 m	177 m	13 Nov. 1977	30 October 1978
LO-5	71°17.0'N	150°44.1'W	99 m	64 m	13 March 1978	7 October 1978
LO-6	71°17.7'N	150°37.9'W	203 m	68 m	11 March 1978	4 September 1978
LO-6	"	"	203 m	188 m	"	14 September 1978
FLAX-1	70°43.6'N	146°00'W	59 m	39 m	22 Feb. 1979	22 July 1979
FLAX-1	"	"	59 m	49 m	"	"
OL-1	71°10.0'N	148°52.7'W	60 m	40 m	21 Feb. 1979	6 March 1980
OL-1	"	"	60 m	50 m	"	"

Influx from the Bering Sea. In summer the most prominent hydrographic signal on the shelf is a subsurface temperature maximum, generally found seaward of about 40-50 m. An example is given in Figure 4, showing a temperature section across the shelf at 150°W during August 1972 (from Mountain, 1974). This temperature maximum is associated with the eastward flow of water originating in the Bering Sea. The influx was first described by Johnson (1956), and it has since been discussed by Hufford (1973), Mountain (1974), Paquette and Bourke (1974) and others.

The warm water that enters the Beaufort Sea has come through eastern Bering Strait and followed the Alaskan coast around Barrow. This intrusion is in fact composed of two water masses, called Alaskan coastal water and Bering Sea water by Mountain (1974). The former can have summer temperatures west of Barrow as high as 5-10°C, but the salinities are low, being less than 31.5‰. The Bering Sea water is more saline and is contained in the density range 25.5 to slightly over 26.0 (in sigma-t), as has been demonstrated in the detailed analyses of Mountain (1974) and Coachman, Aagaard and Tripp (1975). Figures 5 and 6 are adapted from Mountain (1974) and show the temperature on density surfaces associated with the two intruding water masses. The restriction of the eastward flow to the outer continental shelf and slope is clear, as is the difference in extent of influence of the two water masses. The Alaskan coastal water mixes rapidly with the ambient surface water as it moves eastward and is not clearly identifiable east of about 147-148°W. On the other hand, the Bering Sea water, with its deeper temperature maximum (in the sigma-t range 25.5-26.0), can be traced at least as far as Barter Island at 143°W.

BEST DOCUMENT AVAILABLE

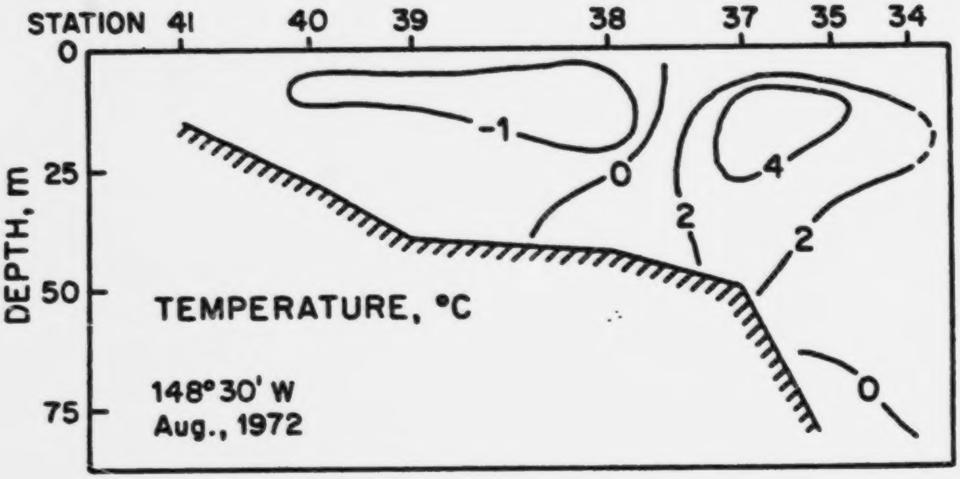

Figure 4. Summer temperature section across the shelf. From Mountain (1974).

BEST DOCUMENT AVAILABLE

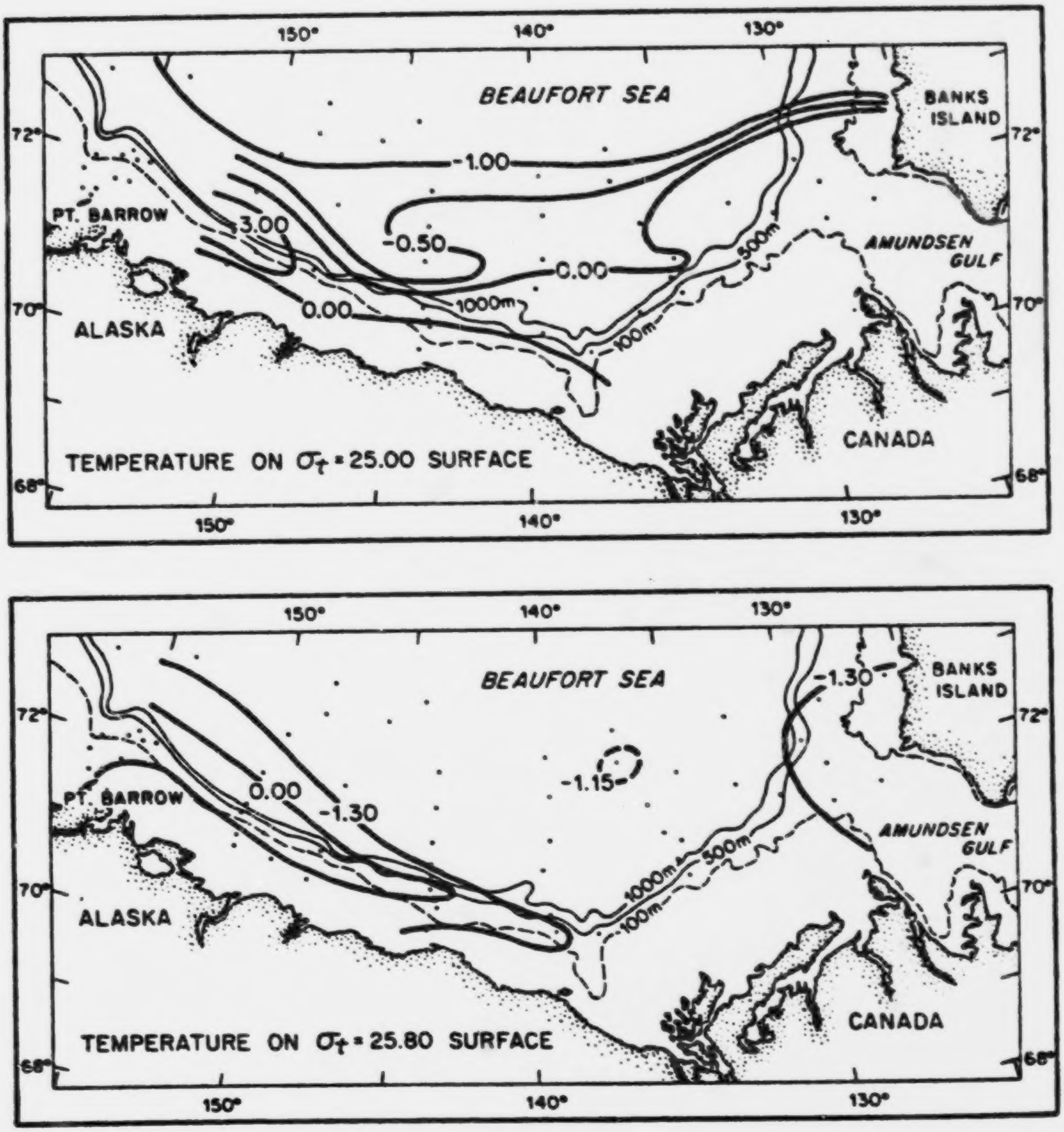
150°
140°
130°
BEAUFORT SEA
BANKS ISLAND
72°
-1.00
PT. BARROW
3.00
-0.50
0.00
500m
AMUNDSEN GULF
1000m
70°
0.00
100m
ALASKA
CANADA
TEMPERATURE ON σ_t = 25.00 SURFACE
68°
150°
140°
130°
BEAUFORT SEA
-1.30
BANKS ISLAND
72°
-1.15
PT. BARROW
0.00
-1.30
AMUNDSEN GULF
500m
1000m
100m
70°
ALASKA
CANADA
TEMPERATURE ON σ_t = 25.80 SURFACE
68°

Figure 5. Temperature on density surfaces corresponding to Alaskan coastal water (σ_t = 25.00) and Bering Sea water (σ_t = 25.80), August-September 1951. Adapted from Mountain (1974).

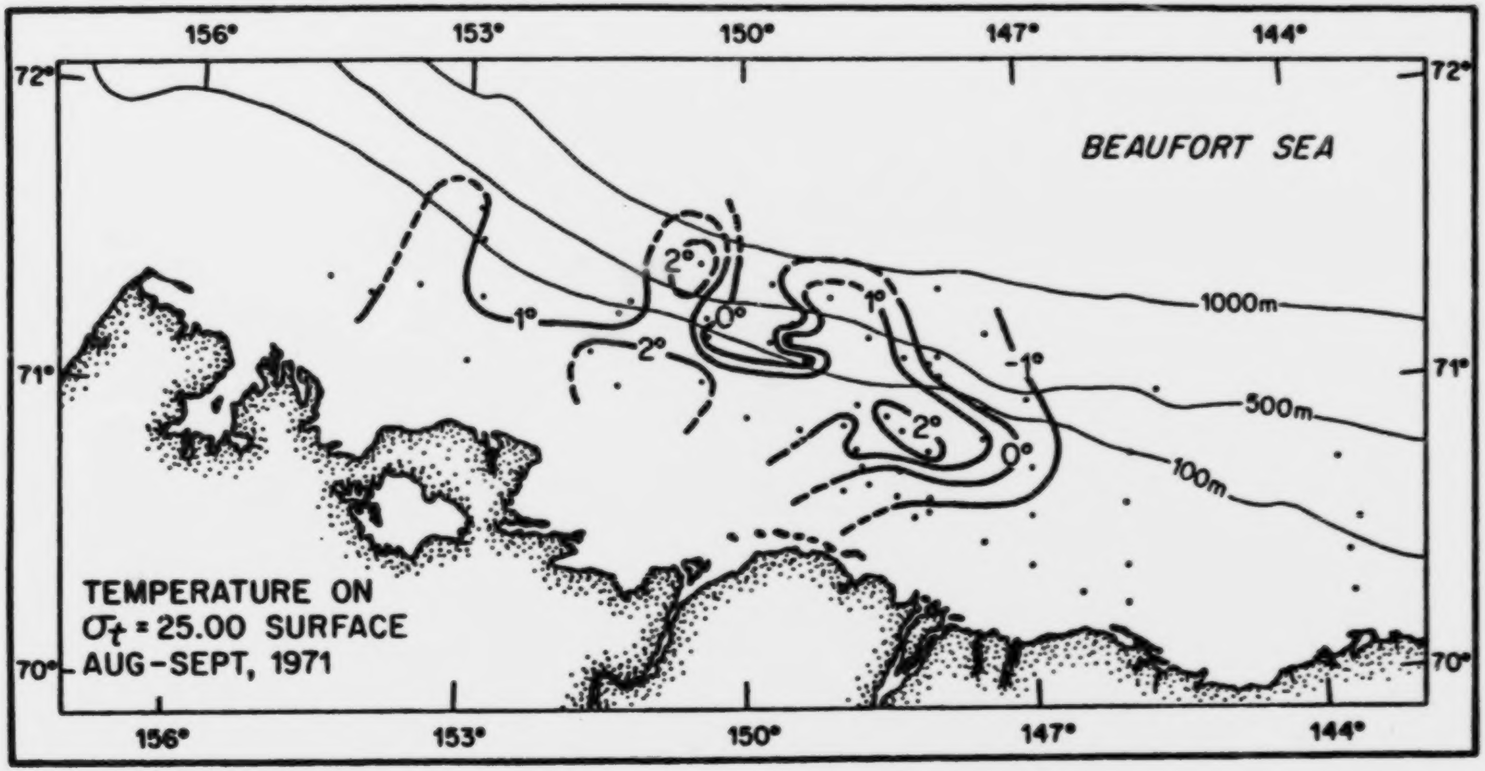
156°
153°
150°
147°
144°
72°
71°
70°
BEAUFORT SEA
1000m
500m
100m
2°
1°
0°
-1°
TEMPERATURE ON
σ_t = 25.00 SURFACE
AUG-SEPT, 1971

Figure 6. Summer temperature on density surface $\sigma_t = 25.00$. Adapted from Mountain (1974).

BEST DOCUMENT AVAILABLE

The patchiness of the temperature distribution in Figure 6 is of particular interest. Mountain (1974) has attributed such features to variations in the influx of warm water onto the Beaufort shelf, and in fact the appropriate variability has been observed upstream along the Chukchi Sea coast. In Mountain's view the eastward flow over the Beaufort shelf is driven externally by the momentum flux of the upstream flow, with its attendant pulsations. While both scale analysis and observations available at that time suggested that the interpretation may be reasonable, it is not clear why such a flow should follow the isobaths eastward, as it appears to do (e.g., cf. Figure 5), for the geometry is such as to destabilize an eastward flow attempting to conserve potential vorticity.

The temperature maximum on the shelf is primarily a summer phenomenon. Figure 7 shows the T-S correlation at two stations in the LW section. Station W 25-19 was taken in early November 1976 and W 27-1 at the same location the following March. The temperature maximum of about −0.9°C at 43 m at station 19 occurred at $\sigma_t = 25.8$ and represents Bering Sea water having rounded Point Barrow earlier in the year at a higher temperature. Sometime later in the winter, the Bering Sea temperature signal is effectively erased on the shelf, as shown by the T-S correlation in the upper 50 m at station W 27-1: down to about 40 m, where the density is 26.5 m in sigma-t, the water is at the freezing point. Such low temperatures extending into or past the density range of the core of Bering Sea water are typical on the shelf in winter, and in fact these conditions can readily be found already in November. One can therefore in general probably not trace the Bering Sea water on the Beaufort shelf much past freeze-up in the fall. We should also note that after that time the new water entering the Beaufort Sea from the Chukchi is itself near the freezing point after being cooled in its fall and winter transit northward.

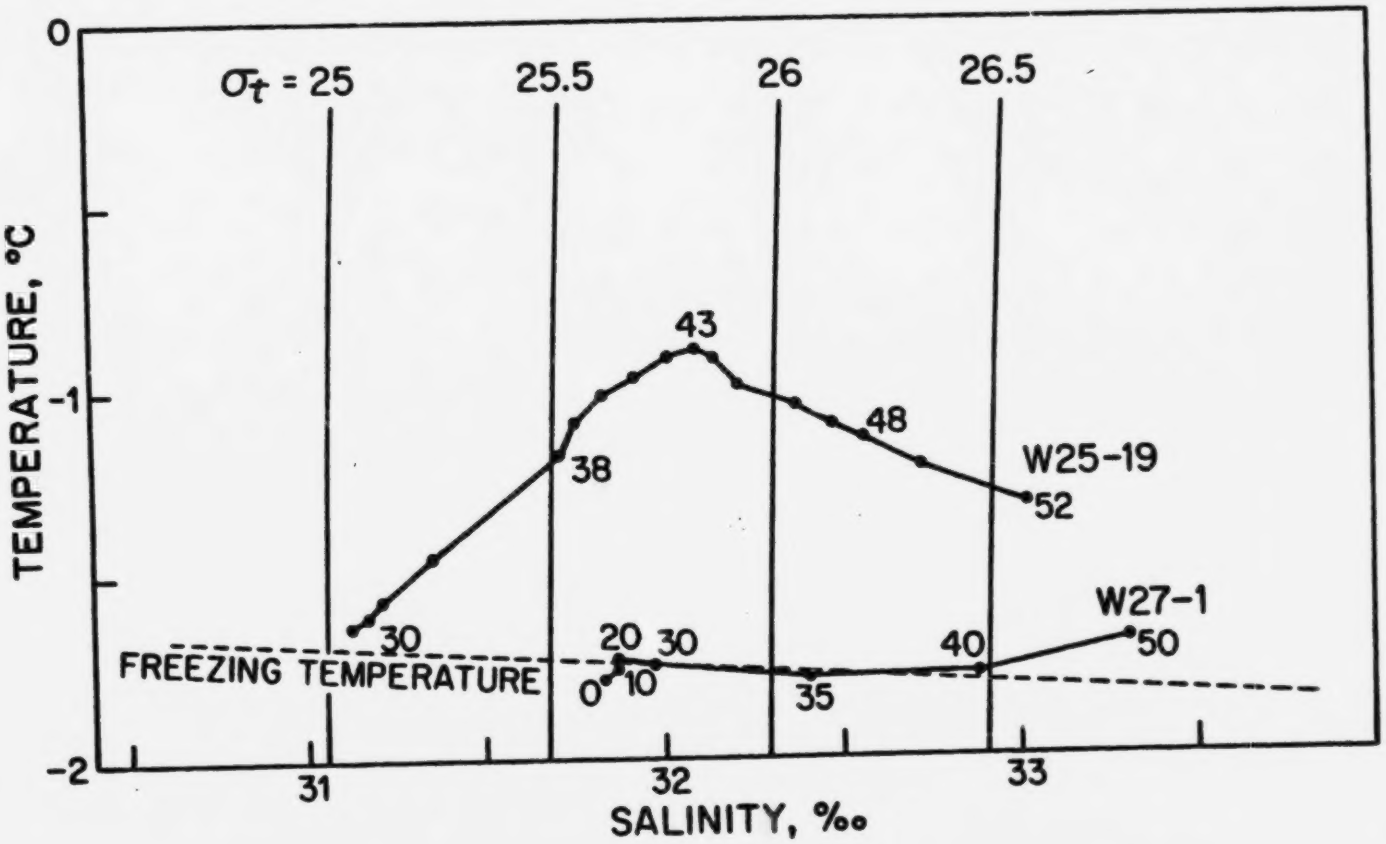

Figure 7. Temperature-salinity correlations at a fall and winter station in Section LW.

BEST DOCUMENT AVAILABLE

Upwelling. There are also other hydrographic signals which provide significant information on the shelf circulation. Among these are the various indicators of upwelling. That is, water has been found on the shelf with characteristics appropriate to a location relatively deep offshore. Such hydrographic anomalies may occur in temperature, salinity, oxygen, nutrients, and other fields. An example from the eastern Alaskan Beaufort shelf during summer was described by Hufford (1974), who found evidence for upwelling from about the 125 m level offshore (cf. Figure 8). He ascribed the upwelling to easterly winds driving a coastal Ekman divergence during periods of open water.

We have observed what appears to be a very different kind of upwelling, with the upwelled water derived from offshore depths of 200 m or more. Figure 9, showing sections LW and OE during October-November 1976, provides an example. Note that in the OE section, water warmer than 0°C and more saline than 34.5°/oo was observed as shallow as 91 m. Comparison with conditions the following winter at the same location (Figure 10) shows that such water is found offshore at about the 200 m level during undisturbed conditions (no upwelling). Note further that at section LW, some 120 km to the west, upwelling was also observed, with relatively warm and saline water apparent even at the innermost station, where the bottom 10 m were warmer than -1°C and more saline than 34°/oo. The upwelling is therefore not a strictly local phenomenon, but can occur over long stretches of the shelf. However, it is important to note that neither during nor within at least 10 days prior to the section occupations in the fall of 1976 were there strong or prolonged easterly winds, so that the elevated isopleths are not readily explainable as representing a wind-driven coastal upwelling event.

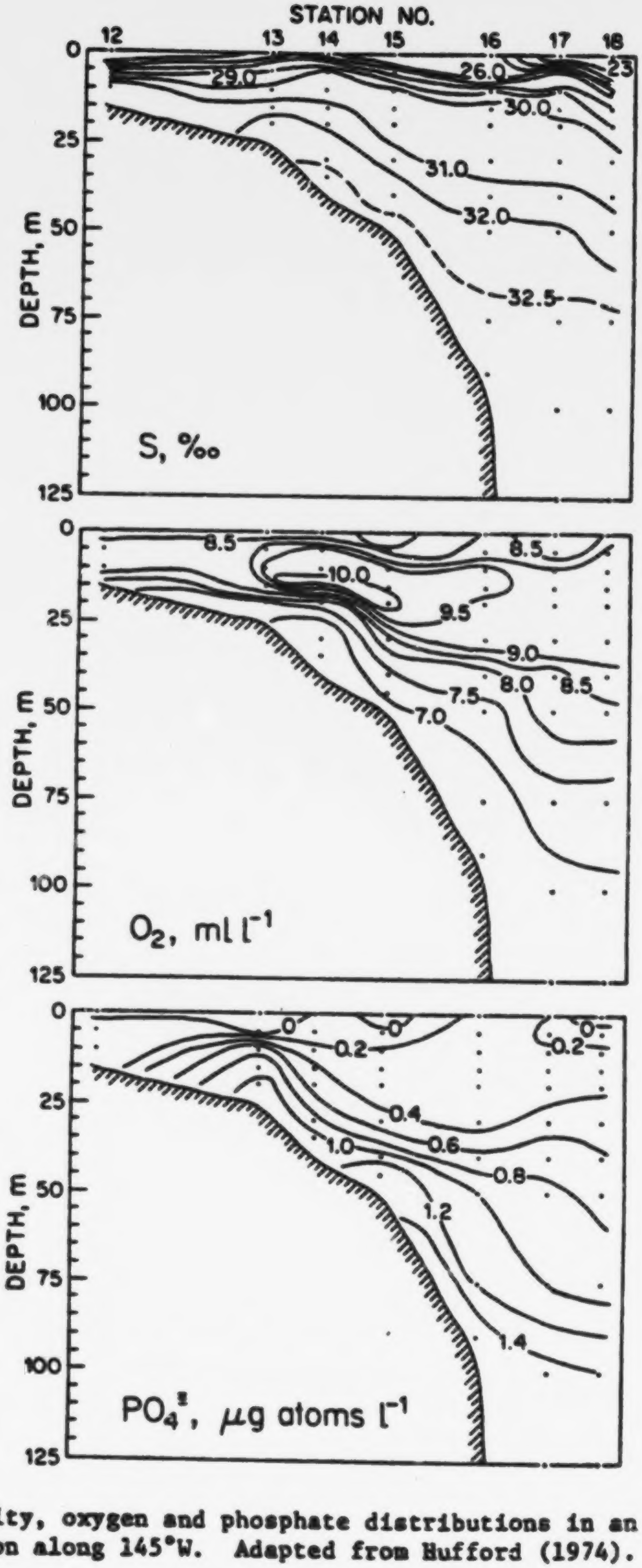

Figure 8. Salinity, oxygen and phosphate distributions in an August 1972 section along 145°W. Adapted from Hufford (1974).

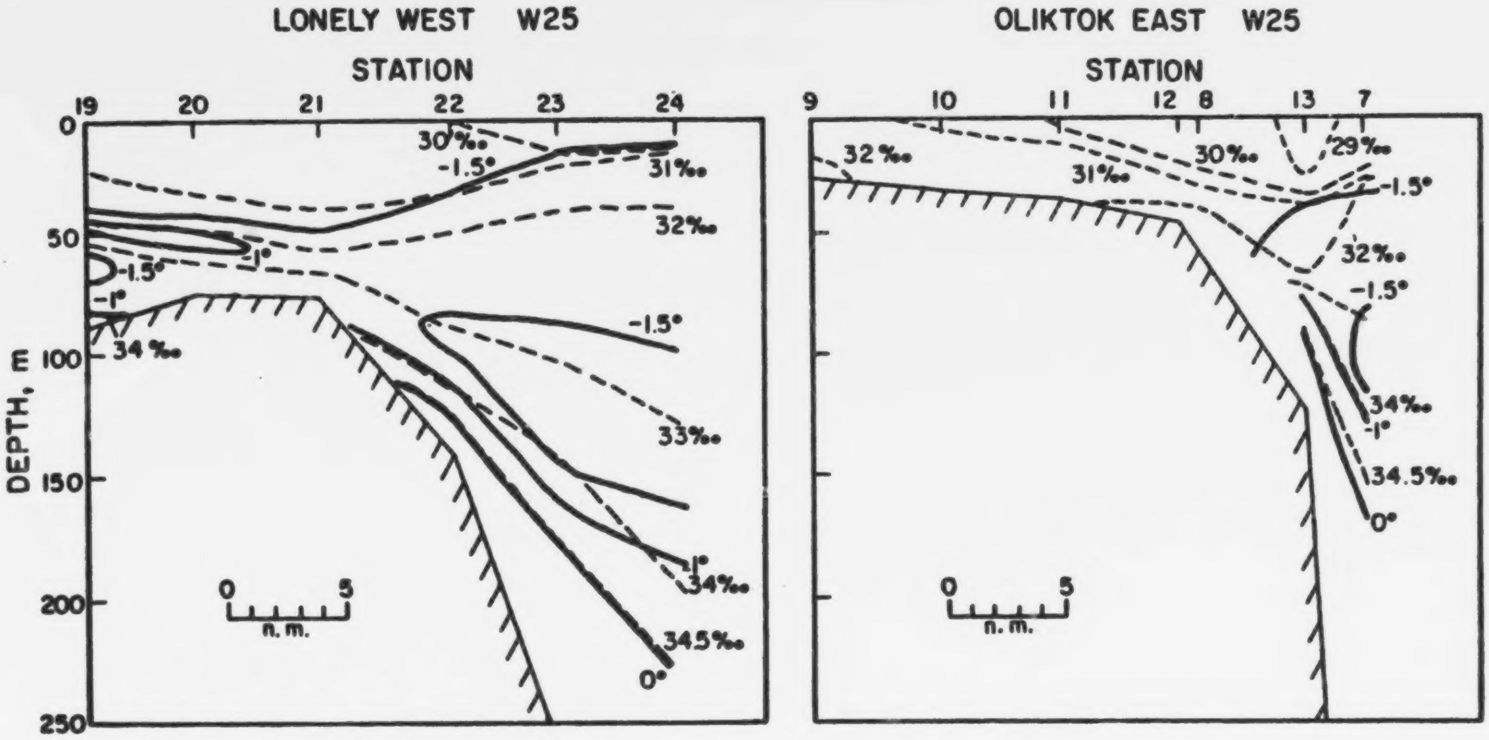

Figure 9. Temperature and salinity distribution along Sections LW and OE, October-November 1976.

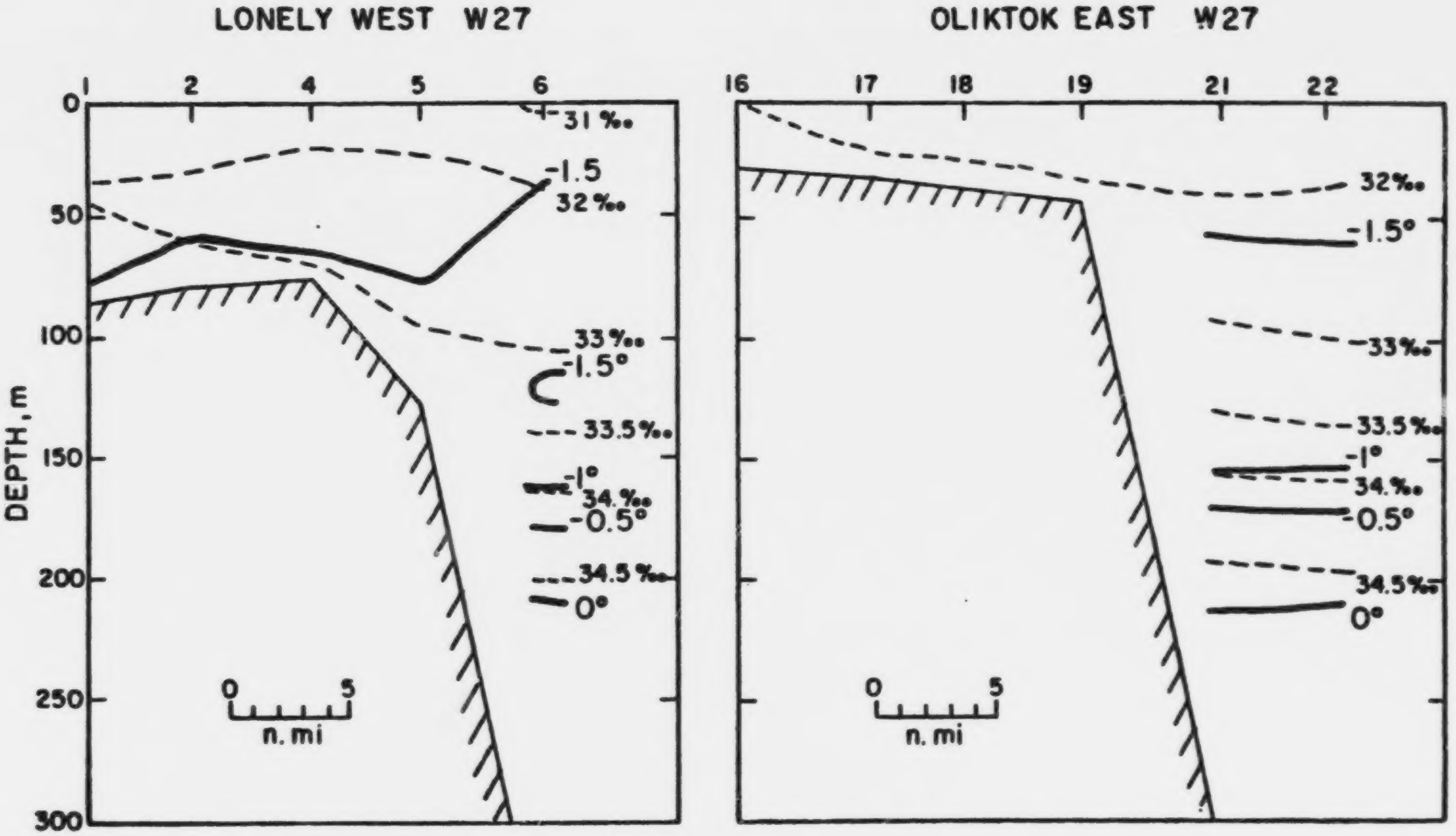

Figure 10. Temperature and salinity distribution along Sections LW and OW, March 1977.

BEST DOCUMENT AVAILABLE

We have seen the deep isopycnals sloping upward toward the shelf in a sufficiently large number of the sections to suggest that the penomenon is relatively common. Furthermore, there is often a change in the sign of the vertical geostropic shear at the outermost stations in these sections. Typically, this occurs at a depth of 50-80 m, and while the geostrophic flow field cannot be uniquely determined from these measurements alone, a reasonable reconstruction is that a core of relatively dense water at mid-depth (50-100 m) was moving westward with a component up-slope. The core speed at such times may be quite high, as suggested by a geostrophic velocity difference between 70 and 200 db of 55 cm sec^{-1} at the time of the stations in Figure 9.

Cross-shelf circulation. A third feature of the hydrography also has implications for the shelf circulation, *viz.* the seasonal change in the cross-shelf salinity gradient in the upper layer. During summer the salinity in the upper layer increases seaward across the shelf. This situation persists into the fall as a relic feature, but by mid-winter the gradient has reversed, with salinity decreasing seaward. An example is seen in Figures 11 and 12, respectively showing the HB section in November 1975 and February 1976. In Figure 11 the remnants of the summer situation are still dominant, with the near-surface salinity increasing outward across the shelf by 2°/oo. However, in Figure 12 the situation is reversed, the salinity decreasing from 30.7°/oo at station 18 to 29.9°/oo at station 24.

While the summer salinity distribution almost certainly represents the effect of fresh water runoff, the winter distribution likely results from a cross-shelf circulation component. Two possibilities suggest themselves.

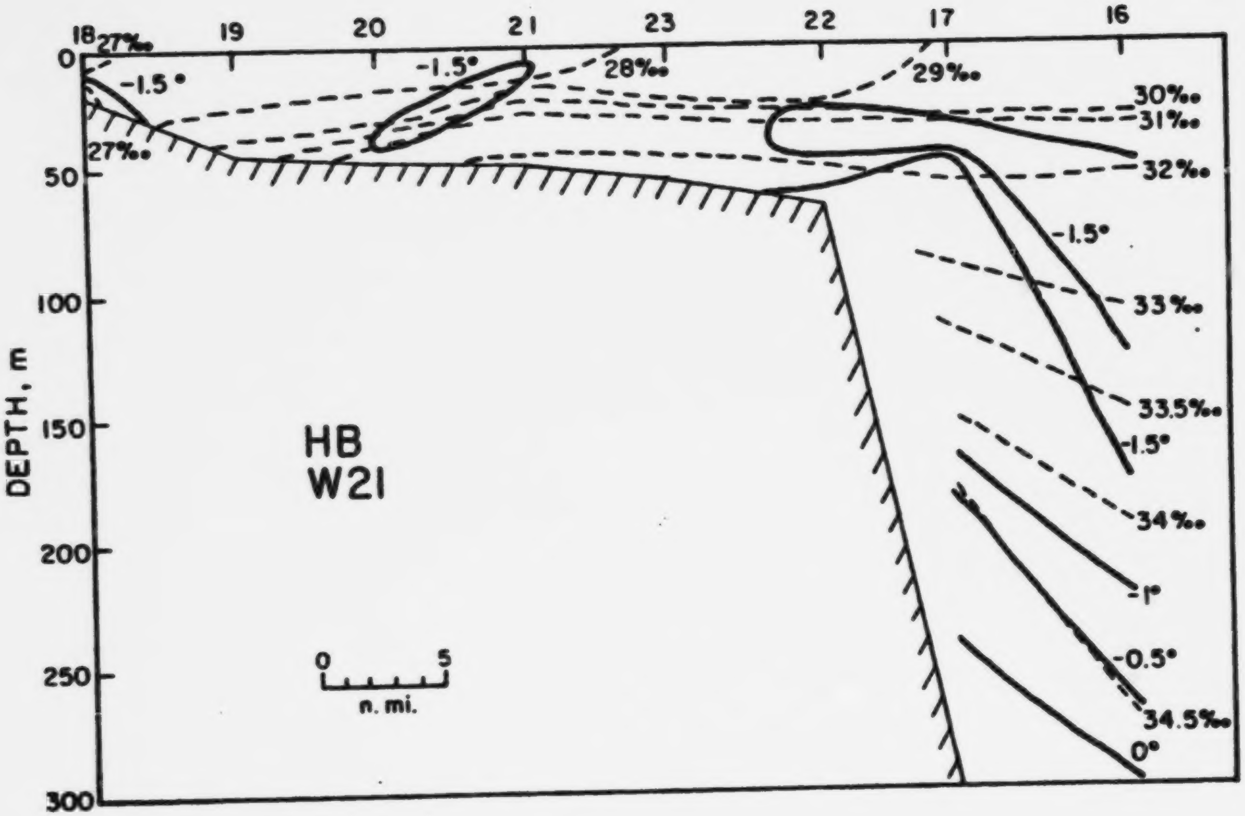

Figure 11. Temperature and salinity distribution along Section HB, November 1975.

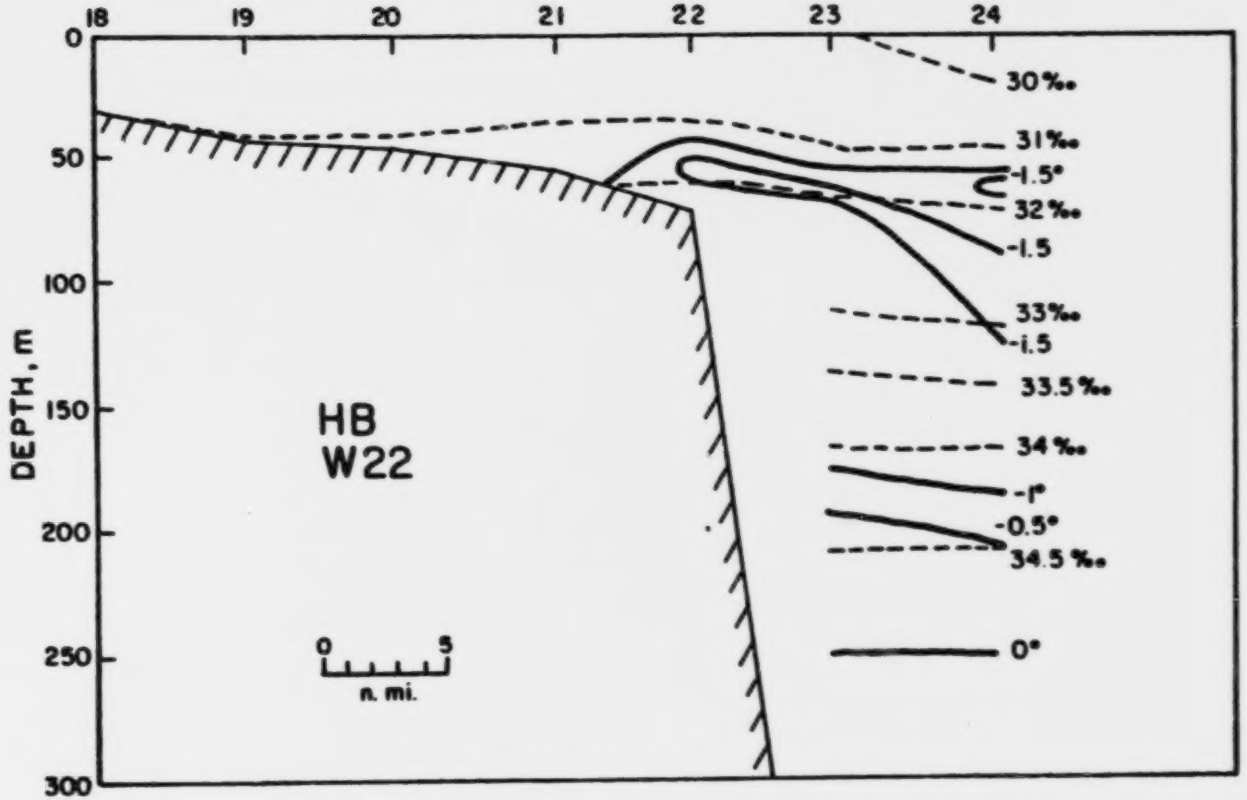

Figure 12. Temperature and salinity distribution along Section HB, February 1976.

One is that relatively dense water sinking from the upper layer above the shelf moves into the Arctic Ocean at mid-depth and is replaced by less saline water moving inshore in the upper layer. Such a transverse circulation is in the counter-clockwise sense (looking westward along the shelf) and would be driven by a shallow salt source on the shelf. Freezing is of course an obvious example of such a salt source, its relatively greater intensity inshore conceivably being due either to the volume of water underlying a given surface area being less there, or to the amount of ice actually formed on the shelf being greater than offshore, for example due to a wind-driven divergence along the coast such as has been shown to be of major import in the Bering and Chukchi seas (Aagaard, Coachman and Carmack, in press). Speaking against the latter possibility is the fact that the Beaufort coast does not typically show persistent ice-free areas in winter. Alternatively, relatively saline water being advected onto the shelf from the Chukchi Sea and later sinking from the shelf could also drive such a transverse circulation. Regardless of the details, a counter-clockwise circulation involves some form of free gravitational convection and is driven by a source of dense water on the shelf. The importance to the climatology of the Arctic Ocean of such mechanisms operating in the shelf seas has recently been discussed by Aagaard, Coachman and Carmack (in press).

The second possible mechanism responsible for the observed salinity distribution is upward movement of saline water onto the shelf from deeper levels in the Arctic Ocean. This water would have to flow in near the bottom and then be subjected to a relatively effective vertical mixing on the inner or middle shelf. Such a transverse circulation is in the clockwise sense (looking westward) and would in effect be driven by a deep salt source seaward of the shelf. It thus represents a forced convection. We have already discussed the evidence that such upwelling actually occurs, and in a later consideration of the temperature records from the moored instruments we shall see that it is a frequent occurrence throughout the year.

As a word of caution, we should not assume that the cross-shelf circulation is merely in a transverse mode, for there are rotational constraints on the dynamics. For example, for the case of a salt source on the shelf, the dense, saline waters attempting to flow off the shelf will be deflected by the effect of the Earth's rotation until geostrophic equilibrium is reached. Therefore the actual feeding of the dense shelf water into the Arctic Ocean likely would either depend on transport in the bottom Ekman layer or on channeling by submarine bathymetry. Once the dense water crosses the shelf break, it must eventually sink to the depth where its density matches that of the ambient oceanic waters, at which point it will detach from the bottom and spread into the interior ocean.

Mixed-layer depth. A final winter hydrographic feature with implications for the ~~hydrography~~ circulation is that the depth to which a layer is mixed (in the sense that above this depth the density is nearly uniform) is considerably shallower than the depth to which the water is at the freezing point. Two examples are shown in Figure 13, one a fall and the other a winter station. At both stations a notable pycnocline (caused by a salinity gradient) of about 0.05 in σ_t per meter begins at about 20 m, while the water is at the freezing point to more than twice this depth. Thus, water that has clearly been conditioned by the freezing process can subsequently be found within or below the pycnocline. In effect, the water must have moved obliquely down to the depth locally

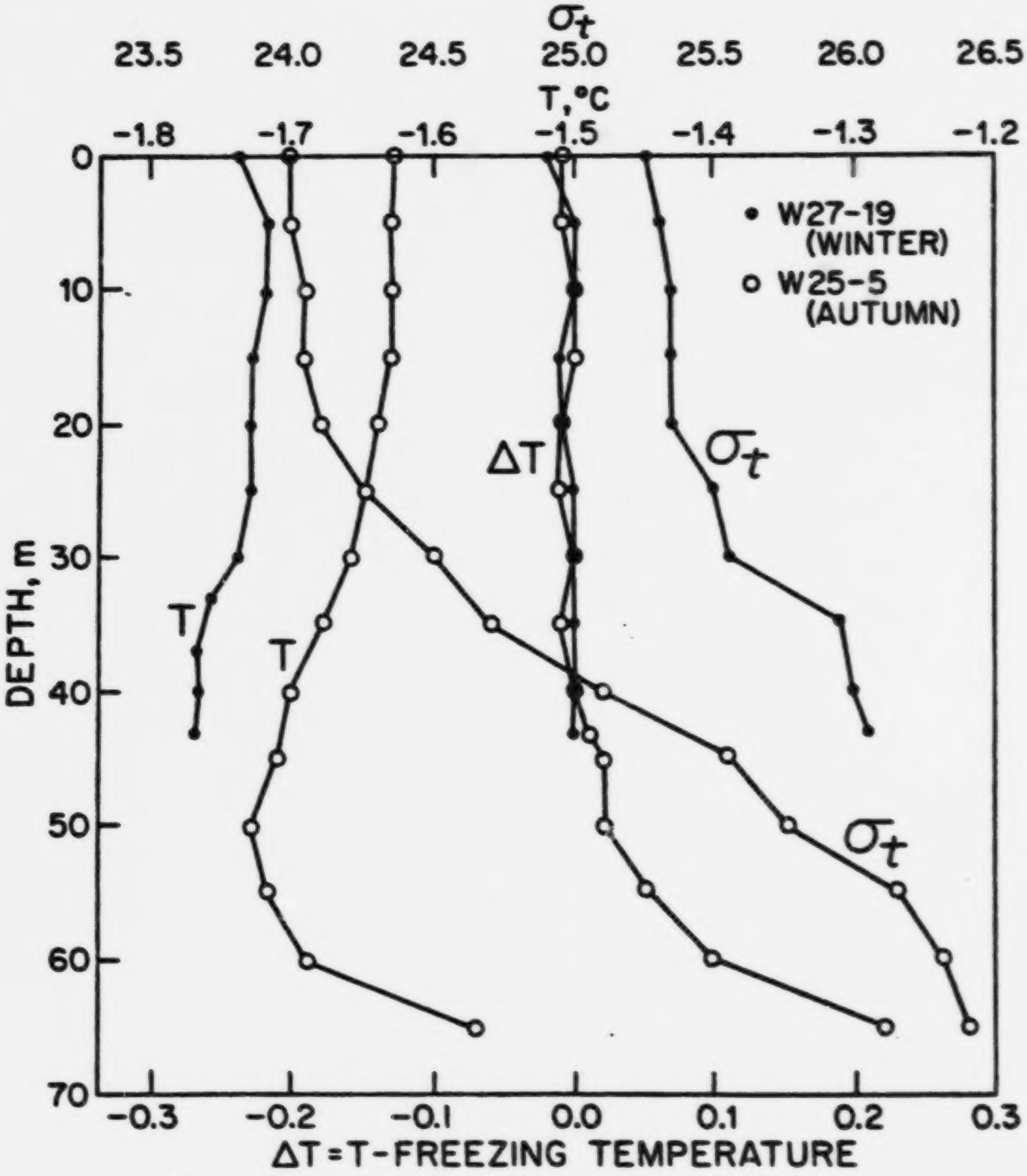

Figure 13. Vertical distributions of temperature, density (σ_t), and departure from freezing point at a fall and winter station on the shelf.

appropriate to its density. An observed winter water column on the shelf is thus not simply representative of a local and vertically extensive mixing process driven by freezing, but rather it represents a layering of waters that may have been influenced by freezing at a variety of locations and times. After being cooled, and probably also having their salinity altered, the various parcels of water then arrange themselves in a stably stratified layer through differential motion. In other words, the hydrography shows that the time history of a column of water involves considerable vertical shearing even in winter.

The inner shelf

We noted earlier that the water moving eastward from the Chukchi Sea is normally found seaward of the 40-50 m isobaths. This depth range proves to be a convenient demarcation zone, separating two different circulation regimes, *viz.* the inner and outer shelf. We shall treat the inner shelf first.

Current measurements on the inner shelf are extremely sparse, largely because of the difficulty of maintaining moorings in ice-covered shallow waters; the moorings are simply ripped away by the drifting ice. However, in March-April of 1976 we obtained two three-week records on the inner shelf, NAR-1 and -2 in, respectively, just under 30 and 40 m of water (cf. Figure 3 and Table 1). In each case an instrument was suspended at 10 m depth from fast ice.

Figure 3 shows the current roses for these two instruments, as well as for the other current records obtained on the shelf under our OCSEAP work. Note that at each indicated mooring site, the current rose for a particular instrument (instrument depth given adjacent to the rose) represents both the mean speed and the direction, the latter in terms of the frequency of occurrence of the current in each sector of angular measure 20 degrees of arc. For example, at mooring LO-5 on the outer shelf, which recorded from 13 March to 7 October 1978 (cf. Table 1), the current was predominantly toward 100 ± 10°T. It registered in this sector 43% of the time, and the mean speed over the nearly 7 months was about 15 cm $\sec^{-1}$. At the same location the next most commonly observed current was in the reciprocal direction, and in the mean it was about 2 cm $\sec^{-1}$ slower (i.e., 13 cm $\sec^{-1}$). Note that Figure 3 by itself provides no information on observational time spans, and must therefore be examined together with Table 1. For example, at site LO-1 the rather round current rose at 78 m represents just over a week of measurements, whereas the elongated elliptical rose at 152 m represents nearly seven months and is therefore in a probabilistic sense far more representative of the current conditions.

Consider now the NAR-1 and -2 records in Figure 3. It is apparent both that the flow was quite slow and that there was little net motion. Examination of the individual records shows that the currents never exceeded 10 cm $\sec^{-1}$ and were generally less than 5 cm $\sec^{-1}$. The mean flow during the three weeks was essentially negligible, being only 0.1 cm $\sec^{-1}$ at NAR-2 and 0.3 cm $\sec^{-1}$ at NAR-1; both were directed WSW.

The two instruments were separated by only 14 km, and the progressive vector diagrams (Figure 14) show that the low-frequency variability was quite similar at the two sites. For example, after some initial motion NE, both instruments showed SW motion from about 1-6 April, followed by some irresolute wandering (but with a small net northward displacement) until 14 April, when two days of stronger motion toward the east occurred. Finally, from 16 April

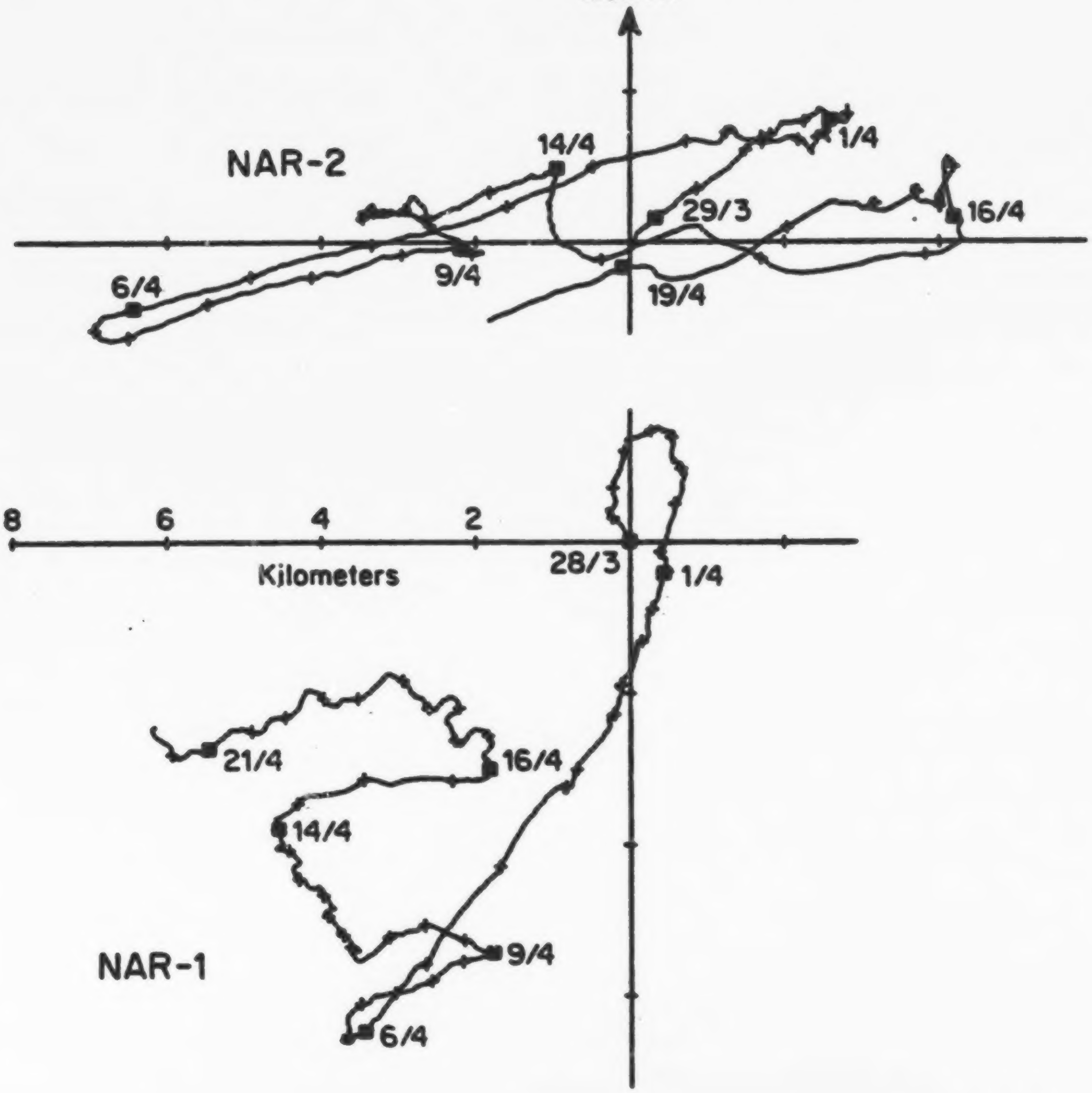

Figure 14. Progressive vector diagrams at NAR-1 and NAR-2.

until the end of the record the motion was westerly. A comparison with the simultaneous wind record from Narwhal Island suggests that the flows were in fact wind-driven. That is, the winds the last few days of March were from the WSW up to 14 knots. Then followed a long period of NE winds with speeds to 13 knots. From 6-13 April the wind was variable, but from 13-15 April strong winds (to 18 knots) blew from between NW and SW. Finally, from late on 15 April until the end of the record, generally E or NE winds prevailed. Comparison with the wind statistics of Searby and Hunter (1971) and Hufford, Lissauer and Welsh (1976) shows these observed wind conditions to be climatically representative in the distributions both of speed and direction. While it might appear puzzling at first why the currents under fast ice should reflect the wind conditions so well, the key probably lies in the instruments being quite close to the edge of the fast ice. (In fact, during the last few days of the NAR-2 record, the ice from which the current meter was suspended broke loose and was in motion.) Close to the edge, the water may, for example, be moved by lateral entrainment. We should expect a decreasing wind response landward of the fast ice edge, as the shore is approached, and in fact Figure 14 suggests that this is indeed the case. That is, the indicated water displacements at the inshore site (NAR-1) under strengthened wind conditions are appreciably less than at the offshore site (NAR-2). For example, contrast the displacements at the two sites from 14-16 April under relatively strong W winds and from 16 April onward under E winds.

The suggestion of a relatively direct wind-driven regime in winter near- and offshore from the fast ice edge is in accord with the observed summer situation on the inner shelf. For example, Barnes and Reimnitz (1974); Barnes, Reimnitz and McDowell (1977); Drake (1977); Hufford and Bowman (1974);

Hufford, Fortier, Wolfe, Doster and Noble (1974); Hufford, Thompson and Farmer (1977); and Wiseman, Sukeyda, Hsu, and Walters (1974) have all shown evidence of such wind-driven effects. In general there is a westward water motion corresponding to the prevailing easterly winds, but the circulation responds rapidly to changing wind conditions, such that under westerly winds (which is the secondary wind mode) the motion is eastward. An interesting summer feature that has been pointed out by Barnes and Toimil (1979) is that east of about 146°W the nearshore flow appears to be predominantly easterly. They suggested that it is associated with the more frequent occurrence of westerly winds in the eastern Beaufort Sea than in the western portion. If this is in fact so, then the tendency should be greatest in winter, when the westerly winds achieve their greatest prominence as a result of mountain barrier baroclinicity (Schwerdtfeger, 1974).

In any case the clear suggestion of our very sparse winter flow measurements on the inner shelf is that even though the kinetic energy levels are suppressed in winter (at least under the fast ice), the circulation is predominantly wind-driven throughout the year. How far inshore under the fast ice the wind effects persist, is not known.

Neither can we at this point say anything conclusive about the transverse circulation on the inner shelf. In addition to the direct driving by the wind, at least three possible mechanisms are available for forcing such a circulation. The first is an estuarine effect, in which in the pure case the upper-layer flow is driven seaward by the accumulated effect of runoff; there would normally be a compensating deeper landward flow in all but the shallowest water. Because of the extremely seasonal character of the runoff, this mechanism could only be of significance during peak runoff in early summer. [For example, note the absence of an effluent plume off the Colville River in August in the work of Hufford and Bowman (1974).] Furthermore, the lack of lateral constraints on the flow means that rotational effects would give rise to primarily a longshore current rather than one normal to the coast. Under these circumstances the cross-shelf transport would have to be accomplished in an Ekman layer, or by turbulent diffusion, or by some other non-estuarine means.

A second possible mechanism for cross-shelf circulation is wind-driven upwelling (or downwelling) at the edge of the fast ice. For example, under easterly winds, a surface Ekman layer divergence at the ice edge would drive upwelling, the water for which in the net would have to be supplied by an onshore flow at lower levels. Experimental evidence for the existence of such upwelling along a free ice edge has been found by Buckley, Gammelsrød, Johannessen, Johannessen and Røed (1979). Under westerly winds the effect would be reversed, with a deep offshore flow.

The third mechanism for a transverse circulation is the production during ice formation of very dense water inshore, which in some manner has to flow seaward. We have already discussed this process in an earlier section, and while there is reason to doubt the existence of a large circulation mode of this kind on the Beaufort shelf (primarily because of the absence of large areas of thin ice or open water in winter), certainly the existence of very dense water in restricted shallow areas during winter could make the mechanism locally important. For example, salinity values of 80-100‰ are common in May in Simpson Lagoon.

The outer shelf

Mean flow. We turn now to the area seaward of the 40-50 m isobaths, *viz.* the outer shelf. Again Figure 3 provides a useful starting point. The principal feature of the indicated velocity field is the predominance of relatively strong flow locally aligned with the isobaths. Note, for example, the nearly E-W orientation of the prevailing currents at OL-1, corresponding to the orientation of the depth contours at that point, whereas at LO-1 and LO-4 the isobaths and major current axes are both aligned SE-NW. (While Figure 3 suggests the local isobath trend at LO-4 to be about 120°T, other more detailed bathymetric constructions for the area indicate a southwestward indentation in the topography in this area. The local isobath orientation may therefore well be more SE-NW, as the current measurements at both LO-1 and LO-4 suggest.) Because of the regional variation in isobath trend, the actual orientation of the prevailing current varies by about 45° over the area, but for simplicity we shall consider the entire octant E-SE as easterly and W-NW as westerly. Note further in Figure 3 both that the statistically prevailing current direction at each site is easterly and also that this sector contains the strongest currents (except at FLAX-1). The net motion is therefore everywhere toward the east (cf. Table 2). This is particularly notable since descriptions of flow in the area have generally considered the mean motion of both water and ice to be westward, representing the southern edge of the anti-cyclonic Beaufort Sea gyre (e.g., compare Figure 17 in Coachman and Aagaard, 1974 with Figure 11 in Hibler, 1979).

The reason for the mean eastward flow over the outer shelf is not entirely clear, although it is obviously of fundamental importance to understanding and modeling the shelf circulation. Certainly the mean winds over the southern Beaufort Sea are easterly, so that local wind driving is not a viable mechanism for the eastward flow. Neither do the regional circulation schemes, whether based on the large-scale dynamic topography or on Sverdrup-type calculations using the curl of the wind stress, indicate anything but westerly flow in the area (cf. Newton, 1973, pp. 19-25 and 39-50). Mountain (1974) has argued that a mean eastward motion might be driven by the momentum flux of the upstream flow, i.e., the flow through Bering Strait, which continues northward along the Chukchi coast of Alaska, and a similar opinion was advanced by Hufford (1975). In this view the outer shelf flow in the Beaufort Sea would be strongly inertial, with the local momentum balance being maintained by the advective influx of momentum (inertia), the retarding effect of bottom friction, and the augmenting or retarding effect of winds, depending on whether they are westerly or easterly. Mountain (1974) showed through a scale analysis that in the absence of favorable (i.e., westerly) winds, such an inertial current likely would be restricted by the bottom friction to lie west of about 143°-145°W. Since the prevailing winds in fact are easterly and the wind effects are very important to the momentum balance, we should not expect an inertially driven flow to continue eastward into the Canadian Beaufort Sea (east of 141°W), even if Mountain's scaling had overestimated the effects of bottom friction.

There are, however, a number of indications that a mean eastward flow over the outer shelf extends not only across the entire Canadian Beaufort Sea, but continues northward along the west coast of Banks Island and then turns eastward into M'Clure Strait, probably extending eastward through Lancaster Sound and into Baffin Bay. For example, such a circulation is compatible with the current schemes of Bailey (1957), Collin (1963), and Herlinveaux (1974, adapted in Walker, 1977). More convincingly, the moored current measurements made at a number of sites on the outer shelf of the Canadian Beaufort Sea between 137°-129°W by Huggett, Woodward, Stephenson, Hermiston, and Douglas (1975) showed mean flow toward the northeast of up to 8 cm sec^{-1} over 3½ months during 1975. They speculated (p. 11) that this flow "is part of a large-scale circulation which is as yet unknown." If in fact the generally eastward mean flow is continuous from the Chukchi Sea through the Canadian Archipelago, then an inertial-frictional momentum balance cannot satisfactorily account for the dynamics. Rather, there must be an important local driving force, almost certainly in the form of an alongshore pressure gradient. (The gradient is probably too small for leveling along the north Alaskan coast to demonstrate its existence, and as Mountain (1974) has pointed out, steric anomaly values calculated from hydrographic data on the shelf have given no indication of it.)

Taken to its ultimate conclusion, the present argument leads to the hypothesis that the mean eastward flow over the outer Beaufort Sea shelf is ascribable to the difference in sea level between the Atlantic and Pacific oceans. In effect, the higher stand of the Pacific drives a flow through Bering Strait, a portion of which is constrained in its course toward the Atlantic to skirt the edge of the large-scale wind-driven Beaufort gyre, running eastward in a thin ribbon along the shelf edge. While this construction is obviously only speculative, there seems little doubt that the surface of the Bering Sea stands higher than that of the Arctic Ocean, probably by something like 1 m (cf. pp. 146-152 in Coachman, Aagaard and Tripp, 1975). Likewise Muench (1970, p. 108) has suggested that the surface of the Canadian Basin of the Arctic Ocean stands higher than that of Baffin Bay by at least one-third of this.

In one sense these speculations are peripheral to the Beaufort Sea shelf circulation. However, because the mean eastward flow is such a prominent feature on the shelf, and because no model of the Arctic Ocean to date has recognized this feature, it is of very great importance to ascertain its origin. Indeed, if the above argument is approximately correct, then this rather intense narrow current is conditioned by nothing less than the global climatology which maintains the Atlantic and Pacific oceans at their present different levels.

The discussion so far has been restricted to the subsurface flow. We do not, of course, have current measurements on the outer shelf above about 40 m depth, so that we cannot be sure of the motion near the surface. It is in fact quite possible that the mean surface motion is westward. Not only are the prevailing easterly winds appropriate to such driving, but the baroclinic structure on the outer shelf is also appropriate. For example, in the 17 CTD sections we took across the shelf, the dynamic topography over the outer shelf was, in about 80% of the cases, such as to sustain a geostrophic shear in which the motion at the surface was westward relative to that at 40 db. A mean geostrophic velocity difference between these levels (excluding cases of reversed shear) was about 7 cm sec^{-1}. Examination of Table 2 shows that this roughly corresponds to the mean easterly flows calculated from the current records, suggesting little or no mean geostrophic motion at the surface. Note also in Table 2 that at the shallowest of the paired measurements made in the strong eastward flow, *viz.* OL-1, the observed long-term mean shear (2 cm sec^{-1} over 10 m) is just about what we calculated above as the mean baroclinic effect (7 cm sec^{-1} over 40 m). The geostrophically balanced baro-

Table 2
Outer Shelf Mean and Maximum Currents

Mooring	Instrument depth (m)	Record length (days)	Mean velocity Speed (cm sec^{-1})	 Direction (°T)	Maximum speed (cm sec^{-1})
OL	100	95	12.8	099	56
LO-1	78	9	record too short for meaningful statistics		
LO-1	152	205	2.3	154	61
LO-4	177	352	4.8	142	66
LO-5	64	208	3.8	100	66
LO-6	68	172	6.4	112	60
LO-6	188	188	6.9	102	57
FLAX-1	39	149	1.0	067	34
FLAX-1	49	149	1.3	073	33
OL-1	40	380	7.0	089	73
OL-1	50	380	9.2	082	70

clinicity in the upper layer may therefore by itself be sufficient to offset the deeper mean eastward flow. Note further that this baroclinic structure results from an upper-layer salinity that decreases seaward, such as we discussed earlier in the section on hydrography. The interesting possibility thus arises that a mean westward motion in the upper layer, if it exists, may be due as much to the presence of dense water on the shelf (whether by brine formation or upwelling) as to direct wind effects. Appropriate models would in that case have to be both thermohaline and wind-driven.

Low-frequency variations. While both the mean and the strongest motion are seen to be eastward on the outer shelf, at least below the surface layer, Figure 3 shows the secondary mode to be westerly and to contain the next-fastest flow. Figure 15, showing the daily mean current over a year at LO-4, illustrates the characteristics of these flows. The figure can be taken as representative of the low-frequency longshore flow on the outer shelf. The motion is seen to alternate sharply between about 140°T (the primary mode) and 320°T (the secondary mode). The consistently parallel orientation of the velocity vectors is remarkable and in this respect resembles the flow found on narrow shelves elsewhere (e.g., cf. Hickey, 1979). The nominally easterly flow (actually SE) is, as noted earlier, both the fastest and the most persistent of the two principal flow directions, so that we are seeing a mean easterly motion upon which is superimposed a strong reciprocating low-frequency signal, the typical period of which is in the neighborhood of 3-10 days (Figure 15).

Figure 16 shows the (energy-conserving) spectral characteristics for the first six months of the LO-4 record. The reference coordinates for the current

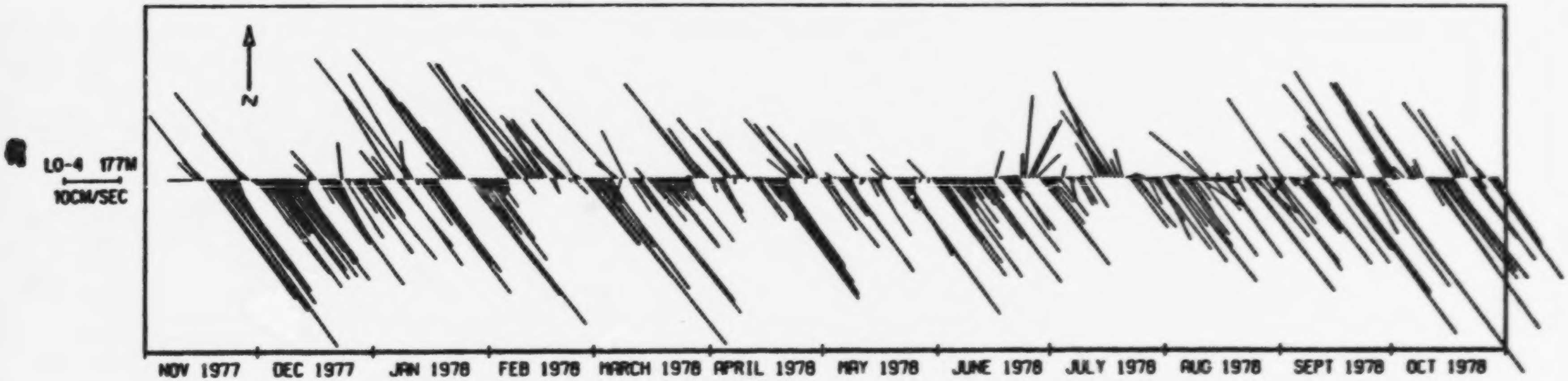

Figure 15. Daily mean current at LO-4.

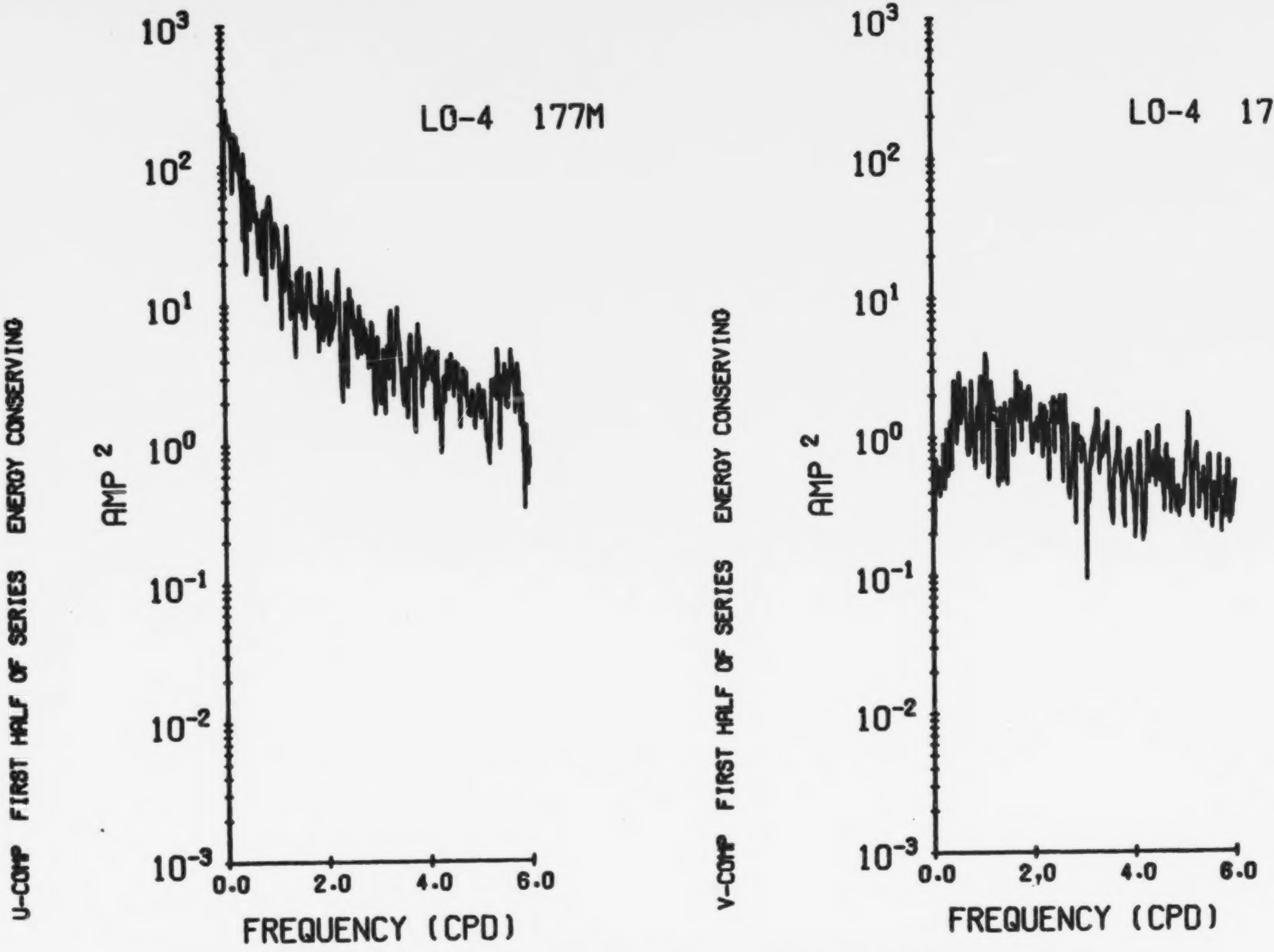

Figure 16. Energy-conserving spectra for first one-half of LO-4 current record. U-component is longshore (140°T) and V-component offshore (050°T).

BEST DOCUMENT AVAILABLE

have been rotated 50° clockwise, such that the u-component is oriented in the direction 140°T, i.e., parallel with the principal current axis (and presumably also parallel with the isobaths). The energy is seen to be almost entirely contained in the longshore mode (u-component), and then principally at the lowest frequencies. By contrast, the already low energy level in the cross-shelf (v) component drops off even further at frequencies less than about 0.5 cpd. A more detailed representation of the frequency band between about 0.1-0.4 cpd (Figure 17a) reveals considerable spectral structure, and comparison with the similar representation for the second six months of the LO-4 record (Figure 17b) shows notable differences between the two portions of the record. The low-frequency statistics are thus non-stationary. In effect, the dynamics of this current regime appear to have a rather broad low-frequency forcing and admittance, such as, for example, would be expected for a wind-driven regime.

Coherence calculations reveal some further characteristics of the reciprocating motion. Figure 18 shows the coherence and phase for the u-component at the two LO-6 instruments. Again, the coordinates have been rotated such that the u-axis coincides with the principal current axis for that mooring (as was done in Figures 16-18 for LO-4); we shall utilize this procedure in the remainder of this report unless otherwise noted. The low-frequency band is seen in Figure 18 to be both coherent and nearly in phase vertically over a depth of 120 m. Furthermore, examination of both the daily means and the energy spectra for the two instruments shows that while there are minor differences, the low-frequency energy levels are overall not sub-

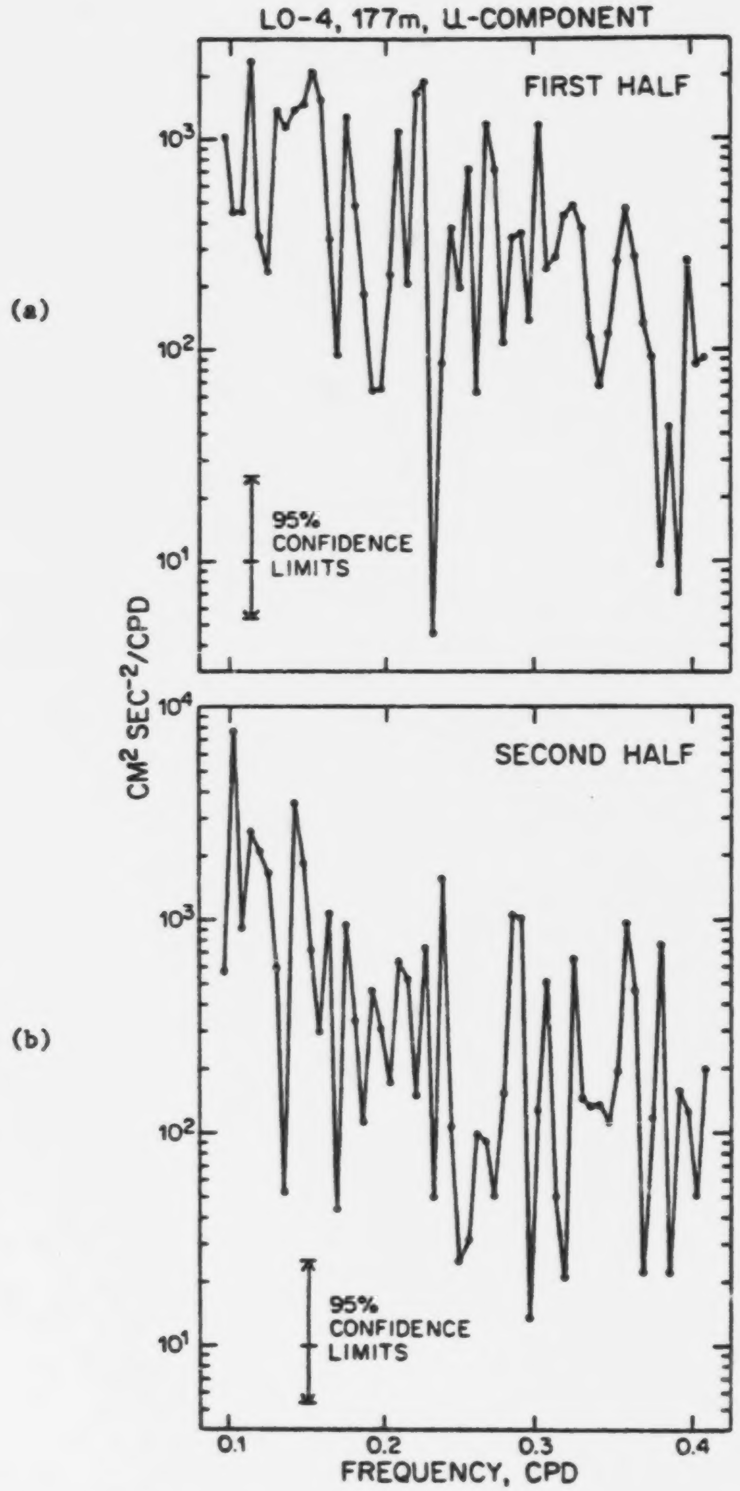

Figure 17. (a) Power spectrum for first one-half of LO-4 current record, U-component, over frequency range 0.1-0.4 cpd.

(b) Power spectrum for second one-half of LO-4 current record, U-component, over frequency range 0.1-0.4 cpd.

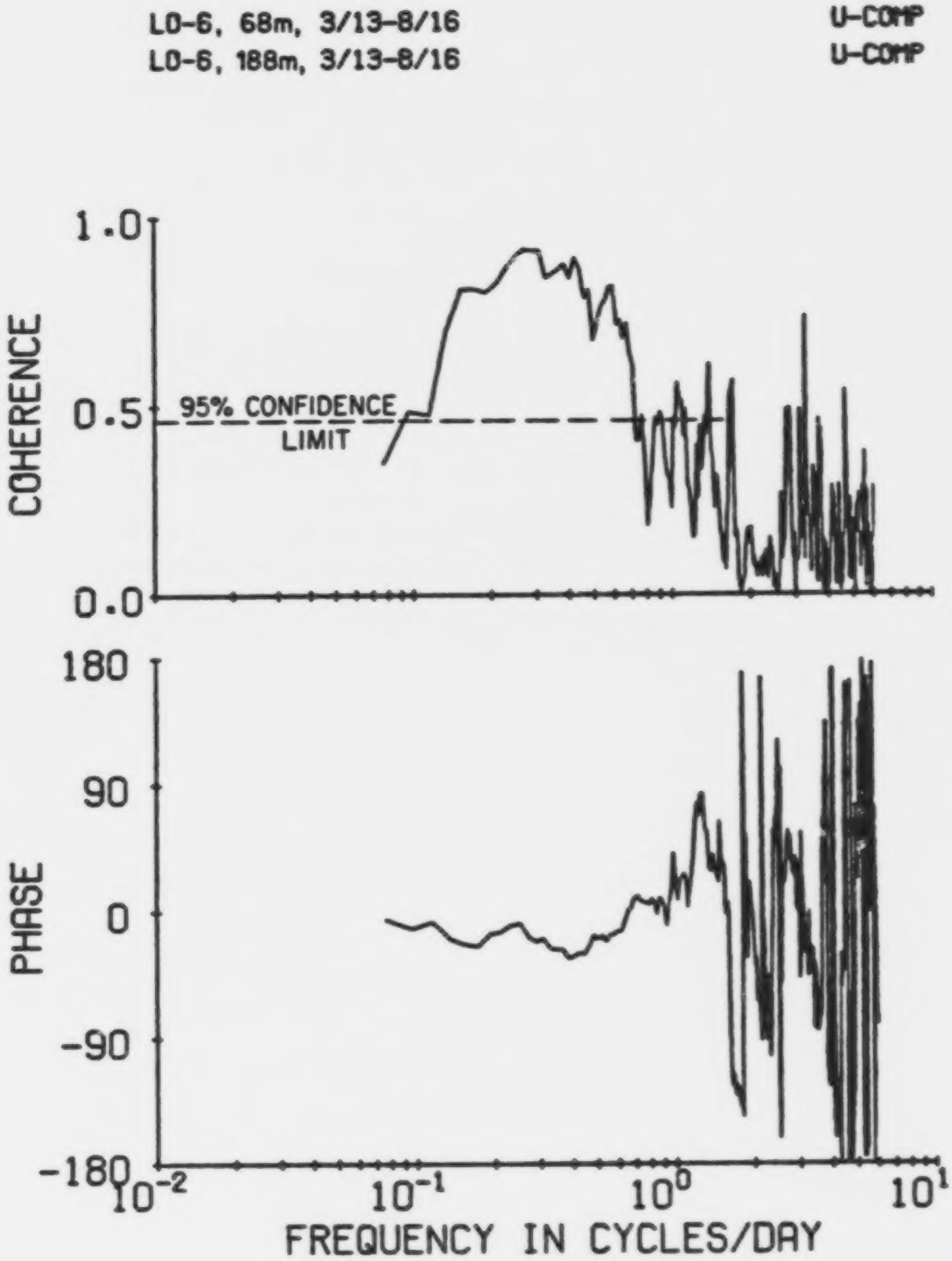

Figure 18. Coherence and phase relations for the upper and lower current records at LO-6, U-component (longshore, directed 105°T).

stantially different (cf. also Table 2). The suggestion is therefore that the entire water column between these levels responds as a single unit. Since the largest density stratification occurs above the level of the upper instrument, this is dynamically reasonable. That is, in the observed depth range we may, for example, be seeing a barotropic signal, or an internal wave in a two-layer stratified system.

Figure 19 shows the extremely high low-frequency coherence between the u-components at the LO-5 and upper LO-6 instruments. These current meters were separated by only 4 km, although they represent somewhat different total water depths, LO-5 being in 99 m of water and LO-6 in 203 m. Note that each instrument was at the same depth below the surface, however. The phase spectrum suggests that the current at LO-5 leads by an amount that increases with the frequency; the phase difference converts to a relatively constant lead time over the low-frequency band of 15-20 hrs. The LO-5 mooring was actually located about 3.5 km upstream of LO-6 (in the sense of the projection of their separation distance on the isobath trend), so that if the phase difference is due to an eastward longshore signal propagation, it implies a very slow phase velocity of only 5-6 cm sec^{-1}. This is less by an order of magnitude than would be expected for even the slowest long waves propagating along the coast, and even if the distance between LO-5 and LO-6 were in error by 3-4 km, it could at most increase the calculated phase speed to about 10 cm sec^{-1}. This can be contrasted with, for example, an internal Kelvin wave propagating along the slope. For a two-layer model with density structure corresponding approximately to a winter station near the mooring site (e.g., station W 27-25), the phase velocity of such a wave would be close to 65 cm

BEST DOCUMENT AVAILABLE

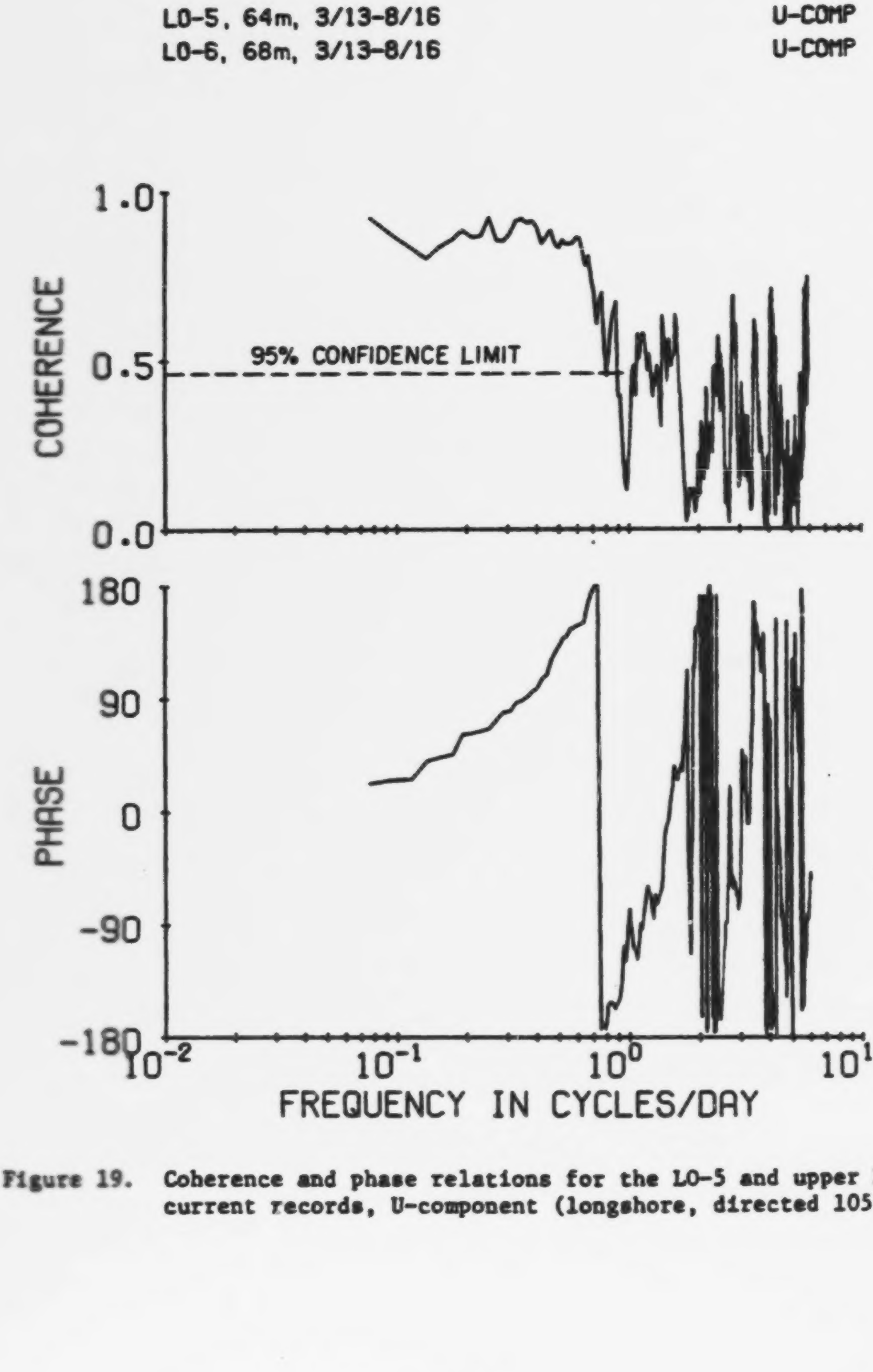

Figure 19. Coherence and phase relations for the LO-5 and upper LO-6 current records, U-component (longshore, directed 105°T at LO-5).

sec^{-1}. While we cannot preclude a wave explanation for the low-frequency variability, based on this rather meager observational basis, certainly such an explanation faces a substantial initial difficulty in the large observed phase difference. Note, however, that a signal propagation of about 5 cm sec^{-1} is close to the mean velocity (cf. Table 2), suggesting that flow events may be carried with the mean current. In that case, the inertial terms in the momentum equation would be important in locally accelerating the flow, as was initially suggested by Mountain (1974) and was discussed earlier in connection with the mean easterly flow.

At large horizontal separations the longshore coherence tends to break down more rapidly than would be expected. Figure 20 shows the coherence between the LO-4 and deep LO-6 records; the moorings were separated by 65 km. The lack of coherence is surprising, since both long waves and wind driving as explanations for the low-frequency variability would require coherence at this spatial scale. For example, the wave length of an internal Kelvin wave of phase speed 65 cm sec^{-1} (see above) and period 0.2 cpd would be 270 km, i.e., over four times the mooring separation. Similarly, major wind events capable of forcing a circulation along the shelf, would have a spatial scale of several hundred kilometers. In either case, the velocity field in the ocean should be coherent at lesser distances.

Therefore, if the lack of coherence is real, it presents major conceptual problems, probably resolvable only by resorting to such mechanisms as flow instability. However, examination of the individual time series at LO-4 and LO-6 suggests an alternate explanation. Figure 21 shows the daily mean u-components at the two instruments. It is clear that much of the variability is in fact quite coherent, as for example is the case for the events from

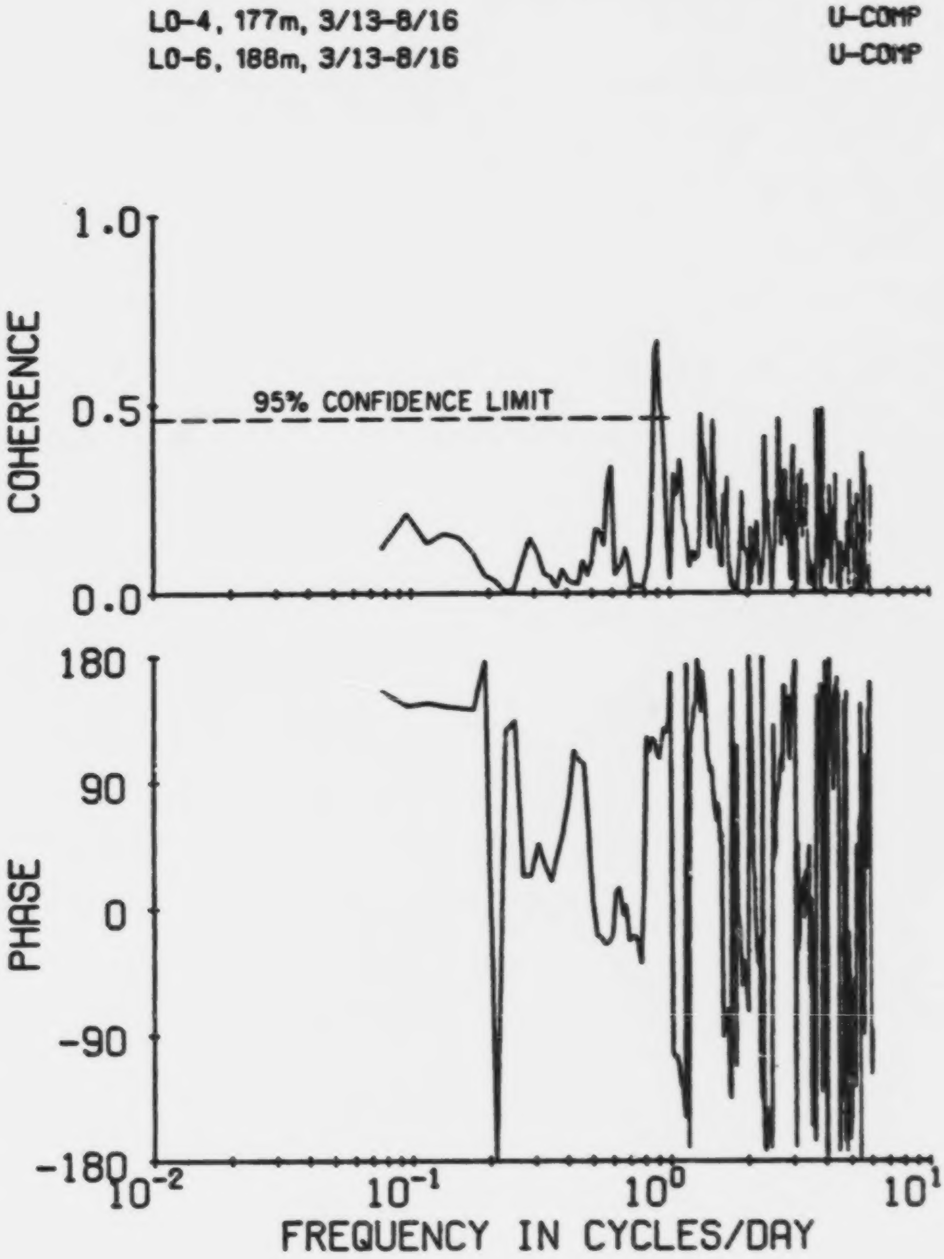

Figure 20. Coherence and phase relations for the LO-4 and lower LO-6 current records, U-component.

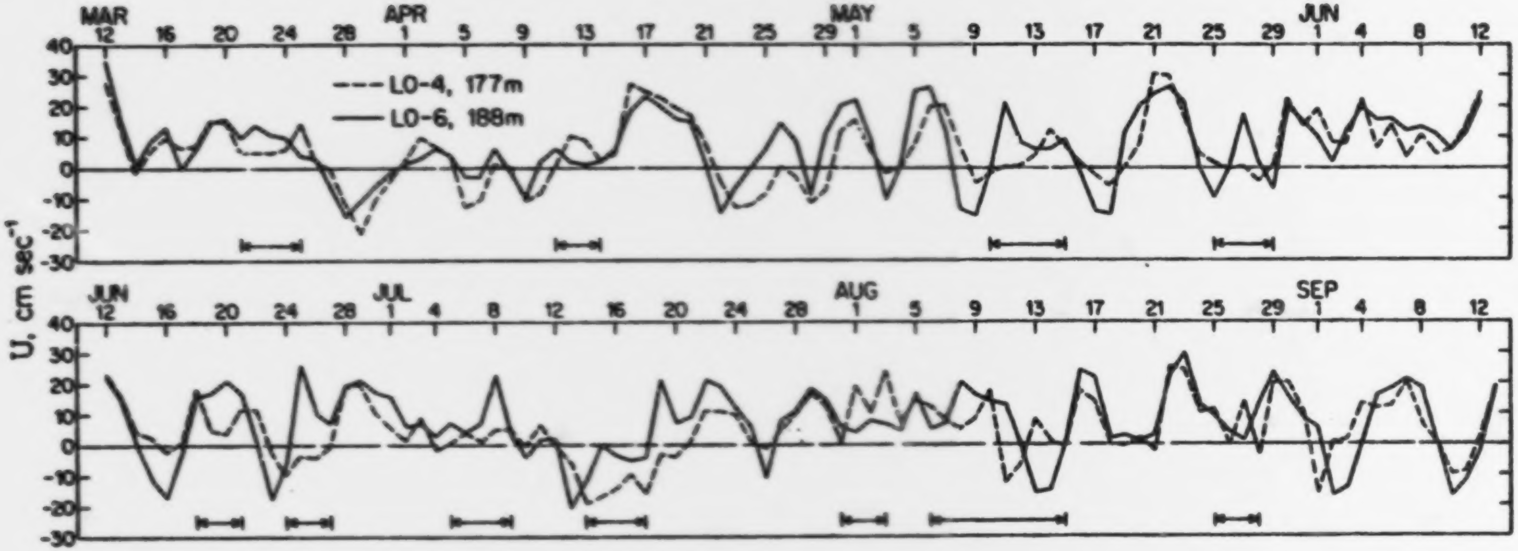

Figure 21. Daily mean U-component at the LO-4 and lower LO-6 instruments. The bracketed arrows indicate times when the signals were visibly uncorrelated.

14 April-9 May. However, about 25% of the time, events were obviously dissimilar, as was true during 6-15 August. Therefore, while the majority of the low-frequency events are coherent over these spatial scales, as one would expect to be the case, there are a sufficient number of uncorrelated events to degrade the coherence statistics. Figure 21 also suggests that the majority of the coherent events are in phase to within about one day. For the given station separation, this means a phase propagation of at least 70 cm sec^{-1}, which in turn means that the signals are not inertially transmitted. We thus have an indication that is quite different from that of the LO-5/LO-6 phase relationship.

As we shall presently see, there is evidence that at least a portion of the low-frequency variability on the outer shelf is related to the wind field. However, before examining that relationship, we'll consider another indication of the possible role of advective momentum transport. During 25 August 1976-10 August 1977, we had a current meter moored west of Cape Lisburne in the Chukchi Sea. Designated NC-7 (cf. Coachman and Aagaard, in press), it was located in the core of the northerly flow along the Chukchi coast. Note that it overlaps in time the LO-1 record during the period 29 March-10 August 1977. Comparison of these two records initially suggested no relationship. However, if the time scale is shifted about 106 days, so that 14 December 1976 in the NC-7 record coincides with 29 March 1977 in the record from LO-1 (cf. Figure 22), then there is a remarkable similarity. Specifically, at the beginning of the LO-1 record, there were two long periods of nearly uninterrupted westward flow, 24 and 28 days in duration and separated by six days of eastward flow. Each major period of reversed flow had 4-5

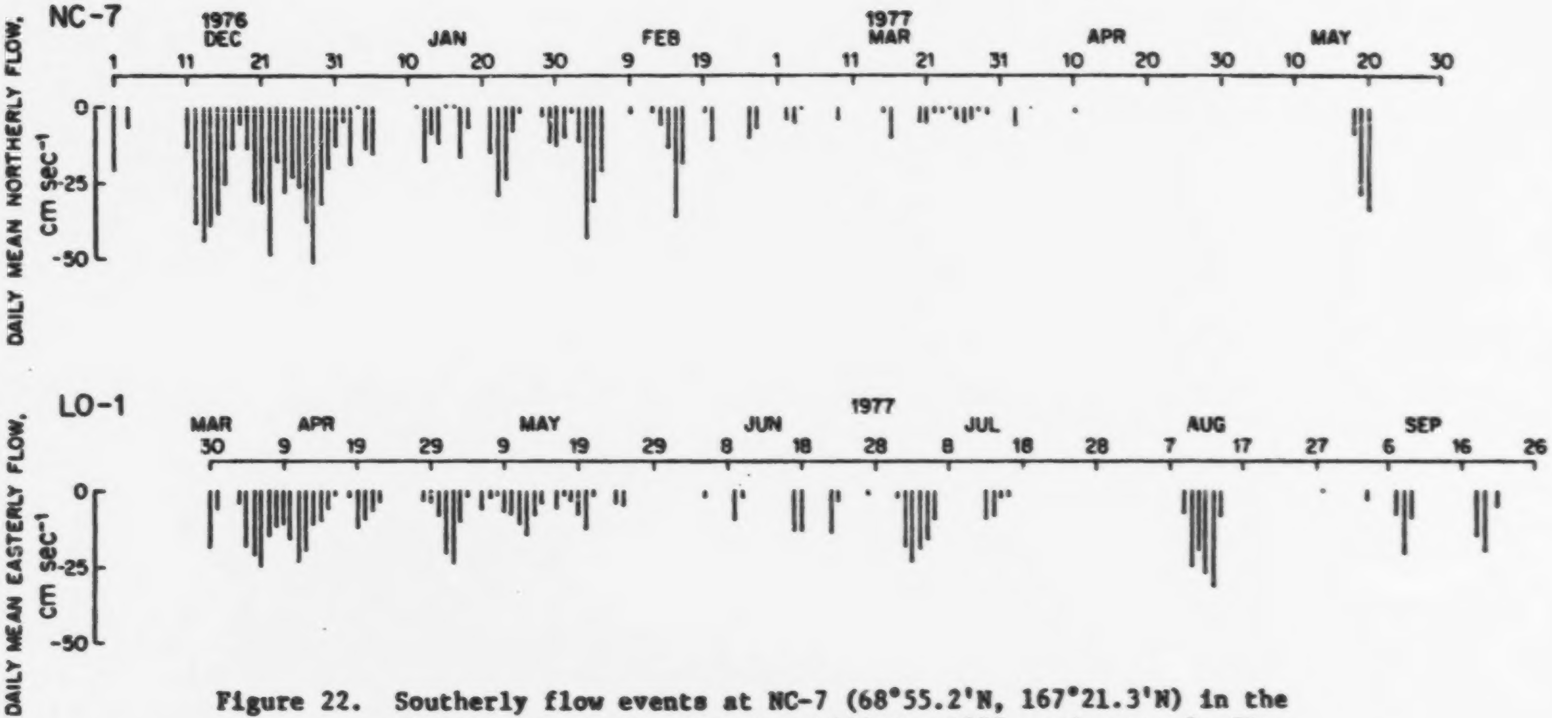

Figure 22. Southerly flow events at NC-7 (68°55.2'N, 167°21.3'N) in the Chukchi Sea during December 1976-May 1977, and westerly flow events at LO-1 during March-September 1977. Note that the time scales are offset.

subordinate oscillations within it. These major reversals are unique in our Beaufort Sea records, as there are no other reversals of comparable duration. Similarly, beginning 11 December 1976 there were two 26-day long periods of southward flow at NC-7, again interrupted by six days of normal flow. Each major reversal had 4-5 embedded subordinate oscillations. There were no other reversals of comparable duration at any time during the year-long record, nor anywhere else at a large number of mooring sites farther west in the Chukchi Sea, in Bering Strait, and in the northern Bering Sea, other than at the mooring immediately west of NC-7 (NC-6), which was also in the core of the mean northward flow along the Chukchi coast. Finally, there is nothing in the wind records (from Barrow) to suggest local wind forcing as the cause of the prolonged LO-1 current reversals. Winds during the period 30 March-25 May 1977 were from the easterly sector about 75% of the time, but were very light, reaching 5 m sec^{-1} on only one day and were usually in the range 1-3 m sec^{-1}. The similarity between the two current records with respect to these unusual events is therefore such that one cannot discount the possible dynamic importance of momentum advection by the mean flow in at least these instances. That is, the long periods of reversed flow at LO-1 may in large degree reflect the absence of momentum input during a period that was determined by upstream events. Note further that NC-7 and LO-1 were separated by about 650 km, suggesting a signal propagation ratio of 7 cm sec^{-1}, i.e., roughly comparable to the long-term mean flow in the area.

Wind influence. We turn now to the role of the wind in promoting the low-frequency variability. Wind records suitable for comparison with the current measurements are available in the form of calculated geostrophic winds at 72°N, 150°W during 18 February-31 July 1979, i.e., at a nominal point about 100 km from OL-1 and 200 km from FLAX-1; the calculations were made by T. Kozo. Surface winds (and pressures) are also available from Barter Island, over 100 km to the east of FLAX-1, during 23 February-4 May 1979 and 30 May-22 July 1979. We shall refer to these latter two periods as parts 1 and 2 of the surface wind records.

Statistically, the wind and current records are moderately correlated at low frequencies. For example, Figure 23 shows the coherence and phase spectra between the u-components of current at the upper FLAX-1 instrument and of the surface wind at Barter Island during part 1. Likewise, Figure 24 shows the coherence between the u-component at the upper OL-1 instrument and the geostrophic wind. (The records from the lower instruments at each mooring are very similar to those from the upper.) While the correlation with the geostrophic wind is somewhat poorer than with the surface wind, the overall suggestion of the two figures is of a current moderately coherent with the wind at time scales longer than about 2-3 days. Figure 23 shows no statistically significant phase difference, while Figure 24 suggests a changing phase relation, with the current lagging the wind at the lowest frequencies, but leading at frequencies greater than about 0.2 cpd. Note, however, that except close to the coherence and phase peaks near 0.3 cpd, the positive phase difference is not statistically significant. (The 95% confidence phase limits for a coherence of 0.46, which is the 95% confidence limit on coherence, is about ± 39°.) In this connection it should also be noted that there was no significant positive phase difference between the current and the surface wind during part 2 of the Barter Island wind record.

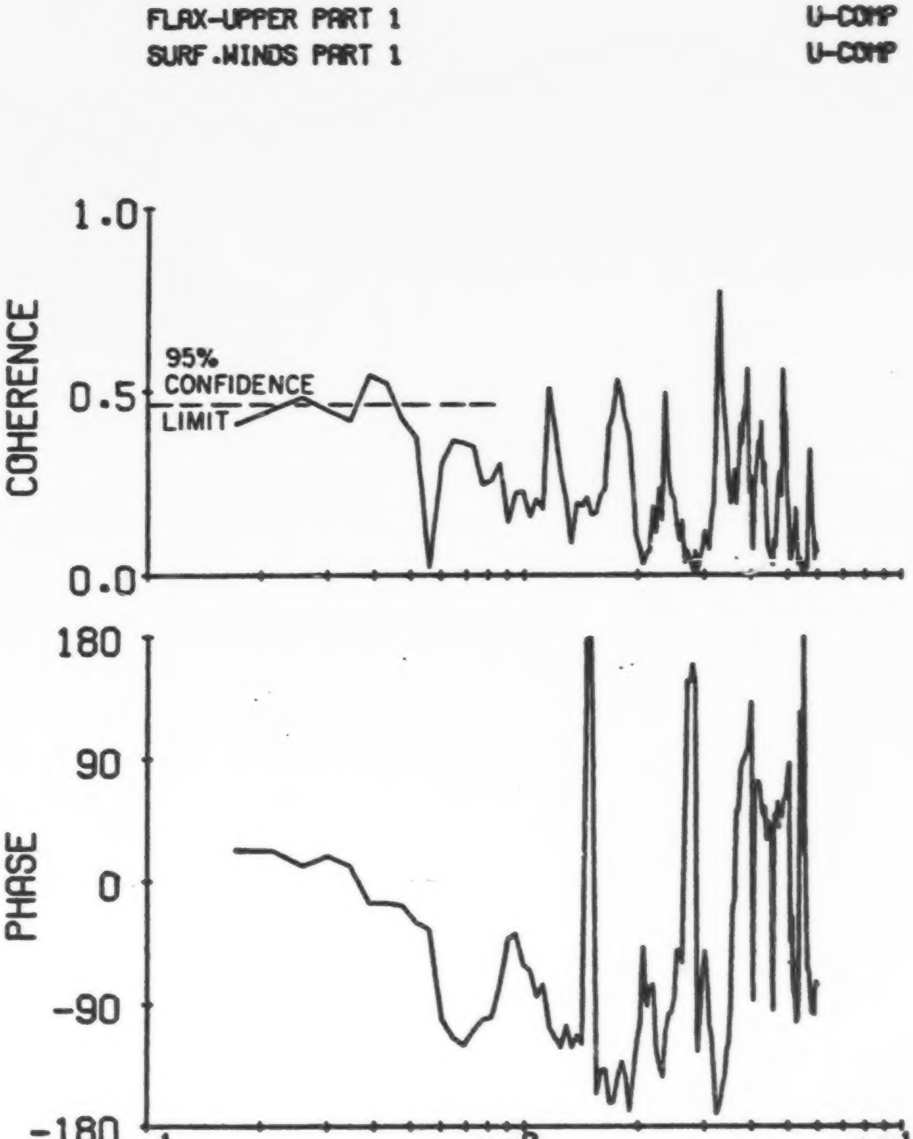

Figure 23. Coherence and phase relations for the upper FLAX-1 current record and the Barter Island surface winds, 23 February-4 May 1979, U-component (longshore, directed 105°T).

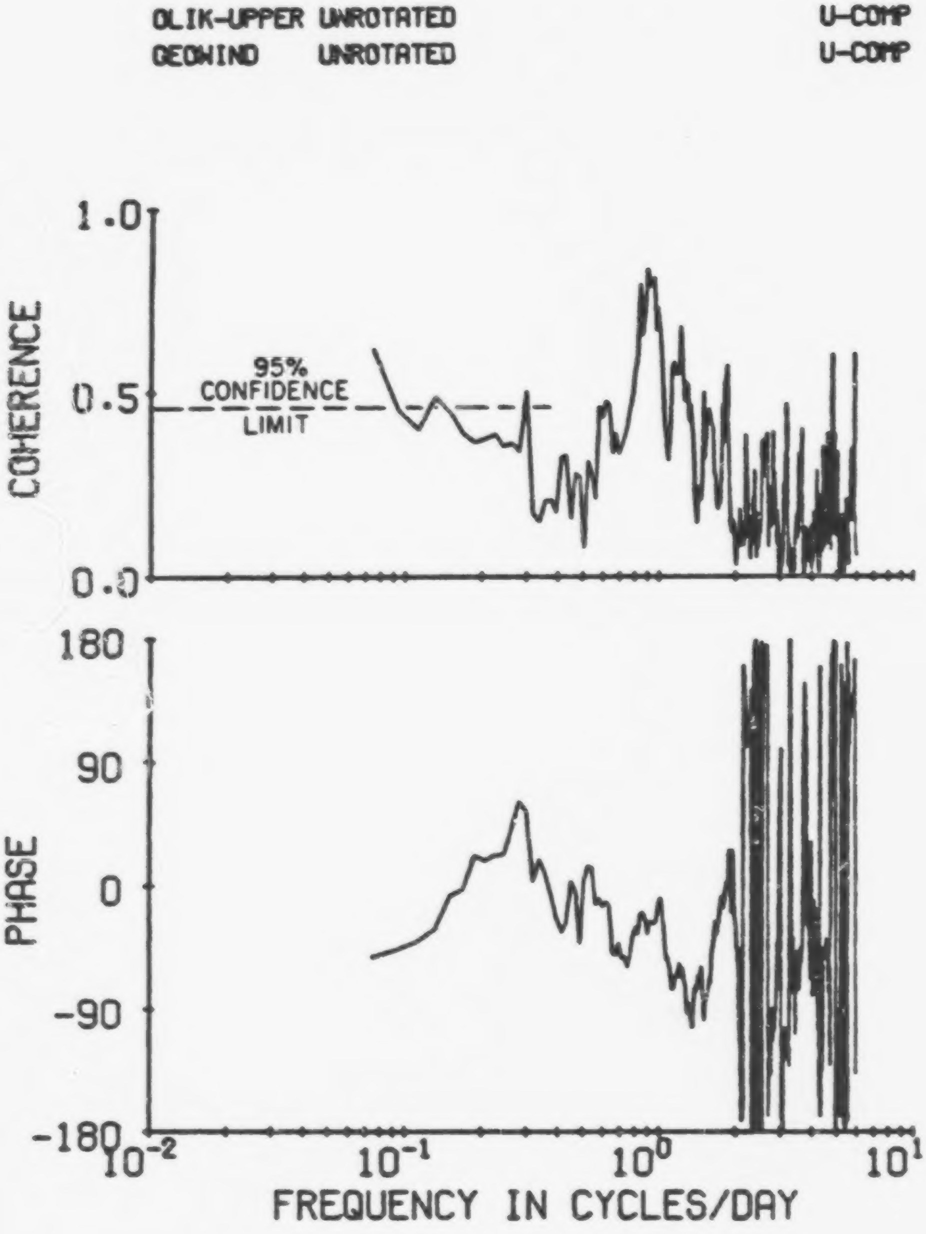

Figure 24. Conerence and phase relations for the upper OL-1 current record and the geostrophic wind at 72°N, 150°W, 18 February-31 July 1979, U-component (longshore, directed 090°T).

Except for a significant (but slightly smaller) correlation between the east component of current and the north component of wind (zero phase difference), no other wind and current combinations prove coherent. The implication of these calculations is therefore that a portion of the low-frequency variability in the longshore current is wind-driven, primarily by the longshore wind component, with which it is nearly in phase. Whether the governing mechanism is one of direct wind stress application to a two-dimensional flow, or whether it involves a coastal (or fast-ice edge) Ekman layer divergence and geostrophically induced longshore flow, or whether it is governed by still some other set of dynamics, is not clear. However, the presence of large, presumably at least in part wind-driven, variability over the outermost shelf, a considerable distance seaward of the coast or the fast ice edge, suggests that the second mechanism is unlikely. This is also the implication of the near-zero phase lag, since the spinup time for a geostrophic longshore current is typically the order of a few days (Allen, 1973), which would correspond to a substantial phase difference.

Examination of individual events in the current records also suggests wind forcing as contributing to the low-frequency variability. For example, comparison of the Barter Island winds with the OL-1 and FLAX-1 current records shows that under strong easterly winds the current normally reverses. This appears to hold in about 75-80% of the instances when the easterly winds exceed 8-10 m sec^{-1}. On the other hand, current reversals also occur that are not obviously related to the wind. Figure 25 shows an example of both kinds of events, depicting surface winds and OL-1 and FLAX-1 currents during 22 February-8 March 1979. Initially, winds and currents were in the same

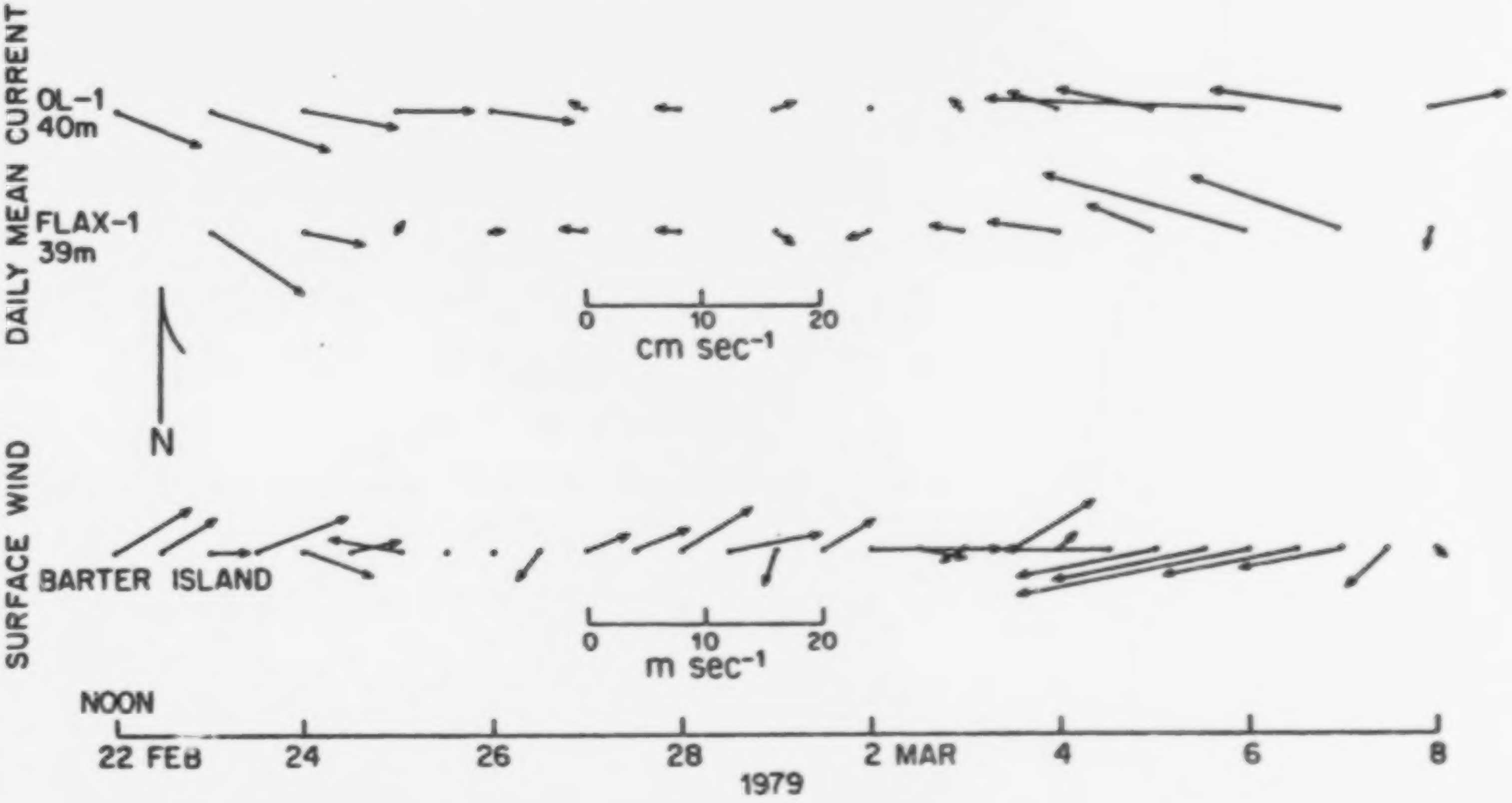

Figure 25. Daily mean current at the upper OL-1 and FLAX-1 instruments and surface wind at Barter Island, 22 February-8 March 1979.

BEST DOCUMENT AVAILABLE

direction (eastward), but during the period centered around 28 February, the currents were weak and variable (and included some westward motion), while the winds continued moderately strong toward the east. About 4 March the currents entered an increasingly pronounced reversed mode which peaked on 6 March. The winds at Barter Island, meanwhile, began blowing toward the west at midnight on 4 March; they reached their maximum strength on 6 March, coincident with the current peak.

The conclusion from these considerations is that the longshore wind plays an important, but certainly not all-prevailing, role in the low-frequency variability of the subsurface longshore flow. The wind appears to be particularly important in flow reversals. Specifically, when the winds are easterly at 8-10 m sec^{-1} or more, the currents over this part of the shelf will normally reverse and set westerly. Ascertaining the dynamics of the wind-driven flow with some certainty and detail will require special experiments, the most difficult part of which undoubtedly will be to obtain good measurements of the offshore wind field. Quite possibly the high noise level in the present wind/current coherence calculations is in fact due to an inadequate definition of the wind stress.

Seasonal variability. Our present current records should be long enough to get an indication of variability on the seasonal time scale. Figure 26 shows the three-week mean longshore currents over two different years at two different locations. There is no apparent seasonal signal, and in fact both the strongest eastward and westward mean currents occurred in late January-early February. A distribution-free "runs-test" indicates that the three-week means in fact constitute a random sequence. There is, however, some

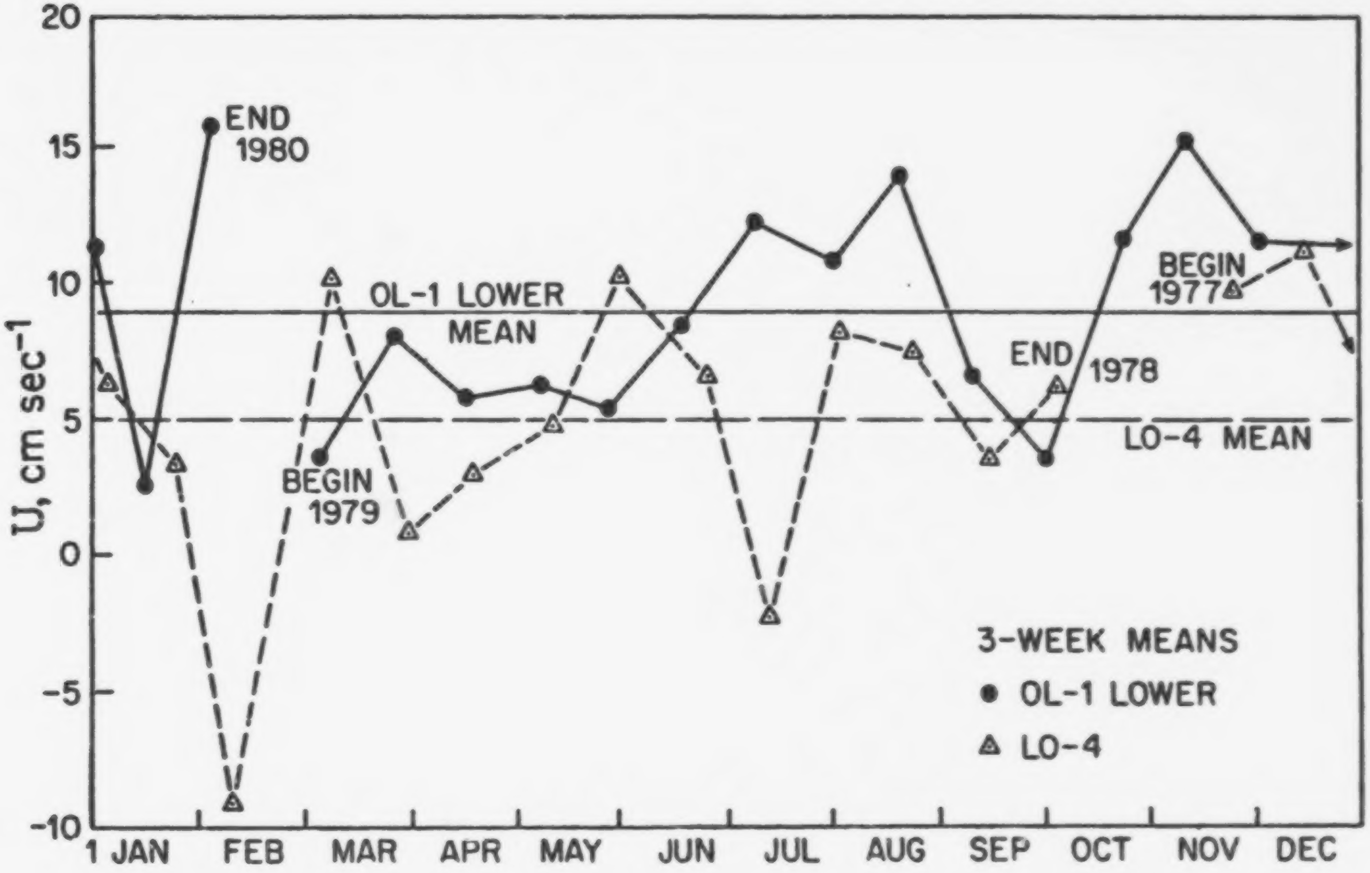

Figure 26. Three-week mean current, U-component, at the LO-4 and lower OL-1 instruments. The horizontal lines represent the annual mean at each location.

tendency toward the lower significance limit on the number of runs, i.e., there is some indication of a persistence of currents weaker or stronger than the mean, on time scales several multiples of the three-week time base.

Overall, the impression is of a long-term mean easterly flow which, although variable on extremely long time scales, does not exhibit any regular seasonal variations. Rather, there are random fluctuations on a time scale of 1-2 months or more.

Upwelling. We discussed earlier the hydrographic evidence for deep upwelling, i.e., from offshore depths of 200 m or more. Such upwelling events are characterized by the elevation of abnormally warm and saline water onto the shelf. Since the current meters are equipped with recording temperature sensors, they provide long time series of thermal evidence for possible upwelling. As an example, Figure 27 depicts the temperature at 177 m at LO-4. Over the year the temperature fluctuated between near-freezing and about 0.3°C; the record is marked by a large variability with a typical time scale of a few weeks. Vertical temperature gradients at this depth are characteristically in the range 0.01-0.03°C m^{-1}, but may reach 0.05°C m^{-1} in extreme upwelling situations (compare Figures 9-12). Since the major thermal events of Figure 27 have an amplitude of order 1°C, this represents a vertical excursion of 30-100 m. Alternatively, since in the absence of upwelling the 0°C isotherm is located below about 200-250 m on the slope (cf. Figures 10 and 12), the elevation of this isotherm in Figure 9 to 90-120 m over the outer shelf, represents a deep upwelling of about 100 m. Figure 27 suggests that upwelling events are common and that their thermal effects typically persist at a location for a week or more.

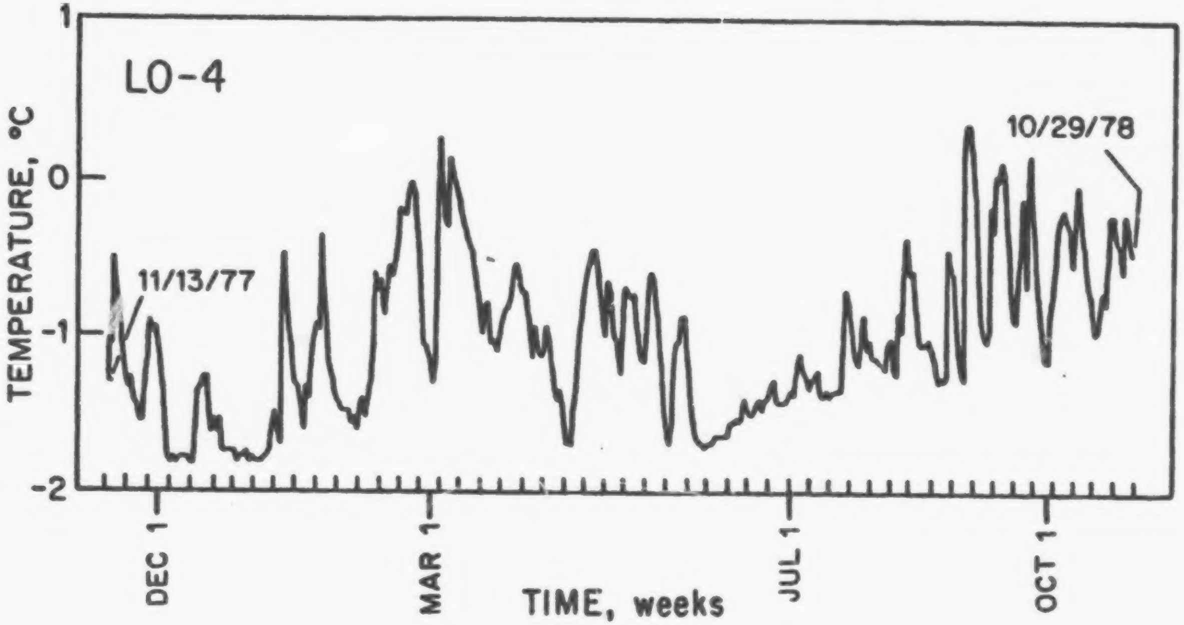

Figure 27. Temperature at LO-4 (177 m).

Inspection of the temperature records from other instruments shows that the thermal influence of upwelling is restricted to the area seaward of about the 60 m isobath. For example, no identifiable upwelling events occurred at the FLAX-1 site (59 m sounding) and only two probable upwelling events were seen at the OL-1 site (60 m sounding). While no upwelling was seen at LO-5 (99 m sounding) the temperature sensor was located 35 m off the bottom and may therefore have been too high in the water column to detect a temperature signal. Certainly Figure 9 shows upwelled water inshore of the 90 m isobath in Section LW.

Upwelling events are widespread in the longshore direction, as was apparent in our earlier examination of the hydrography (recall that Sections LW and OE in Figure 9 were separated by about 120 km). Similarly, inspection of the temperature records from 177 m at LO-4 and 188 m at LO-6 (separated by 65 km) shows them to be remarkably coherent over most of the record; they are also in phase. The chief difference between the two records is a stronger upwelling signal at LO-6. The reason for this difference is not clear, since the moorings were in comparable depths of water (192 and 203 m) and the instruments were located 15 m off the bottom in both instances; conceivably, differences in the local bathymetry are involved.

Comparison of the various temperature records also shows that while the vertical extent of the upwelling is limited (e.g., it did not show at the LO-6 instrument at 68 m depth, some 135 m off the bottom), the upwelled water is probably not restricted to a bottom boundary layer, as would be the case if its influx were due to onshore movement within an Ekman layer driven by a westward longshore geostrophic flow. For example, at LO-1 the temperature sensor was located 40 m off the bottom, but upwelling events are still clearly evident, although not as pronounced as at LO-4, 15 m off the bottom. Taken together with the evidence from the CTD sections (cf. Figure 9), the temperature records suggest a vertical extent above the bottom of the upwelled water of perhaps 50 m. This is most likely outside the bottom Ekman layer (which is probably of order 10 m). Support for this conclusion comes from examination of the current roses for LO-6 (Figure 3), which do not show any onshore turning of the deep current vector, relative to the shallow vector, during periods of westerly flow, even though the deep current meter was only 15 m off the bottom. We therefore conclude that onshore transport within the bottom boundary layer is not a likely primary cause of upwelling, although it may be a contributing factor.

Coherence calculations between the velocity and temperature fields show that at the instruments where frequent upwelling was indicated, the longshore current and the temperature are coherent at time scales of 1-2 weeks; the current lags by about 90° (but close to 135° at 188 m at LO-6), or equivalently, westerly currents are followed by increasing temperatures one-quarter (three-eights at LO-6) cycle later. As an example, Figure 28 shows the coherence and phase spectra for the first one-half of the longshore velocity component and temperature records at LO-4. We saw earlier that strong easterly winds, such as might be expected to produce coastal upwelling, normally could reverse the prevailing eastward current. However, the wind and current were essentially in phase during such events, and since the longshore current and temperature are approximately in quadrature (90° out of phase), we are almost certainly not seeing wind-driven coastal upwelling. Note that we had tentatively arrived at the same conclusion in our earlier discussion of

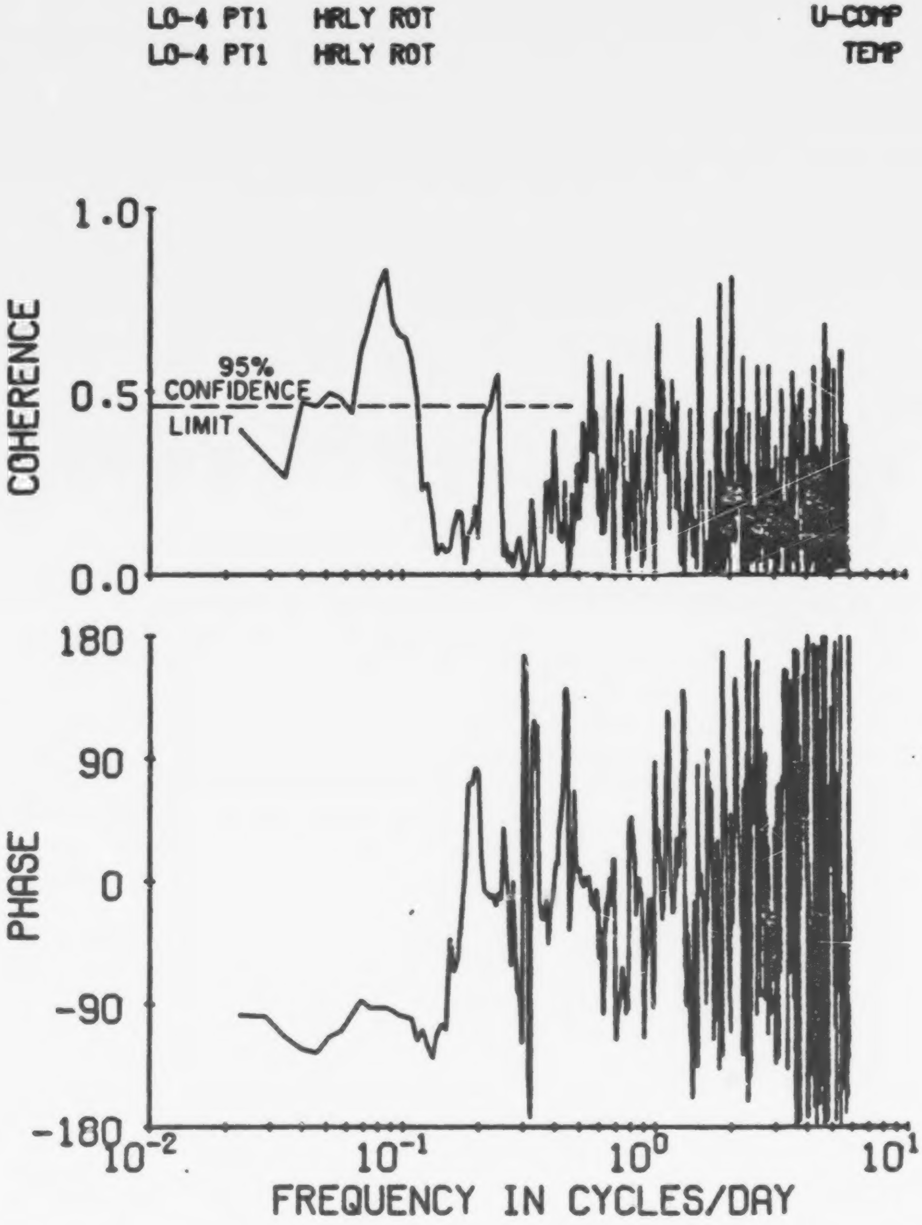

Figure 28. Coherence and phase relations for the first one-half of the records of U-component of velocity and of temperature at LO-4.

the hydrographic evidence for upwelling.

The simultaneous invasion of upwelled water over very long stretches of the shelf (certainly over more than 100 km) also precludes purely local causes, such as quasi-geostrophic eddies. Within these constraints (i.e., that the upwelling is regional in extent, not directly wind-driven, and probably not restricted to a bottom boundary layer), there are still several different conceptual models possible. Consider, for example, the following sequence of events. In the mean state, geostrophic equilibrium requires a pressure gradient directed southward on the southern flank of the Beaufort gyre, and directed northward over the outer shelf, where the mean flow is eastward (possibly reduced near the surface due to the baroclinicity discussed earlier in the section on mean flow). A nominally east-west topographic trough would therefore exist somewhat seaward of the shelf break, and the eastward flow in effect forms a barrier between the Beaufort gyre and the shelf. Suppose now that the flow begins to reverse toward the west. The previously geostrophically adjusted pressure gradient must also change, so that at some point it is directed southward. An ageostrophic onshore flow component could then exist over a limited time, during which the deeper onshore flow would encounter the upward-sloping bottom and be forced to upwell. The presence of the coast would limit the shoreward penetration of this motion, effectively through continuity requirements leading to a pressure gradient directed offshore. At some later time the westward longshore flow will be fully developed and geostrophically balanced so that the southward-directed pressure gradient which forms the dynamic south wall of the Beaufort gyre will extend in over the outer shelf. The effect of the upwelled water on the shelf is to reduce the horizontal pressure gradient with depth, so that the westward geostrophic flow would also be reduced.

While this construction is somewhat intuitive, there are in fact data that are consistent with it. Consider, for example, Figure 29, showing the daily mean velocity at the two LO-6 instruments, along with the temperature record from the deeper one. (The temperature in Figure 29 is probably uniformly too high by 0.1-0.2°C.) The upwelling events are generally preceded by westward flow, and this westward flow is normally both stronger and more frequent at the upper instrument, as would be expected in a baroclinic flow. As further evidence, Figure 30 shows the dynamic topography of the 70 db surface relative to 200 db during the upwelling event observed at the W 25 sections. We do not, of course, know the stage of the upwelling at the time of the sections, but the dynamic topography corresponds to a strong westward baroclinic current, such as might be expected to occur after the main onshore upwelling movement. The geostrophic shear above 70 db reverses, so that Figure 30 portrays the probable current core. (The apparent lack of dynamic relief inshore of Stations 6 and 7 is an artifact due to the lack of inshore stations deeper than 200 m; examination of the gradients across the shelf break at shallower levels in Sections OW and OE suggests very strong currents.) As a final line of evidence, the two probable upwelling events at OL-1, in early October and late January, were both associated with abnormally strong westerly flow. The October event followed 7 days of westerly current up to 57 cm $\sec^{-1}$, and the January event began about a day after the start of a five-day period of westerly flow of up to 62 cm $\sec^{-1}$.

Other conceptual models of the upwelling are also possible, involving, for example, geostrophically balanced onshore flow associated with a longshore

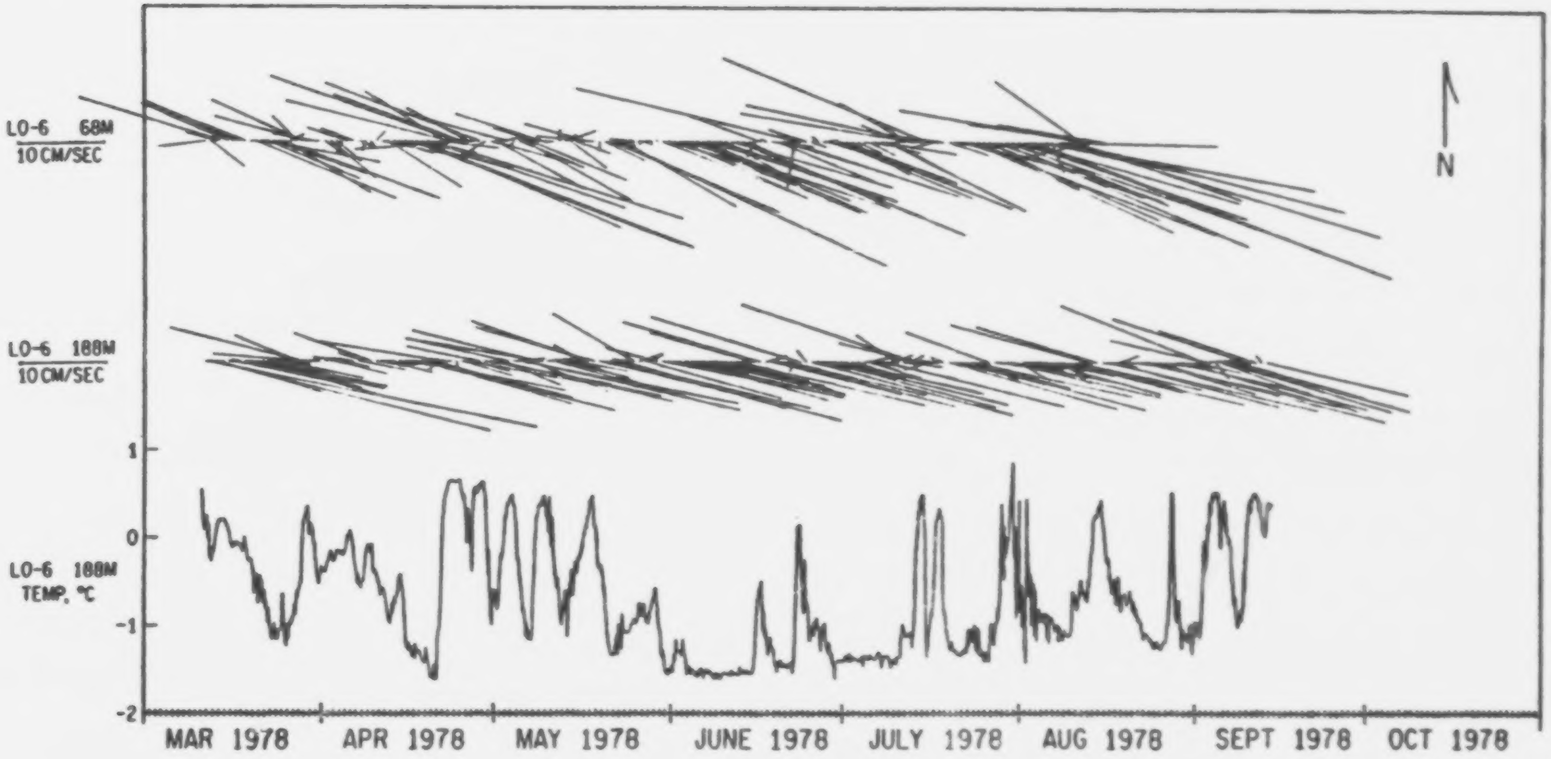

Figure 29. Daily mean current at LO-6 and temperature at 188 m at LO-6.

BEST DOCUMENT AVAILABLE

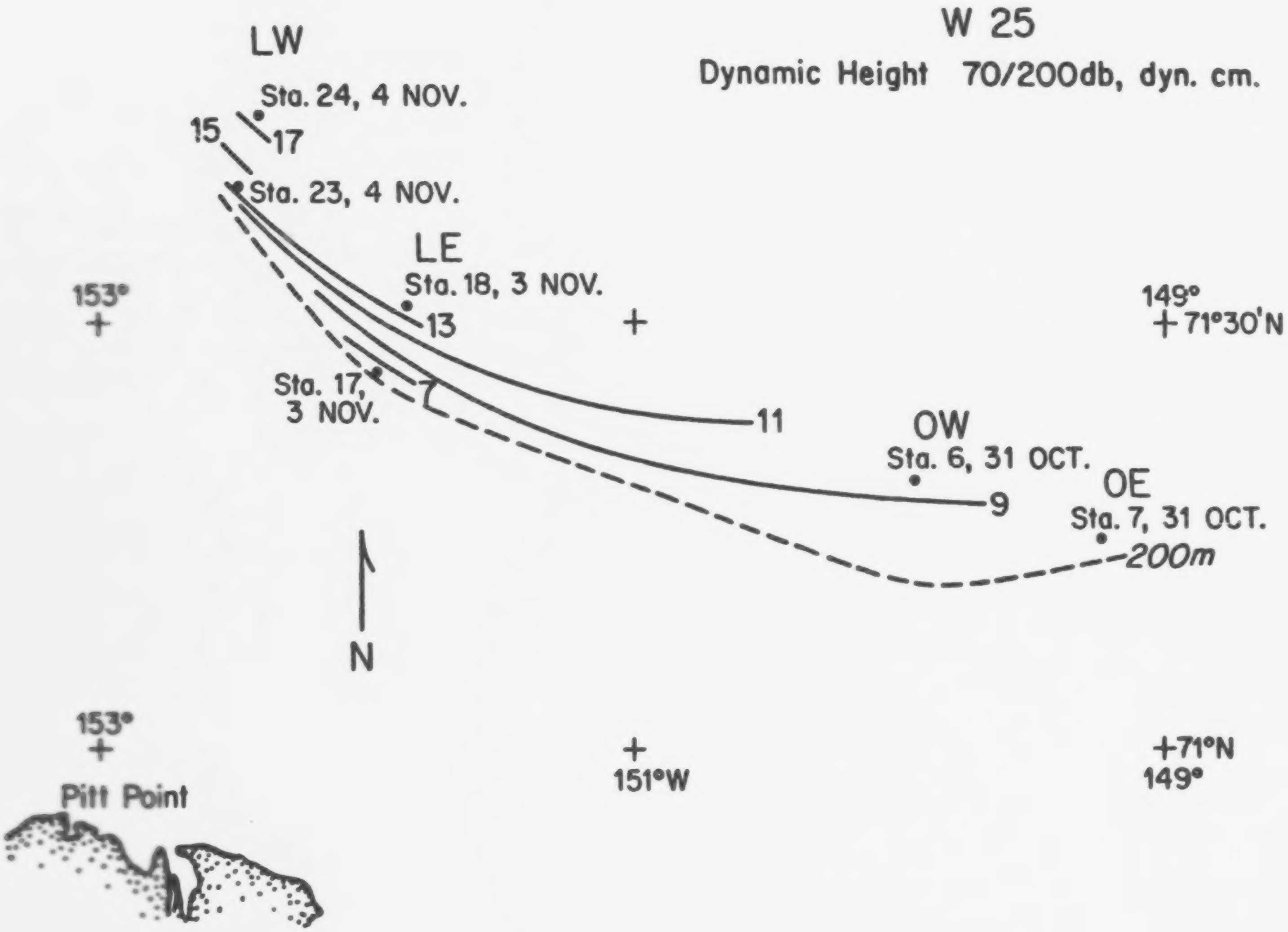
W 25
Dynamic Height 70/200db, dyn. cm.
LW
Sta. 24, 4 NOV.
15
17
Sta. 23, 4 NOV.
LE
Sta. 18, 3 NOV.
13
153°
149°
71°30'N
Sta. 17, 3 NOV.
11
OW
Sta. 6, 31 OCT.
9
OE
Sta. 7, 31 OCT.
200m
N
153°
151°W
71°N
149°
Pitt Point

Figure 30. Dynamic topography, 70/200 db, seaward of the shelf break during W-25.

BEST DOCUMENT AVAILABLE

pressure gradient. Note that in Figure 30 the dynamic topography does in fact stand higher toward the west, suggesting an onshore geostrophic flow, so that a variety of combinations of dynamics are possible. Certainly, the further clarification of the dynamics of deep upwelling on the Beaufort shelf will require both designated experiments and modeling efforts.

A final implication of the moored temperature records relates to the depth of influence of the Bering Sea water. Mountain's (1974) data suggest that this influence probably does not extend below about 100-125 m. However, comparison of the records from LO-6 show the likelihood that even at the lower instrument, at 188 m, the arrival of the Bering Sea water in late July can be seen in the temperature signal: the initial very large temperature pulse signaling the influx of the Bering Sea water at 68 m is duplicated with somewhat reduced amplitude at 188 m. An occasional direct Bering Sea influence should therefore be expected to extend to the bottom even on the outer shelf.

The transition zone

At some offshore distance over the shelf there must be a transition from the outer to the inner shelf regime, e.g., to a regime that is more nearly isotropic in its current distribution, or in which the invasion of Bering Sea water is relatively rare. In one sense, of course, we should not dwell unduly on the concept of a transition zone, for it is not necessarily a dynamically unique region. More likely it is simply an area of the shelf where at one time, the motion resembles that of the outer shelf, and at another time it is more like that of the relatively shallow and flat inner shelf. Nonetheless, Figure 3 suggests that the FLAX-1 mooring is close to such a transition area, since the current roses have a markedly less bimodal

BEST DOCUMENT AVAILABLE

directional character than at other installations further seaward. (This may also be true at OL-1, but to a lesser extent). Since FLAX-1 was located in 59 m depth, our earlier estimated demarcation between the outer and inner shelf regimes near the 40-50 m isobaths is probably not far removed from a useful rule-of-thumb.

Figure 31 shows the daily mean current at FLAX-1. It is obvious that off-shore flow events were more common than onshore ones (compare also the current roses in Figure 3), were fairly strong (daily means frequently exceeded 5 cm sec^{-1}), and typically had a duration of three days or more. Identifying a likely cause of the offshore events has thus far been futile. Offshore flow occurred most frequently during the first three months, although there is no obvious reason why this should be so. Most surprisingly, there appears to be no significant correlation between the cross-shelf flow and either wind component. Conceivably this may be due to an inadequate representation of the local wind field, but while a wind-driven origin of such cross-shelf flow events cannot be entirely discounted on the basis of the present data, it seems unlikely. Speculation as to other causes remains just that.

Concluding remarks

An important facet of the outer shelf circulation (say, seaward of the 50 m isobath) is that it is energetic throughout the year. Not only is there large variability at time scales of days to weeks, but because of the relatively large long-term mean flow, there is an intimate connection between the shelf and areas far removed from it. Specifically, the strong longshore current on the outer shelf is a very efficient transport mechanism. This

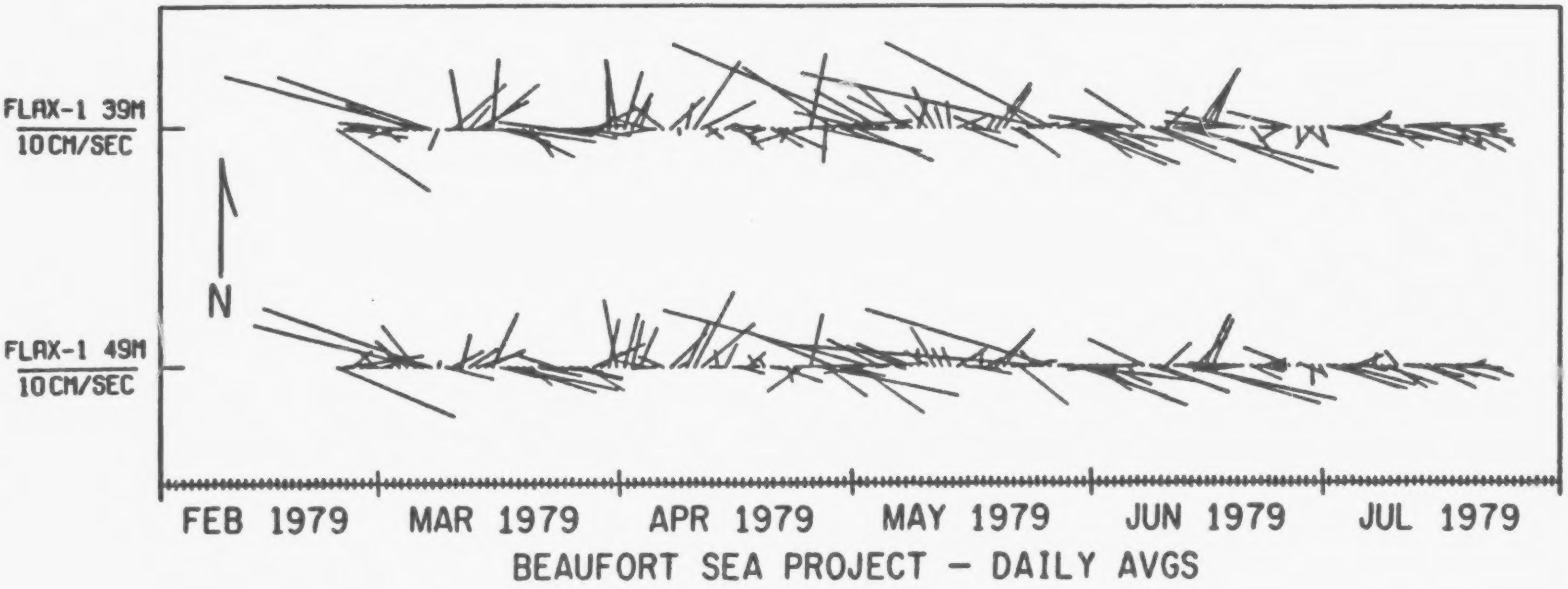

Figure 31. Daily mean current at FLAX-1.

means not only that events on the Alaskan shelf can propagate long distances, e.g., into the Canadian Beaufort, and probably through the Canadian Archipelago as well, but it also means that events in other places affect the north Alaskan shelf. For example, water from the Bering Sea has a major impact on the Beaufort shelf hydrography and undoubtedly also on the biota.

There is also clear communication with the Arctic Ocean, most dramatically through the relatively frequent upwelling events. To illustrate how far-reaching such connections can be, I venture to predict that within the next 2-3 decades, tracer sampling of upwelling events on the outer shelf will yield ^{137}Cs/^{90}Sr ratios of 2 or more. These would be unequivocal evidence of influx from the British Windscale nuclear fuel processing plant in the Irish Sea, entering the Arctic Ocean with the Atlantic water that flows northward through the Norwegian and Greenland seas. The point of these remarks is that only on relatively short time scales (say, a month or less) could the north Alaskan shelf be considered self-contained.

A second important facet of the shelf circulation is that there are frequent cross-shelf motions (in addition to the upwelling events). These are probably of several different types and origins, each with its own characteristics. There is therefore ample opportunity for inshore events to propagate offshore and *vice versa.* In the long-term mean, there must of course be a small offshore net flow due to runoff. However, the inshore sinks and sources of buoyancy and water (e.g., winter brine production and summer river discharge) are certainly not uniform line sources. Coupled with longshore differences in bathymetry, these non-uniformities will almost certainly lead to preferred local avenues of cross-shelf exchange. Such preferred regions might be of quite small lateral extent.

A third matter is that while tidal currents have been outside the thrust of this discussion of the shelf circulation, it's important to note that they may be sufficiently large on the shelf to figure in certain mixing and dispersion problems. For example, the FLAX-1 records show a semi-diurnal component in the range 5-10 cm $\sec^{-1}$. This contrasts with Mountain's (1974) estimate for Barrow Canyon of less than 1 cm $\sec^{-1}$ and with 1-2 cm $\sec^{-1}$ at the NAR-1 and -2 sites in winter, but is similar to values at our outer shelf moorings.

Finally, it is important to point out that there are a great many voids in our knowledge. These range from the most basic descriptive deficiencies (this is probably most pronounced on the inner shelf, where there is a remarkable lack of the long time series necessary to establish useful statistics) to an understanding of the dynamics that at present is largely conjectural. While filling the most glaring of these voids is certainly a major exercise, there is no doubt that the skills and experience exist to do so. What in fact has been achieved these past five years is 1) a first-level understanding that is both sufficiently broad and quantitative to let us ask intelligent and meaningful questions, and 2) the demonstrated experimental ability to answer such questions.

References

Aagaard, K., L.K. Coachman and E.C. Carmack. In press. On the halocline of the Arctic Ocean. *Deep-Sea Res.*

Aagaard, K., C. Darnall and F. Karig. 1978. Measurements with moored instruments in ice-covered waters. *Deep-Sea Res.*, *25*, 127-128.

Allen, J.S. 1973. Upwelling and coastal jets in a continuously stratified ocean. *J. Phys. Oceanogr.*, *3*, 245-257.

Bailey, W.B. 1957. Oceanographic features of the Canadian Archipelago. *J. Fish. Res. Board, Canada*, *14*(5), 731-769.

Barnes, P., E. Reimnitz, and D. McDowell. 1977. Current meter and water level observations in Stefansson Sound, Summer 1976. *U.S.G.S. Open-file Report* 77-477, 7 pp.

Barnes, P.W. and L.J. Toimil. 1979. Inner shelf circulation patterns, Beaufort Sea, Alaska. *U.S.G.S. Miscellaneous Field Studies Map* MF-1125.

Barnes, P. and E. Reimnitz. 1974. Sedimentary processes on arctic shelves off the northern coast of Alaska. Pp. 439-476 in *The Coast and Shelf of the Beaufort Sea*, J.C. Reed and J.E. Sater, eds., Arctic Institute of North America, Arlington, VA 750 pp.

Buckley, J.R., T. Gammelsrød, J.A. Johannessen, O.M. Johannessen and L.P. Røed. 1979. Upwelling: oceanic structure at the edge of the arctic ice pack in winter. *Science*, *203*(4376), 165-167.

Coachman, L.K. and K. Aagaard. 1974. Physical oceanography of arctic and subarctic seas. Pp. 1-72 in *Marine Geology and Oceanography of the Arctic Seas*, Y. Herman, ed., Springer-Verlag, New York, 397 pp.

Coachman, L.K. and K. Aagaard. In press. Re-evaluation of water transports in the vicinity of Bering Strait. In *Oceanography of the Bering Sea Shelf*, D. Hood, ed.

Coachman, L.K., K. Aagaard and R.B. Tripp. 1975. *Bering Strait: The Regional Physical Oceanography*. University of Washington Press, Seattle, 172 pp.

Collin, A.E. 1963. Waters of the Canadian Arctic Archipelago. Pp. 128-139 in *Proceedings of the Arctic Basin Symposium*, Arctic Institute of North America, Washington, D.C., 313 pp.

Drake, D. 1977. Suspended matter in nearshore waters of the Beaufort Sea. *U.S.G.S. Open-file Report* 77-477, 13 pp.

Henry, R.F. 1975. Storm surges. *Tech. Rept. No. 19, Beaufort Sea Project.* Dept. Environment, Victoria, B.C. 41 pp.

Herlinveaux, R.M. 1974. Surface movements in Canadian arctic waters with some accompanying temperature and salinity observations. Unpublished manuscript, *Pacific Marine Science Report*, Marine Sciences Directorate, Pacific Region, Environment Canada, Victoria, B.C., 36 pp.

Hibler, W.D.,III. 1979. A dynamic thermodynamic sea ice model. *J. Phys. Oceanogr.*, *9*(4), 815-846.

Hickey, B.M. 1979. The California Current system. *Prog. Oceanogr.*, *8*, 191-279.

Hufford, G.L. 1973. Warm water advection in the southern Beaufort Sea August-September 1971. *J. Geophys. Res.*, *78*(15), 2702-2707.

Hufford, G.L. 1974. On apparent upwelling in the southern Beaufort Sea. *J. Geophys. Res.*, *79*, 1305-1306.

BEST DOCUMENT AVAILABLE

Hufford, G.L. 1975. Some characteristics of the Beaufort Sea shelf current. *J. Geophys. Res., 80*(24), 3465-3468.

Hufford, G.L. and R.D. Bowman. 1974. Airborne temperature survey of Harrison Bay. *Arctic 27*(1), 69-70.

Hufford, G.L., S.H. Fortier, D.E. Wolfe, J.F. Doster and D.L. Noble. 1974. Physical oceanography of the western Beaufort Sea. In *Marine Ecological Survey of the Western Beaufort Sea.* U.S.C.G. Oceanogr. Rept. CG-373.

Hufford, G.L., I.M. Lissauer and S.P. Welsh. 1976. Movement of spilled oil over the Beaufort Sea, a forecast, *U.S.C.G. Oceanogr. Rept. CG-D-101-76,* 87 pp.

Hufford, G.L., B.D. Thompson and L.D. Farmer. 1977. Surface Currents of the northeast Chukchi Sea. *Annual Report RU 81 OCSEAP Arctic Project,* unpublished manuscript.

Huggett, W.S., M.J. Woodward, F. Stephenson, W. Hermiston and A. Douglas. 1975. Near bottom currents and offshore tides. *Tech. Rept. No. 16, Beaufort Sea Project.* Dept. of Environment, Victoria, Canada. 38 pp.

Johnson, M.W. 1956. The plankton of the Beaufort and Chukchi Sea areas of the Arctic and its relation to the hydrography. *Arctic Institute of North America, Tech. Pap. No. 1,* 32 pp.

Matthews, J.B. 1971. Long period gravity waves and storm surges on the Arctic Ocean continental shelf. *Proc. Joint Oceanogr. Assembly, Tokyo 1970.* D1-I-7, 332.

Mountain, D.G. 1974. Bering Sea water on the north Alaskan shelf. Unpublished thesis, University of Washington, 153 pp.

Newton, J.L. 1973. The Canada Basin; mean circulation and intermediate scale flow features. Unpublished thesis, University of Washington, 157 pp.

Paquette, R.G. and R.H. Bourke. 1974. Observations on the coastal current of arctic Alaska. *J. Mar. Res.*, *32*(2), 195-207.

Schaeffer, P.J. 1966. Computation of a storm surge at Barrow, Alaska. *Archiv für Meteorologie, Geophysik und Bioklimatologie, Ser. A Meteorologie und Geophysik*, *15*(3-4), 372-393.

Schwerdtfeger, P.J. 1974. Mountain barrier effect on the flow of stable air north of the Brooks Range. Pp. 204-208 in *Climate of the Arctic*, Geophysical Institute, University of Alaska, Fairbanks.

Searby, H.W. and M. Hunter. 1971. Climate of the North Slope of Alaska. *NOAA Tech. Memo. NWS AR-4*, Anchorage, 53 pp.

Walker, E.R. 1977. Aspects of oceanography in the Archipelago. IOS Note 3, Institute of Ocean Sciences, Patricia Bay, Sidney, B.C., 186 pp.

Walker, H.J. 1973. Spring discharge of an arctic river determined from salinity measurements beneath sea ice. *Water Resources Res.*, *9*(2), 474-480.

Wiseman, W.J., J.N. Suhayda, S.A. Hsu and C.D. Walters. 1974. Characteristics of nearshore oceanographic environment of Arctic Alaska. Pp. 49-64 in *The Coast and Shelf of the Beaufort Sea*, J.C. Reed and J.E. Sater, eds., Arctic Institute of North America, Arlington, VA 750 pp.

BEST DOCUMENT AVAILABLE

NOAA Technical Memorandum ERL PMEL-22

PHYSICAL OCEANOGRAPHIC AND METEOROLOGICAL CONDITIONS IN THE NORTHWEST GULF OF ALASKA

Robin D. Muench
James D. Schumacher

Contributors:
C. A. Pearson
R. M. Reynolds
R. Overstreet

Pacific Marine Environmental Laboratory
Seattle, Washington
October 1980

UNITED STATES DEPARTMENT OF COMMERCE
Philip M. Klutznick, Secretary

NATIONAL OCEANIC AND ATMOSPHERIC ADMINISTRATION
Richard A. Frank, Administrator

Environmental Research Laboratories
Joseph O. Fletcher, Acting Director

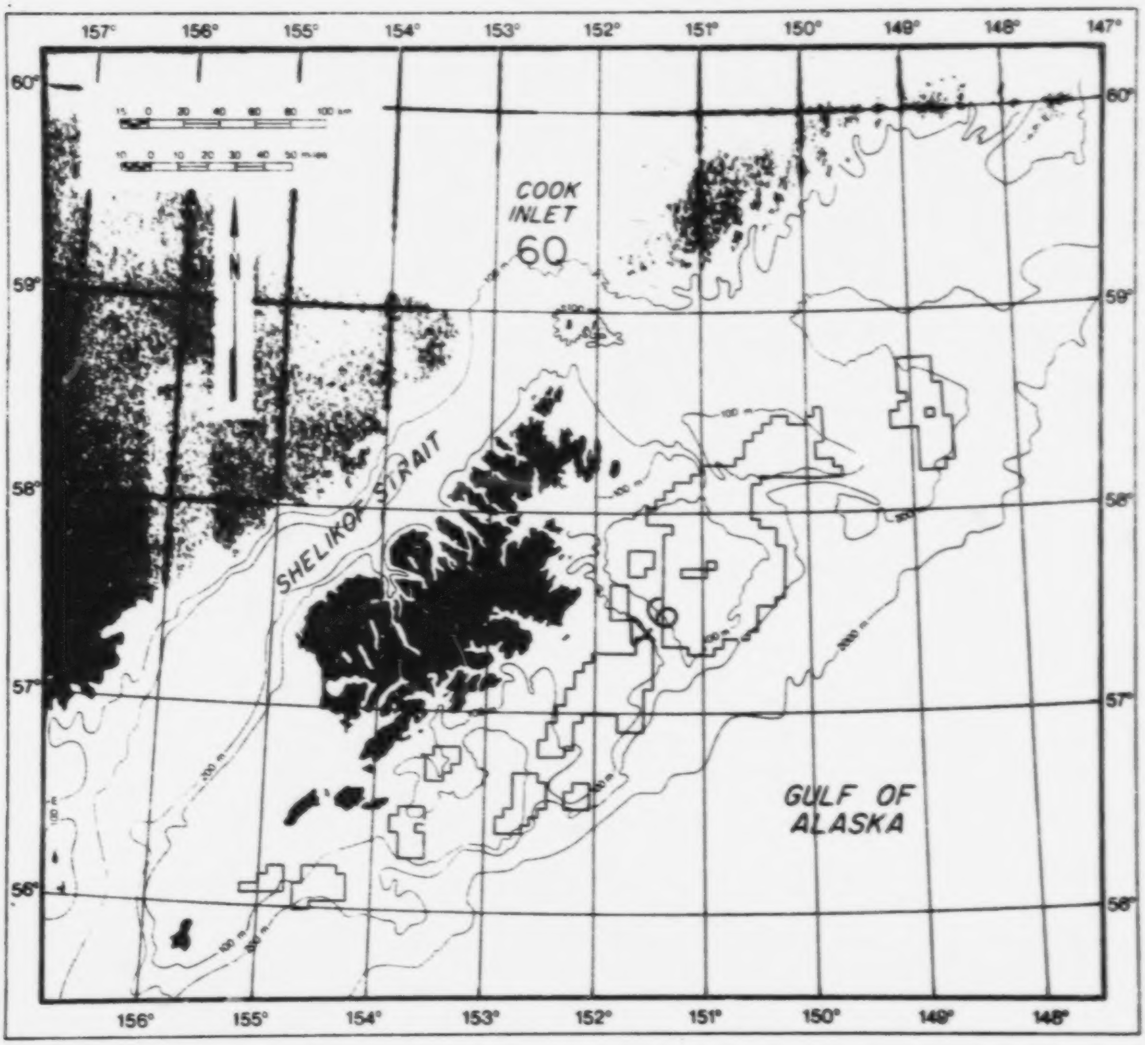
157°
156°
155°
154°
153°
152°
151°
150°
149°
148°
147°
60°
59°
58°
57°
56°
COOK INLET
60
SHELIKOF STRAIT
GULF OF ALASKA
100 m
200 m
2000 m

Frontispiece. Geographical locations in the northwest Gulf of Alaska, showing specific locations of present Outer Continental Shelf lease areas south of Kodiak Island (Sale 46) and general location of present lease area in lower Cook Inlet (Sale 60).

TABLE OF CONTENTS

EXECUTIVE SUMMARY 79

1. INTRODUCTION 84

  1.1 Statement of Purpose 84

  1.2 Geographical Setting 89

  1.3 History of Past Research 94

  1.4 Oceanographic and Meteorological Setting 97

2. OBSERVATIONAL PROGRAM 103

  2.1 Program Rationale 103

  2.2 Current Observation Program 104

    2.2.1 Taut-Wire Moorings 104

    2.2.2 Drift Card Studies 112

    2.2.3 Satellite-Tracked Buoys 113

    2.2.4 Wave Radar (CODAR) Observations 114

  2.3 Temperature and Salinity Observations 116

  2.4 Meteorological Observations 117

3. RESULTS AND DISCUSSION 121

  3.1 Mean Currents, Seasonal Variability and the Temperature, Salinity and Density Fields 121

    3.1.1 Introduction 121

    3.1.2 The General Northwestern Gulf Region 121

    3.1.3 The Kenai Current 124

    3.1.4 Shelikof Strait and Lower Cook Inlet 135

    3.1.5 The Bank and Trough Region 142

  3.2 Behavior of Low-Frequency Current Fluctuations 150

    3.2.1 Introduction 150

BEST DOCUMENT AVAILABLE

3.2.2 The Bank-Trough Region 150

3.2.3 Shelikof Strait 154

3.2.4 Lower Cook Inlet 162

3.3 Tidal Currents 172

3.4 Partitioning of Current Energy with Frequency 183

3.5 Wind Observations 190

3.5.1 Orographic Control 190

3.5.2 Lower Cook Inlet Meteorology 191

4. ACKNOWLEDGEMENTS 214

5. REFERENCES 215

6. APPENDIX A: Current Meter Statistics for Northwest Gulf of Alaska Moorings 219

APPENDIX B: Release and Recovery Information for Draft Cards Released in the Kodiak Island Region During 1978 222

APPENDIX C: Release and Recovery Information for Seabed Drifters, Including Returns Through February 1980 228

APPENDIX D: CTD Stations used in NWGOA Program, Listed by Cruises 230

EXECUTIVE SUMMARY

This report presents a summary of the major findings of Outer Continental Shelf Environmental Assessment Program research into physical oceanographic conditions in the northwest Gulf of Alaska. The stress is on circulation features, since water circulation plays a major role in the path and dispersal of surface contaminants, a problem of major impetus for the OCSEAP program. Reference is made throughout this summary section to Figure i, which summarizes the net circulation regime as deduced from this study. On the figure, arrows depict sense of net flow while the numbers represent a typical range of current speeds, in centimeters per second, which might be encountered in that region. In general, the smaller numbers represent spring-summer conditions while the larger numbers represent autumn-winter conditions. It is stressed here that instantaneous flow observed at a given time need not agree with our simplified graphical depiction. The patterns shown are, rather, indicative of mean conditions and of a normal response to the dynamics which we feel exert dominant control over the system.

The results can be summarized as follows:

1. The Alaskan Stream is a major regional oceanic circulation feature. It flows southwesterly, roughly coincident with the shelf break and slope, with mean speeds of 50-100 cm sec^{-1}. Its width is about 50 km, and its computed annual mean baroclinic volume transport is about 12×10^6 m^3 sec^{-1}. There was no significant annual variability detected either in baroclinic current speed or volume transport. There were eddy-like perturbations observed in the current, at times, which appeared to be related to bottom

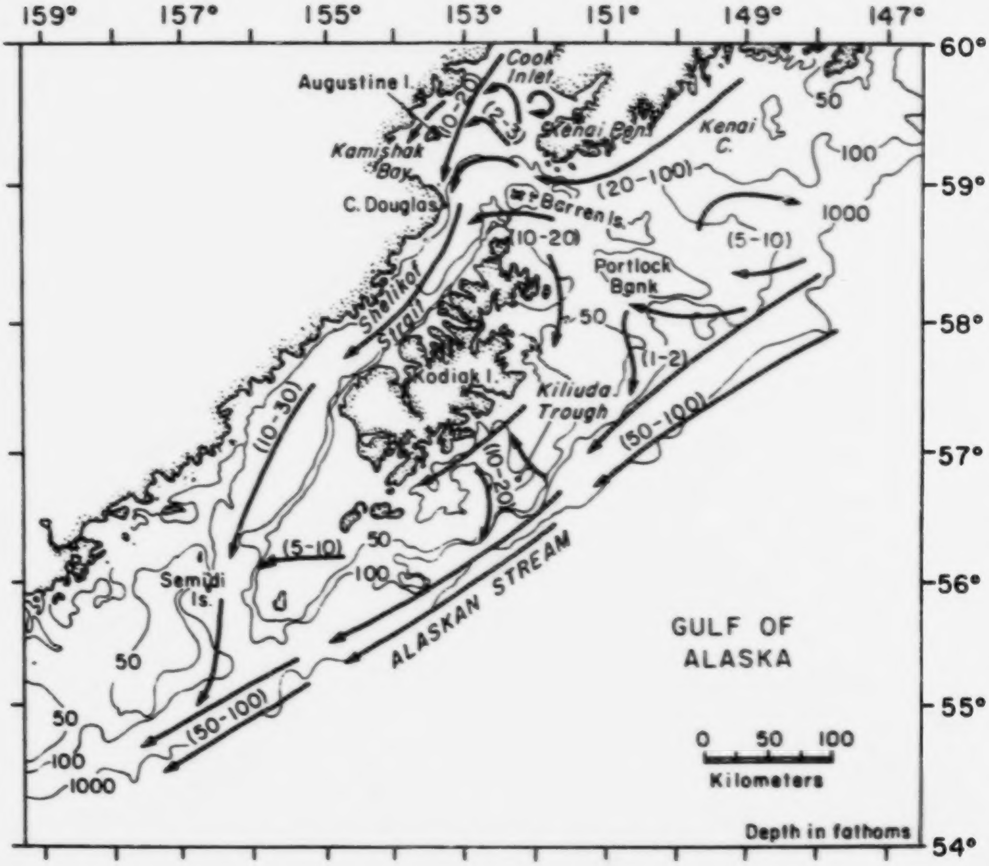
159°
157°
155°
153°
151°
149°
147°
60°
59°
58°
57°
56°
55°
54°
Cook Inlet
Augustine I.
Kamishak Bay
(10-20)
(2-3)
Kenai Pen.
Kenai C.
50
100
(20-100)
C. Douglas
Barren Is.
1000
(10-20)
(5-10)
Portlock Bank
Shelikof Strait
50
(1-2)
Kodiak I.
Kiliuda Trough
(10-30)
(50-100)
(10-20)
(5-10)
50
100
Semidi Is.
ALASKAN STREAM
GULF OF ALASKA
50
50
(50-100)
-100
-1000
0 50 100
Kilometers
Depth in fathoms

Figure i. Schematic diagram of net circulation in the northwest Gulf of Alaska. Arrows indicate direction of mean surface flow, and numbers in parentheses indicate approximate range of speeds in cm sec^{-1}.

topography. A principal driving force for the Alaskan Stream is the wind stress curl over the Gulf of Alaska, which forces the North Pacific subarctic gyre. The Alaskan Stream is the intensified, northwestern leg of this gyre.

2. Dominant circulation on the banks south and southeast of Kodiak Island is predominantly driven by the Alaskan Stream. This includes a poorly defined, weak (5-10 cm sec^{-1}) anticyclonic circulation over Portlock Bank, and a complex flow regime connected with the bank-trough region to the southwest. This bank-trough flow, which apparently represents a bathymetric effect upon the inshore edge of the Alaskan Stream, consists of shoreward flow along the upstream (northeastern) sides of the troughs and a compensatory seaward flow along the downstream (southwestern) sides. The coastal southwesterly flow at the head of Kiliuda Trough reflects this residual circulation, but is probably also due in part to a baroclinic coastal wedge consequent to freshwater input along the south coast of Kodiak Island.

3. A nearshore southwesterly flow along the Kenai Peninsula, the Kenai Current, is a baroclinic coastal current driven by the density field created by freshwater input along the Alaskan coast. This flow is 20-30 km in width and attains maximum current speeds in autumn following the annual period of maximum coastal precipitation and freshwater input. This flow is at its annual minimum during spring and early summer.

4. Flow through Shelikof Strait is southwesterly, with observed speeds during winter (~20 cm sec^{-1}) twice those in summer (~10 cm sec^{-1}). No flow reversals were observed during winter; during summer, the weaker mean flow was accompanied by occasional reversals. This flow is driven in part by the Kenai current upstream and in part by a large-scale alongshore pressure gradient established by the Alaskan Stream. The flow through Shelikof Strait continues to the southwest in a well-defined channel bounded by

relatively shallow banks, merging with the Alaskan Stream some 200 km southwest of Kodiak Island.

5. Circulation in lower Cook Inlet is dominated by the southwesterly flow into Shelikof Strait, which is constrained by bottom topography to traverse an arcuate east-west path across the lower Inlet. Off Cape Douglas, this flow merges with a weaker southward current generated by the freshwater input to upper Cook Inlet, creating a particularly intense southward flow in the region off Cape Douglas. Flow in the central lower inlet out of these two well-defined currents is weak and highly variable.

6. Currents throughout the study region are characterized by speed and direction fluctuations having time scales between about 2 days and a week. These fluctuations are probably related either to meteorological factors or to propagation of ocean eddies across the shelf, though the exact mechanisms are uncertain. In regions such as Shelikof Strait, with a strong mean flow, these fluctuations are of lesser significance relative to the mean flow, leading to speed fluctuations but only minor perturbations to direction. In regions of weak mean flow, such as in central lower Cook Inlet and on Portlock Bank, the fluctuations both in speed and direction are the dominant flow characteristics.

7. Tidal currents vary widely in magnitude throughout the study region. Tidal current effects in Shelikof Strait are minimal because of the standing wave nature of the tidal wave there, and tidal currents become small as the coast is approached south of Kodiak Island. Lower Cook Inlet is characterized, conversely, by large tidal currents particularly in the passages north and south of the Barren Islands due to the near-resonant conditions which lead to extremely large tides in upper Cook Inlet. Tidal currents are also significant in comparison with mean flow on the banks south of Kodiak Island.

8. Winds are controlled by the interaction between large-scale northeastward migrating cyclonic low pressure systems and regional topography. Over the banks south of Kodiak Island, observed winds appear to agree reasonably well with geostrophic winds computed from the atmospheric surface pressure distributions. In lower Cook Inlet, winds are orographically channelled into two orthogonal paths whose axes are aligned with upper Cook Inlet-Shelikof Strait and Barren Islands-Kamishak Bay. This leads to a complex wind pattern there which results from the interaction between these orthogonal flows. Katabatic (drainage) winds may be important locally, particularly in lower Cook Inlet and Shelikof Strait, and wake effects perturb the wind field downstream from such features as Augustine Island.

The picture presented here of major circulation features in the northwest Gulf of Alaska is one of extreme complexity. The various possible combinations of mean, low frequency fluctuating and tidally fluctuating flow lead to a regime wherein prediction of instantaneous flow is impossible. We believe, however, that the flow field has been sufficiently well defined to allow a good prediction of seasonal mean flow. Combined with knowledge of the local and regional wind field, this allows at least an approximate predictability of contaminant dispersion and trajectory.

BEST DOCUMENT AVAILABLE

PHYSICAL OCEANOGRAPHIC AND METEOROLOGICAL CONDITIONS IN THE NORTHWEST GULF OF ALASKA[1]

Robin D. Muench[2] and James D. Schumacher

1. INTRODUCTION

1.1 Statement of Purpose

1.1.1. Objectives

The primary objective of the Alaska OCS Environmental Studies Program is to provide background information for management decisions that may be necessary to protect the OCS marine environment from damage during oil and gas exploration and development. Meaningful data must be readily available in useable form so that informed management decisions can be made before serious or irreversible damage occurs. Protection of the marine and coastal environment is a direct outgrowth of the National Environmental Policy Act of 1969.

In an assessment of the potential impact of OCS development on the marine environment, transport and transformation of petroleum-related contaminants is of key significance. Petroleum or other contaminants introduced into the environment can be transported in the atmosphere, water column and sea ice. During transport, oil and other contaminants undergo continual physical and chemical change brought about by such processes as evaporation, flocculation, emulsification, weathering, biodegradation, and chemical decomposition.

Transport studies are specifically designed to provide data that will enable the Department of the Interior and other agencies to:

- Plan stages and siting of offshore petroleum development so as to minimize potential risk to environmentally sensitive areas.

---

[1] Contribution No. 482 from the NOAA Pacific Marine Environmental Laboratory

[2] Now at SAI/Northwest, 13400B Northrup Way #36, Bellevue, WA 98005

- Provide trajectory, coastal landfall, and impact predictions required for cleanup operations in the event of an oil spill or the introduction of other contaminants.
- Assist in planning the locations of long-term environmental monitoring stations in the study area.

The programmatic objectives described above have resulted in several disciplinary studies of which one element, coastal oceanography and meteorology, directly addresses the problem of movement of contaminants in continental shelf waters.

The primary objective of the OCSEAP oceanography/meteorology studies in the western Gulf of Alaska is to provide, through experimental and theoretical studies, a capability to predict movement and distribution of contaminants introduced into the marine environment through OCS oil and gas development activities. Specific program elements have required the development of methodologies and implementation of studies designed to supply information on:

- Energetics and temporal and spatial variability of coastal ocean circulation in the northwestern Gulf of Alaska;
- Energetics and spatial variability of tidal currents;
- Local wind fields and their influence on coastal circulation;
- Influence of the seasonal heat budget, runoff and precipitation on coastal and estuarine circulation and water mass structure;
- Bathymetric influence on tidal and nontidal circulation and turbulent mixing; and
- Ways to apply data to the prediction of pathways and impact areas of potential pollutants (especially oil) that will aid the assessment of vulnerability of biotic resources and the design of more effective cleanup strategies.

This presents an integrated description of the oceanography and meteorology of the western Gulf of Alaska continental shelf. This description includes the rationale for the various elements of the study program and a presentation of results, analysis techniques and interpretive procedures by which these program elements have been combined to provide an improved understanding of coastal circulation and winds and their likely influence on pollutant transport.

1.1.2 Rationale

Development of an information base that permits prediction, in a probabilistic sense, of the spatial and temporal distribution of petroleum-related contaminants following hypothetical release in coastal waters is a primary function of the OCSEAP transport studies. Such information, in conjunction with seasonal and spatial description of potentially vulnerable marine resources, provides a critical input to the Bureau of Land Management's (BLM's) environmental assessment process. Insofar as this assessment concerns the potential impacts of OCS-related pollutants, BLM's major effort is focused on spilled oil and its subsequent movement on the water surface.

In the Draft Environmental Impact Statement (DEIS), which is to be prepared by the Bureau of Land Management, the most readily apparent use of the oceanographic and meteorological study results is the oil spill risk analysis performed by the U.S. Geological Survey. However, problems of oil incorporation into the water column and sediments and potential impacts of drilling muds, toxic metals, formation waters and other potential pollutants are also of concern. Hence the oceanographic and meteorological studies provide information on both surface and subsurface phenomena that have bearing on the overall problem of contaminant distributions on the continental shelf. Similarly the modeling activities, aside from producing information for the calculation of spilled oil trajectories, also perform important roles in data synthesis, hypothesis formulation and field study design.

Prior to OCSEAP, no systematic studies had addressed mesoscale oceanographic features on the Gulf of Alaska continental shelf. Oceanographic knowledge was limited to a description of large-scale circulation obtained almost exclusively from water mass analyses based on irregular, widely spaced hydrographic data. While knowledge of large-scale flow features such as the Alaska Current and Alaskan Stream was useful in providing a gross picture of Gulf of Alaska circulation, it furnished little insight into smaller scale features present on the continental shelf and responsible for near-coastal transport of contaminants. A need for such information has required the development, through OCSEAP, of a systematic program of mesoscale physical oceanographic and meteorological studies on the continental shelf.

Oceanographic studies in the western Gulf of Alaska cover the geographic region comprising the present Kodiak (Sale 46) and lower Cook Inlet-Shelikof Strait (Sale 60) OCS lease areas shown on the frontispiece. The region consists of the Alaska continental shelf area between Seward and Mitrofania Island on the Alaska Peninsula, including Shelikof Strait and that portion of Cook Inlet south of Kalgin Island.

Oceanographic field studies have employed a variety of techniques including seasonal hydrographic surveys, time series observations of currents, pressure and water properties, Lagrangian current observations, HF Doppler radar current observations, and drift cards. The primary purpose of these studies is to provide the information necessary to develop a picture of continental shelf circulation and mixing processes, including significant temporal and spatial variability scales, relevant to the transport of pollutants.

The importance of local wind forcing to the dynamics of continental shelf waters and to the subsequent movements of potential contaminants was recognized from the program's beginning. It was also recognized that local winds along the Gulf of Alaska coast can differ significantly, because of the effects of coastal orography and land-sea boundaries, from those determined from synoptic weather charts or land-based stations. These differences can lead to substantial errors in pollutant transport predictions based on traditional synoptic geostrophic wind calculations or inappropriately located (for OCSEAP's requirements) weather stations. Consequently, the oceanographic program has been accompanied by concurrent coastal meteorological investigations that include an expanded network of shore stations, over-the-water wind and pressure measurements from meteorological data buoys and ships of opportunity, and computer simulations of coastal winds. These studies have resulted in the development of a technique for determination of mesoscale wind fields that consists of (1) derivation of a synoptic weather pattern climatology in the form of a limited number of surface pressure distributions, based on historical data and judged adequate in number to characterize the region; (2) development of appropriate synoptic climatology statistics, including pattern durations and transition probabilities; (3) calculation, via a combination of direct observations and modeling, of the mesoscale wind field most likely to be associated with and driven in part by each synoptic pattern; and (4) use of (1) - (3) above to derive a statistical description of the local wind climatology. This technique attempts to correlate local wind patterns with regional synoptic distributions which have a statistically meaningful data base and are routinely observable.

Oceanographic and meteorological field studies in the western Gulf of Alaska have been accompanied by computer simulation models of coastal circulation patterns and likely pollutant trajectories. Models employed to date have been of three general types: (1) a diagnostic circulation model utilizing observed winds and hydrography as input and observed currents as calibration data; (2) a tidal model; and (3) an empirical model based on observed currents and winds. Specific model application has depended on the study area in question and the driving forces and physical mechanisms believed to be dominant in that region. These models have been used both in a predictive sense and as vehicles for the synthesis and interpretation of observed data.

Collectively, the modeling activities and oceanographic field studies have been employed in an interactive fashion to provide an improved understanding of coastal circulation patterns and dynamical processes.

1.2 Geographical Setting

In discussing physical oceanographic processes in the northwestern Gulf of Alaska, we focus primarily upon coastal and continental shelf regimes. Physical factors which are known to exert primary controls over circulation in such regions include bottom depth and slope, continental shelf width, and orientation of the coastline relative to north. On a smaller scale, coastline and bottom topographic irregularities can exert significant influence over local circulation features. Since we address a broad range of both temporal and spatial scales of oceanographic processes, it is necessary to discuss in some detail those geographical and bottom features which we expect *a priori* to significantly affect oceanographic conditions.

The northern Gulf of Alaska is an arcuate, east-west trending bight which forms the northern boundary of the northeastern Pacific Ocean (Fig. 1). We are concerned here with the portion of the Gulf extending from the shoreline seaward to the continental shelf break, as defined approximately

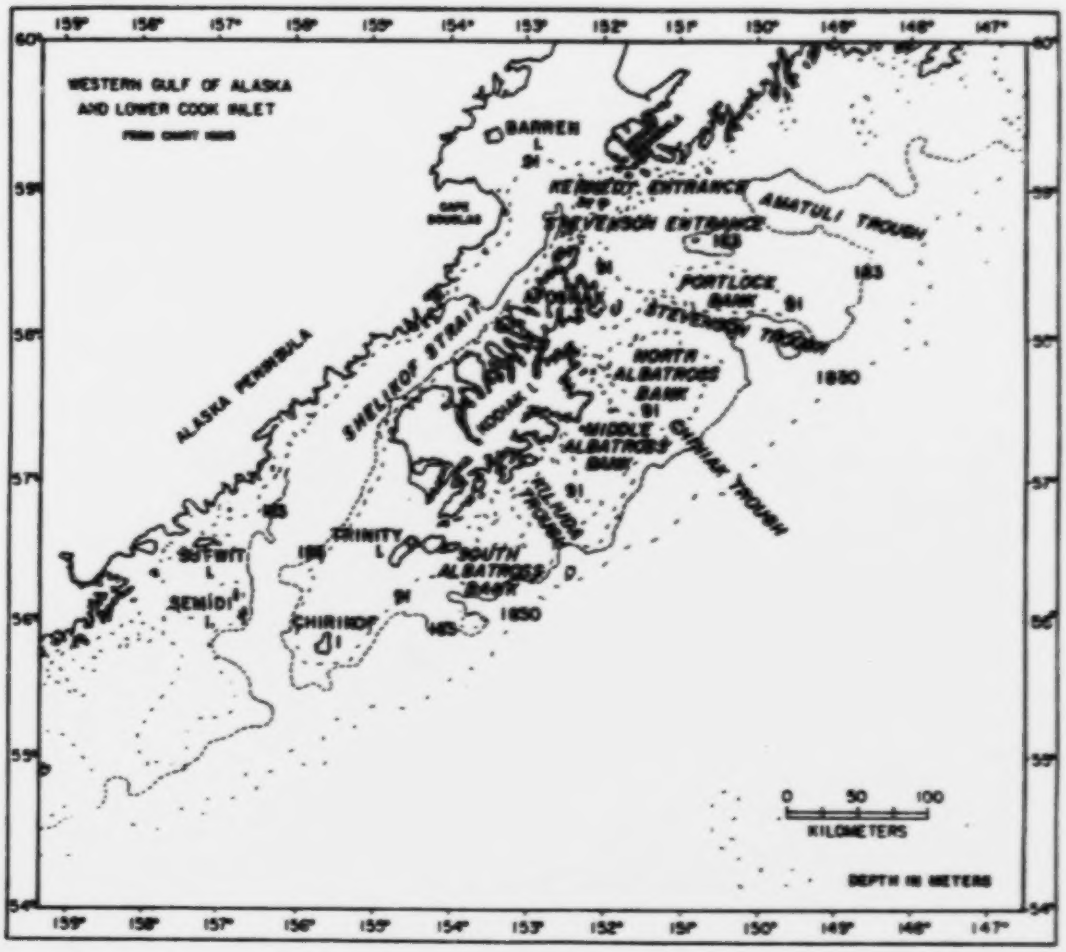
WESTERN GULF OF ALASKA
AND LOWER COOK INLET
159°
158°
157°
156°
155°
154°
153°
152°
151°
150°
149°
148°
147°
60°
59°
58°
57°
56°
55°
54°
BARREN I.
91
CAPE DOUGLAS
KENNEDY ENTRANCE
STEVENSON ENTRANCE
AMATULI TROUGH
183
PORTLOCK BANK
STEVENSON TROUGH
1830
NORTH ALBATROSS BANK
MIDDLE ALBATROSS BANK
CHINIAK TROUGH
KILNUDA TROUGH
KODIAK I.
SHELIKOF STRAIT
ALASKA PENINSULA
SUTWIK I.
SEMIDI I.
TRINITY I.
SOUTH ALBATROSS BANK
CHIRIKOF I.
1830
183
0
50
100
KILOMETERS
DEPTH IN METERS

Figure 1. Northwest Gulf of Alaska regional bathymetry and geographical locations.

by the 200-m isobath, and westward from 148°W to about 160°W. This area encompasses a segment of continental shelf characterized by complex shoreline and bottom topography which includes numerous embayments and channels, banks and troughs. The shelf is about 175 km wide throughout our study region. Kodiak Island, along with its smaller adjacent islands, may be viewed as a barrier to flow which is centrally located on the shelf and surrounded by a system of relatively shallow banks. Alternately, the shelf may be considered to occupy the region southeast and east of Kodiak Island, with Shelikof Strait being a major channel separate from the shelf proper. (Both viewpoints will be used, depending upon the context.) Cook Inlet extends northeasterly from the shelf directly north of Kodiak Island; the lower Cook Inlet-Shelikof Strait system comprises a complex system of deep channels. Overall alongshore orientation of this continental shelf system is northeast-southwest. Seaward of the 200-m deep shelf break, the bottom drops abruptly to attain maximum depths of 5000-6000 m in the Aleutian Trench.

The continental shelf area southeast of Kodiak Island is about 60 km wide. Bottom topography there and to the northeast is dominated by four relatively shoal (~90 m) areas separated from one another by deeper channels which transect the shelf in a direction roughly normal to the coastline (Fig. 1). The shoals are, from northeast to southwest, Portlock and North, Middle and South Albatross Banks. At the northeastern extremity of this system of banks, Amatuli Trough trends east-west with depths exceeding 200 m. At its western end, this trough bifurcates to form the deeper portions of the channels entering Cook Inlet via Kennedy and Stevenson Entrances and, in so doing, provides a relatively deep access (~100 m) from the shelf break to the waters of lower Cook Inlet. To the south of Amatuli Trough lies Portlock Bank, which has depths of less than 50 m and is separated from

North Albatross Bank to the southwest by Stevenson Trough. At its shallowest point, in the narrow channel west of Portlock Bank, Stevenson Trough is about 110 m deep. Depths on North Albatross Bank are 70-90 m. North and Middle Albatross Banks are separated by Chiniak Trough, which has maximum depths of about 145 m. Minimum depths on both Middle and South Albatross banks are about 30 m and are found at the seaward boundary of the banks. Kiliuda Trough separates Middle and South Albatross Banks, has maximum depths of about 150 m, and near the coastline turns and trends southwest to form an inverted L-shaped depression with generally complex topography. Maximum vertical relief in this system of banks and troughs is found surrounding Kiliuda Trough.

Shelikof Strait lies between Kodiak and Afognak Islands and the Alaska Peninsula and is uniformly about 45 km wide, forming a major channel for alongshore flow. At its northern end it is connected to the open shelf via Kennedy Entrance north of the Barren Islands, and via Stevenson Entrance between the Barren Islands and Afognak Island. Kennedy Entrance is the narrower of the two but has greater depths (~200 m). Maximum depths in Stevenson Entrance are about 120 m. The northeastern half of Shelikof Strait is somewhat shallower than the southwestern half, or about 180 m as compared to 200 m. The extension of the Strait across the shelf southwest of Kodiak Island is bounded on both sides by banks and has maximum depths of about 200 m. The adjacent banks are 30-40 m deep to the southeast and 100 m deep to the northwest where they shoal to form Sutwik and the Semidi Islands.

Cook Inlet is a broad (70-90 km), shallow (mean depth about 60 m), elongate embayment extending northeastward from the confluence between Shelikof Strait and Kennedy and Stevenson Entrances (Fig. 2). This study deals only with the lower portion of the Inlet defined as that region

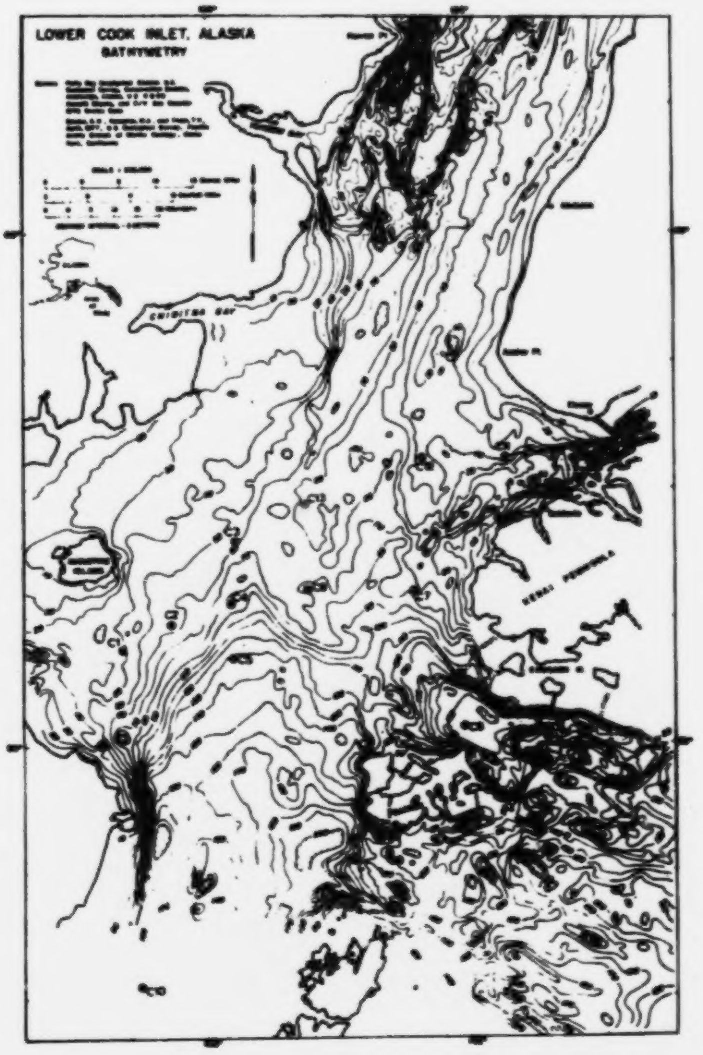
LOWER COOK INLET, ALASKA
BATHYMETRY
CHINITNA BAY
KENAI PENINSULA

Figure 2. Detail of lower Cook Inlet bathymetry.

bounded on the north by the Forelands and on the south by Kennedy and Stevenson Entrances and Shelikof Strait. At the northern end of lower Cook Inlet, Kalgin Island and its associated shoals reduce water flow in the western half of the Inlet. In the central portion of the lower Inlet, bottom depths are 60-80 m. Depth increases to the south in regular fashion except for a prominent ramp-like feature which traverses the inlet from east to west in arcuate fashion along the 100-m isobath. Maximum depths in the inlet occur in a depression just west of Stevenson Entrance. Several embayments extend laterally from the Inlet.

Land areas surrounding the northwestern Gulf of Alaska are extremely mountainous. On Kodiak Island, these mountains rise to elevations of 1000-2000 m, while along the northern shores of Cook Inlet and Shelikof Strait elevations are 2000-3000 m. The mountains are transected by valleys, many containing glaciers or snowfields at their heads. This rugged topography surrounding the study region is of interest because it exerts a marked effect upon local winds, which in turn can affect water circulation.

1.3 History of Past Research

Prior to commencement of the OCSEAP studies, little information was available concerning physical oceanographic conditions on the northern Gulf of Alaska shelf. Few field data were available from the shelf region, since early investigations were confined primarily to the Alaskan Stream or the Gulf of Alaska subarctic gyre. The Alaskan Stream is an offshore boundary current which flows southwestward along the shelf break, forming the northwestern branch of the subarctic gyre. The single exception to this was the early work of McEwen, et al. (1930), who used temperature and salinity data obtained along sections normal to the coastline in the northeast Gulf of Alaska to describe and analyze temperature, salinity and current structures over the shelf and shelf break.

Some three decades following the work of McEwen, et al. (1930), acquisition of substantial sets of new field data allowed investigators to concentrate on the northwestern Gulf. Resulting manuscripts used temperature and salinity data to address circulation processes in the Alaskan Stream southwest of Kodiak Island and westward along the Aleutian Islands (Dodimead et al., 1963; Favorite, 1967; Roden, 1969; Favorite et al., 1976). These analyses led to definition of the Alaskan Stream as a western boundary current which acts as a return flow for the wind-driven circulation in the northern Gulf of Alaska (Favorite et al., 1976), an observation which was subsequently supported by the theoretical work of Thomson (1972). Reed and Taylor (1965) computed peak baroclinic surface speeds in the Alaskan Stream of order 100 cm sec^{-1}, and presented evidence that the flow was predominantly baroclinic and in geostrophic balance. Ingraham et al. (1976) computed Sverdrup transports in the Gulf of Alaska using calculated geostrophic winds, and concluded that transports in the Alaskan Stream can vary from about 20×10^6 m^3 sec^{-1} in winter to less than 5×10^6 m^3 sec^{-1} during summer. Reed et al. (1980) have used OCSEAP temperature and salinity data to show, however, that a mean baroclinic transport of about 12×10^6 m^3 sec^{-1} in the Alaskan Stream does not reflect the large annual variation of wind stress curl over the Gulf of Alaska.

Direct observations of circulation in the Gulf of Alaska are sparse, consisting primarily of the drift-card studies carried out by Favorite (1964) and Favorite and Fisk (1971) which provided qualitative support for cyclonic circulation in the Gulf of Alaska and a westerly flow south of the Aleutians. An excellent summary of subarctic Pacific oceanography was prepared by Favorite et al. (1976). Most recently Reed (1980) used satellite-tracked drogued buoys to document the closed gyre circulation in the Gulf of Alaska.

Prior to inception of the OCSEAP research program, acquisition of new temperature and salinity data from the Gulf of Alaska continental shelves allowed characterization of seasonal variations in the water column (Royer, 1975). Royer and Muench (1977) discussed some large-scale features in the surface temperature distribution and related these to the regional circulation and to vertical mixing regimes on the shelf. Hayes and Schumacher (1976) and Hayes (1979) described and discussed the interrelations between winds, currents and bottom pressures on the continental shelf in the northeastern Gulf. Their work suggests that oceanic forcing is dominant at the shelf break, but that inner shelf or coastal circulation is primarily dependent upon other factors. This was substantiated by Royer et al. (1979), who provided evidence for a coastal flow extending some 500 km east from Prince William Sound in a 15- to 20-km wide coastal band. Royer (1979) discussed the impact that extensive precipitation and runoff can have on the near-coastal circulation. In related work Schumacher et al. (1978; 1979) indicated that for the northwest Gulf of Alaska shelf the Alaskan Stream acts as an offshore feature whose typically high speeds (50-100 cm sec^{-1}) do not extend appreciably onto the shelf. However, they indicate that the hydrographic data show a shoreward flux of heat and salt over the shelf.

Previous work in Cook Inlet, which forms a major embayment on the northwest Gulf of Alaska shelf and is especially subject to pollution problems because of active petroleum activities and other industrial development, has been limited primarily to unpublished manuscripts from various sources (e.g. Kinney et al. 1970a, 1970b; Knull and Williamson, 1969; Wright et al., 1973; Gatto, 1976; Burbank, 1977). Previous field activities focused primarily upon the upper portion of the Inlet (e.g. Kinney et al., 1970a, 1970b). Studies using surface drifters have attempted to define the circulation in Kachemak Bay (Knull and Williamson, 1969) and in the lower Inlet (Burbank, 1977). Landsat data, which qualitatively indicate suspended sediment distributions in near-surface waters, have led to several qualitative expositions on Cook Inlet surface circulation (Wright et al., 1973; Gatto, 1976). In the most recent work on lower Cook Inlet, Muench et al. (1978) used summer 1973 oceanographic data obtained by the National Ocean Survey of NOAA to qualitatively discuss circulation and hydrography in the lower Inlet.

At the time of preparation of this report, then, much is known of the general, large-scale circulation on the northwest Gulf of Alaska continental shelf and in lower Cook Inlet, a major appended embayment. Our goal has been to synthesize this general information while at the same time incorporating the data from our experimental and theoretical studies.

1.4 Oceanographic and Meteorological Setting

In order to clarify the rationale used for field sampling, it is necessary to discuss in general fashion the main physical features which control regional oceanographic processes. The major oceanographic feature in the northwest Gulf of Alaska is the Alaskan Stream, an intense, southwestward-flowing current lying along the continental shelf break and slope to the southeast of Kodiak Island (Fig. 3). This current is the northwestern branch of the closed subarctic Pacific gyre which occupies the Gulf of Alaska and is driven primarily by the wind-stress curl over the North Pacific (Reed et al., 1980). The current is generally most intense near the shelf break, where it can attain daily mean surface speeds of order 100 cm sec^{-1} or more. Speeds taper off to seaward, and the current width from the shelf break to the point where speeds approach zero is of order 50 km. Baroclinic

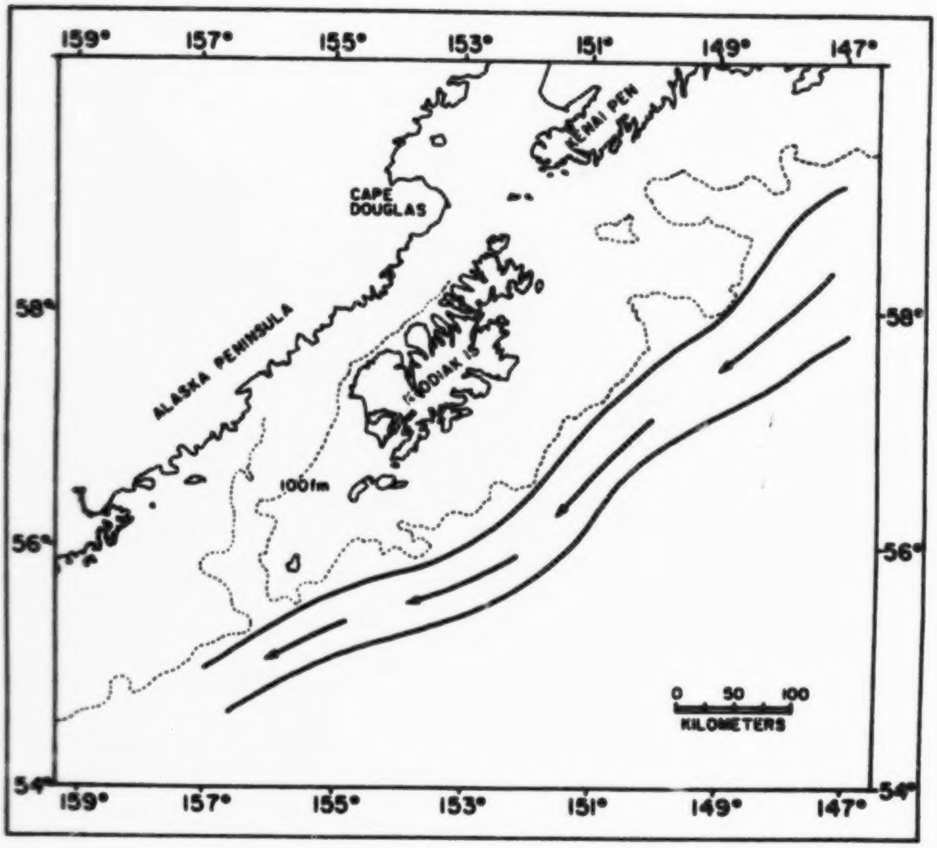
159°
157°
155°
153°
151°
149°
147°
58°
56°
54°
CAPE DOUGLAS
KENAI PEN
ALASKA PENINSULA
KODIAK IS
100fm
0 50 100
KILOMETERS

Figure 3. Approximate location of the Alaskan Stream along the shelf edge in the northwest Gulf of Alaska.

volume transport in the Alaskan Stream averages about 12 x 10^6 m^3 sec^{-1}, as computed using available temperature and salinity data; there does not appear to be a significant seasonal signal in this transport, contrary to what we would expect considering the large annual variation in wind-stress curl over the Gulf of Alaska (Reed et al., 1980). Since there are few direct observations of current in the Alaskan Stream, magnitude of the total volume transport remains uncertain.

Flow on the continental shelf and in Shelikof Strait is toward the southwest throughout the year. This flow is driven primarily by a combination of alongshore sea-level slope, consequent to the presence along the shelf break of the westward-flowing Alaskan Stream, and the baroclinic field established by freshwater input along the Alaskan coast (Muench et al., 1978; Schumacher and Reed, 1980).

Annual variability of shelf water properties in the northern Gulf of Alaska has been characterized by Royer (1975) (Figure 4). During winter, intensification of cyclonic atmospheric circulation over the Gulf of Alaska leads to easterly coastal winds and a downwelling tendency. At the same time, wind and thermohaline processes contribute to vertical mixing. Consequently, the water is characterized during winter by vertical near-homogeneity, elevated salinities and low temperatures. During summer, coastal winds diminish to allow relaxation of downwelling and create a weak upwelling tendency, and freshwater input and solar insolation act to increase stratification. As a result, the coastal waters are stratified in temperature, salinity and density during summer and fall, during which time temperature and salinity attain their maximum and minimum values, respectively, with respect to the annual cycle.

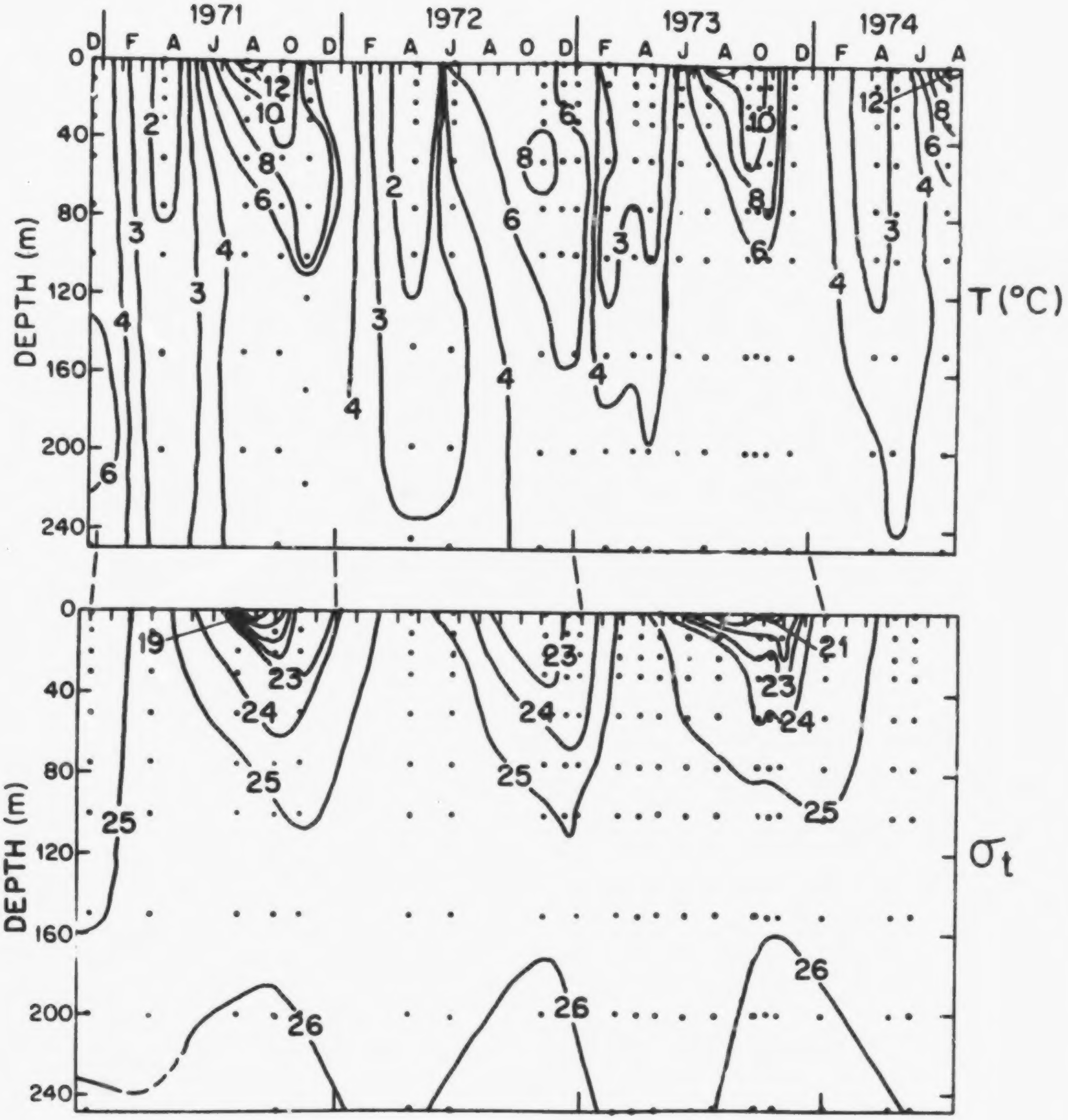

Figure 4. Variation of temperature and density (as sigma-t) at a location on the northern central Gulf of Alaska shelf (after Royer, 1975).

Regional meteorology is dominated by the Aleutian atmospheric low pressure system. During winter this system intensifies and intense, cyclonic low pressure systems migrate northeasterly off Kodiak Island. During summer, the North Pacific atmospheric high pressure region dominates, and the intensity and frequency of cyclonic storms decreases, leading to weak and variable winds. Air temperatures are occasionally below 0°C. during winter, but rise to well above freezing during summer. A useful summary of such regional climatological data has been prepared by Brower et al. (1977).

A final factor which can be significantly effective upon continental shelf circulation is freshwater input from continental sources. This input is not generally well known along the northwestern Gulf of Alaska coast, due to the scarcity of gaging stations. It is known, however, that there are generally two annual peaks in runoff. The first, or spring peak, results from melting of the previous winter's snow cover. The second, or autumn, peak occurs with the onset of severe storms which bring large quantities of rain to coastal regions. This second peak drops off once air temperatures have become low enough so that the precipitation occurs as snow rather than rain. In some areas, one of the peaks may be negligible, or the low-flow period between peaks may disappear. The latter is true of major river input into upper Cook Inlet because of the long duration of the spring snow-melt peak, which actually continues well into summer, coupled with low summer rainfall (cf. Muench et al., 1978).

Sea ice is not generally encountered in the northern Gulf of Alaska. The exception is in Cook Inlet, where low air temperatures and a high freshwater content due to river input lead to local ice formation in the upper Inlet. Some landfast and floe ice also occurs in Kachemak Bay during extreme winters. In Kamishak Bay, a combination of landfast ice in the embayments and floes from the upper Inlet can result in heavy winter ice accumulation. Much of this ice is advected southward along the western shore of the Inlet by wind and water circulation, and is occasionally found as far south as Cape Douglas.

The factors summarized in this section, in conjunction with bathymetric features discussed in Section 1.2, ultimately determine the physical oceanographic characteristics of the northwestern Gulf of Alaska shelf.

2. OBSERVATIONAL PROGRAM

2.1 Program Rationale

The OCSEAP field observation program in the Gulf of Alaska was designed to define and explain the fields of wind and water motion as they affect contaminant trajectories and dispersion. At the outset of the study, little was known either of local winds or of water motion on the Gulf of Alaska continental shelf. Therefore, the initial phases of the program attempted a large-scale definition of motion and the associated temperature-salinity-density (for water) and pressure (for winds) fields needed to address the regional oceanographic and meteorological dynamics. Early phases of the program involved field work extending from east of Kodiak Island westward to Unimak Pass in the Aleutians, but were of too coarse a resolution to define specific local features. Once large-scale winds and water flow on the shelf had been defined, specific process-oriented experiments such as the meteorological-oceanographic study of lower Cook Inlet and the intensive oceanographic study of the bank and trough region off Kodiak Island were undertaken. In this way the field program evolved continually, with new phases of the field work being determined by the outcome of previous phases. The emphases were always on more localized, process-oriented studies as time progressed. Thus, the general survey of oceanic circulation on the shelf between Kodiak Island and Unimak Pass evolved into separate process studies in Cook Inlet, in Shelikof Strait and in the Kiliuda Trough area south of Kodiak Island. Results from the general scientific literature, obtained from experiments in other parts of the world ocean, were also used in planning the process studies and in attempting to foresee results. Results of the studies were integrated with related results from other regions to comprise contributions to basic science, as well as further knowledge of the northern Gulf of Alaska. Aspects of this development will be further clarified in the following discussion.

2.2 The Current Observation Program

Currents were observed in the northwest Gulf of Alaska using moored current meters deployed on subsurface arrays, surface drift cards, satellite-tracked, drogued drifters and HF radar. The first method yielded time series of currents at fixed locations, or Eulerian measurements. The second method provided us with points of release and recovery which, in turn, allowed crude estimation of Lagrangian drift trajectories. The third method provided us with Lagrangian drift trajectories which approximate those followed by a water parcel. The final method yielded actual observations of surface water motions.

2.2.1 Taut-Wire Moorings

Moored current meters were deployed using taut-wire moorings and acoustic releases (Fig. 5). Aanderaa RCM-4 recording current meters were used for all moorings. These use Savonius rotors to measure current speed and vane/compass assemblies for determining current direction relative to magnetic north.

The pattern for deployment of the moorings can be divided into subsets. The first set of moorings was designed to investigate large-scale (~500 km) alongshelf flow seaward of Kodiak Island and as far southwest as Unimak Pass (Fig. 6). Durations of these observations, broken down according to individual instruments on each mooring, are indicated in Appendix A. These moorings carried the prefix designation "WGC".

The second set of moorings was designed to investigate circulation around Kodiak Island, and included deployments in Shelikof Strait and on the banks southeast of the island (Fig. 7).

BEST DOCUMENT AVAILABLE

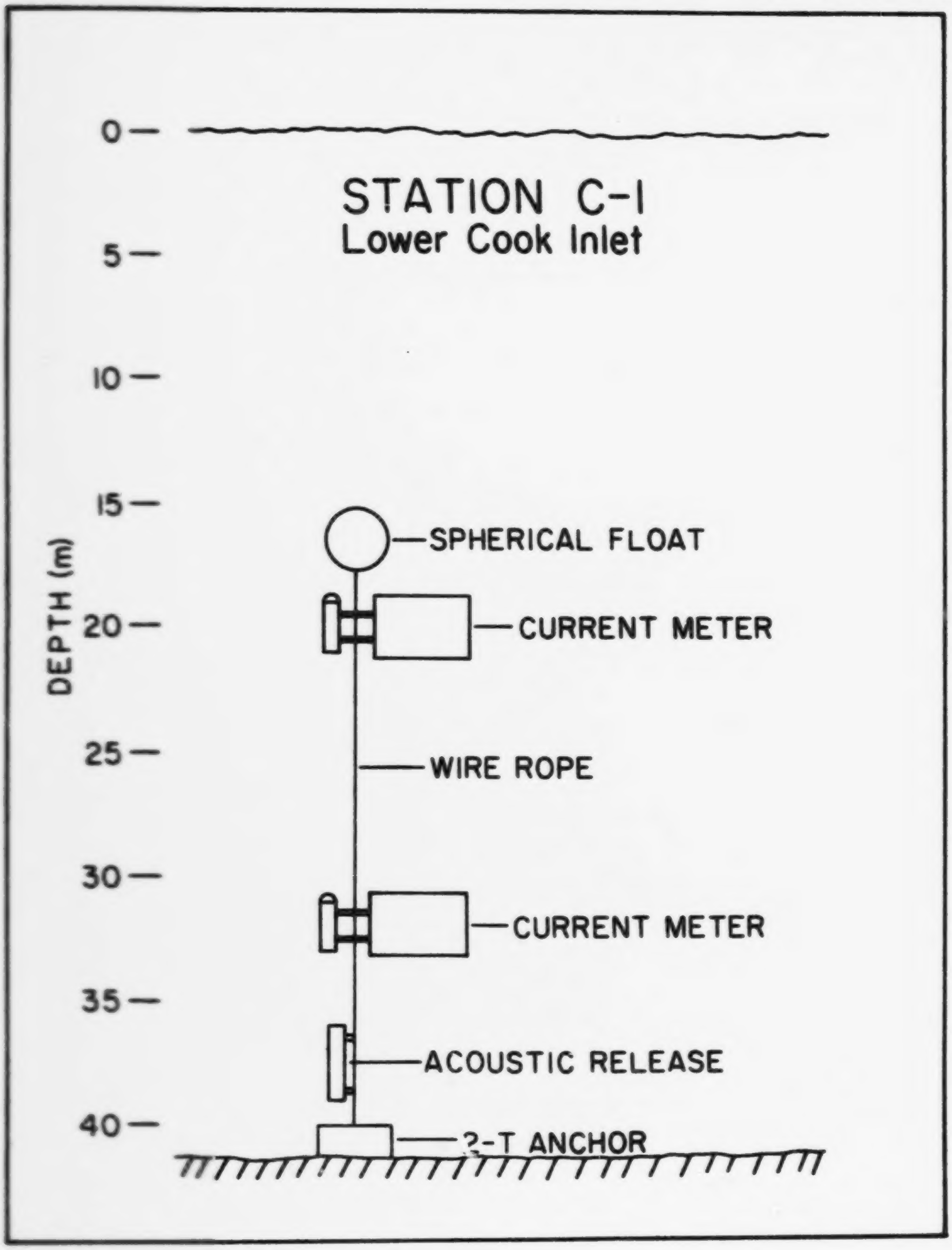

0
5
10
15
20
25
30
35
40
DEPTH (m)
STATION C-1
Lower Cook Inlet
SPHERICAL FLOAT
CURRENT METER
WIRE ROPE
CURRENT METER
ACOUSTIC RELEASE
2-T ANCHOR

Figure 5. Example of configuration of taut-wire current meter mooring used in the northwest Gulf of Alaska. Number of meters and their vertical spacing varied with different stations and depended upon such factors as water depth and stratification.

BEST DOCUMENT AVAILABLE

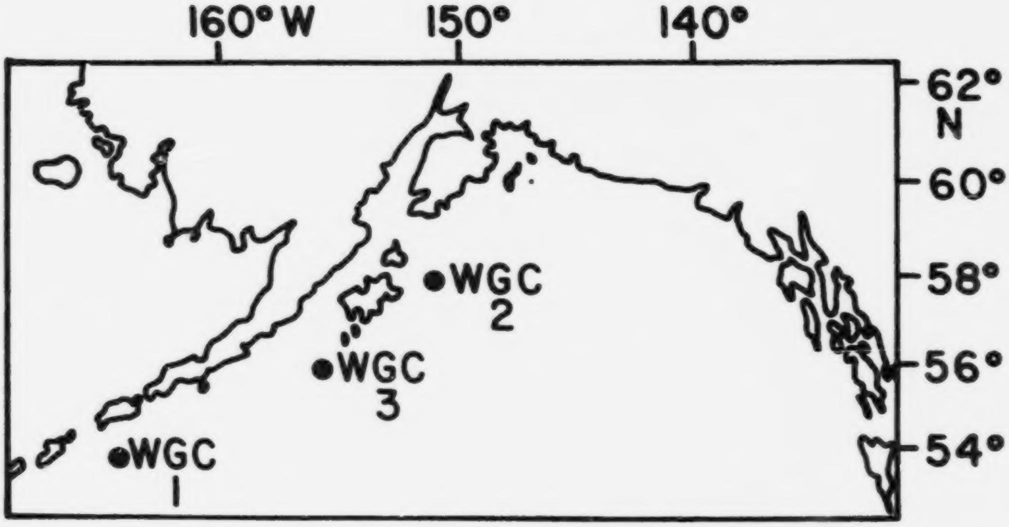
160° W
150°
140°
62° N
60°
58°
56°
54°
WGC 1
WGC 2
WGC 3

Figure 6. Current meter mooring locations for preliminary, large-scale investigations of shelf flow in the northwest Gulf of Alaska. Mooring statistics are given in Appendix A.

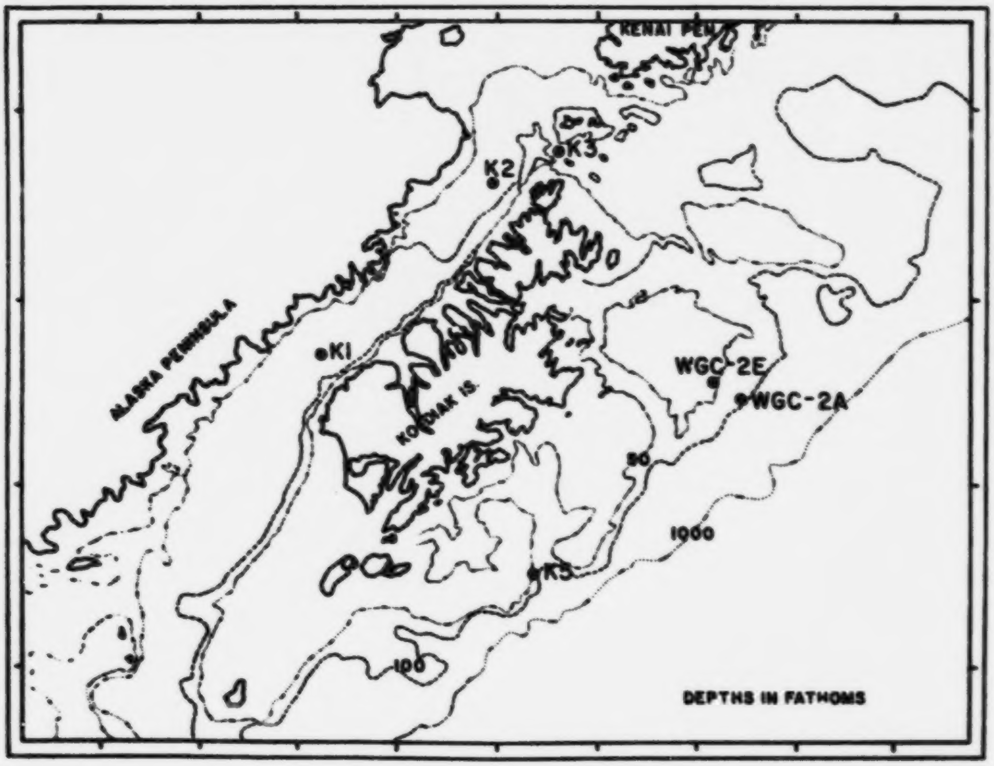
KENAI PEN.
K3
K2
K1
ALASKA PENINSULA
KODIAK IS.
WGC-2E
WGC-2A
50
1000
K5
100
DEPTHS IN FATHOMS

Figure 7. Locations of current meter moorings deployed during winter 1976-77 in the region surrounding Kodiak Island. Mooring statistics are given in Appendix A.

A third set of moorings was deployed on two separate occasions, approximately 5-mo periods in winter 1977-78 and again in summer 1978. These moorings encompassed three separate process-oriented studies. Moorings C1-C13 were deployed in lower Cook Inlet in an attempt to better understand circulation connected with the bathymetry and in the region of convergence defined by Muench et al. (1978) (cf. Section 3.2)(Fig. 8). Moorings K6-K13 were deployed in the region surrounding Kodiak Island as an extension of the experiment initiated with K1-K5 to investigate circulation around the island (Fig. 9). A particularly important aim of this experiment was investigation of circulation in the region south of Kodiak Island where the shelf is transected by banks and troughs. Finally, moorings M1-M4 were deployed, during winter 1977-78 only, in the coastal region off Mitrofania Island southwest of Kodiak Island to attempt a comparison between the coastal dynamics there and in the northeast Gulf of Alaska where a similar experiment had been carried out (cf. Hayes, 1979) (Fig. 10). Failure to recover the shelf break mooring M3 severely limited the usefulness of this data set, however.

The current meters sampled at 15- or 20-min intervals. Raw data were low-pass filtered to remove high-frequency noise; this filter passed more than 99% of the amplitude at periods greater than 5 h, 50% at 2.86 h and less than 0.5% at 2 h. This series was then further filtered to remove most of the tidal energy; the second filter passed more than 99% of the amplitude at periods of more than 55 h, 50% at 35 h and less than 0.5% at 25 h. This second, low-pass filtered series was then resampled at 6-hr intervals and was used for examining nontidal circulation. Details of this processing are discussed in Charnell and Krancus (1976).

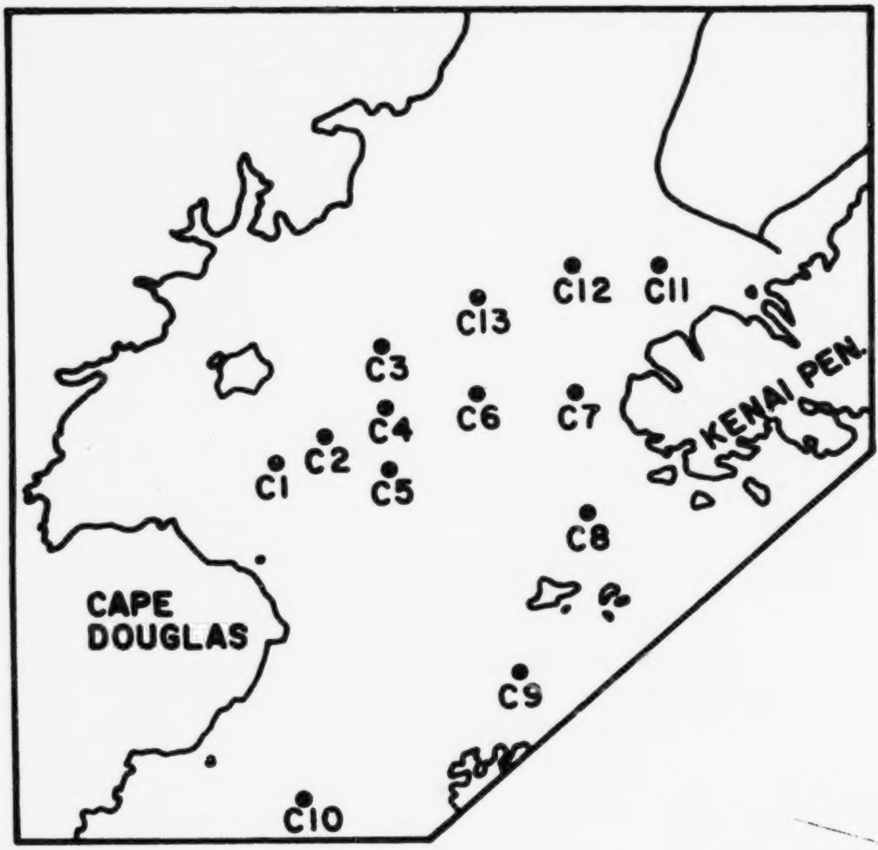
C12
C11
C13
C3
C6
C7
KENAI PEN.
C4
C2
C1
C5
C8
CAPE DOUGLAS
C9
C10

Figure 8. Locations of current meter moorings in lower Cook Inlet in 1977-78. Mooring statistics are given in Appendix A.

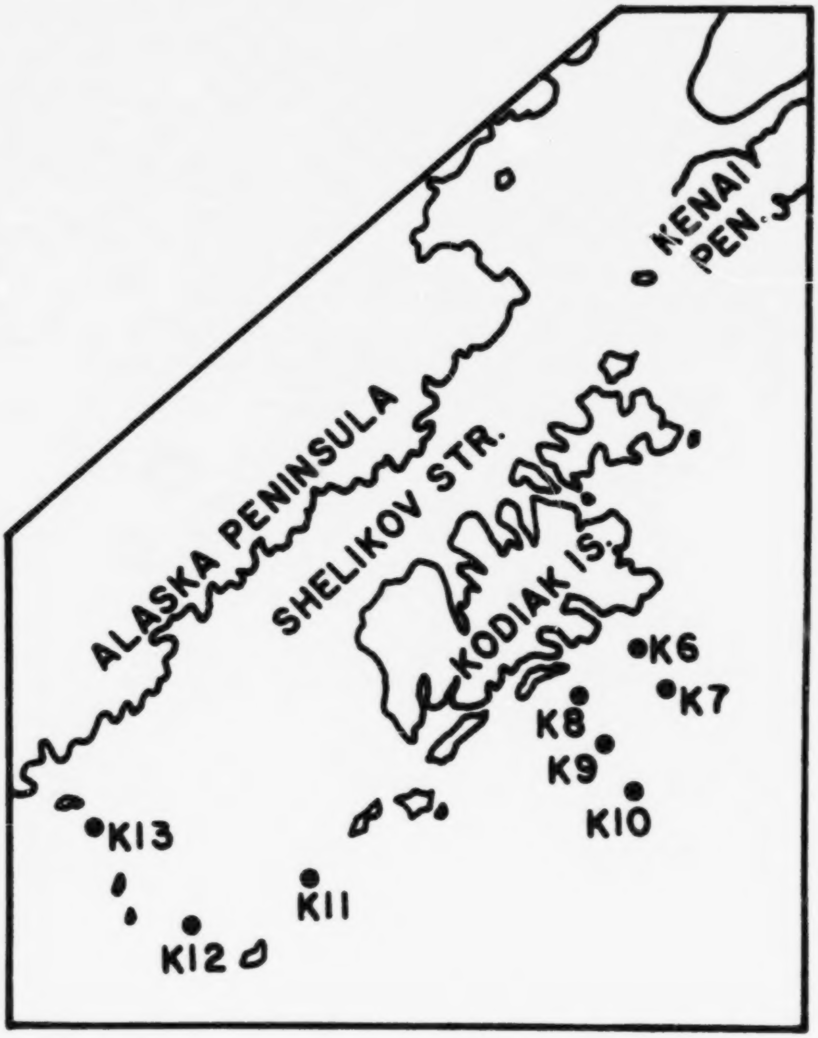
KENAI PEN.
ALASKA PENINSULA
SHELIKOV STR.
KODIAK IS.
K6
K7
K8
K9
K10
K11
K12
K13

Figure 9. Current meter mooring locations south and west of Kdiak Island in 1977-78. Mooring statistics are given in Appendix A.

BEST DOCUMENT AVAILABLE

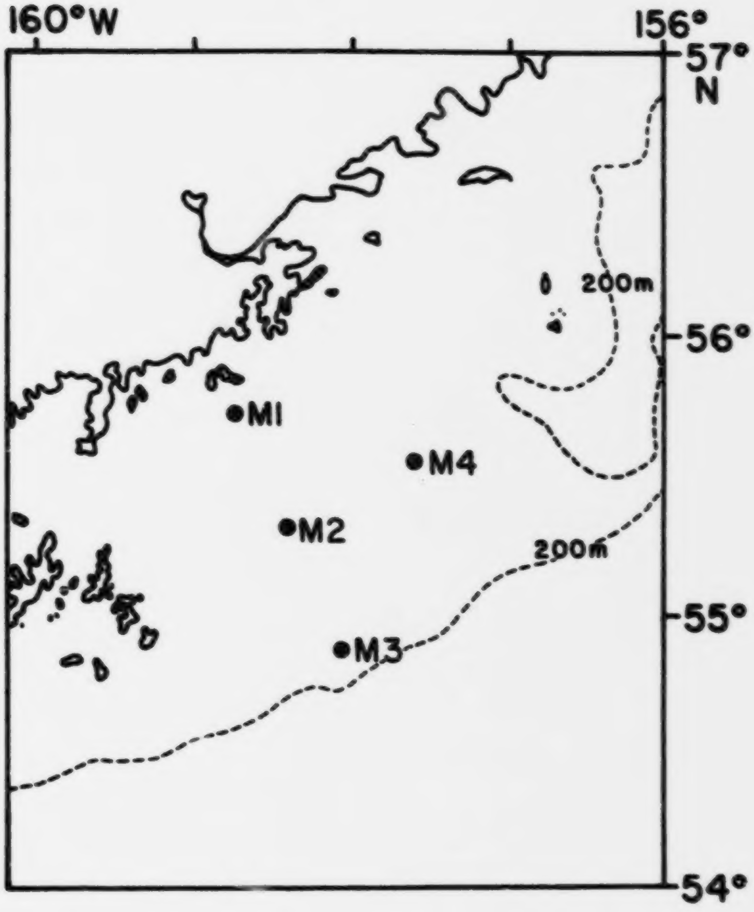
160°W
156°
57° N
56°
55°
54°
200m
200m
M1
M2
M3
M4

Figure 10. Locations of current meter moorings used for the winter 1977-78 Mitrofania Island experiment.

2.2.2 Drift-Card and Seabed Drifter Studies

Since a major objective of the program in the northwest Gulf of Alaska was to provide information that would aid in prediction of the ultimate fate of an oil spill, it was decided to deploy drift cards which float at the surface and which should behave similarly to an oil spill and indicate where beaching might occur. Cards used for this purpose were made of plastic, were 3" x 5" in size and had a specific gravity of about 0.9 which caused them to float nearly submerged at the water surface. The resultant low above-water profile minimizes wind effect upon the cards, consequently movements should be representative of surface water motions. It should be stressed that the cards were not intended to yield actual trajectories, rather to provide, by distribution of their recoveries, a description of possible areas for grounding of an oil spill occurring at a given location. No attempts were made to compute transit times, since there was no way of knowing how long the cards had lain upon the beaches from which they were recovered. This was particularly true in our study region, where the beaches are relatively uninhabited.

Three sets of cards were released: 1400 cards in early March 1978, 1000 cards in late May 1978 and 2000 cards in early October 1978. The release locations were situated to sample flow in three localities: (1) along the Kenai Peninsula; (2) through the entrances to lower Cook Inlet; and (3) along the Kodiak Island shelf. By the end of 1978 the number of responses to the request for recovery information had reached 137 or 3% of the total number of cards released. This was a surprisingly high recovery rate in view of the remote nature of the sampled area. Overall drift-card returns as of the end of 1978 are listed in Appendix B.

In an attempt to define near-bottom water motion on the bank and trough region south of Kodiak Island, sea-bed drifters were deployed by NMFS/NOAA during winter 1977-78 (Dr. Gene Dunn, NMFS/NOAA, personal communication).* These drifters follow water motions within about 1 m of the seabed. Release and recovery data are tabulated in Appendix C.

2.2.3 Satellite-Tracked Drift Buoys

Surface buoys having subsurface window-shade drogues were deployed at various locations in the eastern (i.e. upstream) part of the study region. The buoys, designed and constructed at Nova University on contract to the NOAA Data Buoy Office, were fiberglass spars about 5 m long attached to a 2-m x 10-m window-shade drogue by a 30-m long nylon tether. The designed center of drogue resistance was therefore near a depth of 35 m. Location of the buoys was determined by means of the Random Access Measurements System (RAMS) of the NIMBUS-6 satellite (Levanon, 1975). At the latitude of the northern Gulf of Alaska, the system provided up to five locations per day for each buoy, but at irregular times.

The rms location error was about 4 km. Each satellite overpass provided data for an ambiguous pair of locations. Between sequential orbits it was usually, but not always, possible to identify the proper location. Hence in addition to the location error arising from uncertainties in the satellite orbit, Doppler measurement, etc., individual errors of tens or even hundreds of kilometers were present in the data. These erroneous locations were removed by an objective routine that checked each location for displacement from preceding and succeeding locations, then rejected all locations that implied velocities in excess of an assignable criterion. For this Gulf of Alaska data set we used 150 cm sec^{-1} as the criterion, which retained 70 to 80% of the original data. To facilitate automated computation of

---

*NMFS/NOAA, Seattle, WA 98105.

velocity time series and plotting of results, the position component data were smoothed and interpolated to 6-hr intervals by piecewise least-square fit to a low-order (usually cubic) polynomial. Velocity series were additionally smoothed by a simple three-point triangular filter. The result of this procedure was a set of trajectories and associated velocity time series comparable to what would be done by a skilled subjective analyst, and in which features having a time scale of about 2 days were retained. Tidal flows and inertial currents, where important, were suppressed along with other rapid accelerations.

2.2.4 Wave Radar (CODAR) Observations

Investigations of surface currents were carried out in lower Cook Inlet using a Doppler-shift radar method which is fully described by Barrick *et al.* (1977). This method utilizes the Doppler shift of surface waves under the effect of a current to measure the current field, and has the advantage of providing an instantaneous picture of actual surface currents, an observation virtually impossible by other means. These observations covered the region just off Kachemak Bay and the area between Cape Douglas and Augustine Island (Fig. 11). The observation periods were short in duration compared to the moored current meter measurements, of order 1 week or less, and provided both instantaneous and daily mean values of surface currents in the indicated regions.

BEST DOCUMENT AVAILABLE

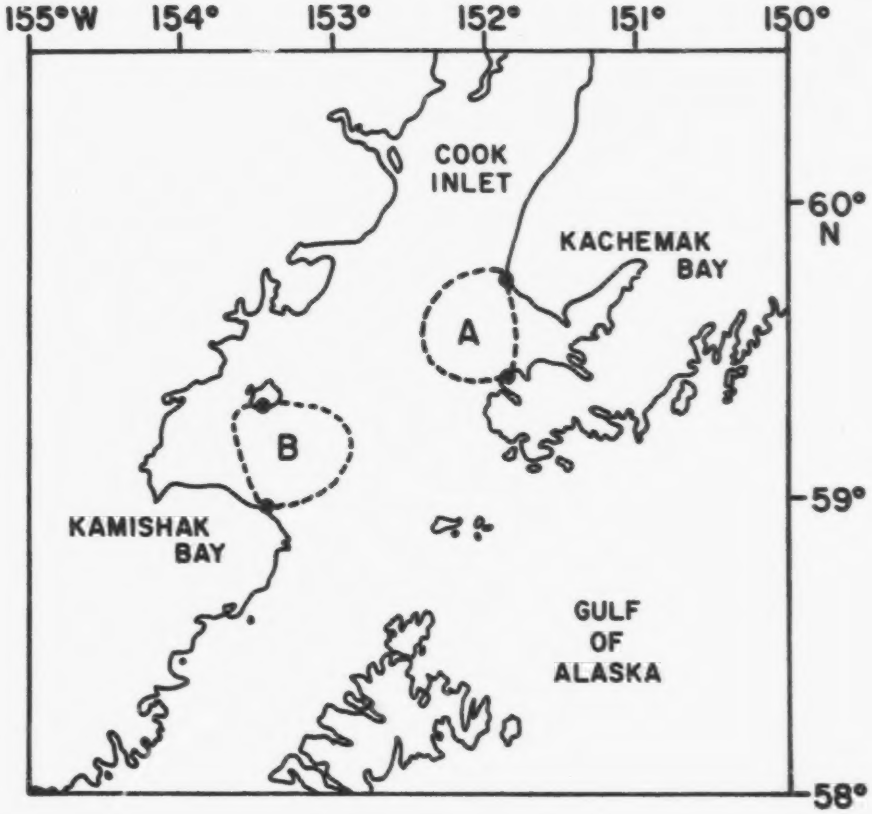
155°W
154°
153°
152°
151°
150°
60° N
59°
58°
COOK INLET
KACHEMAK BAY
A
B
KAMISHAK BAY
GULF OF ALASKA

Figure 11. Areas, designated A and B, where surface current observations were carried out using the Doppler-shift wave radar (CODAR) unit. Solid circles indicate locations at which radar units were deployed.

2.3 Temperature and Salinity Observations

Temperature and salinity data were obtained from shipboard using Plessey Model 9040 conductivity/temperature/depth (CTD) profiling systems. These data were recorded during the downcast, and descent rate was held to about 1 m sec^{-1} or less to minimize error in the recorded data due to thermal lag in the sensors in regions where large vertical temperature gradients were present. In some areas, the descent rate during the upper 200 m of the cast was limited to 0.5 m sec^{-1} due to extreme vertical gradients.

Since the Plessey systems are subject to drift and other possible problems, it was necessary to provide data calibration at frequent intervals. To this end, water samples were obtained and analyzed for conductivity and temperature at roughly half of the CTD stations. These samples were obtained using a rosette sampler equipped with calibrated reversing thermometers. Conductivity was measured aboard ship using a portable salinometer calibrated with standard seawater. These calibration data confirmed an overall accuracy for the CTD temperature and salinity values of ±0.02°C and ±0.02°/oo, respectively.

Temperature and salinity data were used for water mass analyses and for computing geostrophic current speeds and transports, therefore, it is of interest to consider the accuracy of the derived parameters used in these analyses. Given temperature and salinity accuracies of ±0.02°C and ±0.02°/oo, density may be computed to an accuracy of ±0.02 kg m^{-3}. Use of these density values in calculating dynamic heights led to an accuracy of within 1.0 dyn cm referred to the 1500 db level. Using these values to compute surface current speed between two stations spaced 40 km apart, the results were accurate to ±4 cm sec^{-1}.

Temperature and salinity data obtained during the OCSEAP program in the northwest Gulf of Alaska bracket all seasons for the 1976-78 period. Appendix D lists stations occupied according to cruise number and date. All data are archived at, and available on request from, the National Oceanographic Data Center.

2.4 Meteorological Observation Program

This program was designed to define the dominant meteorological features in three specific coastal subregions in the northwest Gulf of Alaska: lower Cook Inlet, Kiliuda Bay and Albatross Bank (Fig. 12). Data sources for this study include land based weather stations, moored data buoys, oil drilling platforms, NOAA research vessels, ships of opportunity, ferries, AMOS stations and remote weather recording installations which were deployed as part of this study (Table 1). The data base also includes information in the form of synoptic data from the U. S. Navy's Fleet Numerical Weather Central (FNWC) analyses. The data collection effort occurred primarily during early 1978 (Table 2), a period which coincided with intensive current observation programs in the lower Cook Inlet and Kodiak Island areas.

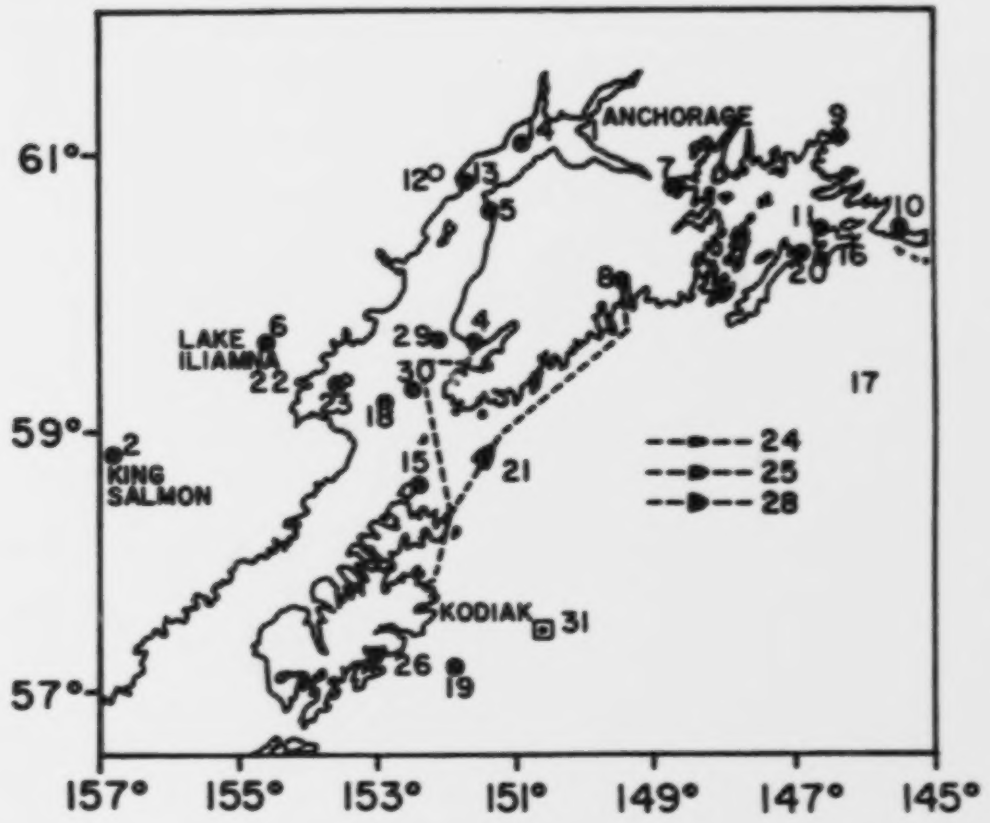
ANCHORAGE
9
14
12°
13
5
7
11
10
16
20
8
6
LAKE ILIAMNA
29
4
30
22
23
18
17
2
KING SALMON
15
21
24
25
28
KODIAK
31
26
19
61°
59°
57°
157°
155°
153°
151°
149°
147°
145°

Figure 12. Map of the study area showing sources of data which are included in this study. Names of numbered stations, sources of data and time periods of data collection are given in Tables 1 and 2.

TABLE 1

Listing of meteorological data collection stations shown on Figure 12.

1.	Anchorage	NWS[1]
2.	King Salmon	NWS
3.	Kodiak	NWS
4.	Homer	NWS
5.	Kenai	NWS
6.	Iliamna	NWS (part-time AMOS[2])
7.	Whittier	NWS
8.	Seward	NWS
9.	Valdez	NWS
10.	Cordova	NWS
11.	Johnston Point	NWS (Air Force)
12.	Big River Lake	NWS (contract)
13.	"Dolly Varden"	Oil Platform
14.	"Phillips"	Oil Platform
15.	Shuyak	NWS (remote wind)
16.	Cape Hinchinbrook	NWS (AMOS)
17.	Middleton Island	NWS (AMOS)
18.	EB-346007	NDBO[3]
19.	EB-46008	NDBO
20.	EB-46009	NDBO
21.	*TUSTUMENA*	Alaska State Ferry
22.	Contact Point	NOAA/PMEL remote[4]
23.	Augustine Island	NOAA/PMEL remote
24.	*SURVEYOR*	NOAA vessel
25.	*DISCOVERER*	NOAA vessel
26.	Kiliuda Bay	NOAA/PMEL remote
27.	Copper River	NOAA/PMEL remote
28.	Ships of opportunity	Miscellaneous
29.	"Diamond M. Dragon"	Oil Platform
30.	"Ocean Bounty"	Oil Platform
31.	FNWC[5]	Computer

[1] National Weather Service, NOAA.
[2] Automatic weather station.
[3] National Data Buoy Office, NOAA.
[4] Remote recording weather station.
[5] Fleet Numerical Weather Central.

BEST DOCUMENT AVAILABLE

TABLE 2

Summary of status of meteorological data base listed according to station location shown on Figure 12. Data indicated by heavy solid lines are available in the automated data base system, While dashes indicate data which are available at PMEL/NOAA.

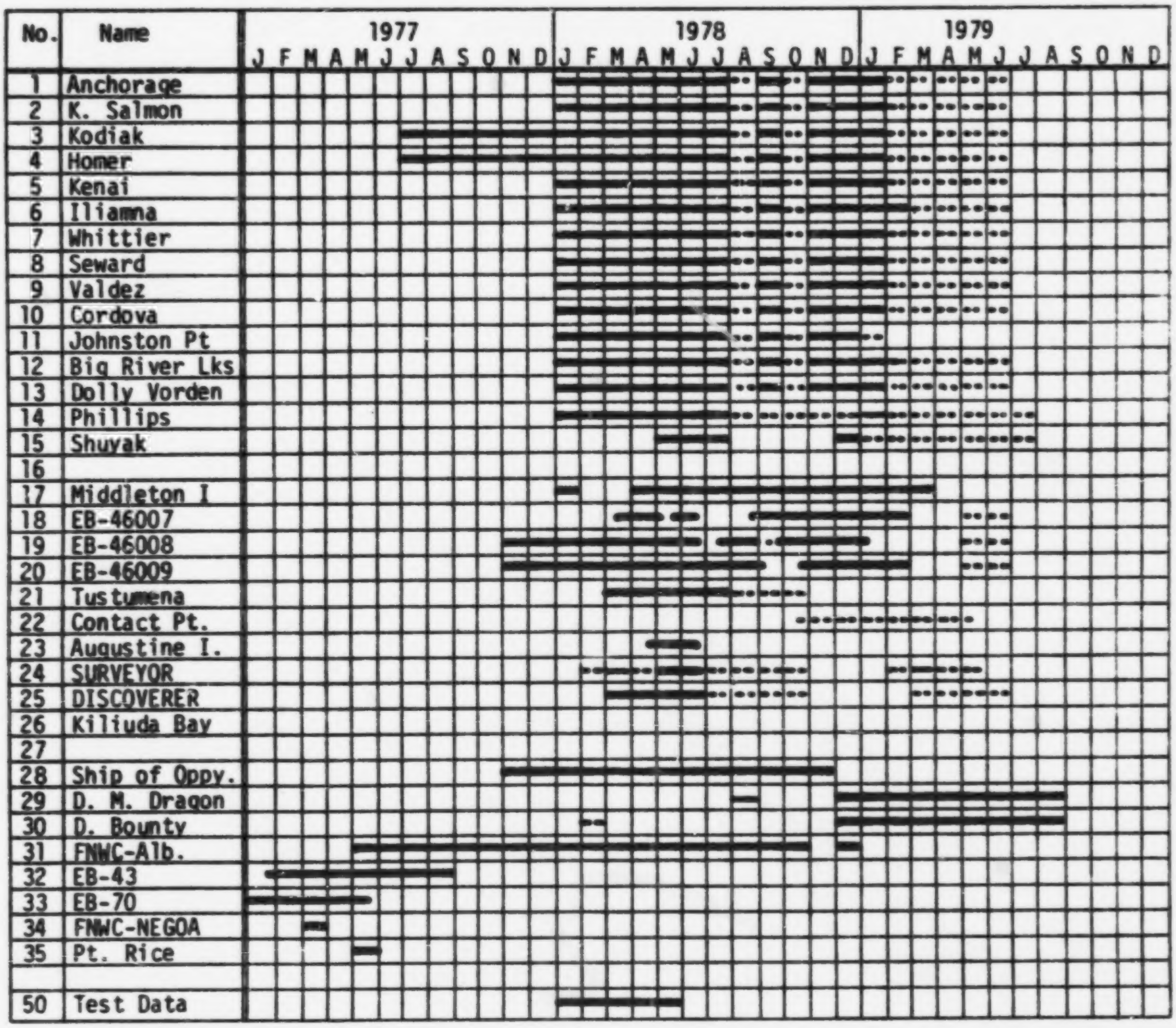

3. RESULTS AND DISCUSSION

3.1 Mean Currents, Seasonal Variations and the Temperature, Salinity and Density Fields

3.1.1 Introduction

The internal density structure of an oceanic system reflects the baroclinic portion of the total time-averaged mean flow. Because of the time interval required for readjustment of this density field following any change in current patterns, the density field reflects time-averaged circulation and can be used to detect seasonal variability. It does not generally reflect, however, the 2- to 10-day period events or tidal fluctuations which are prominent in the northwest Gulf (cf. Section 3.2).

Mean flow can be obtained only by computing a time average of measured current, where the observation and averaging time must extend over a long enough period to allow averaging out of prominent low-frequency fluctuations such as those to be discussed in Section 3.2. In the present study this generally required a record at least 1 mo in length. Since the time scale for seasonal events is of order 3 mo, records longer than 3 mo but shorter than several years record conditions spanning more than one season but still not representing a true annual mean. As our current moorings generally were deployed for periods of 4-5 mo, this limitation must be borne in mind. Lengths of the individual current records are listed in Appendix A.

3.1.2 The General Northwestern Gulf Region

Winter net flow is well represented by the observed mean current vectors depicted on Figure 13. The southwesterly flow at the shelf break at 20 m was about 35 cm sec^{-1} (Station WGC2A). This agreed with a later drogue trajectory (cf. drogue 1220, Fig. 14), which indicated net summer speeds

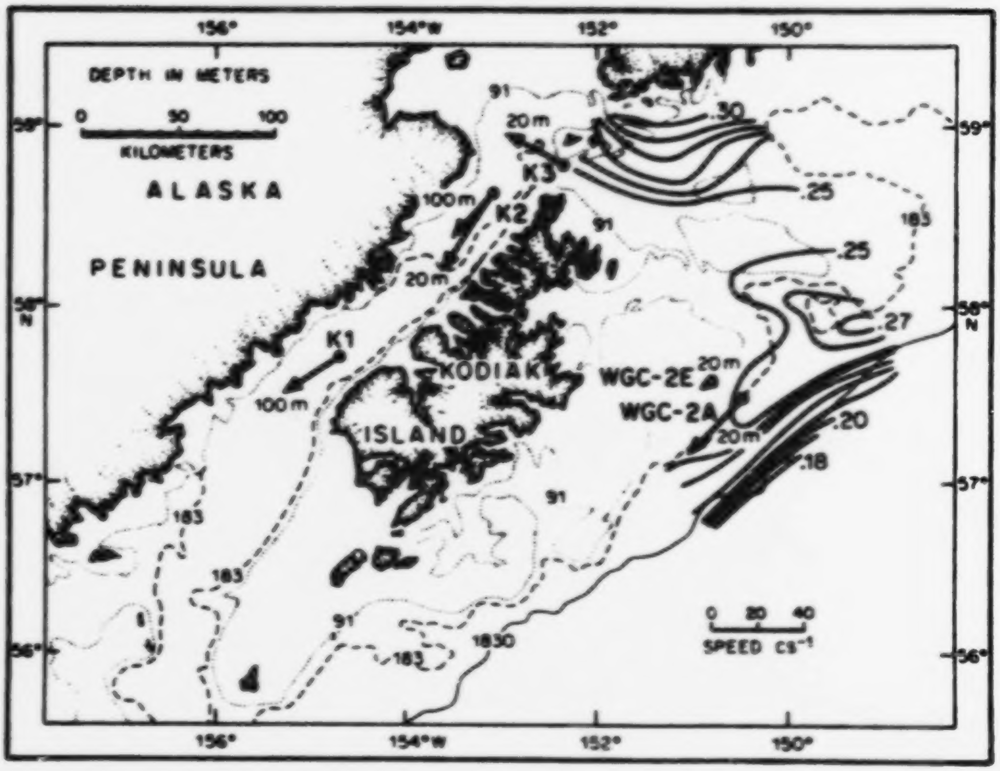
156°
154°W
152°
150°
DEPTH IN METERS
0
50
100
KILOMETERS
ALASKA
PENINSULA
KODIAK
ISLAND
K1
K2
K3
WGC-2E
WGC-2A
20m
100m
91
183
1830
.30
.25
.25
.27
.20
.18
59°
58° N
57°
56°
0
20
40
SPEED cs⁻¹

Figure 13. Mean winter 1976-77 current speed vectors at five locations on the northwest Gulf of Alaska shelf. Actual mooring periods are given in Appendix A. The dynamic topography has a contour interval of 0.01 dyn m and was constructed using March 1977 data.

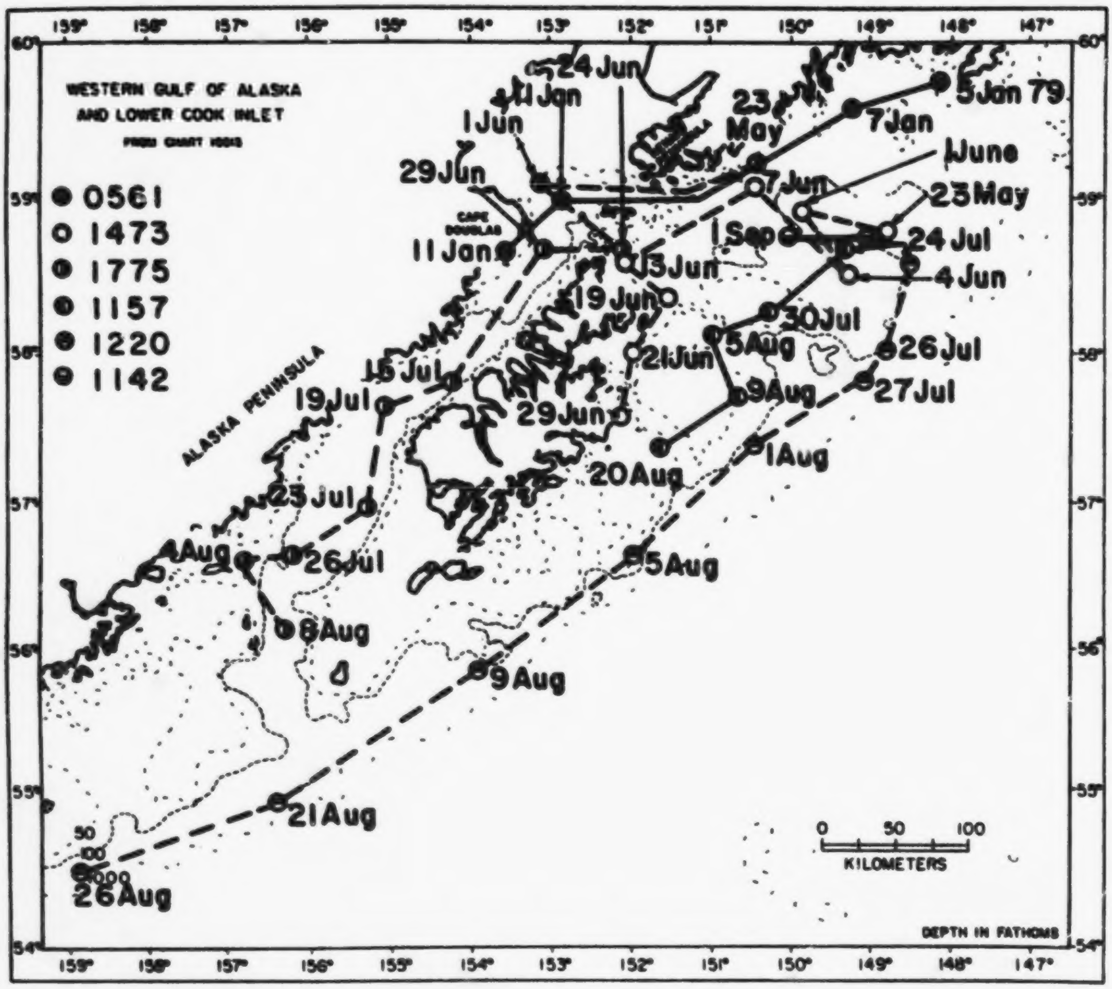
WESTERN GULF OF ALASKA
AND LOWER COOK INLET
● 0561
○ 1473
● 1775
● 1157
● 1220
● 1142
159°
158°
157°
156°
155°
154°
153°
152°
151°
150°
149°
148°
147°
60°
59°
58°
57°
56°
55°
54°
ALASKA PENINSULA
CAPE DOUGLAS
24 Jun
11 Jan
1 Jun
29 Jun
11 Jan
23 May
5 Jan 79
7 Jan
1 June
7 Jun
23 May
1 Sep
24 Jul
13 Jun
4 Jun
19 Jun
30 Jul
5 Aug
26 Jul
21 Jun
9 Aug
27 Jul
15 Jul
19 Jul
29 Jun
20 Aug
1 Aug
23 Jul
4 Aug
26 Jul
5 Aug
8 Aug
9 Aug
21 Aug
50
100
1000
26 Aug
0
50
100
KILOMETERS
DEPTH IN FATHOMS

Figure 14. Satellite-tracked drogue trajectories in the northwest Gulf of Alaska. Drogued buoys were deployed in 1978, and were drogued to track at a water depth of about 25 m.

in the Alaskan Stream of about 40 cm sec^{-1} off Kodiak Island. At a later period the mooring had been moved about 20 km farther inshore (to WGC2E), due to repeated damage from fishing activity at the original location. At the new location, mean speed had dropped to about 5 cm sec^{-1}, still in a southwesterly direction. These two moorings bracketed the zone of large horizontal shear at the inshore edge of the Alaskan Stream.

Moorings K1-K3 were deployed in Shelikof Strait as shown (Fig. 7) during the same period as WGC2E. These indicated a mean 100-m deep flow through Shelikof Strait of about 25 cm sec^{-1} to the southwest. At 20-m depth mean flow was somewhat higher, about 35 cm sec^{-1}, and also southwesterly. These observations were the first current measurements obtained in the region and indicated a general southwesterly flow with its most intense region manifested as the Alaskan Stream along the shelf break. This southwesterly flow, both through Shelikof Strait and south of Kodiak Island, was qualitatively demonstrated by the results of the satellite-tracked buoy and drift card programs (Figs. 14-18).

3.1.3 The Kenai Current

During March, September and October-November 1977 (Fig. 19, 20 and 21), two baroclinic flow regimes were evident on these dynamic topographies: (1) the southwestward-flowing Alaskan Stream over the continental slope south and east of Kodiak Island, accompanied by apparent inshore counterflows east of Portlock Bank; and (2) a well-defined westerly coastal flow along the Kenai Peninsula, designated by Schumacher and Reed (1980) as the Kenai Current. Generally weak and variable circulation occurred between these two relatively well-organized flows. This was supported by summer drogue data, which

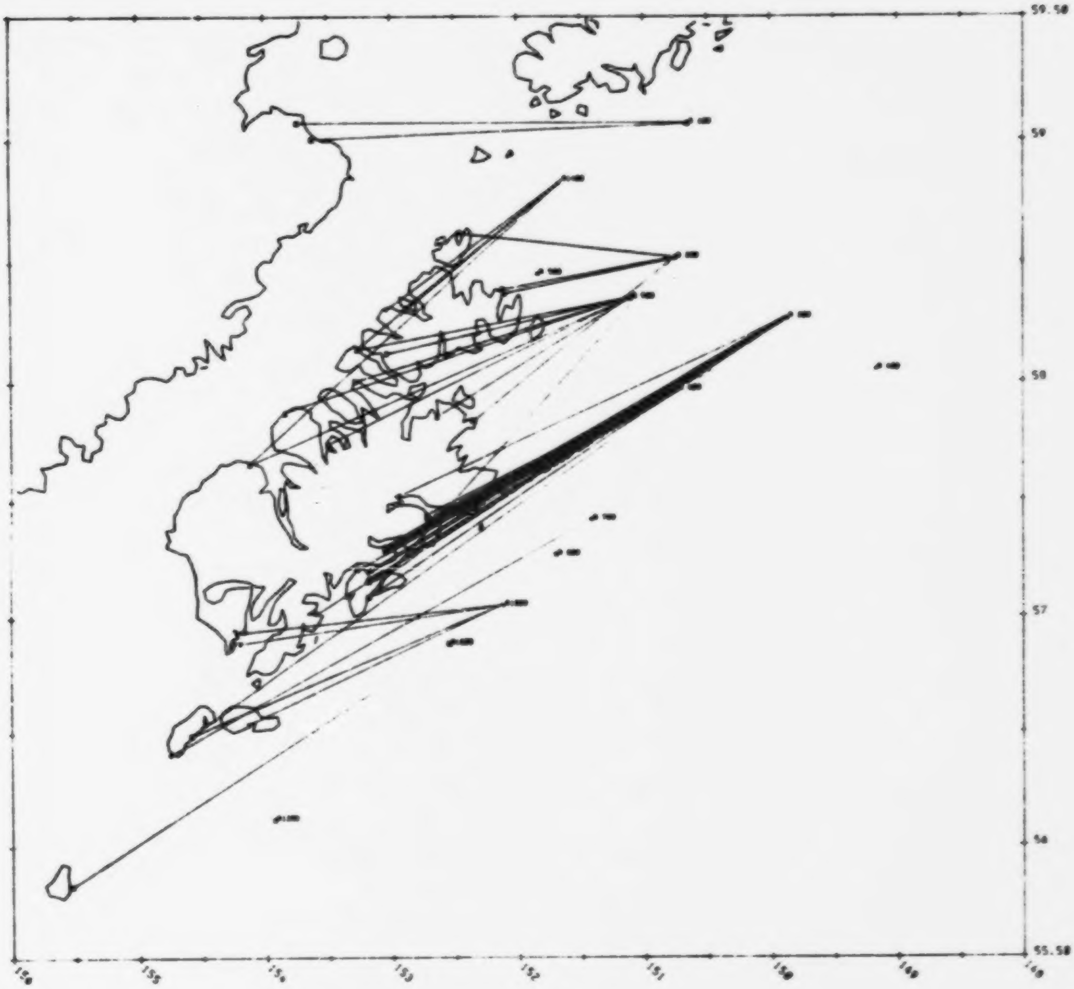
59.50
59
58
57
56
55.50
156
155
154
153
152
151
150
149
148

Figure 15. Summary of recovery and release points for drift cards released in March 1978.

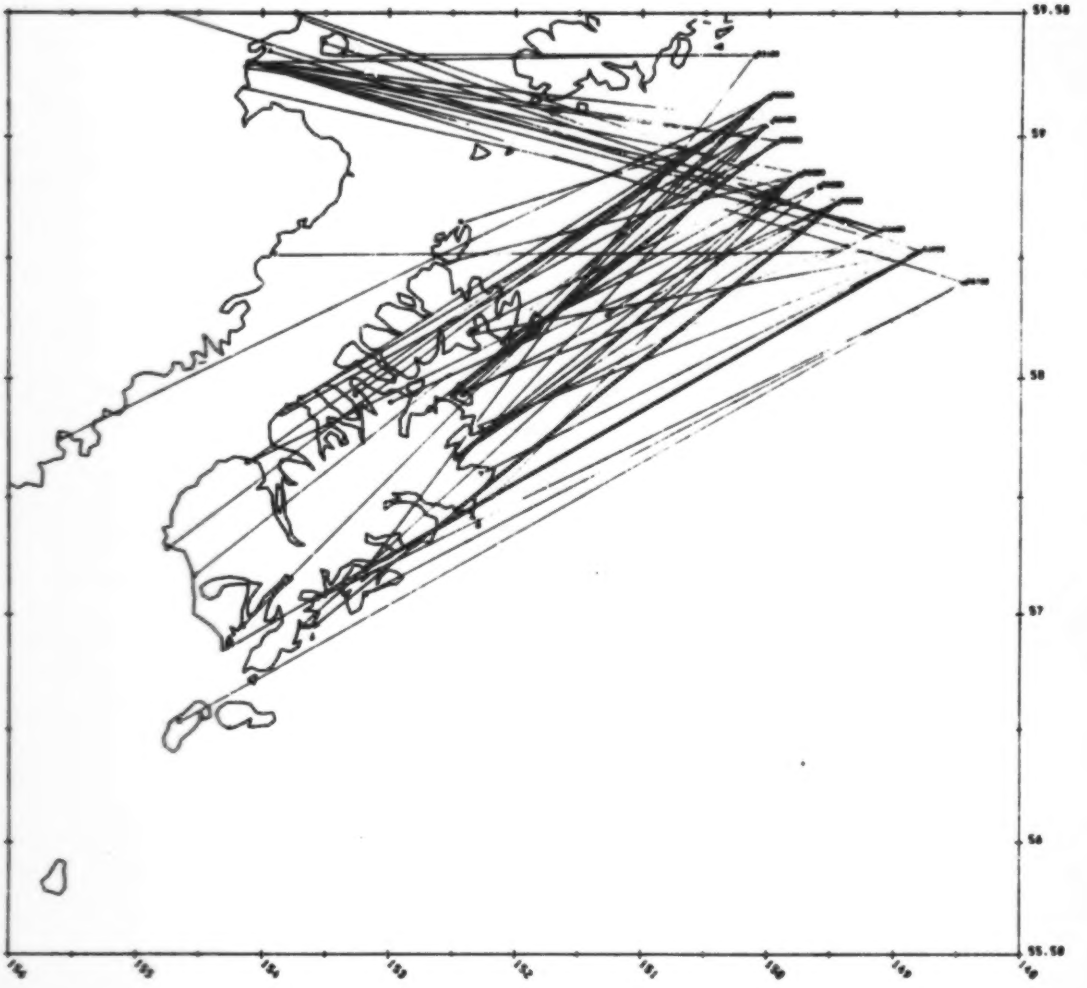
59.50
59
58
57
56
55.50
156
155
154
153
152
151
150
149
148

Figure 16. Summary of recovery and release points for drift cards released in May 1978.

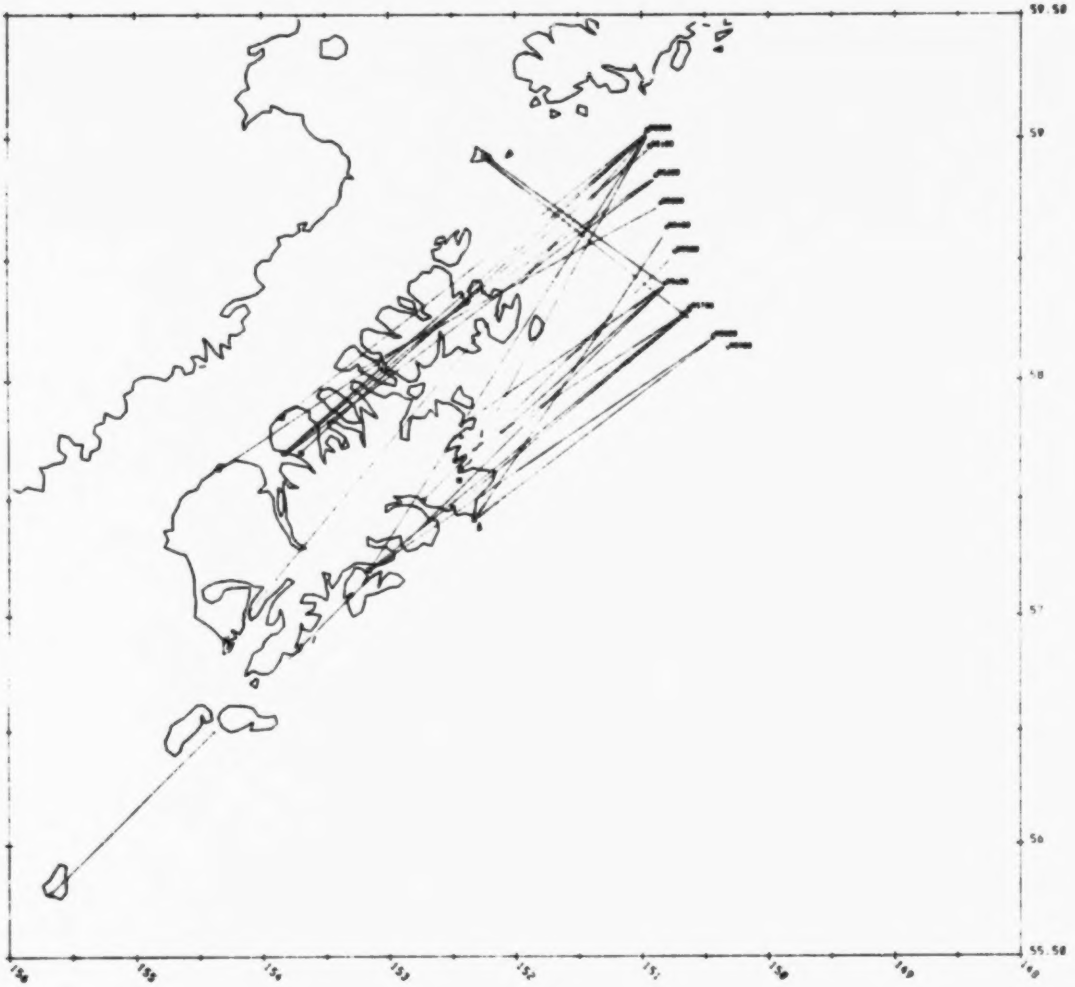
59.50
59
58
57
56
55.50
156
155
154
153
152
151
150
149
148

Figure 17. Summary of recovery and release points for drift cards released in October 1978.

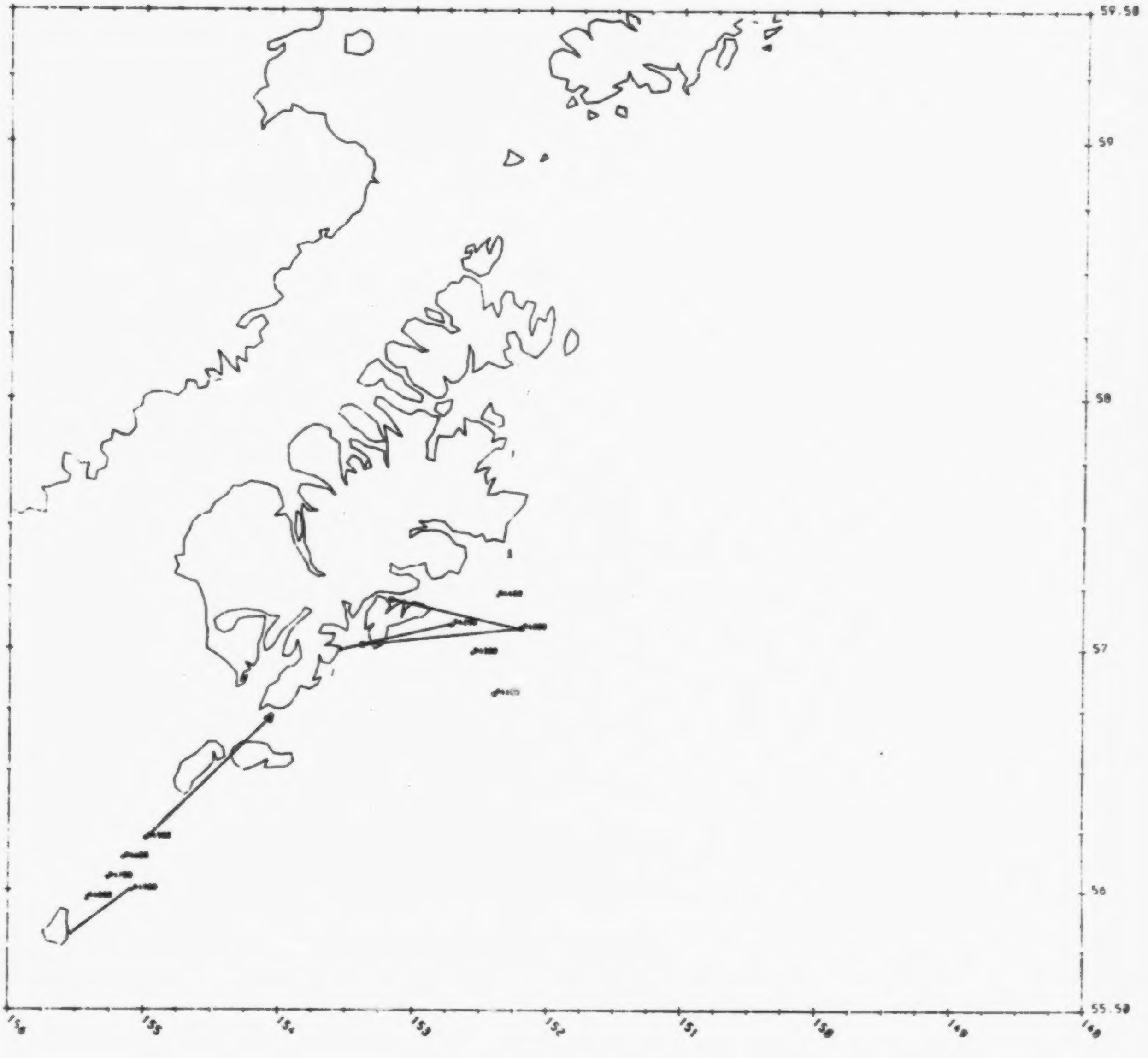
59.50
59
58
57
56
55.50
156
155
154
153
152
151
150
149
148

Figure 18. Summary of recovery and release points for drift cards released in October 1978.

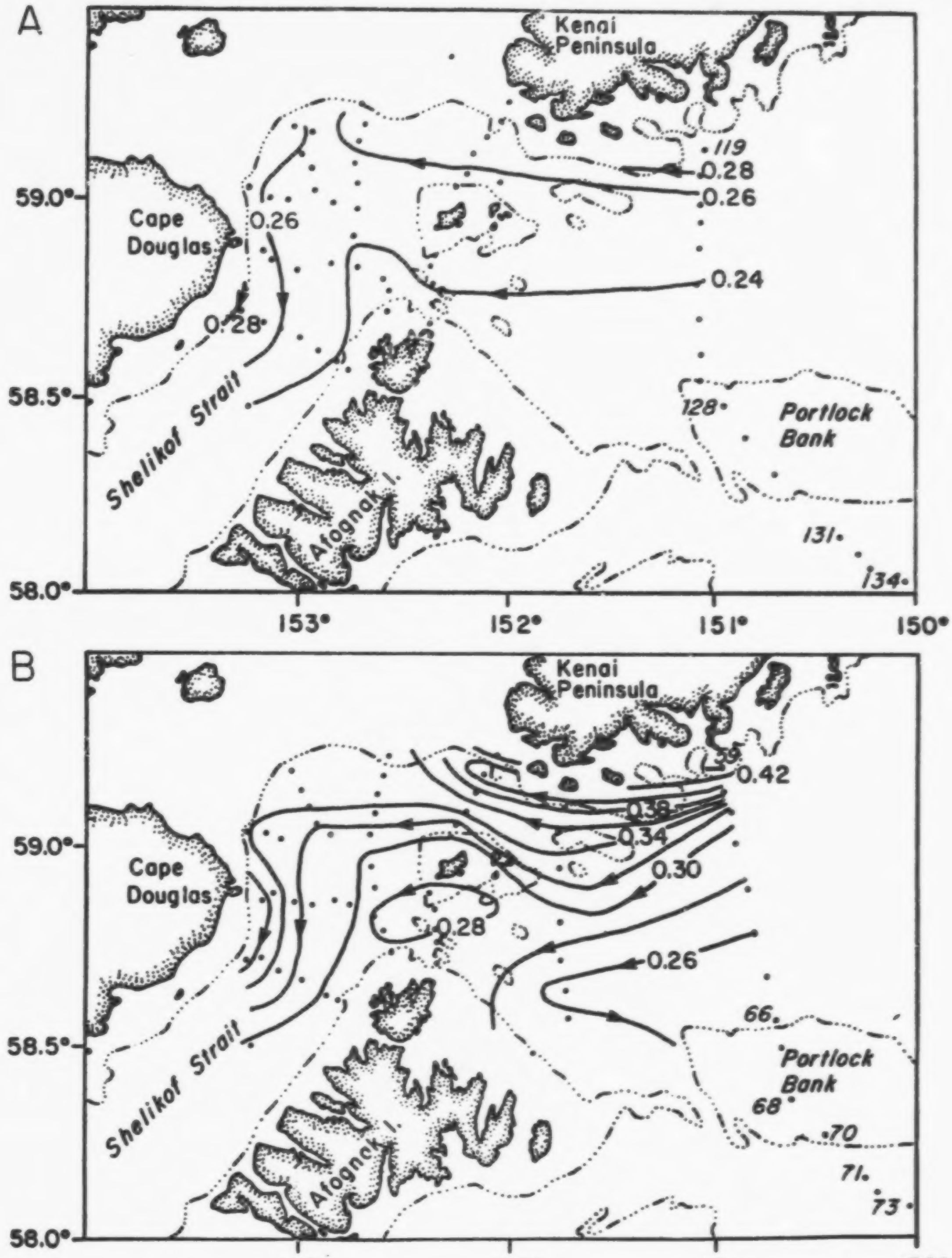
A
Kenai Peninsula
119
0.28
0.26
Cape Douglas
0.26
0.28
0.24
59.0°
58.5°
58.0°
Shelikof Strait
Afognak
128
Portlock Bank
131
134
153°
152°
151°
150°
B
Kenai Peninsula
59
0.42
0.38
0.34
0.30
Cape Douglas
0.28
0.26
66
Portlock Bank
68
70
71
73
59.0°
58.5°
58.0°
Shelikof Strait
Afognak
153°
152°
151°
150°

Figure 19. Dynamic topographies depicting flow in the Kenai Current and into lower Cook Inlet during March (upper) and October (lower) 1978.

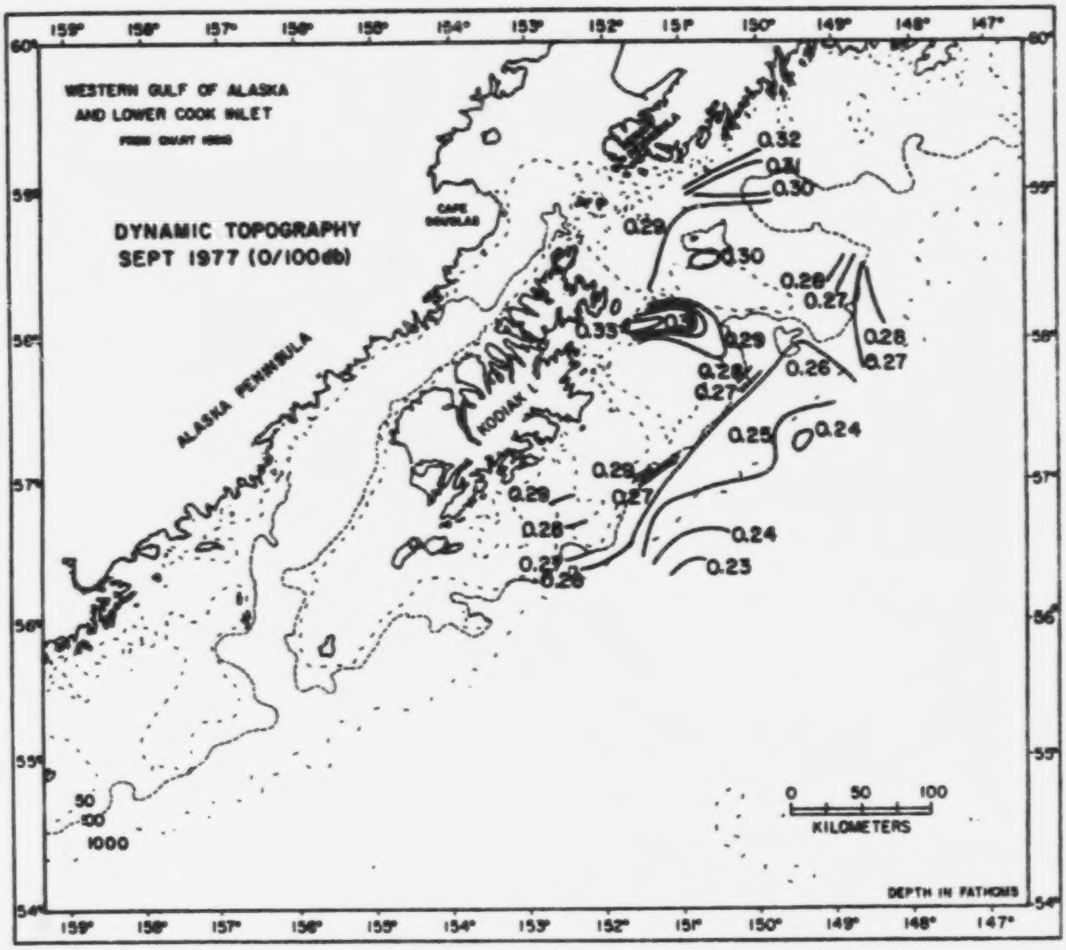
159°
158°
157°
156°
155°
154°
153°
152°
151°
150°
149°
148°
147°
60°
59°
58°
57°
56°
55°
54°
WESTERN GULF OF ALASKA
AND LOWER COOK INLET
DYNAMIC TOPOGRAPHY
SEPT 1977 (0/100db)
CAPE DOUGLAS
ALASKA PENINSULA
KODIAK I.
0.32
0.31
0.30
0.29
0.30
0.28
0.27
0.33
0.29
0.28
0.27
0.28
0.27
0.26
0.25
0.24
0.29
0.27
0.29
0.28
0.27
0.26
0.24
0.23
50
100
1000
0 50 100
KILOMETERS
DEPTH IN FATHOMS

Figure 20. Dynamic topography of the 0/100-db surface in the northwest Gulf of Alaska in September 1977. Contour interval is 0.01 dyn m.

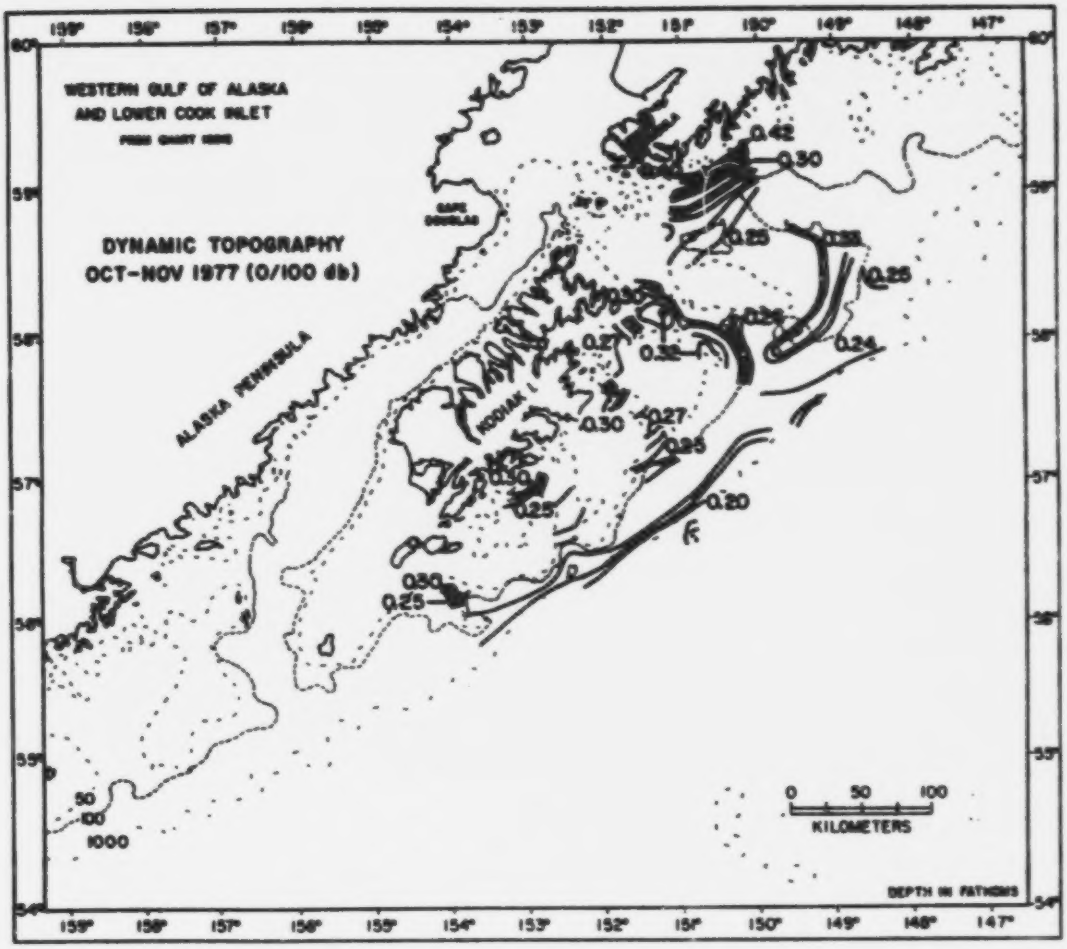
WESTERN GULF OF ALASKA
AND LOWER COOK INLET
DYNAMIC TOPOGRAPHY
OCT-NOV 1977 (0/100 db)
ALASKA PENINSULA
KODIAK I.
0.42
0.30
0.25
0.33
0.25
0.30
0.29
0.27
0.32
0.24
0.30
0.27
0.25
0.30
0.25
0.20
0.30
0.25
50
100
1000
0
50
100
KILOMETERS
DEPTH IN FATHOMS
159°
158°
157°
156°
155°
154°
153°
152°
151°
150°
149°
148°
147°
60°
59°
58°
57°
56°
55°
54°

Figure 21. Dynamic topography of the 0/100-db surface in the northwest Gulf of Alaska in October-November 1977. Contour interval is 0.01 dyn m.

revealed erratic flow directions and weak net speeds (~5 cm sec^{-1}) (cf. drogues 1473 and 1157, Fig. 14). During September and October a southward extension of this coastal flow appeared east of Kodiak and Afognak Islands and may have contributed to formation of a well-developed (relief of about 0.04 dyn m) gyre-like feature between Portlock and North Albatross Banks. Relief across the coastal flow itself was about 0.05 dyn m in March and September, but had increased threefold by October. The salinity distribution (not shown) suggested that this increase in dynamic relief was due to coastal freshwater addition which resulted in depressed salinities along the coast. This was in agreement with Favorite and Ingraham (1977), who suggested westward baroclinic flow near the entrances to lower Cook Inlet and Shelikof Strait during April-May 1972.

Vertical sections of temperature, salinity, and sigma-t along the CTD sections off the Kenai Peninsula (stations 59-68, 70-73 in October 1978; stations 119-134 in March 1978) are presented in Figures 22 and 23. The October sections display a narrow band (~20 km) of warm, dilute, low-density water adjacent to the Kenai Peninsula; this strong baroclinicity coincided with the westward coastal flow entering Shelikof Strait. Indications of relatively weak westward flow extend, however, south of this band to about the northern flank of Portlock Bank. The three stations (67, 68, and 70) over Portlock Bank show weak vertical stratification, and the water at station 68 (63-m depth) was completely mixed. South of Portlock Bank, varying isopycnal slopes suggest that peak speeds in the Alaskan Stream occurred seaward of station 73. In March (Fig. 23), gradients across the coastal flow were much weaker than in fall. There were no indications of significant baroclinicity elsewhere. Minimum temperatures were near the surface, rather than near-bottom as in October, and there was significantly

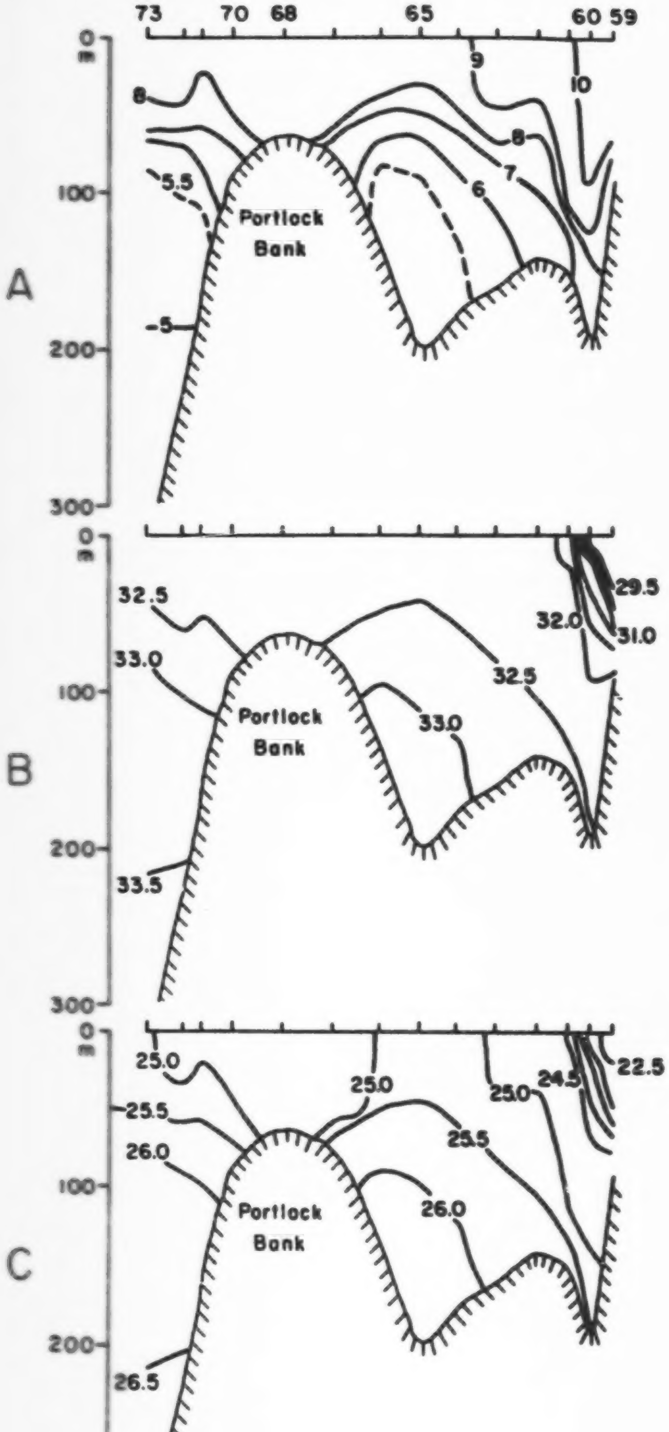

Figure 22. Cross sections of temperature (A), salinity (B) and density as sigma-t (C) across the Kenai Current and Portlock Bank in October 1978. Right-hand side of the section is north.

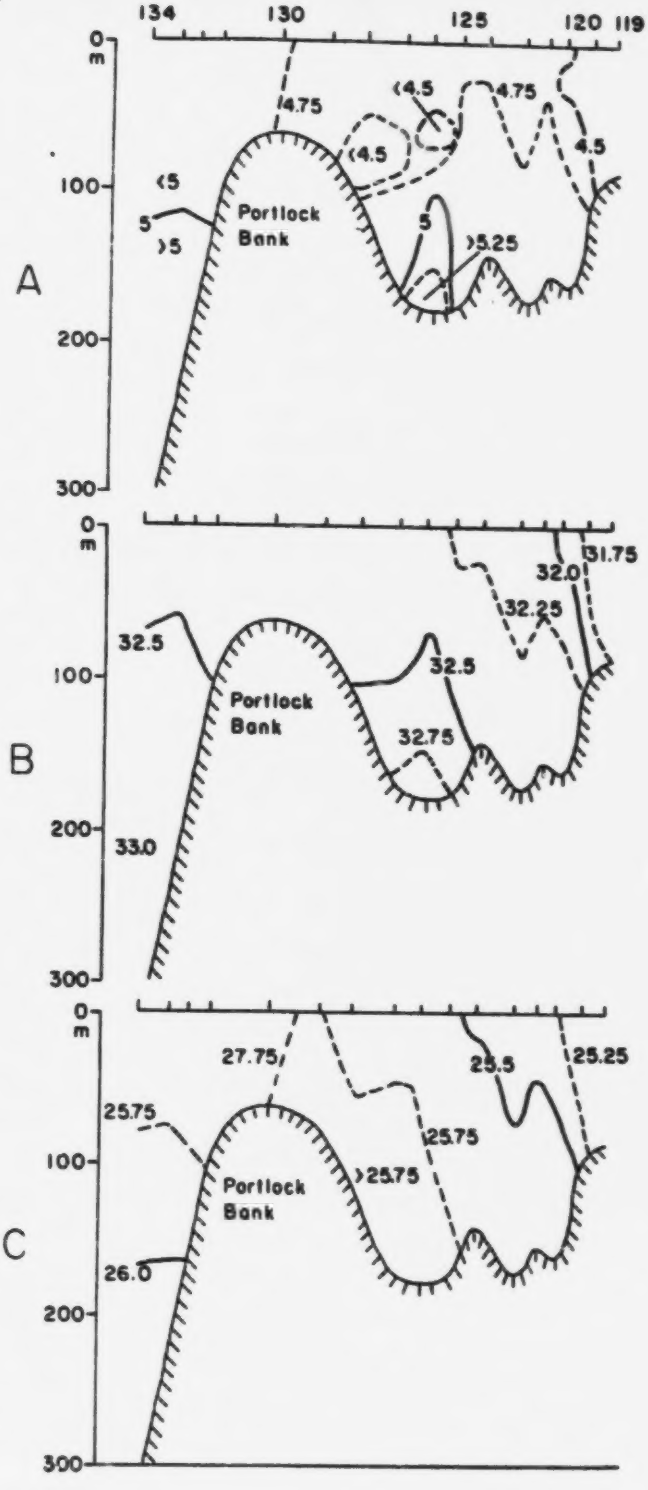

Figure 23. Cross sections of temperature (A), salinity (B) and density as sigma-t (C) across the Kenai Current and Portlock Bank in March 1978. Right-hand side of the section is north.

lower stratification than that observed in fall. The homogeneous water atop Portlock Bank extended about 15 m deeper than in October, which suggests that total mixing (presumably a combination of wind mixing near the surface and tidal mixing near the bottom) was more pronounced in winter than in summer-fall, a result consistent with physical reasoning. The intermediate and deep parts of the water column were more saline in October than in March, while coastal flow near the Kenai Peninsula was more dilute during October. This pattern of decreased surface salinity and increased intermediate and deep salinity during fall is consistent in our data and suggests that the saline water is "drawn up" during periods of peak transport in the Kenai Current, perhaps as an interior upwelling in conjunction with buoyancy flux (Pietrafesa and Janowitz, 1979) similar to estuarine circulation.

3.1.4 Shelikof Strait and Lower Cook Inlet

The flow through Shelikof Strait was measured for 5-mo periods during winter 1977-78 and summer 1978. These observations reaffirmed the southwesterly flow and revealed that mean speeds during summer were about half those during winter; winter 1977-78 speeds were in agreement with those measured in 1976-77. We therefore conclude that mean winter currents in Shelikof Strait flow southwest at about 20-30 cm sec^{-1} with slightly higher speeds at the surface than at depth. Limited evidence has also been presented by Schumacher et al. (1978; 1979) that these observed mean flows agreed with baroclinic flow inferred from the 0/100-db dynamic topography (Figs. 19-21).

Baroclinic coastal flow in the Kenai Current has a significant effect on flow through lower Cook Inlet and Shelikof Strait. This is illustrated by 0/100-db geopotential topographies which encompassed both regions during March and October 1978 (Fig. 21). In March, the baroclinic coastal flow had a dynamic relief of about 0.06 dyn m. It entered Shelikof Strait through passages north and south of the Barren Islands and veered south off Cape Douglas. In October the flow was considerably stronger, with a dynamic relief of about 0.20 dyn m, and a portion of the flow appeared to turn south near Afognak Island without entering Shelikof Strait.

Inflow into northern Shelikof Strait due to the influence of the Kenai Current was supported by the moored current meter observations. Additional evidence was available in the form of satellite-tracked, drogued drift buoy results (Fig. 14), which showed direct evidence of the westward flow through the year. Buoy 0561 indicated a mean speed of about 55 cm sec^{-1} in January. Buoys 1775 and 1473 indicated much lower mean speeds, about 20 cm sec^{-1}, in May-June. The early spring lowering in speed is in agreement with our hypothesis that this flow is largely baroclinic and driven by coastal freshwater input; in early spring, freshwater content in the coastal waters is near its annual minimum.

The persistent westward flow of the Kenai Current into Shelikof Strait exerts a primary control on circulation in lower Cook Inlet. This was first recognized by Muench et al. (1978), who derived a qualitative circulation scheme for lower Cook Inlet using summer 1973 current and temperature-salinity observations (Fig. 24). The prominent westward flow in the southern Inlet is topographically controlled; it follows the path depicted and turns to the south off Cape Douglas. The southward flow from the upper Inlet is due to freshwater input; this flow merges with the westerly flow off Cape Douglas to produce a strong southerly current there. Flow elsewhere throughout the inlet is weak and variable. More recent current data have corroborated this circulation pattern and quantified the mean winter current speeds. Vectors showing the observed mean winter 1977-78 currents in lower Cook Inlet are

BEST DOCUMENT AVAILABLE

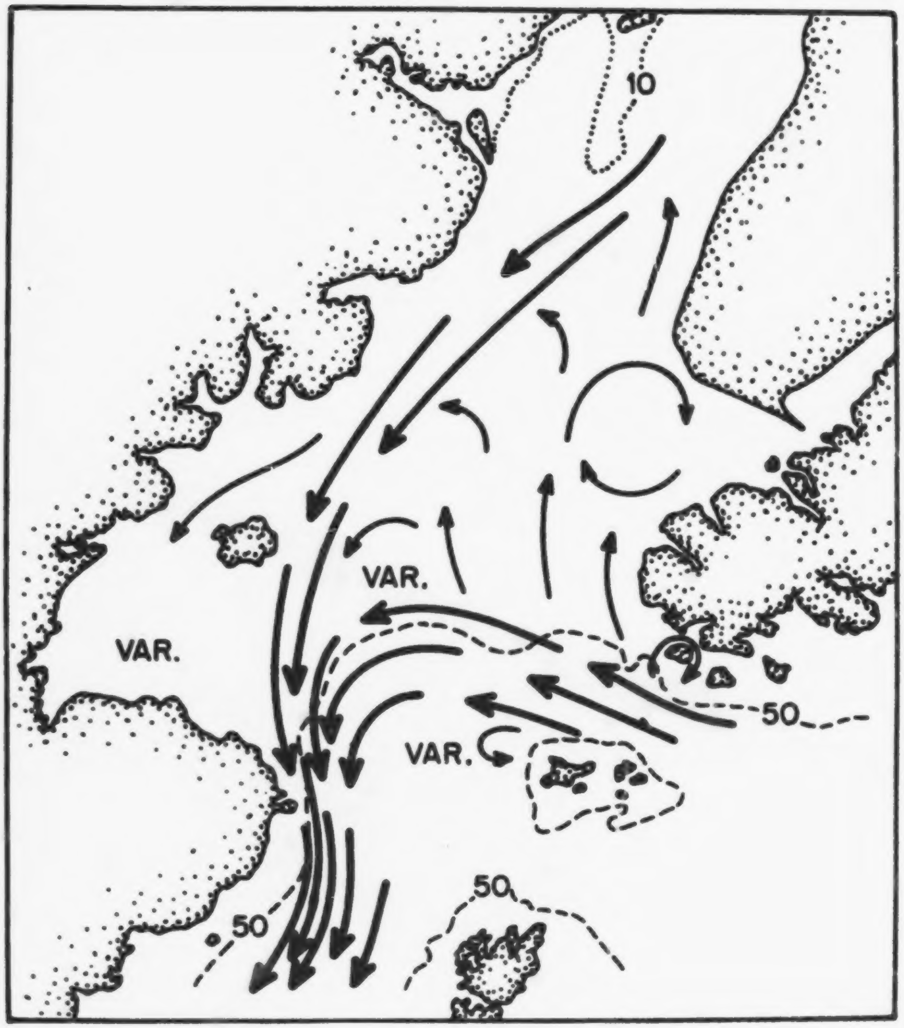

Figure 24. Depiction of qualitative mean flow pattern in lower Cook Inlet derived by Muench et al. (1977) from summer 1973 temperature, salinity and current data. Depths are in fathoms.

depicted on Figure 25. Westerly mean flow across the lower Inlet was about 20 cm sec^{-1}, while southward flow in the western Inlet was 5-10 cm sec^{-1}. Away from these two major flows, mean speeds were only 1-2 cm sec^{-1}.

A similar current observation program was carried out during summer 1978. Preliminary examination of these data has indicated that the flow pattern is the same as during winter. The westerly flow was smaller during summer, and the southerly flow in the western Inlet somewhat larger. Surface current observation carried out in summer 1978 using the CODAR (cf. Section 2.2.4) further substantiated this current pattern; an example of their results is shown in Figure 26.

The circulation depicted on Figure 24 for lower Cook Inlet was also corroborated by drogue results. Westerly drift across the lower Inlet was shown in January, with a mean speed of about 65 cm sec^{-1} (Fig. 14). This relatively high speed, compared with computed mean speeds obtained from moored current meters (Fig. 25), may indicate a current pulse during the observation period. A June drogue track plotted on the same scale did not show sufficient detail for speed computation. The same drogue track was plotted on an expanded scale, however, and compared to a second track on Figure 27. Drogue 1775 followed the bathymetry until 1 June, at which time the data became incomplete. Failure of drogue 1473 to enter Stevenson Entrance from the east suggests that a counterflow may have occurred during June. Drogue 1421 also indicated a westerly flow, though somewhat north of the earlier track and with apparent cross-isobath flow from 1-9 June. We would expect to see this sort of departure of drogue tracks from our conceptual mean flow; the drogues follow instantaneous flow. Both drogues yielded mean westward speeds of order 15 cm sec^{-1}, in agreement with summer mean flows observed using moored current meters.

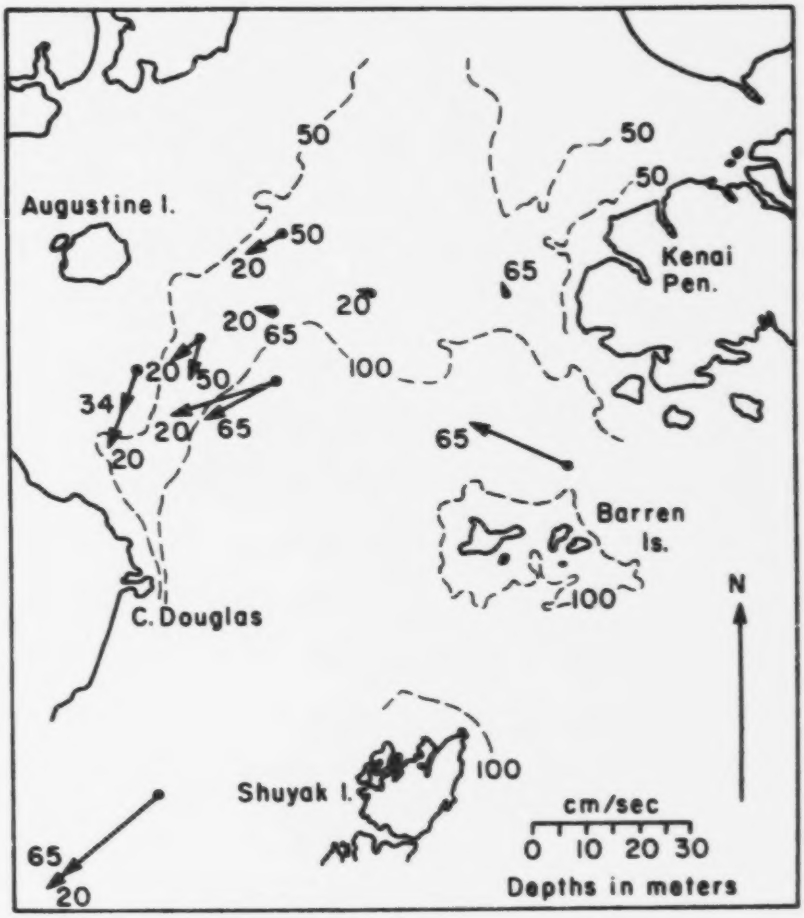
50
50
50
Augustine I.
50
20
65
20
Kenai
Pen.
20
65
100
20
50
34
20
65
20
65
Barren
Is.
100
C. Douglas
N
100
Shuyak I.
cm/sec
0 10 20 30
Depths in meters
65
20

Figure 25. Observed mean current vectors in the lower Cook Inlet region during winter 1977-78. Statistics for individual moorings are given in Appendix A. Numbers indicate current meter depths in meters.

BEST DOCUMENT AVAILABLE

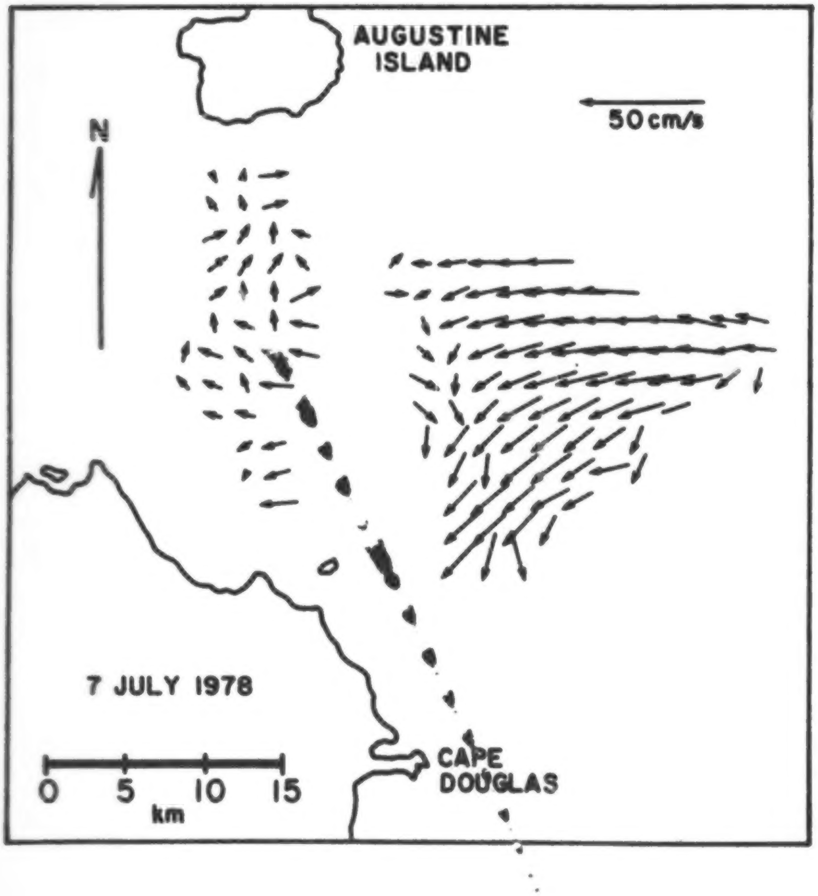
AUGUSTINE ISLAND
50 cm/s
N
7 JULY 1978
0
5
10
15
km
CAPE DOUGLAS

Figure 26. Twenty-four-hour mean surface currents observed on 7 July 1978 in lower Cook Inlet using the surface wave radar unit. Data are from Dr. A. S. Frisch, NOAA/WPL.

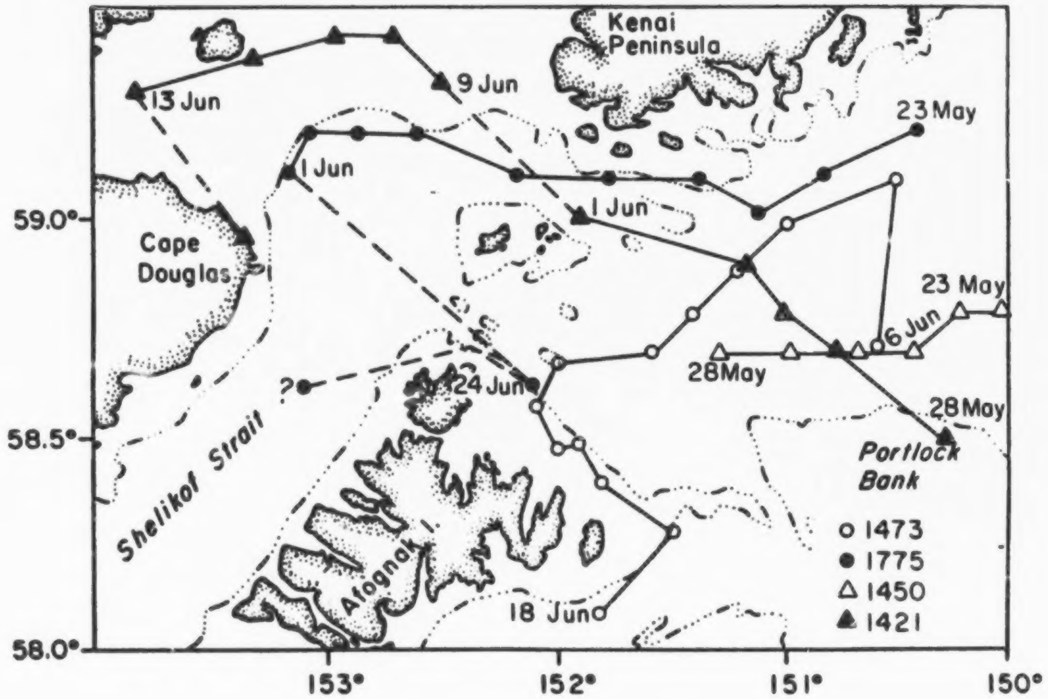
Kenai Peninsula
9 Jun
13 Jun
23 May
1 Jun
1 Jun
59.0°
Cape Douglas
23 May
6 Jun
28 May
?
24 Jun
28 May
58.5°
Shelikof Strait
Portlock Bank
○ 1473
● 1775
△ 1450
▲ 1421
Afognak
18 Jun
58.0°
153°
152°
151°
150°

Figure 27. Details of drogued buoy trajectories in the lower Cook Inlet region in 1978. Buoy locations are plotted at 1-day intervals.

3.1.5 The Bank and Trough Region

The area of complex bank and trough bathymetry south of Kodiak Island is of interest because we expect *a priori* that the topography exerts a control both on currents and on vertical mixing processes. To supplement the current data obtained from mooring WGC2 (cf. Fig. 13), moorings were deployed in the Kiliuda Trough region during winter 1977-78 and summer 1978 (cf. Section 2.2).

Whereas results from WGC2 located approximately the inshore edge of the Alaskan Stream, moorings in Kiliuda Trough defined the effect of the bank-trough-bank configuration on currents. Winter mean currents observed are shown on Figure 28. There was a clearly defined shoreward flow on the up-stream (northeastern) side of Kiliuda Trough, just inside the 91-m (50 fm) isobath. Current speeds here were of order 10 cm sec^{-1}. Along the axis of the trough, there was a weak (~5 cm sec^{-1}) shoreward mean flow which showed a tendency to curve left toward the head of the trough. Inward flow into the trough was supported qualitatively by release and recovery data from seabed drifters which indicated a shoreward flow of bottom water into the trough (Fig. 29). Flow at the head of the trough was dominated by a relatively strong (~20 cm sec^{-1}) southwesterly alongshore flow. The overall tendency was for a cyclonic circulation pattern over the trough. This is reasonable dynamically because of the high-latitude tendency for stream-lines to parallel isobaths and hence conserve potential vorticity. The inshore portion of the Alaskan Stream would, in tending to follow isobaths, flow shoreward along the northeastern side of the trough as observed. The southwesterly coastal flow near the head of the trough may be, in part, a baroclinic effect due to coastal freshwater addition, either locally or more likely as part of the Kenai Current. This tends to augment the topographically controlled flow.

BEST DOCUMENT AVAILABLE

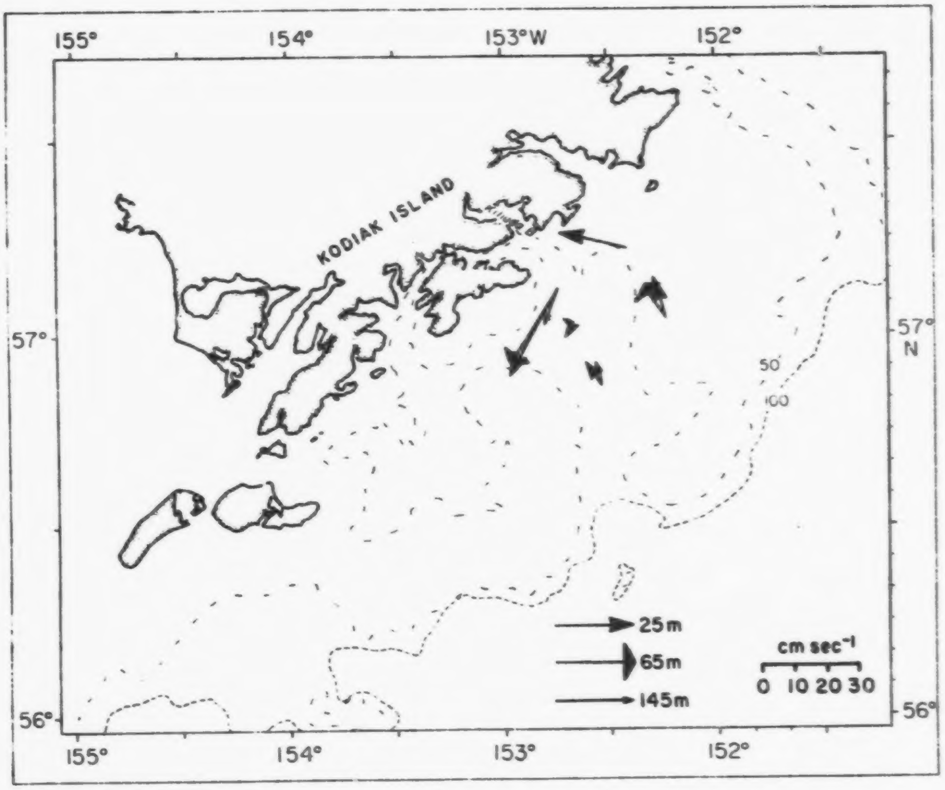
155°
154°
153°W
152°
KODIAK ISLAND
57°
57° N
50
100
25m
65m
145m
cm sec⁻¹
0 10 20 30
56°
155°
154°
153°
152°

Figure 28. Mean currents observed in the bank-trough region south of Kodiak Island during winter 1977-78. Mooring statistics (moorings K6-K10 A-series) are given in Appendix A.

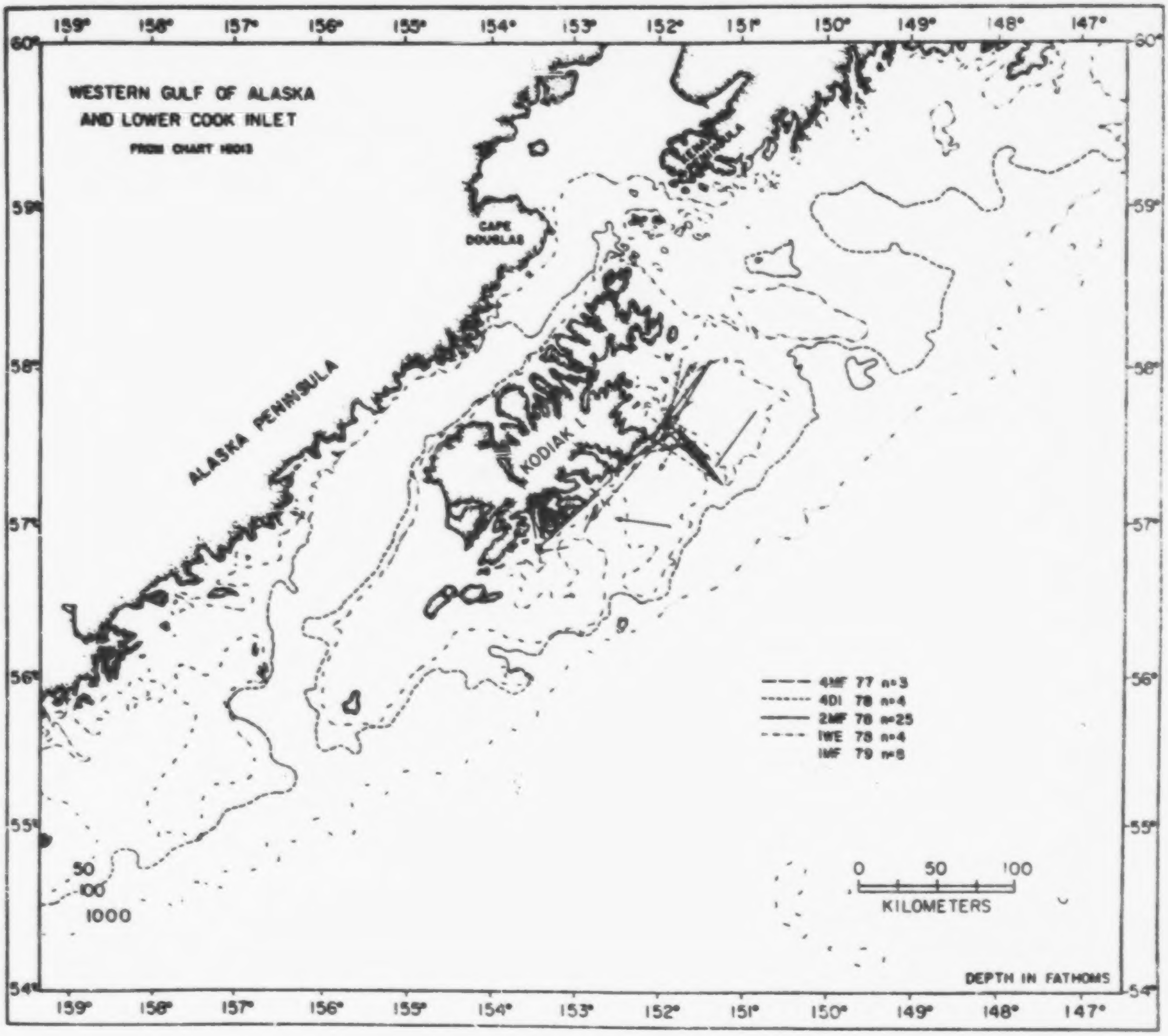
WESTERN GULF OF ALASKA
AND LOWER COOK INLET
FROM CHART 16013
CAPE DOUGLAS
ALASKA PENINSULA
KODIAK I.
4MF 77 n=3
4DI 78 n=4
2MF 78 n=25
1WE 78 n=4
1MF 79 n=8
0
50
100
KILOMETERS
50
100
1000
DEPTH IN FATHOMS
159°
158°
157°
156°
155°
154°
153°
152°
151°
150°
149°
148°
147°
60°
59°
58°
57°
56°
55°
54°

Figure 29. Deployment and recovery locations of seabed drifters, showing inferred directions of movement. Specific positions and dates of deployment and recovery are listed in Appendix C. The figure includes drifters recovered through September 1979, while Appendix C contains recoveries as recent as February 1980.

Sufficient temperature and salinity data were obtained on the banks east of Kodiak Island to allow speculation on processes which influence temperature and salinity distribution. As these banks are bounded on the north by the Kenai Current and on the south by the Alaskan Stream, we might expect considerable complexity there. Of major interest is the vertical density stratification, which reflects vertical mixing processes and mechanisms (such as freshwater input) that act to maintain stratification. With precipitation (>130 cm yr^{-1}) exceeding evaporation (<50 cm yr^{-1}), a net dilution of surface waters occurs (Jacobs, 1951), so that surface changes in salt content usually provide a positive buoyancy flux. During times of minimum precipitation, surface exchange of heat may result in a negative buoyancy flux. Under conditions of negative buoyancy flux, wind and wave mixing at the surface and tidal mixing from the bottom act to stir the entire water column; conversely, with a sufficient positive buoyancy flux, stratification occurs.

We present the distribution of the sigma-t difference between 50 m and the surface (Figs. 30 and 31) compiled from the two cruises having the most complete spatial coverage. The sigma-t differences for September 1977 are representative of summer conditions, whereas those for October-November 1977 represent fall.

The greatest stratification was associated with the Kenai Current. This was caused primarily by dilute (low density) near-surface water, and values were reduced somewhat by enhanced tidal mixing near the Kenai Peninsula and over the banks. During September 1977, the sigma-t distribution suggests that some portion of the Kenai Current did not enter Shelikof Strait but instead turned south near Afognak Island. The effect of more dilute Kenai Current water, in concert with locally added fresh water, was manifested by increased $\Delta\sigma_t$ along Kodiak Island and southwest extension over Middle

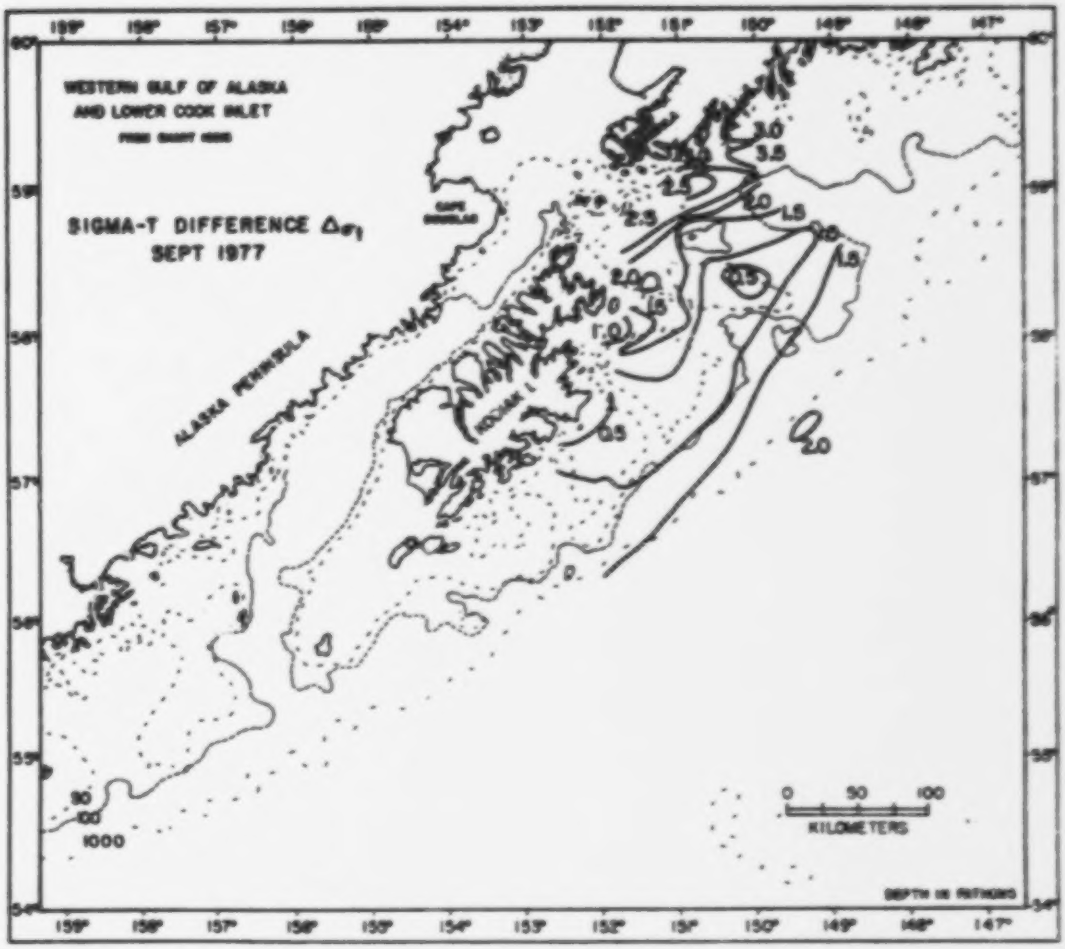
WESTERN GULF OF ALASKA
AND LOWER COOK INLET
SIGMA-T DIFFERENCE $\Delta\sigma_t$
SEPT 1977
ALASKA PENINSULA
KODIAK I.
159°
158°
157°
156°
155°
154°
153°
152°
151°
150°
149°
148°
147°
60°
59°
58°
57°
56°
55°
54°
3.0
3.5
2.5
2.5
2.0
1.5
2.0
1.5
2.0
1.5
1.0
0.5
2.0
0
0
50
100
1000
0 50 100
KILOMETERS
DEPTH IN FATHOMS

Figure 30. Difference in density (as sigma-t) between the surface and 50-m depths on the banks south and east of Kodiak Island in September 1977.

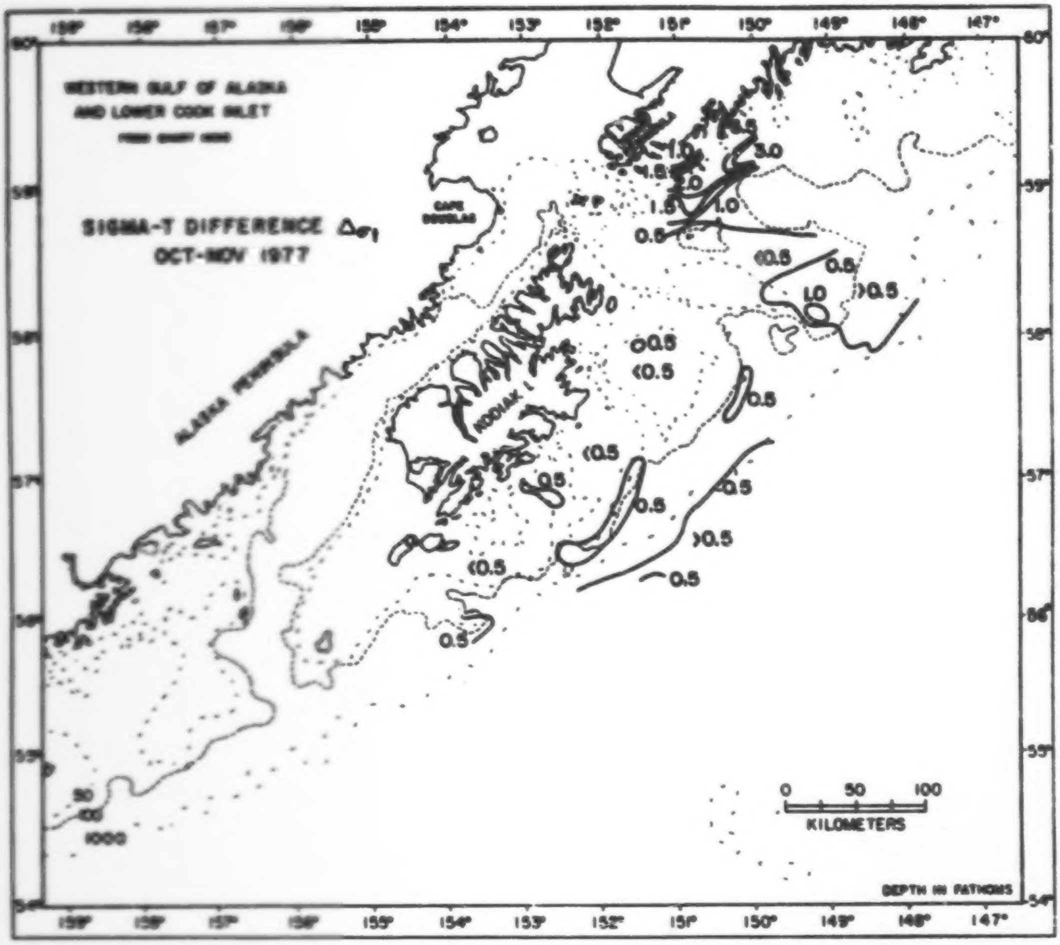
WESTERN GULF OF ALASKA
AND LOWER COOK INLET
SIGMA-T DIFFERENCE Δ_{σ_t}
OCT-NOV 1977
CAPE DOUGLAS
ALASKA PENINSULA
KODIAK I.
1.0
1.5
2.0
3.0
1.5
1.0
0.5
<0.5
0.5
1.0
>0.5
<0.5
<0.5
0.5
<0.5
0.5
0.5
0.5
>0.5
0.5
<0.5
0.5
50
100
1000
0
50
100
KILOMETERS
DEPTH IN FATHOMS
155°
154°
153°
152°
151°
150°
149°
148°
147°
60°
59°
58°
57°
56°
55°
54°

Figure 31. Difference in density (as sigma-t) between the surface and 50-m depths on the banks south and east of Kodiak Island in October-November 1977.

Albatross Bank. During October-November 1977 the wind stress changed from weak northeast to strong southwest, surface cooling became an important factor, and stratification was reduced.

Mechanisms other than thermohaline convection can influence stratification. For example, on 17 October, after occupation of stations 203 and 202.1 over Portlock Bank (Fig. 32), work was discontinued because of high winds from the north (wind speeds > 25 m sec^{-1}). These two stations were reoccupied 41-42 hours later. The storm had produced marked cooling and an increase in salinity of the upper ocean. Although the cooling rates are plausible as a result of surface heat exchange (about 0.6 cal cm^{-2} min^{-1} was estimated from bulk formulas), the large changes in salinity and almost complete homogeneity of the water suggest that a combination of processes including localized upwelling and vertical turbulent mixing occurred in response to the storm. These data point out that the upper ocean may vary widely over short time spans.

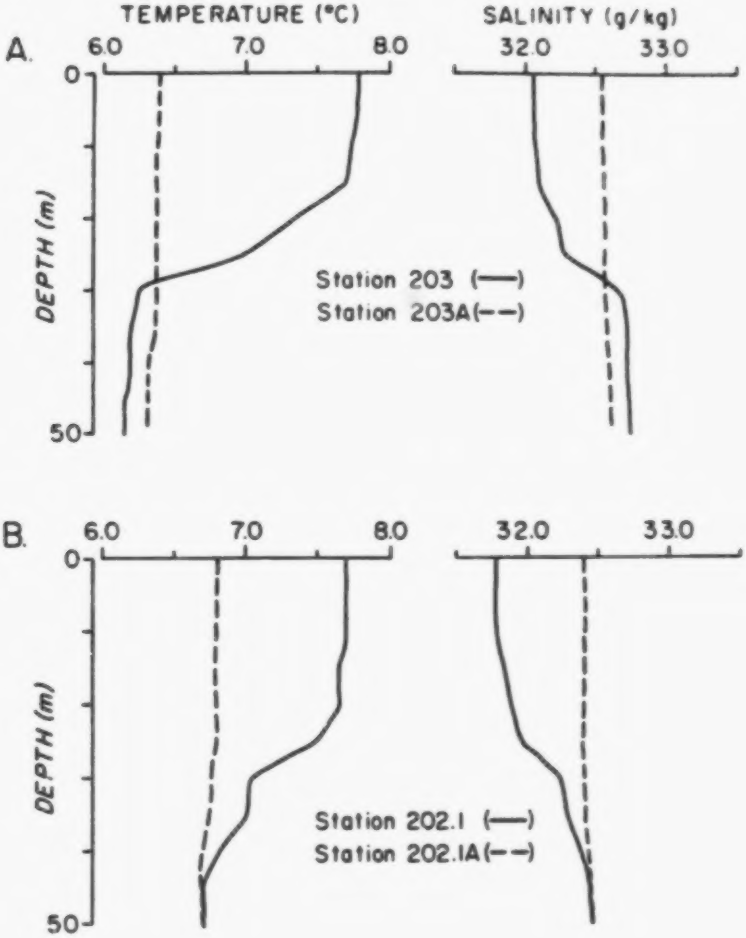

Figure 32. Vertical profiles of temperature and salinity before (solid line) and following (dashed line) a severe storm over Portlock Bank.

3.2 Behavior of Low-Frequency Current Fluctuations

3.2.1 Introduction

In this section, we discuss prominent current fluctuations having periods longer than diurnal tidal, or about 24 hours, but less than seasonal. Currents throughout the northwest Gulf of Alaska and into lower Cook Inlet are characterized by these fluctuations, which attain dominant control over the flow in regions having weak mean currents. For example, in some locations in lower Cook Inlet and on Albatross Bank where the mean flow was small (< 5 cm sec^{-1}) these fluctuations accounted for more than 90% of the kinetic energy in the nontidal water motion, so they must be of paramount importance in material transport. In regions of strong mean flow (> 20 cm sec^{-1}), such as Shelikof Strait, the fluctuations are relatively less important when compared with the mean flow. Figure 33 illustrates the nature of these fluctuations and exemplifies the pattern found throughout the northwestern Gulf. Time scales for the fluctuations are on the order of a week, though they have no clearly defined periodicity. The records used here as illustration are from near-bottom, minimizing biasing of the current records by surface wave noise or mooring motion.

The way in which these low-frequency fluctuations propagate through the northwestern Gulf of Alaska shelf region is of particular interest. We approach this by discussing selected aspects of the fluctuations in specific subregions, commencing with the outer and mid-shelf regions southeast and south of Kodiak Island (Fig. 1).

3.2.2 The Bank-Trough Region

Winter and summer subtidal current variance spectra from outer Albatross Bank (Station WGC2 on Fig. 6) are shown on Figure 34. These spectra are representative of conditions on the banks seaward of Kodiak Island. Most of

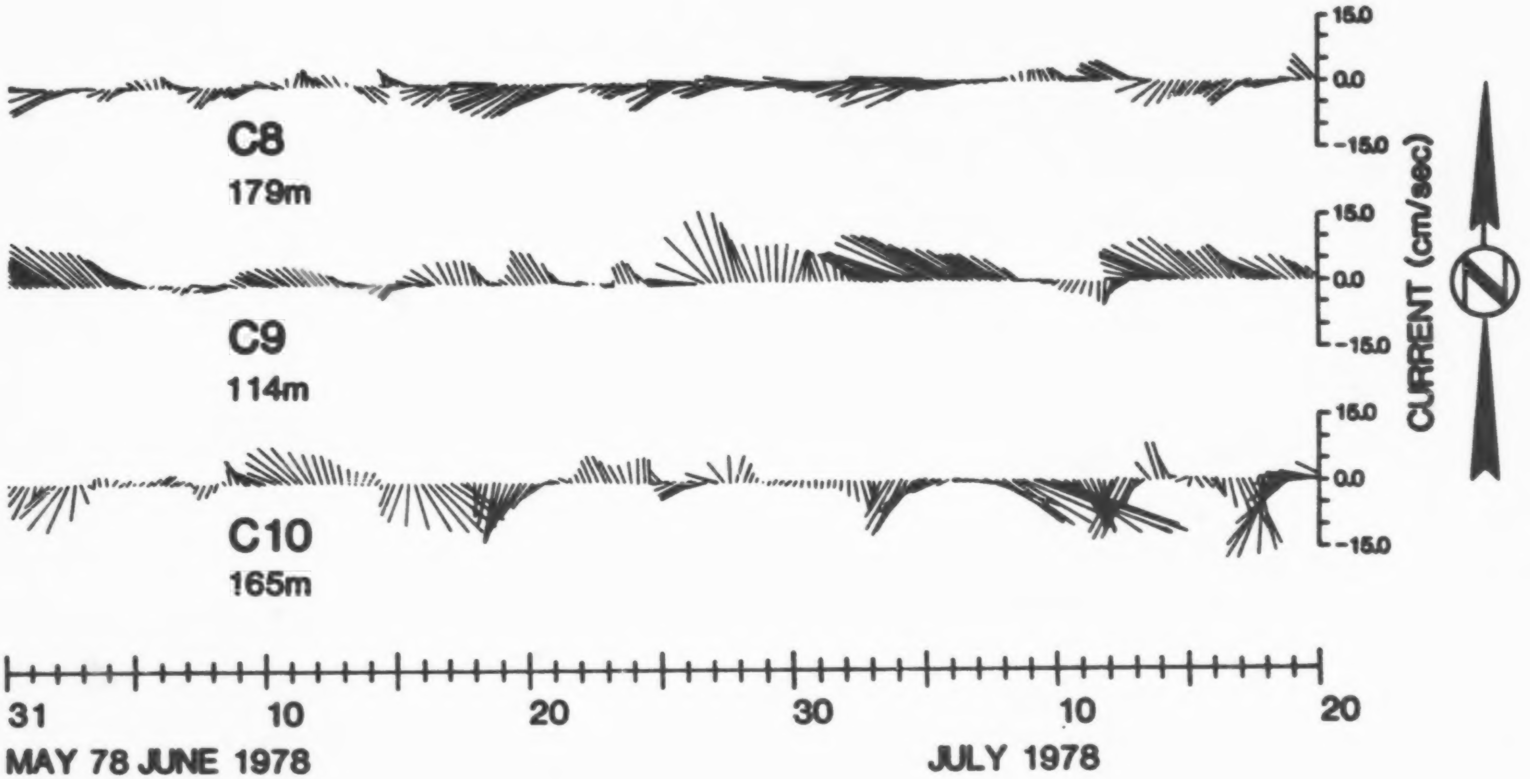

Figure 33. Representative time-series segments of near-bottom currents in Kennedy Entrance (C8), Stevenson Entrance (C9) and northern Shelikof Strait (C10). These records have been low-pass filtered through a 35-h filter to remove the tidal signals.

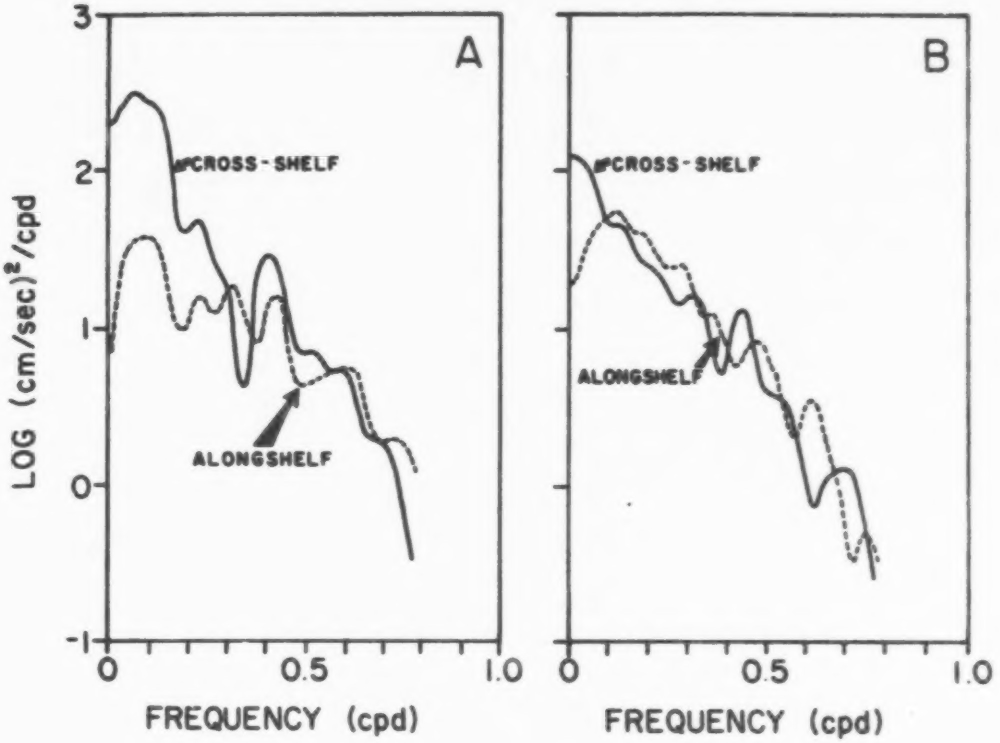

Figure 34. Winter variance spectra at station WGC2 on the banks southeast of Kodiak Island (left) and at station WGC3 off the entrance to Shelikof Strait southwest of Kodiak Island. Both current records were from about 24-m depths. Station locations are indicated on Figure 6.

the low-frequency variance energy is contained in bands below 0.5 cpd, and very low relative amounts of energy occur at 0.75 cpd, the high frequency cutoff. There was a marked change in slope of the spectra at about 0.5 cpd, with variance energy dropping off more sharply at higher frequencies. Shallower observations at the same location indicated higher overall energy levels, while deeper observations showed lower energy levels; the characteristic shapes of the spectra were the same. For comparison purposes, we also show subtidal variance spectra obtained from observations at Station WGC3 just seaward of the southern extremus of Shelikof Strait. The shapes of the spectra at the two locations are similar, though energy levels differ somewhat.

Spectral analyses of the current data from mooring WGC2 on the shelf south of Kodiak Island (Fig. 6) indicated only one significant energy peak; this occurred at about 0.4 cpd or at a period of about 2.5 days and is shown most clearly on the cross-shelf spectra (Fig. 34). Analysis of the current records from moorings WGC1, 2, and 3 have indicated that this peak was coherent in the alongshelf direction, and that motions of this period propagate to the northeast with speeds of about 5 m sec^{-1}. The peak was most pronounced in the cross-shelf component, being in many cases absent entirely from the alongshore component. It decreased in magnitude with increasing depth of observation. It is impossible to discern whether this peak was more energetic on Albatross Bank than elsewhere; overall energy levels were lower on Albatross Bank, and it is possible that a 2.5-day peak of similar magnitude existed at other locations (such as at WGC3 off Shelikof Strait) but was masked by the higher overall spectral energy.

While the WGC series of current moorings were designed to obtain long-term, large-scale information on alongshelf coherency south of Kodiak Island, a more recent series of moorings was deployed in the complex topographic bank and trough region southeast of central Kodiak Island (cf. Fig. 9), providing further definition of the low frequency flow. The low-pass (35-h) filtered current time series from the 1977-78 winter experiment is shown in Figures 35 and 36. The characteristic low-frequency pulses were clearly present but were manifested in different fashions at different locations relative to the banks and troughs. At stations 6 and 7 on the bank and particularly at station 8 in the shoreward portion of the trough, the pulses were primarily in speed with little directional variation. In the central portion of the trough at stations 9 and 10, however, the pulses were manifested as large variations in both speed and direction leading to frequent reversals. While the records from stations 6 and 7 over the bank suggested that events there were correlated, pulses in the trough were not. It is possible that the instruments deployed in the trough were sampling different flow regimes, as these instruments were in the vicinity of an apparent transition from alongshelf flow on the open shelf to cross-shelf flow connected with the trough.

Analysis of variance contained in different frequency bands in the bank-trough region indicated a flatter distribution than observed farther offshore at WGC2. Subtidal variance was distributed approximately evenly across the band, with a more gradual tapering off of energy levels at higher frequencies than was observed at WGC2, and there were no spectral peaks significant at the 95% confidence level.

3.2.3 Shelikof Strait

Shelikof Strait may be defined as an alongshore channel, and we suspect that, due to its confining lateral boundaries, its fluctuating flow might have somewhat different characteristics than to the southeast upon the open shelf. A winter 1976-77 current observation program in Shelikof Strait obtained

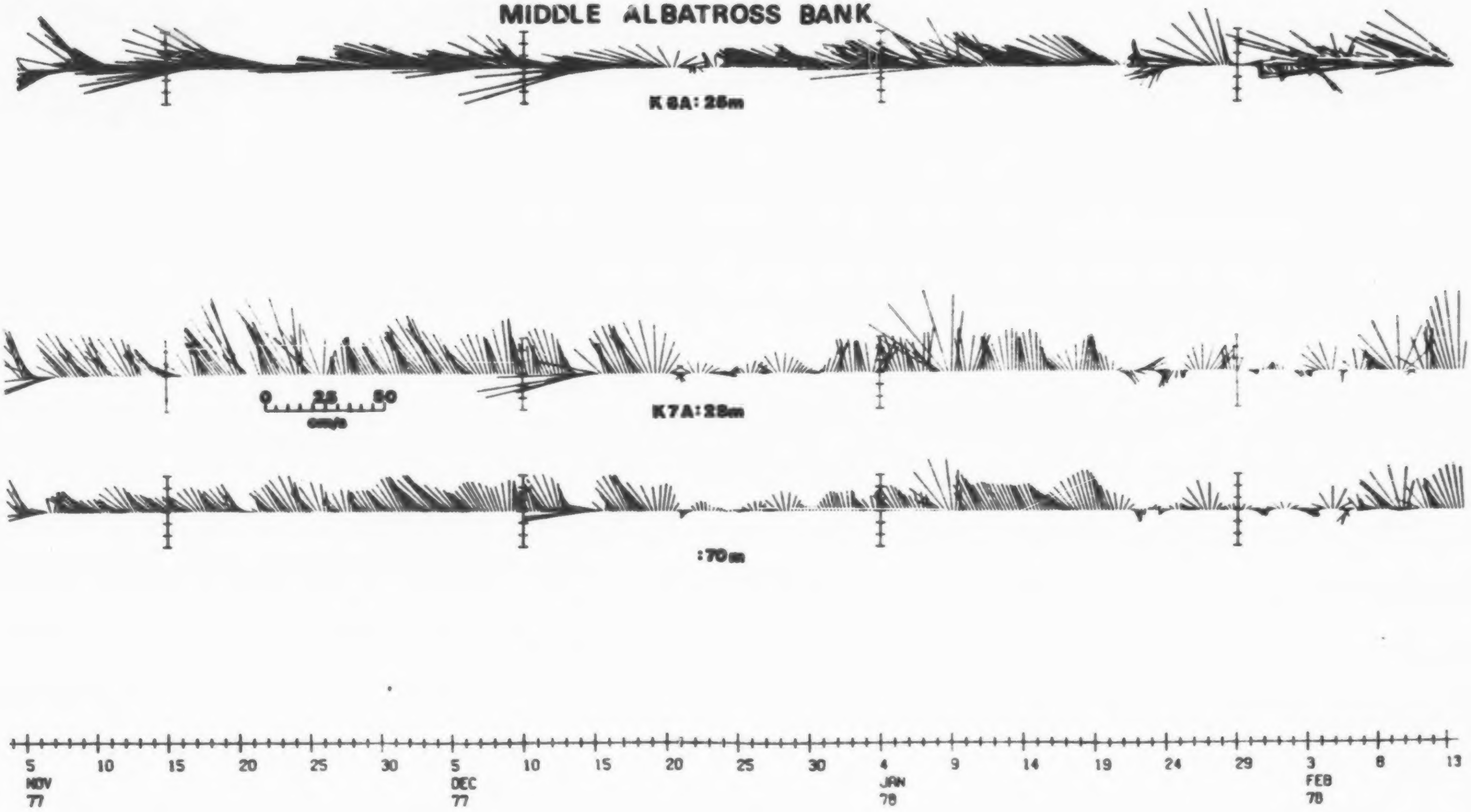

Figure 35. Low-pass (35-h) filtered currents during winter 1977-78 over the bank area south of Kodiak Island. Station locations are indicated on Figure 9.

BEST DOCUMENT AVAILABLE

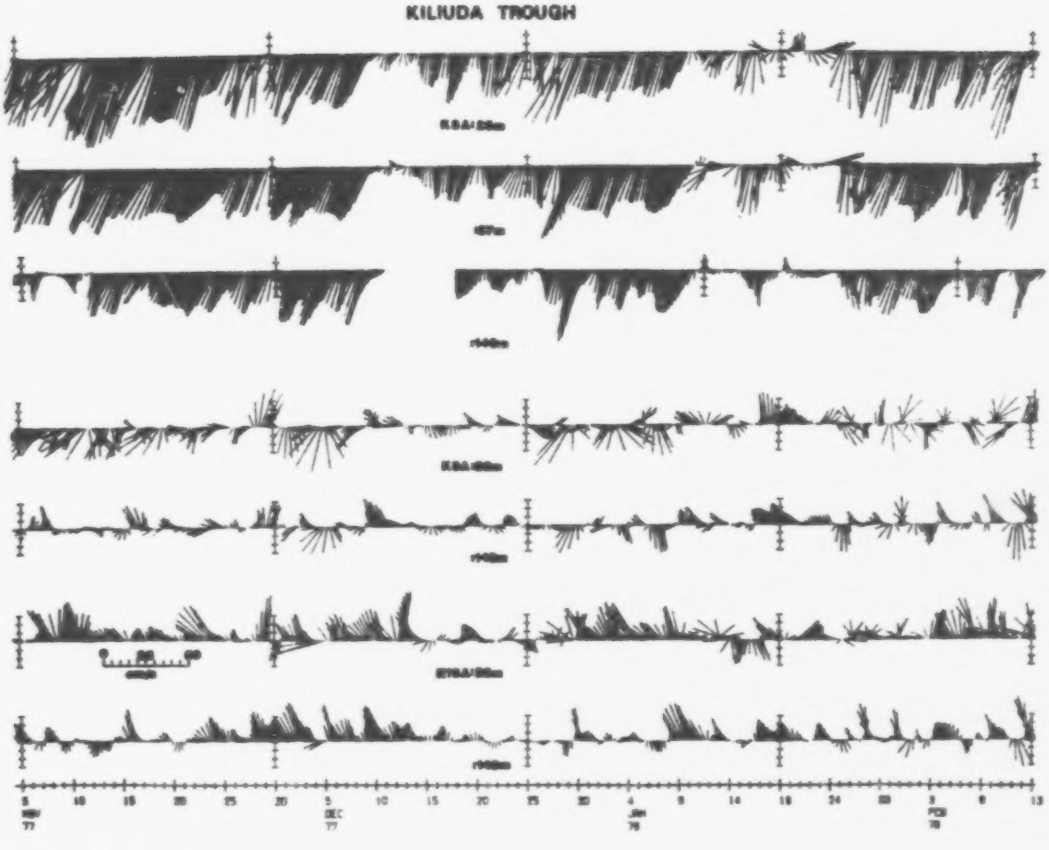

Figure 36. Low-pass (35-h) filtered currents during winter 1977-78 in Kiliuda Trough south of Kodiak Island. Station locations are indicated on Figure 9.

time-series records from the northeast and southwest ends of the Strait, providing data for a comparison of motions through the Strait (cf. Fig. 7). Representative segments of the low-pass (35-h) filtered time series from the two ends of the Strait are shown in Figure 37. Due to the strong winter mean flow through the Strait, the fluctuations were evidenced as pulses in speed rather than as changes in direction. A generally good visual correlation is evident between the records at both ends of the Strait, as we would expect due to the confining lateral boundaries; volume continuity requires that an inflowing pulse at the upstream end of the Strait result in a corresponding outflow at the downstream or southwestern end.

Spectral analyses have been applied to the records from K1 and K2 and indicate a significant shift in cross-channel variance energy from higher and lower frequencies toward a spectral band between 0.1 and 0.3 cpd (Fig. 38). In general, subtidal variance was greater at the downstream than at the upstream end of the Strait. This downstream amplification of cross-channel fluctuations in flow was indicated also on infrared satellite photographs. A representative image is shown in Figure 39, and reveals a wave-like feature defined by the boundary between the low-temperature water from Cook Inlet and the warmer water from the Gulf of Alaska. This boundary appears to oscillate with larger amplitudes towards the southwest end of the Strait before it loses its identity. The same feature has been commonly observed on satellite imagery by G. Hufford (NOAA/NESS, Anchorage, AK 99510). We point out that although the temperature boundary which we use as a tracer loses its identity, it does not necessarily follow that the wave-like feature has ceased to exist.

Application of coherency analyses to the 100-m deep records from K1 and K2 at opposite ends of the strait reveals a confusing picture (Fig. 40).

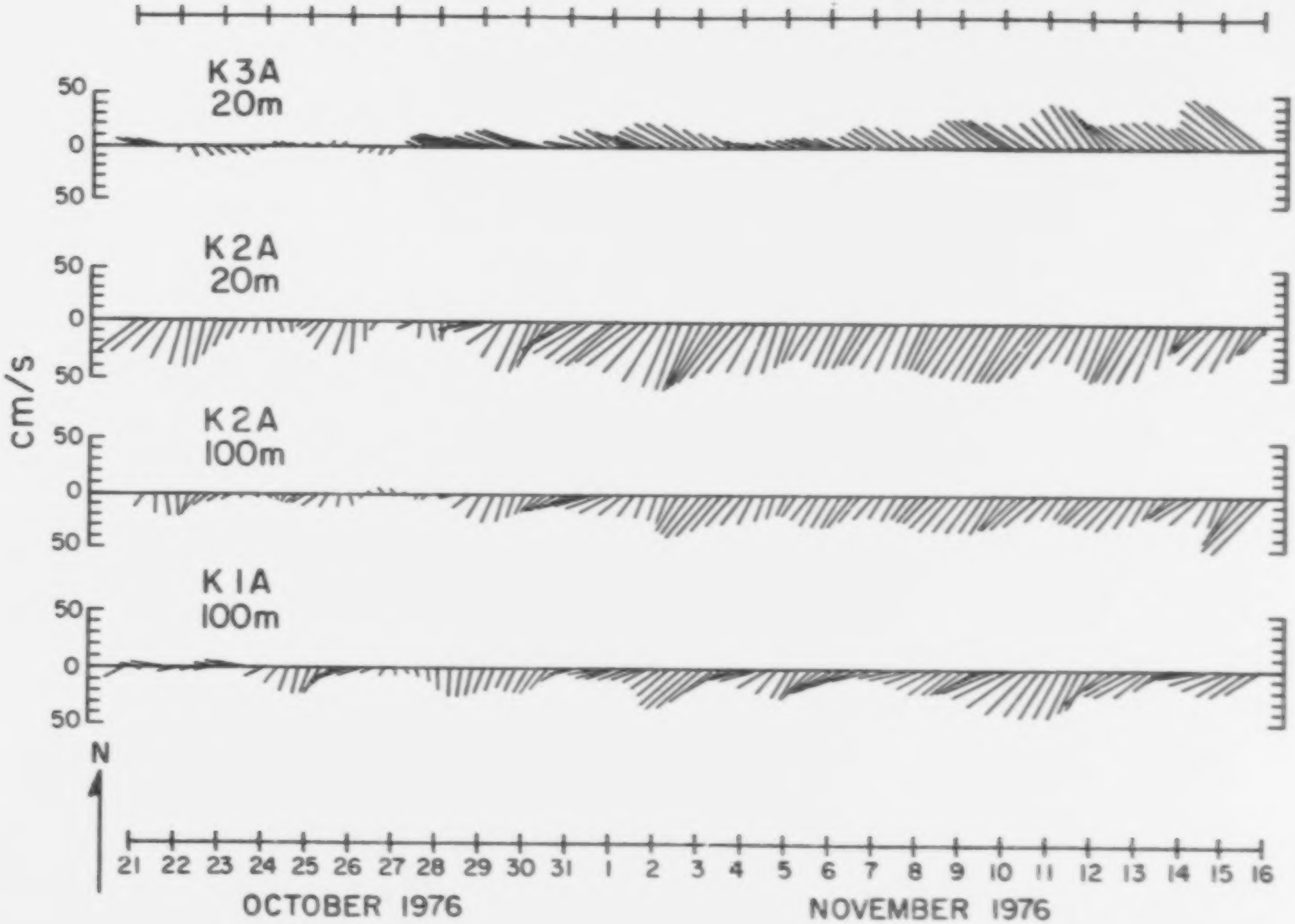

Figure 37. Representative winter segments of low-pass (35-h) filtered current data from northeastern Shelikof Straight (K2A and K3A) and from the southwestern end of the strait (K1A), illustrating continuity of low-frequency flow events through the Straight. Station locations are indicated on Figure 7.

BEST DOCUMENT AVAILABLE

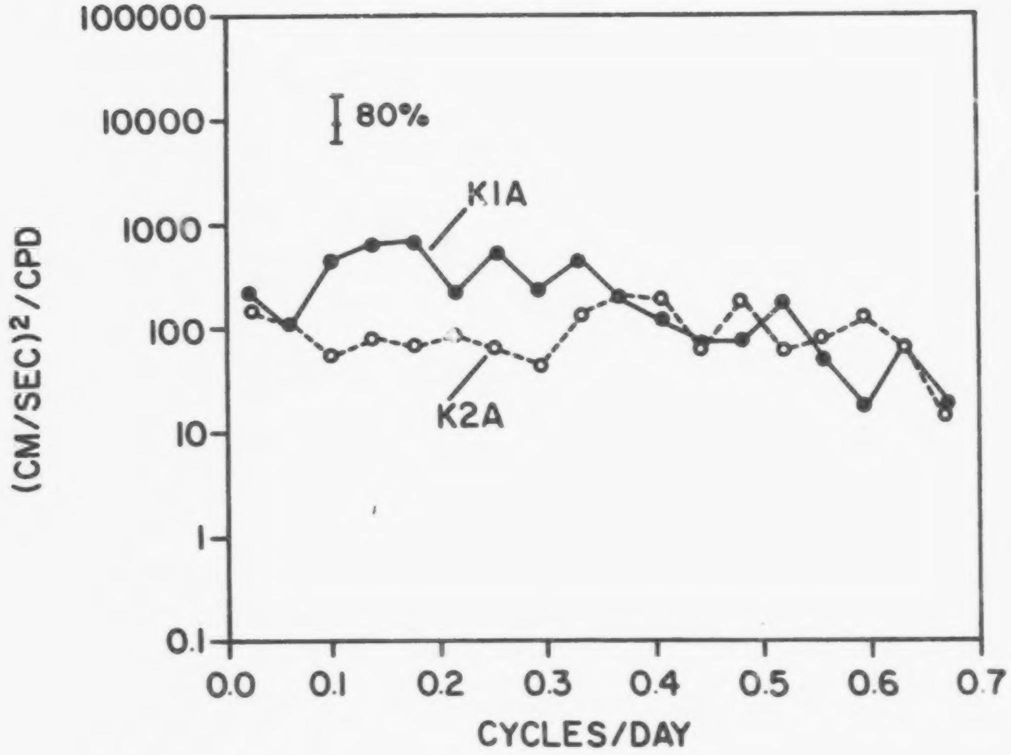

Figure 38. Variance spectra from the northeastern end (K2A) and the southwestern end (K1A) of Shelikof Strait for the cross-channel component of the 100 m deep records, showing the shift of energy into the 0.1-0.35 cpd band from K2A to K1A. Data were obtained during winter 1976-77, and station locations are indicated on Figure 7.

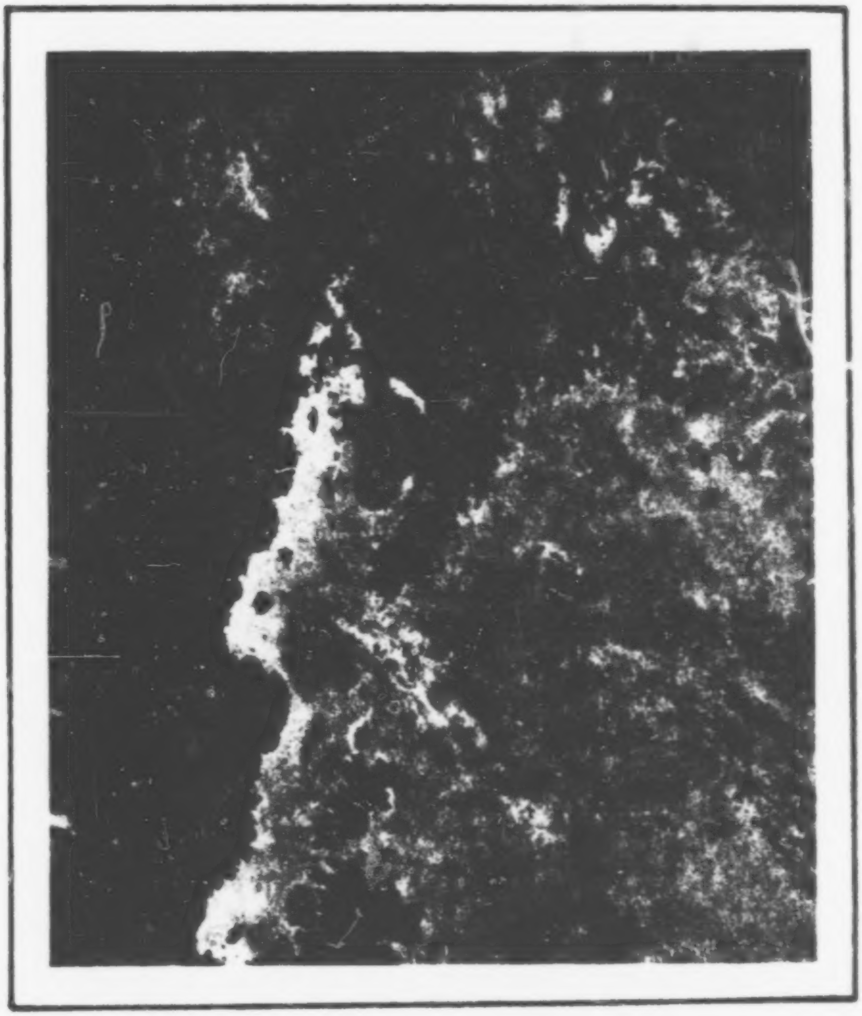

Figure 39. Infrared satellite image of the northwest Gulf of Alaska on 25 February 1977, showing undulating feature defined in northeastern Shelikof Strait by the boundary between cold water (light colored) from Cook Inlet and warmer (darker) water from the Gulf of Alaska.

BEST DOCUMENT AVAILABLE

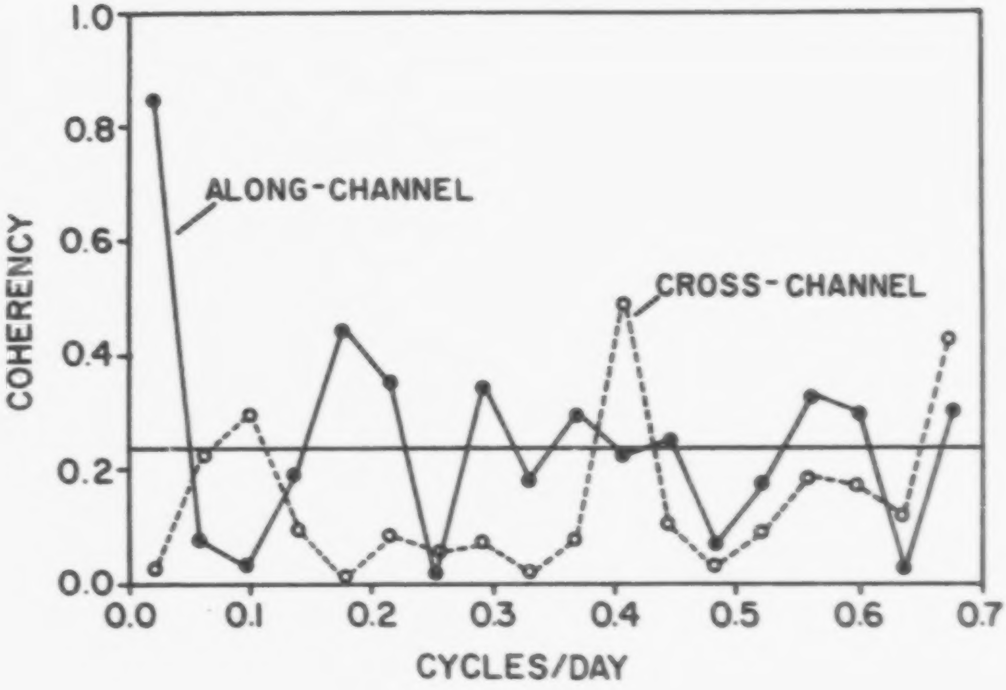

Figure 40. Coherency between cross-channel flow components at northeastern end (K2A) and southwestern end (K1A) of Shelikof Straight using winter 1976-77 data. Station locations are indicated on Figure 7.

The along-channel flow was coherent, as expected, at very low frequencies. The only other significant peaks were at about 0.2 cpd, and at about 0.4 cpd where a cross-channel peak corresponded to our ubiquitous 2.5-day peak. The correlations which are apparent from the time series shown in Figure 37 apparently relate to nonperiodic phenomena, and do not lend themselves to stationary statistical analysis. Based on the above, we conclude that there is generally a good correlation between the along-channel current fluctuations through Shelikof Strait, and that there is a significant coherency between the cross-channel fluctuations at 2.5-day periods. The 2.5-day period pulses are periodic in nature, and manifest themselves in the surface temperature field as wave-like features observable on satellite imagery.

Data obtained from northeastern Shelikof Strait during winter 1977-78 were adequate to test for vertical coherency in the fluctuating flow. Coherency analysis of the entire 5-months record indicated that the flow was vertically coherent throughout the subtidal frequencies. We conclude from this that these pulses are primarily barotropic in nature.

3.2.4 Lower Cook Inlet

A somewhat more detailed analysis of low-frequency fluctuations was possible for lower Cook Inlet than for other regions because of the relatively dense array of current meters used there (Fig. 8). Representative segments of the low-pass filtered currents from six stations in the lower Inlet are shown on Figure 41. It is clear from these plots that the time scales of variability are the same as for other regions considered, on the order of a week, and that the fluctuations are the controlling features of nontidal currents in lower Cook Inlet. At station C4, for instance, it is impossible

BEST DOCUMENT AVAILABLE

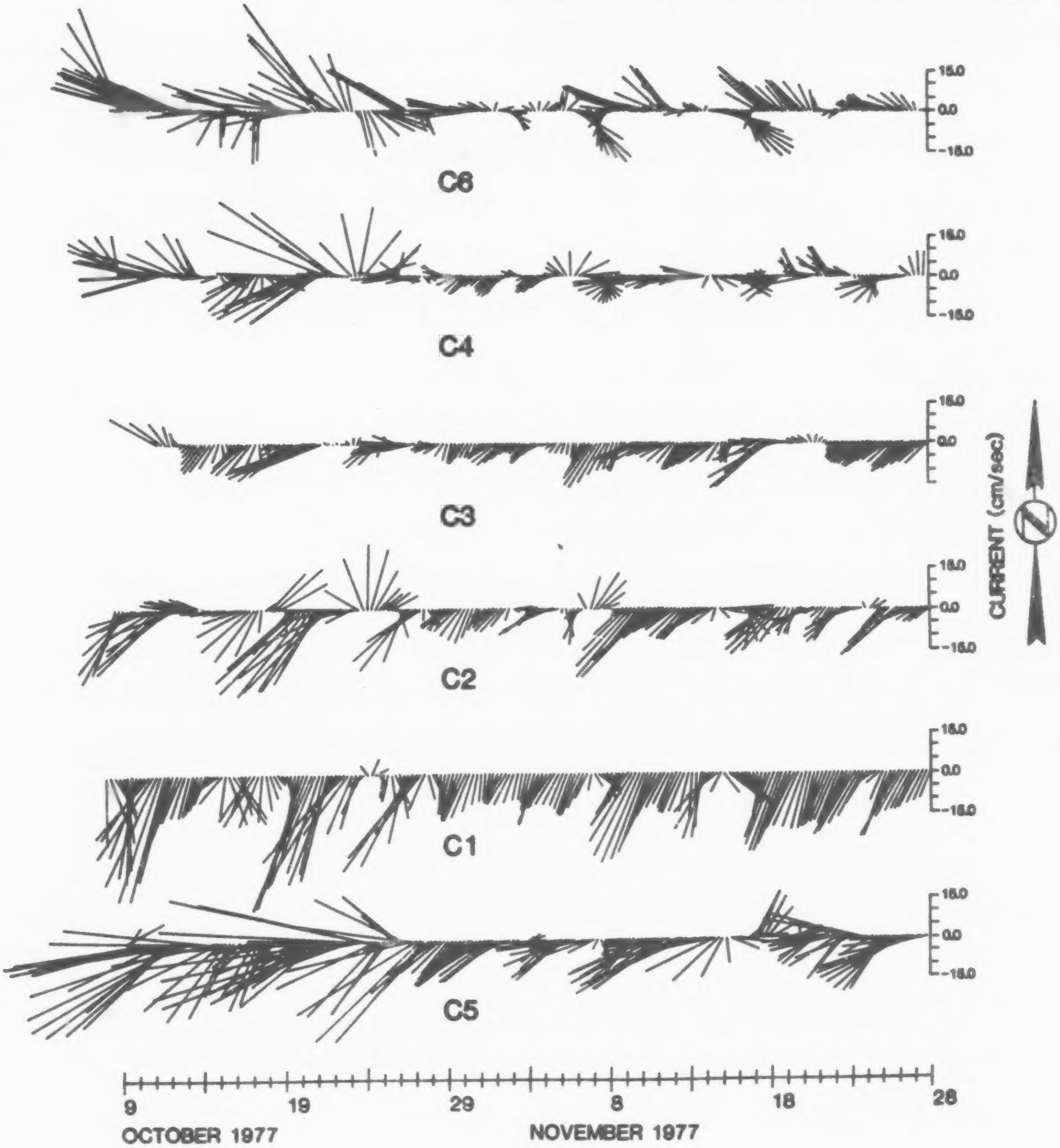

Figure 41. Representative segments of low-pass (35-h) filtered current records obtained from 20 m in lower Cook Inlet. Station locations are indicated on Figure 8.

to detect mean flow direction from a visual inspection of the time-series plot, as the flow was dominated by events. Comparison between the time series shown on Figure 41 reveals a confused pattern of correlation between fluctuations at different locations. For example, a northerly flow event occurred on about 25 October at stations C1, C2 and C4 but not elsewhere. Station C3 showed, in particular, little correlation with events elsewhere in the lower Inlet. Computation of horizontal coherencies between the 20-m records produced no consistent results.

Vertical correlations between the low-frequency pulses varied over the Inlet. At stations C3 and C4 vertical correlations were poor (Fig. 42), even though the records were vertically separated by only 30 and 45 m, respectively. Station C1 showed, conversely, excellent visual correlations in the vertical (Fig. 43) during winter, with correlations somewhat less evident during summer. Station C10, in northern Shelikof Strait, showed high visual correlation in the vertical during both winter and summer. Further analyses are in progress.

Seasonal changes in the low-frequency fluctuations are illustrated by the records from stations C1 and C10 (Fig. 43 and 44). The fluctuations were larger in winter than summer, as evidenced particularly well at station C1. There was no significant seasonal change, however, in time scales or in the lack of horizontal correlation.

In an attempt to further "filter" the current data, 7-day running means of speed were computed. These values, plotted in Figures 45 and 46, allow a better visual definition of correlation between the flow events having time scales longer than 1 week, and also reveal the longer term trends. During the winter observations (Fig. 45) the autumn decrease in flow was evident at all stations except C3. A slight increase later in the winter, particularly

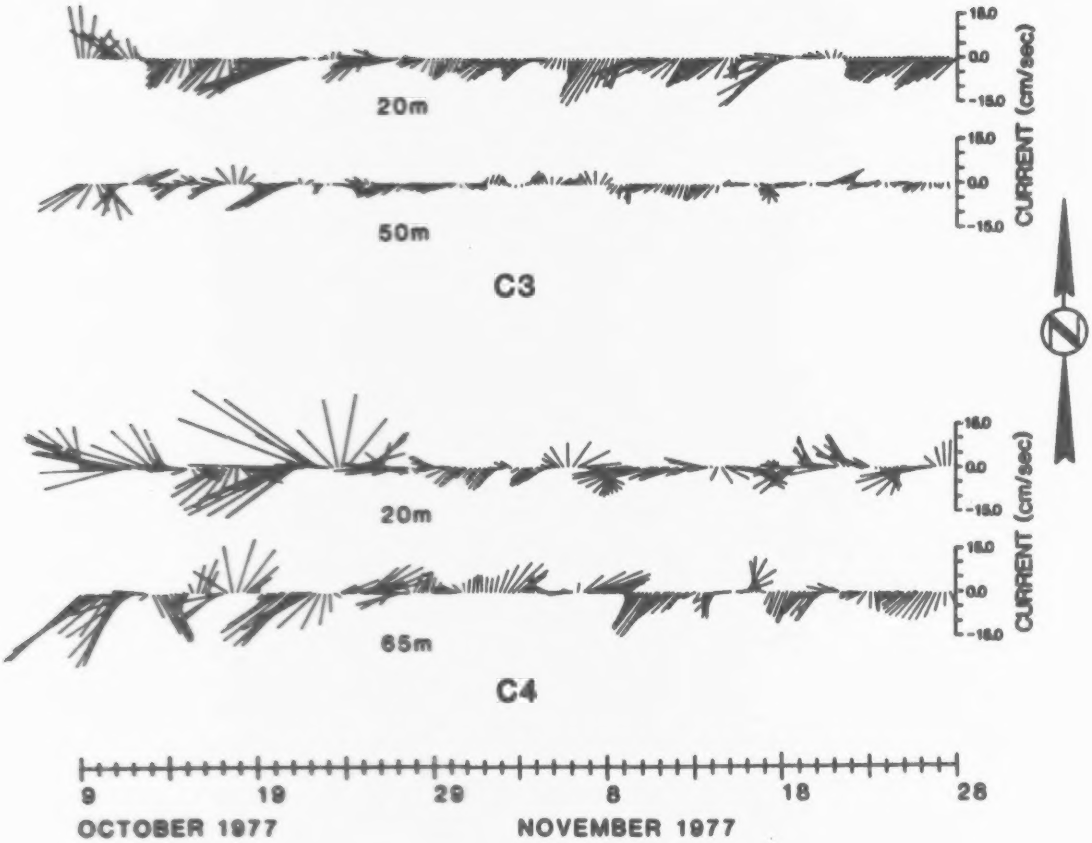

Figure 42. Vertical comparison of low-pass (35-h) filtered current records during winter from two locations in lower Cook Inlet. Mooring locations are indicated on Figure 8.

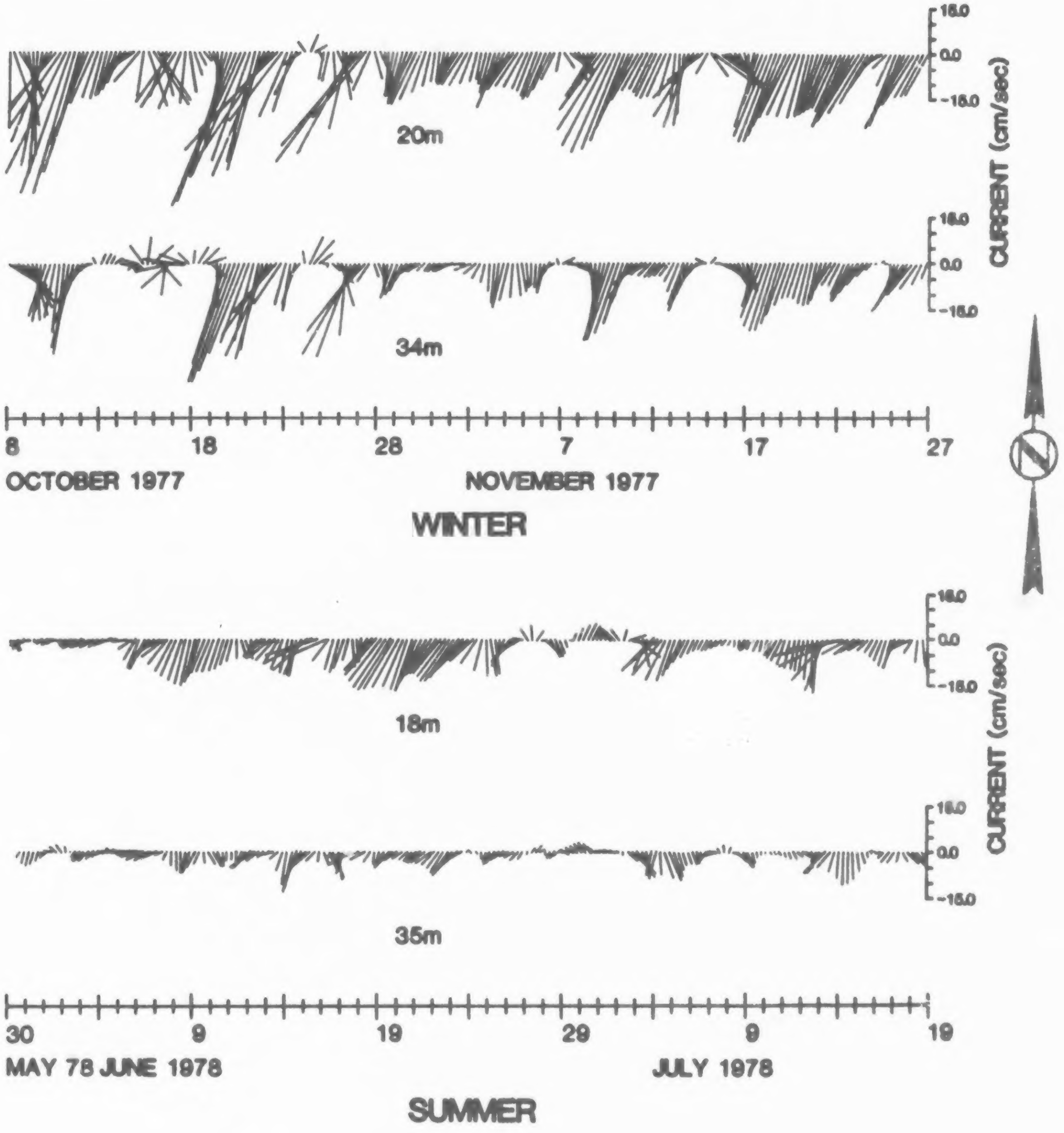

Figure 43. Seasonal comparison of low-pass (35-h) filtered current records from station C1 in lower Cook Inlet at two different depths. Mooring location is indicated on Figure 8.

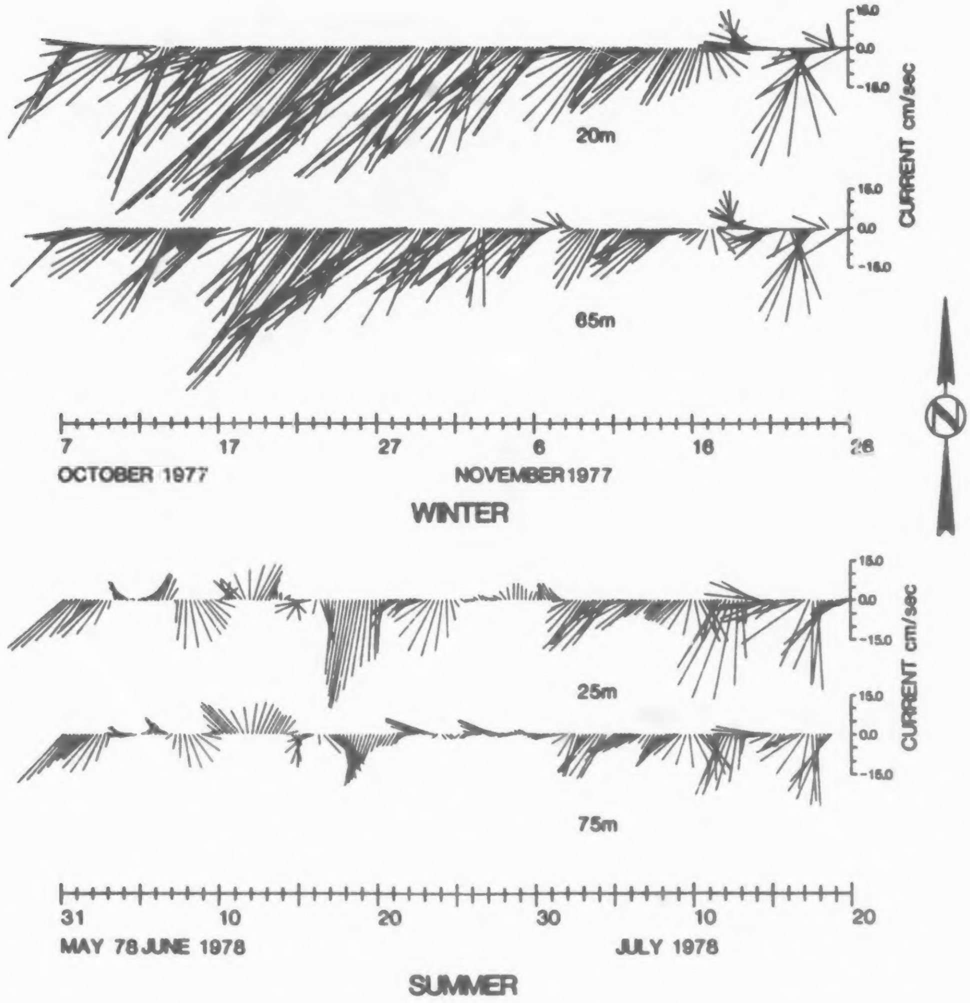

Figure 44. Seasonal comparison of low-pass (35-h) filtered current records from station C10 in northern Shelikof Strait. Mooring location is indicated on Figure 8.

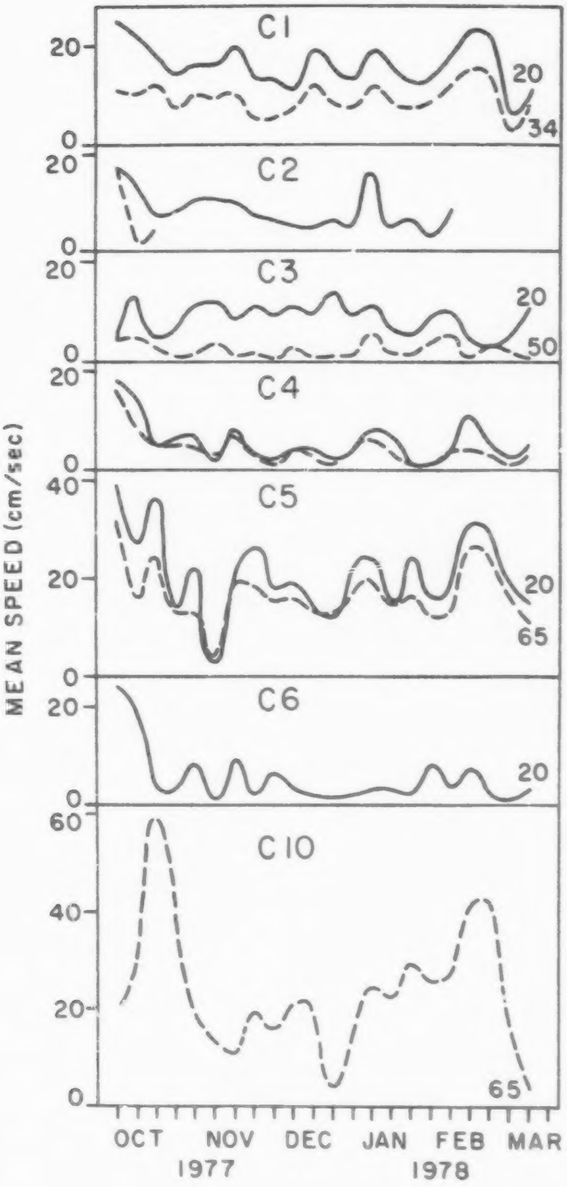

Figure 45. Seven-day running mean speeds at seven stations in lower Cook Inlet. Numbers at right-hand ends of curves indicate observation depths in meters. Station locations are indicated on Figure 8.

BEST DOCUMENT AVAILABLE

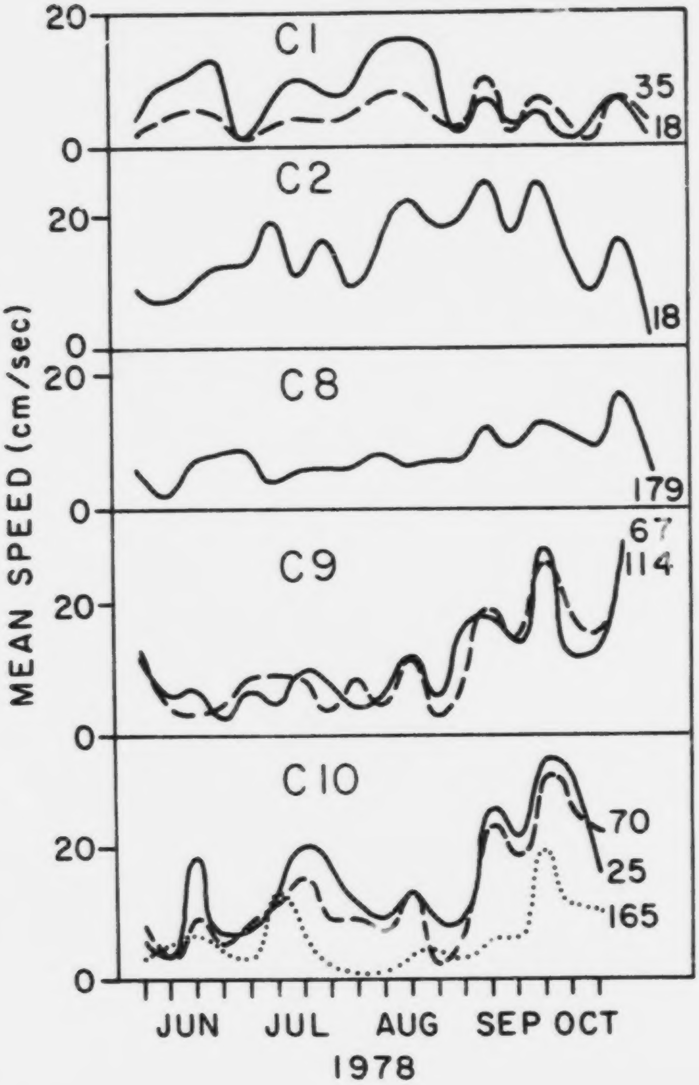

Figure 46. Selected 7-day mean speeds at five stations in lower Cook Inlet during summer 1978. Numbers at right-hand ends of curves indicate observation depths in meters. Station locations are indicated on Figure 8.

apparent at stations C5 and C10, may have been a reflection of winter spin-up of the coastal currents. In addition to the seasonal changes, there were several shorter period (order of weeks) fluctuations that were always correlated at more than one location but rarely at all of them. Stations C5 and C10 were the best correlated, while C3 showed the least correlation with the other records. Generally, vertical correlations were good except for station C3.

Summer current records were relatively incomplete, but indicate the same general patterns that were observed during winter (Fig. 46). The later portion of the records clearly indicates the autumn flow increase consequent to freshwater addition along the Alaskan coast to the east of lower Cook Inlet (Schumacher and Reed, 1980).

The behavior of low-frequency fluctuations in lower Cook Inlet suggests that the pulses tend to follow the same path as the mean flow, that is, an acurate east-west path paralleling the bathymetry. This was manifested as a generally good visual correlation between events at stations C8, C9, C10 and C5. However, these pulses penetrated northward into Cook Inlet only part of the time, so that the frequency of events which can be correlated with those at C5 becomes lower as we progress northward into the Inlet and reaches its lowest value at the northernmost station C3. Conversely, it seems likely that some flow events might be generated in, and confined primarily to, the upper Inlet; these might be evident at the northern stations but not in Shelikof Strait.

The cause of the predominantly aperiodic, low-frequency fluctuations discussed here is uncertain, but is probably related in part to atmospheric forcing. To test for causal factors, selected large events were compared with the local and regional meteorological parameters. Results of these comparisons were inconclusive, and it is felt that this was probably due at least in part to inadequate meteorological data. As discussed in Section 3.5, the atmospheric pressure field is not necessarily representative of actual winds either inside or outside the Inlet. The existing shore stations have also been shown to bear little relation to over-water winds.

Research into the nature of similar flow fluctuations in other large estuarine systems has revealed that such systems are strongly responsive to atmospheric forcing on the continental shelf outside the mouth of the estuary (Wang and Elliot, 1978; Wang, 1978; Winant and Beardsley, 1979; Holbrook et al., 1979). The meteorology of the lower Cook Inlet region is dominated, particularly in winter, by the northeastward migration of intense atmospheric low-pressure systems. We would expect the coastal sea-level variations attendant upon these cyclonic storms to drive significant flow through lower Cook Inlet and Shelikof Strait. Propagation of these pulses northward into the Inlet would then be subject to modification by bathymetry, stratification and local winds. While we have sufficient information on both the bathymetry and stratification to address this problem, the local wind field during our current observations was not defined due to malfunction of environmental buoy EB-46007, which was located centrally in the lower Inlet so as to define the general wind field there. We retain the hypothesis that the fluctuations are driven primarily by atmospheric events over the continental shelf, with local modification to the flow due to stratification, bathymetry and local winds within the lower Inlet itself. Based on work elsewhere, eddies propagating across the shelf could also contribute to these fluctuations. Quantification of these mechanisms awaits further analysis of current data from within the lower Inlet in combination with regional and local wind data.

3.3 Tides and Tidal Currents

The pressure gage data were analysed for tidal components using the Munk-Cartwright Response method (Munk and Cartwright, 1966) with the tide potential as reference series. Results of these analyses are given in Table 3. These analyses were used, along with historical harmonic constants found in Pearson (1973), Rapatz and Huggett (1977), the International Hydrographic Bureau tables (1966), unpublished National Ocean Survey data, and information obtained from the Tide Tables, to describe tidal characteristics and tidal wave propagation in the study area.

Empirical cotidal charts have been constructed for the M_2 (principal lunar semidiurnal) and K_1 (luni-solar diurnal) constituents (Fig. 47 and 48, respectively). These charts show lines of equal phase, or times of high water, and equal amplitude for each constituent. They have been constructed by interpolation between observed values where stations were close-spaced relative to the tidal wavelength, and by estimation in areas where data were sparse. The M_2 and K_1 are the largest of, and generally representative of, semidiurnal and diurnal constituents, respectively.

Both the diurnal and semidiurnal tides propagate from east to west in the Gulf of Alaska in Kelvin wave fashion as part of a north Pacific amphidromic system. According to the cotidal charts of Luther and Wunch (1975) for the central Pacific, the M_2 amphidrome is located at approximately 25°N and 135°W, and the K_1 amphidrome is at 21°N and 177°E. On the outer shelf, M_2 amplitudes decrease from about 110 cm in the vicinity of Middleton Island to 80 cm near Mitrofania Island. Amplitudes increase to about 160 cm up Shelikof Strait toward Cook Inlet. Large amplitudes are found in Cook Inlet, where the semidiurnal tides are near resonance. Amplitudes are largest on the east side in concurrence with Kelvin wave dynamics (Matthews and Mungall,

TABLE 3

Tidal components derived from pressure gage data using the Munk-Cartwright response method (Munk and Cartwright, 1966) with the tide potential as reference series.

Station	LAT	LONG	O1	P1	K1	N2	M2	S2	FROM	TO	DAYS
K8A	57 07	152 45	24.3 261	12.1 273	36.6 274	19.1 276	92.8 299	29.7 329	77 292	78 001	74
K9A	57 01	152 37	25.4 260	12.9 272	39.2 273	19.0 275	92.7 298	30.5 327	77 292	78 068	141
K10A	56 51	152 26	27.0 260	13.9 273	42.2 274	18.9 275	92.6 298	30.5 328	77 292	78 059	133
C1B	59 11	153 19	32.1 271	16.6 286	50.6 287	36.7 303	172.9 326	64.6 002	78 148	78 291	144
C4A	59 17	152 54	34.0 269	17.6 284	53.6 286	37.7 303	177.0 327	65.5 002	77 280	78 074	160
C9B	58 47	152 16	31.8 262	16.0 276	48.8 277	32.4 282	153.6 305	56.1 341	78 149	78 207	58
MIB	55 25	157 59	28.3 267	14.6 280	44.5 281	17.1 291	81.3 314	27.2 343	77 301	78 065	129
WGC2C	57 27	150 30	29.8 256	15.5 271	47.1 273	20.3 271	98.4 295	32.2 325	76 070	76 160	90

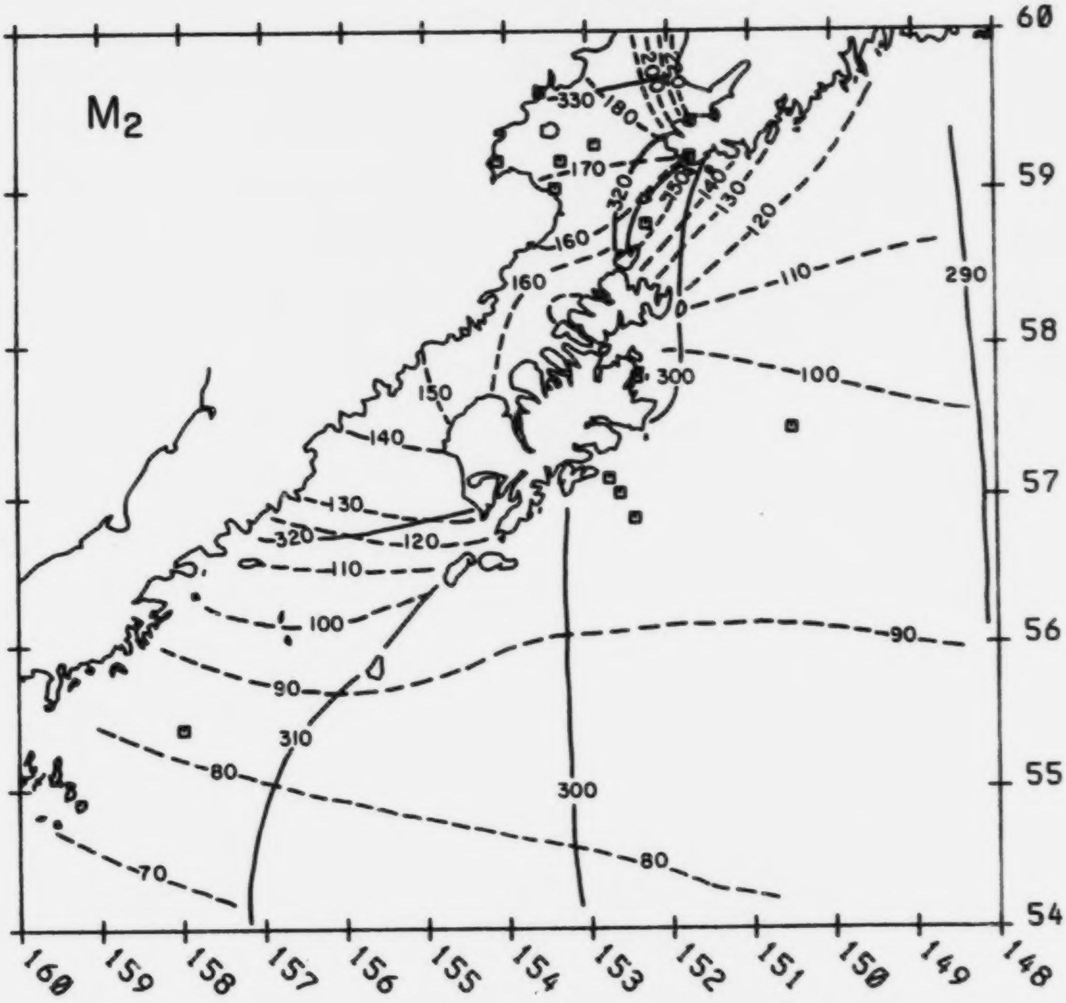
M2
330
180
200
170
320
150
140
130
120
110
160
160
290
150
300
100
140
130
320
120
110
100
90
90
310
80
300
80
70
60
59
58
57
56
55
54
160
159
158
157
156
155
154
153
152
151
150
149
148

Figure 47. Cotidal chart for the M_2 tides. Solid lines are cophase lines referred to Greenwich. Dashes are coamplitude in cm.

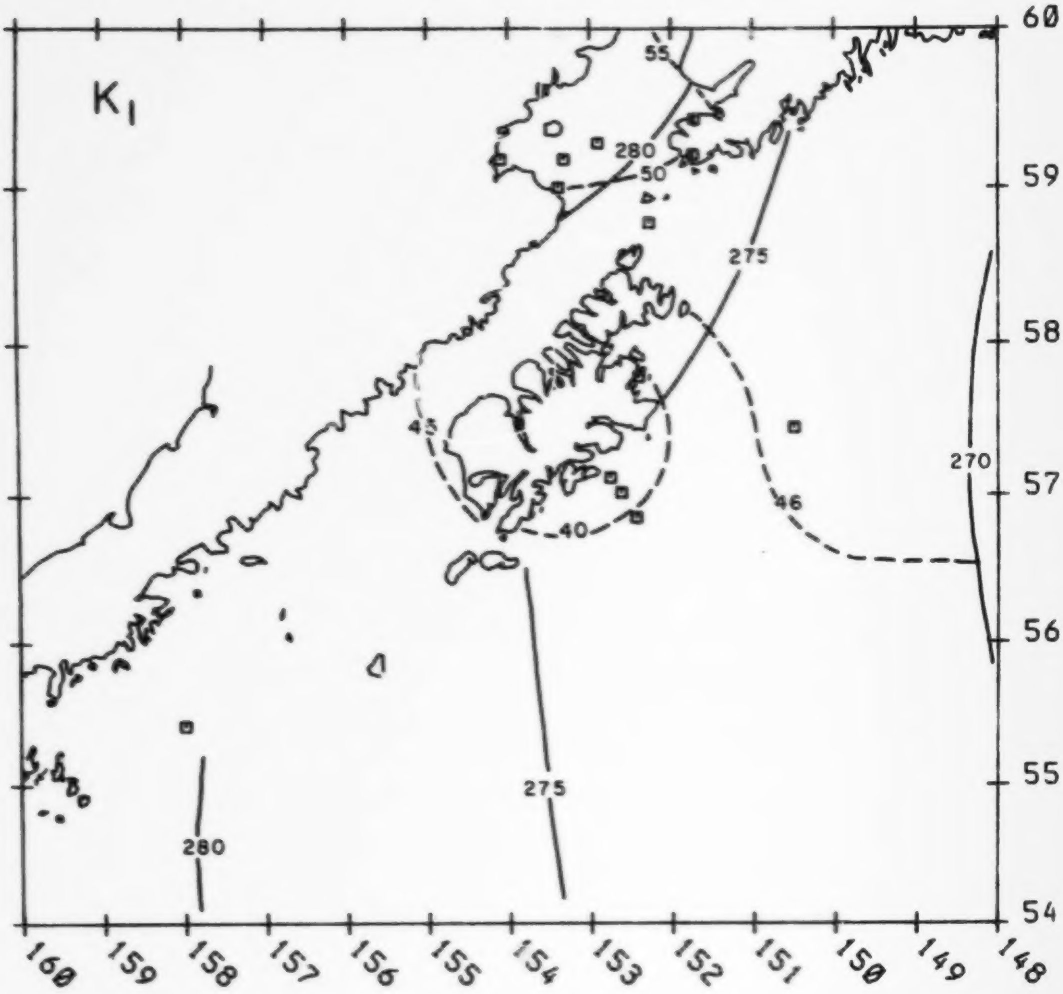
K1
55
280
50
275
45
40
46
270
275
280
60
59
58
57
56
55
54
160
159
158
157
156
155
154
153
152
151
150
149
148

Figure 48. Cotidal chart for the K_1 tides. Solid lines are cophase lines referred to Greenwich. Dashes are coamplitude in cm.

1972). M_2 amplitudes increase from 154 cm at C9 in Stevenson Entrance to 179 cm at C4 in lower Cook Inlet to near 400 cm in the upper Inlet. The K_1 amplitudes are much more uniform in the western Gulf area, ranging from 40 to 50 cm, with somewhat higher values in Cook Inlet.

Tide type may be defined by the ratio of the sums of the amplitudes of K_1 and O_1 to M_2 and S_2:

$$F = \frac{K_1 + O_2}{M_2 + S_2} .$$

F values of 0.25 to 1.5 denote mixed, predominantly semidiurnal tides which are found throughout the Gulf of Alaska region. This type of tide has two high and two low waters per day, but with pronounced inequalities in the high and/or low waters. In the western Gulf, F varies typically from 0.5 to 0.7, with lower values in Cook Inlet where the semidiurnal tide is predominant.

The average spring tide range, defined as $2.1(M_2 + S_2)$, decreases from about 3 m near Middleton Island to 2.5 m near Mitrofania Island, but increases to 5 m and higher in Cook Inlet.

Figure 49 is a plot of the observed bottom pressure for the month of November 1977 at station K9, which is typical of the outer shelf region. The mixed, predominantly semidiurnal tide is evident. Note the large range (3.8 m) observed on the 12th and 13th. This occurred when the new moon, lunar perigee, and extreme lunar declination approximately coincided.

The east and north components of current were analysed for tidal constituents using the response method. Predicted tidal heights from station K9 formed the reference series. The component constituents were then combined in an ellipse representation.

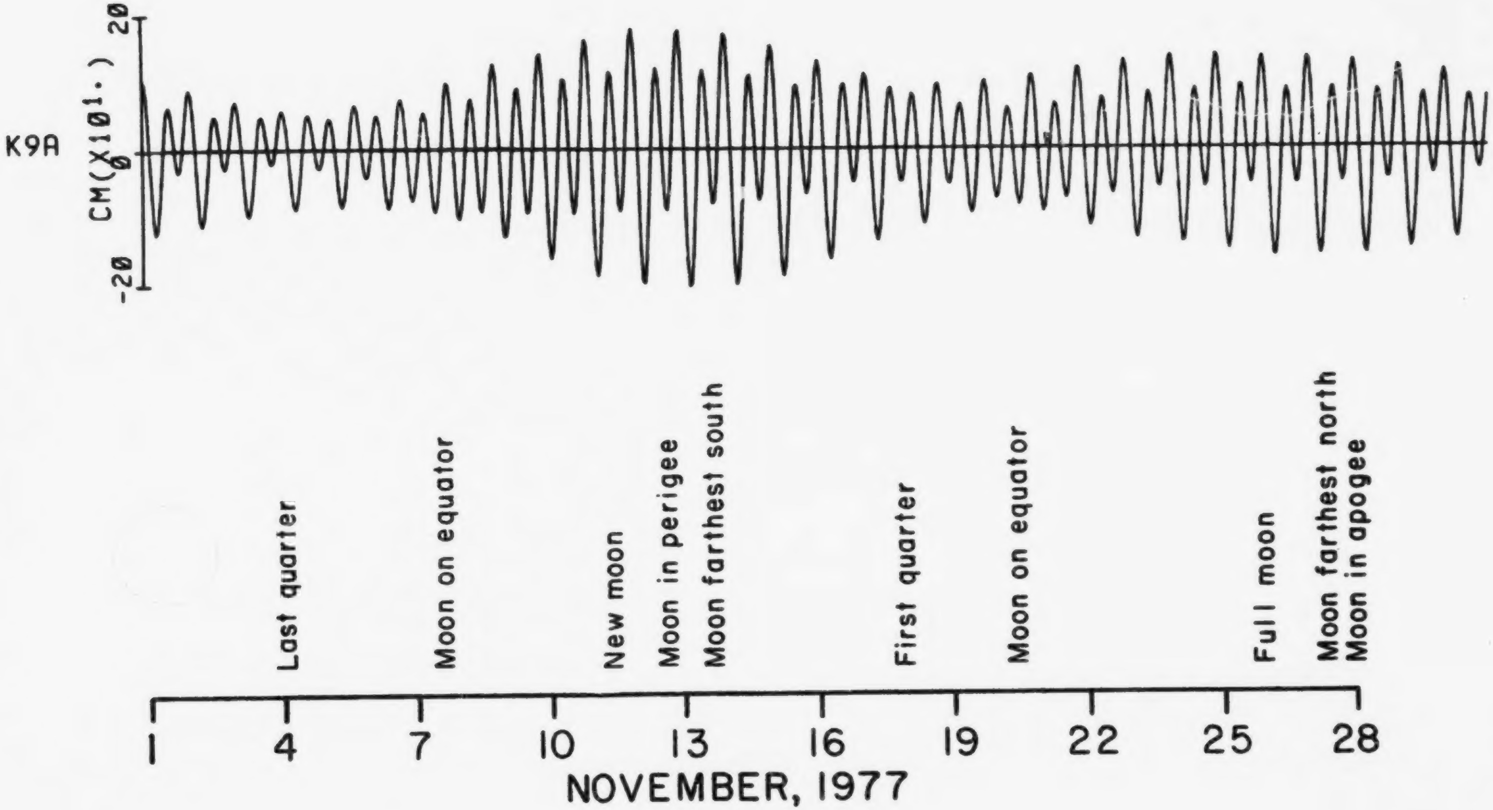

Figure 49. Observed bottom pressure at station K9 for November 1977. Station location is indicated on Figure 9.

In order to minimize possible effects of wave-induced mooring noise, records from summer are presented where possible. However, rotor pumping is not thought to be significant, as discussed in Section 3.1. The results are presented in Table 4. Tidal current ellipses for the M_2 and K_1 constituents are presented in Figures 50 and 51.

The M_2 ellipses show a great deal of spatial variability. Large M_2 tidal currents are found over North Albatross Bank, in Kennedy and Stevenson Entrances and southwest of Kodiak Island. M_2 tidal currents are particularly large in eastern lower Cook Inlet and in upper Cook Inlet. Currents are smaller in central and western lower Cook Inlet, although no further evidence was found of the extremely low tidal currents found at one station in central lower Cook Inlet by Muench et al. (1978). Unusually small M_2 currents are found over Middle Albatross Bank and in northern Shelikof Strait. The small currents over Middle Albatross Bank are evidently the result of Kodiak Island acting as a barrier to the incident tide wave, as the cophase lines roughly parallel the bathymetry there. In northern Shelikof Strait an antinode exists, where the tide wave entering Cook Inlet around the north end of Afognak Island meets the tide wave which has arrived from around the south end of Kodiak Island. The point of meeting, where no M_2 current should exist, is somewhere near station C10. The tidal current there is extremely weak and variable. The semidiurnal tide has standing wave characteristics in Shelikof Strait and over Albatross Bank, while it is more progressive across Portlock Bank and in the entrances to Cook Inlet.

The diurnal K_1 tide exhibits a more uniform speed distribution than M_2. Speeds are very low in Shelikof Strait because, as in the case of the M_2 tide, the waves coming around Kodiak and Afognak islands meet in Shelikof Strait and form an antinode. There is little decrease in the diurnal tidal current

TABLE 4

Tidal current components for four major species derived from current data using the Munk-Cartwright Response method (Munk and Cartwright, 1966) and predicted tidal heights from station K9 as the reference series.

Station	Bottom Depth (m)	Meter Depth (m)	Latitude		Longitude		Start Date (YR/JD)		O_1					K_1					S_2					M_2					Record Length (Days)
									H	Major G	D	Minor H	R	H	Major G	D	Minor H	R	H	Major G	D	Minor H	R	H	Major G	D	Minor H	R	
K1A	228	100	57	45	154	44	76	290	1.2	239	44	0.3	C	3.0	221	51	0	A	5.7	277	49	.1	A	14.9	239	51	3	C	163
K2A	164	20	58	37	153	05	76	290	2.0	222	30	0.1	A	3.7	272	3	.3	C	3.8	199	201	2.6	C	11.8	195	218	5.3	C	164
K5A	95	20	56	33	152	39	76	292	11.6	92	217	5.0	C	18.4	121	223	9.5	C	4.7	246	327	2.5	C	14.1	210	333	7.8	C	158
K6B	82	32	57	14	152	23	78	141	10.2	57	234	4.3	C	17.9	87	239	7.9	C	3.3	350	40	1.9	C	7.9	329	47	6.3	C	138
K7B	84	29	57	06	152	13	78	141	10.5	43	219	4.6	C	16.9	81	227	7.8	C	2.9	14	50	2.6	C	8.0	284	344	6.6	C	136
K8B	155	30	57	07	152	43	78	141	5.2	71	210	0.4	A	7.7	91	223	1.3	A	1.4	311	340	1.3	C	3.5	256	330	2.5	C	136
K9A	157	25	57	01	152	37	77	292	6.7	69	218	0.8	A	13.3	93	224	1.3	A	1.9	284	323	1.3	C	4.5	236	327	2.2	C	141
K10B	153	24	56	50	152	24	78	141	6.4	68	224	1.5	C	11.6	98	226	4.2	C	1.6	335	320	1.1	C	3.7	264	320	[illegible].5	C	136
K11B	83	25	56	02	155	06	78	142	6.8	177	308	.1	A	9.2	206	303	.9	A	20.6	238	329	12.5	C	59.9	208	327	33.6	C	66
K13B	115	28	56	24	156	49	78	142	2.7	155	62	.1	C	4.8	175	62	.2	C	10.4	287	38	2.9	C	24.3	247	41	5.6	C	138
WGC2C	185	24	57	27	150	30	76	070	4.6	150	322	3.8	C	7.7	189	340	6.5	C	5.9	309	304	2.2	C	16.2	289	311	5.6	C	90
WGC2D	93	20	57	34	150	49	76	160	10.4	226	44	7.2	C	16.2	236	34	12.3	C	11.9	298	328	7.3	C	32.4	255	324	22.3	C	132
WGC3D	112	20	55	12	156	57	77	119	3.5	139	24	1.5	C	5.8	178	15	4.2	C	13.8	280	337	8.1	C	36.8	243	341	25.3	C	132
C1B	40	18	59	11	153	19	78	168	3.6	237	34	3.4	C	6.5	229	323	4.8	C	13.6	294	313	5.9	C	33.2	261	306	19.1	C	87
C4A	84	19	59	17	152	55	77	280	6.3	222	14	2.3	C	9.7	242	4	3.7	C	16.8	330	355	5.2	C	46.3	302	357	18.9	C	163
C5A	128	20	59	10	152	56	77	280	3.9	192	355	0.3	A	5.4	222	344	0.5	A	10.2	326	338	0.9	C	28.0	297	338	4.5	C	160
C6B	77	26	59	19	152	38	78	148	6.9	199	8	2.8	C	11.4	213	359	3.7	C	22.7	315	358	7.3	C	57.3	287	356	19.5	C	141
C7B	68	17	59	18	152	10	78	148	8.9	161	358	2.6	C	15.9	184	358	2.5	C	36.8	299	358	4.8	C	98.0	269	357	17.4	C	142
C8B	190	64	59	02	152	03	78	149	8.7	179	301	3.3	A	13.1	207	302	3.7	A	28.0	307	300	2.5	C	70.0	278	295	5.8	C	83
C9B	124	66	58	47	152	16	78	149	10.0	191	293	2.5	C	15.4	205	296	1.9	C	27.2	298	295	1.5	C	70.5	268	291	9.6	C	139
C10B	175	25	58	30	153	12	78	148	2.1	265	58	0.3	A	1.7	307	35	0.1	A	3.3	48	25	1.7	C	8.3	4	35	3.4	C	134
C12A	50	20	59	32	152	14	78	148	9.3	201	9	1.1	C	15.1	212	6	2.0	C	29.8	319	7	0.4	C	79.7	296	6	4.4	C	81
C13A	68	26	59	28	152	41	78	148	9.5	222	23	4.2	C	14.3	235	22	4.5	C	26.5	335	16	9.8	C	74.1	308	13	28.0	C	141
M2	110	50	55	25	157	59	77	301	4.2	179	25	2.2	C	6.9	213	35	3.8	C	6.1	298	5	2.9	C	16.3	263	358	8.4	C	129
M4	118	70	55	46	157	31	77	301	3.9	172	35	1.2	C	5.6	196	33	1.7	C	7.4	295	16	2.6	C	19.6	260	15	7.6	C	129

BEST DOCUMENT AVAILABLE

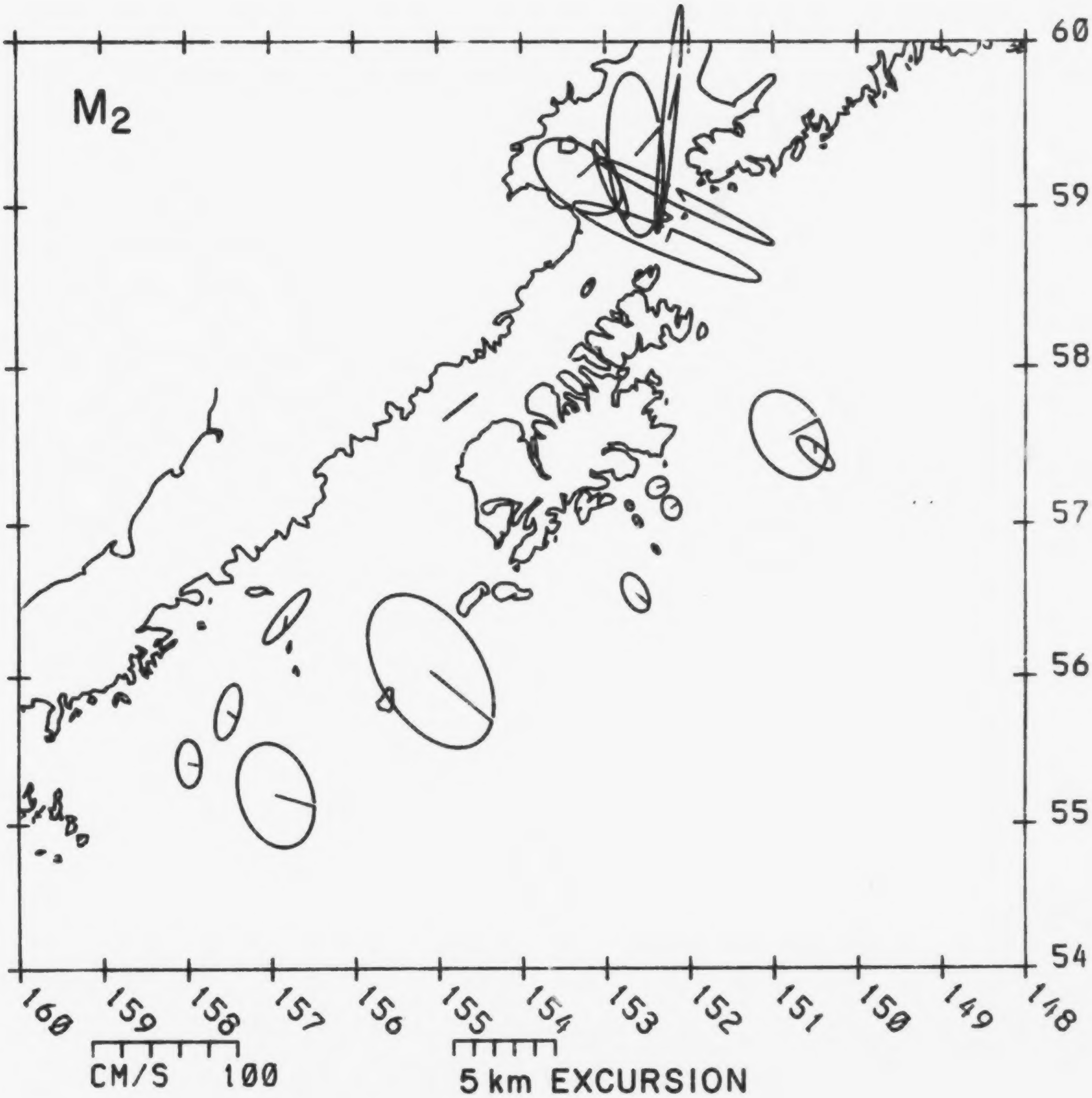
M2
60
59
58
57
56
55
54
160
159
158
157
156
155
154
153
152
151
150
149
148
CM/S 100
5 km EXCURSION

Figure 50. M_2 current ellipses for selected stations in the northwest Gulf of Alaska. Ellipses are centered at station locations; lines radiating from the centers indicate constituent current vectors when the M_2 Greenwich equilibrium phase angle is 0°.

BEST DOCUMENT AVAILABLE

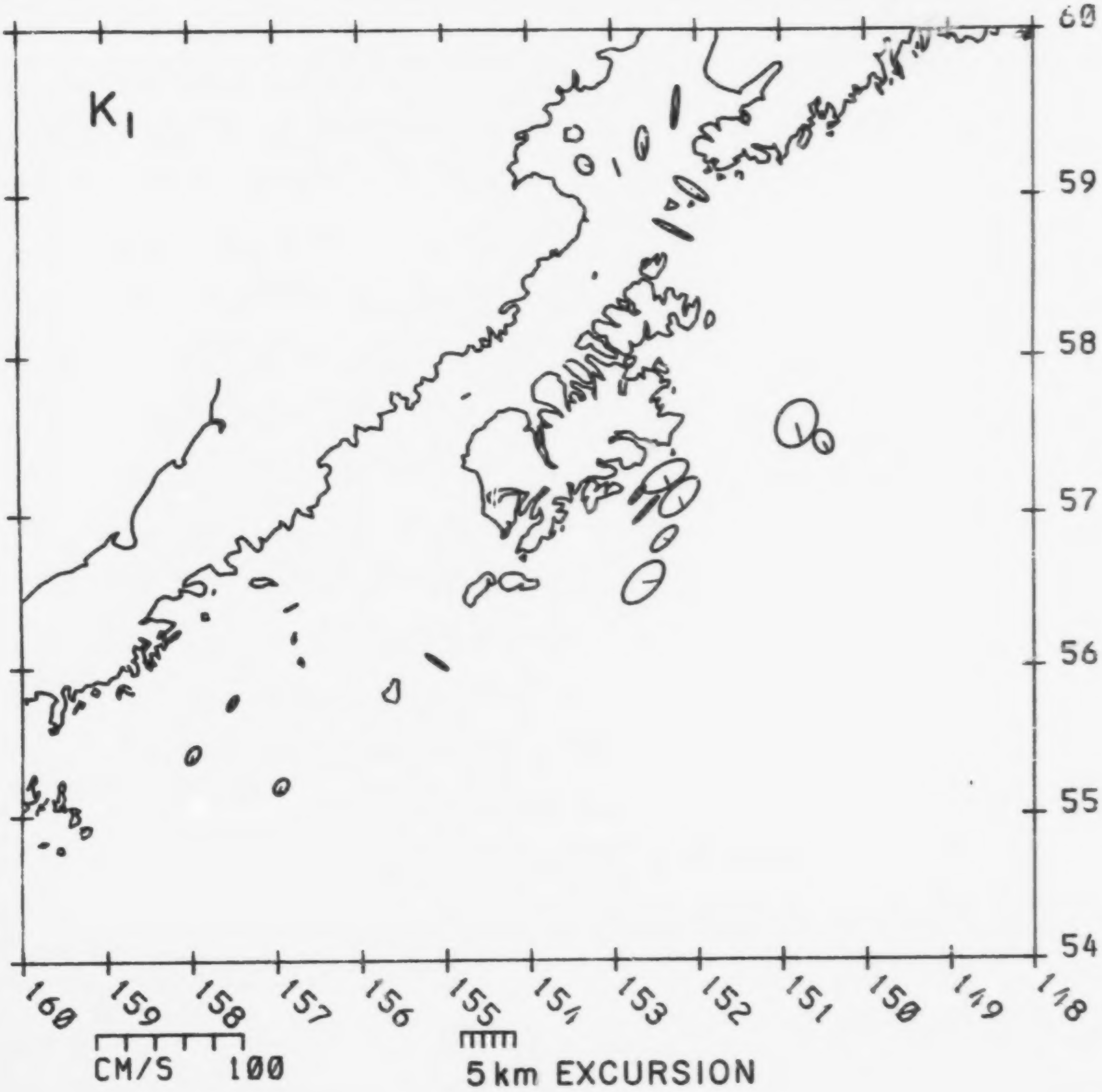
K1
60
59
58
57
56
55
54
160
159
158
157
156
155
154
153
152
151
150
149
148
CM/S 100
5 km EXCURSION

Figure 51. K_1 current ellipses for selected stations in the northwest Gulf of Alaska. Ellipses are centered at station locations; lines radiating from the centers indicate constituent current vectors when the K_1 Greenwich equilibrium phase angle is 0°.

at Middle Albatross Bank, which results in predominantly diurnal tidal currents ($F>1.5$). Elsewhere the currents are mixed predominantly semidiurnal or regular semidiurnal ($F<.25$).

In assessing the environmental impact of pollutants, the tidal excursion is important in relation to the proximity of potential impact areas. The tidal excursion in kilometers, over one-half of a tidal period (the flood tide for instance), is:

$$H\int_{o}^{\pi}\cos\sigma t\,dt = H\frac{T}{\pi}$$

where H is the amplitude, σ is frequency and T is period. For the semidiurnal tide this is approximately 0.14H (H in cm sec^{-1}, and excursion in km). Thus the mean spring tide excursion, where $H = 1.05\ (M_2 + S_2)$, is 20 km at C7 in eastern lower Cook Inlet, 15 km at C8 in Stevenson Entrance, 12 km at K11 southwest of Kodiak Island, and only 1.5 km at C10 in northern Shelikof Strait. At Middle Albatross Bank, where the currents are predominantly diurnal, the excursion is .29H, so during extreme lunar declination when $H = K_1 + O_1$, the excursion over one-half of a diurnal cycle at K7 is about 8 km.

3.4 Current Energy Partition With Frequency

In the following section, we present speed and horizontal kinetic energy (HKE) characteristics from current records collected during the bank-trough experiment (Tables 5 and 6), from North Albatross Bank (Table 7) and from the lower Cook Inlet/Shelikof Strait experiment (Table 6). Coastline and shelf-break orientation are used to define positive alongshelf and cross-shelf as 225°T and 315°T for all records from the bank-trough, north Albatross Bank (WGC series) and C10, 300°T and 030°T for C8B and C9B; and 090°T and 000°T for the lower Cook Inlet records (C3A and 3B and C4A and 4B). Velocities from 35-h filtered records were decomposed along these axes and are presented as speeds. Variance along an axis was used to determine standard deviation as well as subtidal kinetic energy. The 2.9-h filtered data were used to estimate kinetic energy in tidal frequency bands. We note that the latter estimates are averages over several bands, and as such include energy from sources other than tides. The specific tidal frequences do not indicate seasonal trends, as noted also in Section 3.3. The following equations define our parameters:

Kinetic energy of the mean $(\overline{KE}) = \frac{1}{2}(\bar{u})^2 + \frac{1}{2}(\bar{v})^2$

where the bar represents mean axis speed;

Kinetic energy of subtidal flow $(KE') = \frac{1}{2}\sigma_u$ or $\frac{1}{2}\sigma_v$

where σ represent variance along each axis.

Moorings WGC2A to 2C represent conditions on North Albatross Bank (Table 7). These moorings were deployed at the shelf-break at a depth of approximately 190 m and the series WGC2D to 2F were deployed approximately 25 km shoreward in about 85 m of water. This shoreward shift in mooring location resulted in a substantial change in flow characteristics and the distribution of HKE. At the shelf-break, alongshelf $\overline{KE}$ was dominant. At the shoaler location, flow retained some tendency to be alongshelf, however, the dominant energy was

TABLE 5

Current statistics in winter for the bank-trough region southeast of Kodiak Island, and mean alongshelf and cross-shelf wind stress for the current observation period. Mooring locations are indicated on Figure 9.

Mooring (meter depth)	Observed Speed (cm/s)		Horizontal Kinetic Energy Distribution (cm²/s²)					
			Alongshelf			Cross-Shelf		
	Alongshelf	Cross-shelf	Mean	Subtidal	Tidal	Mean	Subtidal	Tidal
BANK								
K6A (23m)	12.3±11.9	19.1±11.2	75.7	70.2	171.5	186.3	62.3	46.1
(65m)	10.6± 8.0	11.4± 6.4	56.2	32.0	88.5	64.8	20.7	17.4
K7A (28m)	-4.1± 8.4	10.7± 9.2	8.4	35.0	173.5	57.2	42.7	62.5
(70m)	-1.5± 4.6	8.0± 5.6	2.3	10.6	76.9	44.0	15.8	25.2
TROUGH								
K8A (25m)	24.3±12.9	-10.1± 7.2	295.3	82.7	35.5	51.0	26.4	20.8
(67m)	20.9±10.1	- 8.3± 6.3	218.4	50.8	31.2	34.5	20.1	9.9
(140m)*	10.1± 7.3	- 6.4± 5.5	51.0	26.4	18.3	20.5	15.2	5.1
K9A (25m)	4.6±10.4	- 0.6± 7.8	10.6	53.8	68.3	0.2	30.1	17.7
(148m)	0.8± 4.7	2.5± 6.2	0.3	11.0	21.4	3.1	18.5	15.1
K10A (25m)	-0.8± 9.4	8.2± 8.8	0.3	44.0	74.1	33.6	39.0	25.8
(144m)	-1.7± 4.1	5.4± 6.8	1.5	8.4	24.5	14.8	22.9	13.2
		Wind Stress (dynes/cm²)						
EB46008		0.76±1.9	0.61±2.0					

*All records 133 days except K8A (140m) which was 66 days. Observation period began in mid-October 1977.

TABLE 6

Current statistics in summer for the bank-trough region southeast of Kodiak Island, and mean alongshelf and cross-shelf wind stress for the current observation period. Mooring locations are indicated on Figure 9.

Mooring (meter depth)	Observed Speed (cm/s)		Horizontal Kinetic Energy Distribution (cm^2/s^2)					
			Alongshelf			Cross-Shelf		
	Alongshelf	Cross-shelf	Mean	Subtidal	Tidal	Mean	Subtidal	Tidal
			BANK					
K6B (32m)	9.6±3.0	12.6±4.8	45.9	17.6	120.2	78.9	11.4	40.3
(72m)	6.6±3.4	5.2±2.6	21.6	1.9	63.1	13.3	3.4	18.5
K7B (29m)	-0.8±4.5	9.0±5.3	0.4	9.9	113.2	40.2	14.0	44.9
			TROUGH					
K8B (30m)	17.6±7.1	-2.9±3.3	154.9	25.0	25.3	4.2	5.3	10.4
(75m)	10.8±4.5	-0.9±3.5	58.5	2.9	21.9	0.4	0.2	10.5
K9B (13m)	4.9±6.3	-0.8±8.1	11.9	19.7	81.4	0.3	32.4	43.5
(58m)	3.5±6.4	2.4±7.5	6.1	20.2	76.1	2.8	27.8	24.7
(142m)	1.5±2.4	3.7±3.1	1.1	2.8	8.8	6.9	4.8	15.8
K10B (24m)	2.1±4.6	4.3±4.9	2.2	10.4	47.9	9.1	12.1	16.2
(69m)	0.8±4.4	5.7±5.5	0.3	9.6	44.6	16.0	15.2	23.4
(149m)	-2.5±2.3	5.8±3.6	3.2	2.7	13.5	16.6	6.5	12.3
	Wind Stress (dynes/cm^2)							
EB46008	-0.18±0.5	0.04±0.4						

*All records are longer than 125 days, and commenced in late May 1978.

TABLE 7

Selected winter and summer current statistics from the lower Cook Inlet region and from the banks southeast of Kodiak Island. Mooring locations are indicated on Figures 7 and 8.

Mooring (meter depth) Record Length(d):Start	Observed Speed (cm/s)		Distribution of HKE (cm^2/s^2)					
			Alongshelf			Cross-Shelf		
	Alongshelf	Cross-shelf	Mean	Subtidal	Tidal	Mean	Subtidal	Tidal
NORTH ALBATROSS BANK								
WGC-2A (100m) 66:75265	25.7± 6.5	-0.40±2.9	330.30	21.0	39.1	0.1	4.3	84.5
WGC-2C (24m) 90:76070	21.8±12.7	0.70±5.6	237.60	80.7	116.1	0.3	15.8	80.5
63:76070 (104m)	24.4± 7.9	4.30±3.6	297.70	21.9	31.7	9.4	6.4	74.1
WGC-2D (20m)	3.0± 4.6	1.10±3.4	4.60	10.4	244.9	0.6	5.7	378.5
133:76160 (80m)	0.9± 2.1	-0.90±1.7	0.30	2.1	90.9	0.3	1.4	136.0
WGC-2E (20m) 156:76293	2.2± 9.7	0.60±6.6	2.50	47.5	303.0	0.2	21.6	478.5
WGC-2F (20m)	4.7± 5.5	-0.40±3.9	10.90	15.0	265.5	0.1	7.6	401.0
167:77084 (80m)	1.9± 2.8	-2.00±2.1	1.90	3.8	103.0	2.0	2.2	149.9
LOWER COOK INLET AND SHELIKOF STRAIT								
C-10 (65m) 151:77278	23.8±17.3	1.90±8.4	283.20	149.4	19.6	1.8	35.3	5.2
C-10B (70) 133:78148	11.9±11.0	-0.70±8.1	70.80	60.3	12.1	0.3	8.1	3.8
C-9B (66m) 133:78150	9.6±10.8	-0.40±4.9	46.10	58.9	1600.1	0.1	11.9	69.9
C-8B (63m) 133:78150	20.4±18.2	-4.70±8.2	208.10	165.8	1953.0	11.1	33.7	100.5
C-4 (65m) 150:77280	-1.3± 6.5	-0.70±6.3	0.90	21.2	40.9	0.3	19.8	373.4
C-4B (64m) 133:78150	0.5± 6.7	-1.20±5.4	0.02	16.3	32.8	0.8	16.1	348.0
C-3 (50m) 159:77280	-1.3± 4.2	-0.90±2.9	0.90	8.9	58.5	0.4	4.1	420.0
C-3B (50m) 93:78148	0.6± 4.1	-0.06±2.8	0.20	8.2	43.1	0.0	3.9	334.0

tidal. The alongshelf speeds were consistent during the observation periods of WGC2D and 2F, whereas during winter 1976-77, alongshelf flow was weaker and more variable. Over the bank, subtidal kinetic energy indicated a threefold variation between winter (WGC2E) and nonwinter records. We attribute this to increased meteorological forcing in winter.

Records from C8, 9, and 10 are representative of the Kenai Current (Table 7). Records from C10 and C10B indicate that during October 1977 to March 1978 (C10) both $\overline{KE}$ and KE' were substantially greater than during May to October 1978. This is consistent with our present understanding of coastal flow in the northwest Gulf of Alaska (Schumacher and Reed, 1980). A peak in baroclinic transport (and speed) occurred sometime in October-November; during this period, 7-day average flow down the axis of Shelikof Strait was observed to be as high as ~70 cm sec^{-1}. In December 1977 through February 1978, observed mean wind stress was ~1.2 dyne cm^{-2} in an alongshore direction. The resulting set-up and barotropic transport (and speed) resulted in 7-day average axial speeds in Shelikof Strait of 20 to 50 cm sec^{-1}. Winds from June-September 1978 did not contribute appreciably to transport, and the baroclinic field suggested transports 0.1 to 0.3 of those observed during peak freshwater addition in fall. Records from the entrances to Shelikof Strait (C8B and C9B) indicate that tidal frequencies dominated HKE. However, at lower frequencies and in a mean sense, there was a significant difference between the two entrances. $\overline{KE}$ was four times greater in Kennedy Entrance than in Stevenson Entrance. As suggested by Schumacher and Reed (1980), current records and hydrographic data indicate that the Kenai Current preferentially flows through Kennedy Entrance.

Within lower Cook Inlet proper (C3 and C4 series, Table 7), net flow was not significant in the total energy balance and tides dominated HKE estimates. We note that subtidal frequencies at both of these locations indicate a less dramatic change from winter (October 1977-March 1978) to summer (May to October 1978) than was observed over the banks. Estimated energy due to subtidal frequencies increased by 25 to 30% in lower Cook Inlet and three- to four-fold over the banks. Orographic effects on the wind field over Lower Cook Inlet appear to diminish seasonal trends, whereas over the banks a strong seasonal change was observed.

The most striking feature of the velocity field is that seasonal differences are small in mean speed components and, in several cases, statistically insignificant. HKE in all three frequency bands is greater in winter, a combination of a more energetic regime or perhaps rotor wave-induced noise. Various authors (e.g., Mayer et al., 1979; Halpern and Pillsbury, 1976) have concluded that rotor pumping can significantly affect speeds recorded by Aanderaa current meters. In order to determine whether the western Gulf current meter data set might be significantly contaminated by such wave-induced noise, successive 29-day harmonic tide analyses were performed for data from the summer (June, July, August) and winter (December, January, February). The following table shows the mean M_2 and standard deviations for those stations which had both summer and winter data at the 20-m depth.

TABLE 8

	C4	C10	WGC2	KG	K7	K8	K10	K.11
Winter Mean	35.2	4.7	30.5	7.4	6.8	2.7	3.8	45.8
S.D.**	.6	.6	.9	.7	.7	.7	.3	.6
Summer Mean	33.3	5.9	29.5	7.4	7.4	2.7	2.4	49.1*
S.D.**	2.8	1.2	2.4	.5	.4	.7	1.0	.8
Winter-Summer	1.9	-1.2	1.0	0	-.6	0	1.4	-3.3

*June-mid July only available
**S.D. = standard deviation.

mean M_2 speeds were computed by

$$A_1 = \frac{U_i^2+V_i^2}{2}^{\frac{1}{2}}$$

where U_i is the major axis M_2 amplitude and V_i is the minor axis amplitude for time period i. Five successive analyses were done for each season, with a 14-day overlap between segments. The A_i's were then averaged to produce the seasonal averages shown in the table.

If it is presumed that wave energy is much greater during the winter (and the windstress values shown in Tables 3 and 4 indicate that it is), then these results suggest that wave-induced noise does not significantly affect the speeds recorded from these data sets, at least on a seasonal average. The difference between these results and those of previous studies probably results from the fact that the subsurface float in our studies was deep enough (usually greater than 20 m) to prevent significant contamination by wave noise.

Over Middle Albatross Bank, HKE was greater near-shore (K6) than over mid-bank (K7), and cross-shelf mean HKE dominated in both seasons (Tables 5-6). Over Kiliuda Trough, a similar pattern occurred; however, the alongshelf mean HKE was dominant. Seaward of K8, current records suggest a dramatic change in velocity-field characteristics. Both tidal and subtidal HKE were larger than mean HKE.

3.5 Wind Observations

Winds over the ocean can be computed from surface pressure maps in conjunction with a boundary layer model. In general, surface winds are weaker than and aligned to the left of the computed geostrophic wind. Researchers have applied this technique with various degrees of sophistication and success. Agreement between computed winds and measured winds from data buoys are generally good except near the coastline, where a variety of additional physical processes become significant. For example, air flow in Lower Cook Inlet is predominantly down-gradient, that is, at right angles to the left of the geostrophic wind.

In the region of Albatross Bank, east of Kodiak, we found measurements from a data buoy approximately 60 km offshore agreed with calculations. We conclude that coastal influence on winds is not seen that far offshore. Lower Cook Inlet winds were completely dominated by the surrounding mountains.

3.5.1 Orographic Control

We have examined data from buoys located off the northeast Gulf of Alaska coast (EB33, EB45, EB72), Kodiak Island (EB46008, formerly EB49), and lower Cook Inlet (EB46007, formerly EB39), and found that within 50-100 km from shore the winds begin to align with the coastal mountains. The size of the mountain range affects this distance. Within about 25 km of the coast, smaller scale features, such as drainage winds, are felt.

The east coast of Kodiak Island is dominated by mountainous estuaries. Wind measurements from Kodiak and Kiliuda Bay confirm the presence of strongly bimodal winds aligned with the estuary axes. In the winter, these winds are predominantly offshore. However, NDBO buoy EB46008, located 60 km offshore, showed little coastal effect; its measurements agreed quite well with surface winds which were computed by the Fleet Numerical Weather Central facility. As the mountains of Kodiak are not particularly high, we expect their offshore effect to be correspondingly reduced; however, without other measurements we cannot determine the extent of reduction.

The wind field over lower Cook Inlet, on the other hand, is completely dominated by mountains. We have made a concentrated study of this region to better understand the processes active in such orographically controlled estuaries.

3.5.2 Lower Cook Inlet Meteorology

The mountainous borders of lower Cook Inlet form natural channels for the flow of air (Fig. 52). The major orographic axis extends from the Susitna Valley in upper Cook Inlet southward and into Shelikof Strait, and is oriented at about 30°T. This channel is bounded on the east by the Talkeetna and Kenai mountains and lesser ranges on Kodiak and Afognak islands. It is bounded on the west by the Alaska and Aleutian ranges. The only breaks in this mountainous barrier to air flow occur at Kennedy and Stephenson Entrances and at the Kamishak Gap, a region of relatively low elevation about 50 km wide between Lake Iliamna and Kamishak Bay.

Orographic Channelling. The prevalence of orographic channelling of winds in lower Cook Inlet is clearly seen in wind fabric diagrams (Davis and Ekern, 1977) constructed using data from environmental buoy EB-46007 (cf. Fig. 52 for buoy location). These diagrams are contoured plots indicating the relative concentrations of observations of wind speed and the direction from which the wind blows during a given month. The observations are 8-min means acquired once every 3 hours. Fabric diagrams for four representative months in 1978 are shown in Fig. 53. Lines have been drawn on the diagrams to indicate the directions of the four major orographic axes as seen from the

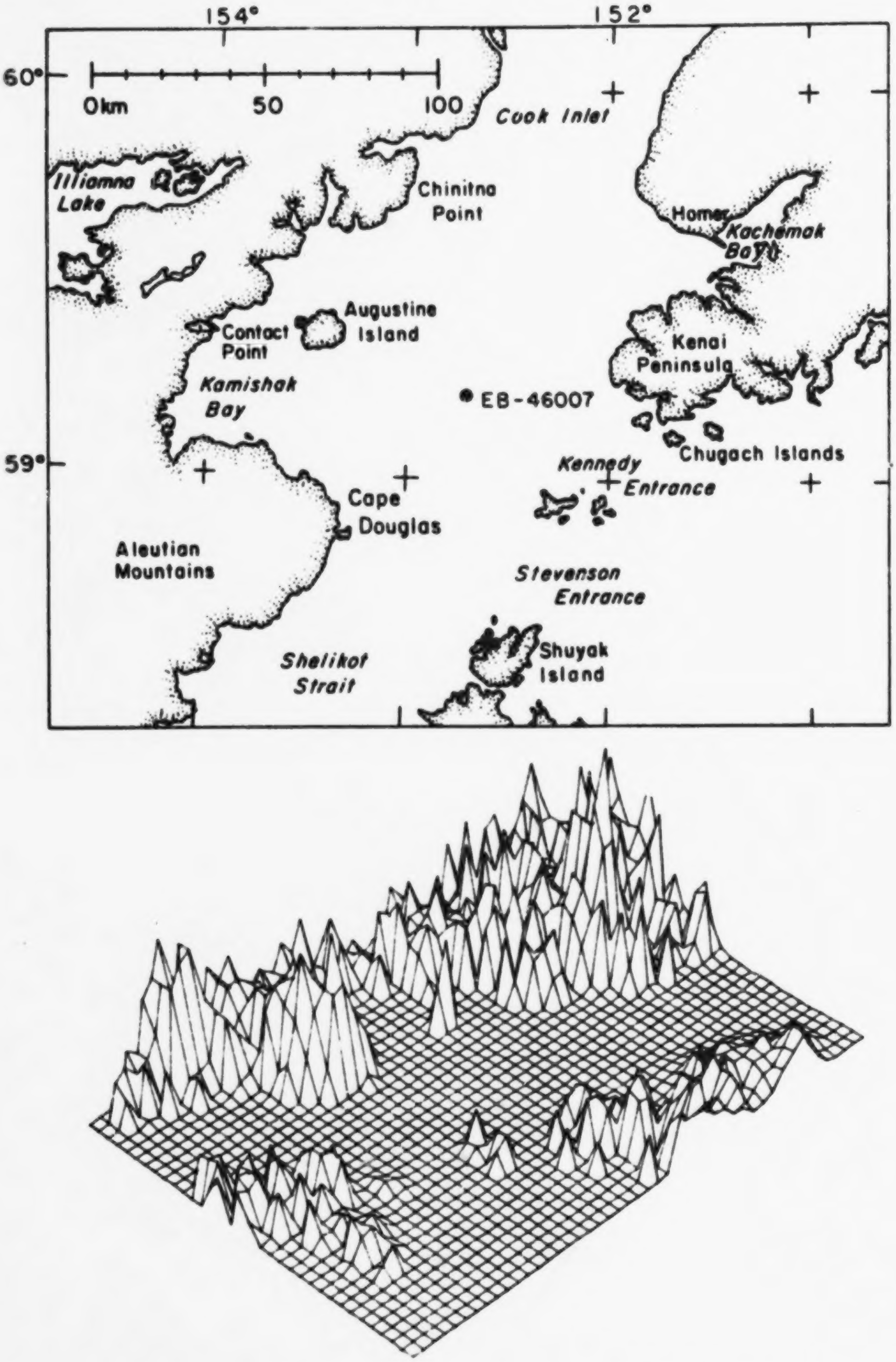
154°
152°
60°
59°
0km
50
100
Cook Inlet
Iliamna Lake
Chinitna Point
Homer
Kachemak Bay
Augustine Island
Contact Point
Kenai Peninsula
Kamishak Bay
EB-46007
Kennedy Entrance
Chugach Islands
Cape Douglas
Aleutian Mountains
Stevenson Entrance
Shelikof Strait
Shuyak Island

Figure 52. Geographical locations in the lower Cook Inlet region and (lower) a relief map of the same area. The black dot indicates the location of environmental buoy EB-46007.

BEST DOCUMENT AVAILABLE

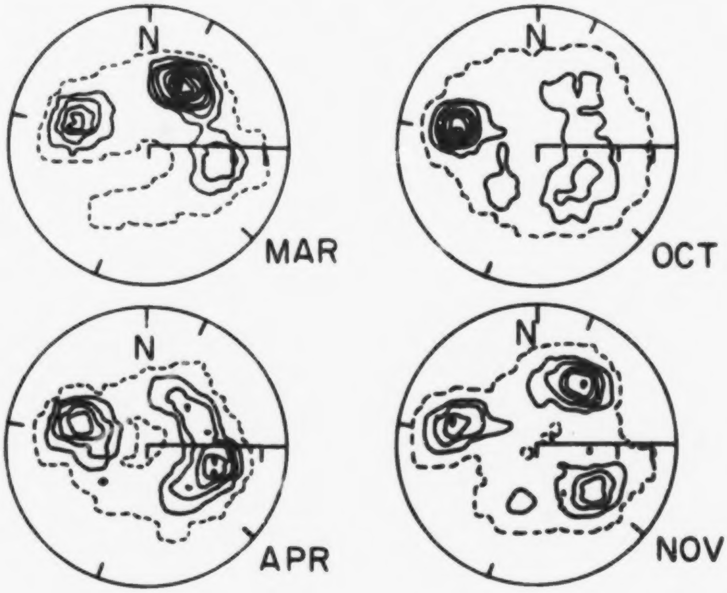

Figure 53. Wind fabric diagrams for EB-46007 in lower Cook Inlet for four months in 1978. The four tic marks on each circle represent the directions of the four channel axes: upper Cook Inlet; Kennedy and Stevenson entrances; Shelikof Strait; and the Kamishak Gap.

buoy. The contours are in intervals of 2% of the observations per percent of the plot area. In March winds were persistently from upper Cook Inlet and closely aligned with the Inlet axis. In April winds blew in both directions through the Kamishak Gap-Kennedy Entrance channel and to a lesser extent from Kachemak Bay and the upper Cook Inlet. In October, winds were almost exclusively from the Kamishak Gap; in November winds originated from all four of the intersecting channels. Little wind was observed from the northwest or southwest, due to the blocking action of the Alaskan and Aleutian ranges.

Though the 4 months that are shown exhibit orographic channeling particularly well, all data obtained show this channeling effect. Given the four major intersecting channels, it is possible to define a minimum of 16 possible flow patterns. Of these, the two which appear most likely to occur are those resulting from the synoptic scale pressure distribution and from interior drainage winds, especially from the Susitna Valley which enters upper Cook Inlet.

Pressure Gradient Forcing. The Geostrophic wind is given by

$$u_g = -\frac{1}{\rho f}\frac{\partial p}{\partial y}$$

$$v_g = \frac{1}{\rho f}\frac{\partial p}{\partial x}$$

where u_g and v_g are the east-west and north-south components of the geostrophic wind, ρ is the air density, f is the Coriolis parameter, and $\frac{\partial p}{\partial x}$ and $\frac{\partial p}{\partial y}$ are the east-west and north-south pressure gradients.

At least three stations are needed to establish the two-dimensional pressure gradient. If more stations are available a plane may be fitted to the observations using multiple regression techniques. The equation

$$p = ax + by + c$$

is fit where x and y are the positions of each station. The pressure gradients are then

$$\frac{\partial p}{\partial x} = a \quad \text{and} \quad \frac{\partial p}{\partial y} = b$$

If curvature in the pressure field is judged significant, higher order equations may be used. The second order equation is

$$p = a_0 + a_1x + a_2y + a_3x^2 + a_4y^2 + a_5xy,$$

for which a minimum of six stations are required. However, for most applications many more than six stations are needed to adequately define the second order pressure field.

In this study we have used a first-order fit with only three stations: Anchorage, Kodiak, and King Salmon. We would have liked to have used Iliamna, but it reports irregularly and, in addition, a 2-mb bias was found in pressure readings reported for March-June 1978. It was felt that the three chosen stations were spaced around the lower Cook Inlet (Fig. 12) to give a reliable and representative network for determining the regional pressure gradient. There are undoubtedly small-scale gradients that are unresolved by such a widely spaced network. These three stations will also be inadequate when the pressure field is highly curved, for we are assuming that it is well represented by a plane.

The geostrophic wind was determined for 7 months in 1978 and 1979. The hourly pressure readings were filtered with a 3-h triangular filter and sampled every 3 hours. These pressures were then fit with a plane to determine the pressure gradients.

In Figure 54 the direction of the geostrophic wind is plotted against that of EB-46007 for the spring (March through June) and for the winter (November through January). Only points for which the geostrophic wind is

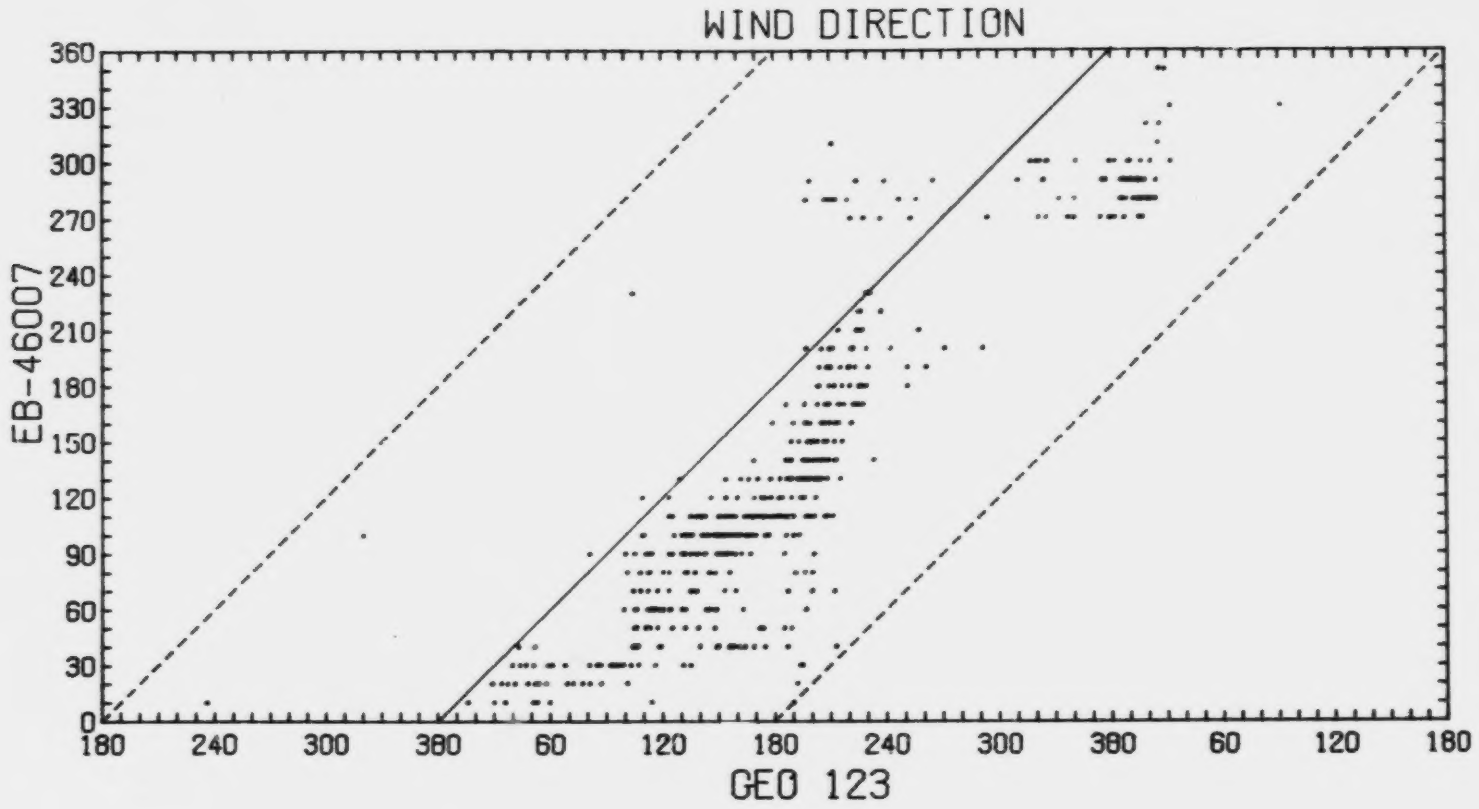

Figure 54. Wind direction at environmental buoy EB-46007 in lower Cook Inlet compared to direction of the geostrophic wind for cases where the geostrophic wind speed was greater than 5 m sec^{-1}.

BEST DOCUMENT AVAILABLE

greater than 5 m sec^{-1} are plotted. The solid line indicates winds which are from the same direction (i.e., the buoy winds are parallel to the isobars); points to the right of the line indicate a component of buoy winds down the pressure gradient, while those to the left indicate a countergradient component.

These figures show clearly the ambiguity often seen in the relation between geostrophic and surface winds in orographically dominated sites; a wide range of surface winds is observed for a given geostrophic wind. For example, with the geostrophic wind from 180° the observed buoy wind can come from virtually any direction. The apparent countergradient flow out of Kamishak Gap may be the result of poor estimation of the local pressure gradient from the three widely spaced stations. Alternately, the pressure field in the Bering Sea could drive air through the Iliamna Gap into lower Cook Inlet and against the pressure gradient there. We have not found that the regional pressure gradient is a good predictor of the local winds. It should be noted, however, that in virtually all cases when the geostrophic wind direction was from 270°-0° in the March-June period or from 240°-40° in the November-December period, westerlies from the Iliamna Gap occurred.

Drainage Winds. Given the presence of adjacent continental land masses whose interior regions are occupied during winter by cold dense air masses, we suspect that drainage or katabatic winds might play an important role in the local wind field in lower Cook Inlet. The magnitude of such winds is dependent upon the cold air reservoir, the external large-scale pressure field and local topographic focussing. These flows are generally colder than the surrounding air and therefore flow beneath the ambient air overlying the water. The distance offshore to which the flow persists depends upon the water-air heat flux and upon the stability of the overlying air. By far the major winter wind feature in lower Cook Inlet is the drainage wind from the Susitna Valley (Fig. 53), which is supplied by a dominant inland high pressure region to the north.

On a smaller scale, drainage winds appear off virtually every glacier and river valley which enters lower Cook Inlet. An example of such a flow was observed in the vicinity of Cape Douglas (Fig. 55), with the wind originating from 2100-m Mt. Douglas and funneling out of a small valley. Width of both the valley mouth and the flow offshore was about 2 km. Vertical potential temperature profiles obtained within this flow and from nearby undisturbed air over northern Shelikof Strait showed similar structure above about 300 m (Fig. 56). The profile off Cape Douglas exhibited, however, a stable layer which was eroded by sea-air heat flux from the surface to a height of 200 m during its passage from the coastline to a point about 10 km offshore. Environmental buoy EB-46007, located about 40 km off this valley, did not reflect the presence of this flow. In general, the buoy data suggest that katabatic flow seldom, if ever, attains the central part of lower Cook Inlet.

Kachemak Bay, across the lower inlet from Cape Douglas, often exhibits drainage winds because several glaciers terminate at its head. At times, these drainage winds resulted in strong ENE winds at Homer, while winds observed at EB-46007 in the lower inlet were westerly. Shipboard observations suggest that the drainage winds in Kachemak Bay are confined to the southern portion of the bay mouth and seldom persist beyond about 20 km from the bay mouth.

BEST DOCUMENT AVAILABLE

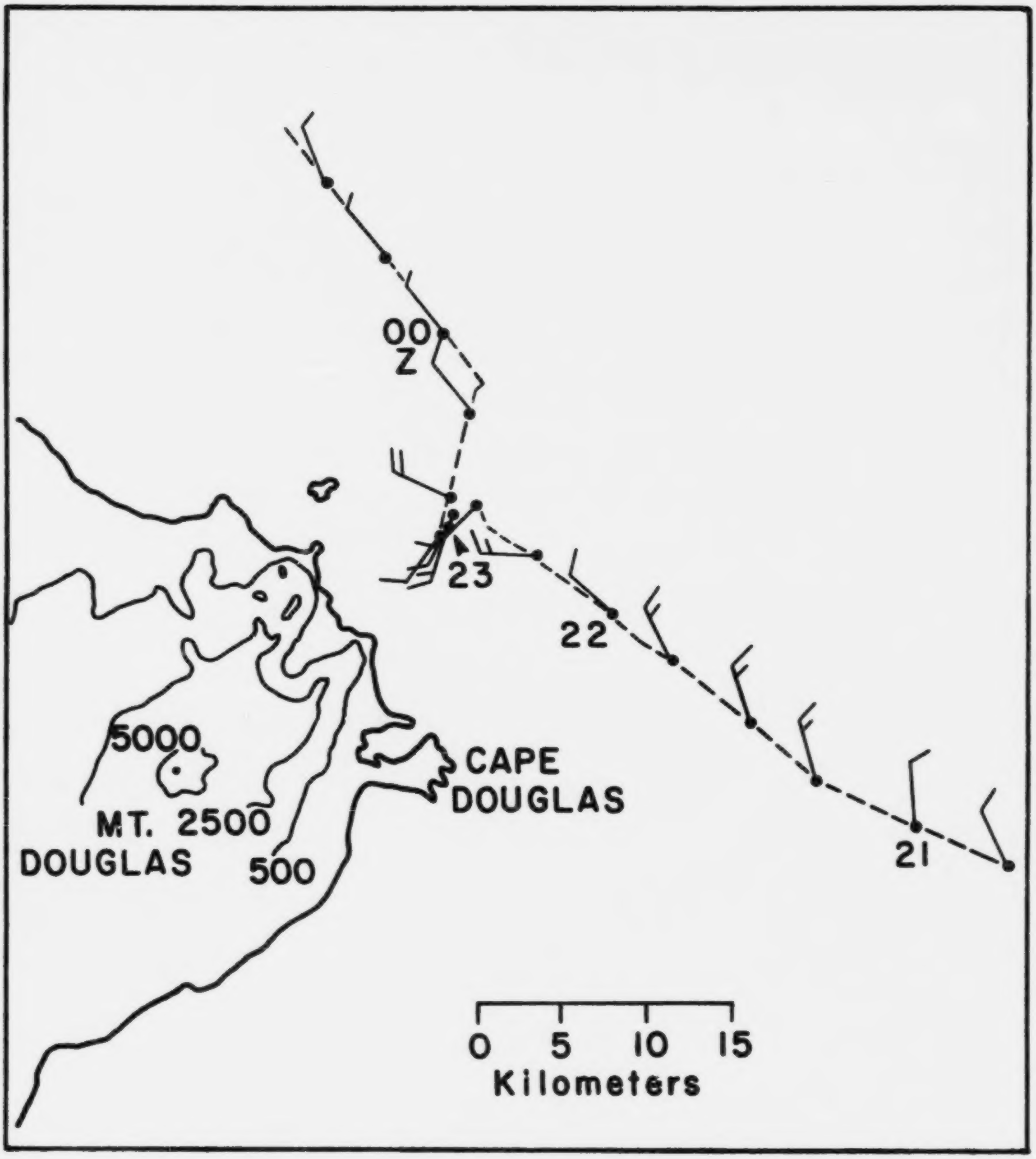
00
Z
23
22
21
CAPE
DOUGLAS
5000
MT. 2500
DOUGLAS
500
0 5 10 15
Kilometers

Figure 55. Observations of surface wind velocity in the vicinity of Cape Douglas, lower Cook Inlet, on 17-18 March 1978. Katabatic flow extended offshore from a mountain valley. Elevation contours are in feet above mean sea level.

BEST DOCUMENT AVAILABLE

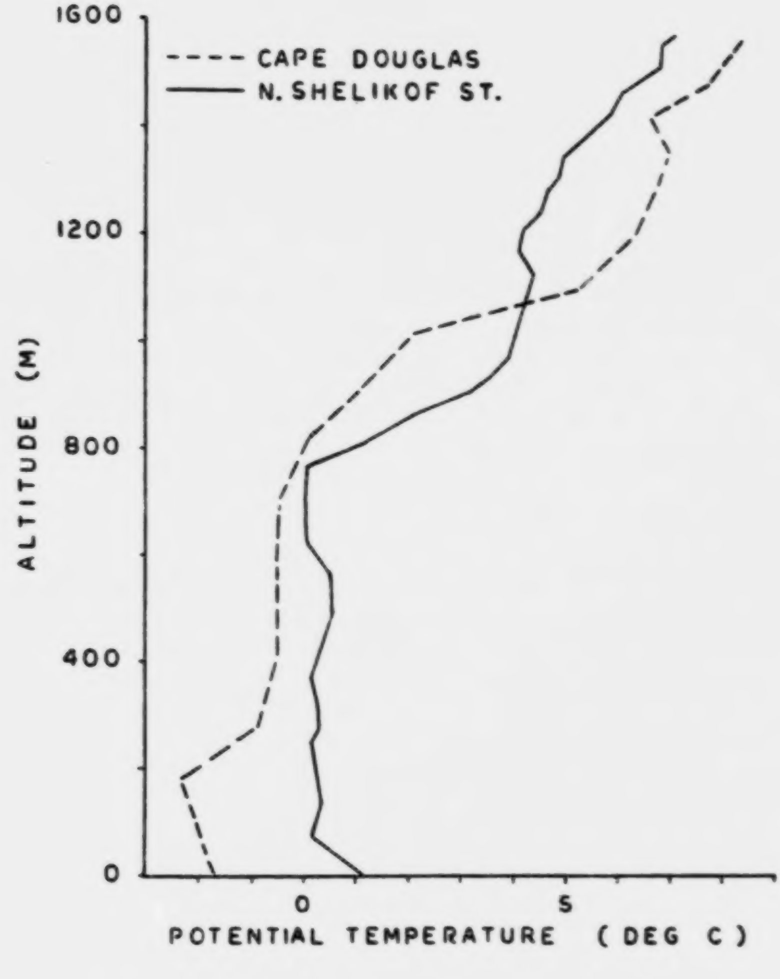

Figure 56. Comparison of vertical potential temperature profiles from airsonde ascents near Cape Douglas and over northeastern Shelikof Strait. A remnant katabatic layer was evident below about 300 m in the sounding from Cape Douglas.

Wake Effects. Given the large vertical relief of land masses surrounding lower Cook Inlet, we would a priori expect to see localized effects of certain of these masses on the air flow. An exceptional example is provided by Augustine Island, which presents a 1300-m high cone-shaped obstacle to local air flow at the eastern edge of Kamishak Bay (Fig. 52). Theoretical and laboratory studies of flow past a cylinder (Hinze, 1959; Batchelor, 1967) have shown that the imposed pressure and velocity distributions generate vortical flow in the lee of the cylinder. Flow on the lee side of an isolated mountain would be expected to show similar characteristics. This supposition was borne out by Scorer (1967), who found that wake effects were present and that the arc sector defining the wake within which lee waves are apparent may vary from 10°-70°. Amplitude of the lee wave disturbances decreases rapidly with increasing height and with distance downstream from the obstacle.

During a period of NNW winds in the lower Inlet, the free stream wind had speeds from 3 to 8 m sec^{-1} and directions from 320-020°T. Assuming a disturbed downstream arc sector of 70° and considering the directional range of the free stream winds, all observed winds to 03 GMT depicted on Figure 57 could be categorized as wake flow. No such confused flow was encountered prior to a station occupation at about 02 GMT some 4 km offshore. Here, in an hour's time and within an area of 2 km^2, wind direction was observed to vary over nearly 360°, suggesting the presence of vortical flow induced by the mountain.

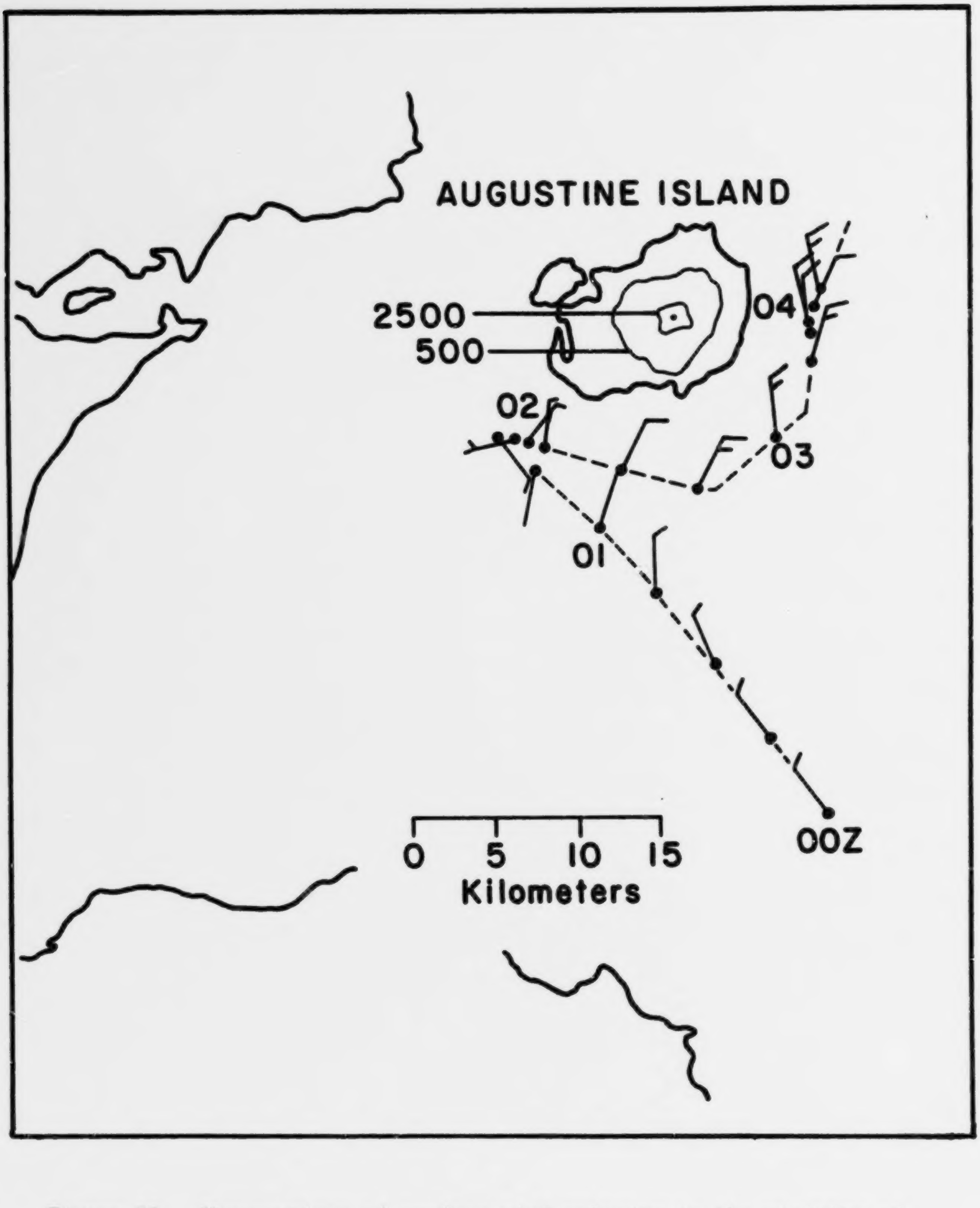
AUGUSTINE ISLAND
2500
500
04
02
03
01
00Z
0 5 10 15
Kilometers

Figure 57. Observations of surface wind velocity in the vicinity of Augustine Island on 18 March 1978. Variable winds at about 02 Z suggest that vortical flow was present in the lee of Mt. Augustine. A quarter flag on the vector shaft designates wind speed below 1.5 m sec^{-1}.

Summary and Conclusion. Winds in lower Cook Inlet are orographically funneled through two perpendicularly oriented channels defined by upper Cook Inlet-Shelikof Strait and Kamishak Bay-Stevenson Entrance. Specific flow patterns appear in most cases to be triggered by the larger scale pressure gradient, though the relationship between geostrophic winds and observed winds is weak and poorly understood at present. Within 20 km of shore, drainage winds emanate from glacier and river valleys. These winds are nearly continuously occurring, but are quickly eroded over water by the sea-air heat exchange. On a yet smaller scale, vortical circulation has been observed in the lee of Augustine Island, a major, centrally located topographic feature in the lower Inlet.

In an effort to provide a more realistic wind input to oil spill trajectory models, we drew surface wind patterns for the lower Cook Inlet based on the weather types of Putnins (1966). Putnins determined 22 different generalized weather classifications for Alaska based on 18 yr of daily synoptic weather charts. For each type he reproduced a representative surface weather chart. For each weather chart, we drew a sketch of what our interpretation of the wind patterns in the lower Cook Inlet would be. This interpretation was based on the data we have analyzed and on our experience in the area. It was, of necessity, tentative and subjective.

The twenty-two wind patterns could be reduced reasonably to five. These five patterns, labeled I through V, are found in Figures 58-62. The wind speeds are indicated in m sec^{-1}. The major guiding principle in the formulation of these patterns is that the wind is predominantly channeled by the orography of the region. We have good evidence that this is true from EB-46007. We have also noted examples where this was not apparently the case, in which the winds seem to be passing across the Kenai Mountains.

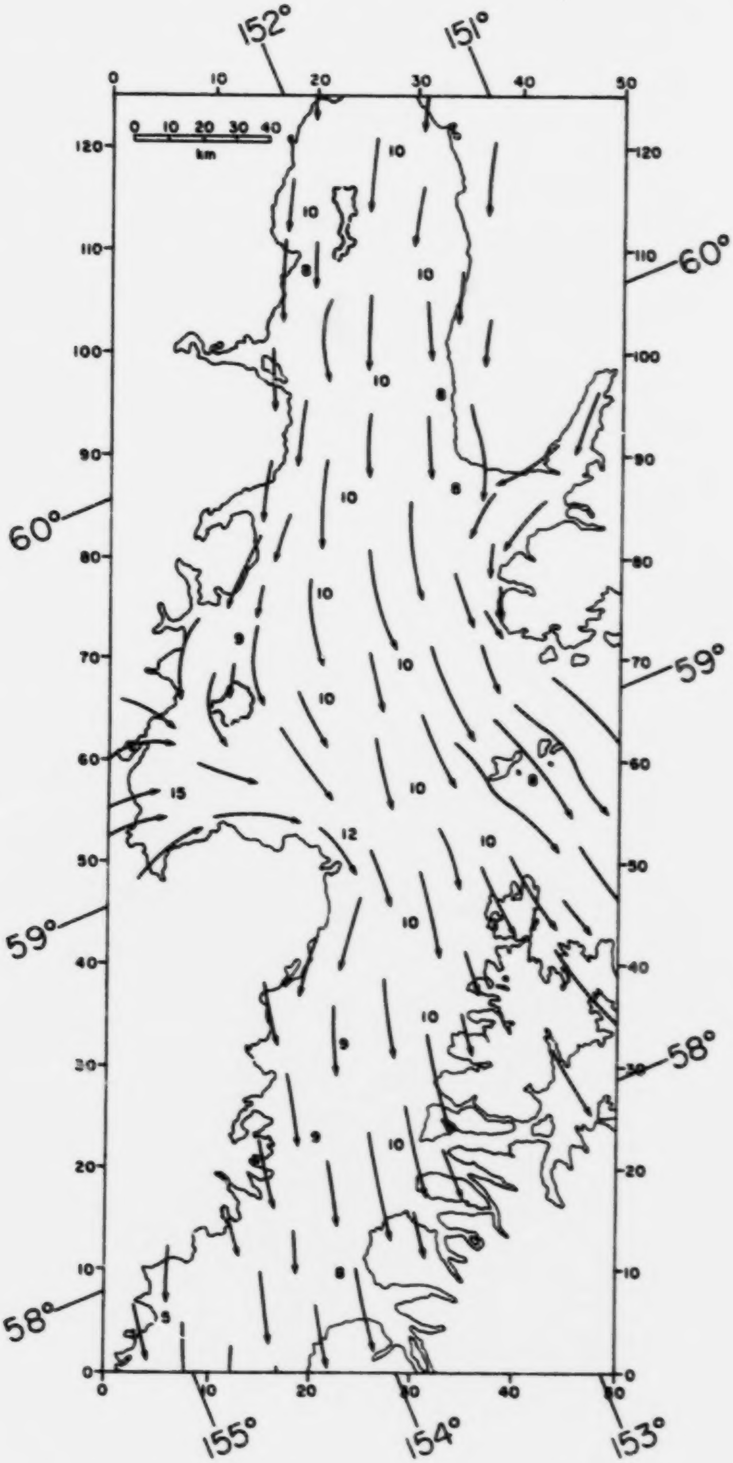

152°
151°
60°
60°
59°
59°
58°
58°
155°
154°
153°
0 10 20 30 40
km
0
10
20
30
40
50
60
70
80
90
100
110
120
10
10
10
8
10
10
8
10
8
10
10
9
10
10
15
12
10
10
8
10
10
10
9
9
10
8
5

Figure 58. Map I of Putnins' wind type for lower Cook Inlet.

BEST DOCUMENT AVAILABLE

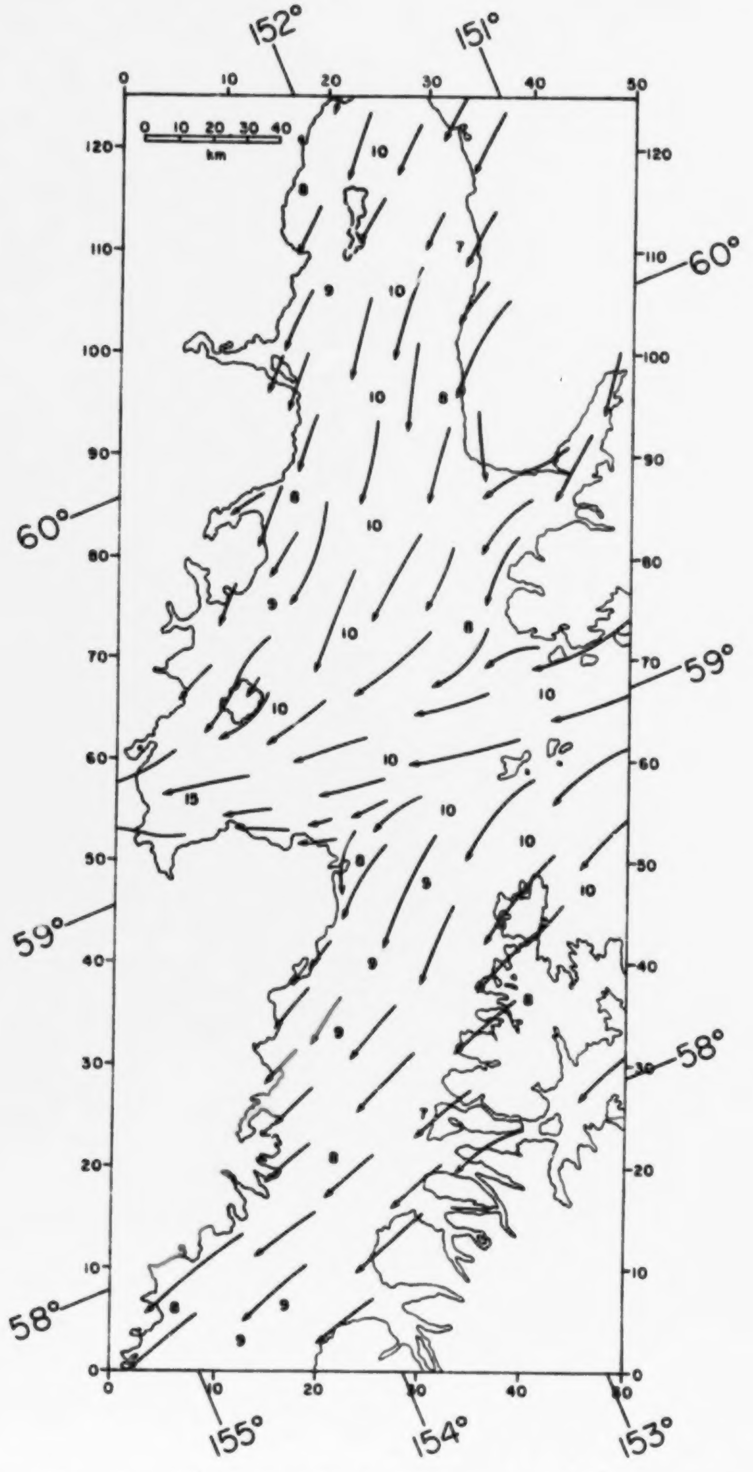
152°
151°
60°
60°
59°
59°
58°
58°
155°
154°
153°
0 10 20 30 40
km
0
10
20
30
40
50
60
70
80
90
100
110
120
10
9
7
15
8

Figure 59. Map II of Putnins' wind type for lower Cook Inlet.

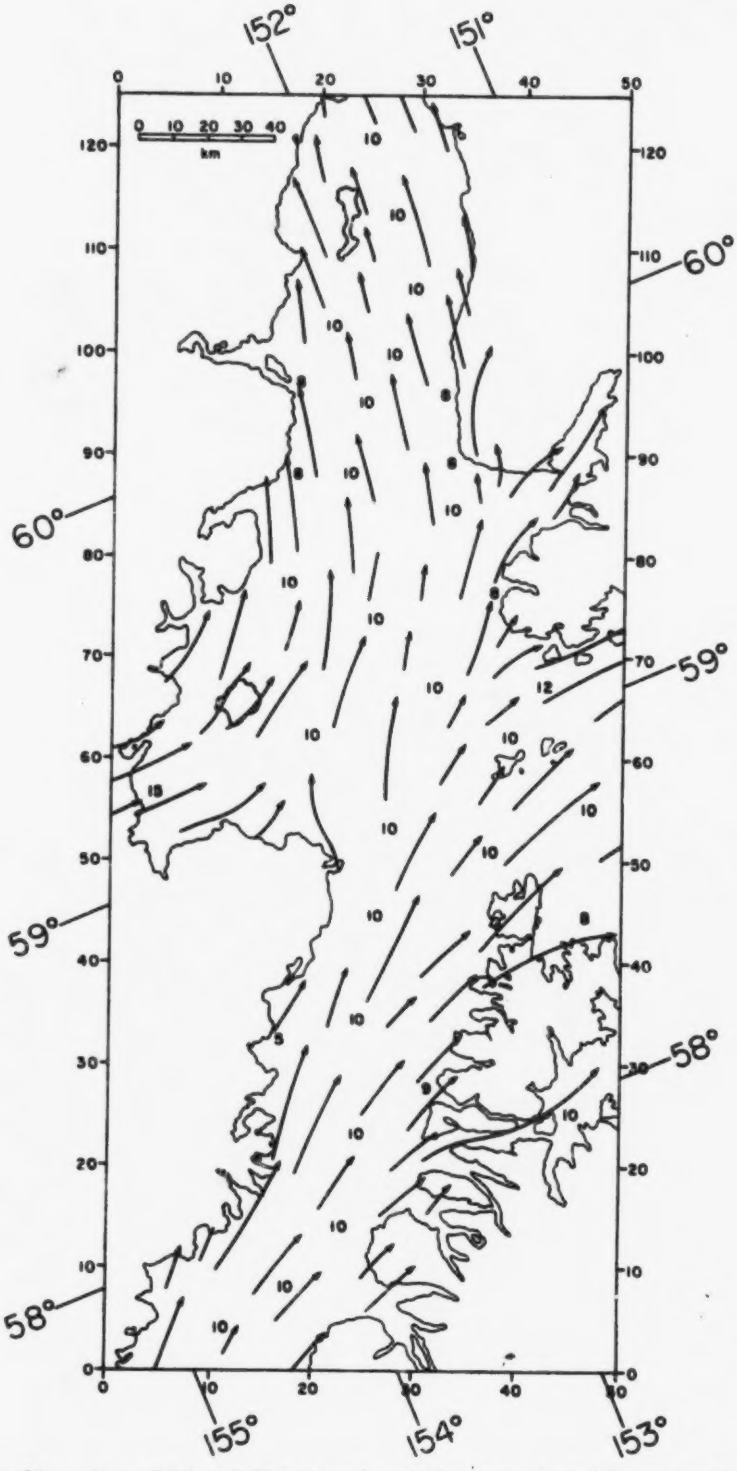
152°
151°
0
10
20
30
40
50
0 10 20 30 40
km
120
110
100
90
80
70
60
50
40
30
20
10
60°
59°
58°
155°
154°
153°
10
8
12
15
5

Figure 60. Map III of Putnins' wind type for lower Cook Inlet.

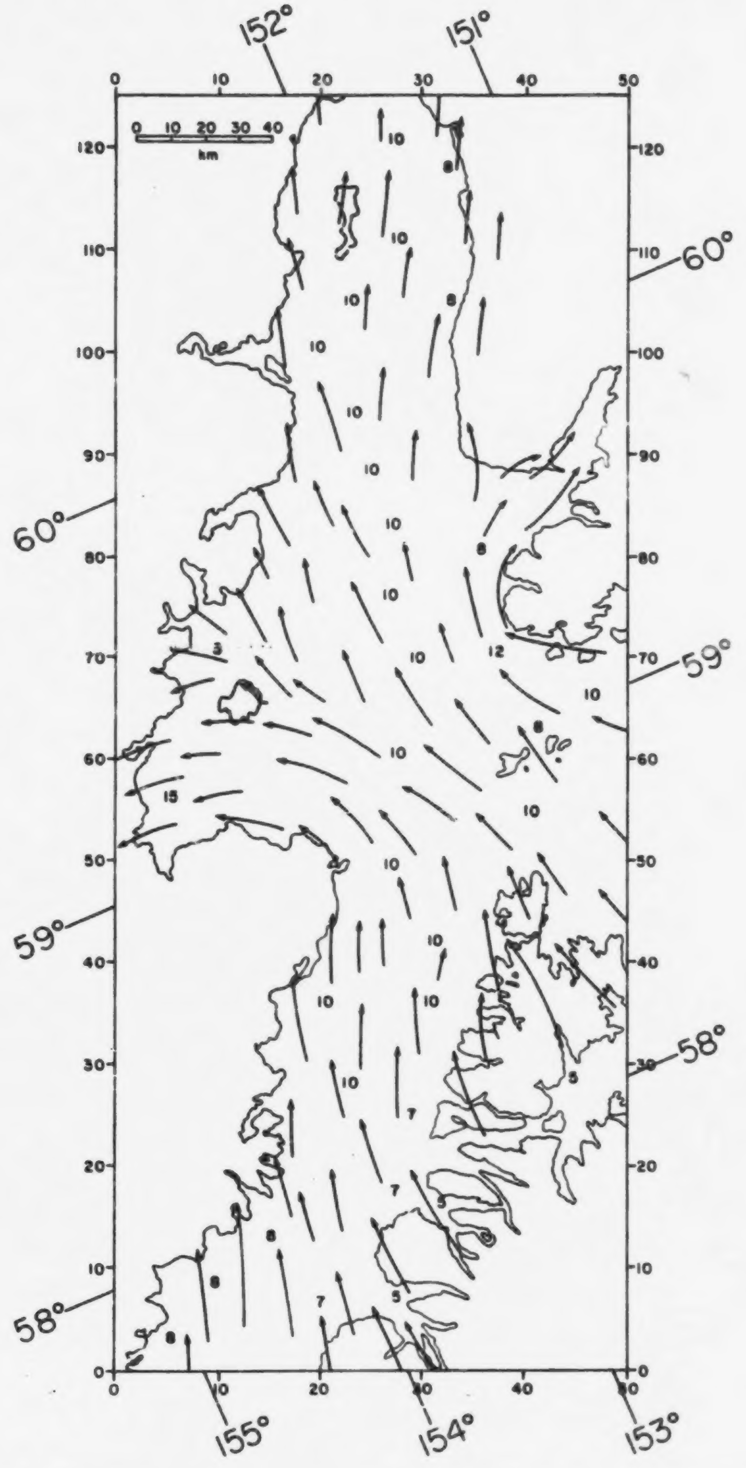
152°
151°
60°
59°
58°
155°
154°
153°
0
10
20
30
40
50
60
70
80
90
100
110
120
0 10 20 30 40
km

Figure 61. Map IV of Putnins' wind type for lower Cook Inlet.

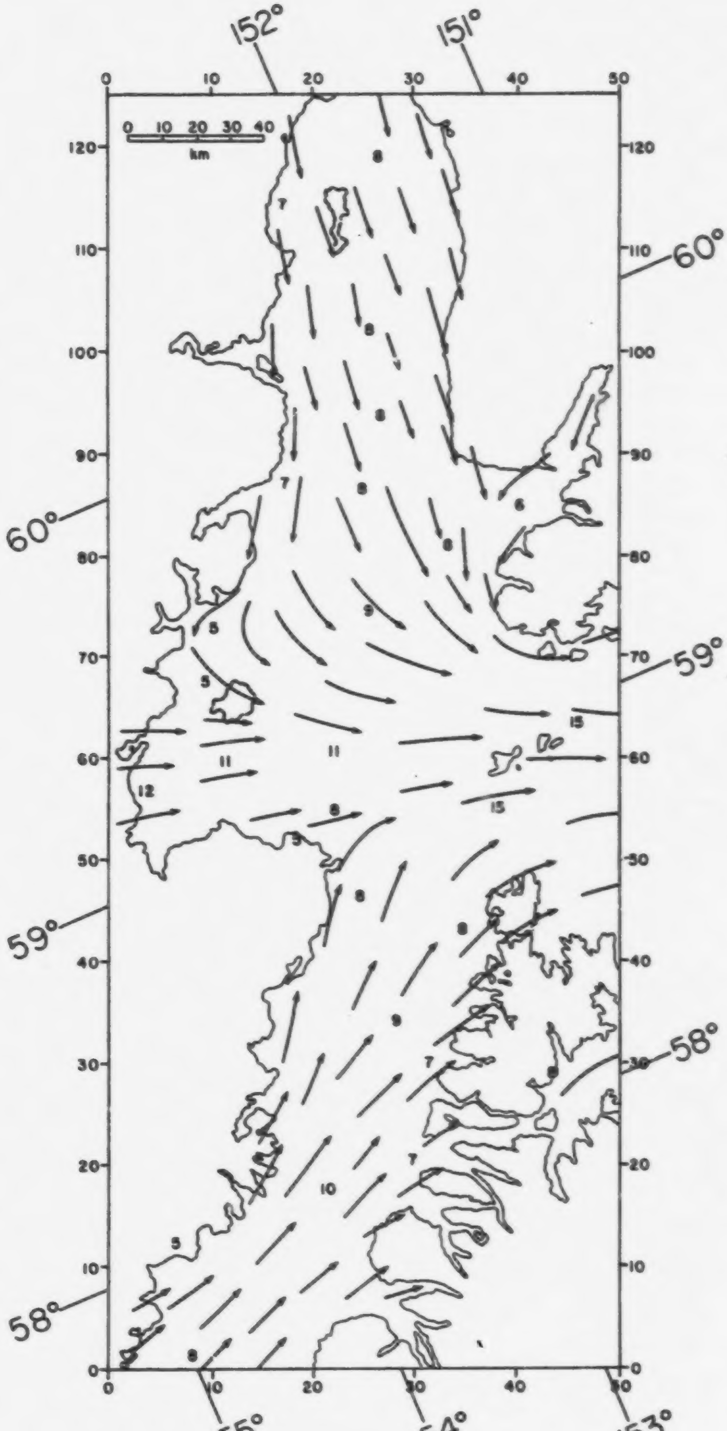
152°
151°
60°
59°
58°
155°
154°
153°
0 10 20 30 40
km
0
10
20
30
40
50
100
110
120
11
12
15
10

Figure 62. Map V of Putnins' wind type for lower Cook Inlet.

There are undoubtedly many situations which would not be well approximated by one of the five patterns, but nevertheless we feel these patterns show the dominant winds.

Each of Putnins' types is assigned a wind pattern map and a scaling factor for the wind speeds in Table 9. In Table 10 the Putnins types associated with each map are listed with their annual percentage occurrence and the total annual percentage occurrence for each map.

An approximate transition matrix was compiled from Putnins' report. He lists the number of times each classification was followed by each of the other classifications on a month-by-month basis for the 18 yr of records. For example, in January type D (101 occurrences) was repeated 73 times, when followed by type E_1 6 times, by type E 5 times, and by type H 4 times. The compilation was somewhat incomplete in that Putnins ignored sequences that occurred rarely. We summed these monthly figures to give the total number of occurrences of each sequence for the whole 18 yr of record. This matrix was then normalized to give the percent probability of each type following each other type (Table 11).

The above scheme provided a transition matrix based on a long historical record. The study by Putnins was the only one available. There are, however, a number of weaknesses to this approach, especially when applied to the lower Cook Inlet region alone. First, each of Putnins' classifications includes a broad range of different weather situations that may produce quite different local winds. The synoptic map reproduced by Putnins for each type is nothing more than a representative sample, and it cannot be presumed that all situations of the same type will produce similar winds in lower Cook Inlet even though that is our working assumption. It is a bit disheartening to note that the most common type, A', has the least well defined pressure gradients

TABLE 9

Assignation of Putnins' wind types according to patterns (cf. Fig. 58-62), and scaling factors for wind speeds

Type	Map	Scaling Factor
A	II	1.5
A	II	1.5
A^{c}	V	1.0
A''	III	1.0
A'''	IV	1.0
A_1	I	1.5
A_2	IV	1.0
A_3	III	0.3
B	I	1.0
C	II	0.5
D	II	1.0
D'	I	1.5
D_1	II	1.0
E	IV	0.5
E'	IV	0.5
E''	II	0.5
E_1	V	0.5
E_1'	IV	0.5
F	III	1.2
F_1	II	1.0
G	V	1.0
H	I	1.0

TABLE 10

Putnins' wind types associated with each map (Fig. 58-62), annual percentage occurrence of each type, and total annual percentage occurrence for each map

Map	Types and % Annual Occurrence							Total %
I	A_1	B	D'	H				
	6.7	1.0	1.2	7.1				16.0
II	A	A_c	C	D	D_1	E''	F_1	
	7.5	3.7	1.3	6.3	3.6	0.8	0.7	23.9
III	A''	A_3	F					
	5.2	1.1	1.1					7.4
IV	A'''	A_2	E	E'	E_1'			
	1.6	5.9	6.3	8.2	5.3			27.3
V	A'	G	E_1					
	23.2	1.0	1.0					25.2

BEST DOCUMENT AVAILABLE

TABLE 11

Normalized matrix showing the percent probability of each of the Putnins' wind types following each other type.

	A	A'	A''	A'''	A_1	A_2	A_3	A_c	B	C	D	D'	D_1	E	E'	E''	E_1	E'_1	F	F_1	G	H
A	50.7	36.0	4.1		1.1			1.9					1.4	0.5	1.1			2.2				
A'	3.8	68.2	6.0	0.4	7.6	4.5	0.5	1.0						0.7	1.5			1.2				4.6
A''			13.0	39.1		15.3				10.8		4.3	6.6	10.9								
A'''			13.0	39.2		15.2				10.9		4.3		6.5	10.9							
A_1		15.5			50.3	0.7			0.7	5.5	6.9		1.4		3.8			0.7		1.4		13.1
A_2	6.2	21.8	1.9		1.9	49.8		1.2			1.2			1.9	13.8			0.8				1.5
A_3		14.3				20.0	65.7															
A_c	3.5	34.5			6.5	1.7		50.4													1.7	1.7
B		25.0	35.0						20.0					20.0								
C		22.5		6.5	10.0	6.4			6.4	35.4		6.4		6.4								
D							0.6				71.4		1.9	8.2	8.2			5.0		1.6		3.1
D'			5.7		5.7	5.7					11.4	48.6	8.6	8.6	5.7							
D_1	11.4	3.6			1.8								59.6		2.5			1.8				19.3
E	10.0	13.7	4.7	2.3		2.0								40.5	17.6			9.4				
E'	1.7	4.1	1.2		0.5	7.0					6.0		1.2	19.2	54.0	0.5		4.6				
E''																50.0		25.0				25.0
E_1		42.9															57.1					
E'_1	18.2	24.0				1.8		3.1					1.3	7.6	5.8			38.2				
F					26.7	13.4							13.4						46.5			
F_1	50.0																		50.0			
G					100.0																	
H	1.7	16.1			5.8	1.6		5.0					9.8		1.7			3.6				54.7

in the lower Cook Inlet area and is most subject to allowing small changes in the positions of low pressure centers to produce large local wind changes. Furthermore, we have only a limited basis for assigning local wind conditions based on a specific baric situation. Finally, and of the least consequence, the transition matrix determined from Putnins' compilation of monthly sequences was not complete and produced some distortion of the overall frequency of occurrence. For example, type A' occurred 23.2% of the time, while the transition matrix is based on an occurrence of 27.3% of the time.

6. ACKNOWLEDGEMENTS

We acknowledge the aid of a large number of persons, not only in the preparation of this document but in carrying out the field work and analyses which have led to its existence. Of these, special thanks must go to the officers and crews of the research vessels DISCOVERER, SURVEYOR, ACONA, MOANA WAVE and MILLER FREEMAN for laboring under less than ideal conditions to carry out an ambitious field program; the first of this magnitude ever undertaken in these stormy waters. Lynn Long, Sharon Wright, Sally Dong, Cindy Loitsch, Jean Chatfield, Phyllis Hutchens, Joy Golly, and Gini May Flake of NOAA/PMEL are due thanks, also, for their help in analyzing the data and preparing the document. Dr. Tom Royer of the University of Alaska and Mr. Ronald K. Reed of PMEL/NOAA have contributed suggestions which have aided preparation of the manuscript. This study was supported in part by the Bureau of Land Management through interagency agreement with the National Oceanic and Atmospheric Administration, under which a multiyear program responding to needs of petroleum development of the Alaskan continental shelf has been managed by the Outer Continental Shelf Environmental Assessment Program (OCSEAP) Office.

7. REFERENCES

Barrick, D. E., M. W. Evans, and B. L. Weber (1977): Ocean surface currents mapped by radar. Science, Vol. 198, 138-144.

Batchelor, G. K. (1967) An Introduction to Fluid Dynamics. University Press, New York, N.Y., 615 pp.

Brower, W.A., Jr., H. F. Diaz, A. S. Prechtel, H. W. Searby, and J. L. Wise (1977) Climatic Atlas of the Outer Continental Shelf Waters and Coastal Regions of Alaska, Vol. 1, Gulf of Alaska. NOAA/OCSEAP Final Rept. Ru No. 347 (unpublished manuscript). 439 pp.

Burbank, D. C. (1977) Circulation studies in Kachemak Bay and lower Cook Inlet, Alaska. Dept. of Fish and Game, Anchorage, AK (unpublished manuscript). 207 pp.

Charnell, R. L. and G. A. Krancus (1976) A processing system for Aanderaa current meter data. NOAA Tech. Memo. ERL-PMEL 6, NOAA, Boulder, CO. 50 pp.

Davis, B. L. and M. W. Ekern (1977) Wind fabric diagrams and their application to wind energy analysis. J. Appl. Meteor., 16: 522-531.

Dodimead, A. J., F. Favorite and T. Hirano (1963) Review of oceanography of the subarctic Pacific region. Bull. Int. N. Pacific Fish. Comm., 13: 1-195.

Favorite, F. (1964) Drift bottle experiments in the northern North Pacific Ocean, 1962-1964. J. Oceanog. Soc. Japan, 20: 160-167.

Favorite, F. (1967) The Alaskan Stream. Bull. 21, Int. N. Pac. Fish. Comm., Vancouver, B. C. 1-20.

Favorite, F. and D. M. Fisk (1971) Drift bottle experiments in the North Pacific Ocean and Bering Sea 1957-60, 1962, 1966, and 1970. NOAA/ NMFS Data Rep. 67, U.S.D.O.C., Washington, D. C. 20 pp.

Favorite, F., A. J. Dodimead and K. Nasu (1976) Oceanography of the subarctic Pacific region, 1960-1972. Bull. Int. N. Pacific Fish. Comm., 33: 1-187.

Favorite, F. and W. J. Ingraham (1977) On flow in the northwestern Gulf of Alaska, May 1972. J. Oceanog. Soc. Japan, 33: 67-81.

Gatto, L. W. (1976) Baseline data on the oceanography of Cook Inlet, Alaska. Rept. 76-25, U. S. Army Cold Regions Res. and Eng. Lab., Hanover, N.H. 84 pp.

Halpern, D., and R. D. Pillsbury (1976) Influence of surface waves on subsurface current measurements in shallow water. Limnolog. and Oceanog., 21: 611-616.

Hayes, S. P. (1979) Variability of current and bottom pressure across the continental shelf in the Northeast Gulf of Alaska. J. Phys. Oceanog., 9: 88-103.

Hayes, S. P. and J. D. Schumacher (1976) Description of wind, current and bottom pressure variations on the continental shelf in the northeast Gulf of Alaska from February to May 1975. J. Geophys. Res., 81: 6411-6419.

Hinze, J. O. (1959) Turbulence. McGraw-Hill, New York, N.Y., 586 pp.

Holbrook, J. R., R. D. Muench and G. A. Cannon (1979) Seasonal observations of low-frequency atmospheric forcing in the Strait of Juan de Fuca. Proc. Fjord Oceanog. Workshop, Plenum Press, New York, 305-317.

Ingraham, W. J., A. Bakun and F. Favorite (1976) Physical oceanography of the Gulf of Alaska. Environmental Assessment of the Alaskan Continental Shelf, 11, NOAA/ERL, Boulder, CO. (unpublished manuscript).

International Hydrographic Bureau (1966) Tides, Harmonic Constants. Spec. Publ. No. 26, Monaco. 260 pp.

Jacobs, W. C. (1951) The energy exchange between the sea and atmosphere and some of its consequences. Bull. Scripps Inst. Oceanog., 6: 27-122.

Kinney, P. J., D. K. Button, D. M. Schell, B. R. Robertson and J. Groves (1970a) Quantitative assessment of oil pollution problems in Alaska's Cook Inlet. Rept. R-169, Inst. Mar. Sci., Univ. of Alaska, Fairbanks. 125 pp.

Kinney, P. J., J. Groves and D. K. Button (1970b) Cook Inlet environmental data, R/V Acona cruise 065 - May 21-28, 1968. Rept. R70-2, Inst. Mar. Sci., Univ. of Alaska, Fairbanks. 120 pp.

Knull, J. R. and R. Williamson (1969) Oceanographic survey of Kachemak Bay, Alaska. Man. Rept. 60, Bur. Comm. Fish. Lab., Auke Bay, Alaska. 54 pp.

Levanon, N. (1975) (Editor) Special issue on data collection from multiple earth platforms. IEEE Trans. on Geoscience Electronics, Vol. 13.

Luther, D. S. and C. Wunsch (1975) Tidal Charts of the Central Pacific Ocean. J. Phys. Oceanog., 5: 222-230.

Matthews, J. B. and J. C. Mungall (1972) A numerical tidal model and its application to Cook Inlet, Alaska. J. Mar. Res., 30: 27-38.

Mayer, D. A., D. V. Hansen, and D. A. Ortman (1979) Long-term current and temperature observations on the middle Atlantic shelf. J. Geophys. Res., 84: 1776-1792.

McEwen, G. F., T. G. Thompson and R. Van Cleve (1930) Hydrographic sections and calculated currents in the Gulf of Alaska, 1927 to 1928. Rept. Int. Fish. Comm., No. 4. 36 pp.

Muench, R. D., H. O. Mofjeld and R. L. Charnell (1978) Oceanographic conditions in lower Cook Inlet; spring and summer 1973. J. Geophys. Res., 83: 5090-5098.

Muench, R. D. and J. D. Schumacher (1980) Some observations of physical oceanographic conditions on the northeast Gulf of Alaska continental shelf. NOAA Tech. Memo. ERL PMEL-17, NOAA/ERL, Boulder, CO. 84 pp.

Munk, W. H. and D. Cartwright (1966), Tidal Spectroscopy and Prediction. Phil. Trans. Roy, Soc. London A, 259, 533-581.

Pearson, C. A. (1973) Deep sea tide and current observations in the Gulf of Alaska and northeast Pacific. NOAA Tech. Memo. NOS16, NOAA/NOS, Rockville, MD. 18 pp.

Pietrafesa, L. J. and G. S. Janowitz (1979) On the effects of buoyancy flux on continental shelf circulation. J. Phys. Oceanog., 9: 911-918.

Putnins, P. (1966) Studies on the Meteorology of Alaska: First Interim Report (The sequences of baric weather patterns over Alaska). U. S. Dept. Commerce, ESSA/EDS, Silver Spring, MD (unpublished manuscript).

Rapatz, W. J. and W. S. Huggett (1977) Pacific Ocean offshore tidal program. Proc. XV Int. Cong. Surv., Stockholm. 47-80.

Reed, R. K. (1980) Direct measurement of recirculation in the Alaskan Stream. J. Phys. Oceanog., Vol. 10 (in press).

Reed, R. K. and N. E. Taylor (1965) Some measurements of the Alaska Stream with parachute drogues. Deep-Sea Res., 12: 777-784.

Reed, R. K., R. D. Muench and J. D. Schumacher (1980) On baroclinic transport of the Alaskan Stream near Kodiak Island. Deep-Sea Res., Vol. 27 (in press).

Roden, G. I. (1969) Winter circulation in the Gulf of Alaska. J. Geophys. Res., 74: 4523-4534.

Royer, T. C. (1975) Seasonal variations of waters in the northern Gulf of Alaska. Deep-Sea Res., 22: 403-416.

Royer, T. C. and R. D. Muench (1977) On the ocean temperature distribution in the Gulf of Alaska, 1974-1975. J. Phys. Oceanog., 7: 92-99.

Royer, T. C. (1979) On the effect of precipitation and runoff on coastal circulation in the Gulf of Alaska. J. Phys. Oceanog., 9: 555-563.

Royer, T. C., D. V. Hansen and D. J. Pashinski (1979) Coastal flow in the northern Gulf of Alaska as observed by dynamic topography and satellite-tracked drogued drift buoys. J. Phys. Oceanog., 9: 785-801.

Scorer, R. S. (1967) Causes and consequences of standing waves. Proc. Symp. on Mountain Meteorology, Atmos. Sci. Paper 122, Colorado State Univ., Fort Collins, CO, 75-101.

Schumacher, J. D., R. Sillcox, D. Dreves and R. D. Muench (1978) Winter circulation and hydrography over the continental shelf of the northwest Gulf of Alaska. NOAA Tech. Rept. ERL 404-PMEL 31, NOAA, Boulder, CO. 16 pp.

Schumacher, J. D., R. K. Reed, M. Grigsby and D. Dreves (1979) Circulation and hydrography near Kodiak Island, September to November 1977. NOAA Tech. Memo. ERL-PMEL-13, NOAA, Boulder, CO. 49 pp.

Schumacher, J. D. and R. K. Reed (1980) Coastal flow in the northwest Gulf of Alaska: the Kenai Current. J. Phys. Oceanog., 85 (in press).

Thomson, R. E. (1972) On the Alaskan Stream. J. Phys. Oceanog., 2: 363-371.

Wang, D. P. and A. J. Elliott (1978) Non-tidal variability in the Chesapeake Bay and Potomac River: evidence for non-local forcing. J. Phys. Oceanog., 8: 225-232.

Wang, D. P. (1978) Subtidal sea level variations in the Chesapeake Bay and relations to atmospheric forcing. J. Phys. Oceanog., 8: 413-421.

Winant, C. D. and R. C. Beardsley (1979) A comparison of some shallow wind-driven currents. J. Phys. Oceanog., 9: 218-220.

Wright, F. F., G. D. Sharma, and D. C. Burbank (1973) Erts-1 observation of sea surface circulation and sediment transport, Cook Inlet, Alaska. Proc. Symp. on Significant Results Obtained from the Earth Resources Technology Satellite-1, NASA, Washington, D. C., 1315-1322.

BEST DOCUMENT AVAILABLE

Appendix A. Current meter statistics for northwest Gulf of Alaska moorings.

					"In" Water OBS			2.86 hr. Net Drift		33 hr. Net Drift		2.86 Mean	35 Mean	2.86	33	Temp.		Pressure		Salinity	
Mooring	Lat.	Long.	Meter Depth	Bott. Depth	Date	Per. 'Days'	Meter #	Speed	Direc.	Speed	Direc.	Speed	Speed	Var.	Var.	Mean	Var.	Mean	Var.	Mean	Var.
C1A	59.18	153.30	20	42	77-279	160	1810	16.26	198.8	15.94	198.7	38.96	16.93	247.18	90.82	4.52	4.91	26.12	1.48	31.12	0.36
C1B	59.18	153.31	18	40	78-148	87	2504	9.15	202.4	9.34	203.5	31.54	10.38	162.59	27.72	8.64	2.77	20.39	1.48	31.40	0.31
C1A	59.18	153.30	34	42	77-279	160	2512	9.04	198.4	8.98	198.7	25.07	10.73	146.52	51.81	4.66	4.65	40.41	1.85	31.08	0.25
C1B	59.18	153.31	35	40	78-148	143	3286	4.36	193.5	4.34	192.7	18.15	6.22	83.56	15.04	9.04	2.21	38.03	1.02	30.45	0.78
C2A	59.23	153.09	20	64	77-279	128	2355	8.18	226.6	8.14	226.6	35.45	11.64	256.60	65.48	5.79	3.72	28.39	1.70	31.37	0.25
C2B	59.23	153.13	18	62	78-148	143	3176	14.64	218.3	14.57	218.4	40.81	17.42	416.01	83.94	9.07	2.07	18.53	1.60	30.33	1.92
C2A	59.23	153.03	50	64	77-279	21	2498	8.03	196.4	10.04	197.1	25.15	18.39	163.79	79.10	8.55	0.12	58.47	2.38	31.52	0.11
C2B	Bad data		48				2505														
C3A	59.40	152.89	20	59	77-280	159	2494	8.21	234.2	8.30	233.6	46.35	9.51	380.48	27.25	5.23	3.68	25.43	2.19	31.42	0.26
C3B	59.41	152.89	25	64	78-146	143	598	17.14	231.8	17.25	231.8	52.16	18.82	603.78	54.93	9.10	1.98	23.49	1.77	0.00	0.00
C3A	59.40	152.89	50	59	77-280	159	2359	1.59	230.9	1.70	229.7	28.62	6.49	212.49	8.86	5.32	3.26	53.89	2.41	31.38	0.11
C3B	59.41	152.89	55	64	78-148	97	3180	0.58	109.8	0.64	94.9	24.56	4.09	179.98	7.89	8.15	1.38	51.08	1.82	30.96	0.76
C4A	59.28	152.90	20	84	77-280	159	1452	3.19	272.9	3.15	273.1	40.11	9.03	317.37	48.24	5.80	2.94	19.32	1.87	31.43	0.26
C4B	59.28	152.92	19	83	78-153	138	3294	2.90	243.7	2.97	265.7	26.40	5.56	551.80	27.38	0.00	0.00	0.00	0.00	0.00	0.00
C4A	59.28	152.90	65	84	77-280	159	1672	1.56	241.3	1.55	238.8	26.35	7.07	217.17	33.56	5.95	2.68	65.14	2.97	31.65	0.07
C4B	59.28	152.92	64	83	78-150	141	3290	1.41	166.4	1.33	157.8	26.95	6.61	199.31	29.01	8.27	1.26	62.69	1.50	31.13	0.48
C5A	59.17	152.94	20	128	77-280	159	1804	20.77	249.8	20.96	250.3	34.95	23.93	289.56	162.62	6.04	2.59	17.49	1.46	31.52	0.25
C5B	59.17	152.90	27	135	78-148	115	2156	18.96	251.6	19.06	251.8	44.81	23.14	796.84	258.46	8.40	1.68	0.00	0.00	28.63	1.68
C5A	59.17	152.94	65	128	77-280	159	1981	16.15	240.1	16.29	240.1	30.61	19.03	148.49	87.95	6.10	2.27	62.33	2.09	31.73	0.09
C5B	Bad data		72				3184														
C5A	Bad data		122				2168														
C5B	59.17	152.90	127	135	78-148	123	1815	2.35	199.1	2.46	199.8	15.05	6.18	85.23	23.02	7.00	0.54	128.55	1.78	32.06	0.07
C6A	59.30	152.64	20	71	77-280	162	1817	2.41	280.5	2.48	275.0	46.34	9.09	444.15	66.96	5.96	3.00	21.72	2.16	31.57	0.21
C6B	59.31	152.63	26	77	78-148	142	3173	0.88	256.9	0.65	256.1	46.31	7.49	518.61	38.89	8.84	2.01	0.00	0.00	25.74	1.81
C6A	Bad data		65				1818														
C6B	59.31	152.63	71	77	78-148	143	3295	3.09	119.2	3.22	118.7	25.38	5.66	193.44	11.60	8.41	1.33	70.82	1.81	30.89	0.75
C7A			20			Not recovered															
C7B	59.31	152.18	17	68	78-148	142	2249	4.19	310.0	4.17	310.0	71.69	7.48	1505.49	42.07	8.61	1.84	31.39	0.39	21.87	1.82
C7A	59.32	152.20	65	71	78-281	118	1986	1.48	343.0	1.52	352.8	53.43	4.16	902.31	7.52	6.59	2.13	63.02	2.25	0.00	0.00
C7B	59.31	152.18	62	68	78-148	142	2500	1.80	237.3	1.81	237.2	38.91	3.56	598.15	4.68	8.31	1.16	67.52	1.68	31.86	0.21
C8A	Lost		20				1806														
C8B	59.0	152.06	63	190	78-149	138	3179	22.26	287.3	22.09	287.4	61.54	23.50	1607.82	353.61	7.79	0.82	63.53	5.67	31.96	0.04
C8A	59.04	152.06	65	191	77-277	19	1681	28.10	295.9	27.34	294.0	52.83	29.34	866.77	96.04	8.12	0.17	72.07	61.37	32.05	0.04
C8B	59.03	152.06	64	190	78-149	82	2252	14.24	284.2	14.21	283.8	51.96	15.55	978.58	70.36	7.26	0.57	63.96	3.85	31.95	0.03
C8A	Inst. Failed		100				1680														
C8B	59.03	152.06	179	190	78-149	138	1682	7.84	258.3	7.84	258.7	39.83	8.63	262.40	20.18	6.65	0.27	179.39	1.63	32.39	0.03
C9A	Lost		20																		
C9B	58.78	152.27	66	124	78-149	138	1973	10.84	299.9	10.58	299.6	52.51	13.18	965.86	102.87	6.78	0.47	66.82	1.69	32.22	0.05
C9A	Lost		65																		
C9B	58.77	152.27	67	124	78-149	138	2501	10.64	297.3	10.38	296.8	52.11	13.05	976.83	104.88	6.76	0.46	68.24	1.99	32.28	0.05
C9A	Lost		107																		
C9B	58.78	152.27	114	124	78-149	138	2248	11.68	300.3	11.35	300.5	34.38	12.04	362.54	74.83	6.09	0.33	115.55	1.13	32.41	0.07
C10A	58.50	153.19	20	170	77-278	159	1683	27.66	228.9	27.80	229.6	33.20	31.01	470.82	382.87	5.82	1.69	26.44	1.66	31.92	0.21
C10B	58.50	153.20	25	175	78-148	134	3171	14.70	221.6	14.43	221.6	20.08	17.67	182.55	118.26	8.59	1.77	21.26	2.00	31.19	1.07
C10A	58.50	153.19	65	170	77-278	159	1982	23.36	228.8	23.43	229.4	27.29	25.73	294.65	254.31	5.87	1.06	72.26	1.46	32.15	0.05
C10B	58.50	153.20	70	175	78-148	134	3175	12.48	221.3	11.95	221.4	17.15	15.28	119.84	94.07	7.36	0.97	66.25	2.14	31.52	0.78
	Bad data		157				1824														
C10B	58.50	153.20	165	175	78-148	134	1669	4.77	201.8	4.28	200.4	11.13	9.29	67.06	49.37	5.42	0.26	18.08	0.39	32.49	0.03
C11A	Lost		34																		
C11B	59.56	151.66	82.4	87	78-149	20	1451	1.37	336.4	1.39	333.7	10.23	1.61	13.72	0.77	5.54	0.04	80.01	2.78	32.04	0.00
C12A	59.53	152.23	20	50	78-148	81	2358	4.03	41.4	3.85	42.4	54.82	4.55	990.82	4.21	7.93	1.31	19.98	2.80	31.76	0.14
C13A	59.47	152.68	26	68	78-148	141	3293	5.14	190.6	5.15	189.2	59.65	8.92	704.34	22.41	8.92	1.79	22.21	1.50	31.08	0.23
C12A	59.53	152.23	46	50	78-148	141	3291	4.02	31.0	3.97	30.1	42.81	4.60	651.61	4.25	8.73	1.71	46.71	2.14	30.58	1.47
C13A	Bad data		56.6				2356														

BEST DOCUMENT AVAILABLE

Appendix A. Continued

"In" Water OBS.								2.86 hr. Net Drift		35 hr. Net Drift		2.86 Mean	35 Mean	2.86	35	Temp.		Pressure		Salinity	
Mooring	Lat.	Long.	Meter Depth	Bott. Depth	Date	Per. 'Days'	Meter #	Speed	Direc.	Speed	Direc.	Speed	Speed	Var.	Var.	Mean	Var.	Mean	Var.	Mean	Var.
E1A	Inst. failed		20				1988														
E1A	57.75	154.73	100	228	76-290	164	1820	27.12	237.8	27.55	237.3	32.87	31.05	247.26	135.66	6.47	0.35	108.94	1.00	32.15	0.03
E2A	58.62	153.08	20	164	76-290	165	1975	41.92	214.3	42.50	214.0	46.17	43.96	588.39	408.45	6.52	0.80	29.24	2.03	31.80	0.12
E2A	58.62	153.08	100	164	76-290	165	2163	26.21	223.2	26.73	228.0	30.19	28.55	249.26	180.05	6.46	0.42	111.02	1.62	32.06	0.03
E3A	58.76	152.17	20	198	76-289	37	1451	33.34	296.6	32.38	296.8	61.12	33.58	1352.74	266.94	7.41	0.35	24.82	3.32	31.88	0.14
E3A	Bad data		100				1806														
E4A	Lost mooring						1816														
E4A	Lost mooring						1976														
E5A	56.55	152.66	20	95	76-292	157	2359	14.73	191.9	15.04	192.1	29.75	18.11	140.44	73.29	10.75	0.43	0.06	0.00	28.30	0.01
E5A	56.55	152.66	80	95	76-292	157	1800	13.30	184.0	13.49	184.2	19.04	14.49	110.78	67.47	5.72	0.15	92.23	0.25	32.70	0.05
E6A	57.22	152.43	23	75	77-292	141	2249	21.63	282.6	21.52	282.9	33.17	24.32	178.69	145.05	5.02	1.41	23.47	0.52	32.40	0.06
E6B	57.23	152.39	32	82	78-141	137	3296	15.72	278.1	15.63	278.0	23.16	16.21	117.16	41.39	7.77	1.38	31.03	0.75	31.38	1.75
E6A	57.22	152.43	65	75	77-292	141	2248	14.67	272.5	14.53	272.5	21.23	16.18	91.98	62.67	5.27	1.21	66.25	0.32	32.43	0.03
E6B	57.23	152.39	72	82	78-141	137	1676	8.31	263.1	8.26	263.0	16.27	8.57	55.76	13.12	0.00	0.00	70.14	2.32	0.00	0.00
E7A	57.06	152.30	28	80	77-292	142	2245	10.52	336.7	10.59	337.1	25.27	13.96	133.08	72.35	5.30	1.01	22.97	0.68	32.40	0.05
E7B	57.09	152.22	29	84	78-141	135	2513	8.77	318.9	8.99	318.8	19.79	10.11	71.32	26.63	7.99	1.21	28.70	0.59	32.11	0.05
E7A	57.06	152.30	76	80	77-292	142	1984	7.65	325.5	7.66	325.8	16.58	9.25	66.92	26.84	5.20	0.75	70.16	0.66	33.00	0.05
E7B	Bad data		74				1675														
E8A	57.12	152.75	25	150	77-292	141	2500	25.04	201.6	25.08	201.8	29.64	26.47	176.69	156.64	5.14	1.53	22.52	0.77	32.36	0.07
E8B	57.11	152.72	30	155	78-141	135	3174	17.90	216.3	17.87	216.1	19.82	18.23	86.12	47.23	8.36	1.63	27.16	0.64	32.14	0.12
E8A	Incomplete		67				1829														
E8B	57.11	152.72	75	155	78-141	135	1827	10.52	220.7	10.66	220.5	13.87	11.36	35.21	16.72	0.00	0.00	0.00	0.00	0.00	0.00
E8A	57.12	152.75	140	150	77-292	65	1827	11.47	199.8	12.22	199.3	15.85	16.04	103.59	67.87	0.00	0.00	143.57	1.30	0.00	0.00
E9A	Incomplete		25				2505														
E9B	56.99	152.56	13	146	78-141	137	3172	4.82	218.1	5.04	221.5	19.47	9.81	77.42	35.93	9.53	1.99	11.04	0.76	31.77	0.56
E9A	57.01	152.02	67	86	77-292	141	1978	0.00	150.1	0.00	150.1	0.00	0.00	0.00	0.00	5.17	1.03	67.89	2.71	32.50	0.02
E9B	56.99	152.56	58	146	78-141	137	3185	6.38	260.3	6.35	260.4	17.97	9.09	60.70	30.33	6.37	0.37	56.78	0.44	32.49	0.01
E9A	57.01	152.62	148	86	77-292	141	1808	2.81	300.2	2.79	299.7	10.80	6.86	29.64	17.46	0.00	0.00	152.55	0.73	0.00	0.00
E9B	56.99	152.56	142	146	78-141	137	2498	3.77	292.0	3.84	293.0	8.49	4.72	20.09	7.54	4.93	0.02	142.30	0.56	32.89	0.02
E10A	Incomplete		25				1811														
E10B	56.83	152.39	24	153	78-141	136	2512	4.60	291.5	4.74	291.0	13.57	6.91	38.16	18.24	8.68	1.88	23.74	0.53	32.31	0.03
E10A	56.85	152.43	144	154	77-292	141	1987	5.62	332.0	5.57	332.1	11.64	7.75	45.80	31.55	5.21	0.07	143.87	0.18	33.02	0.09
E10B	56.83	152.39	69	153	78-141	136	2502	5.78	307.9	5.82	306.8	14.56	7.93	32.58	18.73	5.86	0.08	69.03	0.19	32.43	0.01
E10B	56.83	152.39	149	153	78-141	136	3287	6.21	338.3	6.30	338.6	9.89	6.69	27.41	12.82	4.82	0.03	149.50	0.42	0.00	0.00
E11A	Incomplete		31				390														
E11B	56.03	155.10	25	60	78-142	67	2355	10.02	224.6	10.12	223.9	54.85	10.70	370.86	33.60	6.38	0.39	23.97	0.55	32.46	0.01
E12A	55.99	156.30	18	213	77-297	135	1815	24.30	201.5	24.59	202.6	45.26	32.36	637.94	354.75	4.72	1.36	16.69	1.85	31.86	0.09
E12B	Bad data		24				3183														
E12A	55.99	156.30	203	213	77-297	135	1673	6.45	179.1	6.86	181.6	21.31	14.71	158.53	64.59	5.04	0.05	202.86	0.24	33.29	0.24
E12B	Bad data		208				1671														
E13A	Not deployed						1988														
E13B	56.40	156.82	28	115	78-142	138	3178	13.62	221.1	13.88	220.4	25.17	16.50	234.33	72.66	8.13	2.61	32.69	1.14	31.44	0.35
E13A	Incomplete		102				2356														
E13B	56.40	156.82	111	115	78-142	138	3269	2.65	200.7	2.68	201.5	12.67	5.82	42.50	8.65	5.79	0.78	114.94	0.18	32.02	0.02
MI-A	55.79	158.65	51	71	77-301	130	2504	15.87	219.0	16.07	219.0	21.82	17.88	123.58	89.41	6.67	2.34	55.25	0.73	31.61	0.10
MI-B	Incomplete		50				1833														
MI-B	55.76	157.52	50	118	77-301	16	1826	12.19	318.1	11.24	316.1	20.95	12.18	93.63	22.46	7.25	0.07	56.47	0.45	31.34	0.02
MI-B	55.42	157.98	90	110	77-301	129	2501	7.44	29.2	7.27	28.6	17.27	10.36	96.14	30.47	5.08	1.46	92.76	0.50	32.12	0.04
MI-D	55.76	157.52	90	118	77-301	33	2502	10.09	320.3	10.13	320.7	18.72	11.41	104.51	18.27	6.90	0.42	97.32	0.21	31.70	0.03
MI-D	55.76	157.52	70	118	77-301	129	603	10.65	323.5	10.64	323.6	21.05	12.91	109.45	39.88	4.81	1.71	73.39	0.00	32.10	0.06

BEST DOCUMENT AVAILABLE

Appendix A. Continued

	"In" Water OBS.							2.86 hr. Net Drift		35 hr. Net Drift		2.86 Mean	35 Mean	2.66	35	Temp.		Pressure		Salinity	
Mooring	Lat.	Long.	Meter Depth	Bott. Depth	Date	Per. 'Days'	Meter #	Speed	Direc.	Speed	Direc.	Speed	Speed	Var.	Var.	Mean	Var.	Mean	Var.	Mean	Var.
WGC-1A	54.03	163.0	20	188	75-248	57	1678	27.13	263.6	27.17	263.6	35.67	29.54	206.10	184.94	7.97	0.78	19.23	0.37	31.93	0.03
WGC-1B	54.02	163.0	20	194	75-306	131	1455	11.94	243.0	12.22	243.0	17.58	15.68	176.55	138.38	4.31	0.51	0.00	0.00	0.00	0.00
WGC-1A	54.03	163.0	103	188	75-248	57	1677	15.22	256.8	14.93	257.2	21.15	16.22	57.55	65.51	5.41	0.33	100.47	1.04	32.96	0.06
WGC-1B	54.02	163.0	100	194	75-306	58	645	20.99	262.8	21.47	262.8	28.07	23.95	330.86	348.98	5.10	0.86	112.50	2.21	32.13	3.83
WGC-1C	54.02	163.0	20	186	76-073	90	1982	25.33	253.8	25.13	253.5	32.48	26.73	162.34	123.85	2.68	0.99	11.55	0.42	32.23	0.07
WGC-1D	54.02	163.0	20	89	76-164	110	1973	11.15	253.2	11.17	252.9	22.20	12.97	88.94	59.20	8.02	1.61	17.41	0.30	32.04	0.04
WGC-1C	54.02	163.0	50	186	76-073	90	1978	24.36	254.7	24.42	254.1	30.77	25.38	102.88	110.13	2.73	0.51	42.03	0.43	32.38	0.11
WGC-1D	54.02	163.0	50	89	76-164	110	598	10.23	254.6	10.33	254.6	20.48	11.66	55.53	39.50	4.57	1.32	49.97	20.87	31.87	0.01
WGC-1C	54.02	163.0	100	186	76-073	90	1985	18.98	263.1	19.06	262.8	24.19	19.99	58.98	76.47	3.07	0.22	91.96	0.32	33.06	0.06
WGC-1C	54.02	163.0	175	186	76-073	90	1832	7.56	225.3	7.66	225.2	11.37	9.06	52.71	37.02	4.57	0.27	171.19	14.87	32.13	0.07
WGC-1E	54.05	163.1	18	88	76-275	209	2245	23.32	258.5	23.63	258.2	39.41	28.76	227.11	162.84	5.57	2.08	0.00	0.00	31.59	0.04
WGC-1F	54.06	163.1	20	88	77-120	131	1825	16.29	261.5	16.16	262.1	26.31	17.58	98.07	61.92	8.00	5.41	11.19	0.36	31.56	0.06
WGC-1E	54.05	163.1	78	88	76-275	78	2249	12.46	250.5	12.19	250.3	19.42	14.05	81.49	45.25	6.72	0.42	0.00	0.00	0.00	0.00
WGC-1F	54.06	163.10	76	88	77-119	131	1973	6.86	249.6	7.07	248.8	12.65	8.50	33.49	12.78	5.54	0.78	75.55	0.16	32.09	0.04
WGC-2A	57.45	150.49	20	185	75-265	56	1684	32.96	226.8	33.51	226.5	43.29	34.16	270.82	74.74	7.24	1.87	16.73	0.64	32.14	0.07
WGC-2B	Lost mooring																				
WGC-2A	57.45	150.49	100	185	75-265	56	1683	25.64	224.3	25.73	224.1	30.16	25.91	109.46	41.70	5.31	0.07	96.84	0.33	33.04	0.09
WGC-2B	Lost mooring																				
WGC-2C	57.45	150.49	24	185	76-070	90	1977	21.63	226.6	21.80	226.9	30.10	23.41	160.37	119.84	4.86	0.82	19.20	0.81	32.40	0.05
WGC-2D	57.56	150.82	20	92	76-160	132	1678	3.27	242.4	3.23	244.6	33.79	5.52	223.78	12.10	7.85	1.44	21.02	0.72	31.23	3.47
WGC-2C	57.45	150.49	54	185	76-070	90	1825	23.83	232.3	24.06	232.2	30.21	25.08	122.38	100.38	4.53	0.38	49.15	0.33	32.46	0.01
WGC-2D	57.56	150.82	50	92	76-160	132	1808	3.81	234.0	3.69	235.4	31.62	4.89	177.03	8.06	6.92	0.76	47.99	0.71	31.90	0.91
WGC-2C	57.45	150.49	104	185	76-070	61	1818	25.54	235.3	24.80	235.0	30.19	25.13	164.33	60.17	4.28	0.16	98.87	0.53	32.78	0.02
WGC-2D	57.56	150.82	80	92			1455	1.19	181.1	1.20	181.0	19.77	2.52	104.14	2.10	6.63	0.50	0.00	0.00	32.18	0.20
WGC-2C	57.45	150.49	179	185	76-070	90	1837	12.77	182.5	13.05	182.3	25.36	15.07	195.43	55.97	4.76	0.10	175.05	0.27	33.17	0.07
WGC-2E	57.56	150.82	20	90	76-293	155	1807	2.49	239.5	2.31	240.6	41.13	10.43	219.60	33.93	6.06	0.80	17.24	0.85	32.27	0.16
WGC-2F	57.57	150.83	20	90	77-084	167	1815	34.08	7.04	246.27	17.75	4.68	218.7	4.69	22.04	7.46	5.06	18.89	0.51	31.97	0.27
WGC-2E	57.56	150.82	80	90			1816	0.05	280.7	0.05	287.05	1.47	0.29	0.01	0.05	2.46	0.29	78.23	0.84	36.10	0.02
WGC-2F	57.57	150.83	80	90	77-084	167	1826	2.83	178.3	2.80	178.6	20.38	3.93	114.56	4.36	6.06	0.90	77.96	0.61	32.12	0.09
WGC 3A	Lost mooring																				
WGC-3B	55.19	156.97	20	111	76-162	129	1817	21.35	255.0	21.41	255.7	43.78	22.95	412.01	101.55	8.17	2.21	18.28	0.37	32.90	0.16
WGC-3C	55.20	156.95	28	112	76-292	138	1829	26.19	239.7	26.07	238.8	50.46	33.50	485.54	219.17	6.17	0.60	20.77	34.00	0.00	0.00
WGC-3B	Inst. failed						1834														
WGC-3C	55.20	156.95	90	112	76-292	153	2168	19.59	231.8	19.81	231.6	34.96	20.79	242.37	131.11	6.00	0.37	99.75	0.16	32.90	0.11
WGC-3B	Inst. failed						1831														
WGC-3D	55.20	156.96	20	112	77-191	131	1682	23.82	254.6	24.11	254.9	43.29	25.71	401.53	87.75	7.79	5.57	9.82	0.13	32.06	0.16
WGC-3D	Inst. failed						1803														

BEST DOCUMENT AVAILABLE

Appendix B. Release and recovery information for drift cards released in the Kodiak Island region during 1978.

RELEASED	RECOVERED				
	CARD	DATE	LATITUDE	LONGITUDE	COMMON NAME
101 - 200	107	05/29/78	57 24.0N	156 22.0W	SLAUGHTER ISL
03/06/78	123	07/24/78	59 0.0N	153 37.0W	KAMISHAK BAY
59 4.6N	155	07/24/78	59 0.0N	153 37.0W	KAMISHAK BAY
150 39.4W	171	05/30/79	59 4.0N	153 44.0W	CAPE DOUGLAS
201 - 300	219	04/10/78	58 37.8N	152 27.5W	CARSHAN PT
03/06/78	245	06/18/78	58 22.4N	152 6.5W	SEAL BAY
58 31.8N	250	07/08/78	58 23.3N	152 7.5W	TOLSTOI PT
150 45.0W	263	05/15/78	57 50.2N	152 21.0W	MILLER PT
	268	07/24/78	57 5.2N	153 11.7W	OCEAN BAY
	292	07/08/78	58 23.3N	152 7.5W	TOLSTOI PT
301 - 400	306	07/22/78	57 18.1N	153 0.0W	KILUDA BAY
03/06/78	319	04/09/78	57 27.8N	152 27.0W	PASAGSHAK BAY
58 15.2N	325	05/08/78	57 27.8N	152 27.0W	PASAGSHAK BAY
149 52.0W	342	04/22/78	57 5.3N	153 11.0W	OCEAN BEACH
	343	04/09/78	57 27.8N	152 27.0W	PASAGSHAK BAY
	352	07/22/78	57 10.0N	153 8.5W	PORT HOBRON
	365	07/01/78	56 29.3N	154 35.8W	TUGIDAK ISL
	366	04/05/79	57 31.0N	152 56.0W	HIDDEN BASIN
	371	06/04/78	57 18.0N	153 3.0W	KILUDA BAY
	372	10/10/78	57 9.0N	153 11.0W	PORT HOBRON
	380	07/22/78	57 1.0N	153 36.0W	KIAVAK BAY
	388	05/13/79	57 31.5N	152 16.6W	SACROMENTO RIVER
	392	03/27/79	57 12.0N	153 10.0W	MCCHORD RANCH
	395	04/26/78	57 17.9N	153 3.0W	KILUDA BAY
401 - 500	454	10/14/78	56 52.0N	158 54.0W	STROGNOFF PT
03/06/78	464	06/12/79	59 41.7N	140 17.5W	POINT MANBY
58 3.6N					
149 10.3W					
501 - 600					
03/10/78					
58 27.6N					
151 50.0W					
601 - 700	609	07/22/78	57 12.5N	153 16.0W	OLD HARBOR
03/10/78	625	08/03/78	57 26.0N	152 43.0W	EAGLE COVE
57 58.3N	628	02/22/79	57 12.0N	153 10.0W	MCCHAORD RANCH
150 44.6W	630	04/09/78	57 27.8N	152 27.0W	PASAGSHAK BAY
	634	10/09/78	57 25.2N	152 43.0W	EAGLE HARBOR
	644	04/29/78	57 17.9N	153 3.0W	KILUDA BAY
	664	04/12/78	57 27.8N	152 27.0W	PASAGSHAK BAY
	671	09/12/78	57 9.0N	153 11.0W	MCCORD RANCH
	695	03/27/79	57 12.0N	153 10.0W	MCCHORD RANCH

BEST DOCUMENT AVAILABLE

Appendix B. Continued

RELEASED	RECOVERED				
	CARD	DATE	LATITUDE	LONGITUDE	COMMON NAME
701 - 800 03/13/78 57 25.8N 151 25.8W	743	07/24/78	56 24.0N	154 45.0W	TUGIDAK ISL
	777	10/01/78	56 30.0N	160 0.0W	PORT HEIDEN
	798	05/05/79	59 21.0N	146 25.0W	MIDDLETON ISL
801 - 900 03/14/78 57 16.3N 151 42.2W					
901 -1000 03/10/78 58 21.4N 151 6.9W	904	11/23/78	57 51.0N	152 38.0W	CANNONS BEACH
	908	04/20/78	58 8.8N	153 16.8W	NORTH BEACH
	910	05/17/78	57 24.0N	156 22.0W	WIDE BAY
	920	11/06/78	57 52.0N	153 50.0W	CP UGAT
	958	07/11/78	57 44.0N	153 30.0W	PACKERS SPIT
	966	04/20/78	58 8.8N	153 16.8W	NORTH BEACH
	973	08/02/79	58 0.0N	153 17.0W	OUTLET CAPE
	985	06/19/78	57 39.0N	154 7.0W	7 MILE BEACH
	998	10/22/78	58 7.0N	153 2.0W	
1001-1100 03/14/78 57 3.1N 152 7.8W	1010	06/30/78	56 32.0N	154 8.0W	SITKINAK ISL
	1022	07/22/78	56 53.0N	154 12.0W	LAZY BAY
	1046	07/01/78	56 29.3N	154 35.0W	TUGIDAK ISL
	1062	05/02/78	56 56.1N	154 10.0W	AKHIOK VILLAGE
1101-1200 03/14/78 56 53.6N 152 33.0W	1133	11/10/78	54 36.0N	164 52.0W	CAPE SARICHEF
	1165	07/04/79	55 49.5N	155 32.0W	CHIRIKOF ISL
1201-1300 03/14/78 56 53.6N 152 33.0W	1242	10/01/78	56 30.0N	160 0.0W	PORT HEIDEN
	1243	10/17/79	53 27.0N	166 55.0W	SW. UNALASKS ISL
1301-1400 03/16/78 56 7.5N 153 56.2W	1322	08/15/79	52 56.0N	168 54.0W	NIKOLSKI
1401-1500 03/10/78 58 50.0N 151 39.0W	1413	05/05/79	56 0.0N	161 16.0W	NELSON LAGOON
	1423	05/03/78	58 18.1N	153 2.0W	CP PARAMANOF
	1448	05/02/78	58 18.4N	153 2.7W	CP PARAMANOF
	1452	04/20/78	58 8.8N	153 16.8W	NORTH BEACH
	1464	05/14/78	58 18.4N	153 2.7W	CP PARAMANOF
	1486	06/26/78	57 39.1N	154 7.0W	7 MILE BEACH
	1495	07/26/78	58 17.0N	152 55.5W	CP PARAMANOF

BEST DOCUMENT AVAILABLE

Appendix B. Continued

RELEASED	RECOVERED				
	CARD	DATE	LATITUDE	LONGITUDE	COMMON NAME
3001-3100 05/23/78 58 48.3N 149 36.1W	3036	07/04/78	57 39.1N	154 7.0W	7 MILE BEACH
	3058	07/30/78	57 40.0N	152 28.0W	MIDDLE BAY
3101-3200 05/23/78 59 20.3N 150 7.3W	3102	08/01/78	59 32.0N	153 46.2W	URSUS COVE
	3107	07/03/78	60 21.0N	152 0.0W	KALGIN ISL
	3111	07/25/78	59 18.4N	154 6.0W	AMAKDORI BEACH
	3144	03/27/79	57 12.0N	153 10.0W	MCCHORD RANCH
	2156	07/01/78	59 20.0N	153 22.0W	ST AUGUSTINE
3201-3300 05/23/78 58 51.3N 149 45.4W	3203	12/31/78	58 12.0N	152 21.0W	KITOI BAY
	3221	06/21/79	56 57.0N	153 41.0W	JAP BAY
	3221	06/21/79	56 57.0N	153 41.0W	UPPER JAP BAY
	3228	09/19/78	57 25.5N	152 20.0W	NARROW CAPE
	3242	11/01/78	58 16.0N	151 16.0W	MARMOT ISL.
	3267	07/25/78	59 16.4N	154 6.0W	AMAKDEDORI BEACH
	3276	10/29/78	58 9.0N	152 6.0W	PILLAR CAPE
	3278	07/25/78	59 18.4N	154 6.0W	AMAKDEDORI BEACH
	3294	07/31/78	57 40.0N	152 28.0W	MIDDLE BAY
	3297	09/22/78	58 29.3N	152 33.9W	DAYLIGHT HRB
	3297	09/22/78	58 29.3N	152 33.9W	DAYLIGHT HRB
3301-3400 05/23/78 58 59.9N 149 56.7W	3322	11/12/78	57 52.6N	152 41.2W	CRAG PT
	3346	11/01/78	57 51.0N	153 51.0W	CAPE UGAT
	3351	08/22/78	57 57.0N	152 29.0W	SPRUCE ISLAND
	3366	09/04/78	59 17.0N	154 8.0W	KAMISHAK
3401-3500 05/23/78 59 4.6N 149 54.9W	3412	07/25/78	59 18.4N	154 6.0W	AMAKDEDORI B
	3415	07/23/78	58 39.0N	152 26.0W	MIDDLE BAY
	3418	07/31/78	57 56.0N	152 25.0W	PINAPPLE COVE
	3419	08/11/78	57 55.0N	153 42.0W	MINERS PT
	3436	04/18/79	57 6.0N	156 30.0W	PORT WRANGLE
	3446	06/27/78	57 10.5N	154 32.5W	AGAKULIK RIVER
	3483	07/12/78	57 40.0N	152 26.5W	MIDDLE BAY
3501-3600 05/23/78 58 44.7N 149 27.5W	3507	08/18/78	57 54.8N	152 59.5W	DRY SPRUCE BAY
	3508	07/25/78	59 18.4N	154 6.0W	AMAKDEDORI B
	3511	07/31/78	57 56.0N	152 25.0W	PINAPPLE COVE
	3520	08/13/78	59 32.0N	153 46.2W	URSUS COVE
	3527	06/22/79	56 33.0N	157 9.0W	SUTWIK ISL
	3535	04/15/79	57 40.0N	152 28.0W	
	3546	09/21/78	56 57.5N	153 35.5W	KNOLL BAY
	3583	09/06/78	59 30.0N	153 44.0W	URSUS COVE
	3585	08/21/78	57 27.5N	152 27.0W	PASAGSHAK BAY

BEST DOCUMENT AVAILABLE

Appendix B. Continued

RELEASED	CARD	DATE	LATITUDE	LONGITUDE	COMMON NAME
	RECOVERED				
3601-3700	3610	07/19/78	59 12.5N	154 8.1W	CHENIK LAGOON
05/23/78	3657	09/09/79	57 46.9N	152 21.5W	WOODY ISL
58 37.8N	3673	10/11/78	57 56.5N	152 29.0W	W SIDE SPRUCE ISL
149 7.5W	3684	08/05/78	59 21.3N	153 57.5W	CONTACT PR
	3686	06/25/78	60 11.0N	151 26.0W	CLAM GULCH
	3689	07/25/78	59 18.4N	154 6.0W	AMAKDEDORI R
	3690	07/24/78	59 30.8N	154 45.3W	URSUS COVE
	3691	07/14/78	59 18.0N	154 6.7W	AMAKDEDORI R
	3698	08/11/78	59 23.0N	153 31.0W	W ST AUGUSTINE
	3700	07/25/78	59 18.8N	154 6.0W	AMAKDEDORI R
3701-3800	3719	08/02/78	57 5.3N	153 11.0W	OCEAN BAY
05/23/78	3792	09/09/79	56 32.5N	154 39.0W	TUGIDAK ISL
58 24.5N	3794	03/25/79	57 4.0N	153 34.0W	KAISIGNAK BAY
146 27.0W	3800	08/03/78	57 53.7N	153 48.0W	RINER CREEK
3801-3900	3612	07/01/78	56 57.0N	154 9.0W	MOSER BAY
05/23/78	3823	10/22/78	57 56.5N	152 29.0W	SPRUCE ISLAND
59 10.3N	3826	06/12/78	57 45.0N	155 36.5W	PAULF BAY
150 .7W	3841	10/28/78	57 17.5N	154 45.0W	GURNEY BAY
	3642	07/21/78	57 39.1N	154 7.0W	7 MILE BEACH
	3873	06/26/78	57 56.5N	153 16.0W	VIEKODA BAY
3901-4000	3902	10/14/78	57 36.0N	152 16.0W	LONG ISL
05/23/78	3904	08/10/78	59 32.0N	153 46.2W	URSUS COVE
58 32.0N	3906	08/01/78	59 32.0N	153 46.2W	URSUS COVE
148 48.2W	3913	08/09/78	58 11.2N	152 22.0W	KITIO BAY
	3914	08/29/78	58 31.0N	153 54.0W	CHINIAK BAY
	3915	07/13/78	59 29.0N	153 42.8W	ROCKY COVE
	3943	08/01/78	59 32.0N	153 46.2W	URSUS COVE
	3945	06/27/78	59 50.0N	151 48.0W	WHISKEY GULCH
	3960	07/08/78	57 47.8N	152 21.8W	MISSION BEACH
	3978	09/26/78	56 52.0N	154 14.0W	CAPE AKHIOK
	3982	06/09/79	57 12.0N	153 10.0W	PORT HOBRON
	3987	07/25/78	59 18.4N	154 6.0W	AMAKDEDORI R
4001-4100	4027	09/17/79	57 12.0N	153 10.0W	SITKALIDAK
10/03/78	4030	10/07/78	57 1.6N	153 23.8W	NATALIA PENN
57 5.6N	4031	10/07/78	57 1.6N	153 23.8W	NATALIA PENN
152 12.9W	4046	07/10/79	57 12.0N	153 10.0W	PORTHOBRON
	4051	10/07/78	57 1.6N	153 23.8W	NATALIA PENN
	4065	10/07/78	57 1.6N	153 23.8W	NATALIA PENN
	4077	10/07/78	57 1.6N	153 23.8W	NATALIA PENN
	4078	10/07/78	57 1.6N	153 23.8W	NATALIA PENN
	4087	10/07/78	57 1.6N	153 23.8W	NATALIA PENN
	4091	10/07/78	57 1.6N	153 23.8W	NATALIA PENN

Appendix B. Continued

```
RELEASED                                     R E C O V E R E D
---------     -------------------------------------------------------------------------
              CARD        DATE         LATITUDE       LONGITUDE       COMMON NAME
              ----      --------       --------       ---------       -----------
4101-4200
10/04/78
56 49.4N
152 24.3W

4201-4300     4239      11/05/78       57    .2N      153 33.0W       KIAVAK BAY
10/04/78      4259      04/05/79       57    .3N      153 33.0W       KIAVAK BAY
57  6.4N      4276      11/03/78       57    .2N      153 33.0W       KIAVAK BAY
152 43.9W     4277      11/08/78       57    .2N      153 33.0W       KIAVAK B
              4288      11/04/78       57    .2N      153 33.0W       KIAVAK BAY
              4292      04/07/79       57    .3N      153 33.0W       KIAVAK BAY

4301-4400     4338      03/17/79       56 34.0N       169 38.0W       ST GEORGE ISL
10/05/78      4340      08/26/79       55 44.0N       159 54.0W       DENT POINT
56 59.6N
152 34.0W

4401-4500
10/05/78
57 13.6N
152 23.1W

4501-4600     4549      08/15/79       56 43.0N       154  4.0W       ATAKALIK ISL
10/07/78
56 13.2N
154 59.0W

4601-4700     4677      03/26/79       56 34.0N       169 38.0W       ST GEORGE ISL
10/07/78
56  8.5N
155  9.6W

4701-4800
10/08/78
56  3.9N
155 15.3W

4801-4900
10/08/78
55 58.4N
155 25.8W

4901-5000     4960      07/07/79       55 49.5N       155 32.0W       CHIRICOF ISL
10/07/78
56   .7N
155  5.1W
```

Appendix B. Continued

RELEASED	CARD	DATE	LATITUDE	LONGITUDE	COMMON NAME
5001-5100	5011	01/14/79	57 35.5N	152 27.5W	KALSIN BECH
10/10/78	5013	11/01/78	57 51.0N	153 51.0W	UGAT CAPE
59 2.8N	5019	10/30/78	57 42.2N	153 50.2W	SPIRIDON BAY
150 57.2W	5053	10/30/78	57 42.2N	153 50.2W	SPIRIDON BAY
	5064	07/08/79	56 54.0N	154 18.0W	ALITAK LAGOON
	5088	10/30/78	57 42.2N	153 42.2W	SPIRIDON BAY
	5099	01/17/79	57 12.0N	153 10.0W	MCCHORD RANCH
5101-5200	5134	10/30/78	57 42.2N	153 50.2W	SPIRIDON BAY
10/10/78	5180	10/30/78	57 42.2N	153 50.2W	SPIRIDON BAY
58 58.1N	5168	10/30/78	57 42.2N	153 50.5W	SPIRIDON BAY
150 56.2W	5200	10/30/78	57 42.2N	153 50.2W	SPIRIDON BAY
5201-5300	5203	10/30/78	57 42.2N	153 50.2W	SPIRIDON BAY
10/10/78	5208	06/06/79	57 38.0N	154 21.0W	CAPE UYAT
58 51.6N	5235	12/14/78	57 42.2N	153 50.5W	SPIRIDON BAY
150 53.0W	5278	10/30/78	57 42.2N	153 50.2W	SPIRIDON BAY
5301-5400	5323	11/10/78	58 3.5N	153 14.0W	ONION BAY
10/10/78	5328	11/08/78	59 21.2N	151 55.3W	ENGLISH BAY
58 44.9N					
150 51.6W					
5401-5500	5467	03/18/79	57 25.5N	152 20.0W	
10/10/78					
58 38.6N					
150 48.0W					
5501-5600	5516	05/10/79	57 30.0N	152 44.0W	SALTERY COVE
10/10/78					
58 32.3N					
150 44.9W					
5601-5700	5636	06/27/79	55 47.0N	155 41.0W	S. CHIRIKOF ISL
10/10/78	5615	03/21/79	57 49.0N	152 26.0W	MONASHKA BAY
58 24.5N	5649	01/06/79	57 46.8N	152 26.5W	GIBSON COVE
150 49.0W	5675	05/01/79	58 55.8N	152 12.4W	USHAGAT ISL
	5683	01/20/79	57 38.5N	152 26.0W	BROAD PT
5701-5800	5732	12/27/78	57 24.2N	152 30.0W	CAPE CURRENT
10/10/78	5742	07/08/79	55 20.0N	160 26.0W	POPOFF ISL
58 18.8N	5748	03/27/79	57 12.0N	153 10.0W	MCCHORD RANCH
150 37.8W	5782	04/12/79	57 40.0N	152 29.0W	MIDDLE BAY
5801-5900	5807	05/27/79	57 12.0N	153 10.0W	PORT HOBORN
10/10/78	5819	01/15/79	58 56.0N	152 15.0W	USHAGAT ISL
58 11.3N	5851	03/18/79	57 25.5N	152 20.0W	
150 26.6W					

BEST DOCUMENT AVAILABLE

Appendix C. Release and recovery information for seabed drifters, including returns through February, 1980.

Cruise Number	Date Released	Release Location Latitude N	Release Location Longitude W	Recovery Date	Recovery Location Latitude N	Recovery Location Longitude W
4MF 77	5 Nov 77	58°02'	151°38'	Jan 79	Nataliu Bay	
	5 Nov 77	56°53'	153°04'	8 Jan 78	56°50'	153°18'
	2 Nov 77	57°37'	151°55'	-	57°03'	152°48'
4DI 78	9 Apr 78	57°07'	153°00'	Jan 79	Nataliu Bay	
	8 Apr 78	57°47'	151°41'	19 May 78	57°25'	152°30'
	9 Apr 78	57°28'	152°10'	30 Sep 78	57°32'	151°42'
	29 Mar 78	58°04'	151°45'	-	-	-
	29 Mar 78	58°04'	151°45'	23 Sep 79	Chiniak Gulley	
2MF 78	24 Jun 78	56°55'	153°22'	29 Jan 79	57°08'	153°25'
	24 Jun 78	57°04'	153°03'	11 Nov 78	Ocean Bay, Sitkalidak Isl.	
	26 Jun 78	57°16'	151°17'	18 Sep 78	57°34'	151°51'
	26 Jun 78	56°59'	152°55'	17 Sep 78	57°08'	152°44'
	24 Jun 78	56°55'	153°22'	17 Nov 78	57°05'	153°26'
	26 Jun 78	57°16'	151°17'	6 Dec 78	57°38'	151°52'
	26 Jun 78	57°16'	151°17'	28 Sep 78	57°32'	151°42'
	22 Jun 78	57°36'	151°48'	21 Sep 78	57°32'	151°40'
	22 Jun 78	57°36'	151°48'	24 Sep 78	57°25'	151°26'
	27 Jun 78	57°43'	150°54'	26 Sep 78	57°22'	151°22'
	24 Jun 78	57°12'	152°44'	27 Sep 78	56°52'	153°26'
	24 Jun 78	57°19'	152°24'	27 Oct 78	57°24'	152°24'
	24 Jun 78	56°55'	153°22'	15 Sep 78	57°03'	153°25'
	24 Jun 78	56°55'	152°22'	23 Sep 78	57°03'	153°25'
	26 Jun 78	57°00'	151°55'	29 Sep 78	57°03'	152°30'
	26 Jun 78	57°16'	151°17'	29 Sep 78	57°38'	151°58'
	21 Jun 78	58°03'	151°25'	20 Jan 79	57°40'	151°50'
	24 Jun 78	56°55'	153°22'	6 Dec 78	57°05'	153°26'
	24 Jun 78	56°55'	153°22'	23 Oct 78	57°05'	153°26'
	27 Jun 78	57°43'	150°54'	-	-	-
	24 Jun 78	57°04'	153°03'	18 Feb 79	Ocean Bay, Sitkalidak Isl.	
	22 Jun 78	57°37'	151°47'	18 Feb 79	57°21'	152°33'
	21 Jun 78	58°03'	151°25'	11 Feb 79	57°31'	152°17'
	24 Jun 78	56°55'	153°22'	28 Feb 79	57°10'	153°20'
	24 Jun 78	56°55'	153°22'	26 Feb 79	57°10'	153°19'
	24 Jun 78	56°55'	153°22'	24 Feb 79	57°09'	153°21'
	22 Jun 78	58°18'	150°12'	8 Jan 79	-	-
	30 Jun 78	56°26'	153°44'	11 Apr 79	-	154°32'
	24 Jun 78	57°04'	153°03'	3 Feb 80	56°37'	153°06'
	27 Jun 79	57°43'	150°55'	20 Nov 79	57°43'	152°20'
	27 Jun 78	57°43'	150°55'	27 Oct 79	Cape Chiniak on NE Side Kodiak	
	22 Jun 78	58°18'	150°12'	4 Jul 79	57°16'	150°46'
	22 Jun 78	58°18'	150°12'	19 Oct 79	Chiniak Gully	

Appendix C. Continued

1WE 78	28 Oct 78	56°55'	153°22'	17 Mar 79	57° -	153°25'
	28 Oct 78	57°16'	151°17'	2 Feb 79	Silver Bay, Cape Chiniak	
	1 Nov 78	57°36'	151°46'	5 Jan 79	57°25'	152°00'
	28 Oct 78	56°55'	153°22'	28 Jan 79	57°07'	153°25'
	27 Oct 78	57°29'	152°07'	19 Jan 80	56°53'	152°35'
	2 Nov 78	58°03'	151°27'	6 Jan 80	57°32'	151°44'
	1 Nov 78	57°45'	151°28'	3 Jan 80	Cap Chiniak	
	1 Nov 78	58°18'	150°12'	31 Dec 79	57°34'	151°49'
	1 Nov 78	57°37'	151°47'	29 Dec 79	57°33'	151°48'
	1 Nov 78	58°18'	150°12'	24 Nov 79	57°38'	152°20'
1MF 79	15 Feb 79	57°04'	153°04'	29 Mar 79	Ocean Bay,Sitkalidak Isl.	
	15 Feb 79	57°04'	153°04'	29 Mar 79	"	"
	18 Feb 79	57°45'	151°28'	25 Mar 79	57°56'	151°57'
	15 Feb 79	57°04'	153°04'	4 Apr 79	Ocean Bay,Sitkalidak Isl.	
	15 Feb 79	57°04'	153°04'	4 Apr 79	"	"
	15 Feb 79	57°04'	153°04'	4 Apr 79	"	"
	15 Feb 79	57°04'	153°04'	4 Apr 79	"	"
	18 Feb 79	57°45'	151°28'	23 Sep 79	"	"
	15 Feb 79	57°04'	153°02'	12 Jan 80	56°58'	153°29'
	22 Feb 79	58°04'	151°24'	19 Jan 80	57°08'	152°31'
	22 Feb 79	58°04'	151°24'	29 Dec 79	57°20'	152°30'
	18 Feb 79	57°29'	152°06'	31 Oct 79	57°14'	152°54'
	15 Feb 79	57°04'	151°02'	11 Nov 79	56°46'	153°29'
	7 Mar 79	58°18'	150°12'	2 Nov 79	Loran:31402-11697-7960 32070-43168-9990	
	15 Feb 79	57°04'	153°02'	12 Oct 79	Newman Bay Loran-31228-32535	

BEST DOCUMENT AVAILABLE

Appendix D. CTD stations used in NWGOA program, listed by cruises.

Cruise ID	Vessel	Dates	No. Casts
RP4-DI77C2	Discoverer	4-12 Oct 77	186
RP4-DI77C3	Discoverer	13-21 Oct 77	97
RP4-DI77C4	Discoverer	27 Oct-5 Nov 77	127
RP4-SU77B5	Surveyor	6-15 Sep 77	130
RP4-SU77C2	Surveyor	4-17 Nov 77	46
RP4-DI77A2	Discoverer	2-10 Mar 77	58
Acona 245	Acona	30 June-16 Jul 77	109
RP4-DI76A	Discoverer	13 May-2 June 76	130
RP-DI76BL6	Discoverer	14-23 Oct 76	39
RP4-DI77A3	Discoverer	15 Mar-1 Apr 77	141
RP4-DI77A4	Discoverer	5-22 Apr 77	106
RP4-DI76A	Discoverer	7-13 Apr 76	27
DS5	Discoverer	9-16 Nov 77	94
Acona 205	Acona	13 Feb 75	3
814	Uncertain	30 Oct-13 Nov 75	116
MW3	Moana Wave	20 Apr-1 May 76	99
RP4-SU78A2	Surveyor	4-17 Mar 78	179
RP4-DI78A1	Discoverer	6-24 Mar 78	180
RP4-DI78A2	Discoverer	14-20 Apr 78	26
RP4-DI78A4	Discoverer	26 May-7 June 78	135
OP 343603	Silas Bent	1-26 Sep 75	127
MW4	Moana Wave	7-20 May 76	94
MW5	Moana Wave	22 Jul-1 Aug 76	69
RP4-DI78A2	Discoverer	28 Mar-14 Apr 78	91
RP4-DI78B4	Discoverer	6-22 Oct 78	171
RP4-MF77A4	Miller Freeman	3-7 April 77	25
RP4-MF78A4	Miller Freeman	20 Jun-5 Jul 78	106
RP4-SU78A3	Surveyor	24-27 Mar 78	21
RP4-DI78A3	Discoverer	25 Apr-5 May 78	42
RP4-MF78A1	Miller Freeman	9-12 May 78	20
RP4-MF78A5	Miller Freeman	13-18 Jul 78	53
RP4-SU78B1	Surveyor	14-18 Aug 78	36
RP4-MF78A3	Miller Freeman	7-11 June 78	49
Wekoma-78	Wekoma	27 Oct-13 Nov 78	94
RP4-MF78A	Miller Freeman	20-30 May	107
RP4-SU79B	Surveyor	5-14 Aug	79
RP4-SU79A	Surveyor	23 Mar-3 Apr 79	141
248IMS	Acona	10-16 Aug 77	20
SU41MS	Surveyor	21 Sep-2 Oct 76	79
IMS79A	Surveyor	9-21 Feb 79	133
241IMS	Acona	24 Apr 77	5
FN9IMS	Miller Freeman	29 Mar-2 Apr 77	32
254IMS	Acona	28 Nov-2 Dec 77	9
FN8IMS	Miller-Freeman	12-18 Nov 76	87
FN7IMS	Miller Freeman	10-19 Nov 76	24
IMS812	Discoverer	10-15 Oct 75	24
MW6	Moana Wave	13-19 Oct 76	22

FINAL REPORT--TASK 1
OIL SPILL TRAJECTORY SIMULATION
LOWER COOK INLET - SHELIKOF STRAIT, ALASKA

BERING SEA - GULF OF ALASKA PROJECT OFFICE
OUTER CONTINENTAL SHELF ENVIRONMENTAL
ASSESSMENT PROGRAM

JOB NO. 06797-014-88
June 13, 1980

LOS ANGELES, CALIFORNIA

June 13, 1980

Outer Continental Shelf Environmental
Assessment Program
Bering Sea - Gulf of Alaska Project Office
Post Office Box 1808
Juneau, Alaska 99802

Attention: Herbert E. Bruce, Ph.D.
OCSEAP Project Manager

Gentlemen:

Final Project Report
Oil Spill Trajectory Simulation
Lower Cook Inlet and Shelikof Strait, Alaska
For National Oceanic and Atmospheric Administration

We are pleased to submit our final project report on oil spill trajectory simulation in Lower Cook Inlet and Shelikof Strait, Alaska. This report has incorporated and responded to comments received from your Juneau staff, as well as the Bureau of Land Management (BLM) in Anchorage, Alaska, and the United States Geological Society (USGS) in Reston, Virginia.

We wish to express our appreciation to the Pacific Marine Environmental Laboratory (PMEL) in Seattle, Washington for their assistance during the meteorological and oceanographic data collection phase of this project.

An Executive Summary has been prepared which presents the essential results and conclusions of this study. This Executive Summary is designed to be self-sufficient documentation of the project for those who may not be interested in the full, detailed report.

It has been a pleasure to work on this phase of our 1980 fiscal year contract with your Juneau staff. Please do not hesitate to contact us if you have questions regarding the contents or findings of this study.

Very truly yours,

DAMES & MOORE
Marine Services Group

Roger S. Schlueter, Ph.D.
Managing Principal-in-Charge

Charles I. Rauw

Charles I. Rauw
Project Manager

RSS:CIR:sms

PREFACE

This report describes a study of oil spill trajectory simulation in Lower Cook Inlet and Shelikof Strait, Alaska. The work was performed under Contract No. NA80RAC00075 between Dames & Moore and the National Oceanic and Atmospheric Administration.

This study was supported by the Bureau of Land Management through through interagency agreement with the National Oceanic and Atmospheric Administration, under which a multi-year program responding to needs of petroleum development of the Alaskan continental shelf is managed by the Outer Continental Shelf Environmental Assessment Program (OSCEAP) Office.

Executive Summary

The primary objective of this study, one of a continuing series focusing on the behavior of spilled oil, was to perform trajectory simulations of spilled oil in Lower Cook Inlet and Shelikof Strait, Alaska. Trajectories of the centroid of hypothetical surface slicks originating from selected launch sites throughout the study area represented slick behavior. Physico-chemical processes such as spreading, evaporation, and sinking were neglected. Trajectory driving forces included winds, tidal and net currents.

A total of 38 hypothetical launch sites were specified by the U.S. Geological Survey (USGS) as representing locations of potential transportation routes, drilling and production sites within the study area. Also included in these sites were five open water boundary launch sites which allowed the results presented here to be interfaced with a complementary USGS Gulf of Alaska trajectory model.

Wind fields in the area of interest were defined by five spatially dependent flow patterns and six intensity factors. These patterns were prepared by the Pacific Marine Environmental Laboratories (PMEL, 1980) and represent refinements to the five primary wind fields developed and presented in Dames & Moore, 1979. The wind patterns and intensity factors were correlated by PMEL to the 22 baric weather patterns developed in Putnins, 1966a. A catalog of approximately 19 continuous years of daily baric weather patterns (Putnins, 1966b) was converted to a corresponding wind pattern and intensity catalog.

Surface currents were divided into two spatially varying components, a time-dependent tidal flow and a constant net surface circulation. The tidal flow field for Lower Cook Inlet was the same as that developed in Dames & Moore, 1979 and represents average tidal current velocities based on harmonic analyses of current measurements in combination with the results of a tidal flow hydrodynamic model. The tidal flow field was expanded to include Shelikof Strait using harmonic analyses of current measurements from two moorings within the strait.

The net surface circulation was represented by winter and summer net current patterns derived from analyses of current measurements, published literature, and a previously developed net circulation pattern (Dames & Moore, 1979).

In order to obtain a statistically significant sample of trajectory impact locations for subsequent risk analyses by the USGS, 200 trajectories were initiated at each launch site for both summer and winter seasons for a total of 15,200 trajectories. The winter season was defined from October through March and the summer season was defined from April through September. The basis for the seasonal designation was limited by the knowledge of the seasonal variation of net surface currents.

Each trajectory was initiated by randomly selecting a day/month/year within the desired season and entering the converted wind catalog for that date. The wind field was then sequenced from the initial starting date, every 24 hours according to the following observed weather pattern. The net current pattern for that season was held constant for the duration of trajectory simulation. The tidal current pattern was time dependent with the initial tidal phase incremented 30 degrees for each sequential trajectory.

A limited analysis was performed on the trajectory impact locations by season for all sites combined and for two selected sites individually. The results are presented in terms of the percent frequency of boundary impact per kilometer along discrete reaches of the shorelines of Lower Cook Inlet and Shelikof Strait.

The primary results from the present oil spill trajectory simulation were the 15,200 trajectories delivered to the USGS for use in their oil spill risk assessment study (LaBelle, 1980). These trajectories represent the most comprehensive set of descriptors of surface transport behavior available in Lower Cook Inlet and Shelikof Strait.

Two major improvements in the data base allowed consideration of seasonal effects on trajectory movement to be made for the first time. The availability of processed and analyzed winter net current data resulted in the ability to estimate winter and summer net current patterns. In addition, the use of Putnins' continuous daily weather catalog coupled to revised local wind fields over Lower Cook Inlet and Shelikof Strait also provided the ability to evaluate seasonal effects of the meteorological component of the trajectory driving forces.

The inclusion of variability of the wind fields resulted in complex trajectory behavior considering each trajectory independently. However, collectively the trajectories moved and/or impacted the shoreline in preferred directions or locations based primarily on launch site and season. Considering all sites combined and ignoring impacts along open water boundaries, the following areas experienced relatively high frequencies of shoreline impacts:

1. The northern and central shorelines of Shelikof Strait
2. Augustine Island
3. The Barren Islands
4. Kalgin Island
5. The western shoreline of Kamishak Bay
6. The western shoreline of Lower Cook Inlet between Iniskin Bay and Chisik Island
7. The shoreline of Lower Cook Inlet directly west of Kalgin Island
8. The eastern shoreline of Lower Cook Inlet between Anchor Point and Ninilchik

The major overall seasonal effect observed in the trajectories was a northward shift of the paths and impact locations during the summer season. This is a direct result of the decreased magnitude of the net current through Shelikof Strait and the increased frequency of northerly wind fields during the summer.

Further improvements in trajectory simulation for Lower Cook Inlet and Shelikof Strait using the deterministic approach taken in Dames & Moore (1976, 1979), and the present study should focus primarily on refining the temporal and spatial accuracy of the data bases. Incorporating diurnal variations in the wind fields would add to the dispersion of trajectories observed in the present study and would increase the ability to realistically model the meteorological forcing of surface transport.

The knowledge and accuracy of net surface currents in northern Lower Cook Inlet has not been improved over those used in the 1979 study. Unprocessed current meter records exist and analysis of these records would significantly improve the accuracy and reliability of the resulting trajectories in this portion of the study area. The variability of the net surface currents over periods of time as short as 24 hours have been observed to be significant both in terms of magnitude and direction. Incorporation of this effect would also add to the dispersive nature of trajectory paths and impact locations and would also increase the ability to realistically model the forcing fields.

These and other improvements would require significant committments of time and resources to perform field programs and data analyses. With the exception of the currents in northern Lower Cook Inlet, it is questionable whether the improvements if incorporated would provide cost effective increases in the present knowledge of surface transport characteristics in Lower Cook Inlet and Shelikof Strait. If the emphasis shifts from large regional studies of trajectory behavior to those local areas of concern identified by the regional studies, then those improvements in the data base would become mandatory. Local effects, such as a diurnal sea breeze, drainage winds, near coast circulation features, would need to be examined in detail as well as the variability of these features on a shorter time interval. This is a direct result of the fact that as the length scale of the area of interest becomes smaller, the time scale of the features modeled must be decreased (if the magnitudes of the forcing functions remain relatively constant) to provide the level of detail necessary to accurately evaluate the resulting trajectory movement.

It is also concluded that continued studies on a regional level of the behavior of spilled oil should begin to examine the physical characteristics of spills such as spreading, weathering, sinking and interactions with winds, waves and ice. These studies will provide more specific information from which environmental effects of spilled oil can be assessed.

CONTENTS

Page

I. Introduction 244

Purpose 244

Scope 244

Objectives 245

II. Modeling Approach 246

Oil Spill Model 246

Grid Coverage 247

Oil Spill Scenarios 248

III. Input Data Development and Application 250

General 250

Putnins' Weather Catalog 251

Wind Fields 254

Net Current Patterns 255

Tidal Current Pattern 260

IV. Simulation Results 262

V. Conclusions and Recommendations 273

Bibliography 277

Appendix A - Wind Field & Intensity Catalog Input Data File 318

Appendix B - Wind Field Input Data File 323

Appendix C - Net Current Field Input Data File 334

Appendix D - Tidal Current Field Input Data File 342

LIST OF FIGURES

Figure

279

1 Grid System 279

2 Trajectory Launch Sites 280

3 Wind Field 1 281

4 Wind Field 2 282

5 Wind Field 3 283

6 Wind Field 4 284

7 Wind Field 5 285

8 Winter Net Current Pattern 286

9 Summer Net Current Pattern 287

10 Tidal Current Phase Distribution 288

11 Tidal Current Pattern - Phase = 0° 289

12 Tidal Current Pattern - Phase = 90° 290

13 Tidal Current Pattern - Phase = 180° 291

14 Tidal Current Pattern - Phase = 270° 292

15-18 Sample Trajectories, Site P7, Winter 293 - 296

19-22 Sample Trajectories, Site P7, Summer 297 - 300

23-26 Sample Trajectories, Site P3, Winter 301 - 304

27-30 Sample Trajectories, Site P3, Summer 305 - 308

31-32 Base Case Trajectories, Site 8, Dames & Moore (1979) 309 - 310

33 Boundary Impact Frequency, Site P7, Winter 311

34 Boundary Impact Frequency, Site P7, Summer 312

35 Boundary Impact Frequency, Site P3, Winter 313

36 Boundary Impact Frequency, Site P3, Summer 314

37 Annual Percent Probability of Exposure, Site 8, Dames & Moore (1979) 315

38 Boundary Impact Frequency, All Sites, Winter 316

39 Boundary Impact Frequency, All Sites, Summer 317

LIST OF TABLES

Table

I Conversion Factors From Putnins' Weather Typology to PMEL's Wind Field and Intensity Factors 252

II Wind Field Frequency of Occurrence 256

III Wind Field Frequency of Occurrence Accounting For Intensity 257

IV Percentage of Trajectories Exceeding Upper Time Limit of 10 Days 271

I. Introduction

Purpose

This study was initiated by the Outer Continental Shelf Environmental Assessment Program (OCSEAP) on behalf of the Bureau of Land Management. Two previous oil spill trajectory analyses covering the Lower Cook Inlet area were performed for the OCSEAP (Dames & Moore, 1976; Dames & Moore, 1979). These studies provided information on probable shoreline impact areas and associated time to impact of hypothetical oil spills originating from a total of 21 selected point spill locations within Lower Cook Inlet.

The present study extended the areal coverage to include Shelikof Strait and provided significant improvements in the environmental data fields. The calculated trajectories were supplied to the USGS for their use in an oil spill risk assessment study (LaBelle, 1980).

Scope

This study was conducted in accordance with the scope of services for Task I detailed in the Dames & Moore proposal, "Oil Dispersion Analysis, Lower Cook Inlet and Shelikof Strait, Alaska," RFx41-436-2905, for National Oceanic and Atmospheric Administration, July 19, 1979 and "Proposal Addendum, Oil Spill Dispersion Analysis," RFx41-436-2905, October 15, 1979, subsequently amended in a letter dated February 4, 1980.

Objectives

The primary elements of the scope of services for Task 1 presented in the above documents are summarized below:

1. Expand the areal coverage of the modeling effort to incorporate Shelikof Strait.
2. Update and extend the net and tidal current fields based on information supplied by Pacific Marine Environmental Laboratories (PMEL).
3. Revise and extend surface wind patterns developed by PMEL corresponding to specific baric weather patterns identified by Putnins (1966a and 1969).
4. Calculate trajectories from sites specified by the USGS using a daily sequence of wind patterns corresponding to historically observed baric weather patterns (Putnins, 1966b).
5. Provide trajectory information to the USGS in a computer compatible format as input to a risk assessment study.
6. Evaluate the applicability of a first order wind field transition matrix to represent historically observed sequences and variability of wind fields as applied to trajectory simulation.

Elements 1-5 are reported upon here; results of the analyses conducted under element 6 are in preparation and will be reported in a separate submittal.

II. Modeling Approach

Oil Spill Model

The theoretical basis of the oil spill model used in this study is the same as employed in the two previous OCSEAP oil spill trajectory analyses performed for the Lower Cook Inlet area (Dames & Moore, 1976; 1979). Modifications to the computer program embodying the model were necessitated to allow implementation on a UNIVAC 90/60 computer. Additional modifications were performed to facilitate an increased efficiency in handling input/output requirements that were significantly larger due to expanded grid coverage, time variability of the wind fields and increased number of trajectory runs. Model verification was performed and was in agreement with the verification reported in Appendix A of Dames & Moore, 1979.

Movement of the spill centroid in the Dames & Moore model was considered to be governed by the independent effects of wind and water currents. Second-order forces such as waves and wind-wave current interaction were neglected. The wind-induced velocity vector of the trajectory centroid was taken to be colinear with the wind vector and proportional to the wind speed. The proportionality constant has been experimentally found in the range from 1 to 5 percent (Oceanographic Institute of Washington, 1977) and was taken to be 3 percent for this study. There is some question as to whether the wind and slick vectors should be colinear due to the considerable scatter in relevant field data. However, the evidence is not conclusive on this issue and, hence, this study assumed colinearity.

In the absence of winds, the slick centroid was modeled to move at the same velocity as the underlying current. As with the wind-driven component, there is no conclusive set of evidence which documents that this is the best approach. However, alternative schemes (i.e., Swartzberg, 1971) have major flaws or have been subjected to limited validation.

For this study, the current field was divided into two components, a net surface component and a tidal component. Hence, the centroidal velocity vector can be written as:

$$\bar{U}_{oil} = 0.03\ \bar{U}_{wind} + \bar{U}_{tidal} + \bar{U}_{net} \qquad (1)$$

With input data available to the model, a trajectory was generated by evaluating Equation (1) over a sequence of finite time steps (Δt = 30 minutes) until the centroid reached a boundary or exceeded an upper limit on time.

Grid Coverage

Operational implementation of the oil spill model was based on a grid system that overlapped the area of interest as illustrated in Figure 1. The grid system served multiple purposes: (1) definition of the Cook Inlet and Shelikof Strait geometry, (2) input of wind and current information, and (3) definition of shoreline impact locations.

This grid system was oriented along the main axis of Lower Cook Inlet and Shelikof Strait with each grid cell being 3 km on a side. Characteristic features required by the model, such as land and water areas and open water boundaries, were prescribed by assigning to each cell an index that defined the predominant feature of that cell. Land boundaries were chosen to represent the best approximation of the geometric extent of the inlet.

The boundary of the grid system shown in Figure 1 ignored those bays, inlets and channels that were not considered major features of the Lower Cook Inlet and Shelikof Strait system. The surface winds and water motions within these areas are dominated by local effects that cannot be determined from the regional wind and flow patterns developed for the larger open water areas of Lower Cook Inlet and Shelikof Strait. Without detailed oceanographic and meteorological data in each embayment, inlet, or channel, it was not possible to accurately simulate the movement of a spill centroid for these areas. Therefore, for those cases where the trajectory intersected one of these boundary conditions, the trajectory was terminated. It was concluded that oil would have entered the bay, inlet, or channel, but its subsequent behavior is unknown.

Oil Spill Scenarios

The locations of oil spill launch sites for the trajectory study were specified by the USGS since the results of the trajectory analysis were to be used by the USGS in an oil spill risk assessment (LaBelle, 1980). The launch sites specified were substantially different from those used in the previous trajectory analyses (Dames & Moore, 1979; 1976). Except for one point site, all launch sites were designated as line sources as shown in Figure 2. These line sources represent launch sites that cover potential platform locations, tanker or pipeline transportation routes, or water grid boundaries. The water grid boundary launch sites were selected by USGS to allow them to pick up a trajectory moving out of the boundary and continue the trajectory simulation beyond the Dames & Moore grid system.

From each launch site shown in Figure 2, 400 trajectories were initiated. For the line sources, the trajectory starting locations were evenly distributed along the total length of the line. Two hundred trajectories were launched from each site during a summer and winter season for a total of 400 trajectories per site. The number of trajectories per site per season was specified by the USGS as being the minimum number of trajectories required to obtain statistical significance for their risk assessment. The total number of trajectories that were calculated for the Lower Cook Inlet and Shelikof Strait area was 15,200 (38 sites x 200 trajectories per site per season x 2 seasons). This represented an increase of approximately 20 times the number of trajectories that were run in the 1979 Dames & Moore trajectory analysis. The results of these trajectories were supplied on computer compatible magnetic tape to the USGS.

III. Input Data Development and Application

General

The primary emphasis on input data development for the present study was to improve the wind fields and implement a technique that would realistically approximate their variability. Recommendations made at the conclusion of the 1979 trajectory analysis recognized this simulation deficiency and concluded, "the results of this project indicate that the wind fields and their simulated behavior are the most limiting aspect of the environmental data base" (Dames & Moore, 1979).

Secondary emphasis was placed on improvements in the net current field made possible by the availability of analyzed winter current measurements and ongoing studies of the general circulation features of the Lower Cook Inlet and Shelikof Strait system. The availability of winter current data provided the potential for development of at least two seasonal net current patterns, winter and summer. The ongoing circulation studies provided information that would allow refinement of the spatial features of the previously developed net circulation pattern.

Due to the inclusion of Shelikof Strait, which increased the study area nearly two-fold, another aspect of input data development was to collect and analyze the necessary information to expand both the wind and current fields to cover Shelikof Strait.

All of the above input data improvements were to be extracted from available OCSEAP reports. However, during the course of the study, certain data was not available in the requisite format. This necessitated additional data analyses to develop the required fields. Detailed discussion of the input data development is provided in the following sections.

Putnins' Weather Pattern Catalog

The original intent of the meteorological input data was to utilize variable wind fields with improved spatial resolution developed by PMEL. The variability of the wind fields was to be prescribed by a transition matrix also developed by PMEL based on their meteorological data and analyses in the Lower Cook Inlet and Shelikof Strait area. Based on a preliminary meeting, it became apparent that these data products were not going to be available in time to incorporate them into the trajectory analysis. It was agreed that PMEL would revise the Putnins' wind fields used in the previous trajectory studies (Dames & Moore, 1979; 1976) and provide a transition matrix based on Putnins' work (Putnins, 1966a; 1969). Review of the Putnins' transition matrix provided by PMEL revealed that it was incomplete and overemphasized the more frequently occurring weather patterns. A solution to this problem was obtained by utilization of Putnins' unpublished tabulations of approximately 19 years of daily baric weather patterns (Putnins, 1966b).

Putnins developed 22 specific baric weather patterns describing mesoscale weather situations over Alaska. These 22 baric weather patterns were related to 5 wind fields and 6 wind field intensities as developed by PMEL and shown in Table I (PMEL, 1980). These wind patterns and intensity conversions allowed two approaches to the utilization of Putnins' catalog of daily baric weather patterns. The first approach was to use the

TABLE I

CONVERSION FACTORS FROM PUTNINS' WEATHER TYPOLOGY TO PMEL'S WIND FIELD AND INTENSITY FACTORS

Putnins Type		PMEL Type
A	=	25
A_C	=	25
A'	=	53
A"	=	33
A"'	=	43
A_1	=	15
A_2	=	43
A_3	=	31
B	=	16
C	=	22
C_1	=	42
D	=	23
D'	=	15
D_1	=	23
E	=	45
E'	=	42
E"	=	26
E_1	=	22
F	=	43
F_1	=	23
G	=	53
H	=	14

PMEL Type	
(Wind Field /	Intensity Factor)
1 = Figure 3	1 = 0.3
2 = Figure 4	2 = 0.5
3 = Figure 5	3 = 1.0
4 = Figure 6	4 = 1.2
5 = Figure 7	5 = 1.5
	6 = 0.7

Example: PMEL Type 45 represents wind field number 4 as shown in Figure 6 with all magnitudes increased by a factor of 1.5 as denoted by the intensity factor index 5. PMEL Type 45 is equivalent to Putnins' Weather Type E.

catalog directly, entering with a random date and historically sequencing the wind fields as converted by Table I from the weather types given in the catalog. The second approach was to use the catalog to calculate a first order transition matrix and use this matrix to sequence the wind fields. The former method was selected for this trajectory study because certain unresolved questions remained regarding the applicability of a first order transition matrix to the accurate sequencing of weather patterns in Alaska. These questions are currently under study with the results to be presented in a succeeding report.

Seasonal variability of the full suite of trajectory driving forces was limited by the ability to define the seasonal characteristics of the net current pattern. Since only "winter" and "summer" net current patterns could be developed from the data sources, the wind fields were also applied seasonally by "winter" and "summer" conditions defined by the chosen starting date of the catalog. Winter conditions were defined as occurring from October through March, and summer conditions defined as occurring from April through September.

The wind field catalog includes all days from January 1, 1945 through March 31, 1963. The wind field sequencing was initiated by randomly selecting a day, month and year. As the trajectory simulation proceeded, the wind fields were sequenced every 24 hours corresponding to the observed sequence in the catalog. This sequencing continued until the trajectory impacted a boundary or exceeded a time limit of 10 days. The daily catalog of wind fields and intensities that were used for the trajectory simulation is presented in Appendix A.

Wind Fields

As briefly discussed in the previous section, the original intent regarding preparation of the meteorological input data was for PMEL to develop representative wind fields over Lower Cook Inlet and Shelikof Strait as a direct result of their ongoing meteorological programs. The required products were not available within the schedule limitations of the trajectory simulation study. This necessitated a less rigorous treatment of the wind fields and it was agreed that PMEL would provide revisions to wind fields previously developed by Dames & Moore for use with Putnins' typology. PMEL's direct exposure to local wind characteristics, derived during their meteorological field measurement program and data analysis, would provide added confidence in the wind field development. The five wind fields developed by PMEL were reviewed in Anchorage, Alaska on February 6, 1980 during a combined meeting with PMEL, Dames & Moore and local meteorologists.

The revised wind fields included the spatial variability of wind speed and direction over Lower Cook Inlet and Shelikof Strait. In addition, wind intensity scaling factors were assigned to each wind field to account for the relative strength or weakness of the wind pattern as related to a particular Putnins' baric weather pattern. The intensity scaling factors that were applied to each wind field essentially multiplied all speeds by a constant factor; the direction was unaffected by this scaling process.

The five basic wind fields are shown on Figures 3 through 7, and the relationship between intensity, wind field and baric weather pattern is presented in Table I. The digitized input data files for the five basic wind fields are presented in Appendix B. Table II presents the percent frequency of occurrence for the five basic wind fields for summer, winter and annual conditions. These frequencies were derived from the 19 years of converted daily weather catalog data. Table III presents the percent frequency of occurrence for the 13 specific combinations of wind fields and intensity factors for summer, winter and annual conditions. A comparison of the summer and winter frequencies of occurrence indicates that seasonal variations in percentages are significant.

Net Current Patterns

The net current pattern utilized in the 1979 trajectory analysis (Dames & Moore, 1979) was developed primarily from current measurement data taken by PMEL and NOS during summer months from May to August. Thus, the pattern was representative of summer conditions and seasonal variations of the net surface circulation were not included in the 1979 trajectory analysis.

The objective of developing updated current patterns for the present study was to include seasonal variations based on published information from PMEL. Winter current meter data had been processed and analyzed by PMEL and thus afforded an opportunity to estimate at least a representative average summer and

TABLE II
WIND FIELD FREQUENCY OF OCCURRENCE

PMEL Type (Wind Field)	Percent Frequency of Occurrence		
	Summer (April-Sept)	Winter (Oct-March)	Annual
1	11.60	20.21	15.95
2	17.15	32.33	24.83
3	9.71	2.61	6.12
4	36.40	21.04	28.64
5	25.14	23.81	24.46

TABLE III

WIND FIELD FREQUENCY OF OCCURRENCE ACCOUNTING FOR INTENSITY

PMEL Type (Wind Field/Intensity Factor)	Percent Frequency of Occurrence		
	Summer (April-Sept)	Winter (Oct-March)	Annual
14	3.83	10.42	7.16
15	6.44	9.11	7.79
16	1.34	0.68	1.01
22	2.00	2.73	2.37
23	6.65	14.37	10.55
25	8.29	14.28	11.32
26	0.36	1.10	0.74
31	1.37	0.65	1.01
33	8.35	1.96	5.12
42	15.94	11.07	13.48
43	12.72	5.02	8.82
45	7.74	4.96	6.33
53	24.97	23.67	24.30

winter net surface circulation pattern. Temporal variations of each pattern were not able to be specified from the available data base. The area of coverage was expanded to include Shelikof Strait.

The published reports that were used to develop the winter and summer net current patterns included Muench, et al. (1978, 1980); Schumacher, et al. (1978, 1979); and Reed, et al. (1979). In addition, a visit was made to PMEL to obtain clarification of certain data and results and to extract newly analyzed and unpublished data (Muench, 1979). These data sources were used to modify and expand the representative average net summer circulation pattern presented in Dames & Moore, 1979. An average net winter circulation pattern was also developed from the above data sources. Major features of both the summer and winter net circulation patterns are in agreement with the circulation pattern presented in Muench, et al. (1980). Flow patterns in the northern portion of Lower Cook Inlet, not covered by the pattern presented in Muench, et al. (1980), were extracted from the pattern presented in Dames & Moore (1979). The net circulation pattern for northern Lower Cook Inlet was described in Dames & Moore (1979) as being at best a rough estimate. No new data or analyses were found in the publications used to develop the patterns for this study that would increase the confidence or accuracy of the net circulation pattern in this area of Lower Cook Inlet.

The net surface cirulation patterns for representative winter and summer conditions are shown on Figures 8 and 9, respectively and are presented in digitized form in Appendix C.

Winter is defined as that period from October through March, and summer is defined as that period from April through September.

One important aspect of the net current input data that could not be addressed with the information contained in the publications used to develop the net current patterns is their variability with time. The spatial distribution of current meter moorings within Lower Cook Inlet and Shelikof Strait was not adequate to represent the current variability by using standard deviations of the mean. This technique was used in a limited analysis in conjunction with an assumed normal distribution for selected areas with dense current meter coverage in Lower Cook Inlet for the Dames & Moore 1979 study. For the present study, two current meter moorings are used to describe the currents in Shelikof Strait, and none are available to characterize the surface current variability in northern Lower Cook Inlet. For the present trajectory simulation analysis, the current variability would need to be specified over the entire area of coverage.

The variability of the magnitude and direction of measured currents in Lower Cook Inlet and Shelikof Strait has been discussed in Muench, et al. (1980); Muench, et al. (1978); and Schumacher, et al. (1978). In summary, these publications characterize the current variability in Lower Cook Inlet and Shelikof Strait as having speed and direction fluctuations with time scales of 2 to 7 days. Shelikof Strait has a strong mean flow and experiences fluctuations in speed and direction that are smaller relative to the mean flow compared to regions of weak mean flow, such as in central Lower Cook Inlet, where the fluctuations become the dominant flow characteristic. Attempts to correlate the fluctuations observed from the various current moorings generally revealed a poorly related sequence of flow events. The one exception occurred between the two current meter stations located within Shelikof Strait. This was expected in that Shelikof Strait has confining lateral boundaries which, due to continuity considerations, suggest that a fluctuation at one end would generate a compensating fluctuation at the other end.

Tidal Current Pattern

The tidal current pattern developed in Dames & Moore (1979) was expanded to cover Shelikof Strait. The semidiurnal tide has a standing wave characteristic within Shelikof Strait as a result of the progressive tidal wave entering the strait from both the north and south end as it passes Kodiak Island. This results in an antinode, where no semidiurnal tidal current component would exist, located in the upper third of the strait.

The semidiurnal component of tidal current was selected to represent average tidal current conditions to be consistent with the analyses present in Dames & Moore (1979). The magnitude of both the ebb and flood M_2 tidal current constituent were assumed equal. The spatial distribution of the M_2 tidal current constituent in Lower Cook Inlet was interpolated in the Dames & Moore (1979) study with the aid of a two-dimensional hydrodynamic tidal model (Mungall and Matthews, 1973; and Mungall, 1973). Application of this model over the expanded study area was not conducted since it was believed that the tidal currents within the strait could adequately be interpolated from existing measurements and harmonic analyses by applying basic hydrodynamic principles.

Therefore, the tidal current pattern developed for the present study was based on the pattern developed in Dames & Moore (1979) and expanded to cover Shelikof Strait by interpolating the results of harmonic analyses of current meter data from two mooring locations in Shelikof Strait. Likewise, the spatial distribution of the tidal current phase angle was based on that presented in Dames & Moore (1979) and expanded to cover Shelikof Strait by interpolating the phase relationships of the harmonic analyses of current meter data given in Muench, et al. (1980) and as discussed with Muench (1979). The resulting tidal current phase distribution for the entire study area is shown in Figure 10. Tidal current vector patterns for phase angles of 0, 90, 180 and 270 degrees are shown in Figures 11 through 14, respectively. The zero phase angle was arbitrarily defined for the southern portion of Lower Cook Inlet on a line between Cape Douglas and Cape Elizabeth. The phase relationships shown are representative of peak tidal currents occurring during a mean tidal range with a single value corresponding to an average of the peak ebb and flood tidal current phases. The digitized tidal current field input data file is presented in Appendix D.

IV. Simulation Results

The primary results from the trajectory simulation for Lower Cook Inlet and Shelikof Strait were the computer tapes containing the 15,200 trajectories. These tapes were delivered to the USGS for subsequent use in an oil spill risk assessment. Therefore, no attempt was made to perform a complete trajectory analysis. However, a limited analysis was conducted in order to highlight the major findings, comparisons, and conclusions as a result of the present trajectory simulation study.

The most significant improvement over the trajectory simulation presented in Dames & Moore, 1979 is the inclusion of wind field variability. The 24 hour sequencing of wind fields in the present study more realistically represents the temporal variability of surface winds than the assumed 150 hour constant wind fields used in the 1979 study.

Examples of trajectories calculated in the present study are shown in Figures 15 through 30. These figures present sample trajectories from two launch sites, P7 and P3, for a variety of wind sequences on a seasonal basis. Comparison of these figures with Figures 31 and 32 (reproduced from Figures B-35 and B-53 presented in Dames & Moore, 1979) reveals a significant change in the behavior of a majority of the trajectories calculated in the present study. While persistence of the wind fields is evident for some of the trajectories presented in Figures 15 through 30, total reversals and major changes in direction are observed for the majority of the trajectories. Thus, the results of modeling the variability of the wind fields in the present study reinforces the conclusion reached in the 1979 study that the wind dominates trajectory movement. This conclusion should bear in mind that the variability of the other forcing fields, net and tidal currents, was not incorporated in the trajectory modeling effort for the present study. It would be reasonable to assume that the wind would dominate trajectory movement even if these effects were realistically modeled.

Figures 15 through 18 show sample trajectories from launch site P7 during the winter season. Ten trajectories are plotted on each figure. The trajectories exhibit two preferred directions; to the west into Kamishak Bay and to the southwest into Shelikof Strait. These directions were primarily a result of the vectorial combinations of the winter net current pattern and wind fields 1, 2 and 4. These wind fields occurred approximately 74% of the time during the winter season as shown on Table II. Therefore, trajectories with directions other than into Kamishak Bay and Shelikof Strait would be the exception rather than the rule.

Travel time to impact varied widely depending on many parameters so that no attempt was made to evaluate the elapsed time to impact in detail. The elapsed time to impact for trajectories from launch site P7 during winter conditions ranged from 12 hours up to the simulation time limit of 240 hours (10 days).

Figures 19 through 22 present sample trajectories from launch site P7 during the summer season. Ten trajectories are plotted on each figure. Comparison of the winter and summer trajectories showed a significant shift of overall trajectory movement. The summer trajectories penetrated further up into Lower Cook Inlet than the winter trajectories. This occurred even though the summer net current magnitude in Lower Cook Inlet was greater than in winter. Wind fields 3 and 4 would combine vectorially with the net current field to generate movement up into Lower Cook Inlet. These two wind fields occurred approximately twice as frequently in summer as in winter (46% to 26% of the time) which resulted in the observed change in overall trajectory movement up into Lower Cook Inlet during summer conditions. The elapsed time to impact for trajectories from launch site P7 during summer conditions ranged from 14 to 240 hours.

Trajectories were also examined from site P3. As shown in Figure 2, site P3 is a point source site and was located in very nearly the same location as site 8 from the 1979 study. The selection of site P3 for trajectory analysis in the present study allowed limited qualitative comparisons to be made between the results of the two studies. Sample trajectories are provided in Figures 23 through 30. There are ten sample trajectories plotted on each figure and four figures presented for each season.

Site P3 was located near the north end of Shelikof Strait where the flows from Lower Cook Inlet and through Kennedy and Stevenson Entrances converged to form a strong southwesterly net flow. Based on this net flow and the dominant winter wind fields it would be expected that the primary trajectory movement would be to the southwest into Shelikof Strait during the winter season. In fact, this conclusion was shown to be true for those trajectories presented in Figures 23 through 26. These sets of figures represent sample trajectories calculated during winter conditions. None of the sample trajectories presented in these figures showed movement into Lower Cook Inlet northward of Augustine Island. The elapsed time to impact for trajectories from launch site P3 during winter conditions ranged from 30 to 240 hours.

During summer conditions the net flow into and through Shelikof Strait weakened and the frequency of wind fields 3 and 4, which have north-northeasterly flow in the vicinity of P3, increased significantly. The combination of these two factors should have resulted in an overall shift of trajectories northward with some increase in transport into Lower Cook Inlet. Also, the reduced net current magnitudes through Kennedy and Stevenson Entrances during the summer should have allowed an increase in trajectory movement toward the Barren Islands from site P3. Figures 27 through 30 show in a qualitative sense that the above features were, in fact, observed. These figures show an increase of trajectories moving into Kamishak Bay and around the Barren Islands over that observed during winter. Some trajectories moved north of Augustine Island basically keeping to the middle or western side of Lower Cook Inlet. The elapsed time to impact for trajectories from launch site P3 during summer conditons ranged from 23 to 240 hours.

Since it was not feasible to meaningfully present all trajectories from one site, much less all sites, summary figures were developed showing percent frequency of boundary impact per kilometer of boundary. The shoreline and water boundaries were segmented into representative reaches and the frequency of trajectory impact was calculated for each reach for winter and summer conditions. The frequency of impact per kilometer of reach was displayed by the width of each line segment. This technique provided a qualitative visual aid in evaluating trajectory impact distribution.

Figure 33 presents the percent frequency of boundary impact per kilometer of reach for site P7 for winter conditions. The most obvious feature was the high frequency of impact which occurred near Chenik Head along the west side of Kamishak Bay. This was due primarily to wind fields 2 and 4 which occurred over 53% of the time during winter and had westerly flows that would clearly dominate trajectories in the weak net and tidal current fields existing in Kamishak Bay. Relatively large frequencies of impact also occurred along the western reach of Augustine Island and the northern exposed reach of Uganik Bay. Both shorelines of middle and northern Shelikof Strait were impacted with regular frequency. Other areas that had significant impact frequencies included the Barren Islands and the western shoreline of Lower Cook Inlet from Ursus Cove to just below Chisik Island. No impacts were recorded north of Chisik Island nor along the eastern shoreline of Lower Cook Inlet. This area included Kachemak Bay southward around Cape Elizabeth to the Chugach Islands.

Figure 34 presents the percent frequency of boundary impact per kilometer of reach for site P7 for summer conditions. The high impact frequency near Chenik Head was again apparent, but was lesser in magnitude than that observed during winter conditions. This was presumably due to the stronger southwesterly net flow in central Lower Cook Inlet during the summer conditions as wind fields 2 and 4 maintained a strong 53% combined frequency of occurrence during the summer conditions. The shift in impact location toward the north during summer was evident in this figure. Impacts along both shorelines of Shelikof Strait were observed to diminish during summer. Augustine Island had an increase in impact frequency as did the Barren Islands. Most notably the western shoreline of Lower Cook Inlet from Iniskin Bay to just north of Chinitna Bay displayed a dramatic increase in impact frequency. The northern portion of Lower Cook Inlet was again void of any trajectory impacts, but some trajectories now impacted the eastern shoreline near Anchor Point in Kachemak Bay and along Cape Elizabeth. Rather significant frequency of impacts occurred along the water boundaries of Kennedy and Stevenson Entrances suggesting possible transport into the Gulf of Alaska northeast of Kodiak Island. Impacts also occurred at a lesser frequency along the water boundary between the southern tip of Kodiak Island and the Alaska Peninsula, indicating transport south of Kodiak Island.

Figures 35 and 36 present the percent frequency of boundary impact per kilometer of reach for site P3 for winter and summer conditions, respectively. The winter figure indicated a rather even distribution along the western shoreline of Kamishak Bay and southward along both shorelines of Shelikof Strait. No impacts were recorded north of Augustine Island and the largest impact frequencies occurred along the shorelines in the central portion of Shelikof Strait. This portion of Shelikof Strait, between Cape Gull and Uganik Bay represents the narrowest width of the strait. In addition, this area marks a transition in a slight alignment change between upper and lower Shelikof Strait. Therefore, it would be expected that this region would experience a greater frequency of impact from trajectories moving up or down the strait due to the narrow width and slight change in geometric alignment.

Figure 36 reveals that summer conditions again result in a general northward shift of impact locations compared to those observed during winter conditions. The frequency distribution along the shorelines of Shelikof Strait had lessened in magnitude and extent. The frequency of impacts which occurred along the western shoreline of Kamishak Bay dramatically increased over that observed during winter conditions. The Barren Islands had a high frequency of impact primarily along the western and southern exposure of their shorelines. Impacts also occurred along the southern shoreline of Augustine Island and the western shoreline of Lower Cook Inlet from Iniskin Bay northward beyond Chinitna Bay. A relatively high frequency of impacts occurred along the water boundary of Kennedy and Stevenson Entrances for both winter and summer conditions. However, only winter conditions indicated trajectory movement as far south as the boundary between the southern tip of Kodiak Island and the Alaska Peninsula.

Although a direct comparison of trajectory impact cannot be made for site P3 in the present study and site 8 in the 1979 study, Figure 37 is presented for a qualitative discussion. Figure 37 is reproduced from Figure B-89 of Dames & Moore, 1979, and presents the annual percent probability of shoreline exposure for trajectory impacts from site 8 of that study. Three regions were shown to have high probabilities of trajectory impact. These were the southern shoreline of Augustine Island, Cape Douglas and the northern and western shoreline of Shuyak Island. Also impacted, but to a lesser extent was the shoreline south of Chinitna Point and the shoreline near Anchor Point. The present study agreed with the high frequency of impacts along Shuyak Island and Cape Douglas, but did not indicate as high a relative frequency of impacts on Augustine Island. Within the same areal coverage as the 1979 study, the present study indicated high impact frequencies occurred among the Barren Islands and along the western shoreline of Kamishak Bay. These were areas that the 1979 study did not show as being impacted. The results of the two studies were in agreement with respect to the low frequency of impacts which occurred north of Augustine Island. Both studies showed no impacts near Kachemak Bay.

Figures 38 and 39 present the percent frequency of boundary impact per kilometer of reach for all sites for winter and summer conditions respectively. Again, the most general trend observed was a shift of trajectory impact location from the south to the north when comparing winter to summer conditions. Areas of high frequency of impact included the western shoreline of Kamishak Bay, Augustine Island, the Barren Islands, the western shoreline of Lower Cook Inlet from Iniskin Bay to north of Chinitna Bay and the central and northern shorelines of Shelikof Strait. The relatively high impact frequencies for the water boundary of Kennedy and Stevenson Entrances and the water boundary between the southern tip of Kodiak Island and the Alaska Peninsula were somewhat misleading. This was due to the fact that these boundaries were also used as launch sites for a significant number of the total trajectories simulated. Therefore, the frequencies along these boundaries were expected to be relatively high. Kamishak Bay is shown on both Figures 38 and 39 to have had very low frequencies of impacts. The southern shorelines of Shelikof Strait also had relatively low frequencies of impacts.

These figures provide a visual summary description of the trajectory simulation from a boundary impact viewpoint. However, the location of all launch sites should be kept in mind as they have just as direct an influence of impact location as the forcing fields used to drive the trajectories.

The percentage of trajectories that did not impact a boundary prior to exceeding the upper time limit of 10 days is presented in Table IV for sites P7, P3 and all sites combined for winter and summer conditions. This table shows that the time limitation of 10 days affected only a minor portion of the total number of trajectories run. In addition, the table shows the percentages for summer slightly and consistently higher than those for winter. This may be attributed to the stronger flows throughout most of the study area that occur in winter as well as an increased percent frequency of occurrence of wind fields with higher intensity factors during winter conditions.

TABLE IV

PERCENTAGE OF TRAJECTORIES REACHING UPPER TIME LIMIT OF 10 DAYS

	Percent of Trajectories	
Site	Winter	Summer
P7	6.5	8.5
P3	6.0	9.0
All Sites	6.8	8.2

A brief qualitative discussion of some aspects of the results of this trajectory analyses has been presented to help clarify the methodology and approach. The quantitative aspects of the results are the subject of the USGS risk assessment study (LaBelle, 1980). Tapes of all trajectory runs are being maintained by Dames & Moore if additional analyses are desired.

V. Conclusions and Recommendations

A brief discussion and samples of the results of this trajectory study were presented in the previous section. Without performing a detailed analysis of the trajectory results, only general conclusions can be drawn from this study.

Implementation of wind field variability was one of the primary objectives of this study. The persistence of the wind fields as well as the variability was incorporated through the use of Putnins' weather catalog and marks a significant improvement over the methodology employed in the 1979 study. The second significant improvement was the development and implementation of two seasonal (winter and summer) net current patterns. This allowed, for the first time in Lower Cook Inlet, trajectories to be computed on a seasonal basis. The primary difference was a general shift in trajectories toward the north during summer conditions. Weaker fields occurred during summer conditions which resulted in a slight increase in the number of trajectories that exceeded a 10 day upper limit on trajectory simulation time. It does not appear feasible, considering existing data and planned field efforts, to refine seasonal net current patterns beyond the two seasons developed in this study. The existence of Putnins' daily weather catalog and the coupled wind fields and intensity factors would allow any detail of seasonal breakdown.

The sample results of the trajectory simulation examined in this study once again suggest that the wind drift component of flow dominated trajectory movement. The variability of the wind fields added to this dominance in that the trajectory movement was altered significantly by each shift in the wind field. The seasonal variability of the net current patterns was observed in specific examples to result in an overall shift of trajectories somewhat northward during summer conditions. However, the net current patterns had a secondary (compared to the wind fields) effect on overall trajectory movement. The effect of the tidal current component was important in certain specific trajectories, but overall preferred movement was not significantly affected. It can be concluded that the tidal current component added a measure of dispersion to trajectory movement and impact location and should be included in trajectory simulation for an enclosed coastal region such as Lower Cook Inlet and Shelikof Strait.

If further trajectory simulations using deterministic environmental forcing fields are desired for this area, certain improvements can be suggested as a result of the present study and knowledge of the existing data base. One area of improved simulation would be to account for the diurnal land-sea interaction on the wind fields. Since this is primarily an onshore-offshore effect and would vary with location, the resulting trajectory behavior may be significant; as an example, shorter times to shoreline impact would be expected.

If improved deterministic trajectory simulation is desired, it is recommended that the variability of the net current pattern both in terms of magnitude and direction be evaluated in greater detail. This is particularly important where the variability has been shown to be significant. As discussed in Muench, 1980, flow pulses have been observed with current magnitudes twice as large as the mean and with complete reversals in direction at current moorings located at the northern end of Shelikof Strait. It is doubtful that the existing data base can provide the required spatial and temporal coverage for the parameters needed to specify the current variability. However, the effect of this variability could be examined in an area where adequate coverage existed and recommendations formulated from the results. It is further recommended that the unprocessed NOS current meter records from northern Lower Cook Inlet taken in 1973 be analyzed as the patterns utilized in this study are still uncertain in this area.

While the tidal current pattern used in the present study does not simulate the elliptical nature and lunar phasing of tidal current strength, it is not believed necessary to add these characteristics based on the results of this study as well as those of the 1979 study. A reasonable approximation can be implemented to account for these effects if so desired and would provide an additional source of time and spatial variability to trajectory simulations.

In summary, there are limited improvements that can be made to trajectory simulation using empirical, deterministic environmental forcing fields in the Lower Cook Inlet and Shelikof Strait area from existing data bases. Major improvements would require significant committments of time and resources to conduct and collect the appropriate field programs and data. Such programs might examine the directional and angular coupling of the wind drift component on an actual oil slick. Other field studies may be desired in order to define the surface transport existing in the various embayments and channels that are currently excluded from this grid system.

However, it is recommended that future efforts now begin to focus on those aspects of oil movement beyond the centroidal transport of a hypothetical slick. Mechanisms such as spreading and weathering are believed to be a more important consideration in oil spill assessment than the increased accuracy possibly obtainable in continued trajectory simulations.

BIBLIOGRAPHY

Dames & Moore, 1976. Report, Oil Spill Trajectory Analysis, Lower Cook Inlet, Alaska, for National Oceanic and Atmospheric Administration, Job Number 6797-003-20.

_____, 1979. Report, Oil Spill Trajectory Analysis, Lower Cook Inlet, Alaska, for National Oceanic and Atmospheric Administration, Job Number 6979-011-02.

LaBelle, R.P., W.B. Samuels, K.J. Lanfear, 1980. An Oil Spill Risk Analysis for Cook Inlet and Shelikof Strait (Proposed Sale 60) Outer Continental Shelf Lease Area; U.S. Geological Survey Open File Report 80 - in preparation .

Muench, R.D., H.O. Mofjeld, and R.L. Charnell, 1978. Oceanographic Conditions in Lower Cook Inlet: Spring and Summer 1973. J. Geophys. Res. 83(C10): 5090-5098.

Muench, R.D., 1979. Personal communication. Current meter data, circulation patterns and tidal current harmonics for Lower Cook Inlet and Shelikof Strait.

Muench, R.D., J.D. Schumacher, and R. Sillcox, 1979. Northwest Gulf of Alaska Shelf Circulation, Annual Report, Research Unit #138, U.S. Dept. of Commerce, NOAA/OCSEAP.

Muench, R.D., and J.D. Schumacher, 1980. Physical Oceanographic Conditions in the Northwest Gulf of Alaska, Northwest Gulf of Alaska Synthesis Report for U.S. Dept. of Commerce, NOAA/OCSEAP (in press).

Mungall, J.C.H., and J.B. Matthews, 1973. Numerical Tidal Models with Unequal Grid Spacings. Tech. Rep. R73-2. Institute of Marine Science, Univ. of Alaska, Fairbanks, Alaska.

Mungall, J.C.H., 1973. Cook Inlet Tidal Stream Atlas. Tech. Rep. R73-2. Institute of Marine Science, Univ. of Alaska, Fairbanks, Alaska.

Oceanographic Institute of Washington, 1977. Modeling Methods for Predicting Oil Spill Movement, Oceanographic Commission of Washington, Seattle, Washington, March.

Pacific Marine Environmental Laboratories, 1980. Personal communication. Development of local wind fields corresponding to regional synoptic weather patterns after Putnins, 1966a, R.M. Reynolds, Marine Meteorological Studies Group, NOAA.

Putnins, P., 1966a. Studies on the Meteorology of Alaska: First Interim Report (The sequences of baric weather patterns over Alaska). U.S. Dept. Commerce, ESSA/EDS, Silver Spring, Maryland.

_____, 1966b. Unpublished tabulation of daily baric weather types for Alaska from January 1, 1945 to March 31, 1963, University of Alaska.

_____, 1969. Studies on the Meteorology of Alaska: Final Report (Weather situations in Alaska during the occurrences of specific baric weather), U.S. Department of Commerce, ESSA, Research Laboratories, Boulder, Colorado, 80302, 267 p.

Reed, R.K., R.D. Muench, and J.D. Schumacher, 1979. On Baroclinic Transport of the Alaskan Stream near Kodiak Island. (in preparation for submission to Deep-Sea Res.)

Schumacher, J.D., R. Sillcox, D. Dreves, and R.D. Muench, 1978. Winter Circulation and Hydrography Over the Continental Shelf of the Northwest Gulf of Alaska. NOAA Technical Report ERL 404-PMEL 31, 16 p.

Schumacher, J.D., R.K. Reed, M. Grigsby, and D. Dreves, 1979. Circulation and Hydrography Near Kodiak Island; September - November 1977. (Submitted for publication as an ERL Technical Report.)

Swartzberg, H.G., 1971. "The Movement of Oil Spills," Proc. of the Jt. Conf. on Prev. and Cont. of Oil Spills, published by Amer. Petrol. Inst., Washington, D.C., pp. 489-494.

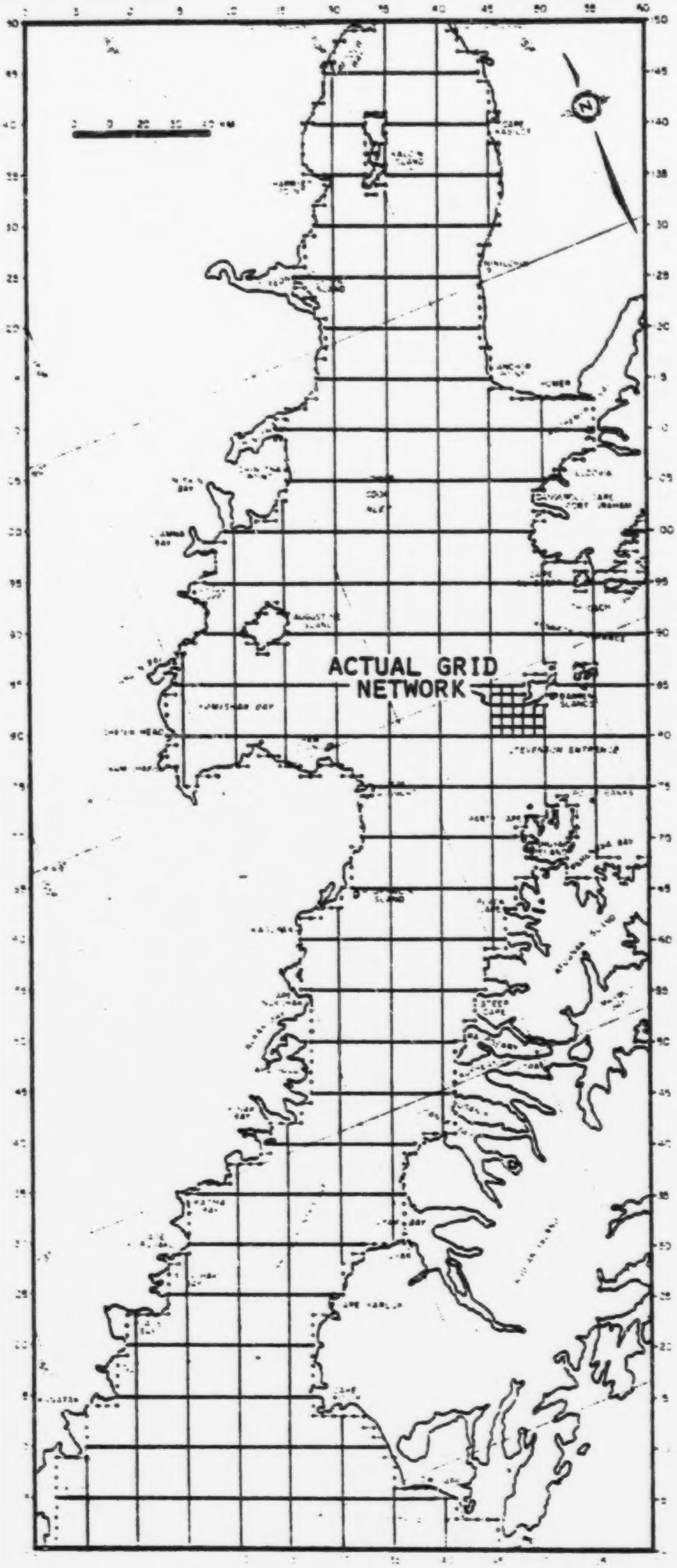
ACTUAL GRID NETWORK

NOTE:
GRID NETWORK OUTLINED
FOR EVERY FIFTH GRID
INTERVAL

FIGURE 1: GRID SYSTEM

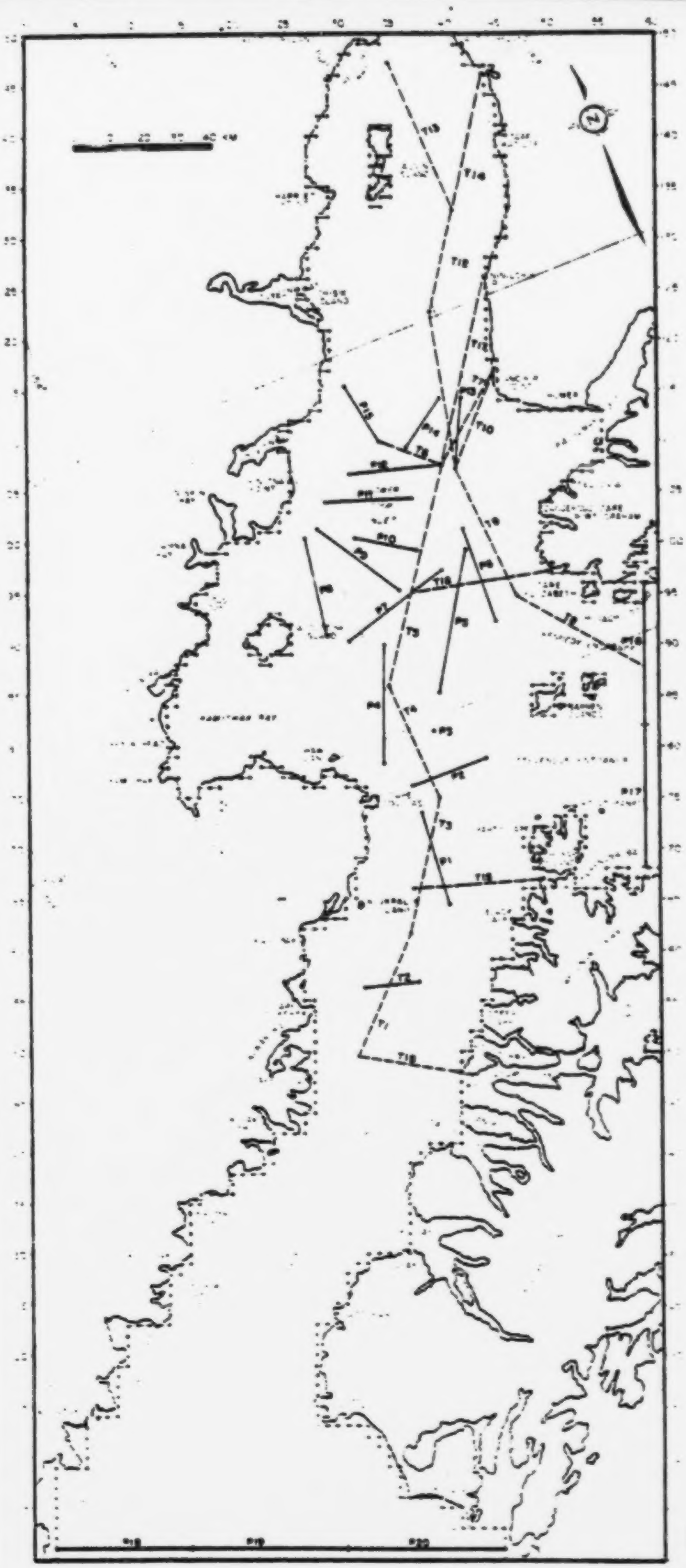
T13
T14
T18
T12
T10
P15
P14
P8
P11
P10
P9
P7
P6
P5
T16
T8
T5
T4
P4
P3
P2
T3
P1
T15
T2
T1
T18
P16
P17
P18
P19
P20

LEGEND:

P1 - P15 PLATFORM LOCATIONS

P16 - P20: WATER GRID BOUNDARIES

T1 - T18: PIPELINE OR TANKER ROUTES

FIGURE 2: TRAJECTORY LAUNCH SITES

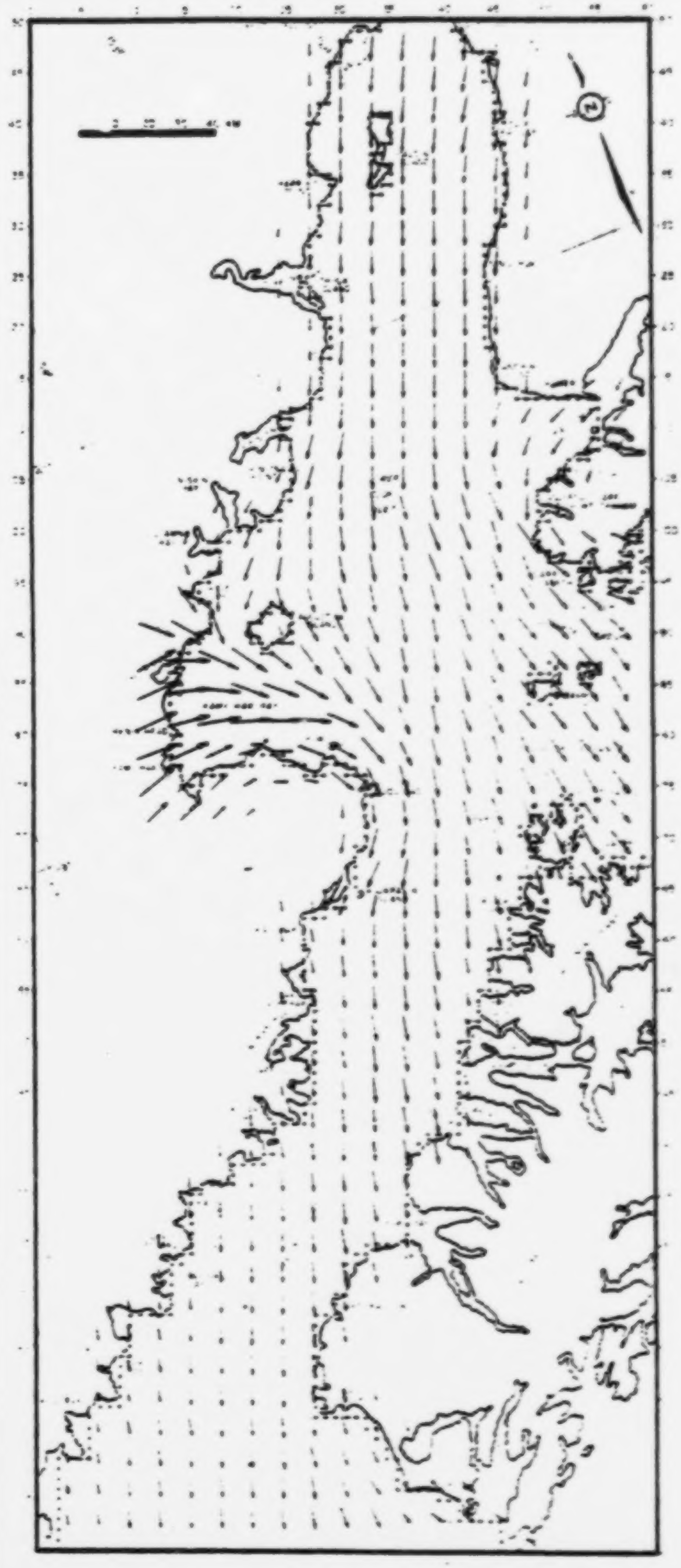

WIND VECTOR MAGNITUDE

→

25 METERS/SECOND

WIND FIELD PROBABILITY

ANNUAL - 15.95%
WINTER - 20.21%
SUMMER - 11.60%

FIGURE 3: WIND FIELD 1

BEST DOCUMENT AVAILABLE

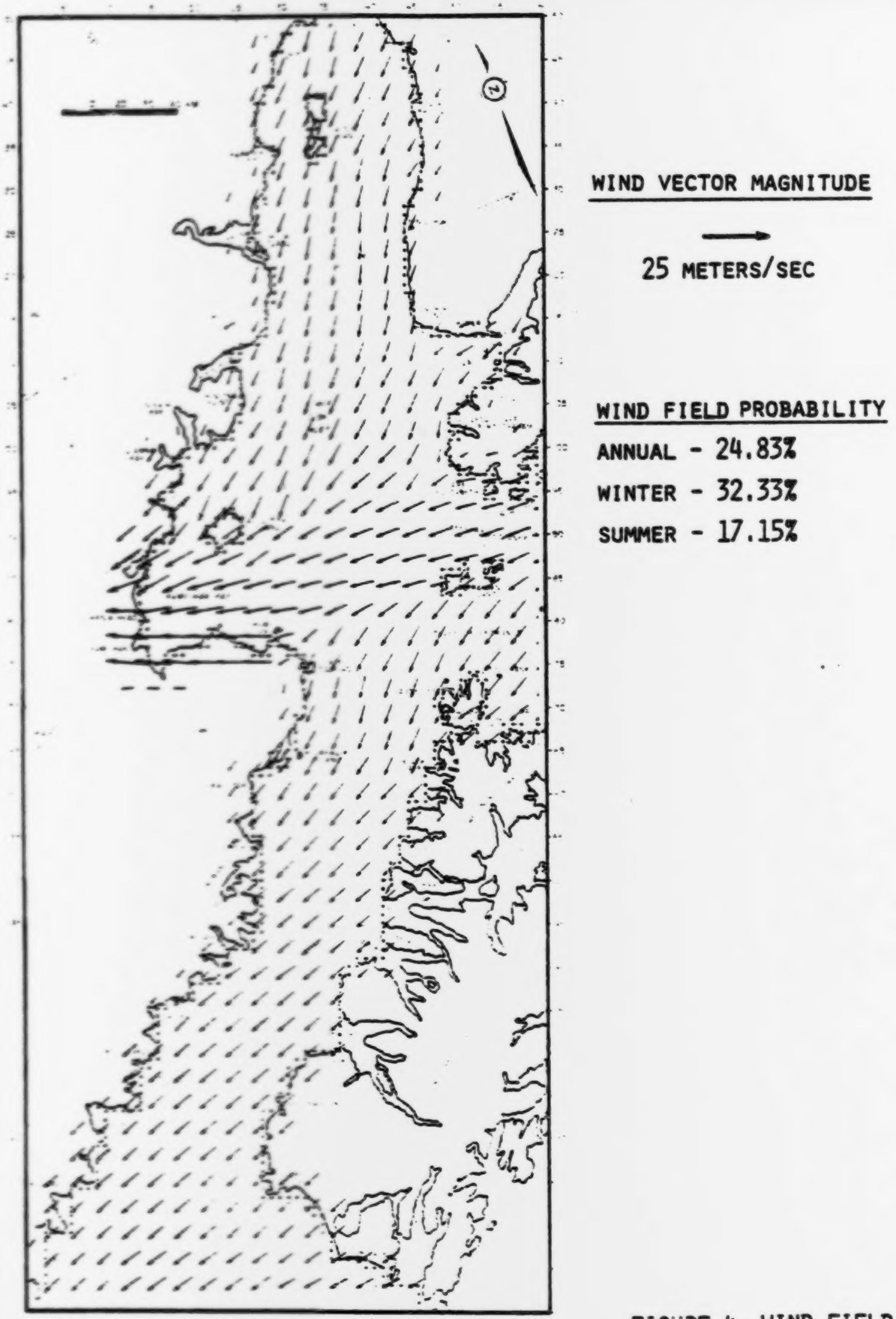
WIND VECTOR MAGNITUDE
25 METERS/SEC
WIND FIELD PROBABILITY
ANNUAL - 24.83%
WINTER - 32.33%
SUMMER - 17.15%
N

FIGURE 4: WIND FIELD 2

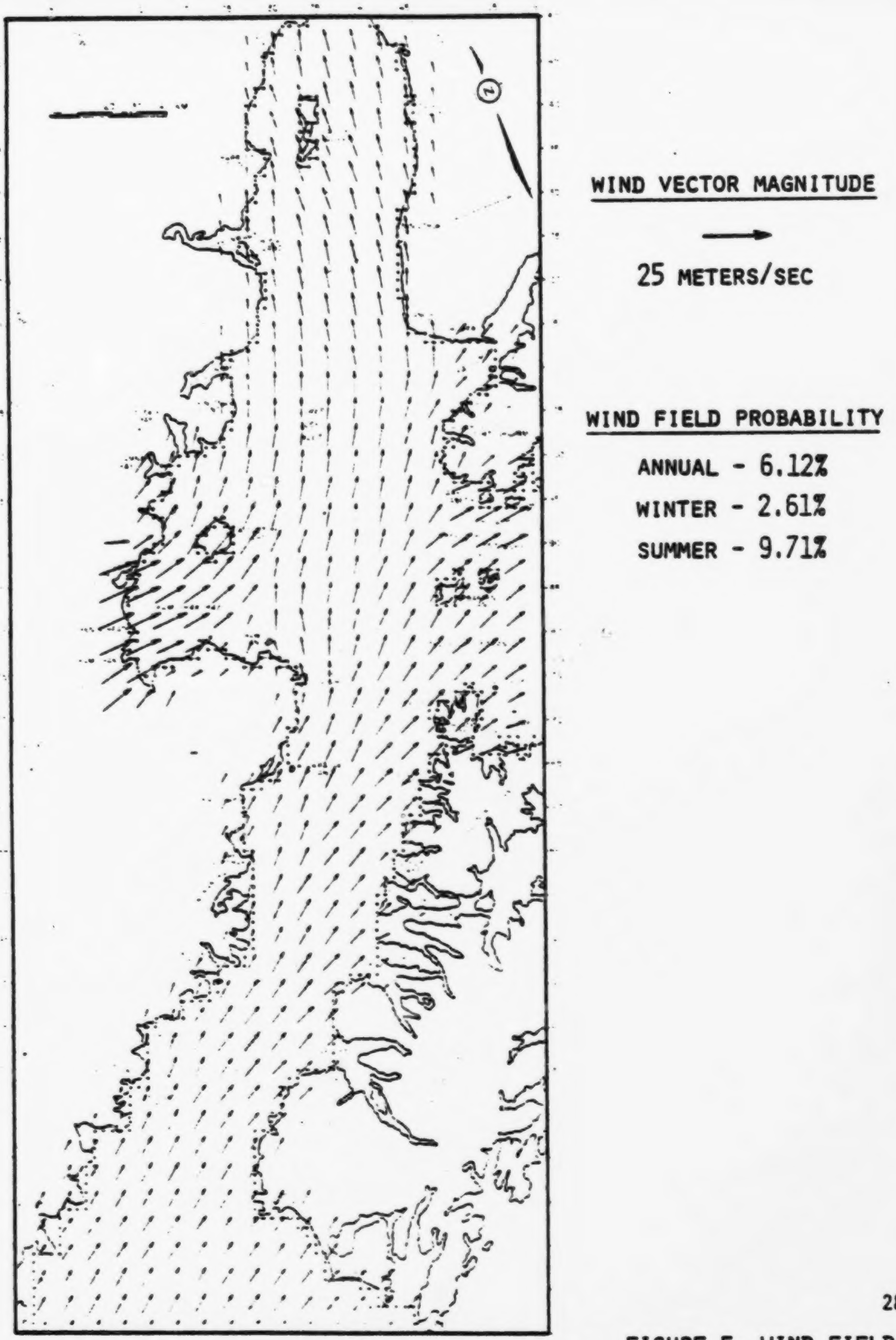
WIND VECTOR MAGNITUDE
25 METERS/SEC
WIND FIELD PROBABILITY
ANNUAL - 6.12%
WINTER - 2.61%
SUMMER - 9.71%

FIGURE 5: WIND FIELD 3

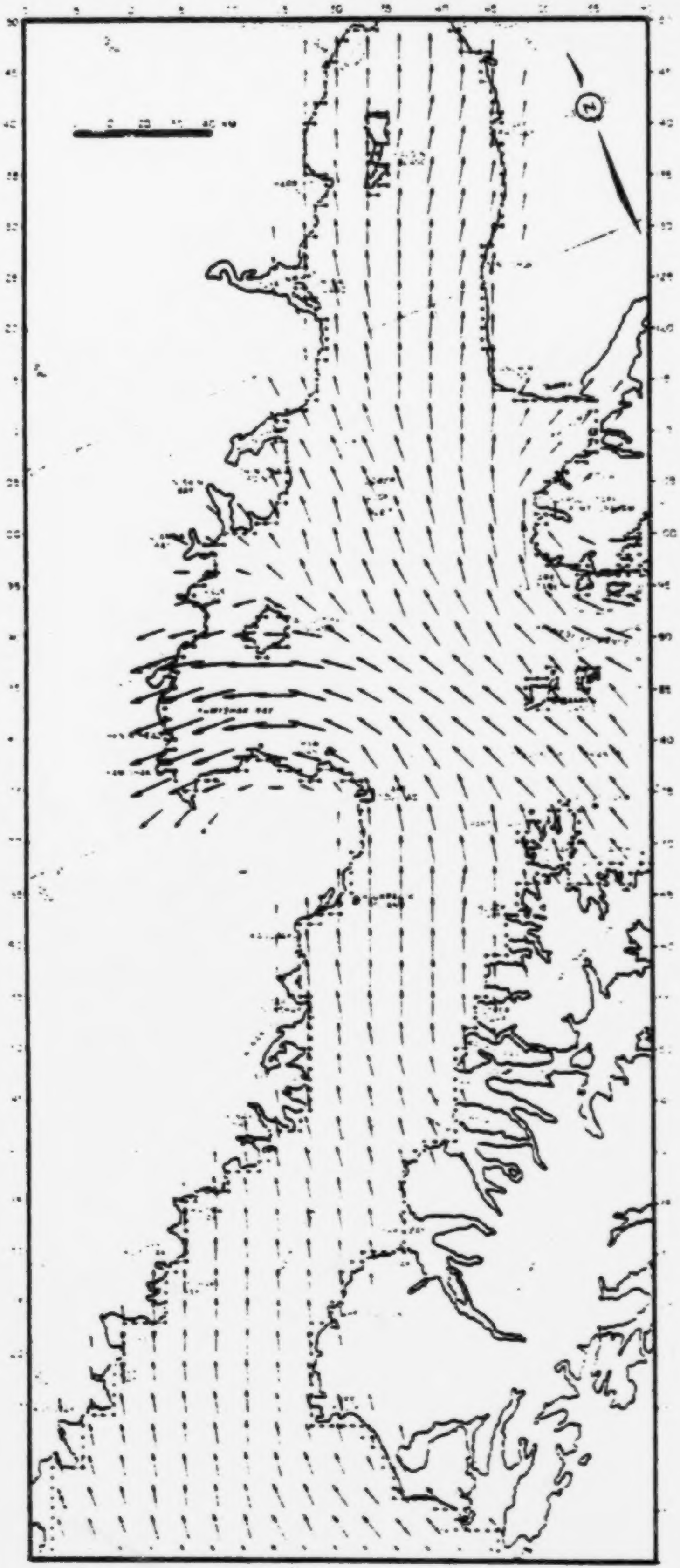

WIND VECTOR MAGNITUDE

→

25 METERS/SEC

WIND FIELD PROBABILITY

ANNUAL - 28.64%
WINTER - 21.04%
SUMMER - 36.40%

FIGURE 6: WIND FIELD 4

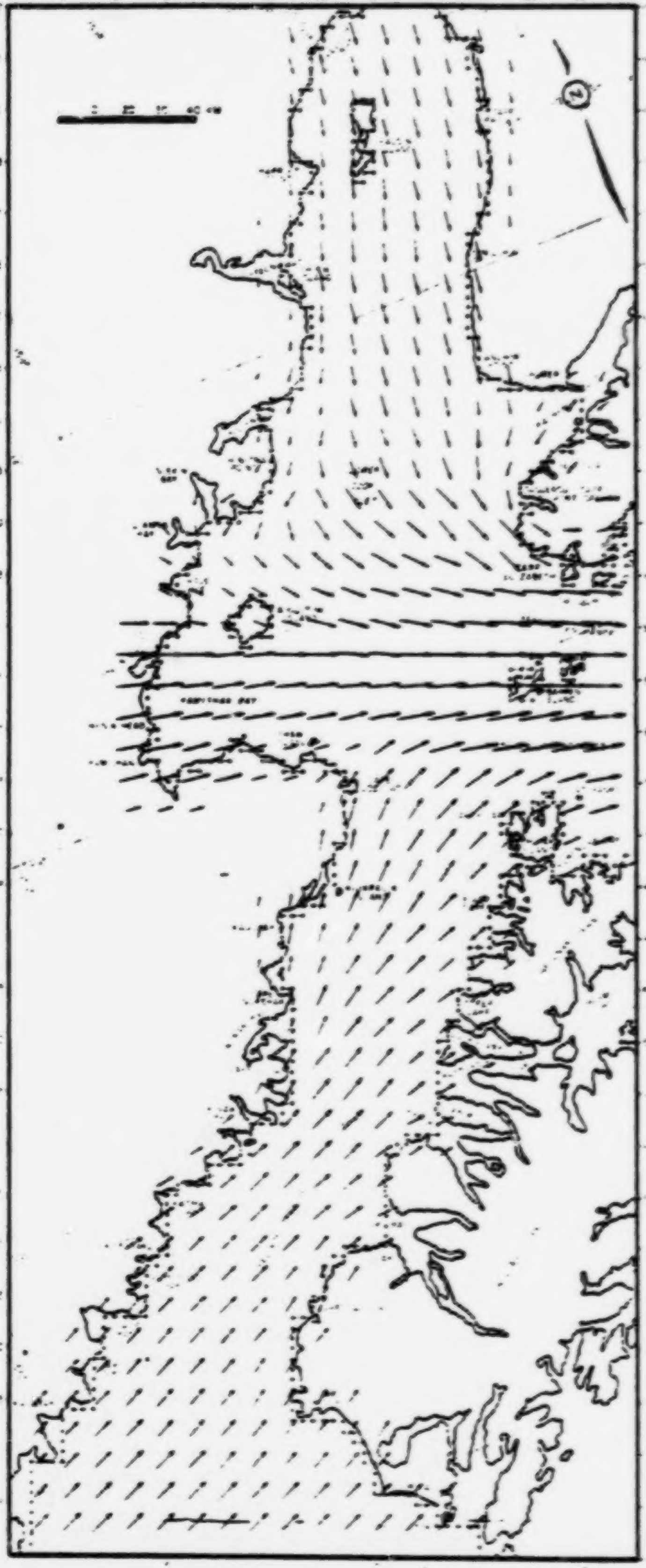

WIND VECTOR MAGNITUDE

25 METERS/SEC

WIND FIELD PROBABILITY

ANNUAL - 24.46%
WINTER - 23.81%
SUMMER - 25.14%

FIGURE 7: WIND FIELD 5

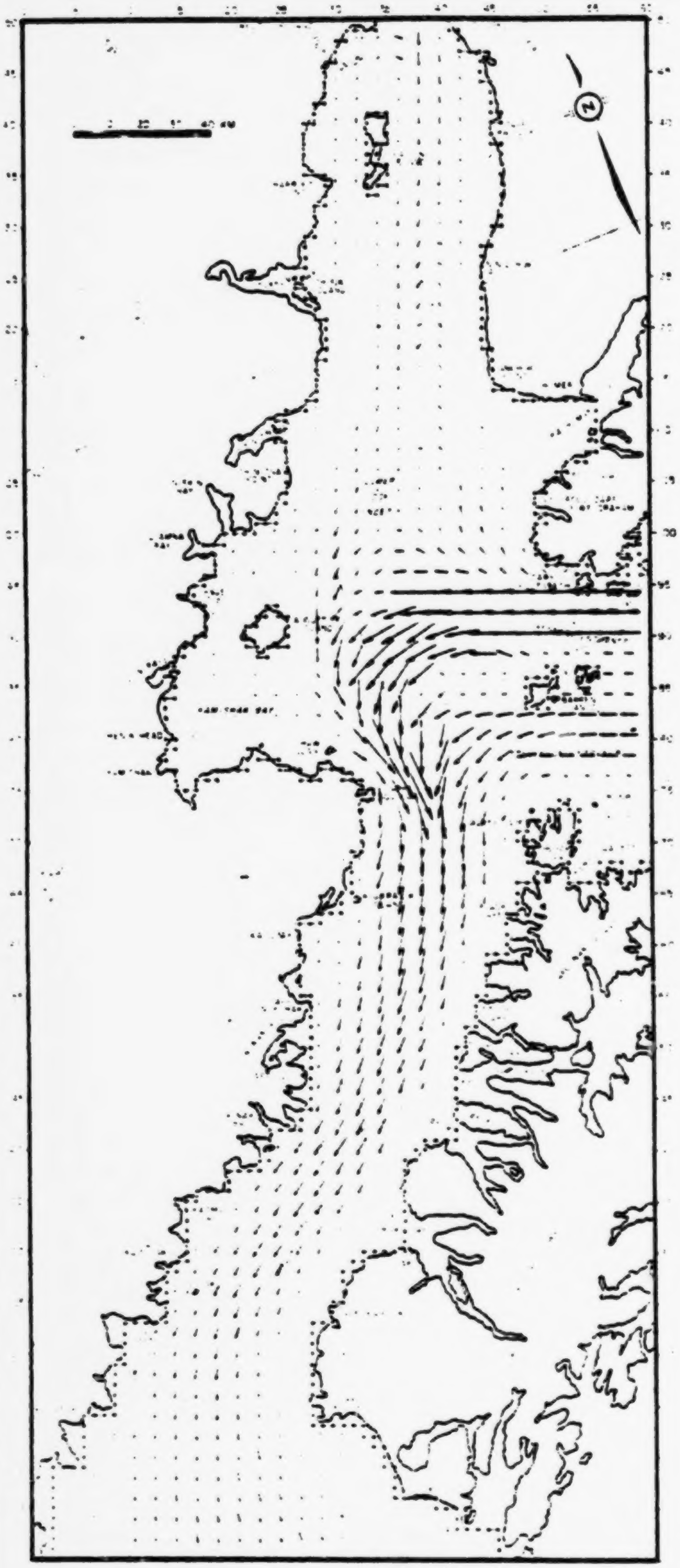
2
NET CURRENT
VECTOR MAGNITUDE
1 METER/SEC

FIGURE 8: WINTER NET
CURRENT PATTERN

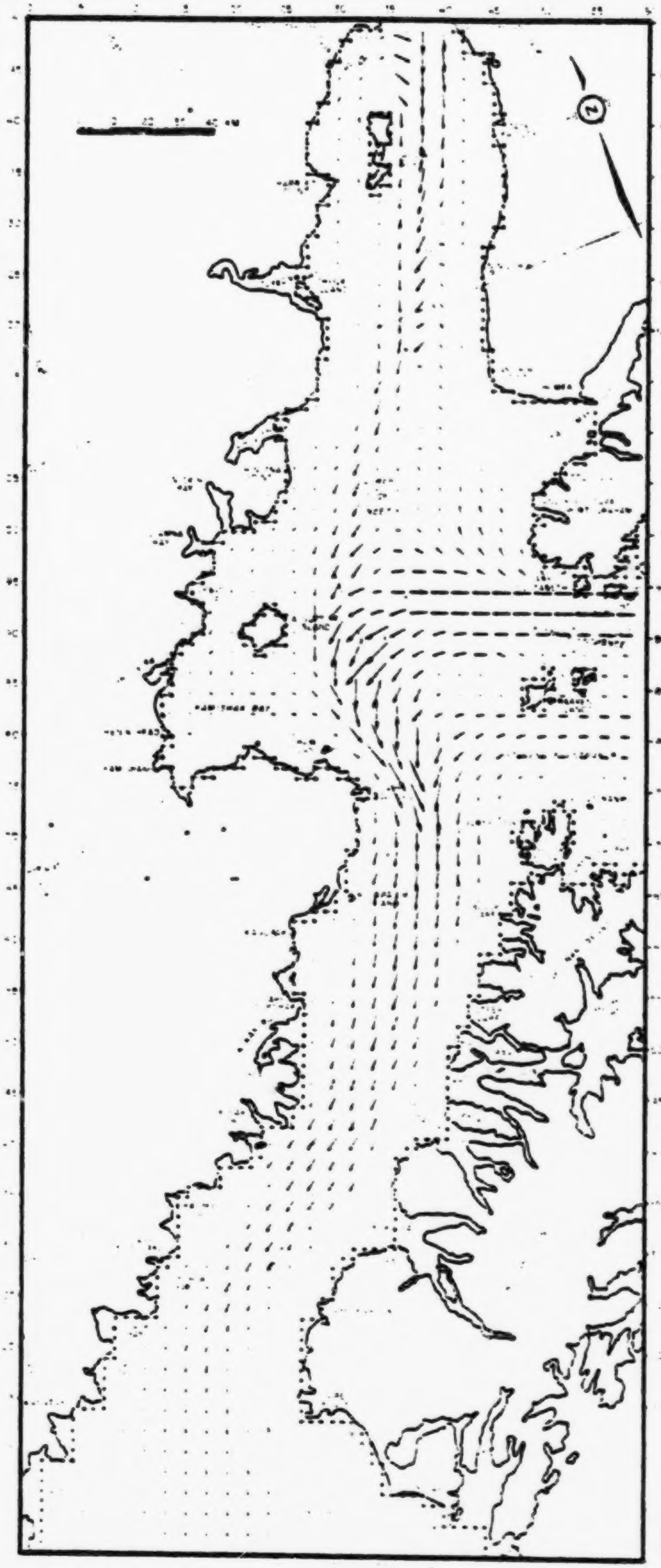
N
NET CURRENT VECTOR MAGNITUDE
1 METER/SEC

FIGURE 9: SUMMER NET CURRENT PATTERN

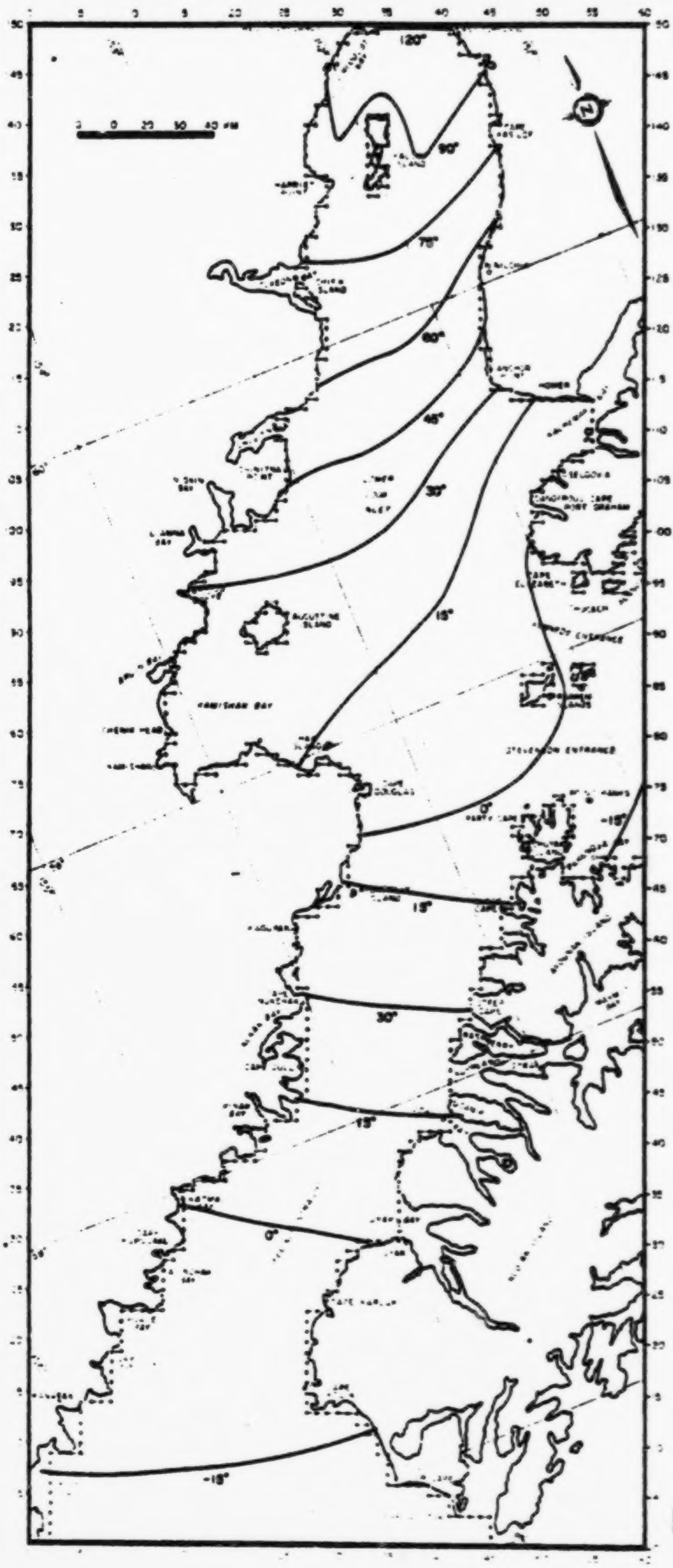

120°
90°
75°
60°
45°
30°
15°
0°
-15°
15°
30°
15°
0°
-15°
KAMISHAK BAY
STEVENSON ENTRANCE

PHASE GIVEN IN DEGREES RELATIVE TO TIDAL CURRENTS AT ENTRANCE TO LOWER COOK INLET. (360° = 12.4 HOURS)

FIGURE 10: TIDAL CURRENT PHASE DISTRIBUTION

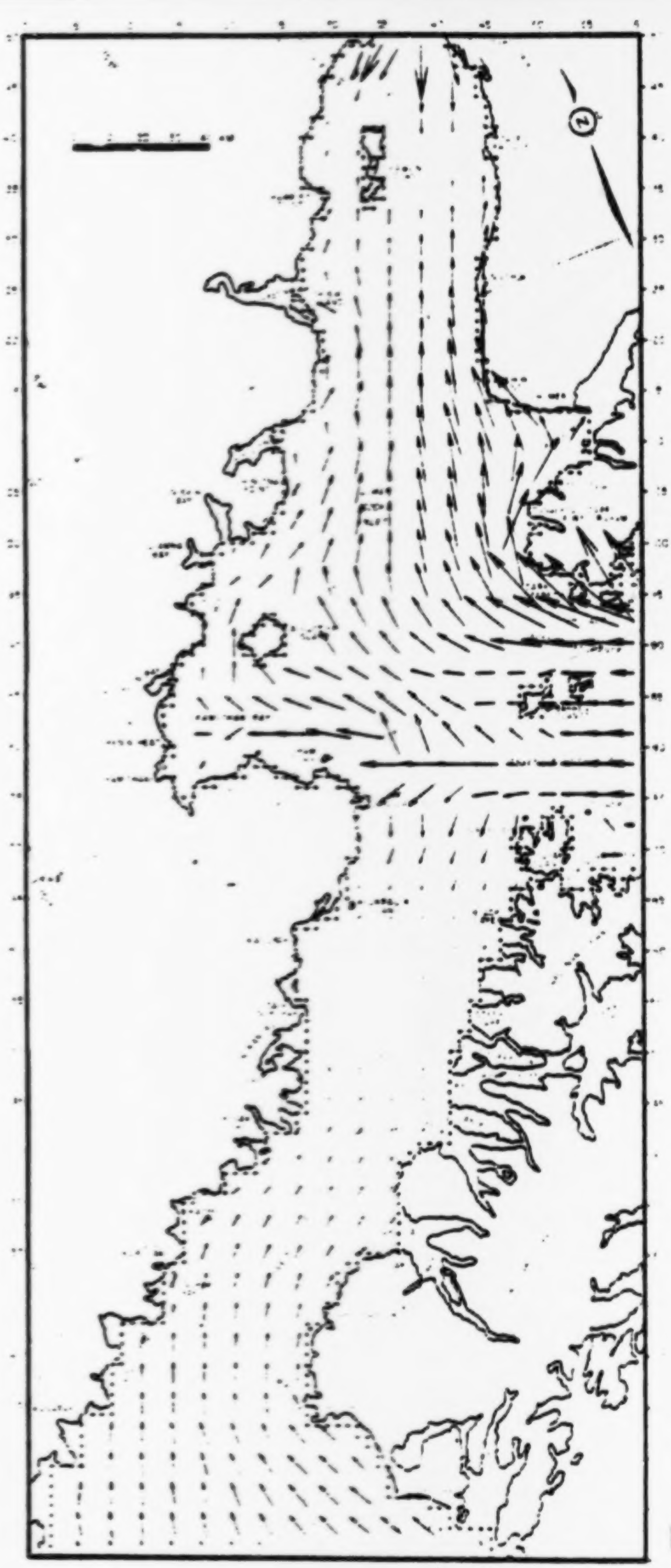
TIDAL CURRENT
VECTOR MAGNITUDE
1 METER/SEC

TIDAL CURRENT PHASE DEFINED BETWEEN CAPE DOUGLAS AND CAPE ELIZABETH

FIGURE: 11 TIDAL CURRENT PATTERN - PHASE = 0°

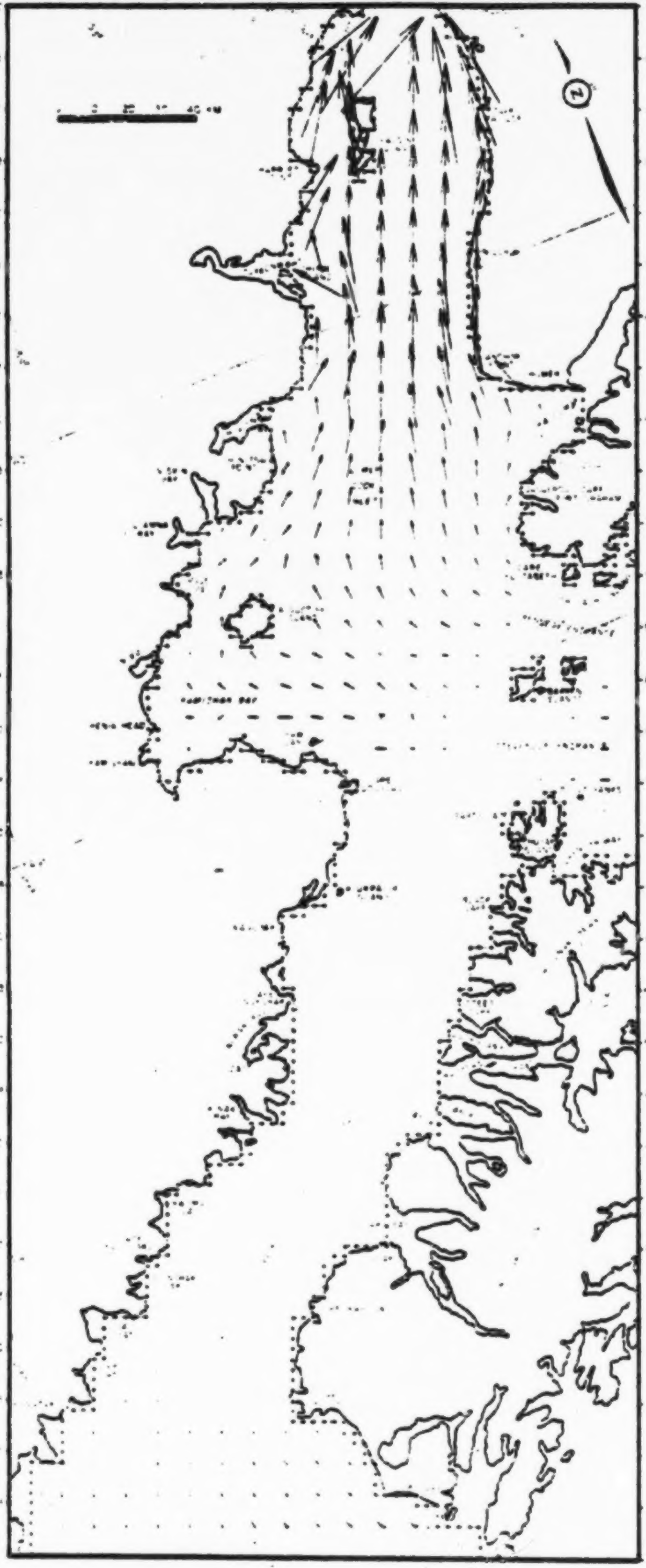

TIDAL CURRENT
VECTOR MAGNITUDE

→

1 METER/SEC

TIDAL CURRENT PHASE DEFINED BETWEEN CAPE DOUGLAS AND CAPE ELIZABETH.

FIGURE 12: TIDAL CURRENT PATTERN - PHASE = 90°

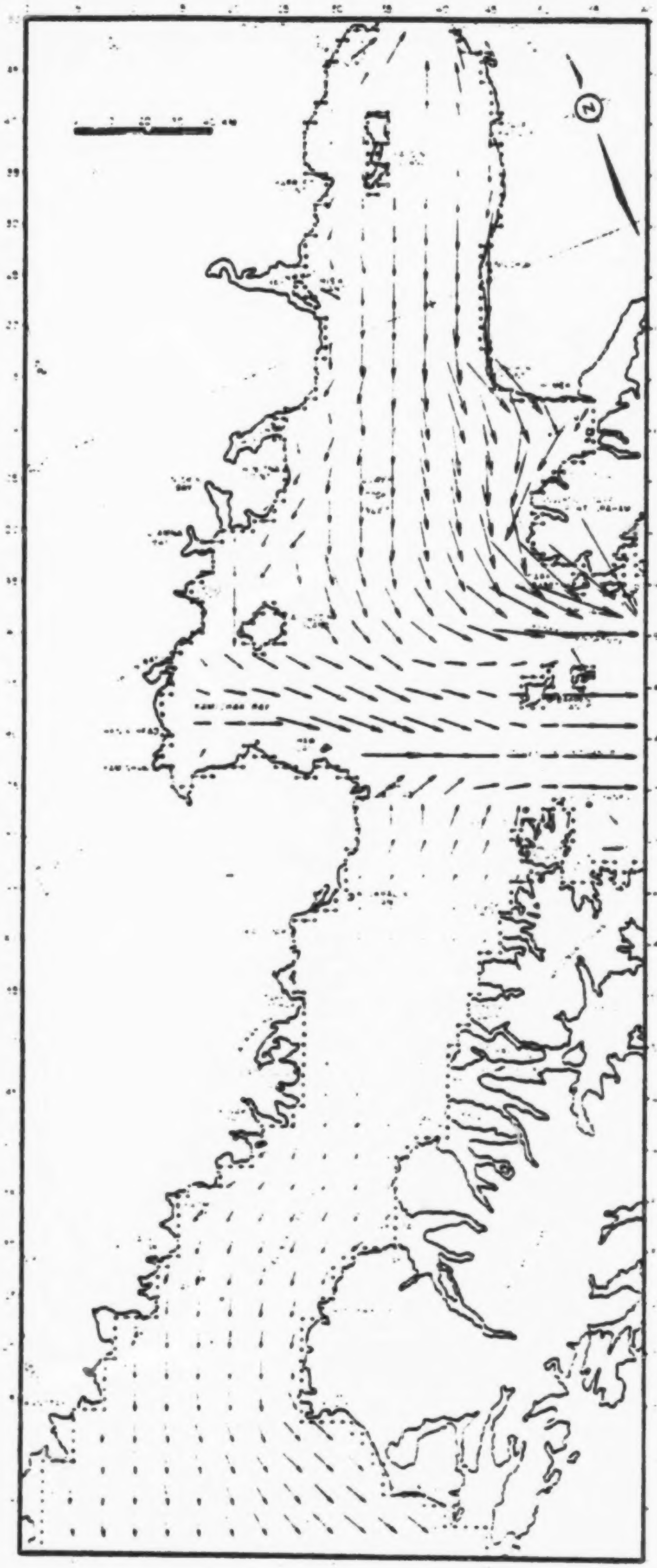

TIDAL CURRENT VECTOR MAGNITUDE

→

1 METER/SEC

TIDAL CURRENT PHASE DEFINED BETWEEN CAPE DOUGLAS AND CAPE ELIZABETH

FIGURE 13: TIDAL CURRENT PATTERN - PHASE = 180°

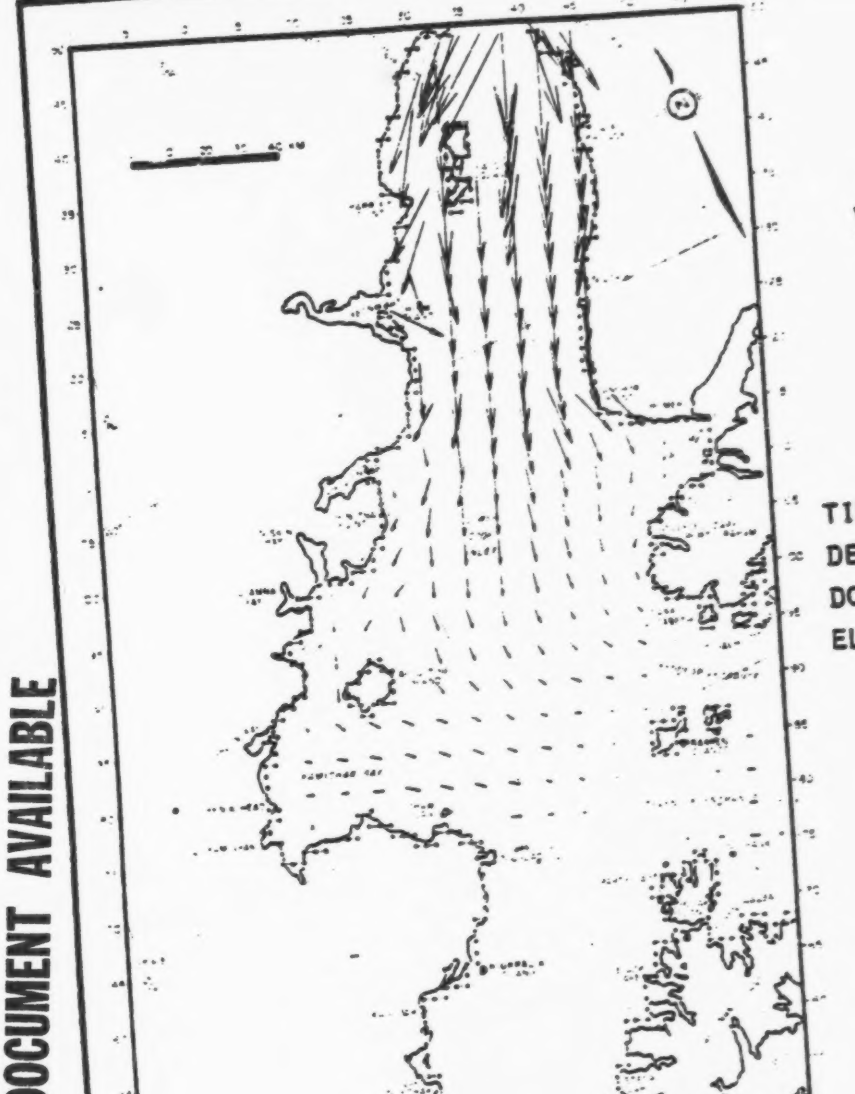
TIDAL CURRENT
VECTOR MAGNITUDE
1 METER/SEC
TIDAL CURRENT PHASE
DEFINED BETWEEN CAPE
DOUGLAS AND CAPE
ELIZABETH

FIGURE 14: TIDAL CURRENT PATTERN - PHASE = 270°

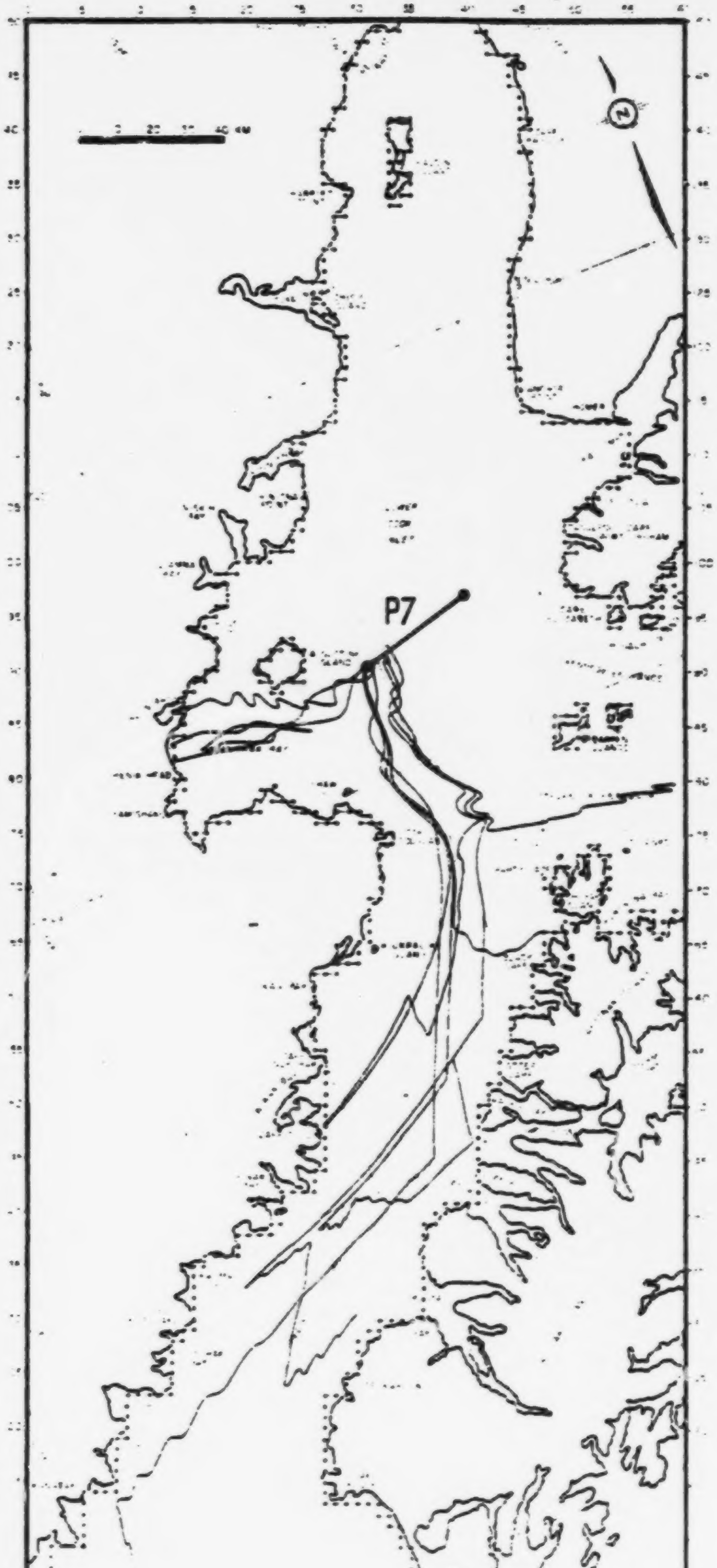
P7
10 20 30 40 KM
N

SITE:

P7

SEASON:

WINTER

WIND FIELD VARIABILITY:

WEATHER CATALOG

FIGURE 15: 10 SAMPLE TRAJECTORIES

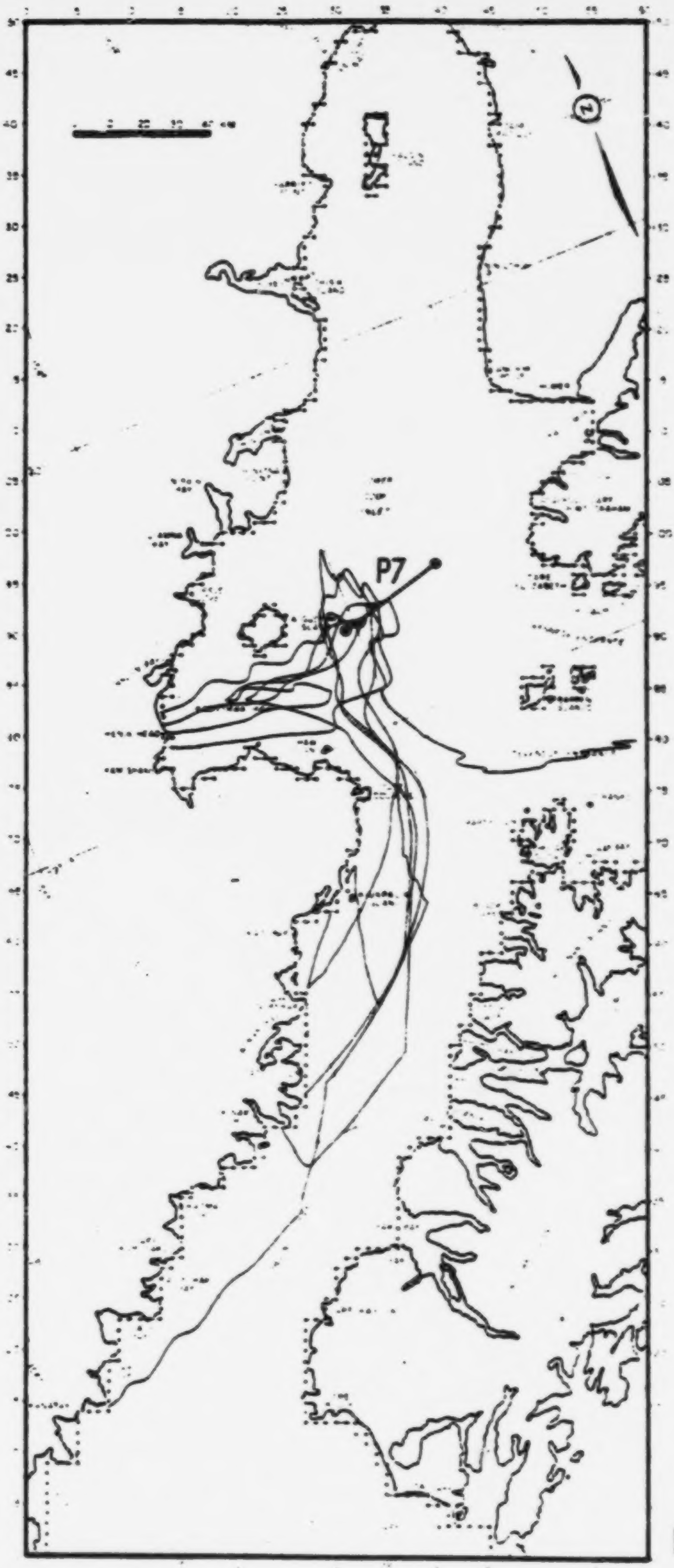

SITE:

P7

SEASON:

WINTER

WIND FIELD VARIABILITY:

WEATHER CATALOG

FIGURE 16: 10 SAMPLE TRAJECTORIES

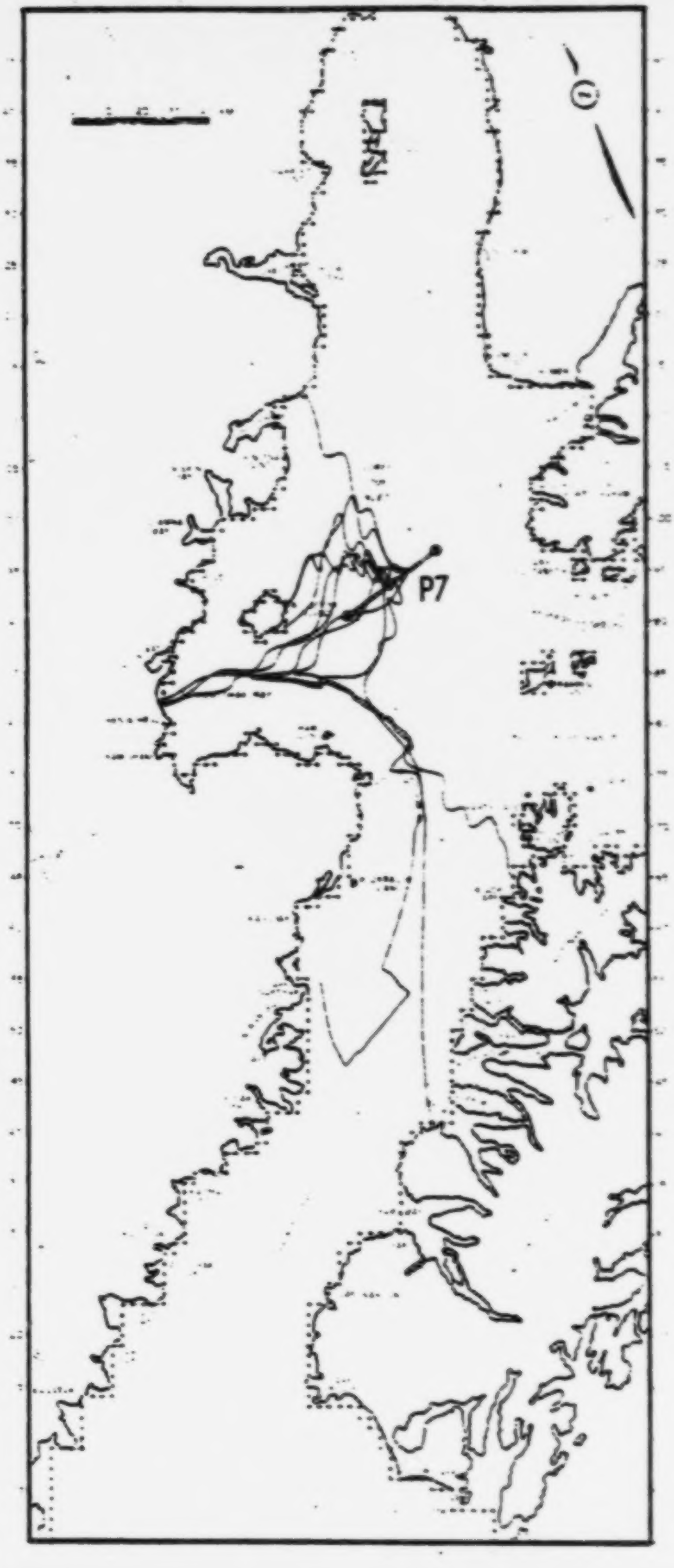

SITE:

P7

SEASON:

WINTER

WIND FIELD VARIABILITY:

WEATHER CATALOG

FIGURE 17: 10 SAMPLE TRAJECTORIES

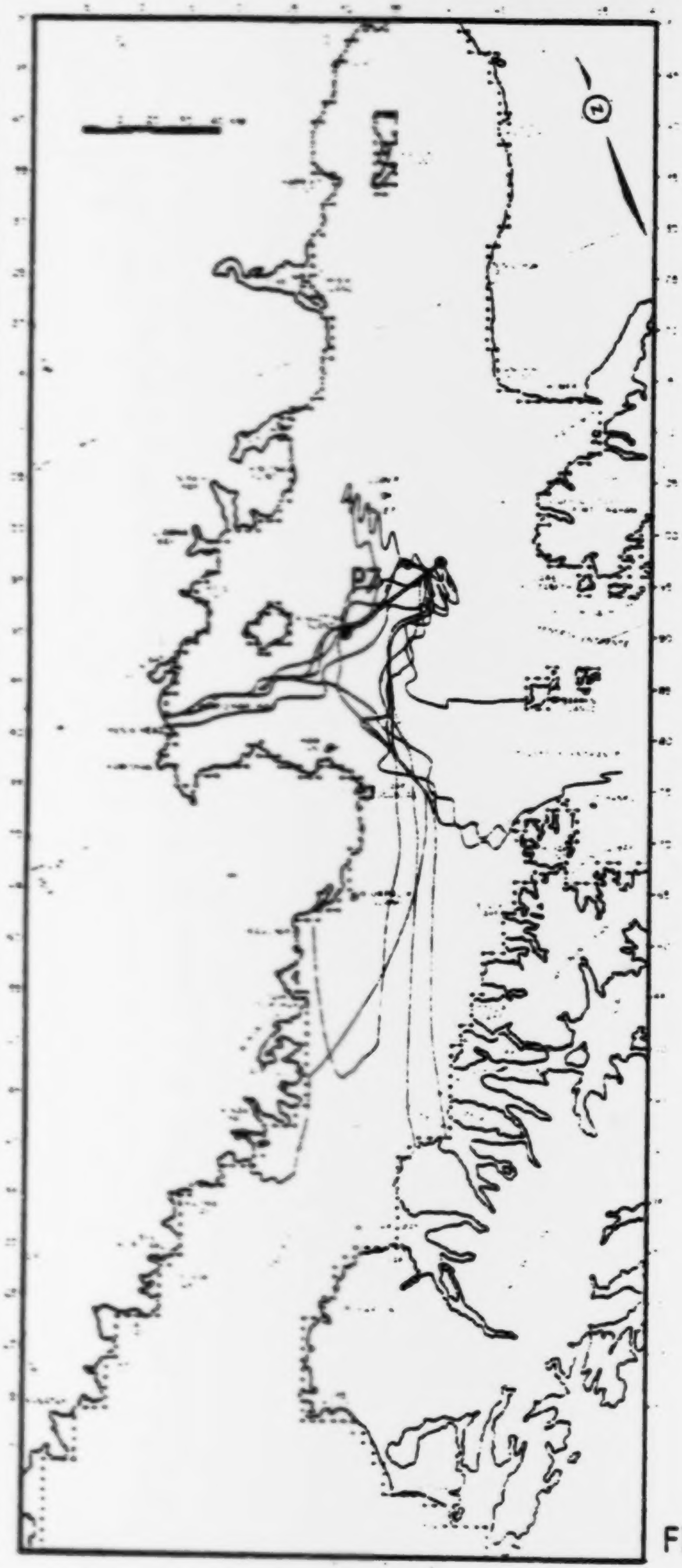

SITE:

P7

SEASON:

WINTER

WIND FIELD VARIABILITY:

WEATHER CATALOG

FIGURE 18: 10 SAMPLE TRAJECTORIES

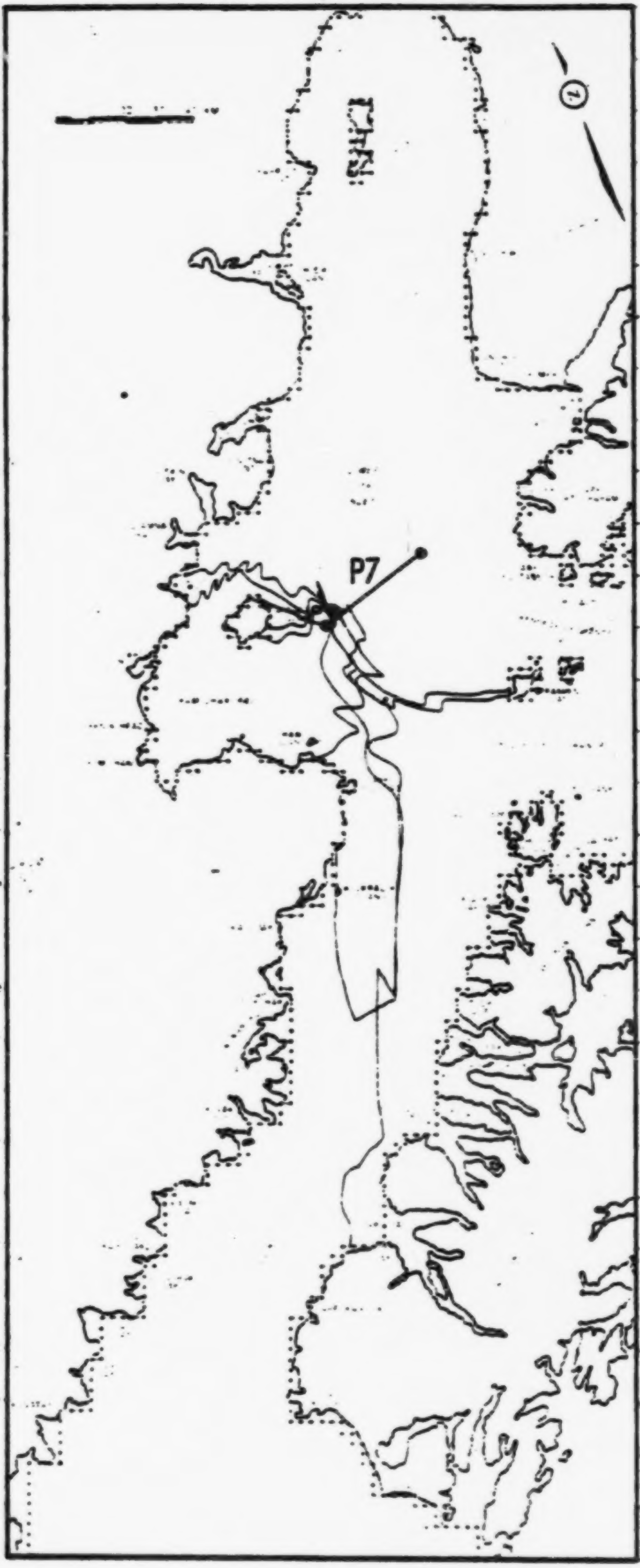

SITE:

P7

SEASON:

SUMMER

WIND FIELD VARIABILITY:

WEATHER CATALOG

FIGURE 19: 10 SAMPLE TRAJECTORIES

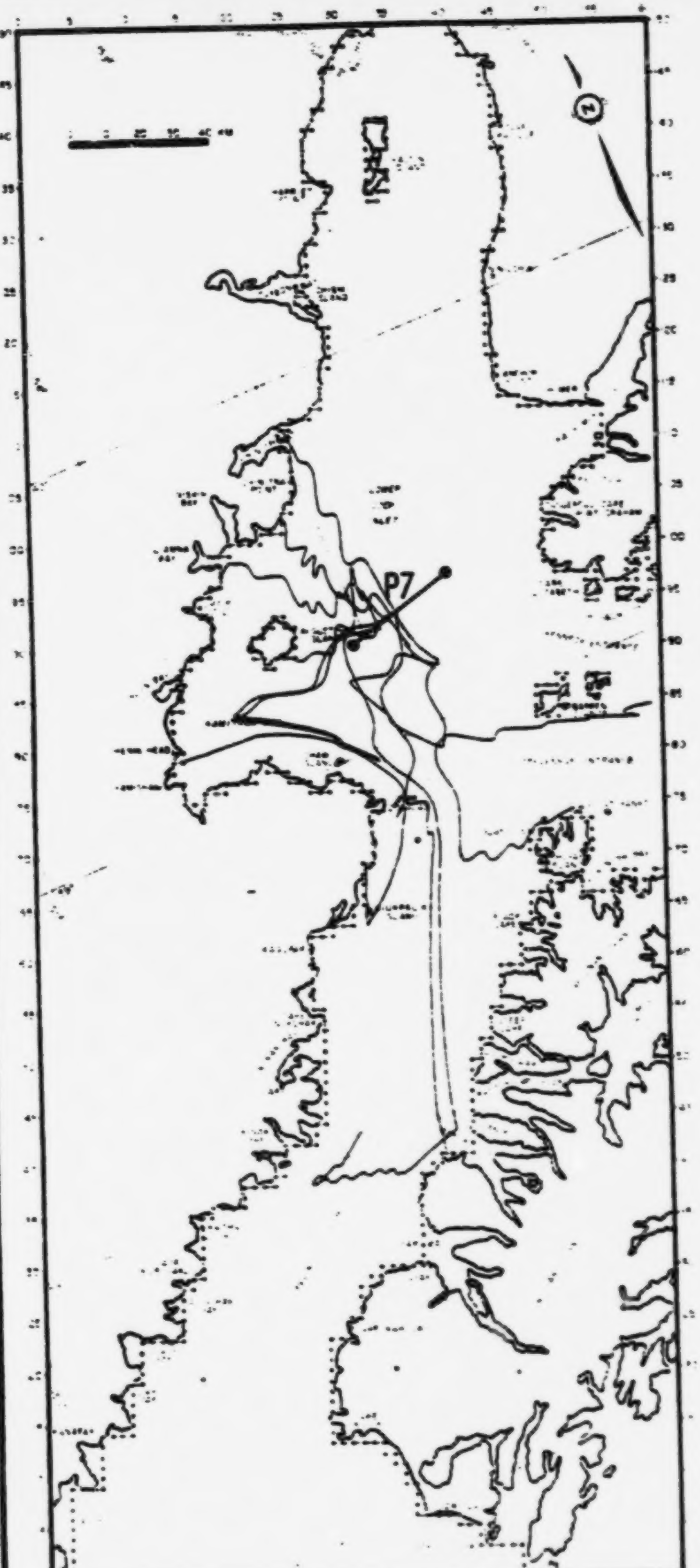

SITE:

P7

SEASON:

SUMMER

WIND FIELD VARIABILITY:

WEATHER CATALOG

FIGURE 20: 10 SAMPLE TRAJECTORIES

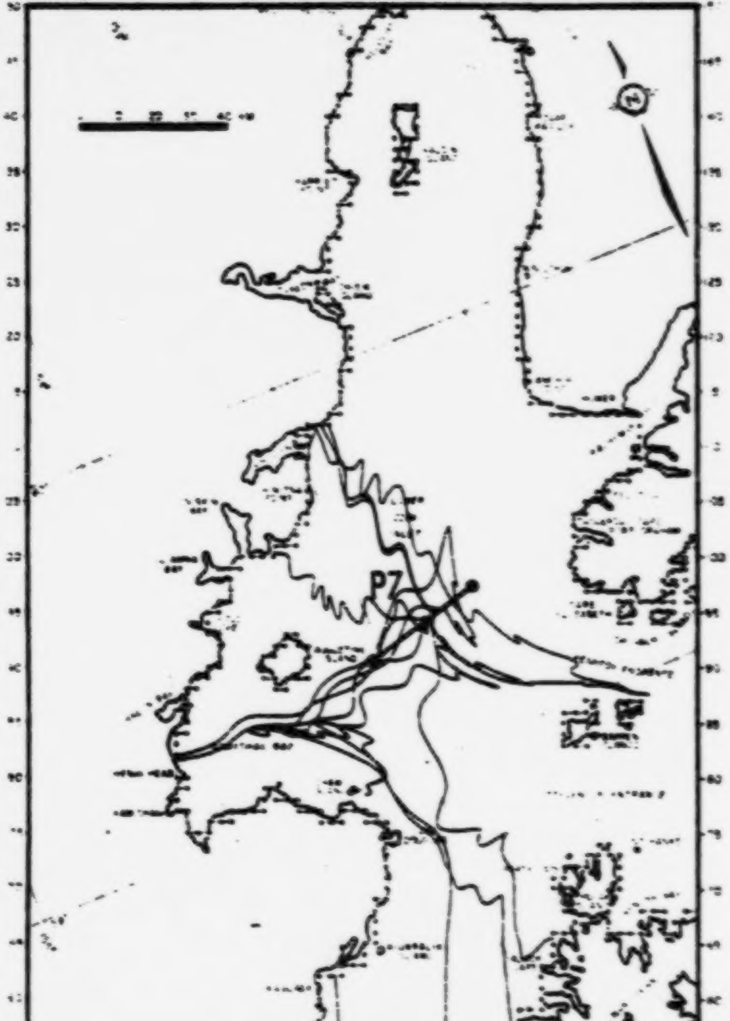

SITE:

P7

SEASON:

SUMMER

WIND FIELD VARIABILITY:

WEATHER CATALOG

FIGURE 21: 10 SAMPLE TRAJECTORIES

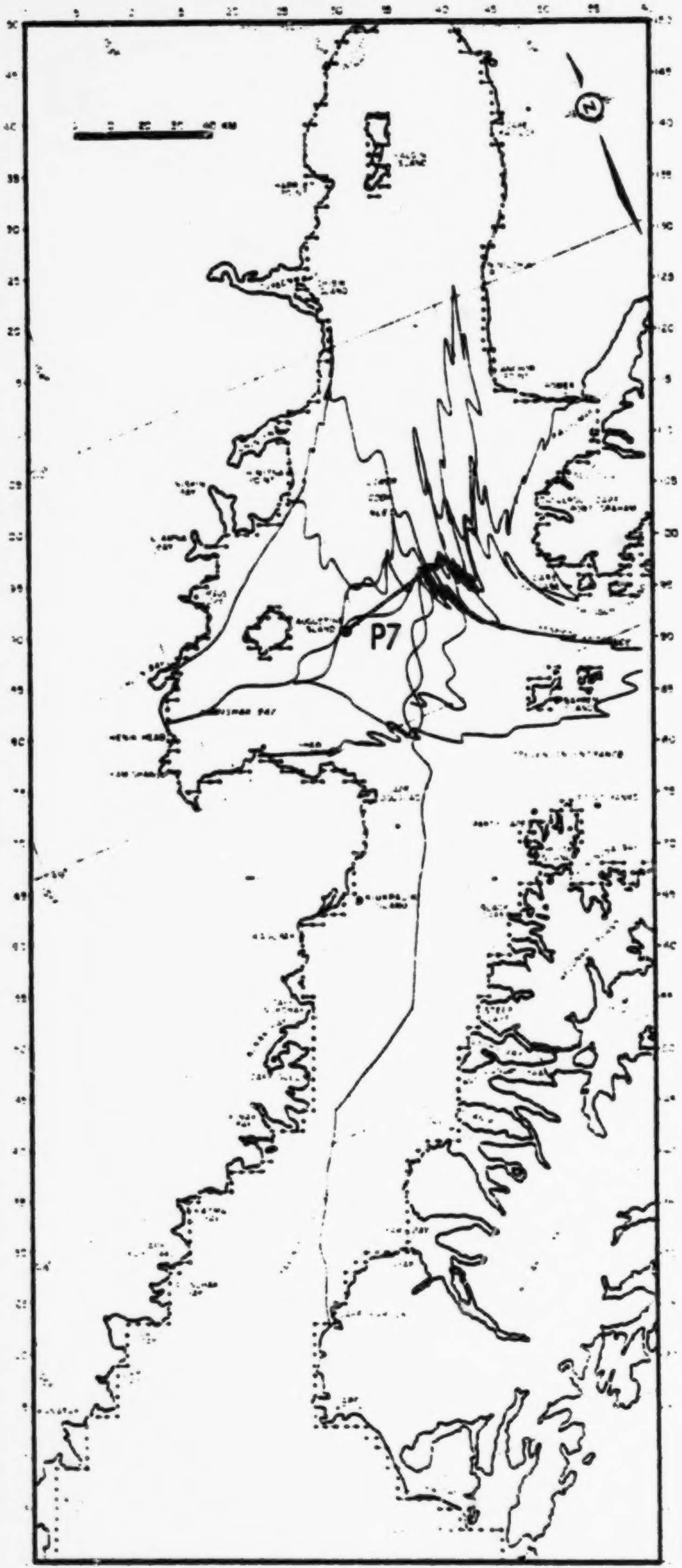

SITE:

P7

SEASON:

SUMMER

WIND FIELD VARIABILITY:

WEATHER CATALOG

FIGURE 22: 10 SAMPLE TRAJECTORIES

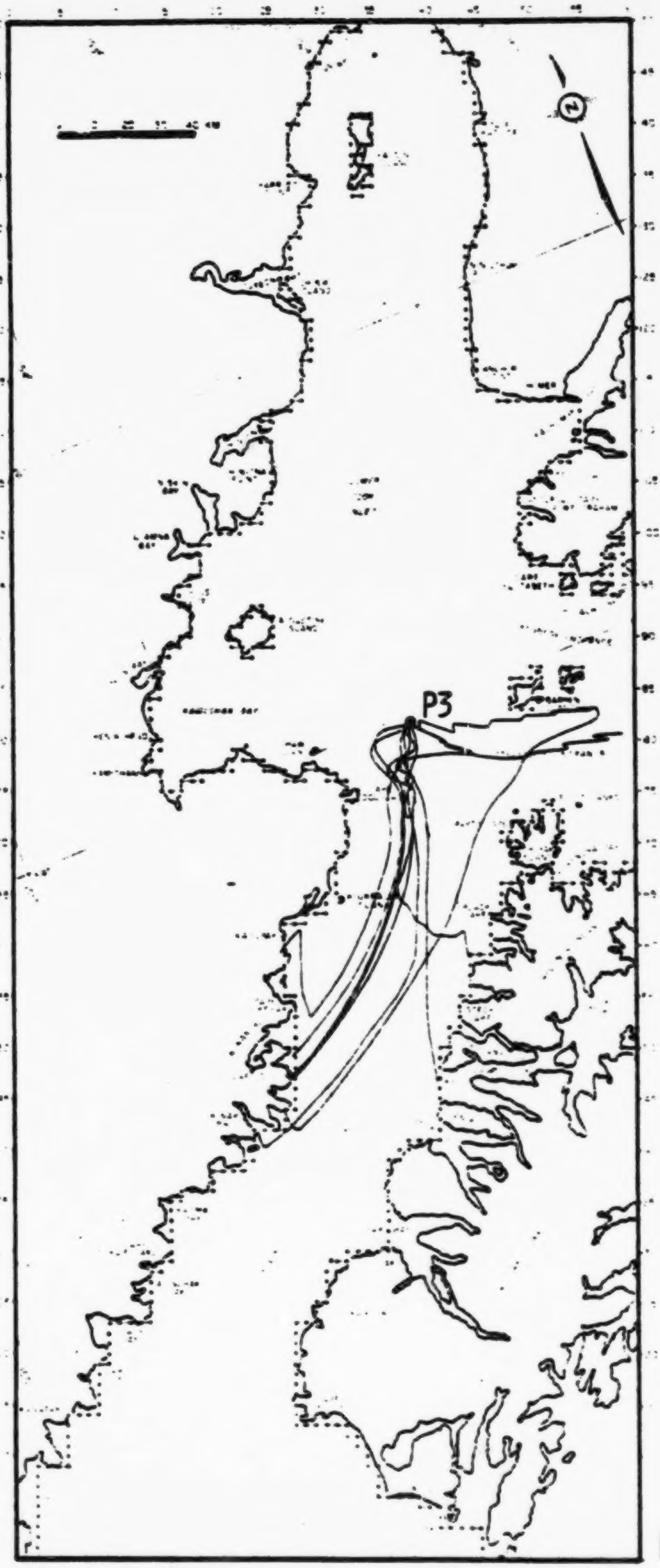

SITE:

P3

SEASON:

WINTER

WIND FIELD VARIABILITY:

WEATHER CATALOG

FIGURE 23: 10 SAMPLE TRAJECTORIES

BEST DOCUMENT AVAILABLE

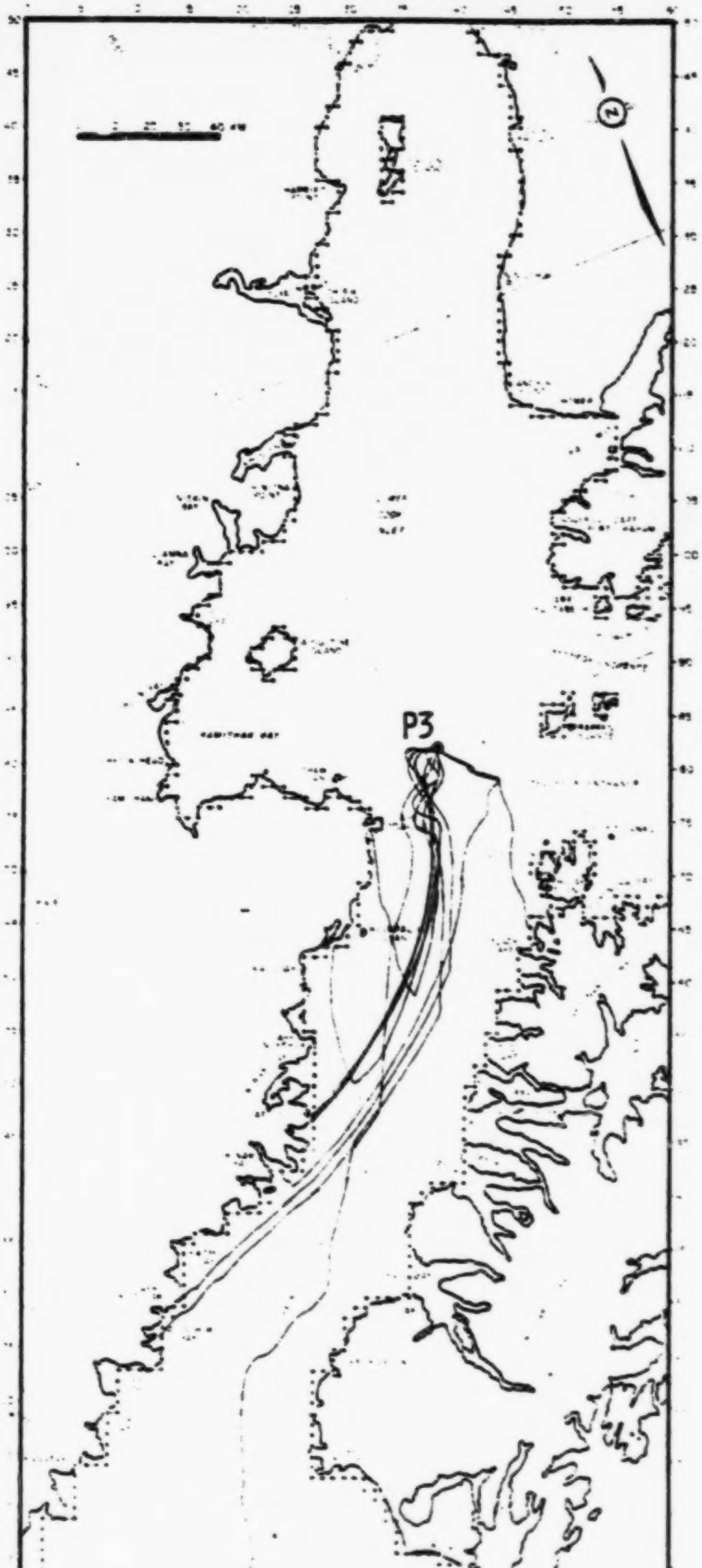

SITE:

P3

SEASON:

WINTER

WIND FIELD VARIABILITY:

WEATHER CATALOG

FIGURE 24: 10 SAMPLE TRAJECTORIES

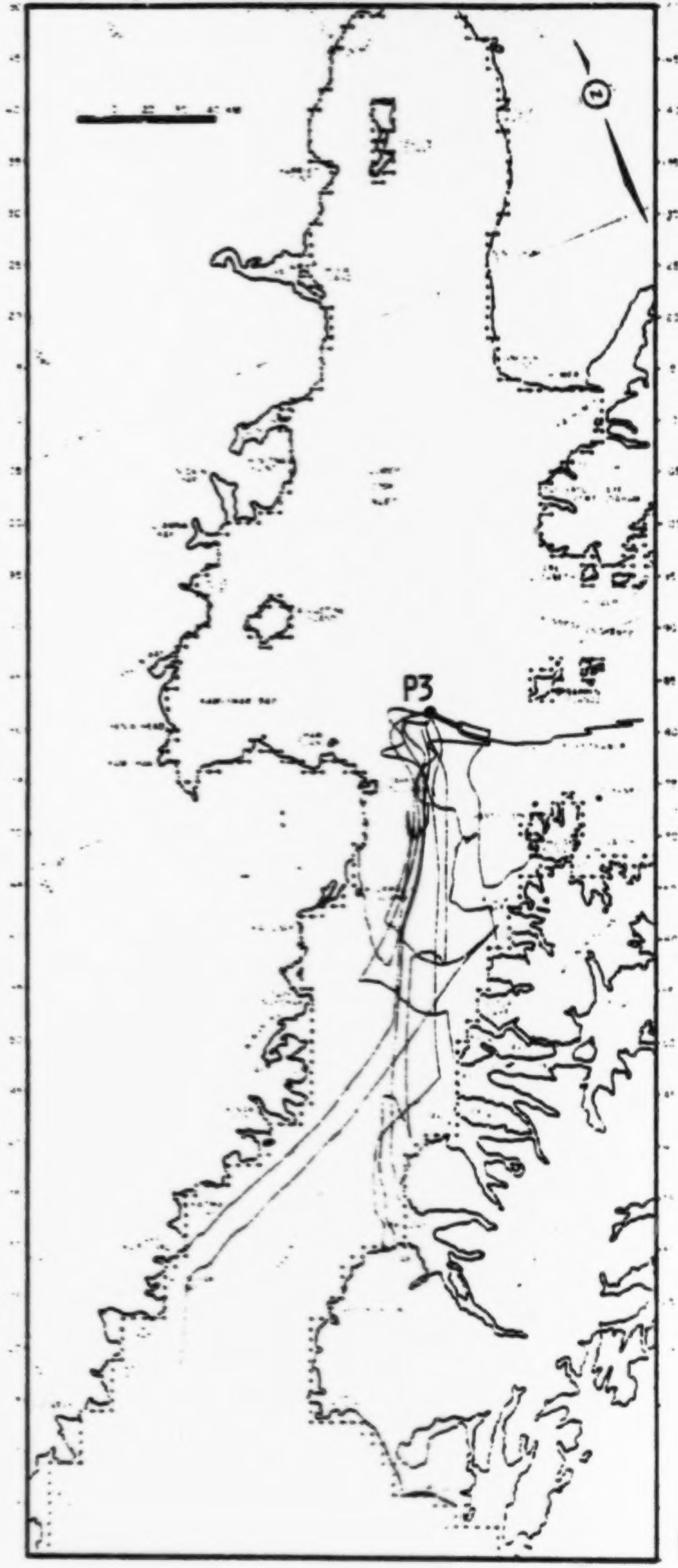

SITE:

P3

SEASON:

WINTER

WIND FIELD VARIABILITY:

WEATHER CATALOG

FIGURE 25: 10 SAMPLE TRAJECTORIES

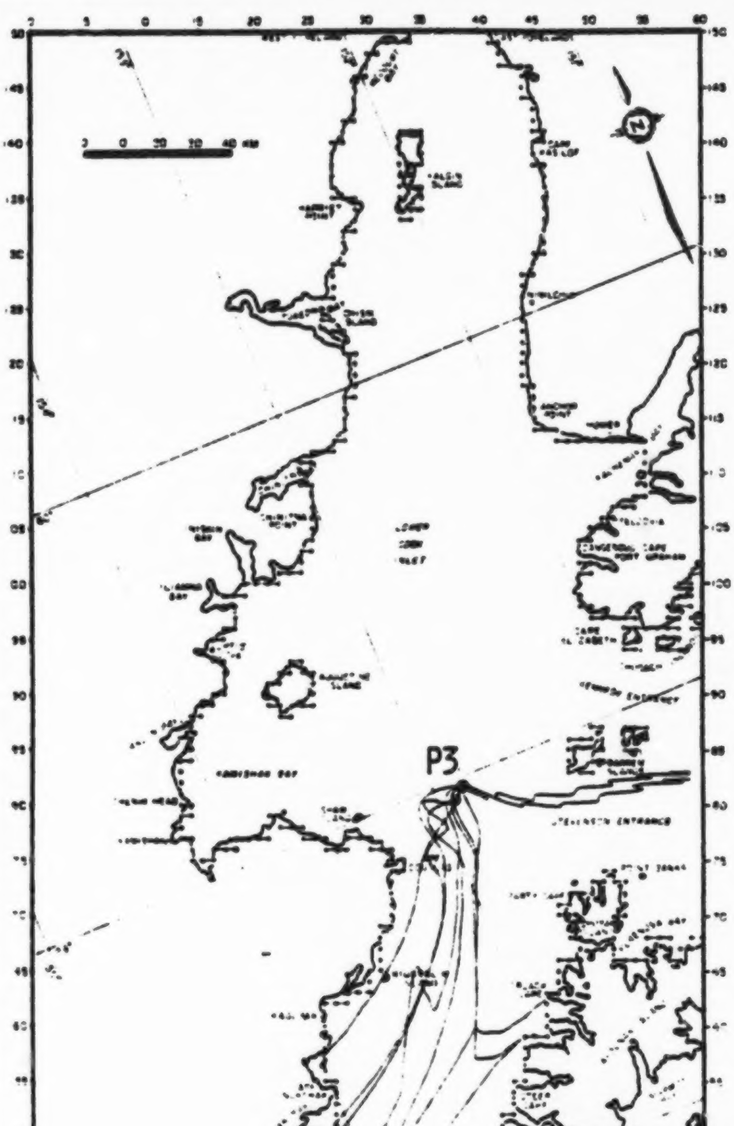

SITE:

P3

SEASON:

WINTER

WIND FIELD VARIABILITY:

WEATHER CATALOG

FIGURE 26: 10 SAMPLE TRAJECTORIES

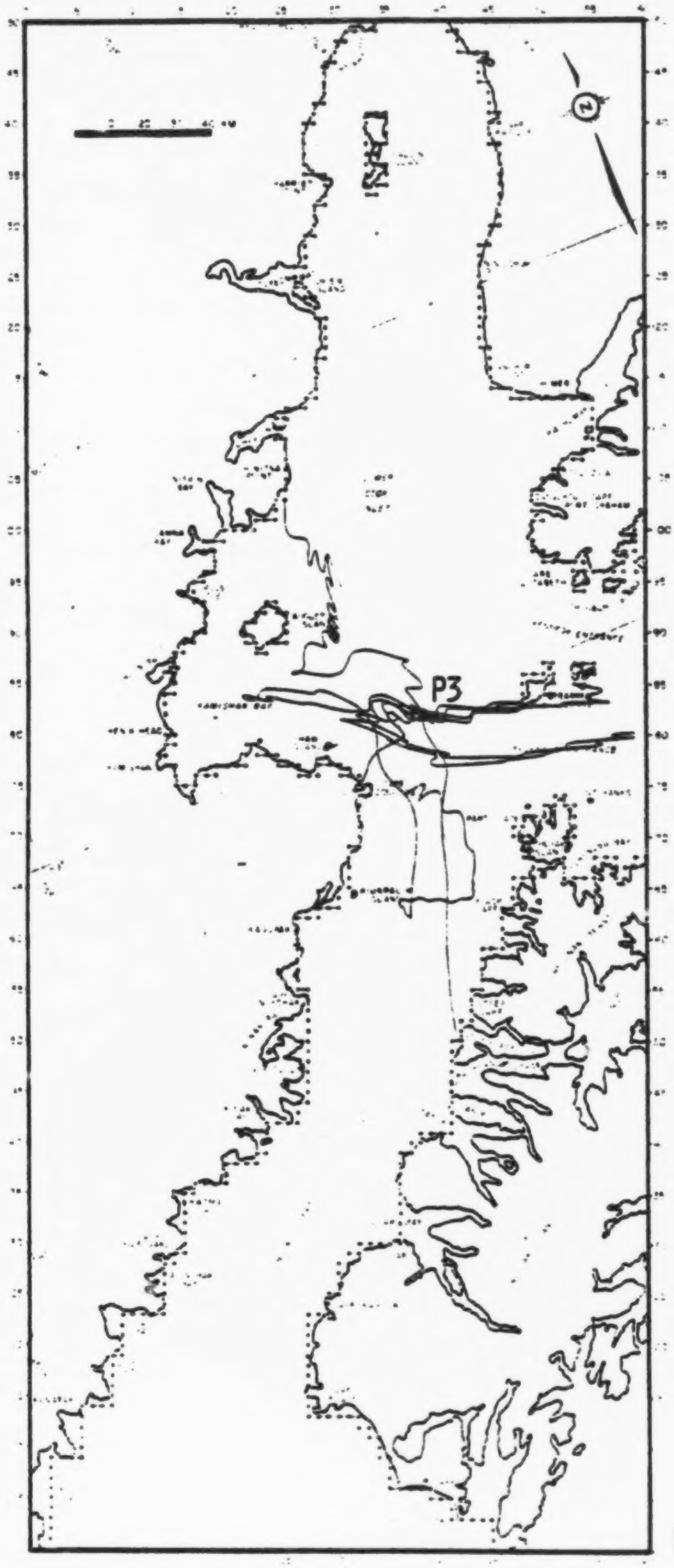

SITE:

P3

SEASON:

SUMMER

WIND FIELD VARIABILITY:

WEATHER CATALOG

FIGURE 27: 10 SAMPLE TRAJECTORIES

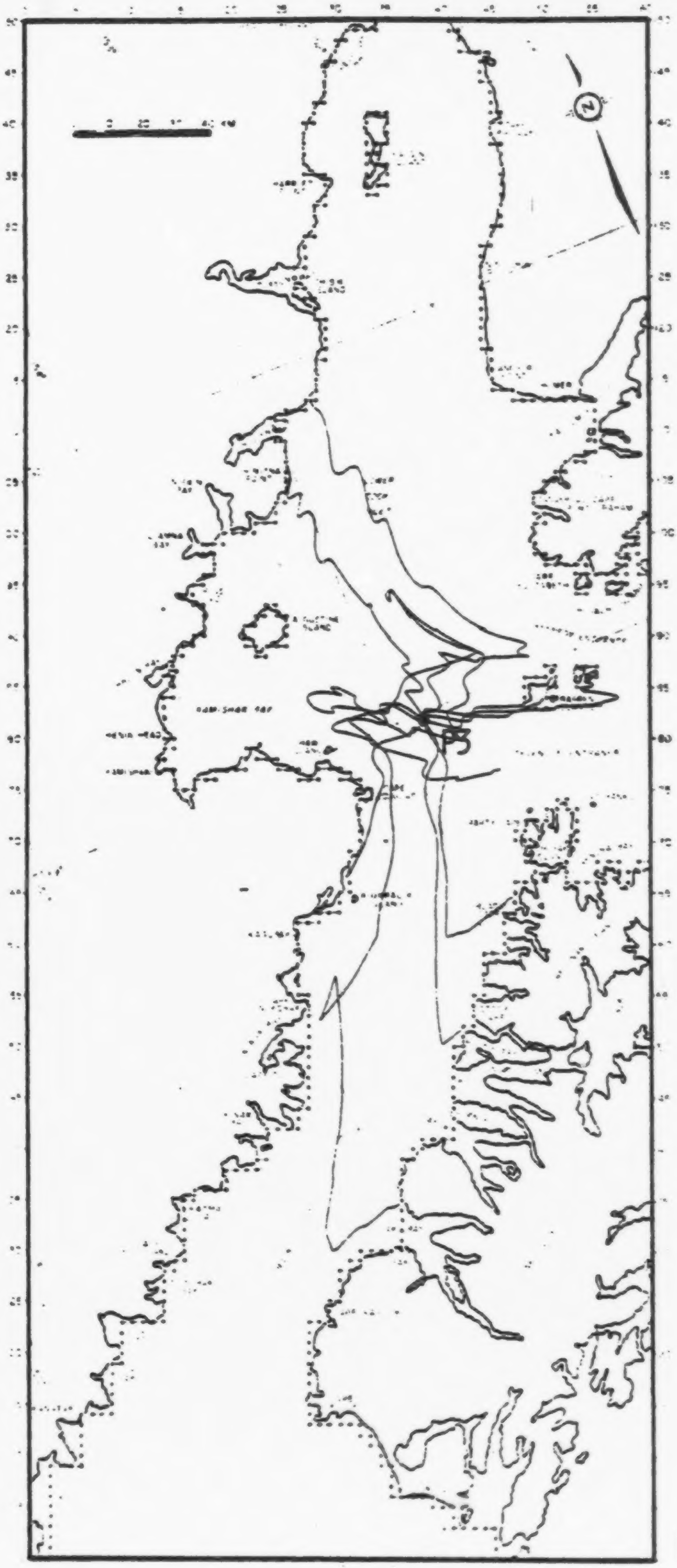
0 20 40 KM
N
P3

SITE:

P3

SEASON:

SUMMER

WIND FIELD VARIABILITY:

WEATHER CATALOG

FIGURE 28: 10 SAMPLE TRAJECTORIES

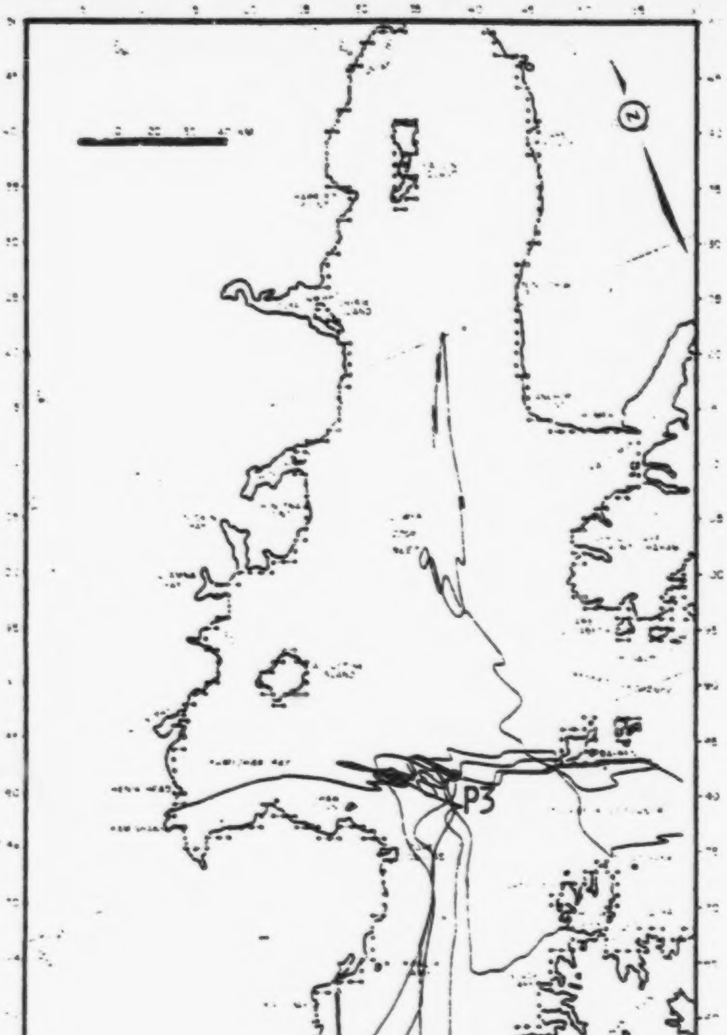

SITE:

P3

SEASON:

SUMMER

WIND FIELD VARIABILITY:

WEATHER CATALOG

FIGURE 29: 10 SAMPLE TRAJECTORIES

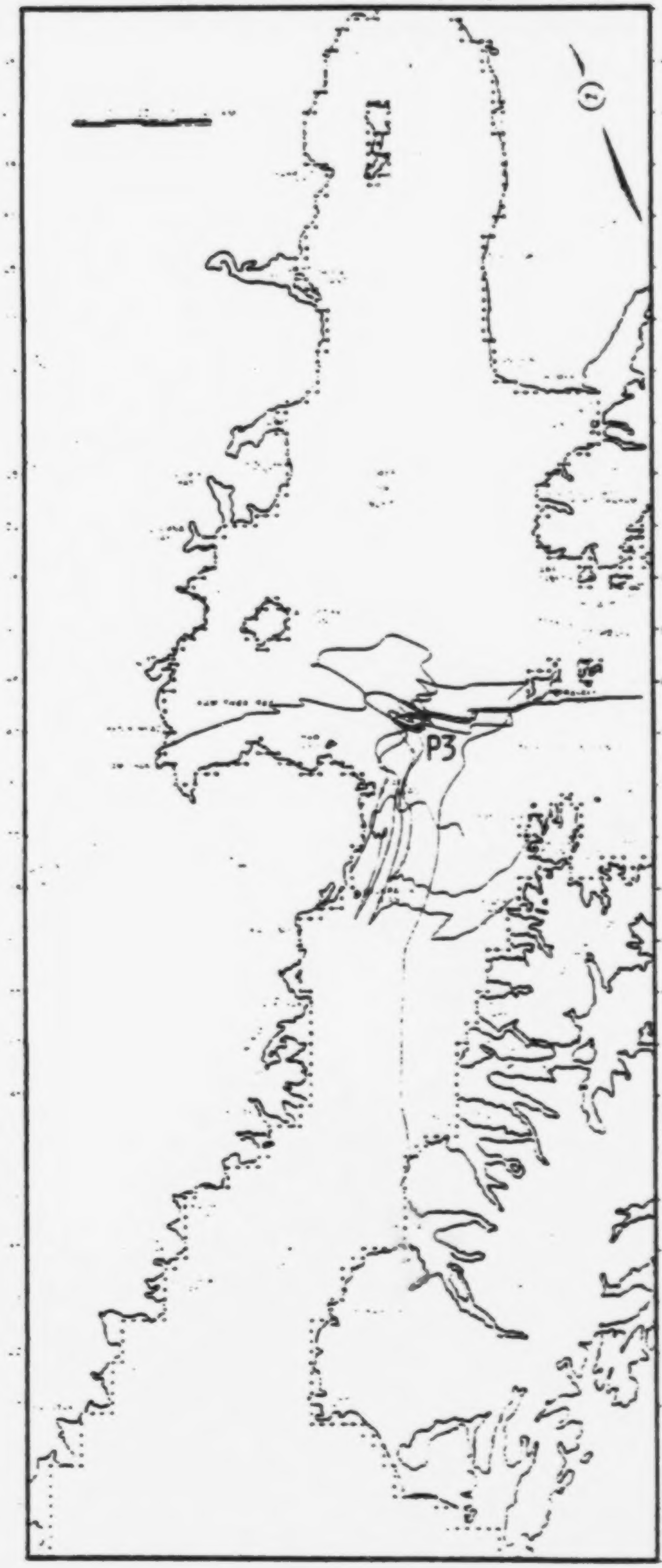

SITE:

P3

SEASON:

SUMMER

WIND FIELD VARIABILITY:

WEATHER CATALOG

FIGURE 30: 10 SAMPLE TRAJECTORIES

WIND
4

SITE
8

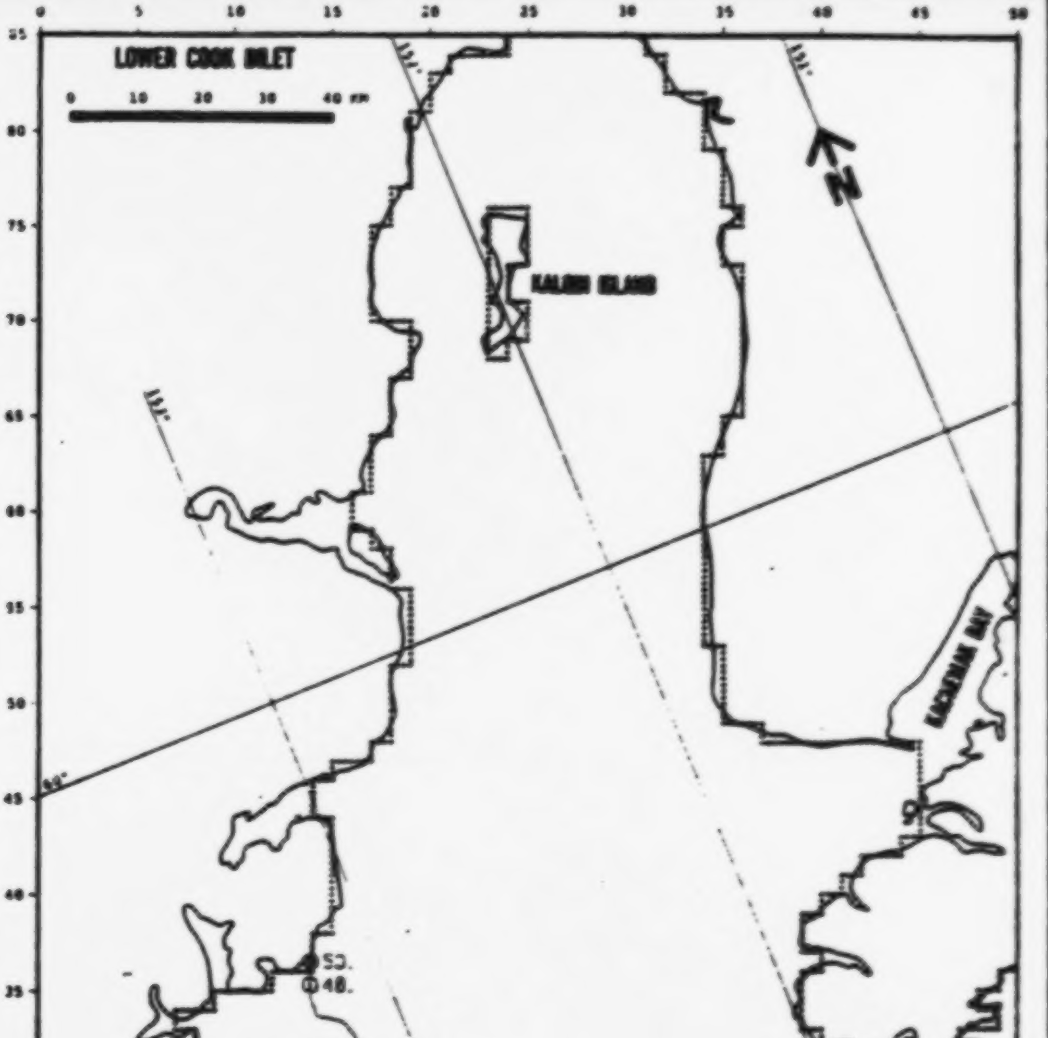
LOWER COOK INLET
0 10 20 30 40 km
N
KALGIN ISLAND
KACHEMAK BAY
KAMISHAK BAY
CAPE DOUGLAS
53.
48.
36.
24.
12.
0 5 10 15 20 25 30 35 40 45 50
0 5 10 15 20 25 30 35 40 45 50 55 60 65 70 75 80 85

FIGURE 31: BASE CASE
(FROM DAMES & MOORE, 1979)

WIND
6

SITE
3

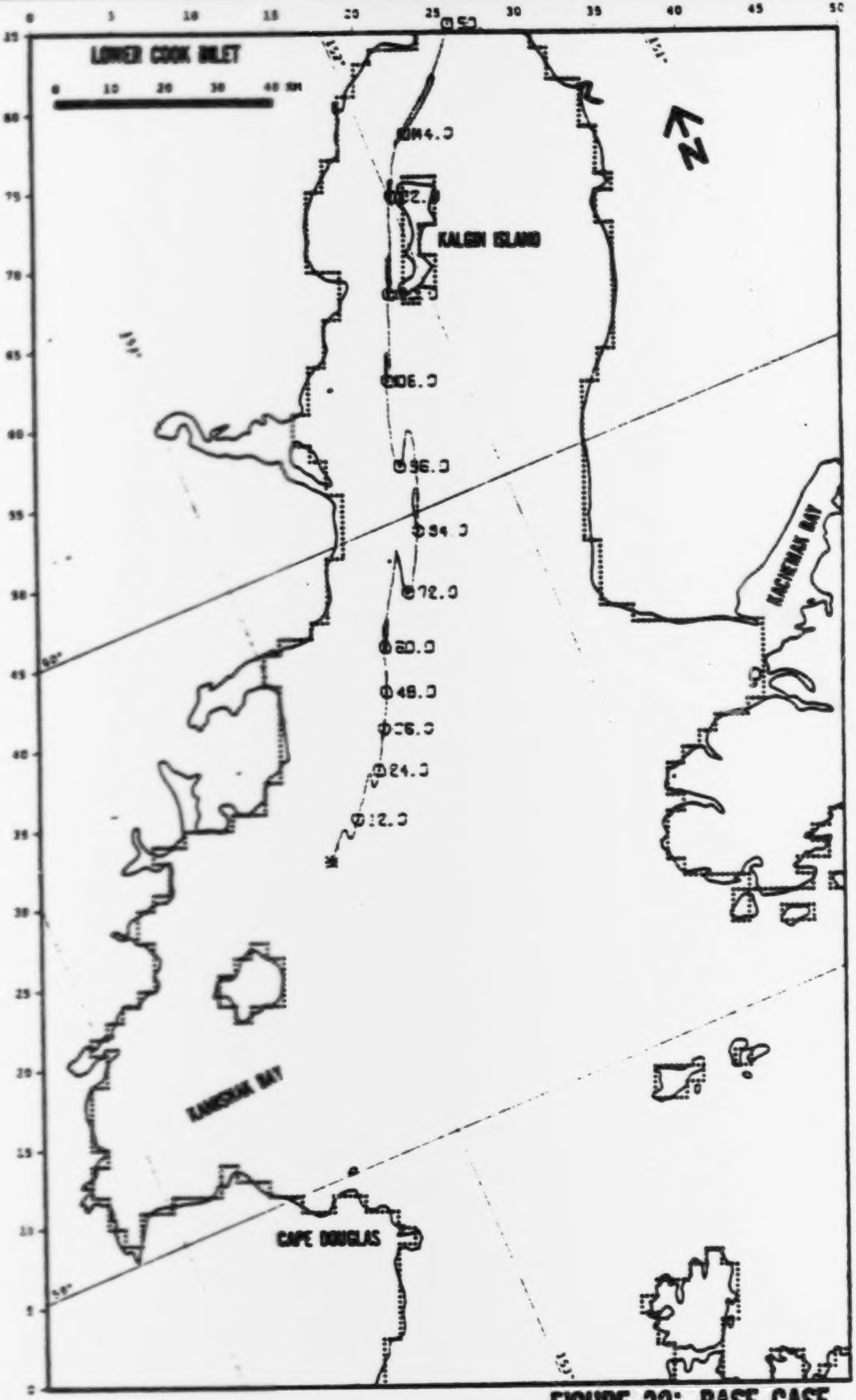

LOWER COOK INLET
0 10 20 30 40 NM
KALGIN ISLAND
KACHEMAK BAY
KAMISHAK BAY
CAPE DOUGLAS
N
0 5 10 15 20 25 30 35 40 45 50
0 5 10 15 20 25 30 35 40 45 50 55 60 65 70 75 80 85
12.0
24.0
36.0
48.0
60.0
72.0
84.0
96.0
06.0
4.0
59°
60°
151°
152°
153°

FIGURE 32: BASE CASE
(FROM DAMES & MOORE, 1979)

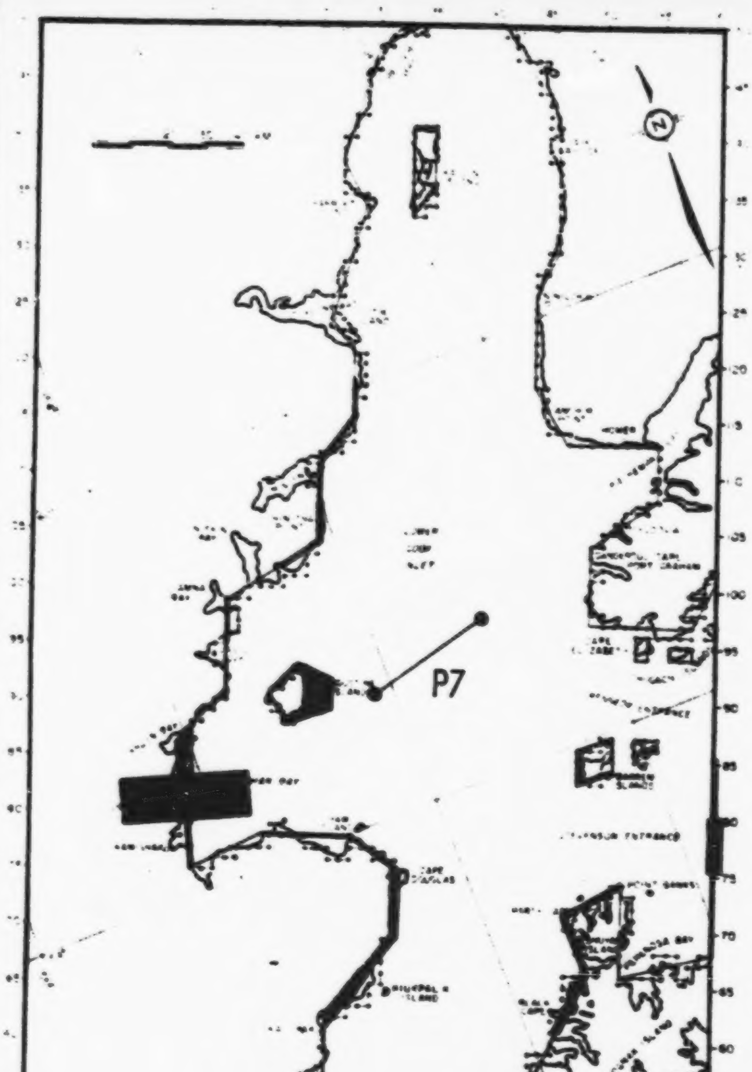

SITE:

P7

SEASON:

WINTER

WIND FIELD VARIABILITY:

WEATHER CATALOG

PERCENT FREQUENCY OF
BOUNDARY IMPACT PER
KILOMETER OF REACH

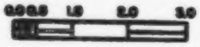

NOTE: WIDTH OF SHADING
ALONG SEGMENTIZED
REACHES REPRESENTS
MAGNITUDE OF PERCENT
FREQUENCY OF BOUNDARY
IMPACT

FIGURE 33: BOUNDARY IMPACT
FREQUENCY

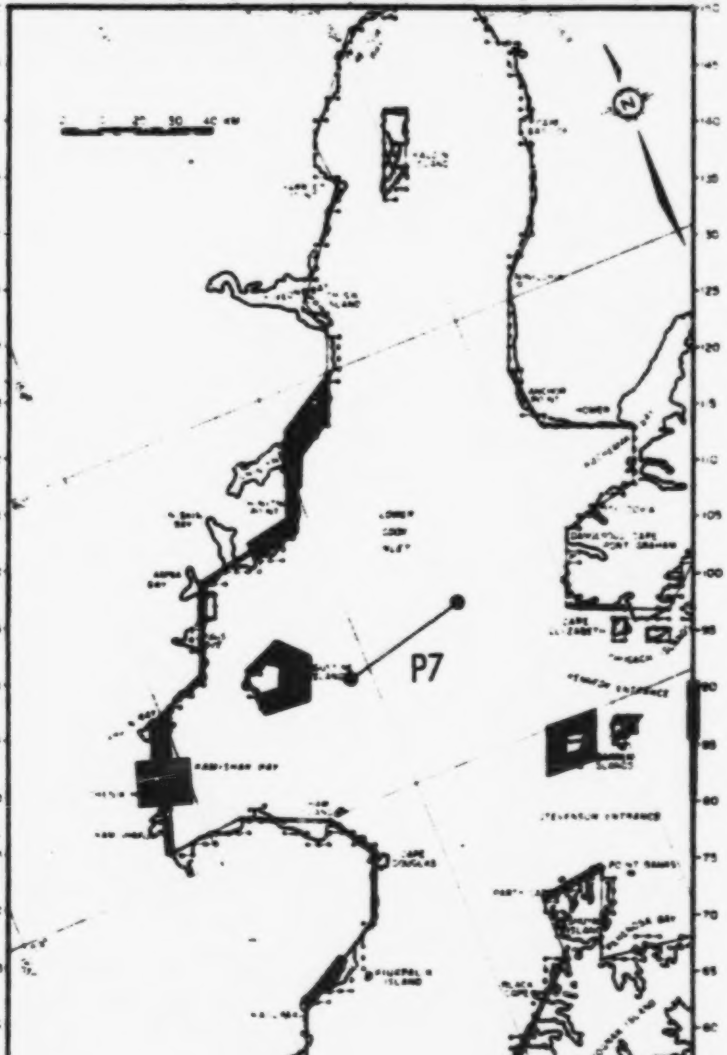

SITE:

P7

SEASON:

SUMMER

WIND FIELD VARIABILITY:

WEATHER CATALOG

PERCENT FREQUENCY OF
BOUNDARY IMPACT PER
KILOMETER OF REACH

0.005 1.0 2.0 3.0

NOTE: WIDTH OF SHADING
ALONG SEGMENTED REACHES
REPRESENTS MAGNITUDE OF
PERCENT FREQUENCY OF
BOUNDARY IMPACT

FIGURE 34: BOUNDARY IMPACT FREQUENCY

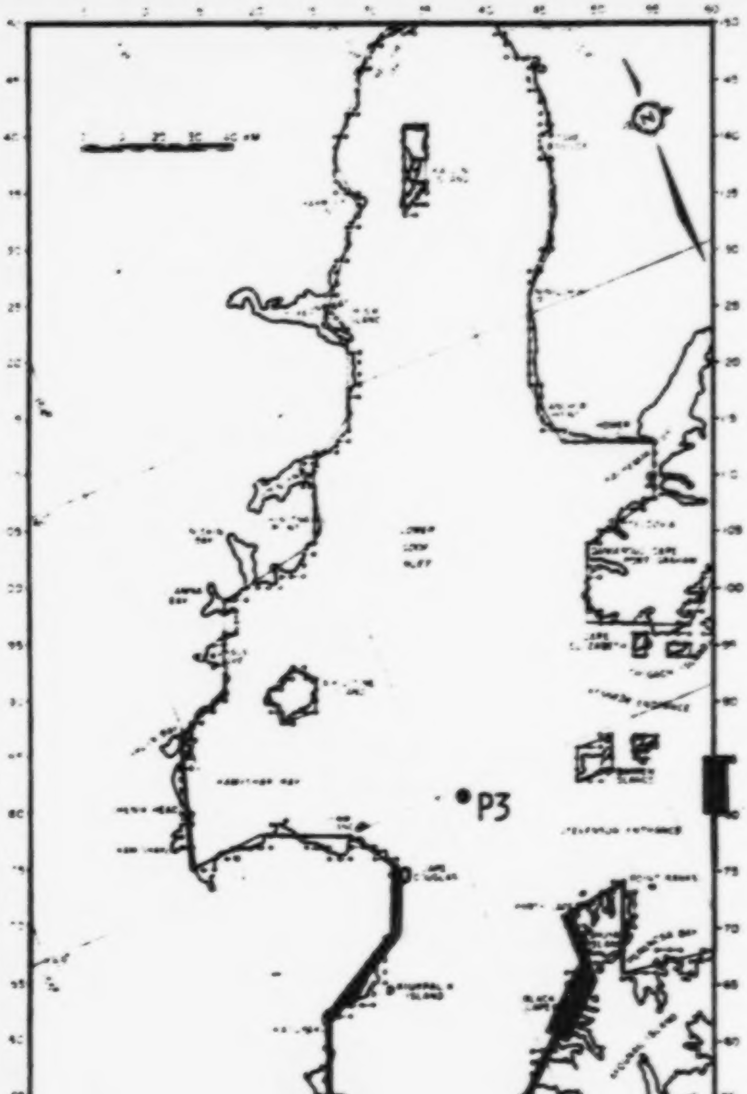

SITE:

P3

SEASON:

WINTER

WIND FIELD VARIABILITY:

WEATHER CATALOG

PERCENT FREQUENCY OF BOUNDARY IMPACT PER KILOMETER OF REACH

NOTE: WIDTH OF SHADING ALONG SEGMENTIZED REACHES REPRESENTS MAGNITUDE OF PERCENT FREQUENCY OF BOUNDARY IMPACT

FIGURE 35: BOUNDARY IMPACT FREQUENCY

BEST DOCUMENT AVAILABLE

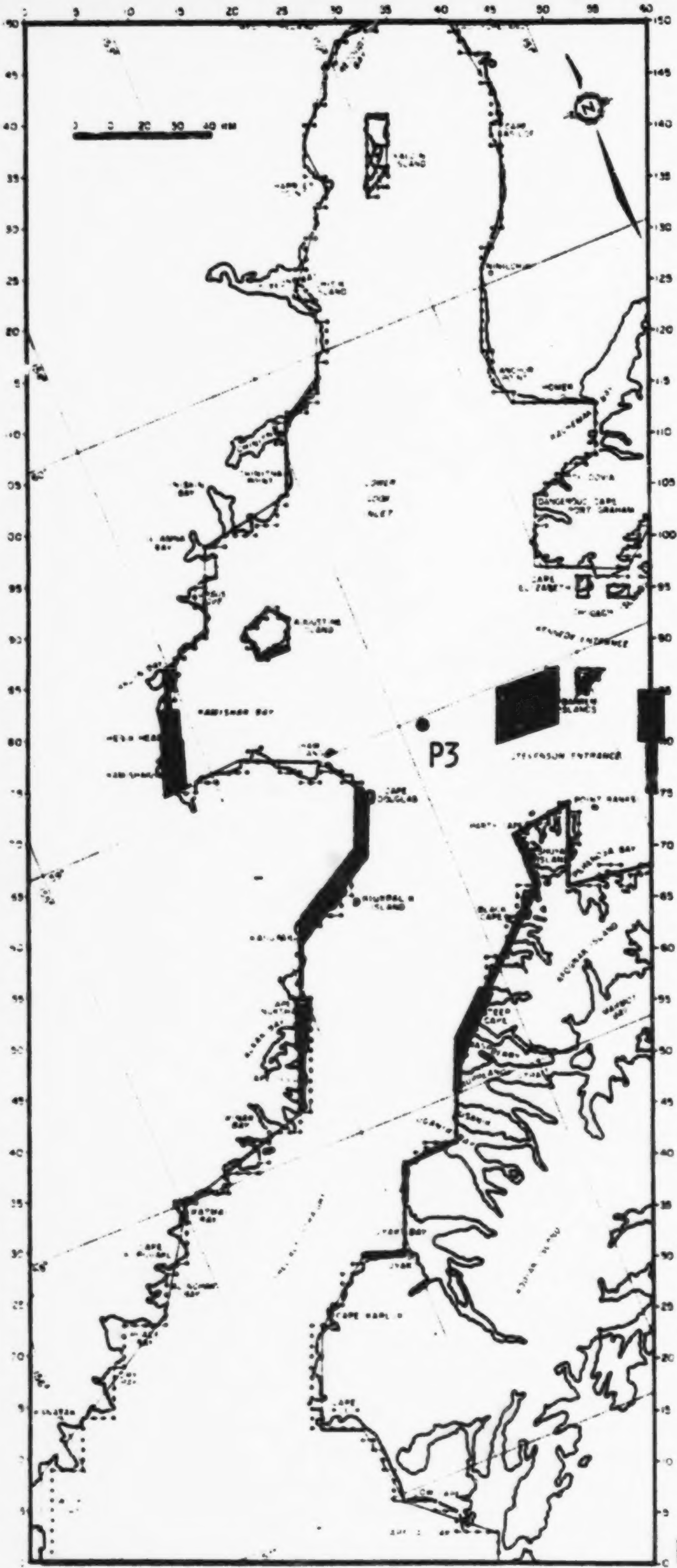
0 10 20 30 40 KM
P3
CAPE DOUGLAS
STEVENSON ENTRANCE
KENNEDY ENTRANCE
HOMER
AUGUSTINE ISLAND
KAMISHAK BAY

SITE:

P3

SEASON:

SUMMER

WIND FIELD VARIABILITY:

WEATHER CATALOG

PERCENT FREQUENCY OF BOUNDARY IMPACT PER KILOMETER OF REACH

0.0 0.5 1.0 2.0 3.0

NOTE: WIDTH OF SHADING ALONG SEGMENTIZED REACHES REPRESENTS MAGNITUDE OF PERCENT FREQUENCY OF BOUNDARY IMPACT.

FIGURE 36: BOUNDARY IMPACT FREQUENCY

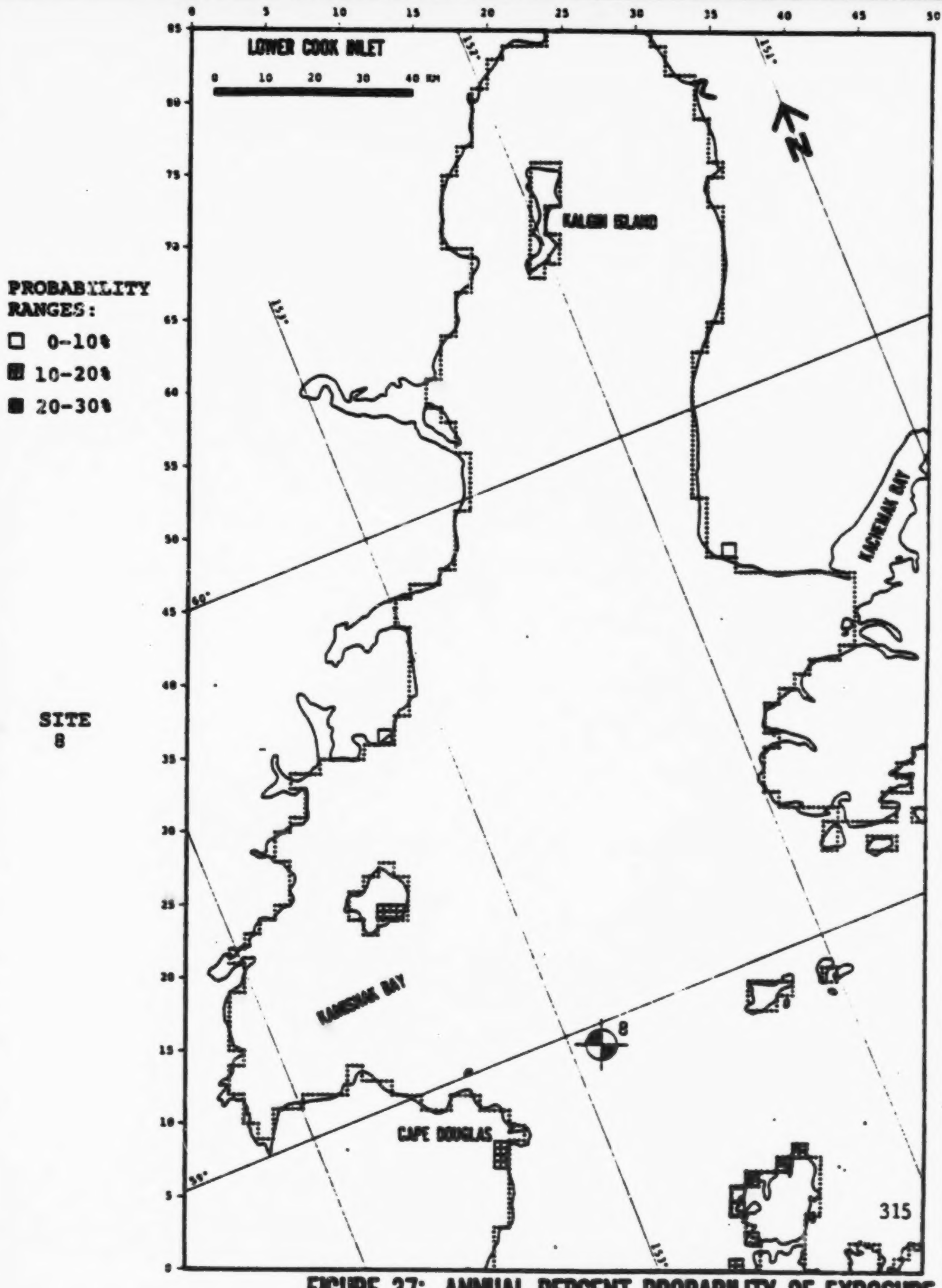
LOWER COOK INLET
0 10 20 30 40 KM
N
KALGIN ISLAND
KACHEMAK BAY
KAMISHAK BAY
CAPE DOUGLAS
152°
151°
153°
60°
59°
8
PROBABILITY RANGES:
☐ 0-10%
▨ 10-20%
■ 20-30%
SITE 8
0 5 10 15 20 25 30 35 40 45 50
0 5 10 15 20 25 30 35 40 45 50 55 60 65 70 75 80 85

FIGURE 37: ANNUAL PERCENT PROBABILITY OF EXPOSURE

(FROM DAMES & MOORE, 1979)

BEST DOCUMENT AVAILABLE

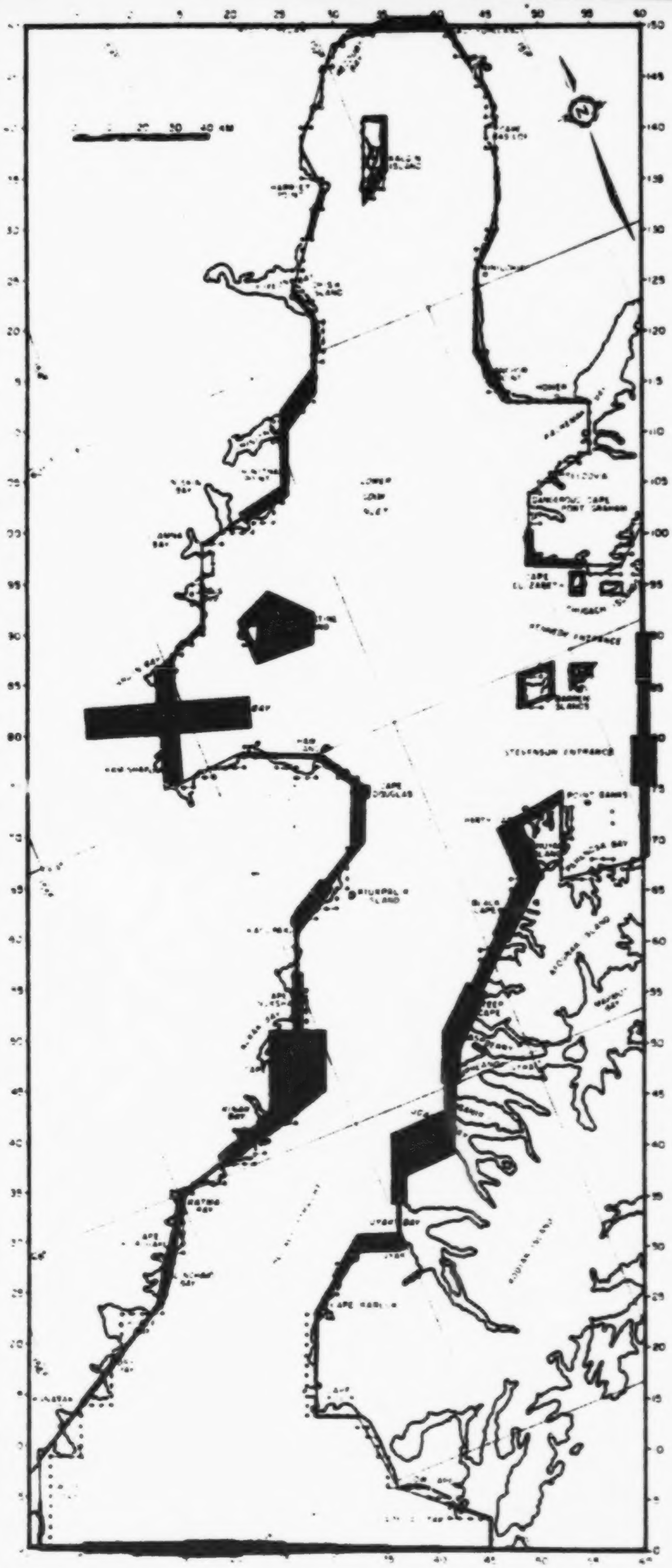

SITE:

ALL

SEASON:

WINTER

WIND FIELD VARIABILITY:

WEATHER CATALOG

PERCENT FREQUENCY OF
BOUNDARY IMPACT PER
KILOMETER OF REACH

0 0.5 1.0

NOTE: WIDTH OF SHADING
ALONG SEGMENTIZED
REACHES REPRESENTS
MAGNITUDE OF PERCENT
FREQUENCY OF BOUNDARY
IMPACT

FIGURE 38: BOUNDARY IMPACT FREQUENCY

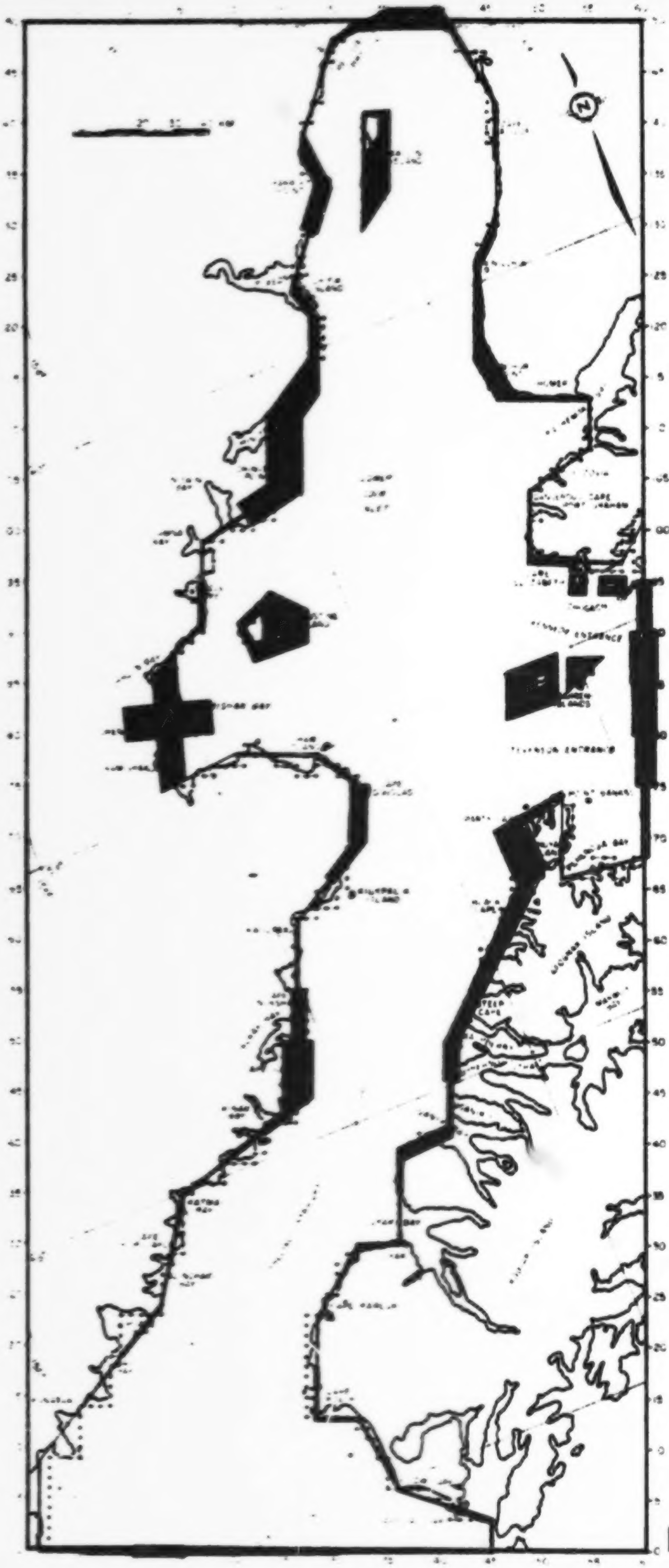

SITE:
ALL

SEASON:
SUMMER

WIND FIELD VARIABILITY:
WEATHER CATALOG

PERCENT FREQUENCY OF BOUNDARY IMPACT PER KILOMETER OF REACH

NOTE: WIDTH OF SHADING ALONG SEGMENTIZED REACHES REACHES REPRESENTS MAGNITUDE OF PERCENT FREQUENCY OF BOUNDARY IMPACT

FIGURE 39: BOUNDARY IMPACT FREQUENCY

APPENDIX A

WIND FIELD & INTENSITY CATALOG INPUT DATA FILE

Input Data File Format: Wind Field and Intensity Catalog

			Assigned Daily Wind Field & Intensity Factor																														
YR	MO	DA	1	2	3	4	5	6	7	8	9	10	11	12	13	14	15	16	17	18	19	20	21	22	23	24	25	26	27	28	29	30	31
XX	XX		XX	XX	XX	XX	XX	XX	XX	XX	XX	XX	XX	XX	XX	XX	XX	XX	XX	XX	XX	XX	XX	XX	XX	XX	XX	XX	XX	XX	XX	XX	XX

Intensity Factor (values 1 → 6)
Wind Field (values 1 → 5)
} See Table II

BEST DOCUMENT AVAILABLE

BEST DOCUMENT AVAILABLE

```
45  1 0053222342231453254253255353531423234242252523254242424225254253
45  2 00232322314535353435353531523424242454553435343452253424245000000
45  3 004542425343535353535353435353531453535353535353221453535353 4542
45  4 0023232315151545452245452253152323535314151522162315151414535300
45  5 003153532323232323232314535353532342424242424242434342424242424342
45  6 004353535342422525252553332323262642425353533353333316335353535300
45  7 0053422323232323232315535353334245224353533353535316535345453323
45  8 0023424243151653333353535343535353434323424245435353535343434242
45  9 00533335353535343452253535345534343221523234545424242424553535300
45 10 0053312525535353535353533153531633252553535325251515234525252553
45 11 0022531515424242252243231414231414535353222253535353151515151500
45 12 0053151415151515141423232525221414424242424242223231453535353531414
46  1 0053255353535314141414424523234242535342452555333454242424342251453
46  2 0053141415151515151542422553532525534253142315232314141425000000
46  3 005342252515225353531453531425255353531453535353535353435323234553
46  4 004314455353535314145314535353535353532553535325254245535353535300
46  5 0053454353534242454545453153535353424542424243144343421414154223
46  6 00424215424242424243434242454522222242424242425315424242424200
46  7 0042333343434223424245534515453315434343424242454343532245535316
46  8 00335343434333333345454553534545535343222223131434545453131224542
46  9 003131232345434545452325535353232525535353531516531414431522151400
46 10 0014535345255353334353535342424542535353535353535316452525535353
46 11 0025253353333335353534353531523232323232323232345455323231522431600
46 12 0053151522535315152215152315151443535353434325155342424214151445
47  1 0042532225432526154533154243255353145353141453531515152323232323
47  2 0014141414144242422323232314144245454545421442424245454223000000
47  3 0023232353535314141614145353531423234242535353532242255323141414
47  4 0023231414532525535353534242424242223231514435353431453535353535300
47  5 0025334245255325255314234353535343535342434545254545424242422323
47  6 0014141453434223235353422553333333535343434333453333154343531500
47  7 00435343424343434343431545454542424242424242434333423353434553
47  8 0053434342422642454243454342434343424243152323234253535353535353
47  9 0053534333535353535353535353333531542535343235315431522453131434300
47 10 0053221645454253535353535353535353535353255353535353535316151525
47 11 0043334243435333345534353535353535353534242422542452553424253434200
47 12 0042424253255353535353255314535325255353535353533353531453145325
48  1 0025253353535353535353144214142525424225252525254245535315142525
48  2 0045432323232323234242432323531423232323231414235353141425250000
48  3 0014231514142323234515535325255353533353532515232345455343425342
48  4 002323234343431523434243454343151522224322533155343434316151500
48  5 0053531414535353142525535315155314535353533333531525454553434343
48  6 00535343224553534223424342424242424245434343434342424243533333433300
48  7 0033333342455343164343535345424242455353534343535333535353533353
48  8 0045454553333353434242434345454333434343424243431642161631313143
48  9 0053223353535342165333434242423353535353252553432553424545422500
48 10 002553535333335353535353535342455353535343535353535353535325353
48 11 0042535353434343433342535353535314221414141414141515262614141400
48 12 0053152222141414224253532645535342533333434353154525535353531515
49  1 0014142553251542454242434343432525424545164245262626422642454245
49  2 0015232343531443141523424343431515232342421414234242421414000000
49  3 0014252525424342454245452323232323232323234225432553535353535325
49  4 005353535353535315161553141443145353535353531514141453535353335300
49  5 00535353531553232314145353333334542454242424242434342424243535353
49  6 0025255333155333221633253333334242435353535343432343161653155300
49  7 0043434343434245264242425333334542454333333333333343535333431653
49  8 0053162222233333353333534353151633333534342422525334533532542425353
49  9 005353535353534343422345425353535353533325535353535353535342232500
49 10 004545252553531425255353535345454526452553535345535353535353535353
49 11 005353151522224343454543154323232323234525535353151545454315434300
49 12 0015431515225353225343425353222323232323231414144225252222141453
50  1 0045424325232343432323234523232323312323232323234323232323232323
50  2 004323232222151514141414141414142222322223142311414141444242000000
50  3 00252553534342424242424242424253535353535353535353532253535343155325
50  4 001415222264516454553252553333333353532553533314535314141453535300
50  5 005315535333532525535353535353531414435333333343425353535333333315
50  6 0015151642424233334333144242424253424525425333423353432216161500
50  7 004242424223421442424545434214424243433322223224253333333333534343
50  8 004342453342424242424222642232323424523424242225252525535353533326
50  9 0053532553533353325254533334242424525255353425353533333345454532500
50 10 0025252525232314432553535353455342224525535345535333335353315353
```

```
50 11 0053531523222243224545431543232323262645252222151526222215434300
50 12 0053531515225353142543452553532626142323231414142345252522144353
51  1 0053141442422525255353435315151414141553151515152623232323232342
51  2 0014141414142314142323454245424225535315424225252322251643000000
51  3 0023232323262323232314532553532653151423534314535325255353141442
51  4 0042255353252525553231515434242424245262323424214432525252525255300
51  5 0043434242232323232323231453255345252525255353534242424242454242
51  6 0042424242424243431453535353534545454245424343434323424245454300
51  7 004242424233334245232342422343424543423353535315154343431515553 31
51  8 0015535353454545434242252525535331534342225353334242252525434323
51  9 0023235325535353235353255353534515252542454223232314145322535300
51 10 0053333353535353531414151522232323232342424242234253333342424242
51 11 0025535325455325251442535322334316532545424242532525252553535532500
51 12 0053535353151514142342432323532223234253334242432342434342452525
52  1 0033432553141514151523425342234253154343431414231425252542142323
52  2 0053535314234242422525151414141442424245425342535314454543450000
52  3 0045231414144242424345425325455353151514144253252553535353151515
52  4 0015151515424242422553155353535325255343252555353422553434353 2200
52  5 0022434333535315144323141553434226422533333531543434345422543 4353
52  6 0053535353334345454242422343434343231443434343434343434345534 34300
52  7 0053433345454253334242424225331543432515422342424243424343334316
52  8 0016454345454242424245431515151543535353531516533343141442424225
52  9 0053421515151542425353155353141414535322451514232325252553531400
52 10 0014144242535343434353531522454553332253532514532345162242255314
52 11 0053535342424242225255353255314252525255534225432545454223142314 00
52 12 0014252514535353535353535353535353531525232325252525252525532553 53
53  1 0053534242424542232323141423141423232553535353152314231414141414
53  2 0053535343141414252543422542255353534225254342422525254225000000
53  3 0053421414141415151414312645252553535353145325252353535353252553 15
53  4 0042535353531515232323232314144253254225535343432325252525231400
53  5 0023142314431414535343145353435323255353252543434342424243424242
53  6 0042234223145343434343534345454553431515151515151515151523434300
53  7 0043434343434331535343151515553531533334343424242422323424242424 2
53  8 0042535353434533433333434343535315432243434533333333333535353 53
53  9 0043161653535353422626535353424253533333535353535353531515232300
53 10 0014141414252553535353535325255353535353535353535353145353141414 1453
53 11 0053531553262622422223232553535353535353421425252525255353424500
53 12 0045255353535353535353535353142242231423232342255325534214142353 14
54  1 0053141414145353535343262626232323232323232323232323231443435353
54  2 0042535325255333332323232314141523144343163131435315151442000000
54  3 0042531622332225531553535315154522151545454343151523232323232323
54  4 0023231543152343151423155333535353434314141515151523234545252500
54  5 0022252553222525424542424243432323232325434315141433144325255323
54  6 0053534342424542424525435353535333422345163333333333343533 1454200
54  7 0042423353434343313133433323224242535331535333434343424543424553
54  8 0031313131424245454553535343433143434545434345454343164533424533
54  9 0045453325313116224343151442454243314343435353535315434242454200
54 10 0042422323231414252553533325252525535353535345455322534225252553
54 11 0053432553535342231414232314145353535353535353534525531645311542 00
54 12 0053431526435353532525535315533131312315535353151515151443313122
55  1 0043255315142542452553424242532514142525532553532525424242141414
55  2 0042535325151515144223535315531543434343432342424242421523000000
55  3 0015424225252515425353152342455345334242224242424222525535314252 5
55  4 0015144215151515553535322221453154542335353535353531414144253 2500
55  5 0042423142532553435353434242424225535353434245252525535343434242
55  6 0053431553334223255353533333333433143434225312542425353535343 00
55  7 0042454543434343422525535345434533333342424342424545535353431515
55  8 0042434343535353532553534353225353154331333343252553333333332325
55  9 0025533315424242424253535353535322222242424545534323454553252500
55 10 0022252553535353151553255333535353535353534525252555353151515 1523
55 11 0023232343431553531542424214141415151553531423264242262642535300
55 12 0053141414232314255315264543234242532323231516152343264331151525
56  1 0015265315232253221523232323232315154315252525251523234245452215
56  2 0025534242434343531515152323422525531515232345535353252515530000
56  3 0015151515141515152342454542532525252542424225251523142214141443
56  4 0014535353151414532525255353535342255353232323234542424242424200
56  5 0025254223234253535353534253535353535314535353534245452543535343
56  6 0053534545535353252543434343423353155353255331313115155343422300
56  7 0023233131313143151523232323233115155342535342232323454343434343
56  8 0015333315164322312342424242225255353535353535353534225535353 43
56  9 0043424242534225424245424545332322435353535353431414424522255300
```

BEST DOCUMENT AVAILABLE

```
56 10 005353535353532222222253534325535353155322531414142222243255353531515
56 11 00162553531523141453531515144343531425532525535342422255325162300
56 12 0015232323232342151415232323422323141525144343313131314242535323
57  1 00232542431515234223232323232323232323422323232345454242452323
57  2 0023424242424343535315152325431514424242232323232525254325000000
57  3 0043251425141414142525151514434242225533333431515141433142323 2323
57  4 0025161523424245454242454545154542424223421414144253535314232300
57  5 0023232342424222323424223232314422525252525534343432314145343 1442
57  6 0042424242232323254342252525333316252515151555353332516535343 4300
57  7 0043433333333316332545424533254545454533333434353534343221515 1542
57  8 0042424545333331542424343535342424222333333151515234242425333 3325
57  9 0042452542255343434343422533454223422553434315235315155353531 500
57 10 0016422342424523432516165333424242421553234545452243432325253 343
57 11 0025252525333454523232325252525424222525454542144253532553252 55300
57 12 0025253325252525253334545333333353531414141425252525531514252 5141553
58  1 0015231443252525331414232323255353152553254242252543252523232323
58  2 0042424223232323232323232323141423232323232525232323252314420000 00
58  3 0042254315453314141442424523162323232345535322531414141414142525
58  4 0025141423424223142323255325252553535322432323454545452323234200
58  5 0014145353535353535353142314535325434545452525424342422323232342
58  6 0042424242424242424243252525334253332342422533333343433333333300
58  7 0053165342424242534353434225333315534253533325535323232525333343
58  8 0043535353535353424353252525255353535353154253535353334322333333
58  9 0033455315161633224242434233531515335353535333252553534315154200
58 10 0025255343433333422222151522455353532525151545142225531522532553
58 11 0053535325252555353151515151545452553531515224542424222525531231400
58 12 0053534542232323232323144223232323232323252525255353234315151515
59  1 0023235353531515151515152323151515152323232314141414142525424242
59  2 0025254543152342432343532345454525425353434315252525252553000000
59  3 0043251514145353531515151515151553531515153153141414235325535325
59  4 0025255315531515252553254243431514431414142323454253533333454500
59  5 0045454542251425255353311414142525252523151542454342234243434343
59  6 0025254353532525151522154242454245452323235353333315155333432200
59  7 0033535325334322223333535353535353532222435353534333434343435353
59  8 0043231515155333153342234543251445454545535333334343424543535353 53
59  9 0053435353535343232515152245425353141414314343254353434245252500
59 10 0033334223232323231414145353534316232323422525535342252543254353
59 11 0033144242535353333323234542454542252525535325534242422525532500
59 12 0053534215155353435353534325252515222514535353535315534325534242
60  1 0042424225255343455353535353535325424223232314232323422323252525
60  2 0053252525252525255353535325252545454522224245424223232323230000
60  3 0023232323231515152353531415532525255315232314421414151423231425
60  4 0053531515535342425353432525252353155353535343535353232323141400
60  5 0023421415232325533316252525251423232353252345252525142523315353
60  6 0053433323234243434353533333535353531543421422224542253325535300
60  7 0053535353535333424215152323232553535333424242424343435353533333
60  8 0033535333253333431515424242424353535353334533333345254553531553
60  9 0043252525155322434353252525434525532542424225252533534543234500
60 10 0033333325254353434253141414252525422322262525252525252553532525
60 11 0053531425535323424226141414145325252525535315151515224222532600
60 12 0026333314424225252525532553424242422323232525252526424242255314
61  1 0014252525255314141423232325252525422342424242454545142323232322
61  2 0053535353255353535353141414141414141414231425154353252500000 0
61  3 0025531423232525232323252543155353532525232314141414141423232525
61  4 0053531443434253434533533343535325535353434245424545531514232300
61  5 0023234223424223262345532214144553532553535314535342425353534242
61  6 0042533353532525531525252553531515151555353314353535353334242420 0
61  7 0043535353531653535322433343533345535353334343454245454245424245
61  8 0043334525535353534245425315433353424545455353533333535325532553
61  9 0053535333452525534545252553535353534233252525252533323454553530 0
61 10 0053535353535342252515141515151514535345452553535353535353254315
61 11 0045451442534315535353532225434225535342535353154253262323422500
61 12 0025535315434215454545252525152515152323261415141515531543432325
62  1 0025162522151523234222152345224515232323232345432315231515151525
62  2 0053532342424242535353531423232323234545421542234242232323000000
62  3 0023422242454553534542231415531415155343151515232525142525422342
62  4 0045421425151522431553161515155343151525251553153333333534343430 0
62  5 0015151542422342454245422553434225334542333345333345452515151533
62  6 0033335343535333333454245453325434343151515154325335353333353420 0
62  7 0042234243424542424525255353425342424242532214424245424242424245
```

```
62  8 00454225535343453333152542424523424343252533333535333454542451643
62  9 00425353421514421533163333353535353534223252525252522533333152500
62 10 00533316333342252515151515141425533333353533345424225532325232323
62 11 00234242422252325252525151523231442422525435353232525531553252500
62 12 005353251515532323234225252525255314535325232345231523232323232323
63  1 0023432515251543432323424222245454545424242234242424223232323232323
63  2 007315151525252525251543232323231515422525252525252325252525000000
63  3 002523425325424242534515425315331425255315223315224543151523232323
```

BEST DOCUMENT AVAILABLE

APPENDIX B

WIND FIELD INPUT DATA FILES

Input Data File Format: Wind Fields

	Grid Coord.		Wind Parameters for (y,x)		Wind Parameters for (y,x+3)		Wind Parameters for (y,x+6)		Wind Parameters for (y,x+9)		Wind Parameters for (y,x+12)		Wind Parameters for (y,x+15)		Wind Parameters for (y,x+18)	
M	y	x	V	Θ	V	Θ	V	Θ	V	Θ	V	Θ	V	Θ	V	Θ
X	XX	XX	XX.	XXX.	XX.	XXX.	XX.	XXX.	XX.	XXX.	XX.	XXX.	XX.	XXX.	XX.	XXX.

M - WIND FIELD NUMBER

(y,x) - GRID CELL LOCATION FOR WIND FIELD DATA

V - WIND VELOCITY AT (y,x) IN METERS/SEC

Θ - DIRECTION OF WIND VELOCITY AT (y,x) IN DEGREES (MEASURED CLOCKWISE FROM NORTH)

BEST DOCUMENT AVAILABLE

```
100000 05.   170.  05.   170.  05.   170.  07.   170.  07.   175.  08.   175.  08.   175.
100021 08.   175.  09.   170.  09.   165.  09.   160.  08.   155.  08.   145.  06.   140.
100042 05.   130.  05.   130.
100300 05.   170.  05.   170.  05.   170.  07.   175.  07.   175.  08.   175.  08.   175.
100321 08.   175.  09.   170.  09.   170.  08.   160.  08.   155.  05.   140.  05.   130.
100342 05.   130.  05.   130.
100600 05.   170.  05.   170.  05.   170.  07.   175.  07.   175.  08.   175.  08.   175.
100621 09.   175.  09.   175.  09.   170.  08.   160.  06.   145.  05.   140.  05.   135.
100642 05.   130.
100900 05.   170.  05.   170.  05.   170.  07.   175.  07.   175.  08.   175.  09.   175.
100921 09.   175.  10.   170.  09.   165.  07.   160.  05.   155.  05.   150.
100942
101200             05.   170.  05.   170.  06.   170.  07.   170.  08.   170.  09.   175.
101221 09.   175.  10.   175.  08.   170.  07.   165.  05.   160.  05.   155.
101242
101500             05.   170.  05.   170.  05.   170.  05.   170.  08.   175.  09.   175.
101521 09.   175.  10.   175.  06.   175.  06.   170.  05.   165.
101542
101800                         05.   170.  05.   170.  06.   170.  08.   175.  08.   175.
101821 09.   175.  10.   175.  08.   175.
101842
102100                         05.   170.  05.   170.  05.   170.  06.   175.  08.   180.
102121 09.   180.  09.   180.  09.   175.  07.   170.
102142
102400                                     05.   170.  05.   170.  05.   175.  08.   180.
102421 08.   180.  09.   180.  09.   175.  07.   170.
102442
102700                                                 05.   170.  05.   170.  08.   180.
102721 08.   180.  08.   180.  09.   175.  10.   170.  08.   170.
102742
103000                                                 05.   170.  05.   170.  08.   180.
103021 07.   180.  08.   180.  08.   175.  10.   170.  08.   170.  05.   170.
103042
103300                                                             05.   175.  05.   180.
103321 07.   180.  08.   175.  08.   175.  10.   175.  08.   170.  05.   170.
103342
103600                                                             05.   180.  05.   180.
103621 05.   175.  08.   175.  08.   175.  08.   175.  08.   170.  05.   170.
103642
103900                                                                         05.   180.
103921 05.   175.  05.   170.  07.   175.  08.   180.  08.   175.  09.   170.  10.   170.
103942 05.   170.
104200
104221 05.   175.  05.   170.  06.   175.  09.   175.  09.   175.  10.   170.  10.   170.
104242 05.   170.
104500
104521             05.   170.  05.   170.  08.   175.  10.   175.  10.   170.  08.   170.
104542 05.   170.
104800
104821                         05.   170.  07.   170.  10.   175.  10.   170.  08.   170.
104842 06.   170.
105100
105121                         06.   170.  08.   170.  10.   170.  10.   170.  08.   170.
105142 06.   170.  05.   170.
105400
105421             05.   170.  06.   170.  08.   170.  09.   175.  10.   175.  10.   170.
105442 07.   170.  05.   170.
105700
105721             05.   170.  05.   170.  08.   175.  09.   175.  10.   175.  10.   170.
105742 05.   170.  05.   170.  05.   170.
106000
106021             05.   170.  05.   170.  07.   180.  09.   180.  10.   175.  10.   175.
106042 10.   175.  08.   165.  05.   165.
106300
106321             05.   170.  05.   170.  08.   200.  09.   190.  10.   180.  10.   175.
106342 10.   175.  08.   165.  05.   165.
106600
106621                                     08.   205.  11.   205.  11.   190.  10.   180.
106642 09.   175.  05.   165.  05.   165.  05.   160.  08.   145.  08.   140.  10.   140.
106900
106921                                     08.   190.  11.   195.  11.   190.  10.   180.
106942 09.   170.  09.   165.  08.   160.  08.   155.  10.   150.  10.   140.  10.   140.
107200                                                 10.   045.  08.   045.  06.   045.
107221 04.   050.                          05.   180.  08.   175.  10.   175.  12.   170.
107242 10.   165.  10    160.  10    155.  10.   150.  10    145.  10.   140.  10.   140.
```

```
107500                                         15.  050. 10.  045. 08.  045.
107521 05.  060. 05.  090. 05.  100. 10.  130. 12.  155. 12.  165. 12.  170.
107542 10.  165. 10.  165. 10.  155. 10.  150. 10.  150. 10.  145. 10.  145.
107800                                         15.  070. 15.  065. 10.  065.
107821 08.  075. 08.  090. 10.  110. 11.  120. 12.  140. 12.  155. 11.  165.
107842 10.  165. 10.  165. 10.  155. 10.  145. 10.  140. 10.  145. 10.  145.
108100                                         15.  065. 15.  075. 15.  080.
108121 14.  085. 13.  090. 13.  095. 12.  115. 11.  140. 11.  160. 10.  170.
108142 10.  160. 10.  155. 08.  140. 08.  140. 10.  145. 10.  150. 10.  150.
108400                                         15.  065. 15.  085. 15.  095.
108421 14.  110. 13.  110. 13.  120. 12.  145. 11.  150. 10.  170. 10.  170.
108442 10.  165. 10.  160. 08.  140. 08.  145. 10.  145. 10.  150. 10.  150.
108700                                         15.  060. 15.  090. 15.  115.
108721 15.  125. 10.  130. 13.  145. 12.  150. 10.  155. 10.  170. 10.  170.
108742 10.  160. 10.  155. 10.  145. 10.  140. 10.  140. 10.  145. 10.  145.
109000                                         13.  110. 13.  120. 11.  160.
109021 08.  170. 05.  160. 10.  150. 10.  155. 10.  160. 10.  170. 10.  170.
109042 10.  160. 10.  150. 10.  140. 10.  135. 10.  140. 10.  135. 09.  130.
109300                                                   11.  145. 09.  180.
109321 08.  200. 09.  165. 10.  165. 10.  165. 10.  170. 10.  165. 10.  165.
109342 10.  165. 10.  160. 10.  150. 10.  140. 10.  130. 10.  110. 10.  100.
109600                                                   05.  160. 05.  200.
109621 09.  200. 09.  190. 09.  180. 10.  170. 10.  170. 10.  170. 10.  160.
109642 10.  160. 10.  160. 10.  160. 10.  130. 08.  090. 08.  090. 08.  090.
109900                                                   05.  200. 05.  210.
109921 08.  200. 09.  185. 09.  180. 10.  175. 10.  175. 10.  165. 10.  160.
109942 10.  160. 11.  165. 12.  145. 08.  145. 06.  130. 06.  110. 06.  090.
110200                                                             05.  210.
110221 05.  210  05.  205. 09   170. 10.  180. 10.  175. 10.  165. 10.  165.
110242 10.  165. 10.  155. 10.  100  05.  170.           05.  090. 05.  090.
110500
110521           05.  205. 09.  195. 10.  185. 10.  180. 10.  180. 10   175.
110542 10.  170. 10.  165. 08.  185. 06.  195. 05.  195.
110800
110821           05.  190. 10   195. 10.  190. 10.  180. 10.  180. 10.  175.
110842 10.  175. 08.  195. 08   200. 08.  215. 06.  215. 05.  215.
111100
111121           05.  190. 08.  185. 10.  185. 10.  180. 10.  180. 10.  180.
111142 10.  180. 09.  195. 07.  210. 07.  225. 07.  225. 06.  225.
111400
111421           05.  185. 08.  185. 10.  185. 10.  180. 10.  180. 10.  180.
111442 10.  180. 08.  180. 05.  180. 05.  250. 05.  235. 05.  210.
111700
111721                     05.  180. 08.  185. 10.  180. 10.  180. 10.  180.
111742 10.  180. 08.  170.
112000
112021                     05.  180. 08.  180. 09.  175. 10.  180. 10.  180.
112042 10.  180. 08.  180.
112300
112321           04.  185. 05.  180. 07.  175. 09.  175. 10.  180. 10.  180.
112342 10.  180. 08.  180.
112600
112621           04.  185. 05.  185. 08.  180. 09.  180. 10.  180. 10.  180.
112642 10.  180. 10.  185.
112900
112921           04.  190. 06.  180. 09.  185. 10.  185. 10.  180. 10.  180.
112942 10.  180. 10.  185. 06.  185.
113200
113221                     06.  180. 09.  180. 08.  180. 10.  180. 10.  180.
113242 10.  180. 10.  180. 06.  185.
113500
113521                     06.  180. 09.  180. 08.  180. 10.  180. 10.  180.
113542 10.  185. 08.  185. 06.  185.
113800
113821                     06.  180. 10.  180. 06.  180. 10.  185. 10.  185.
113842 10.  190. 08.  190. 06.  190.
114100
114121                     06.  180. 10.  180. 06.  180. 10.  185. 10.  185.
114142 10.  190. 08.  190. 06.  190.
114400
114421                     06.  180. 08.  180. 10.  185. 10.  185. 10.  185.
114442 10.  190. 08.  190. 06.  190.
114700
114721                     06.  180. 08.  180. 10.  185. 10.  185. 10.  185.
114742 10.  185. 06.  185.
115000
115021                               06.  180. 08.  185. 10.  185. 10.  185.
115042 08.  185.
```

200000	08.	230.	08.	230.	08.	230.	08	230.	08.	230.	08.	230.	10.	230.
200021	10.	230.	10.	235.	10.	240.	10.	240.	10.	240.	10.	240.	10.	240.
200042	10.	240.	10.	245										
200300	08.	230.	08.	230.	08.	230.	08.	230.	10	235.	10.	235.	10.	235.
200321	10.	235.	10.	235.	10.	235.	08.	240.	08.	240.	08.	240.	08.	240.
200342	08.	240.	08.	240.										
200600	08.	230.	08.	230.	08.	230.	08.	230.	10.	235.	10.	235.	10.	235.
200621	10.	235.	08.	235.	08.	235.	08.	235.	08.	235.	08.	235.	08.	235.
200642	08.	235.												
200900	08.	230.	08.	230.	08.	230.	08.	230.	09.	230.	09.	230.	09.	230.
200921	09.	230.	08.	230.	08.	230.	08.	230.	08.	230.	08.	230.		
200942														
201200			08.	230.	08.	230.	08.	230.	09.	230.	09.	230.	09.	230.
201221	08.	230.	08.	230.	08.	230.	08.	230.	08.	230.	08.	230.		
201242														
201500			08.	230.	08.	230.	09.	230.	09.	230.	09.	230.	09.	230.
201521	08.	230.	08.	230.	08.	230.	08.	230.	08.	230.				
201542														
201800					08.	230.	08.	230.	08.	230.	08.	230.	09.	230.
201821	09.	230.	09.	230.	08.	230.								
201842														
202100					08.	230.	08.	230.	08.	230.	08.	230.	09.	230.
202121	09.	230.	09.	230.	08.	230.	08.	230.						
202142														
202400							08.	230.	08.	230.	08.	230.	09.	230.
202421	09.	230.	09.	230.	09.	230.	08.	230.						
202442														
202700									08.	230.	08.	230.	09.	230.
202721	09.	230.	09.	230.	09	230.	08.	230.	08.	230.				
202742														
203000									08.	230.	08.	230.	08.	230.
203021	09.	230.	09.	230.	09.	230.	09.	230	08.	230.	08.	230.		
203042														
203300											05.	225.	08.	225.
203321	09.	230.	09.	230.	09.	230.	09.	230.	08.	230.	08.	230.		
203342														
203600											05.	225.	08.	225.
203621	09.	230.	09.	230.	09	230.	09.	230.	09.	230.	08	230.		
203642														
203900													05.	225.
203921	05.	230.	08.	235.	09.	235.	10.	235.	09.	230.	08.	230.	06.	230.
203942	06.	230.												
204200														
204221	05.	230.	05.	230.	08.	230.	08.	230	10.	230.	08.	230.	07.	230.
204242	06.	230.												
204500														
204521			05.	230.	08.	230.	08.	230.	09.	230.	08.	230.	07.	230.
204542	06.	230.												
204800														
204821					08.	230.	09.	230.	09.	230.	09.	230.	08.	230.
204842	07.	230.												
205100														
205121					08.	225.	10.	225.	10.	225.	09.	225.	08.	225.
205142	07.	225.	06.	225.										
205400														
205421			05.	225.	08.	225.	09.	225.	09.	225.	08.	225.	08.	225.
205442	07.	225.	05.	225.										
205700														
205721			06.	225.	08	225.	09.	220.	09.	220.	09.	220.	08.	225.
205742	08.	225.	07.	225.	05.	225.								
206000														
206021			05.	220.	08.	220.	09.	215.	09.	215.	09.	220.	09.	220.
206042	09.	225.	08.	225.	05.	225.								
206300														
206321			05.	220.	05.	220.	08.	220.	09.	210.	09.	210.	09.	215.
206342	09.	205.	08.	205.	06.	210.								
206600														
206621							08.	220.	09.	210.	09.	205.	09.	205.
206642	09.	200.	10.	205.	08.	220.	08.	230.	08.	230.	08.	230.	08.	230.
206900														
206921							06.	215.	08.	205.	09.	200.	09.	175.
206942	09.	200.	10.	205.	10.	210.	08.	235.	08.	230.	10.	230.	10.	230.
207200									05.	260.	05.	270.	05.	270.
207221							05.	190.	08.	195.	09.	195.	09.	195.
207242	09.	200	09.	200.	09.	210.	10.	215.	10.	220.	10.	220.	10.	220.

BEST DOCUMENT AVAILABLE

```
207500                                             17.  275.  15.  275.  14.  275.
207521 13.  270.  12.  270.  11.  270.  05.  240.  08.  210   09.  210.  09.  210.
207542 09.  210.  10.  205.  10.  205.  10.  215.  10.  220.  10.  220.  10.  220.
207800                                             17.  275.  17.  270.  15.  270.
207821 14.  270.  13.  270.  12.  270.  08.  255.  08.  230.  10.  215.  10.  215.
207842 10.  215.  10.  210.  10.  210.  10.  215.  10.  220.  10.  220.  10.  220.
208100                                             17.  270.  15.  260.  15.  260.
208121 15.  260.  13.  260.  12.  260.  11.  260.  10.  255.  10.  245.  10.  240.
208142 10.  235.  10.  225.  10.  220.  10.  220.  10.  220.  10.  220.  10.  220.
208400                                             17.  250.  15.  240.  15.  245.
208421 15.  255.  15.  255.  12.  255.  10.  255.  10.  255.  10.  255.  10.  255.
208442 10.  255.  10.  255.  08.  255.  08.  235.  08.  235.  10.  235.  10.  230.
208700                                             15.  235.  15.  240.  13.  240.
208721 11.  250.  11.  245.  11.  235.  10.  250.  10.  250.  10.  250.  10.  250
208742 10.  250.  10.  255.  10.  255.  10.  255.  10.  250.  10.  245.  10.  245.
209000                                             10.  230.  10.  230.  12.  220.
209021 08.  220.  08.  235.  10.  235.  10.  235.  10.  240.  10.  245.  10.  250.
209042 10.  250.  10.  250.  10.  250.  10.  250.  10.  250.  10.  250.  10.  250.
209300                                                        10.  225.  12.  225.
209321 12.  205.  10.  215.  10.  205.  10.  200.  10.  220.  10.  235   10   240.
209342 10.  245.  10   245.  10.  250.  09.  255.  09   255.  09.  250.  09.  250.
209600                                                        08.  220.  08.  220.
209621 10.  215.  10.  215.  10.  215.  10.  205.  10.  210.  10.  220.  10.  230
209642 10.  230.  10.  215   08.  235.  08.  260.  08.  260.  08.  250   08.  235.
209900                                                        06.  215.  08.  215.
209921 08.  210.  09.  220.  10.  215.  10.  205.  10.  205.  10   210.  10.  220.
209942 10.  225.  10.  210.  07.  190.  05.  240.  05.  255   05.  240.  08.  235.
210200                                                                   05.  170.
210221 06.  205   08.  210.  09.  215.  10.  205.  10.  205.  10   205.  10   210.
210242 10.  205.  10   200   08.  190.  05.  200.             05.  225.  05   230
210500
210521            08.  205.  08.  210.  09.  200.  10.  200.  10.  205.  10.  210.
210542 10.  205   10.  205.  08.  205   05.  210.  05.  210.
210800
210821            06.  200.  08.  205.  10.  195.  10.  195.  10.  200.  10.  205.
210842 10.  210.  09.  205.  10.  210.  08.  220.  05.  235.  05.  240.
211100
211121            05.  240.  08.  205.  10.  200.  10.  195.  10.  195.  10.  200.
211142 10.  200.  09.  195.  05.  230.  08.  240.  10.  225.  05.  220.
211400
211421            05.  240.  06.  210.  08.  200.  10.  195.  10.  195.  10.  190.
211442 09.  195.  08.  190.  05.  210.  05.  245.  05.  240.  08.  210.
211700
211721                       06.  205.  08.  200.  10.  195.  10.  195.  10.  190.
211742 09.  190.  08.  190.
212000
212021                       08.  195.  08.  195.  10.  195   10.  190.  10.  185.
212042 09.  190.  08.  200.
212300
212321            05.  200.  07.  200.  08.  195.  10.  190.  10.  190.  10.  185.
212342 09.  190.  08.  205.
212600
212621            05.  200.  08.  200.  09.  200.  10.  195   10.  190.  10.  185.
212642 09.  190.  08.  205.
212900
212921            05.  205.  08.  200.  09.  200.  10.  195.  10.  195.  10.  195.
212942 09.  195.  08.  210.  05.  210.
213200
213221                       05.  200.  09.  200.  08.  200.  10.  195.  10.  195
213242 10.  195.  07.  215.  05.  215.
213500
213521                       08.  205.  09.  205.  08.  205.  08.  205.  10.  205.
213542 10.  205.  07.  210.  05.  210.
213800
213821                       08.  205.  09.  205.  08.  205.  08.  205.  10.  205.
213842 08.  205.  07.  205.  05.  210.
214100
214121                       08.  205.  10.  205.  08.  205.  08.  205.  10.  205.
214142 08.  205.  07.  205.  05.  210.
214400
214421                       06.  206.  08.  200.  10.  195.  10.  195.  10.  205.
214442 10.  205.  07.  205.  05.  205.
214700
214721                       06.  200.  08.  200.  10.  195.  10.  195.  10.  205.
214742 10.  205.  07.  205.
215000
215021                                  08.  200.  10.  195.  11.  195.  11.  205.
215042 08.  205.
```

```
300000 08. 030.   09. 030.   10. 030.   10. 030.   10. 030.   10. 030.   10. 030.
300021 10. 030.   10. 035.   10. 035.   09. 035.   08. 035.   08. 040.   08. 040.
300042 08. 040.   09. 040.
300300 08. 030.   08. 030.   09. 030.   10. 030.   10. 030.   10. 030.   10. 030.
300321 10. 030.   10. 035.   10. 035.   09. 035.   08. 040.   08. 040.   08. 040.
300342 08. 040.   08. 040.
300600 08. 030.   08. 030.   08. 030.   09. 030.   10. 030.   10. 030.   10. 030.
300621 10. 030.   10. 035.   10. 035.   09. 035.   08. 040.   08. 040.   08. 040.
300642 08. 040.
300900 08. 030.   08. 035.   08. 035.   09. 035.   10. 035.   10. 035.   10. 035.
300921 10. 035.   10. 035.   09. 035.   08. 035.   08. 035.   08. 035.
300942
301200            08. 035.   08. 035.   09. 035.   10. 035.   10. 035.   10. 035.
301221 10. 035.   08. 035.   08. 035.   08. 035.   08. 035.   08. 035.
301242
301500            08. 030.   08. 030.   08. 030.   09. 030.   10. 030.   10. 030.
301521 10. 030.   09. 030.   08. 030.   08. 030.   08. 030.
301542
301800                       08. 030.   08. 030.   08. 030.   10. 030.   10. 030.
301821 10. 030.   09. 030.   08. 030.
301842
302100                       07. 030.   07. 030.   08. 030.   10. 030.   10. 030.
302121 10. 030.   10. 030.   08. 030.   08. 030.
302142
302400                                  07. 025.   07. 025.   08. 025.   10. 025.
302421 10. 030.   10. 035.   08. 040.   08. 045.
302442
302700                                             07. 020.   08. 020.   10. 025.
302721 10. 035.   10. 040.   09. 040.   08. 045.   08. 045.
302742
303000                                                        08. 020.   10. 020.
303021 10. 025.   10. 035.   10. 040.   09. 045.   08. 045.   08. 045.
303042
303300                                                        06. 020.   08. 020.
303321 10. 030.   10. 040.   10. 040.   10. 040.   09. 040.   08. 045.
303342
303600                                                        06. 020.   06. 020.
303621 08. 035.   10. 035.   10. 040.   10. 040.   10. 045.   08. 045.
303642
303900                                                                   06. 020.
303921 06. 020.   08. 030.   10. 035.   10. 035.   10. 040.   09. 050.   08. 050.
303942 05. 045.
304200
304221 05. 035.   06. 030.   08. 030.   10. 030.   10. 035.   10. 045.   08. 045.
304242 05. 045.
304500
304521            05. 025.   05. 025.   09. 025.   10. 030.   10. 035.   08. 045.
304542 05. 065.
304800
304821                       08. 020.   09. 025.   10. 030.   10. 035.   09. 040.
304842 08. 045.
305100
305121                       08. 015.   09. 025.   10. 035.   10. 040.   09. 040.
305142 05. 045.   05. 045.
305400
305421            05. 025.   05. 015.   09. 020.   09. 025.   10. 040.   10. 040.
305442 05. 045.   05. 045.
305700
305721            05. 030.   05. 030.   08. 020.   09. 020.   10. 040.   10. 040.
305742 08. 045.   08. 045.   05. 045.
306000
306021            05. 030.   08. 030.   09. 025.   09. 020.   10. 030.   10. 040.
306042 09. 045.   08. 045.   05. 045.
306300
306321            05. 030.   05. 030.   08. 030.   10. 025.   10. 025.   10. 035.
306342 10. 045.   10. 045.   05. 055.
306600
306621                                  08. 030.   09. 030.   10. 025.   10. 025.
306642 10. 045.   10. 045.   09. 040.   08. 065.   08. 070.   08. 075.   08. 080.
306900
306921                                  08. 030.   09. 030.   10. 020.   10. 025.
306942 10. 035.   10. 045.   09. 045.   08. 045.   08. 055.   08. 070.   08. 000.
307200                                             15. 050.   10. 040.   08. 030.
307221                                  05. 020.   05. 010.   10. 015.   10. 025.
307242 10. 030.   10. 040.   10. 045.   08. 045.   08. 050.   08. 060.   08. 070.
```

```
307500                                          15. 055.  15. 060.  05. 060.
307521 05. 060.  05. 050.  05. 030.  05. 000.  08. 345.  10. 000.  10. 025.
307542 10. 030.  10. 035.  10. 040.  10. 045.  08. 050.  10. 055.  10. 055.
307800                                          15. 065.  15. 065.  12. 065.
307821 10. 065.  05. 045.  05. 025.  05. 340.  08. 350.  10. 000.  10. 015.
307842 10. 020.  10. 030.  10. 040.  10. 050.  10. 050.  10. 050.  10. 055.
308100                                          15. 065.  15. 065.  15. 065.
308121 12. 060.  10. 050.  05. 025.  09. 000.  10. 350.  10. 005.  10. 015.
308142 10. 025.  10. 030.  10. 030.  10. 040.  10. 045.  10. 050.  10. 055.
308400                                          15. 065.  15. 065.  14. 060.
308421 13. 055.  12. 050.  10. 040.  09. 000.  10. 005.  10. 010.  10. 015.
308442 10. 025.  10. 030.  10. 030.  10. 040.  10. 045.  10. 050.  10. 055.
308700                                          15. 070.  15. 065.  14. 055.
308721 14. 050.  13. 040.  13. 035.  09. 010.  10. 015.  10. 010.  10. 010.
308742 10. 025.  10. 030.  10. 045.  10. 050.  10. 050.  10. 055.  10. 055.
309000                                          10. 085.  10. 055.  13. 045.
309021 13. 035.  13. 040.  13. 035.  10. 025.  10. 020.  10. 015.  10. 010.
309042 10. 015.  10. 025.  10. 050.  10. 055.  11. 060.  10. 060.  10. 055.
309300                                                    10. 040.  10. 035.
309321 12. 020.  09. 025.  12. 025.  12. 015.  10. 015.  10. 010.  10. 005.
309342 10. 010.  10. 020.  10. 035.  11. 060.  12. 060.  12. 060.  11. 060.
309600                                                    10. 040.  10. 030.
309621 11. 015.  10. 020.  10. 015.  10. 010.  10. 010.  10. 015.  10. 015.
309642 10. 010.  10. 015.  08. 025.  07. 070.  07. 070.  11. 060.  12. 060.
309900                                                    10. 035.  10. 025.
309921 10. 015.  10. 015.  10. 010.  10. 010.  10. 005.  10. 005.  10. 010.
309942 10. 010.  10. 015.  08. 015.  08. 025.  07. 050.  06. 060.  05. 060.
310200                                                              05. 025.
310221 08. 015.  08. 015.  10. 010.  10. 010.  10. 005.  10. 005.  10. 010.
310242 10. 010.  10. 015.  08. 015.  08. 030.            05. 060.  05. 060.
310500
310521           05. 005.  08. 000.  10. 000.  10. 000.  10. 005.  10. 005.
310542 10. 010.  10. 015.  09. 030.  08. 035.  05. 035.
310800
310821           05. 000.  08. 355.  10. 000.  10. 000.  10. 000.  10. 000.
310842 10. 000.  10. 010.  10. 015.  07. 045.  06. 045.  05. 040.
311100
311121           05. 000.  08. 355.  10. 355.  10. 355.  10. 350.  10. 350.
311142 10. 355.  10. 355.  09. 000.  08. 035.  07. 035.  07. 025.
311400
311421           05. 000.  08. 355.  08. 355.  10. 355.  10. 350.  10. 350.
311442 10. 350.  10. 355.  08. 350.  07. 040.  07. 040.  05. 040.
311700
311721                     05. 355.  08. 350.  10. 350.  10. 350.  10. 350.
311742 10. 350.  08. 000.
312000
312021                     05. 350.  08. 350.  10. 350.  10. 350.  10. 350.
312042 10. 350.  08. 000.
312300
312321           05. 350.  08. 350.  08. 350.  10. 350.  10. 350.  10. 345.
312342 10. 345.  08. 350.
312600
312621           05. 350.  08. 355.  08. 355.  10. 345.  10. 345.  10. 345.
312642 10. 345.  08. 350.
312900
312921           05. 350.  08. 355.  08. 355.  10. 340.  10. 340.  10. 345.
312942 10. 345.  08. 345.  05. 345.
313200
313221                     05. 355.  10. 350.  10. 340.  10. 340.  10. 340.
313242 10. 345.  08. 345.  05. 345.
313500
313521                     05. 350.  08. 345.  10. 340.  10. 340.  10. 340.
313542 10. 345.  08. 350.  05. 350.
313800
313821                     05. 345.  08. 340.  10. 340.  10. 340.  10. 345.
313842 10. 350.  08. 350.  05. 350.
314100
314121                     05. 345.  08. 340.  08. 345.  10. 345.  10. 345.
314142 10. 350.  08. 350.  05. 350.
314400
314421                     05. 350.  08. 350.  10. 350.  10. 345.  10. 345.
314442 10. 345.  08. 345.  05. 345.
314700
314721                     05. 350   08. 350.  10. 355.  10. 345.  10. 345.
314742 08. 345.  05. 345.
315000
315021                               08. 355.  10. 355.  10. 345.  10. 345.
315042 08. 345.
```

```
400000 05.   340.  07    340   08.   340   09    340   09.   340.  10.   340.  10.   335.
400021 10.   335   10.   330.  10.   330.  10.   330.  10.   325.  10.   325.  10.   325.
400042 08.   325.  08.   325
400300 05.   340.  07.   340.  08    340.  09.   340.  09.   345.  09.   345.  10.   345.
400321 10.   345.  10.   330.  10    335.  10.   325.  10.   320.  08.   320.  08.   320
400342 08.   320.  08.   320.
400600 05.   340.  07    340.  08.   340.  08.   345.  09.   350.  09.   355.  09.   350.
400621 10.   345.  10.   335.  10.   335.  10.   325.  08    320.  08.   320.  08.   320.
400642 08.   320.
400900 05.   340.  07.   345.  08.   345.  08.   350.  09.   350.  09.   350.  09.   350.
400921 10.   350.  10.   345.  10.   340.  10.   335.  07.   335.  07.   335.
400942
401200             05.   345.  08.   350.  08.   350.  08.   350.  09.   355.  09.   350.
401221 10.   355.  09.   350.  08.   345.  08.   345.  07.   345.  07.   345.
401242
401500             05.   350   05.   350.  08.   350.  08.   350.  09.   350.  09.   350.
401521 10.   355.  08.   350.  07    345.  07.   345.  07    345.
401542
401801                         05.   350.  08.   355.  08.   355.  09.   355.  09.   355.
401821 10.   355.  08.   355.  07.   350.
401842
402101                         05.   350.  07    350.  08.   355.  09.   000.  09.   000.
402121 10.   000.  08.   355.  07.   350.  05.   350.
402142
402400                                     05.   350.  07.   355.  08.   000.  09.   000.
402421 10.   000.  08.   000.  08    355.  07.   350.
402442
402700                                                 08.   000.  08.   000   09.   000.
402721 10.   000.  08.   355.  08.   355.  07.   355.  05.   355.
402742
403000                                                             08.   000.  09.   000.
403021 09.   355.  08.   355.  08.   355.  07.   355   07.   350.  05.   340.
403042
403300                                                             08.   000.  09.   355.
403321 09.   355.  06.   355.  08.   355.  08.   350.  08.   350.  05.   340.
403342
403600                                                             05.   000.  09.   350.
403621 08.   350.  08.   350.  08.   350.  08.   350.  07.   345.  06.   340
403642
403900                                                                         05.   355.
403921 05.   350.  08.   350.  08.   345.  08.   345.  08.   350.  07.   345.  05.   340.
403942 05.   330.
404200
404221 05.   350.  08.   350.  08.   345.  08.   350.  08.   350.  07.   345.  07.   335.
404242 05.   330.
404500
404521             05.   350.  08.   355.  08.   350.  08.   350.  08.   345.  07.   335.
404542 05.   335.
404800
404821                         10.   000.  09.   355.  08.   345.  08.   345.  07.   345.
404842 05.   350.
405100
405121                         10.   000.  09.   355.  09.   350.  09.   355.  08.   355.
405142 07.   350.  05.   345.
405400
405421             05.   000   10.   000.  10.   350.  10.   355.  10.   000.  09.   000.
405442 07.   355.  05.   350.
405700
405721             05.   000.  10.   355.  10.   350   10.   000.  10.   000.  10.   000.
405742 07.   000.  05.   355.  05.   350.
406000
406021             05.   000.  10.   355.  10.   355.  10    000.  10.   000.  10.   000.
406042 10.   000.  05.   355.  05.   350.
406300
406321             05.   000.  10.   355.  10.   000.  10.   000.  10.   000.  10.   000.
406342 10.   005.  07.   000.  05.   350.
406600
406621                                     08.   000.  10.   000.  10.   000.  10.   000.
406642 10.   010.  10.   000.  08.   350.  05.   325.  05.   325.  05.   320.  05.   320.
406900
406921                                     08.   000.  10.   000.  10.   000.  10.   350.
406942 10.   350.  10.   350.  08.   340.  08.   340.  08.   325.  10.   320.  10.   320.
407200                                                 10.   230.  08.   220.  05.   220.
407221                                     05.   000.  08.   355.  10.   350.  10.   345.
407242 10.   345.  10.   350.  10.   340   10.   340.  10.   330.  10.   320.  10.   320.
```

407500									15.	245.	10.	245.	08.	250.
407521	05.	250.	05.	270.	05.	290.	05.	320.	08.	340.	10.	335.	10.	330.
407542	10.	340.	10.	330.	10.	315.	10.	320.	10.	320.	10.	320.	10.	320.
407800									15.	250.	15.	250.	15.	250.
407821	08.	265.	08.	280.	10.	285.	08.	300.	10.	325.	10.	330.	10.	325.
407842	10.	315.	10.	315.	10.	315.	10.	320.	10.	320.	10.	320.	10.	320.
408100									15.	250.	15.	250.	15.	250.
408121	15.	260.	14.	270.	13.	285.	11.	295.	10.	305.	10.	315.	10.	315.
408142	10.	310.	10.	310.	10.	310.	10.	310.	10.	315.	10.	320.	10.	320.
408400									15.	250.	15.	250.	15.	255.
408421	15.	265.	14.	270.	13.	285.	11.	270.	10.	300.	10.	305.	10.	305.
408442	10.	310.	10.	310.	09.	315.	08.	325.	08.	330.	10.	320.	10.	310.
408700									15.	250.	15.	260.	15.	265.
408721	12.	270.	12.	270.	12.	280.	12.	285.	10.	300.	10.	305.	10.	310.
408742	10.	315.	09.	315.	08.	325.	08.	320.	08.	310.	10.	300.	10.	275.
409000									10.	250.	10.	255.	08.	255.
409021	08.	260.	08.	270.	10.	280.	10.	305.	10.	305.	10.	315.	10.	325.
409042	10.	330.	10.	330.	10.	315.	10.	305.	10.	295.	10.	270.	10.	290.
409300											05.	255.	05.	255.
409321	08.	255.	08.	300.	09.	310.	10.	320.	10.	335.	10.	340.	10.	330.
409342	10.	330.	10.	335.	11.	320.	11.	320.	11.	295.	11.	280.	11.	280.
409600											05.	270.	05.	275.
409621	05.	285.	08.	310.	10.	335.	10.	335.	10.	335.	10.	330.	10.	330.
409642	10.	345.	12.	345.	12.	345.	12.	330.	12.	280.	12.	270.	12.	270.
409900											05.	275.	05.	305.
409921	05.	310.	07.	325.	08.	345.	10.	345.	10.	340.	10.	340.	10.	345.
409942	10.	350.	12.	350.	13.	355.	08.	320.	06.	295.	06.	270.	06.	270.
410200													05.	310.
410221	06.	320.	08.	335.	10.	340.	10.	345.	10.	340.	10.	340.	10.	345.
410242	10.	350.	11.	350.	08.	000.	05.	000.			05.	240.	05.	240.
410500														
410521			08.	335.	09.	335.	10.	335.	10.	335.	10.	340	10.	350.
410542	10.	350.	10.	355.	08.	030.	06.	045.	05.	045.				
410800														
410821			05.	330.	08.	330.	10.	335.	10.	335.	10.	340.	10.	350.
410842	10.	000.	10.	005.	08.	030.	06.	045.	05.	045.	05.	045.		
411100														
411121			05.	330.	08.	335.	10.	340.	10.	340.	10.	345.	10.	355.
411142	10.	000.	10.	005.	07.	025.	07.	040.	06.	035.	05.	035.		
411400														
411421			08.	330.	08.	340.	08.	345.	10.	350.	10.	000.	10.	000.
411442	10.	005.	08.	000.	07.	030.	07.	075.	07.	040.	05.	040.		
411700														
411721					06.	355.	08.	355.	10.	350.	10.	000.	10.	000.
411742	10.	005.	08.	000.										
412000														
412021					05.	000.	08.	355.	10.	345.	10.	000.	10.	005.
412042	10.	005.	08.	000.										
412300														
412321			05.	355.	08.	355.	10.	350.	10.	350.	10.	000.	10.	005.
412342	10.	005.	08.	000.										
412600														
412621			05.	355.	08.	355.	10.	350.	10.	355.	10.	000.	10.	005.
412642	10.	010.	08.	010.										
412900														
412921			05.	355.	08.	355.	10.	355.	10.	000.	10.	000.	10.	005.
412942	10.	010.	08.	010.	06.	010.								
413200														
413221					06.	355.	08.	350.	08.	000.	10.	005.	10.	010.
413242	10.	010.	08.	010.	06.	010.								
413500														
413521					06.	355.	08.	350.	08.	000.	08.	005.	10.	010.
413542	10.	010.	08.	010.	06.	010.								
413800														
413821					08.	355.	08.	355.	08.	005.	08.	010.	10.	010.
413842	10.	010.	08.	010.	06.	010.								
414100														
414121					06.	000.	08.	000.	08.	005.	08.	005.	10.	010.
414142	10.	010.	08.	010.	06.	010.								
414400														
414421					06.	000.	08.	000.	08.	000.	10.	000.	10.	005.
414442	10.	005.	08.	005.	06.	010.								
414700														
414721					06.	000.	08.	000.	08.	000.	10.	000.	10.	000.
414742	08.	000.	06.	005.										
415000														
415021							08.	000.	08.	000.	10.	000.	10.	000.
415042	08.	000.												

500000	07.	050.	08.	050.	09.	050.	07.	045.	10.	045.	10.	045.	10.	045.
500021	10.	045.	10.	045.	10	045.	08.	045.	08.	045.	08.	045.	08.	045.
500042	08.	045.	08.	045.										
500300	07.	045.	08.	045.	09.	045.	09.	045.	09.	045.	09.	045.	09.	045.
500321	09.	045.	09.	045.	08.	045.	08.	045.	08.	045.	08.	045.	08.	045.
500342	08.	045.	07.	045.										
500600	07.	045.	07.	045.	08.	045.	09	045.	09.	045.	09.	045.	09.	045.
500621	09.	045.	09.	045.	09.	045.	08.	045.	08.	045.	07.	045.	07.	045.
500642	07.	045.												
500900	07.	045.	07.	045.	07.	045.	08.	045.	09.	045.	09.	045.	09.	045.
500921	08.	040.	08.	040.	07.	040.	07.	040.	07.	040.	07.	040.		
500942														
501200			07.	045.	07.	045.	08.	045.	09.	045.	08.	040.	08.	040.
501221	08.	040.	08.	040.	07.	035.	07.	035.	07.	035.	07.	035.		
501242														
501500			07.	045.	07.	045.	07	045.	08.	040.	08.	040.	08.	040.
501521	07.	040.	07.	035.	07.	035.	07.	035.	07.	035.				
501542														
501800					07.	045.	07.	045.	07.	040.	08.	040.	08.	040.
501821	07.	040.	07.	035.	07.	035.								
501842														
502100			0.	0.	07.	040.	07.	040.	07.	040.	07.	040.	07.	040.
502121	07.	040.	07.	040.	07.	040.	07.	040.						
502142														
502400							07.	040.	07.	040.	07.	045.	08.	045.
502421	08.	045.	07.	045.	07.	035.	07.	025.						
502442														
502700									07.	045.	08.	045.	08.	045.
502721	08.	045.	08.	045.	07.	040.	07.	025.	07.	035.				
502742														
503000									07.	055.	07.	050.	07.	045.
503021	08.	045.	08.	045.	08.	045.	07.	040.	07.	050.	07.	060.		
503042														
503300											07.	060.	07.	055.
503321	08.	050.	08.	045.	08.	045.	08.	050.	08.	055.	05.	065.		
503342														
503600											07.	060.	05.	060.
503621	07.	050.	09.	045.	08.	045.	08.	050.	08.	050.	07.	055.		
503642														
503900													05.	060.
503921	06.	050.	07.	050.	09.	045.	10.	045.	08.	045.	07.	055.	06.	055.
503942	05.	055.												
504200														
504221	05.	050.	08.	045.	09.	040.	10.	045.	10	045.	08.	045.	07.	060.
504242	05.	065.												
504500														
504521			05.	030.	07.	030.	09.	040.	10.	040.	09.	040.	08.	050.
504542	07.	060.												
504800														
504821					07.	030.	09.	040.	09.	040.	09.	040.	07	050.
504842	07.	055.												
505100														
505121					04.	030.	08.	025.	09.	040.	09.	045.	08.	050.
505142	07.	050.	05.	050.										
505400														
505421			04.	015.	05.	010.	08.	025.	09.	035.	09.	045.	08.	050.
505442	07.	055.	05.	055.										
505700														
505721			04.	010.	06.	010.	06.	020.	08.	035.	09.	040.	09.	045.
505742	07.	050.	05.	050.	05.	050.								
506000														
506021			05.	010.	07.	010.	07.	020.	08.	030.	09.	035.	09.	045.
506042	07.	050.	07.	050.	05	050.								
506300														
506321			04.	010.	06.	010.	07.	015.	08.	025.	08.	030.	09.	035.
506342	08.	045.	07.	050.	05.	050.								
506600														
506621							07.	015.	08.	020.	08.	025.	09.	030.
506642	09.	035.	08.	045.	08.	050.	05.	055.	05.	060.	05.	060.	05.	065.
506900														
506921							07.	010.	08.	010.	08.	020.	09.	035.
506942	10.	040.	08.	045.	07.	045.	05.	060.	06.	065.	07.	070.	07.	075.
507200									05.	075.	05.	075.	05.	075.
507221							05.	020.	08.	015.	08.	025.	09.	035.
507242	10.	045.	09.	050.	08.	055.	07.	066.	08.	070.	10.	075.	10.	080.

BEST DOCUMENT AVAILABLE

```
507500                                             10.  075.  10.  075.  10.  075.
507521 10.  075.  05.  075.  05.  075.  05.  050.  05.  035.  09.  045.  10.  045.
507542 11.  050.  11.  055.  11.  060.  10.  065.  10.  075.  12.  080.  12.  085.
507800                                             12.  080.  12.  080.  10.  075.
507821 10.  075.  05.  075.  05.  075.  05.  075.  05.  070.  08.  055.  10.  065.
507842 12.  075.  12.  080.  12.  080.  14.  080.  14.  080.  14.  080.  14.  085.
508100                                             12.  080.  12.  080.  11.  080.
508121 11.  080.  11.  080.  10.  080.  10.  080.  10.  075.  11.  080.  13.  080.
508142 13.  080.  15.  080.  15.  080.  15.  080.  15.  080.  15.  085.  15.  085.
508400                                             12.  085.  12.  085.  11.  085.
508421 11.  080.  11.  080.  11.  085.  11.  085.  11.  085.  11.  085.  12.  085.
508442 13.  085.  14.  085.  10.  090.  10.  090.  10.  090.  12.  090.  15.  090.
508700                                             12.  090.  12.  090.  12.  090.
508721 11.  085.  11.  085.  11.  090.  11.  090.  11.  095.  11.  095.  12.  090.
508742 13.  090.  14.  090.  14.  090.  14.  090.  15.  090.  15.  090.  15.  090.
509000                                             10.  090.  08.  090.  07.  100.
509021 05.  100.  05.  110.  07.  105.  10.  105.  11.  105.  11.  105.  11.  100.
509042 12.  100.  13.  095.  14.  095.  14.  095.  15.  095.  15.  095.  15.  095.
509300                                                        05.  115.  05.  115.
509321 05.  125.  06.  120.  07.  120.  08.  110.  09.  110.  10.  105.  10.  105.
509342 11.  105.  11.  100.  11.  100.  12.  095.  12.  095.  12.  095.  12.  090.
509600                                                        05.  120.  05.  140.
509621 05.  135.  07.  135.  08.  130.  09.  130.  09.  125.  10.  120.  10.  115.
509642 10.  110.  11.  125.  10.  135.  08.  115.  09.  100.  10.  075.  10.  075.
509900                                                        05.  140.  05.  165.
509921 05.  215.  07.  200.  08.  165.  09.  145.  09.  135.  09.  130.  09.  130.
509942 10.  140.  10.  135.  10.  135.  08.  125.  06.  090.  05.  075.  05.  075.
510200                                                                   05.  200.
510221 05.  235.  05.  235.  07.  215.  08.  150.  09.  145.  09.  145.  09.  140.
510242 10.  135.  10.  145.  08.  170.  05.  160.             05.  075.  05.  075.
510500
510521            04.  210.  06.  195.  08.  170.  08.  160.  08.  160.  08.  160.
510542 09.  160.  09.  175.  06.  200.  06.  220.  05.  220.
510800
510821            04.  190.  07.  190.  07.  190.  08.  165.  08.  160.  08.  160.
510842 08.  165.  08.  180.  07.  195.  06.  215.  05.  230.  05.  240.
511100
511121            04.  200.  06.  200.  07.  190.  08.  165.  08.  165.  08.  165.
511142 08.  170.  07.  175.  06.  170.  04.  210.  05.  220.  05.  230.
511400
511421            04.  215.  06.  195.  07.  190.  08.  170.  08.  165.  08.  165.
511442 08.  165.  07.  165.  06.  170.  04.  235.  04.  240.  05.  210.
511700
511721                       05.  185.  07.  180.  08.  170.  08.  165.  08.  165.
511742 08.  165.  06.  165.
512000
512021                       05.  180.  07.  180.  08.  165.  08.  165.  08.  165.
512042 08.  165.  06.  165.
512300
512321            04.  180.  05.  180.  07.  170.  08.  170.  08.  170.  08.  165.
512342 08.  165.  08.  165.
512600
512621            04.  180.  05.  180.  07.  175.  08.  175.  08.  175.  08.  175.
512642 08.  165.  07.  165.
512900
512921            04.  180.  05.  180.  07.  175.  08.  175.  08.  175.  08.  170.
512942 08.  165.  07.  165.  05.  175.
513200
513221                       05.  175.  07.  175.  07.  175.  08.  175.  08.  165.
513242 08.  165.  07.  170.  05.  175.
513500
513521                       07.  175.  07.  170.  07.  165.  07.  165.  08.  165.
513542 08.  170.  07.  170.  05.  175.
513800
513821                       07.  175.  07.  170.  07.  165.  07.  165.  08.  165.
513842 08.  165.  07.  165.  05.  165.
514100
514121                       07.  170.  07.  165.  07.  165.  08.  165.  08.  165.
514142 08.  165.  07.  165.  05.  165.
514400
514421                       07.  165.  07.  165.  08.  165.  08.  165.  08.  165.
514442 07.  165.  07.  165.  05.  165.
514700
514721                       07.  165.  07.  165.  08.  165.  08.  165.  08.  165.
514742 07.  165.  05.  165.
515000
515021                                  07   165.  07.  165.  08.  165.  08.  165.
515042 08.  165.
```

BEST DOCUMENT AVAILABLE

APPENDIX C

NET CURRENT FIELDS INPUT DATA FILE

Input Data File Format: Net Currents

Grid Coordinates		Net Current Parameters for (y,x)			Net Current Parameters for (y, x+2)			Net Current Parameters for (y, x+4)			Net Current Parameters for (y, x+6)			Net Current Parameters for (y, x+8)		
y	X	V_{win}	V_{sum}	θ	V_{win}	V_{sum}	θ	V_{win}	V_{sum}	θ	V_{win}	V_{sum}	θ	V_{win}	V_{sum}	θ
XXX	XX	X.XX	X.XX	XXX.	X.XX	X.XX	XXX.	X.XX	X.XX	XXX.	X.XX	X.XX	XXX.	X.XX	X.XX	XXX.

(y,X) - GRID CELL LOCATION FOR NET CURRENT DATA

V_{win} - NET CURRENT VELOCITY FOR WINTER SEASON IN METERS/SEC

V_{sum} - NET CURRENT VELOCITY FOR SUMMER SEASON IN METERS/SEC

θ - DIRECTION OF NET CURRENT (IN DEGREES, CLOCKWISE FROM NORTH)

BEST DOCUMENT AVAILABLE

```
00002 0.00 0.00 010  0.03 0.02 010  0.05 0.03 010  0.01 0.01 140  0.10 0.05 180
00012 0.10 0.05 180  0.12 0.06 175. 0.15 0.10 170  0.15 0.10 170  0.15 0.10 165
00022 0.15 0.10 165  0.14 0.07 160  0.10 0.05 155. 0.10 0.05 155  0.05 0.02 150
00032 0.02 0.01 140  0.01 0.01 140  0.02 0.01 325  0.02 0.01 325  0.01 0.01 315
00042 0.01 0.01 310  0.01 0.01 310  0.00 0.00 310.
00052
00102 0.00 0.00 010  0.03 0.02 010  0.05 0.03 010  0.01 0.01 140  0.10 0.05 180.
00112 0.10 0.05 180  0.12 0.06 175. 0.15 0.10 170. 0.15 0.10 170  0.15 0.10 165
00122 0.15 0.10 165  0.14 0.07 160  0.10 0.05 155. 0.10 0.05 155. 0.05 0.02 150.
00132 0.02 0.01 140  0.01 0.01 140. 0.02 0.01 325. 0.02 0.01 325  0.01 0.01 315
00142 0.01 0.01 310  0.01 0.01 310. 0.00 0.00 310
00152
00302 0.00 0.00 010. 0.03 0.02 010. 0.05 0.03 015  0.01 0.01 140  0.10 0.05 100.
00312 0.10 0.05 180. 0.12 0.06 175. 0.15 0.10 170  0.15 0.10 170  0.15 0.10 165.
00322 0.15 0.10 165. 0.13 0.06 160. 0.10 0.05 155. 0.08 0.04 150  0.05 0.02 145
00332 0.03 0.01 140. 0.02 0.01 320  0.02 0.01 320. 0.01 0.01 315  0.01 0.01 310.
00342 0.00 0.00 310  0.00 0.00 310.
00352
00502 0.00 0.00 010. 0.03 0.02 010. 0.05 0.03 015. 0.01 0.01 135  0.10 0.05 180
00512 0.10 0.05 180. 0.12 0.06 175. 0.15 0.10 170. 0.15 0.10 170. 0.15 0.10 165.
00522 0.15 0.10 165. 0.12 0.06 160. 0.10 0.05 155. 0.06 0.03 150  0.04 0.02 140.
00532 0.03 0.01 325. 0.03 0.01 325  0.01 0.01 315. 0.01 0.01 290  0.00 0.00 290.
00542
00552
00702 0.00 0.00 025. 0.02 0.01 030  0.05 0.03 030. 0.01 0.01 070  0.10 0.05 180.
00712 0.10 0.05 180  0.12 0.06 180  0.15 0.10 180  0.15 0.10 175  0.15 0.10 170.
00722 0.13 0.07 165. 0.11 0.05 160  0.05 0.04 160  0.05 0.02 155  0.01 0.01 325.
00732 0.04 0.02 325  0.02 0.01 325. 0.00 0.00 335  0.00 0.00 290.
00742
00752
00902 0.00 0.00 090  0.00 0.00 050. 0.03 0.01 035. 0.05 0.02 035  0.08 0.04 190.
00912 0.10 0.05 190  0.12 0.06 185  0.15 0.10 180  0.15 0.10 180  0.15 0.10 175.
00922 0.12 0.06 170  0.10 0.05 165. 0.05 0.02 155  0.01 0.01 330. 0.05 0.02 325.
00932 0.02 0.01 320  0.00 0.00 320.
00942
00952
01102                0.00 0.00 320  0.02 0.01 025  0.04 0.02 035  0.08 0.04 190.
01112 0.10 0.05 190  0.12 0.06 185. 0.14 0.10 180  0.15 0.10 180  0.16 0.11 180
01122 0.12 0.06 175  0.10 0.05 170  0.05 0.02 165  0.05 0.02 310  0.02 0.01 300
01132 0.01 0.01 300  0.00 0.00 300
01142
01152
01302                0.00 0.00 060  0.01 0.01 060  0.02 0.01 075  0.04 0.02 140
01312 0.10 0.05 195  0.13 0.07 190  0.15 0.10 185. 0.16 0.11 185  0.16 0.11 180.
01322 0.10 0.05 175  0.05 0.02 170  0.01 0.01 295  0.00 0.00 275  0.00 0.00 280.
01332 0.00 0.00 280
01342
01352
01502                               0.00 0.00 110  0.00 0.00 210  0.03 0.01 200
01512 0.10 0.05 195  0.13 0.07 195  0.14 0.10 190  0.17 0.11 185  0.14 0.10 185
01522 0.10 0.05 180  0.04 0.02 170  0.01 0.01 165  0.00 0.00 160
01532
01542
01552
01702                                              0.00 0.00 175. 0.02 0.01 200.
01712 0.08 0.04 195. 0.12 0.06 195. 0.16 0.11 195. 0.18 0.12 190. 0.13 0.07 190.
01722 0.10 0.05 185. 0.05 0.02 180. 0.01 0.01 180. 0.00 0.00 180.
01732
01742
01752
01902                                              0.00 0.00 220. 0.01 0.01 215.
01912 0.05 0.02 205. 0.10 0.05 200. 0.15 0.10 200. 0.18 0.12 200. 0.15 0.10 195.
01922 0.10 0.05 190. 0.05 0.02 190. 0.01 0.01 180. 0.00 0.00 180.
01932
01942
01952
02102                                              0.00 0.00 220. 0.01 0.01 215.
02112 0.02 0.01 210. 0.10 0.05 205. 0.12 0.06 205. 0.19 0.13 200. 0.18 0.12 200.
02122 0.12 0.06 200. 0.08 0.04 195. 0.01 0.01 190. 0.00 0.00 190.
02132
```

```
02142
02152
02302                                                                  0.00 0.00 270.
02312 0.00 0.00 270.  0.03 0.01 205.  0.10 0.05 205.  0.15 0.10 205.  0.20 0.15 205.
02322 0.15 0.10 205.  0.10 0.05 205.  0.02 0.01 205.  0.00 0.00 205.
02332
02342
02352
02502
02512 0.00 0.00 120.  0.02 0.01 205.  0.10 0.05 205.  0.13 0.07 205.  0.20 0.15 210.
02522 0.15 0.10 210.  0.12 0.06 210.  0.08 0.04 205.  0.02 0.01 205.  0.00 0.00 205.
02532
02542
02552
02702
02712 0.00 0.00 215.  0.01 0.01 210   0.08 0.04 210.  0.11 0.05 210.  0.15 0.10 210.
02722 0.21 0.15 210.  0.15 0.10 210.  0.10 0.05 210.  0.02 0.01 210.  0.00 0.00 205.
02732
02742
02752
02902
02912                 0.00 0.00 225.  0.02 0.01 215.  0.09 0.05 215.  0.13 0.06 215.
02922 0.20 0.15 215.  0.22 0.16 215.  0.15 0.10 210.  0.12 0.06 210.  0.02 0.01 210.
02932 0.00 0.00 205.
02942
02952
03102
03112                 0.00 0.00 140.  0.01 0.01 180.  0.05 0.02 215.  0.10 0.05 215.
03122 0.15 0.10 215.  0.23 0.17 210.  0.20 0.15 210.  0.15 0.10 210.  0.04 0.02 210.
03132 0.02 0.01 065.  0.01 0.01 050.  0.00 0.00 000.
03142
03152
03302
03312                 0.00 0.00 180.  0.01 0.01 190.  0.02 0.01 210.  0.05 0.02 215.
03322 0.11 0.06 215.  0.20 0.15 215.  0.24 0.17 215.  0.18 0.12 215.  0.15 0.10 215.
03332 0.02 0.01 210.  0.02 0.01 045.  0.00 0.00 000.
03342
03352
03502
03512                                 0.00 0.00 230.  0.01 0.01 270.  0.02 0.01 225.
03522 0.08 0.04 220.  0.11 0.06 220.  0.22 0.16 215.  0.25 0.17 215.  0.21 0.15 215.
03532 0.15 0.15 210.  0.02 0.01 000.  0.00 0.00 000.
03542
03552
03702
03712                                                 0.00 0.00 180.  0.01 0.01 225.
03722 0.02 0.01 225.  0.15 0.10 220.  0.20 0.15 215.  0.25 0.17 215.  0.20 0.15 210
03732 0.20 0.15 210.  0.02 0.01 205.  0.00 0.00 180.
03742
03752
03902
03912                                                                 0.00 0.00 270.
03922 0.00 0.00 225.  0.02 0.01 225.  0.18 0.12 215.  0.23 0.16 215.  0.26 0.18 215.
03932 0.23 0.16 210.  0.20 0.15 205.  0.00 0.00 205.
03942
03952
04102
04112
04122 0.00 0.00 215.  0.01 0.01 230.  0.02 0.01 225.  0.21 0.15 210.  0.25 0.17 210.
04132 0.25 0.17 205.  0.21 0.15 205   0.02 0.01 205.  0.00 0.00 270.  0.00 0.00 270.
04142 0.00 0.00 180.
04152
04302
04312
04322                 0.00 0.00 270.  0.00 0.00 210.  0.15 0.08 210.  0.23 0.16 205.
04332 0.27 0.18 205.  0.23 0.16 205.  0.04 0.02 215.  0.01 0.01 195.  0.01 0.01 225.
04342 0.00 0.00 225.
04352
04502
04512
```

```
04522                                 0.00 0.00 180.  0.08 0.04 205.  0.21 0.15 200.
04532 0.27 0.18 200.  0.24 0.17 200.  0.20 0.15 200.  0.10 0.05 200.  0.01 0.01 185.
04542 0.00 0.00 270.
04552
04702
04712
04722                                 0.00 0.00 180.  0.08 0.04 195.  0.20 0.15 200.
04732 0.24 0.17 200.  0.28 0.19 200.  0.23 0.16 205.  0.15 0.10 205.  0.01 0.01 180.
04742 0.00 0.00 270.
04752
04902
04912
04922                                 0.00 0.00 180.  0.05 0.02 195.  0.18 0.12 200.
04932 0.24 0.17 200.  0.30 0.20 200.  0.25 0.18 205.  0.20 0.15 205.  0.01 0.01 190.
04942 0.00 0.00 180.
04952
05102
05112
05122                                 0.00 0.00 180.  0.03 0.02 195.  0.16 0.11 195.
05132 0.22 0.16 195.  0.28 0.19 195.  0.28 0.19 200.  0.20 0.15 200.  0.05 0.02 200.
05142 0.00 0.00 200.
05152
05302
05312
05322                                 0.00 0.00 180.  0.04 0.02 190.  0.10 0.05 195.
05332 0.20 0.15 195.  0.26 0.18 195.  0.30 0.20 200.  0.24 0.17 200   0.16 0.11 200.
05342 0.01 0.01 200.  0.00 0.00 200.
05352
05502
05512
05522                                 0.00 0.00 180.  0.02 0.01 000.  0.05 0.02 195.
05532 0.20 0.15 195.  0.25 0.17 195.  0.34 0.22 195.  0.28 0.19 195.  0.20 0.15 195.
05542 0.02 0.01 195.  0.00 0.00 200.
05552
05702
05712
05722                                 0.00 0.00 015.  0.05 0.02 020.  0.05 0.02 200.
05732 0.18 0.12 195.  0.25 0.17 190.  0.36 0.24 190.  0.32 0.21 190.  0.21 0.15 195.
05742 0.04 0.02 195.  0.00 0.00 195.
05752
05902
05912
05922                                 0.00 0.00 020.  0.03 0.01 020.  0.04 0.02 200
05932 0.10 0.05 195.  0.22 0.16 190.  0.36 0.24 190.  0.35 0.23 190.  0.25 0.17 195.
05942 0.10 0.05 195.  0.00 0.00 195.
05952
06102
06112
06122                                 0.00 0.00 035.  0.02 0.01 035.  0.04 0.02 035.
06132 0.06 0.03 205.  0.22 0.16 190.  0.36 0.24 190.  0.36 0.24 190.  0.30 0.20 190.
06142 0.20 0.15 195.  0.02 0.01 195.  0.00 0.00 180.
06152
06302
06312
06322                                                 0.00 0.00 045.  0.00 0.00 045.
06332 0.05 0.02 200.  0.21 0.15 190.  0.35 0.24 190.  0.38 0.27 185.  0.35 0.24 185.
06342 0.22 0.16 190.  0.10 0.05 190.  0.00 0.00 180.
06352
06502
06512
06522                                                                 0.00 0.00 190.
06532 0.05 0.02 200.  0.24 0.17 200.  0.35 0.24 190.  0.40 0.30 185.  0.35 0.24 185.
06542 0.25 0.17 185   0.14 0.08 185.  0.02 0.01 180   0.00 0.00 160.  0.00 0.00 180.
06552 0.00 0.00 180   0.00 0.00 325.  0.00 0.00 180.  0.00 0.00 180.  0.00 0.00 180.
06702
06712
06722                                                                 0.00 0.00 190.
06732 0.03 0.01 200   0.28 0.19 195.  0.32 0.21 190.  0.40 0.30 180.  0.40 0.30 180.
06742 0.30 0.20 180.  0.20 0.15 180.  0.02 0.01 175.  0.01 0.01 120.  0.00 0.00 090.
06752 0.01 0.01 045.  0.01 0.01 240.  0.00 0.00 270.  0.00 0.00 240.  0.00 0.00 140.
```

```
06902
06912
06922                                                                 0.00 0.00 190.
06932 0.00 0.00 180.  0.25 0.17 195.  0.35 0.24 180.  0.50 0.35 180.  0.50 0.35 180.
06942 0.35 0.23 185.  0.20 0.15 180.  0.05 0.02 180.  0.00 0.00 180.  0.00 0.00 180.
06952 0.00 0.00 180.  0.01 0.01 215.  0.01 0.01 235.  0.01 0.01 255.  0.01 0.01 265.
07102
07112
07122                                                                 0.00 0.00 190.
07132 0.00 0.00 180.  0.25 0.16 180   0.35 0.24 165.  0.55 0.37 165.  0.50 0.35 175.
07142 0.35 0.18 190.  0.20 0.15 200.  0.10 0.05 220.  0.00 0.00 220.  0.00 0.00 180.
07152 0.00 0.00 180.  0.01 0.01 325.  0.02 0.02 280.  0.02 0.02 270.  0.02 0.02 270.
07302
07312
07322                                                                 0.00 0.00 180.
07332 0.00 0.00 195.  0.20 0.10 175.  0.45 0.32 155.  0.60 0.40 155.  0.50 0.35 190.
07342 0.30 0.15 200   0.16 0.08 205.  0.10 0.05 210.  0.01 0.01 225.  0.00 0.00 230.
07352 0.00 0.00 315.  0.01 0.01 315.  0.02 0.02 305.  0.02 0.02 285.  0.02 0.02 275.
07502
07512 0.00 0.00 180.  0.00 0.00 180.  0.00 0.00 180.  0.00 0.00 180.  0.00 0.00 180.
07522 0.00 0.00 180.  0.00 0.00 180.  0.00 0.00 180.  0.00 0.00 180.  0.00 0.00 180.
07532 0.00 0.00 120.  0.20 0.10 145.  0.60 0.40 150.  0.60 0.40 155.  0.50 0.30 200.
07542 0.30 0.15 210.  0.20 0.10 220.  0.15 0.07 220.  0.12 0.06 235.  0.10 0.05 260.
07552 0.05 0.02 270.  0.05 0.02 275.  0.05 0.02 280.  0.05 0.02 280.  0.05 0.02 275.
07702
07712 0.00 0.00 180.  0.00 0.00 120.  0.01 0.02 060.  0.00 0.00 065.  0.00 0.00 055.
07722 0.00 0.00 180.  0.00 0.00 110.  0.00 0.00 090.  0.00 0.00 070.  0.00 0.00 125.
07732 0.20 0.10 125.  0.55 0.35 140.  0.55 0.35 160.  0.50 0.30 180.  0.40 0.20 200
07742 0.30 0.15 225.  0.25 0.12 225.  0.20 0.10 235.  0.20 0.10 260.  0.15 0.07 265
07752 0.15 0.07 265.  0.15 0.07 270.  0.15 0.07 270.  0.15 0.07 270.  0.15 0.02 270.
07902
07912 0.00 0.00 180.  0.00 0.00 220.  0.01 0.02 110.  0.01 0.02 080.  0.01 0.01 085.
07922 0.00 0.00 090   0.01 0.02 095.  0.01 0.02 095.  0.01 0.02 105.  0.02 0.05 120.
07932 0.25 0.25 140.  0.50 0.35 155.  0.55 0.35 180.  0.40 0.25 180.  0.30 0.15 190.
07942 0.30 0.15 235.  0.20 0.10 235.  0.20 0.10 245.  0.20 0.10 250.  0.20 0.10 255.
07952 0.20 0.10 260.  0.20 0.10 265.  0.20 0.10 270.  0.20 0.10 270.  0.20 0.10 270.
08102
08112 0.00 0.00 180.  0.01 0.02 140.  0.01 0.02 145.  0.01 0.02 115.  0.01 0.00 095.
08122 0.02 0.05 095.  0.02 0.05 095.  0.02 0.05 095.  0.05 0.05 120.  0.15 0.15 140.
08132 0.30 0.30 165.  0.50 0.35 180.  0.50 0.25 180.  0.40 0.20 220.  0.20 0.10 240.
08142 0.20 0.10 250.  0.20 0.10 260.  0.20 0.10 260.  0.20 0.10 260.  0.20 0.10 260.
09152 0.20 0.10 265   0.20 0.10 270.  0.20 0.10 270   0.20 0.10 270.  0.20 0.10 270.
08302
08312 0.00 0.00 180.  0.01 0.02 180.  0.01 0.02 180.  0.02 0.05 140.  0.02 0.05 130.
08322 0.02 0.05 110.  0.02 0.05 095.  0.02 0.05 125.  0.10 0.10 140.  0.30 0.30 150.
08332 0.35 0.35 180.  0.50 0.35 195.  0.48 0.22 205.  0.04 0.20 205.  0.10 0.05 225.
08342 0.05 0.02 255.  0.05 0.02 265.  0.05 0.02 265.  0.00 0.00 265.  0.00 0.00 270.
08352 0.10 0.05 270.  0.10 0.05 270.  0.10 0.05 270.  0.10 0.05 270.  0.10 0.05 270.
08502
08512 0.00 0.00 180.  0.00 0.00 205.  0.01 0.02 215.  0.02 0.05 200.  0.02 0.05 195.
08522 0.01 0.02 225.  0.01 0.02 180.  0.01 0.02 120.  0.10 0.10 150.  0.30 0.30 180.
08532 0.35 0.35 220.  0.48 0.35 220.  0.48 0.22 215.  0.40 0.15 230.  0.05 0.02 125.
08542 0.05 0.02 095.  0.05 0.02 080.  0.05 0.02 050.  0.00 0.00 235.  0.00 0.00 250.
08552 0.05 0.03 330.  0.00 0.00 270.  0.10 0.05 270.  0.10 0.05 270.  0.10 0.05 270.
08702
08712 0.00 0.00 180.  0.00 0.00 180.  0.01 0.02 210.  0.02 0.05 225.  0.01 0.02 180.
08722 0.01 0.02 215.  0.01 0.02 230.  0.01 0.02 200.  0.20 0.20 180.  0.35 0.35 195.
08732 0.35 0.35 205.  0.45 0.35 225.  0.50 0.20 235.  0.40 0.15 240.  0.35 0.15 250.
08742 0.30 0.15 255.  0.30 0.15 270.  0.20 0.10 290.  0.10 0.05 290.  0.05 0.02 280.
08752 0.05 0.02 275.  0.05 0.02 270.  0.10 0.05 270.  0.10 0.05 270.  0.10 0.05 270.
08902
08912                 0.00 0.00 180.  0.00 0.00 230.  0.02 0.05 210.  0.01 0.02 180.
08922 0.00 0.00 180   0.00 0.00 180.  0.01 0.02 235.  0.25 0.20 180.  0.30 0.30 210.
08932 0.30 0.30 225.  0.40 0.30 240.  0.50 0.20 240.  0.40 0.15 235.  0.40 0.15 250.
08942 0.40 0.15 260.  0.35 0.17 270.  0.30 0.15 270.  0.30 0.15 270.  0.30 0.15 270.
08952 0.30 0.15 270   0.30 0.15 270.  0.30 0.15 270.  0.30 0.15 270.  0.30 0.15 270.
09102
09112                                 0.00 0.00 180.  0.02 0.05 205.  0.01 0.02 190.
09122 0.00 0.00 180.  0.00 0.00 180.  0.01 0.02 190.  0.20 0.20 180.  0.20 0.20 220.
09132 0.10 0.20 240.  0.20 0.15 250.  0.40 0.20 250.  0.50 0.20 265.  0.50 0.20 270.
```

```
09142 0.50 0.20 270.  0.50 0.20 270.  0.50 0.20 270.  0.50 0.20 270.  0.50 0.20 270.
09152 0.50 0.20 270.  0.50 0.20 270.  0.50 0.20 270.  0.50 0.20 270.  0.50 0.20 270.
09302
09312                                 0.00 0.00 180.  0.02 0.05 180.  0.02 0.05 205.
09322 0.01 0.02 215.  0.00 0.00 135.  0.02 0.05 155.  0.10 0.10 190.  0.20 0.20 210.
09332 0.10 0.20 245.  0.10 0.10 255.  0.20 0.15 270.  0.30 0.20 270.  0.30 0.20 270.
09342 0.50 0.20 270.  0.50 0.20 270.  0.50 0.20 270.  0.50 0.20 270.  0.50 0.20 270.
09352 0.50 0.20 270.  0.50 0.20 270.  0.50 0.20 270.  0.50 0.20 270.  0.50 0.20 260.
09502
09512                                 0.00 0.00 180.  0.01 0.02 225.  0.04 0.04 220.
09522 0.05 0.05 210.  0.02 0.02 210.  0.02 0.05 190.  0.10 0.10 195.  0.20 0.20 205.
09532 0.10 0.20 215.  0.10 0.10 230.  0.15 0.15 260.  0.15 0.15 270.  0.15 0.15 275.
09542 0.15 0.15 280.  0.10 0.10 295.  0.10 0.10 310.  0.10 0.10 310.  0.05 0.05 315.
09552 0.05 0.05 060.  0.00 0.00 180.  0.00 0.00 230.  0.00 0.00 310.  0.00 0.00 270.
09702
09712                                                 0.00 0.00 180.  0.03 0.03 225.
09722 0.04 0.04 220.  0.05 0.05 215.  0.03 0.05 215.  0.07 0.10 200.  0.20 0.20 205.
09732 0.10 0.20 225.  0.10 0.10 235.  0.10 0.10 270.  0.10 0.10 295.  0.10 0.10 310.
09742 0.10 0.10 310.  0.10 0.10 320.  0.10 0.10 330.  0.05 0.05 330.  0.00 0.00 360.
09752 0.00 0.00 360.  0.00 0.00 360.  0.00 0.00 360.  0.00 0.00 360.  0.00 0.00 360.
09902
09912                                                 0.00 0.00 180.  0.01 0.02 210.
09922 0.02 0.02 220.  0.03 0.03 220.  0.05 0.05 220.  0.03 0.05 210.  0.15 0.15 205.
09932 0.10 0.20 215.  0.05 0.05 225.  0.05 0.05 270.  0.05 0.05 300.  0.05 0.05 330.
09942 0.10 0.10 340.  0.10 0.10 330.  0.05 0.05 330.  0.01 0.01 350.  0.00 0.00 360.
09952
10102
10112                                                                 0.00 0.00 180.
10122 0.00 0.00 180.  0.00 0.00 225.  0.04 0.04 225.  0.05 0.05 215.  0.10 0.10 205.
10132 0.10 0.20 210.  0.05 0.05 210.  0.05 0.05 205.  0.05 0.05 330.  0.05 0.05 340.
10142 0.10 0.10 345.  0.10 0.10 340.  0.05 0.05 330.  0.01 0.01 360.  0.00 0.00 360.
10152
10302
10312
10322                 0.00 0.00 180.  0.02 0.02 225.  0.04 0.05 225.  0.07 0.15 205.
10332 0.10 0.20 205.  0.05 0.05 205.  0.05 0.05 195.  0.05 0.05 355.  0.05 0.05 355.
10342 0.08 0.08 350.  0.05 0.05 340.  0.05 0.05 340.  0.01 0.01 320.  0.00 0.00 360.
10352
10502
10512
10522                 0.00 0.00 180.  0.01 0.02 180.  0.02 0.05 215.  0.03 0.05 225.
10532 0.10 0.20 205.  0.05 0.05 200.  0.05 0.05 205.  0.05 0.05 330.  0.05 0.05 335.
10542 0.02 0.02 355.  0.02 0.02 335.  0.02 0.01 300.  0.02 0.01 230.  0.00 0.00 225.
10552 0.00 0.00 180.
10702
10712
10722                 0.00 0.00 180.  0.01 0.02 175.  0.02 0.02 290.  0.02 0.04 230.
10732 0.08 0.15 205.  0.08 0.10 200.  0.04 0.07 195.  0.04 0.04 270.  0.05 0.05 305.
10742 0.02 0.02 360.  0.02 0.02 330.  0.01 0.01 330.  0.02 0.01 205.  0.01 0.01 205.
10752 0.00 0.00 220.  0.00 0.00 180.
10902
10912
10922                 0.00 0.00 180.  0.01 0.02 325.  0.02 0.02 330.  0.01 0.02 235.
10932 0.05 0.10 205.  0.10 0.20 200.  0.05 0.10 205.  0.02 0.02 270.  0.05 0.05 320.
10942 0.02 0.02 360.  0.02 0.02 360.  0.01 0.01 015.  0.02 0.01 155.  0.01 0.01 170.
10952 0.01 0.01 190.  0.01 0.01 225.  0.00 0.00 180.
11102
11112
11122                 0.00 0.00 180.  0.01 0.01 050.  0.02 0.02 025.  0.02 0.02 025.
11132 0.02 0.04 215.  0.10 0.20 200.  0.05 0.10 205.  0.02 0.02 270.  0.05 0.05 315.
11142 0.02 0.02 360.  0.02 0.02 030.  0.02 0.01 075.  0.02 0.01 140.  0.01 0.01 130.
11152 0.01 0.01 160.  0.01 0.01 180.  0.00 0.00 180.
11302
11312
11322                                 0.00 0.00 360.  0.00 0.00 030.  0.02 0.02 030.
11332 0.02 0.03 210.  0.10 0.20 205.  0.07 0.15 200.  0.02 0.02 270.  0.05 0.05 320.
11342 0.02 0.02 360.  0.01 0.01 060.  0.01 0.01 120.  0.00 0.00 135.  0.00 0.00 180.
11352 0.00 0.00 180.  0.00 0.00 180.  0.00 0.00 180.
11502
11512
```

```
11522                                                       0. 00 0. 00 360.  0. 01 0. 01 040.
11532 0. 01 0. 02 060.  0. 08 0. 20 185.  0. 10 0. 20 195.  0. 02 0. 05 270.  0. 05 0. 05 320.
11542 0. 02 0. 02 360.  0. 01 0. 01 335.  0. 00 0. 00 360.  0. 00 0. 00 360.
11552
11702
11712
11722                                                       0. 00 0. 00 360.  0. 01 0. 01 010.
11732 0. 02 0. 02 050.  0. 05 0. 08 170.  0. 10 0. 20 190.  0. 10 0. 20 225.  0. 05 0. 05 320.
11742 0. 02 0. 02 360.  0. 01 0. 01 360.  0. 00 0. 00 360.
11752
11902
11912
11922                                                       0. 00 0. 00 360.  0. 01 0. 01 360.
11932 0. 02 0. 02 360.  0. 05 0. 07 160.  0. 10 0. 20 185.  0. 05 0. 10 235.  0. 05 0. 05 320.
11942 0. 02 0. 02 360.  0. 01 0. 01 360.  0. 00 0. 00 360.
11952
12102
12112
12122                                                       0. 00 0. 00 360.  0. 01 0. 01 335.
12132 0. 02 0. 02 345.  0. 05 0. 06 175.  0. 10 0. 20 180.  0. 10 0. 20 215.  0. 05 0. 05 320.
12142 0. 02 0. 02 360.  0. 00 0. 00 360.  0. 00 0. 00 360.
12152
12302
12312
12322                                     0. 00 0. 00 360.  0. 00 0. 00 330.  0. 02 0. 02 340.
12332 0. 02 0. 02 345.  0. 03 0. 05 175.  0. 10 0. 15 180.  0. 10 0. 20 215.  0. 05 0. 05 320.
12342 0. 02 0. 02 360.  0. 00 0. 00 360.  0. 00 0. 00 360.
12352
12502
12512
12522                                     0. 00 0. 00 360.  0. 01 0. 01 340.  0. 05 0. 05 345.
12532 0. 02 0. 02 350.  0. 05 0. 05 180.  0. 10 0. 15 185.  0. 10 0. 25 215.  0. 05 0. 05 290.
12542 0. 02 0. 02 010.  0. 00 0. 00 360.  0. 00 0. 00 360.
12552
12702
12712
12722                                     0. 00 0. 00 360.  0. 01 0. 01 010.  0. 05 0. 05 360.
12732 0. 02 0. 02 350.  0. 05 0. 05 185.  0. 00 0. 15 190.  0. 10 0. 25 205.  0. 05 0. 05 280.
12742 0. 05 0. 05 010.  0. 00 0. 00 010.  0. 00 0. 00 360.
12752
12902
12912
12922                                     0. 00 0. 00 360.  0. 00 0. 00 040.  0. 05 0. 05 015.
12932 0. 02 0. 02 350.  0. 05 0. 05 195.  0. 08 0. 15 195.  0. 10 0. 25 200.  0. 02 0. 02 270.
12942 0. 05 0. 05 010.  0. 01 0. 01 020.  0. 00 0. 00 360.
12952
13102
13112
13122                                                       0. 00 0. 00 360.  0. 05 0. 05 015.
13132 0. 02 0. 02 350.  0. 03 0. 03 195.  0. 05 0. 15 190.  0. 10 0. 30 195.  0. 07 0. 10 200.
13142 0. 05 0. 05 360.  0. 01 0. 01 010.  0. 00 0. 00 360.
13152
13302
13312
13322                                                       0. 00 0. 00 360.  0. 05 0. 05 360.
13332 0. 05 0. 05 350.  0. 00 0. 00 220.  0. 05 0. 15 190.  0. 10 0. 30 190.  0. 10 0. 15 195.
13342 0. 05 0. 05 360.  0. 01 0. 01 360.  0. 00 0. 00 360.  0. 00 0. 00 360.
13352
13502
13512
13522                                     0. 00 0. 00 360.  0. 00 0. 00 330.  0. 05 0. 05 350.
13532 0. 05 0. 05 360.  0. 00 0. 00 360.  0. 05 0. 15 185.  0. 10 0. 30 190.  0. 10 0. 15 185.
13542 0. 05 0. 05 350.  0. 01 0. 01 360.  0. 00 0. 00 360.  0. 00 0. 00 360.
13552
13702
13712
13722                                     0. 00 0. 00 360.  0. 01 0. 01 005.  0. 05 0. 05 010.
13732 0. 05 0. 05 360.  0. 00 0. 00 360.  0. 05 0. 15 180.  0. 10 0. 35 185.  0. 10 0. 20 185.
13742 0. 05 0. 05 350.  0. 01 0. 01 350.  0. 00 0. 00 360.
13752
```

BEST DOCUMENT AVAILABLE

```
13902
13912
13922                                      0. 00 0. 00 360.  0. 01 0. 01 020.  0. 05 0. 05 020.
13932 0. 05 0. 05 360.  0. 00 0. 00 360.  0. 05 0. 20 180.  0. 10 0. 35 180.  0. 10 0. 20 180.
13942 0. 05 0. 05 345.  0. 01 0. 01 335.  0. 00 0. 00 360.
13952
14102
14112
14122                                                        0. 00 0. 00 360.  0. 05 0. 05 025.
14132 0. 05 0. 05 030.  0. 00 0. 00 360.  0. 05 0. 20 140.  0. 10 0. 40 180.  0. 10 0. 20 175.
14142 0. 05 0 05 340    0. 01 0. 01 335.  0. 00 0. 00 360.
14152
14302
14312
14322                                                        0. 00 0. 00 360.  0. 02 0. 02 030.
14332 0. 05 0. 05 040.  0. 02 0. 02 050.  0. 05 0. 20 130.  0. 15 0. 40 180.  0. 15 0. 30 175.
14342 0. 05 0. 05 330.  0 01 0. 01 320.   0. 00 0. 00 360.
14352
14502
14512
14522                                                        0. 00 0. 00 360.  0. 01 0. 01 040.
14532 0. 05 0. 05 045.  0. 05 0. 05 055.  0. 10 0. 20 115.  0. 20 0. 40 180.  0. 10 0. 30 175.
14542 0. 05 0. 05 330.  0. 00 0. 00 320.  0. 00 0. 00 360.
14552
14702
14712
14722                                                                          0. 00 0. 00 360.
14732 0. 03 0. 03 055.  0. 05 0. 05 060.  0. 10 0. 20 110.  0. 20 0. 40 180.  0. 05 0. 30 175.
14742 0. 00 0. 00 290.  0. 00 0. 00 360.
14752
14902
14912
14922                                                                          0. 00 0. 00 360.
14932 0. 00 0. 00 090.  0. 00 0. 00 090.  0. 20 0. 40 165.  0. 20 0. 40 180.  0. 01 0. 02 260.
14942 0. 00 0. 00 360.
14952
```

APPENDIX D

TIDAL CURRENT FIELD INPUT DATA FILE

Input Data File Format: Tidal Currents

STARTING COORDINATES		TIDAL CURRENT PARAMETERS FOR (Y, X)				TIDAL CURRENT PARAMETERS FOR (Y, X+3)				TIDAL CURRENT PARAMETERS FOR (Y, X+6)				TIDAL CURRENT PARAMETERS FOR (Y, X+9)			
Y	X	VMAX	FLOOD	EBB	PHASE	VMAX	FLOOD	EBB	PHASE	VMAX	FLOOD	EBB	PHASE	VMAX	FLOOD	EBB	PHASE
XXX	XX	X.XX	XXX	XXX	XXX	X.XX	XXX	XXX	XXX	X.XX	XXX	XXX	XXX	X.XX	XXX	XXX	XXX

(Y, X) - GRID CELL LOCATION FOR TIDAL CURRENT DATA

VMAX - MAXIMUM FLOOD & EBB VELOCITY IN METERS/SEC.

FLOOD - DIRECTION OF FLOOD CURRENT (IN DEGREES, CLOCKWISE FROM NORTH)

EBB - DIRECTION OF EBB CURRENT (IN DEGREES, CLOCKWISE FROM NORTH)

PHASE - PHASE OF TIDAL CURRENT WITH LOCATION RELATIVE TO ZERO BETWEEN CAPE DOUGLAS & CAPE ELIZABETH (IN DEGREES, 360° = 12.4 HOURS)

```
150 02
150 14
150 26                                           0. 00 030 210 120   2. 70 030 210 120
150 38   3. 20 360 180 120   1. 75 335 155 120   0. 00 320 140 120
150 50
147 02
147 14
147 26                       0. 00 030 210 100   1. 20 050 200 108   1. 75 030 210 105
147 38   2. 00 360 180 113   1. 75 345 165 108   1. 10 330 150 103   0. 00 330 150 105
147 50
144 02
144 14
144 26                       0. 00 020 200 090   1. 30 030 200 098   1. 51 040 210 092
144 38   1. 66 360 180 106   1. 70 350 180 104   1. 30 330 180 095   0. 00 360 180 090
144 50
141 02
141 14
141 26   0. 00 020 200 090   1. 10 020 200 087   1. 30 360 180 090   0. 00 360 180 087
141 38   1. 45 360 180 099   1. 66 350 180 097   1. 30 340 180 089   0. 00 360 180 081
141 50
138 02
138 14
138 26   0. 00 360 180 085   1. 10 010 190 085   1. 35 350 180 086   0. 00 360 180 085
138 38   1. 44 360 190 090   1. 50 360 180 090   1. 15 350 180 082   0. 00 360 180 075
138 50
135 02
135 14
135 26                       0. 00 360 180 081   1. 80 360 180 083   0. 00 360 100 082
135 38   1. 15 360 190 090   1. 28 360 180 085   1. 08 360 180 077   0. 00 360 180 068
135 50
132 02
132 14
132 26   0. 00 030 210 080   0. 95 030 210 079   1. 04 360 180 080   0. 95 360 100 079
132 38   1. 05 360 190 082   1. 16 360 180 078   1. 04 010 190 069   0. 00 020 200 060
132 50
129 02
129 14
129 26   0. 00 030 210 078   0. 85 020 200 077   0. 85 360 180 077   1. 00 360 100 077
129 38   1. 10 360 180 075   1. 20 360 180 070   1. 10 010 190 062   0. 00 360 180 058
129 50
126 02
126 14
126 26   0. 00 360 180 075   0 55 345 165 074    0. 86 350 170 073   1. 00 360 180 073
126 38   1. 10 360 180 070   1. 10 360 180 065   1. 00 360 180 056   0. 00 360 180 053
126 50
123 02
123 14
123 26   0. 00 340 160 070   0. 67 300 120 070   0. 82 345 180 069   1. 00 360 180 069
123 38   1. 01 360 180 067   1. 08 355 180 062   0. 85 360 180 051   0. 00 360 180 045
123 50
120 02
120 14
120 26                       0. 00 360 180 066   0. 80 350 180 066   0. 95 360 180 065
120 38   1. 02 360 180 063   1. 00 350 100 060   0. 96 360 100 045   0. 00 360 100 040
120 50
117 02
117 14
117 26   0. 00 010 190 064   0. 73 360 100 062   1. 05 360 100 061   1. 15 360 100 061
117 38   1. 25 360 180 060   1. 11 353 173 051   1. 06 340 168 041   0. 00 360 100 035
117 50
114 02
114 14
114 26   0. 00 020 200 060   0. 55 030 210 058   0. 76 012 192 056   1. 00 360 180 056
114 38   0. 97 356 176 052   1. 00 347 160 045   0. 98 340 140 035   0. 98 320 140 030
114 50   0. 00 270 090 075   0. 00 090 270 015   0. 00 035 215 015
111 02
111 14
111 26   0. 00 360 180 055   0. 30 351 171 053   0. 70 355 175 052   0. 80 360 180 050
111 38   0. 80 350 170 045   0. 84 342 162 038   0. 76 342 162 030   0. 70 339 159 020
111 50   0. 38 336 156 012   0. 36 031 211 013   0. 00 035 215 014
```

```
108 02
108 14                                                              0. 00 360 180 053
108 26  0. 25 350 170 049   0. 52 020 200 048   0. 63 010 190 046   0. 62 368 180 045
108 38  0. 75 350 170 040   0. 75 352 172 030   0. 70 351 171 022   0. 63 007 187 015
108 50  0. 60 029 209 008   0. 00 035 215 009
105 02
105 14                                                              0. 00 040 220 045
105 26  0. 25 030 210 045   0. 52 020 190 043   0. 55 010 180 042   0. 60 360 180 039
105 38  0. 65 350 170 035   0. 65 351 171 026   0. 68 358 178 020   0. 70 015 195 012
105 50  0. 00 035 215 005
102 02
102 14                                          0. 00 060 240 043   0. 10 050 230 041
102 26  0. 36 030 210 039   0. 43 020 180 038   0. 50 010 180 036   0. 58 360 180 034
102 38  0. 58 350 170 030   0. 70 350 170 023   0. 68 350 170 015   0. 80 023 203 008
102 50  0. 00 360 180 000
099 02
099 14                      0. 00 060 240 038   0. 10 020 180 038   0. 25 030 210 036
099 26  0. 32 040 220 034   0. 40 020 100 033   0. 50 010 100 032   0. 55 360 180 030
099 38  0. 58 350 170 026   0. 58 342 162 020   0. 72 345 165 013   0. 85 348 168 006
099 50  0. 00 330 150 000   0. 00 270 090 000   0. 00 270 070 000   0. 00 230 050 -03
076 02
096 14                      0. 00 050 240 033   0. 20 050 180 032   0. 26 045 215 030
096 26  0. 40 010 170 029   0. 43 345 165 029   0. 45 345 165 028   0. 48 350 170 025
096 38  0. 49 341 161 021   0. 55 334 156 015   0. 68 332 152 010   0. 95 318 138 005
096 50  0. 98 314 134 000   1. 00 310 130 000   1. 50 330 150 000   1. 50 325 140 -05
073 02
093 14                      0. 00 360 100 029   0. 41 020 180 028   0. 00 030 210 027
093 26  0. 00 360 180 026   0. 49 330 165 026   0. 45 332 160 025   0. 47 334 154 023
093 38  0. 45 327 147 020   0. 42 320 140 015   0. 60 309 129 010   0. 78 298 118 007
093 50  0. 84 296 116 001   1. 00 290 110 000   1. 00 290 110 000   0. 90 280 100 -05
070 02
090 14                      0. 00 360 180 027   0. 41 360 100 026   0. 00 310 130 025
090 26  0. 00 030 210 024   0. 38 327 147 023   0. 37 320 140 022   0. 40 320 140 020
090 38  0. 40 310 130 017   0. 45 300 117 015   0. 50 290 110 009   0. 60 277 097 006
070 50  0. 60 277 097 003   0. 70 270 070 000   0. 70 270 090 -03   0. 80 270 090 -07
007 02
087 14  0. 00 360 100 028   0. 16 360 140 026   0. 31 360 130 024   0. 34 320 120 023
087 26  0. 34 290 120 022   0. 36 295 115 020   0. 34 301 121 019   0. 32 307 127 017
087 38  0. 29 285 105 015   0 26 275 095 015    0. 23 266 006 009   0. 20 268 080 006
087 50  0. 20 250 070 003   0. 40 270 150 000   0. 00 240 060 -05   0. 70 270 090 -08
034 02
084 14  0. 00 360 180 026   0. 20 320 110 024   0. 30 310 100 023   0. 36 300 105 021
034 26  0. 36 290 110 020   0. 45 290 115 018   0. 45 300 115 017   0. 47 310 115 015
084 38  0. 47 311 105 013   0. 35 300 105 010   0. 23 266 105 008   0. 20 270 070 005
084 50  0. 20 270 090 002   0. 40 270 090 -03   0. 60 270 090 -06   0. 80 270 090 -08
081 02
081 14  0. 00 020 200 026   0 21 270 090 023    0. 28 235 090 021   0. 42 270 070 019
081 26  0. 55 270 105 018   0. 55 280 110 016   0. 56 280 110 015   0. 57 337 110 012
081 38  0. 50 340 110 010   0. 40 320 110 008   0. 30 310 110 006   0. 20 310 100 003
081 50  0. 20 300 070 001   0. 40 270 090 -05   0. 60 270 090 -08   0. 80 270 090 -10
078 02
078 14  0. 00 310 130 026   0. 14 214 034 023   0. 00 260 080 002   0. 00 270 090 019
078 26  0. 00 270 070 016   0. 00 270 070 015   0. 00 270 070 012   0. 71 270 070 010
078 38  0. 50 270 090 008   0. 40 270 070 006   0. 30 270 090 003   0. 20 270 090 001
078 50  0. 20 270 090 000   0. 40 270 090 -05   0. 60 270 090 -08   0. 80 270 090 -12
075 02
075 14                      0. 00 360 180 023
075 26                                          0. 00 180 360 008   0. 40 230 050 005
075 38  0. 40 230 050 003   0. 30 230 050 002   0. 30 260 080 000   0. 30 260 080 000
075 50  0. 20 270 090 -07   0. 40 270 090 -07   0. 60 270 090 -10   0. 80 270 090 -15
072 02
072 14
072 26                                          0. 00 180 360 000   0. 30 180 360 000
072 38  0. 30 180 360 000   0. 30 200 020 000   0. 30 200 020 003   0. 30 190 010 004
072 50  0. 00 190 010 004   0. 00 360 180 -07   0. 20 320 140 -10   0. 40 270 090 -15
069 02
069 14
069 26                                          0. 00 180 360 005   0. 20 200 020 005
069 38  0. 20 200 020 005   0. 20 200 020 005   0. 20 200 020 005   0. 20 180 360 005
069 50  0. 00 180 360 005   0. 00 180 360 -08   0. 20 270 090 -12   0. 20 270 090 -16
```

BEST DOCUMENT AVAILABLE

```
066 02
066 14
066 26                      0.00 210 030 010    0.06 210 030 010    0.10 210 030 010
066 38  0.10 200 020 010    0.12 200 020 010    0.10 200 020 010    0.10 200 020 010
066 50  0.00 200 020 010    0.00 200 020 -15    0.00 180 360 -15    0.00 270 090 -17
063 02
063 14
063 26                      0.00 230 050 015    0.05 220 040 015    0.05 195 015 015
063 38  0.05 195 015 015    0.05 200 020 015    0.05 200 020 015    0.00 200 020 015
063 50
060 02
060 14
060 26  0.00 205 025 022    0.03 205 025 022    0.04 195 015 022    0.04 195 015 021
060 38  0.04 195 015 020    0.04 200 020 018    0.03 225 025 018    0.00 225 025 018
060 50
057 02
057 14
057 26  0.00 230 050 027    0.02 195 015 026    0.03 195 015 025    0.03 195 015 023
057 38  0.03 195 015 022    0.03 195 015 022    0.00 195 015 022
057 50
054 02
054 26  0.00 185 005 030    0.00 185 005 030    0.01 190 010 029    0.02 195 015 028
054 38  0.02 195 015 027    0.01 200 020 025    0.00 200 020 025
054 50
051 02
051 14
051 26  0.00 000 180 024    0.01 000 180 026    0.00 005 185 029    0.00 190 010 030
051 38  0.00 195 015 030    0.00 195 015 030    0.00 195 015 030
051 50
048 02
048 14
048 26  0.00 005 185 020    0.05 005 185 022    0.05 005 185 023    0.04 010 190 024
048 38  0.03 015 195 026    0.00 020 200 027
048 50
045 02
045 14
045 26  0.00 015 195 017    0.07 015 195 018    0.07 020 200 019    0.05 030 210 020
045 38  0.05 035 215 022    0.00 080 260 023
045 50
042 02
042 14                                                              0.00 040 220 014
042 26  0.08 040 220 015    0.09 030 210 016    0.08 030 210 016    0.06 030 210 017
042 38  0.05 055 235 018    0.00 080 310 020
042 50
039 02
039 14                                          0.00 050 230 008    0.10 050 230 008
039 26  0.13 020 200 010    0.12 020 200 012    0.11 025 205 014    0.10 010 170 015
039 38  0.00 010 170 016
039 50
036 02
036 14                      0.00 050 230 005    0.12 050 230 006    0.14 040 220 006
036 26  0.15 035 215 007    0.14 035 215 008    0.13 030 210 010    0.12 005 185 012
036 38  0.00 005 185 012
036 50
033 02
033 14  0.00 040 220 000    0.19 040 220 001    0.18 030 210 002    0.17 030 210 004
033 26  0.17 030 210 005    0.16 030 210 006    0.15 030 210 007    0.13 040 220 008
033 38  0.00 090 270 008
033 50
030 02
030 14  0.00 020 200 -01    0.21 020 200 -01    0.20 020 200 -01    0.20 025 205 000
030 26  0.18 025 205 002    0.18 030 210 002    0.17 050 230 004    0.10 070 250 005
030 38  0.00 120 300 006
030 50
027 02                                                              0.00 020 200 -04
027 14  0.20 020 200 -03    0.23 015 195 -03    0.23 015 195 -02    0.22 015 195 -02
027 26  0.22 015 195 -01    0.20 025 205 -01    0.00 025 205 000
027 38
027 50
024 02                                          0.00 005 185 -07    0.00 005 185 -07
```

```
024 14  0.20 005 185 -06  0.25 005 185 -05  0.25 005 185 -05  0.24 010 190 -04
024 26  0.24 015 195 -04  0.00 015 195 -03
024 38
024 50
021 02                                      0.00 020 200 -07  0.20 020 200 -08
021 14  0.26 000 180 -08  0.26 000 180 -07  0.25 005 185 -06  0.25 005 185 -05
021 26  0.25 010 190 -05  0.00 010 190 -05
021 38
021 50
018 02                    0.00 040 220 -09  0.00 040 220 -08  0.25 000 180 -08
018 14  0.27 000 180 -08  0.27 000 180 -08  0.27 000 180 -08  0.26 000 180 -08
018 26  0.26 000 180 -08  0.00 000 180 -08
018 38
018 50
015 02                    0.00 005 185 -10  0.00 -10 005 185  0.30 000 180 -10
015 14  0.29 000 180 -09  0.29 355 175 -09  0.28 355 175 -09  0.28 355 175 -09
015 26  0.26 335 155 -09  0.00 335 155 -10  0.00 335 155 -10
015 38
015 50
012 02                    0.00 010 190 -13  0.32 005 185 -12  0.32 000 180 -12
012 14  0.31 350 170 -11  0.31 340 160 -11  0.31 340 160 -11  0.31 340 160 -11
012 26  0.31 320 140 -11  0.30 315 135 -11  0.00 315 135 -12  0.00 315 135 -12
012 38
012 50
009 02  0.00 355 175 -13  0.00 005 185 -13  0.33 000 180 -13  0.33 355 175 -13
009 14  0.33 355 175 -13  0.33 345 165 -13  0.33 335 155 -13  0.34 325 145 -14
009 26  0.35 315 135 -14  0.34 315 135 -14  0.30 315 135 -15  0.00 315 135 -15
009 38  0.00 315 135 -15
009 50
006 02  0.00 355 175 -15  0.35 005 185 -15  0.35 000 180 -15  0.35 355 175 -15
006 14  0.35 350 170 -15  0.35 350 170 -15  0.35 340 160 -15  0.35 330 150 -15
006 26  0.35 320 140 -15  0.35 315 135 -16  0.35 310 130 -17  0.00 310 130 -17
006 38  0.00 310 130 -17  0.00 310 130 -17  0.00 000 180 -18
006 50
003 02  0.00 350 170 -17  0.37 350 170 -17  0.37 355 175 -17  0.37 355 175 -17
003 14  0.37 350 170 -17  0.37 350 170 -17  0.37 340 160 -17  0.36 330 150 -17
003 26  0.35 320 140 -18  0.35 315 135 -18  0.35 310 130 -18  0.35 310 130 -18
003 38  0.35 310 130 -18  0.00 330 150 -18  0.00 005 185 -18  0.00 005 185 -20
003 50
000 02  0.00 320 140 -18  0.40 350 170 -18  0.40 355 175 -18  0.40 355 175 -18
000 14  0.40 350 170 -18  0.40 345 165 -18  0.40 340 160 -18  0.40 330 150 -18
000 26  0.40 325 145 -20  0.40 325 145 -20  0.40 320 140 -20  0.40 320 140 -20
000 38  0.40 320 140 -20  0.40 330 150 -20  0.40 340 160 -20  0.00 340 160 -22
000 50
```

BEST DOCUMENT AVAILABLE

FINAL REPORT--TASK I
WIND FIELD TRANSITION MATRIX ANALYSIS
LOWER COOK INLET--SHELIKOF STRAIT, ALASKA
BERING SEA--GULF OF ALASKA PROJECT OFFICE
OUTER CONTINENTAL SHELF ENVIRONMENTAL
ASSESSMENT PROGRAM

JOB NO. 06797-014-88
OCTOBER 31, 1980

LOS ANGELES, CALIFORNIA

October 31, 1980

Outer Continental Shelf Environmental
Assessment Program
Bering Sea--Gulf of Alaska Project Office
Post Office Box 1808
Juneau, Alaska 99802

Attention: Herbert E. Bruce, Ph.D.
OCSEAP Project Manager

Gentlemen:

Final Report--Task I
Wind Field Transition Matrix Analysis
Lower Cook Inlet--Shelikof Strait, Alaska
Bering Sea--Gulf of Alaska Project Office
Outer Continental Shelf Environmental
Assessment Program

We are pleased to submit our final report on an analysis of wind field transition matrices based upon historical data for Lower Cook Inlet and Shelikof Strait, Alaska.

This report has incorporated and responded to comments received from your Juneau staff.

It has been a pleasure to work on this phase of our 1980 fiscal year contract with your staff. Please do not hesitate to contact us if you have questions regarding the contents of this study.

Very truly yours,

DAMES & MOORE
Marine Services Group

Roger S. Schlueter, Ph.D.
Managing Principal

Michael W. Miller

Michael W. Miller
Principal Investigator

RSS:MWM:jh

BEST DOCUMENT AVAILABLE

CONTENTS

Page

1.0 Introduction. 350
  1.1 Background 350
  1.2 Purpose. 351
  1.3 Scope. 351
  1.4 Objectives 352
  1.5 Organization 352

2.0 Data Base: Characterization of Matrices. 353
  2.1 Putnins' Weather Catalog 353
  2.2 Accuracy of Transition Matrices. 355

3.0 Auto Correlation Functions. 357

4.0 Comparison of First- and Second-Order Matrices and the Weather Catalog. 361

5.0 Conclusions and Recommendations 365

References 368

Appendix A: Converted Weather Catalog 369

Appendix B: Statistical Methodology--Matrix Accuracy 378

1.0 INTRODUCTION

1.1 BACKGROUND

This report describes the results of a wind field transition matrix analysis based on historical weather data used in an oil spill trajectory simulation in Lower Cook Inlet and Shelikof Strait, Alaska. The work was performed under Contract No. NA80RAC00075 between Dames & Moore and the National Oceanic and Atmospheric Administration.

This study was supported by the Bureau of Land Management through interagency agreement with the National Oceanic and Atmospheric Administration, under which a multi-year program responding to needs of petroleum development of the Alaskan continental shelf is managed by the Outer Continental Shelf Environmental Assessment Program (OSCEAP) Office.

This study was initiated by the Outer Continental Shelf Environmental Assessment Program (OCSEAP) on behalf of the Bureau of Land Management (BLM). This is one of a series of studies conducted by Dames & Moore to investigate the behavior of hypothetical oil spills within the Alaskan Outer Continental Shelf. The ability to accurately specify the variability of weather for use in an oil spill trajectory model in Lower Cook Inlet and Shelikof Strait has been a subject of continued interest for several years. The availability of a catalog of daily baric weather patterns over a 19-year period has increased the reliability that can be placed in the results of trajectory modeling in Lower Cook Inlet and Shelikof Strait. This catalog has been previously used in a hindcast mode by randomly accessing and using the observed sequences of weather patterns. This is a rather cumbersome method and does not solve the problem of specifying weather variability in a forecast mode. Simplified operations and forecast capabilities could be achieved using a transition matrix calculated from the historical catalog. The desire to use a transition matrix led to the question of whether a first-order transition matrix adequately represents the sequencing of weather patterns in southern Alaska. The answer to this question directly influences studies conceived or being conducted for BLM/OCSEAP in Lower Cook Inlet and Shelikof Strait as well as the Bering Sea.

1.2 PURPOSE

The purpose of this study was to investigate the validity of using a first-order transition matrix to represent the time history of weather patterns in southern Alaska. Other probabilistic approaches considered were: (1) randomly accessing Putnin's 19-year catalog of daily weather patterns to obtain an observed historical sequence; or (2) using a second-order transition matrix to generate sequences of daily weather patterns.

This study dealt with three basic questions: (1) How accurate is the first-order approach? (2) Is there anything to support use of a second-order matrix? (3) Does a first-order matrix generate unrealistic sequences of weather patterns?

1.3 SCOPE

This study was conducted in accordance with the scope of services for Task I detailed in the Dames & Moore proposal, "Oil Dispersion Analysis, Lower Cook Inlet and Shelikof Strait, Alaska," RFx41-436-2905, for National Oceanic and Atmospheric Administration, July 19, 1979 and "Proposal Addendum, Oil Spill Dispersion Analysis," RFx41-436-2905, October 15, 1979, subsequently amended in a letter dated February 4, 1980.

1.4 OBJECTIVE

The primary element of the scope of services relating to the evaluation of the wind field transition matrix presented in the above documents is summarized below:

1. Evaluate the applicability of a first-order wind field transition matrix to represent historically observed sequences and variability of wind fields as applied to trajectory simulation.

1.5 ORGANIZATION

Section 2.0 investigates the accuracy of a first-order transition matrix. The approach was not to look at the matrices as a whole, but to look at individual entries, especially those associated with weather pattern sequences which occur frequently.

An evaluation of the correlation between daily weather patterns using auto correlation functions is presented in Section 3.0. This examination considered the weather patterns both with and without intensity factors.

Section 4.0 presents a comparison of a first- and second-order transition matrix and randomly accessing the weather catalog. This comparison was based on calculating the probabilities that three-day sequences would occur using the three different methods.

Finally, conclusions and recommendations are presented in Section 5.0. Significant implications with respect to oil spill modeling is discussed as well as still unresolved problem areas.

2.0 DATABASE: CHARACTERIZATION OF MATRICES

2.1 PUTNINS' WEATHER CATALOG

The oil spill trajectory studies for Lower Cook Inlet and Shelikof Strait presented in Dames & Moore (1980; 1979; and 1976) have all used the work of Putnins, (1966a) to derive wind field variability. The 1979 and 1976 studies used a deterministic approach in applying the wind fields and therefore, probabilistic wind field generation schemes were not required. One major objective of the 1980 study was to increase the variability of the wind fields used to calculate the wind drift component of surface pollutant transport. This was accomplished by randomly accessing a wind field catalog, based on the work of Putnins (1966a), and sequencing historically observed daily weather patterns. This random accessing was done enough times to provide a statistically significant sample of trajectories from each launch site examined.

Putnins (1966a) developed 22 specific baric weather patterns describing mesoscale weather situations over Alaska. These 22 baric weather patterns were related to 5 wind fields and 6 wind field intensity factors as developed by PMEL and shown in Table 2.1 (PMEL, 1980). This table was used to convert Putnins' unpublished tabulations of approximately 19 years of daily baric weather patterns (Putnins, 1966b) into a wind field catalog (Appendix A).

These wind fields and intensity factors allowed two basic approaches to be used in sequencing weather patterns during the 1980 oil spill trajectory study. The first approach was to use the wind field catalog given in Appendix A, converted from Putnins' data using Table 2.1, entering with a random date and historically sequencing the wind fields. The second approach was to use the wind field catalog to calculate first-order transition matrices (Tables A-1, A-2, A-3, A-4) and use

TABLE 2.1

CONVERSION FACTORS FROM PUTNINS' WEATHER TYPOLOGY TO PMEL'S WIND FIELD AND INTENSITY FACTORS

Putnins Type		PMEL Type
A	=	25
A_c	=	25
A'	=	53
A"	=	33
A"	=	43
A_1	=	15
A_2	=	43
A_3	=	31
B	=	16
C	=	22
C_1	=	42
D	=	23
D'	=	15
D_1	=	23
E	=	45
E'	=	42
E"	=	26
E_1	=	22
F	=	43
F_1	=	23
G	=	53
H	=	14

PMEL Type (Wind Field	/ Intensity Factor)
1 = Figure 3	1 = 0.3
2 = Figure 4	2 = 0.5
3 = Figure 5	3 = 1.0
4 = Figure 6	4 = 1.2
5 = Figure 7	5 = 1.5
	6 = 0.7

Example: PMEL Type 45 represents wind field number 4 as shown in Figure 6 with all magnitudes increased by a factor of 1.5 as denoted by the intensity factor index 5. PMEL Type 45 is equivalent to Putnins' Weather Type E.

these matrices to sequence the wind fields. The former method was used in the 1980 trajectory study because certain unresolved questions remained regarding the applicability of a first-order transition matrix. This report addresses some of the questions that have been raised regarding the accuracy of a first-order transition matrix applied to weather patterns in southern Alaska.

2.2 ACCURACY OF TRANSITION MATRICES

A transition matrix is a statistical tool used to associate probabilities of going from one "state" (in this case, wind pattern) to another "state". The question naturally arises, "How realistic are these probabilities?"

One method which can be used to analyze whether or not the database is large enough to accurately characterize first- and second-order transition matrices is to examine the individual entries in the matrices (as opposed to examining the entire matrix structure).

The problem with this approach lies in the calculation of confidence intervals for each entry. Since confidence intervals are a function of sample size and number of observations, the sampling intervals will vary from entry to entry. However, by concentrating on entries containing a relatively large sample size, i.e., number of observations, it is believed that a reasonable picture of the entire structure can be obtained. This approach is necessary because it is not possible to characterize those entries with only a few observations within reasonable confidence limits. Therefore, confidence intervals about the "major" entries will be used to examine how well the historical data characterizes the entire matrix.

Suppose that a population of three sequences is divided into two categories, those which are 14, 14, 23 and those which do not have this sequence. If in the whole population there is a proportion θ of the above sequence, the probability that in a sample of five individuals picked at random there will be χ with the 14, 14, 23 characteristic, is given by the binomial function

$$f(x) = C(5,x)\ \theta^{x}\ (5-\theta)^{5-x}$$

where

f is the probability density function

χ is the observed number of 14, 14, 23s in this sample, and

θ is the actual proportion of 14, 14, 23s in the entire population

C is the standard combinatorial notation.

The value of θ is usually unknown, but it can be estimated from the sample, and the larger the sample, the more accurate the estimate. If p is defined as the proportion of individuals in the sample having the "characteristic" 14, 14, 23, then $p = x/s$. Obviously, if the sample s is so large that it includes the whole population, p will coincide with θ, but for small samples p will vary from one sample to another.

The expectation of x is given by $\mu = s\theta$, so that, since s is a fixed number (the sample size), the expectation of p is $\mu/s = \theta$. The variance of p is:

$$\mathrm{Var}(p) = \theta(1-\theta)/s$$

Hence, the variance of p naturally diminishes as the sample size increases.

If it is now assumed that x has a certain value, then the probability, that a random sample of size s will have a value of p differing from Θ by any given amount, can be estimated. If the sample is large enough, i.e., ($\geq$ 30), the normal approximation to the binomial will enable an estimate of this probability to be made quite easily. An example of this methodology is presented in Appendix B.

If the confidence limits are examined as percentages of the number of entries in the matrix rather than as a cardinal range, it is seen that there is greater statistical confidence associated with the entries of the first-order matrix as opposed to the second-order matrix.

3.0 AUTO CORRELATION FUNCTIONS

Two tests were run to investigate the correlation of daily weather patterns. Auto correlation functions were generated based upon the historical data. Since the raw data was not continuous (e.g., 14, 15, 16, 22), a simple transformation replaced each data type with an integer from 1 to 13. (Only 13 combinations of the 5 wind patterns and 6 intensities factors were correlated by PMEL to Putnins data.) The auto correlation function was generated for both the whole weather pattern (wind field and intensities) and for the pattern only (wind field only). In addition, as a point of comparison, the autocorrelation function for randomly generated weather sequences was calculated. The results are presented on Plates 3.1 through 3.3.

It is apparent from the figures that, although the correlation is small, the weather patterns are not random events. In addition, the correlation for the form only is a

BY S. VanOtta DATE 9-10-80
CHECKED BY ____________

NOAA
FILE 06797-014-(5105) 88

REVISIONS
BY ________ DATE ____

BEST DOCUMENT AVAILABLE

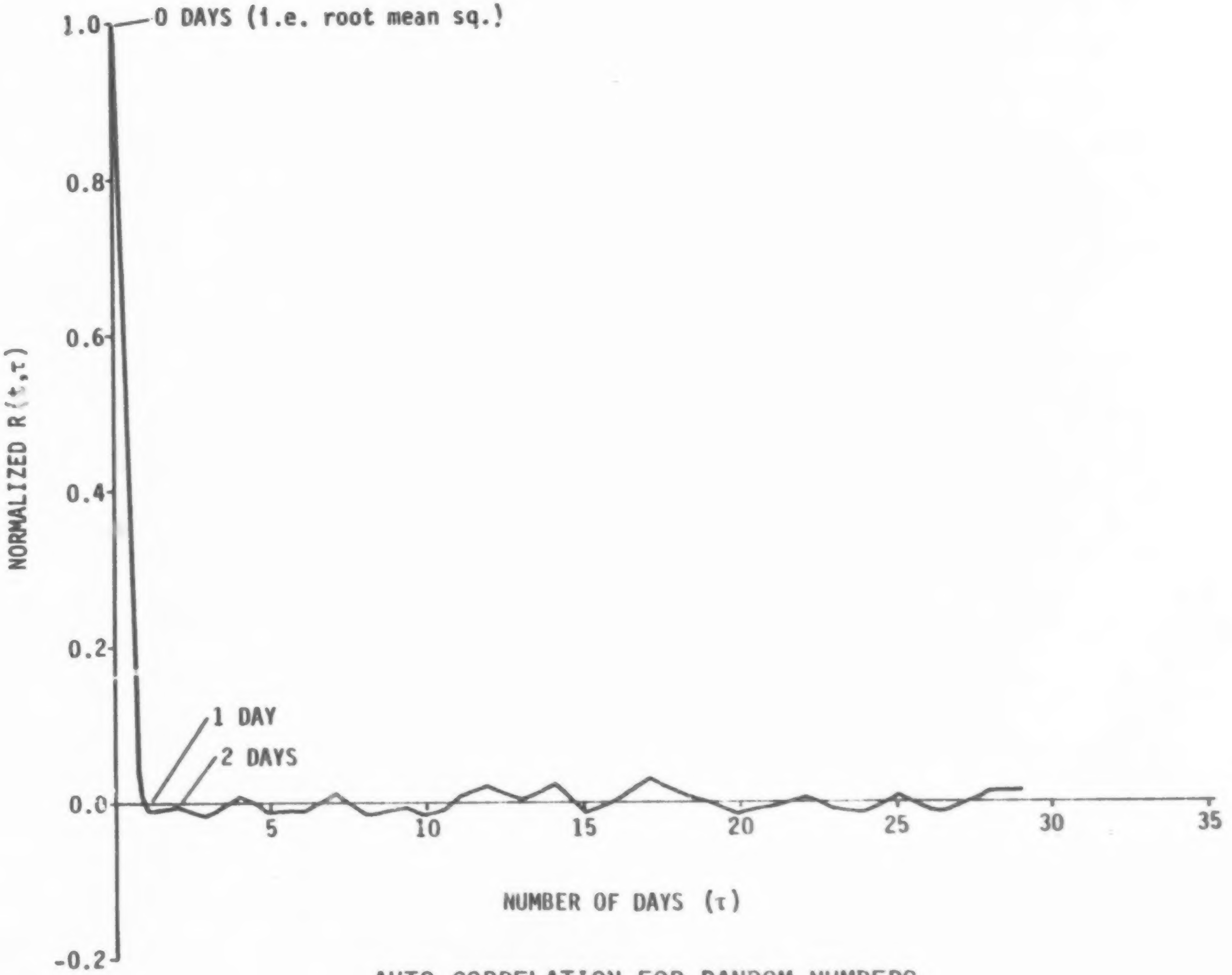

AUTO CORRELATION FOR RANDOM NUMBERS

946.7 (REV. 6-61)

BY S. Van Atta DATE 9-10-80
CHECKED BY ____________

NOAA
FILE 06797-014-88 (5105)

REVISIONS
BY ________ DATE ______

BEST DOCUMENT AVAILABLE

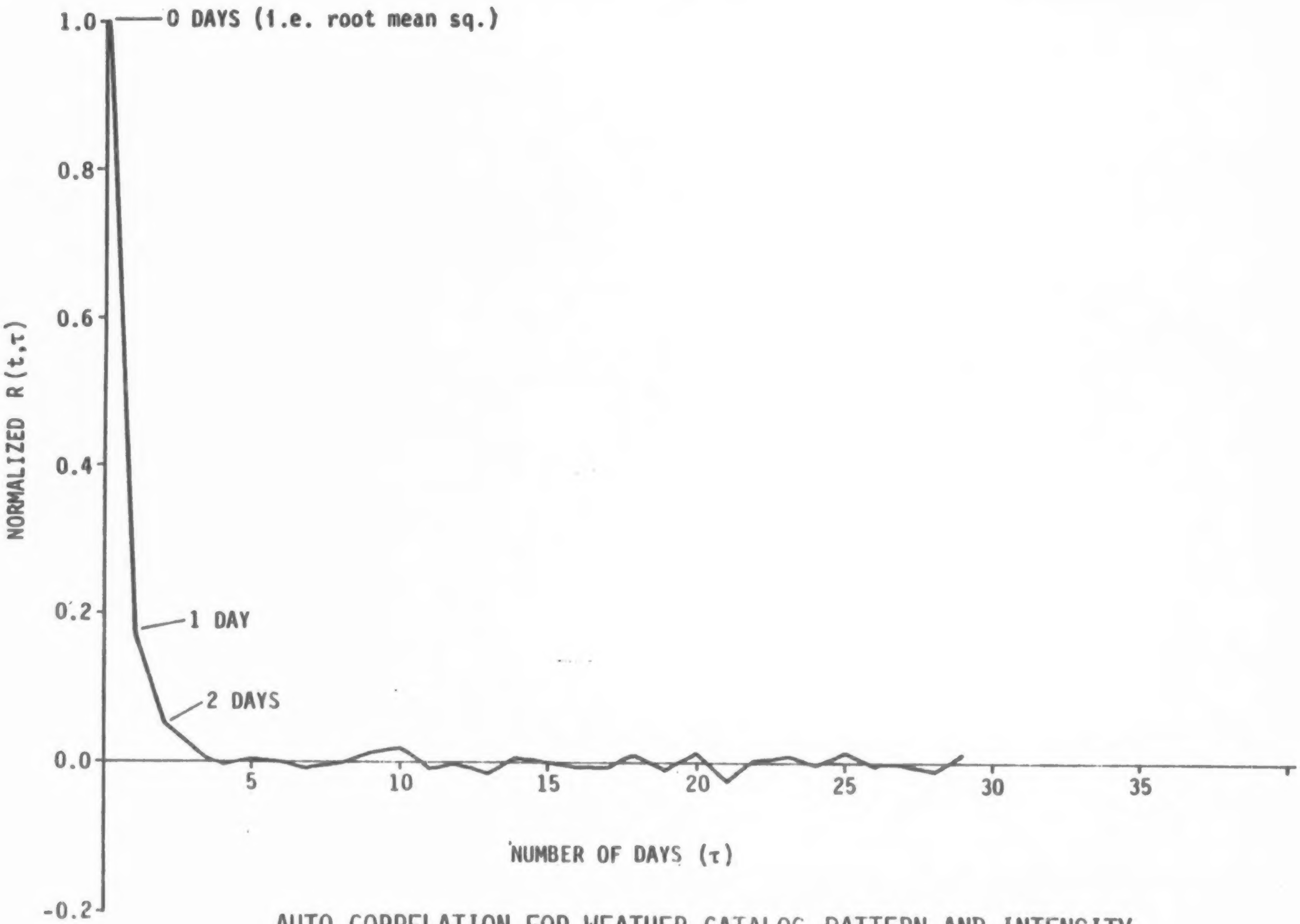

AUTO CORRELATION FOR WEATHER CATALOG PATTERN AND INTENSITY

DAMES & MOORE

PLATE 3.2

.7 (REV. 6-61)

BY__________ DATE 9-10-80
CHECKED BY S. Van Otta

NOAA
FILE 06797-014-(5105)-88

REVISIONS
BY________ DATE ______

BEST DOCUMENT AVAILABLE

DAMES & MOORE

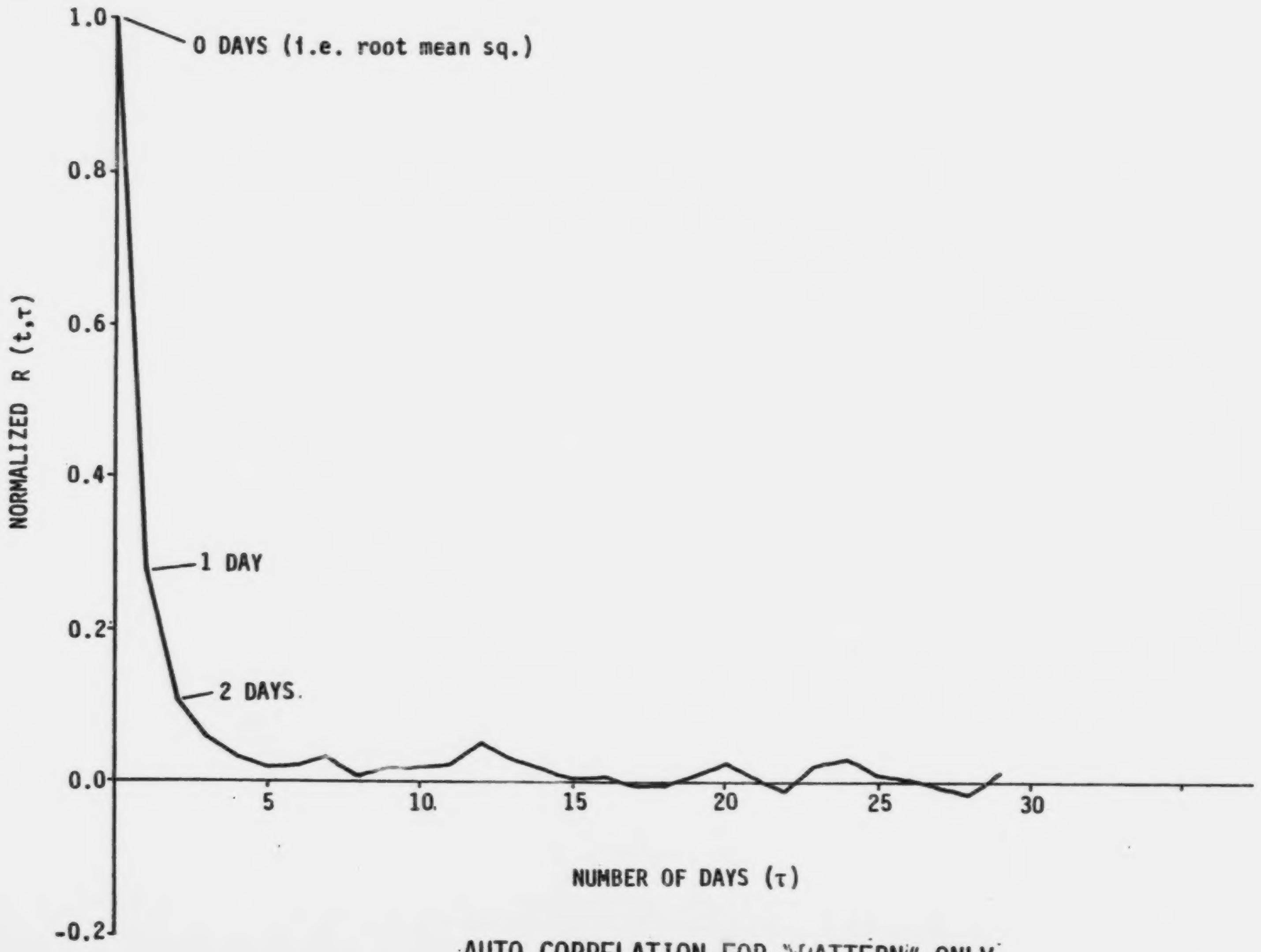

AUTO CORRELATION FOR "PATTERN" ONLY

360

little stronger than that for the form and intensity together. This seems reasonable as it can be expected that wind fields would be somewhat more stable than intensities.

The second step in the correlation analyses was to use a statistical test to determine if the occurrences of weather patterns were independent events or were correlated to the previous days' weather.

Using the first-order transition matrix as a contingency table, a chi square statistic was generated for the table using the method outlined by Freund, et al. (1960). Based upon this statistic, it was concluded that there is some correlation between the present day's weather and the previous day's weather, i.e., the null hypothesis that there is no correlation can be rejected with 95 percent confidence.

4.0 COMPARISON OF FIRST- AND SECOND-ORDER MATRICES AND THE WEATHER CATALOG

The third step in comparing the transition matrices and the weather catalog consisted of calculating the probabilities that three-day sequences would occur using three different methods.

As a first approach, each day's weather was assumed to be an independent event. The frequency of occurrence of each weather pattern was calculated from the historical data. The following analysis assumed that the initial weather pattern was 14.

A 13 x 13 matrix of probabilities was then generated using:

$$P'_{14,A,B} = P(14) \times P(A) \times P(B) \qquad (4.1)$$

TABLE 4.1
PROBABILITY OF WEATHER PATTERN SEQUENCES

1 - P(14) x P(A) x P(B)
2 - P(14) x P(A/14) x P(B/A)
3 = P(14,A) x P(B/14,A)

INITIAL SEQUENCE	TYPE	14	15	16	22	23	25	26	31	33	42	43	45	53
14 14	1	.00037	.00040	.00005	.00012	.00054	.00058	.00004	.00005	.00026	.00069	.00045	.00032	.00125
	2	.01270	.00183	.00006	.00051	.00339	.00252	0.00000	.00012	.00012	.00264	.00150	.00030	.00429
	3	.01321	.00152	.00015	.00045	.00376	.00270	0.00000	.00030	.00030	.00285	.00061	.00015	.00436
14 15	1	.00040	.00043	.00006	.00013	.00059	.00063	.00004	.00006	.00029	.00075	.00049	.00035	.00136
	2	.00039	.00168	.00009	.00021	.00052	.00016	.00005	.00001	.00006	.00027	.00024	.00013	.00052
	3	.00059	.00193	0.00000	.00015	.00059	.00015	0.00000	0.00000	0.00000	.00015	0.00000	0.00000	.00074
14 16	1	.00005	.00006	.00001	.00002	.00008	.00008	.00001	.00001	.00004	.00010	.00006	.00005	.00017
	2	0.00000	.00001	.00001	.00001	.00001	.00001	0.00000	0.00000	.00002	.00001	.00001	.00001	.00003
	3	.00010	0.00000	0.00000	0.00000	0.00000	0.00000	0.00000	0.00000	0.00000	0.00000	0.00000	0.00000	0.00000
14 22	1	.00012	.00013	.00002	.00004	.00018	.00019	.00001	.00002	.00009	.00023	.00015	.00011	.00041
	2	.00008	.00011	.00003	.00020	.00005	.00008	.00002	.00002	.00007	.00011	.00014	.00012	.00019
	3	.00030	0.00000	0.00000	.00030	.00015	.00015	0.00000	0.00000	0.00000	.00030	0.00000	0.00000	0.00000
14 23	1	.00054	.00059	.00008	.00018	.00080	.00086	.00006	.00008	.00039	.00102	.00067	.00048	.00184
	2	.00076	.00029	.00001	.00011	.00441	.00049	.00007	.00005	0.00000	.00097	.00021	.00040	.00025
	3	.00150	.00045	0.00000	0.00000	.00435	0.00000	.00015	0.00000	0.00000	.00075	.00015	.00015	.00060
14 25	1	.00058	.00063	.00008	.00019	.00086	.00092	.00006	.00008	.00041	.00109	.00071	.00051	.00197
	2	.00014	.00027	.00005	.00007	.00017	.00265	.00002	.00002	.00021	.00032	.00025	.00012	.00167
	3	.00015	.00030	0.00000	0.00000	.00015	.00405	0.00000	0.00000	0.00000	.00015	.00015	0.00000	.00105
14 26	1	.00004	.00004	.00001	.00001	.00006	.00006	0.00000	.00001	.00003	.00007	.00005	.00003	.00013
	2	0.00008	0.00000	0.00000	0.00000	0.00000	0.00000	0.00000	0.00000	0.00000	0.00000	0.00000	0.00000	0.00000
	3	0.00000	0.00000	0.00000	0.00000	0.00000	0.00000	0.00000	0.00000	0.00000	0.00000	0.00000	0.00000	0.00000
14 31	1	.00005	.00006	.00001	.00002	.00008	.00008	.00001	.00001	.00004	.00010	.00006	.00005	.00017
	2	.00001	.00002	0.00000	.00001	.00002	.00001	0.00000	.00010	.00001	.00002	.00004	0.00000	.00004
	3	0.00000	0.00000	0.00000	0.00000	0.00000	0.00000	.00015	0.00000	0.00000	0.00000	.00015	0.00000	0.00000
14 33	1	.00026	.00029	.00004	.00009	.00039	.00041	.00003	.00004	.00019	.00049	.00032	.00023	.00089
	2	.00001	.00001	.00001	0.00000	.00001	.00001	0.00000	0.00000	.00010	.00002	.00003	.00002	.00005
	3	.00030	0.00000	0.00000	0.00000	0.00000	0.00000	0.00000	0.00000	0.00000	0.00000	0.00000	0.00000	0.00000
14 42	1	.00069	.00075	.00010	.00023	.00102	.00109	.00007	.00010	.00049	.00130	.00085	.00061	.00235
	2	.00016	.00008	.00001	.00007	.00051	.00063	.00005	.00002	.00009	.00280	.00041	.00075	.00066
	3	.00030	.00030	0.00000	0.00000	.00030	.00030	0.00000	0.00000	0.00000	.00330	0.00000	.00060	.00120
14 43	1	.00045	.00049	.00006	.00015	.00067	.00071	.00005	.00006	.00032	.00085	.00056	.00040	.00154
	2	.00010	.00029	.00007	.00007	.00021	.00023	.00001	.00005	.00015	.00047	.00118	.00017	.00053
	3	.00075	.00015	0.00000	0.00000	.00015	.00060	0.00000	.00015	0.00000	.00015	.00105	0.00000	.00060
14 45	1	.00032	.00035	.00005	.00011	.00048	.00051	.00003	.00005	.00023	.00061	.00040	.00029	.00110
	2	0.00000	.00001	.00001	.00002	.00003	.00007	.00001	.00001	.00004	.00014	.00006	.00022	.00003
	3	0.00000	0.00000	0.00000	0.00000	0.00000	0.00000	0.00000	0.00000	0.00000	.00014	0.00000	.00028	.00028
14 53	1	.00125	.00136	.00017	.00041	.00184	.00197	.00013	.00017	.00089	.00235	.00154	.00110	.00423
	2	.00047	.00073	.00007	.00020	.00016	.00069	.00004	.00008	.00061	.00048	.00078	.00019	.00566
	3	.00045	.00030	0.00000	.00015	.00015	.00135	0.00000	0.00000	0.00000	0.00000	.00045	.00015	.00720

BEST DOCUMENT AVAILABLE

TABLE 4.2
PROJECTED NUMBER OF OCCURRENCES OF GIVEN SEQUENCES
BASED UPON A 19-YEAR RECORD (6,663 DAYS)

1 - P(14) x P(A) x P(B)
2 - P(14) x P(A/14) x P(B/A)
3 - P(14,A) x P(B/14,A)

INITIAL SEQUENCE	TYPE	14	15	16	22	23	25	26	31	33	42	43	45	53
14 14	1	2.4	2.7	.3	.8	3.6	3.9	.3	.3	1.7	4.6	3.0	2.2	8.3
	2	84.6	12.2	.4	3.4	22.6	16.8	0.0	.8	.8	17.6	10.0	2.0	28.6
	3	88.0	10.1	1.0	3.0	25.0	18.0	0.0	2.0	2.0	19.0	4.0	1.0	29.1
14 15	1	2.7	2.9	.4	.9	3.9	4.2	.3	.4	1.9	5.0	3.3	2.4	9.0
	2	2.6	11.2	.6	1.4	3.4	1.1	.3	.1	.4	1.8	1.6	.8	3.5
	3	4.0	12.8	0.6	1.0	4.0	1.0	0.0	0.0	0.0	1.0	0.0	0.0	4.9
14 16	1	.3	.4	0.0	.1	.5	.5	.8	.0	.2	.6	.4	.3	1.2
	2	0.0	.1	.1	.1	.1	.1	0.0	0.0	.1	.1	.1	.1	.2
	3	.7	0.0	0.0	0.0	0.0	0.0	0.0	0.0	0.0	0.0	0.0	0.0	0.0
14 22	1	.8	.9	.1	.3	1.2	1.3	.1	.1	.6	1.5	1.0	.7	2.7
	2	.5	.7	.2	1.3	.4	.5	.1	.2	.5	.7	.9	.8	1.3
	3	2.0	0.0	0.0	2.0	1.0	1.0	0.0	0.0	0.0	2.0	0.0	0.0	0.0
14 23	1	3.6	3.9	.5	1.2	5.3	5.7	.4	.5	2.6	6.8	4.4	3.2	12.2
	2	5.1	1.9	.1	.7	29.4	3.3	.5	.3	0.0	6.5	1.4	2.7	1.7
	3	10.0	3.0	0.0	0.0	29.0	0.0	1.0	0.0	0.0	5.0	1.0	1.0	4.0
14 25	1	3.9	4.2	.5	1.3	5.7	6.1	.4	.5	2.8	7.3	4.8	3.4	13.1
	2	1.0	1.8	.3	.5	1.1	17.6	.1	.2	1.4	2.1	1.7	.8	11.1
	3	1.0	2.0	0.0	0.0	1.0	27.0	0.0	0.0	0.0	1.0	1.0	0.0	7.0
14 26	1	.3	.3	0.0	.1	.4	.4	0.0	0.0	.2	.5	.3	.2	.9
	2	0.0	0.0	0.0	0.0	0.0	0.0	0.0	0.0	0.0	0.0	0.0	0.0	0.0
	3	0.0	0.0	0.0	0.0	0.0	0.0	0.0	0.0	0.0	0.0	0.0	0.0	0.0
14 31	1	.3	.4	0.0	.1	.5	.5	0.0	0.0	.2	.6	.4	.3	1.2
	2	.1	.1	0.0	.1	.1	.1	0.0	.6	.1	.1	.3	0.0	.3
	3	0.0	0.0	0.0	0.0	0.0	0.0	1.0	0.0	0.0	0.0	1.0	0.0	0.0
14 33	1	1.7	1.9	.2	.6	2.6	2.8	.2	.2	1.3	3.3	2.2	1.5	5.9
	2	0.0	.1	0.0	0.0	.1	.1	0.0	0.0	.7	.2	.2	.1	.4
	3	2.0	0.0	0.0	0.0	0.0	0.0	0.0	0.0	0.0	0.0	0.0	0.0	0.0
14 42	1	4.6	5.0	.6	1.5	6.8	7.3	.5	.6	3.3	8.7	5.7	4.1	15.6
	2	1.1	.5	.1	.5	3.4	4.2	.3	.1	.6	18.7	2.7	5.0	4.4
	3	2.0	2.0	0.0	0.0	2.0	2.0	0.0	0.0	0.0	22.0	0.0	4.0	0.0
14 43	1	3.0	3.3	.4	1.0	4.4	4.8	.3	.4	2.2	5.7	3.7	2.7	10.2
	2	.7	2.6	.5	.5	1.4	1.5	.1	.4	1.0	3.1	7.9	1.2	3.5
	3	5.0	1.0	0.0	0.0	1.0	4.0	0.0	1.0	0.0	1.0	7.0	0.0	4.0
14 45	1	2.2	2.4	.3	.7	3.2	3.4	.2	.3	1.5	4.1	2.7	1.9	7.3
	2	0.0	.1	.1	.1	.2	.5	0.0	0.0	.3	.9	.4	1.5	.6
	3	0.0	0.0	0.0	0.0	0.0	0.0	0.0	0.0	0.0	.9	0.0	1.9	1.9
14 53	1	8.3	9.0	1.2	2.7	12.2	13.1	.9	1.2	5.9	15.6	10.2	7.3	28.2
	2	3.1	4.9	.5	1.4	1.1	4.6	.3	.5	4.1	3.2	5.2	1.3	37.7
	3	3.8	2.0	0.0	1.0	1.0	9.0	0.0	0.0	0.0	0.0	3.0	1.0	48.0

where A is the first day's weather, and
B is the second day's weather.

The second approach was to use a first-order transition matrix. Again, the initial weather pattern was assumed to be 14. A second 13 x 13 matrix was generated using:

$$P''_{14,A,B} = P(14) \times P(A/14) \times P(B/A) \qquad (4.2)$$

The third approach was to use a second-order transition matrix. This time it was assumed that the initial weather conditions were specified by 14,A where A is any one of 13 patterns. The third 13 x 13 matrix was generated using

$$P''_{14,A,B} = P(14,A) \times P(B/14,A) \qquad (4.3)$$

The results are presented on Tables 4.1 and 4.2.

In addition, an inquiry was made into the difference between the first- and second-order matrices with respect to the probabilities each associated with similar events. The matrices were compared in two ways. First, the mean and standard deviation were calculated for the differences between each; i.e.,

$$P''_{14,A,B} - P''_{14,A,B}.$$

Overall, the average difference between these is 0.896 days with a standard deviation of 1.462 days.

The most important finding, however, is the fact that 83 3-day sequences of weather patterns are generated by the first-order transition matrix which have not occurred in historical data or as a result of using the second-order transition matrix.

The use of a first-order transition matrix which generates non-observed patterns could have significant effects on the results of an oil spill trajectory analysis. The above finding is especially important since only the sequences beginning with "14" were examined. It is probably safe to assume that weather sequences beginning with other patterns would produce similar results; i.e., 13 x 80 = 1,040 sequences, or 15 percent of the total in this case, which are generated but do not occur. Since the results of the oil spill trajectory analysis are strongly related to the sequences of weather patterns, it would be important to eliminate those sequences of weather patterns which have not occurred historically. This argument becomes more critical when considering results of the auto correlation function, which showed some correlation after two days.

5.0 CONCLUSIONS AND RECOMMENDATIONS

Based upon this analysis, the following conclusions have been reached: (1) use of a first-order transition matrix is an improvement over assuming each day is a random event; (2) use of a second-order matrix is an improvement over the first-order matrix because it eliminates the generations of patterns which historically have not been observed.

There is a definite tradeoff between the accuracy with which a transition matrix can be characterized from a given data base and the number of unrealistic weather pattern sequences which are tolerable. It has been shown that a first-order matrix generates a large number of sequences which, historically, have never occurred. On the other hand, it has been demonstrated that the entries in the first-order matrix are statistically more efficient than those in a second-order matrix. Unfortunately, the question of "How much data is necessary to accurately define a transition matrix?" has not been resolved. However, it has been demonstrated that if enough data is available, a second-order matrix is much preferable to a first-order matrix, simply because of the unrealistic sequences generated by the first-order matrix and the possible effects this may have on oil spill trajectories.

This last conclusion should be tempered with the type of oil spill trajectory study being conducted and the relative importance of other environmental factors. For example, if a first-order transition matrix generates unobserved wind field sequences, the total wind-drift vector will be the same for an observed sequence having the same wind fields. The question still remains as to whether or not unobserved sequences would generate significantly different oil spill trajectory results. If an oil spill trajectory study were conducted in a hindcast-stochastic mode, then the possibility exists that only minor differences would result from using a first- or second-order wind field transition matrix. Where the difference becomes critical would be the use of a first-order transition matrix in a forecasting-stochastic mode where unobserved sequences would give, over the short-term (2 to 3 days), erroneous probabilities and locations for trajectory movement.

If the environmental fields other than wind (tides and net currents) are significant, then unobserved wind field sequences could lead to trajectory end points different than those produced by observed sequences containing the same wind fields. The wind drift vector would combine with net and tidal currents having different gradients and phasing in strength and direction and could result in radically different paths and end points.

The trajectory study presented in Dames & Moore (1980) used historically observed sequences and, therefore, is not subject to the concerns expressed above. However, the methodology used was cumbersome and really only applicable to the hindcast-stochastic mode of operation required for the risk assessment study. In order to take advantage of the efficiency afforded by a transition matrix approach and to be able to operate in a forecasting-stochastic mode, the following recommendations are made:

- Perform a comparison between the end-point locations of trajectories calculated using a first- and second-order wind field transition matrix, as well as those calculated using a random access to historically sequence observed wind fields.

- These comparisons should be performed from launch sites in at least two areas characterized by relatively strong and weak net and tidal current strength and gradients.

- Investigate the frequency of occurrence and wind drift differential associated with 2- or 3-day forecasts containing unobserved sequences generated by a first-order transition matrix compared to a second-order transition matrix.

Completion of the above recommended studies will provide answers to key remaining questions and will lead to more accurate implementation of wind field variability in future oil spill trajectory and/or dispersion studies. The results should also aid in developing simplified strategies in implementation of oil spill contingency plans through knowledge of the relative strength of environmental fields and their resultant effect on surface transport.

REFERENCES

Dames & Moore, 1980. Final Report, Task I, Oil Spill Trajectory Simulation, Lower Cook Inlet and Shelikof Strait, Alaska, for the Bering Sea, Gulf of Alaska Project Office, Outer Continental Shelf Environmental Assessment Program, Job Number 06797-014-88.

__________, 1979. Report, Oil Spill Trajectory Analysis, Lower Cook Inlet, Alaska, for National Oceanic and Atmospheric Administration, Job Number 06979-011-02.

__________, 1976. Report, Oil Spill Trajectory Analysis, Lower Cook Inlet, Alaska, for National Oceanic and Atmospheric Administration, Job Number 06797-003-20.

Freund, John E., Paul E. Livermore, and Irwin Miller, 1960. Manual of Experimental Statistics. Prentice-Hall Mathematics Series, Prentice Hall Inc.

Putnins, P., 1966a. Studies on the Meteorology of Alaska: First Interim Report (The sequences fo baric weather patterns over Alaska). U.S. Dept. of Commerce, ESSA/EDS, Silver Spring, Maryland.

__________, 1966b. Unpublished tabultion of daily baric weather types for Alaska from January 1, 1945 to March 31, 1963, University of Alaska.

__________, 1969. Studies on the Meteorology of Alaska: Final Report (Weather situations in Alaska during the occurrences of specific baric weather), U.S. Department of Commerce, ESSA, Research Laboratories, Boulder Colorado, 80302, 267 p.

APPENDIX A

WIND FIELD & INTENSITY CATALOG INPUT DATA FILE

Input Data File Format: Wind Field and Intensity Catalog

			ASSIGNED DAILY WIND FIELD & INTENSITY FACTOR																														
YR	MO	DA	1	2	3	4	5	6	7	8	9	10	11	12	13	14	15	16	17	18	19	20	21	22	23	24	25	26	27	28	29	30	31
XX	XX		XX	XX	XX	XX	XX	XX	XX	XX	XX	XX	XX	XX	XX	XX	XX	XX	XX	XX	XX	XX	XX	XX	XX	XX	XX	XX	XX	XX	XX	XX	XX

INTENSITY FACTOR (VALUES 1→6) } SEE TABLE II
WIND FIELD (VALUES 1→5)

BEST DOCUMENT AVAILABLE

```
45  1 00532223422314532542532553535314232342422525232542424242225254253
45  2 0023232314535353435353531523424242454553435343452253424245000000
45  3 0045424253435353535353534353535314535353535353532214535353534542
45  4 002323231515154545224545225315222353535314151522162315151414535300
45  5 0031535323232323232314535353532342424242424242434342424242424342
45  6 00435353534242252525255333232326264242535353333533333163353535300
45  7 0053422323232323232315535353334245224353533353535316535345453323
45  8 0023424243151653333353535343535353434323424245435353535343434242
45  9 00533353535353534345225353534553434322152323454542424242424553535300
45 10 0053312525535353535353533153531633252553535325251515234525252553
45 11 0022531515424242252243231414231414535353222253535353151515151500
45 12 0053151415151514142323252522141442424242424242223231453535353531414
46  1 0053255353535314141414424523234242535342452553333454242424342251453
46  2 0053141415151515151542422553532525534253142315232314141425000000
46  3 0053422525152253535314535314252553531453535353535353435323234553
46  4 0043144553535353141453145353535353532553535325254245535353535300
46  5 0053454353534242454545453153535353424542424243144343421414154223
46  6 004242154242424242434342424245452222224242424242531542424242424200
46  7 0042333343434223424245534515453315434343424242454343532245535316
46  8 00335343434333333334545455353454553534322223131434545453131224542
46  9 0031312323454345454523255353532325255353531516531414431522151400
46 10 00145353452553533334353535342424542535353535353535316452525535353
46 11 00252533533333353535343535315232323232323232345455323231522431600
46 12 0053151522535315152215152315151443535353434325155342424214151445
47  1 0042532225432526154533154243255353145353141453531515152323232323
47  2 0014141414144242422323232314144245454545421442424245454223000000
47  3 0023232353535314141614145353531423234242535353532242255323141414
47  4 002323141453252553535342424242422323151443535353431453535353535300
47  5 0025334245255325255314234353535343535342434545254545424242422323
47  6 0014141453434223235353422553333333535343434333453333154343531500
47  7 004353434243434343434315454545424242424242424242434333423353434553
47  8 0053434342422642454243454342434343424243152323234253535353535353
47  9 0053534333535353535353535333531542535343235315431522453131434300
47 10 00532216454542535353535353535353535353535325535353535353535316151525
47 11 00433342434353334553435353535353535353424242254245255342425343420 0
47 12 00424242532553535353532553145353252553535353535353335353145314532 5
48  1 0025253353535353535314421414252542422525252525254245535315142525
48  2 0045432323232323234242432323531423232323231414235353141425250000
48  3 0014231514142323234515535325255353533353532515232345455343425342
48  4 0023232343434315234342434543431515222243225353155343434316151500
48  5 0053531414535353142525535315155314535353533333531525454553434343
48  6 005353432245535342234243424242424242424543434343424243533333433300
48  7 00333333424553431643435353454242424553535343435353335353535333 53
48  8 0045454553333353434242434345454333434343424243431642161631313143
48  9 0053223353535342165333434242423353535353252553432553424545422500
48 10 002553535333333535353535353534245535353534353535353535353535353
48 11 0042535353434343433342535353535314221414141414141515262614141400
48 12 0053152222141414224253532645535342533333434353154525535353531515
49  1 0014142553251542454242434343432525424545164245262626422642454245
49  2 0015232343531443141523424343431515232342421414234242421414000000
49  3 0014252525424342454245452323232323232323422543255353535353535325
49  4 0053535353535315161553141443145353535353531514141453535353335300
49  5 0053535353155323231414535333334542454242424242434342424243535353
49  6 0025255333155333221633255333334242435353535343432343161653195300
49  7 0043434343434245264242425333334542454333333333333435353323431653
49  8 0053162222333333533353435315163333534342422525334533532542425353
49  9 0053535353534343422345425353535353533325535353535353535342232500
49 10 00454525255353142525535353534545452645255535345535353535353535353
49 11 0053531515222243434545431543232323232345255353151545454515434300
49 12 00154315152253532253434253532223232323232314141442252522 2141453
50  1 0045424325232343432323234523232323312323232323234323232323232323
50  2 0043232322221515141414141414141422232222314231141414144242000000
50  3 0025255353434242424242424242425353535353535353532253535343155325
50  4 0014152226451645455325255333333353532553533314535314141453535300
50  5 0053155353335325255353535353531414435333333343425353535333333315
50  6 0015151642424233334333144242424253424525425333423353432216161500
50  7 0042424242234214424245454342144242434333222322425333333333534343
50  8 0043424533424242424242226422323234245234242422525252553535333326
50  9 005353225535333532525453333424242452525535342535353333334545452500
50 10 00252525252323144325535353534553422245255253455353333335353315353
```

BEST DOCUMENT AVAILABLE

```
50 11 0053531523222243224545431543232323262645252222151526222215434300
50 12 0053531515225353142543452553532626142323231414142345252522144353
51  1 0053141442422525255353435315151414141553151515152623232323232342
51  2 0014141414142314142323454245424225535315424225252322251643000000
51  3 0023232323262323232314532553532653151423534314535325255353141442
51  4 0042255353252525532315154342424242452623234242144325252525255300
51  5 0043434242232323232323232314532553452525252553535342424242454242
51  6 0042424242424243431453535353534545454245424343434323424245454300
51  7 0042424242333342452323424223434245434233535353151543434315155331
51  8 0015535353454545434242252525535331534342225353334242252525434323
51  9 0023235325535353235353255353534515252542454223232314145322535300
51 10 0053333353535353531414151522232323232342424242234253333342424242
51 11 0025535325455325251442535322334316532545424242532525255353532500
51 12 0053535353151514142342432323532223234253334242432342434342452525
52  1 0033432553141514151523425342234253154343431414231425252542142323
52  2 0053535314234242422525151414141442424245425342535314454543450000
52  3 0045231414144242424345425325455353151514144253252553535353151515
52  4 0015151515424242422553155353535325255343252553534225534343532200
52  5 0022434333535315144323141553434226422533335315434343454225434353
52  6 0053535353333434545424242223434343432314434343434343434553434300
52  7 0053433345454253334242424225331543432515422342424243424343334316
52  8 0016454345454242424245431515151543535353531516533343141442424225
52  9 0053421515151542425353155353141414535322451514232325252553531400
52 10 0014144242535343434353531522454553332253532514532345162242255314
52 11 0053535342424242252553532553142525252553422543254545422314231400
52 12 0014252514535353535353535353535353152523232525252525252553255353
53  1 0053534242424542232323141423141423232553535353152314231414141414
53  2 0053535343141414252543422542255353534225254342422525254225000000
53  3 0053421414141415151414312645252553535314532525235353535325255315
53  4 0042535353531515232323232314144253254225535343432325252525231400
53  5 0023142314431414535343145353435323255353252543434342424243424242
53  6 0042234223145343434343534345454553431515151515151515151523434300
53  7 0043434343434331535343151515535315333343434242424223234242424242
53  8 0042535353434533433333434343535315432243434533333333333353535353
53  9 0043161653535353422626535353424253533333535353535353531515232300
53 10 0014141414252553535353532525535353535353535353531453531414141453
53 11 0053531553262622422223232553535353535353421425252525255353424500
53 12 0045255353535353535353535314224223142323234225532553421414235314
54  1 0053141414145353535343262626232323232323232323232323231443435353
54  2 0042535325255333332323232314141523144343163131435315151442000000
54  3 0042531622332225531553535315154522151545454343151523232323232323
54  4 0023231543152343151423155333535353434314141515151523234545252500
54  5 0022252553222525424542424243432323232325434315141433144325255323
54  6 0053534342424542424525435353535333422345163333333333435331454200
54  7 0042423353434343313133433323224242535331535333434343424543424553
54  8 0031313131424245454553535343433143434545434345454343164533424533
54  9 0045453325313116224343151442454243314343435353535315434242454200
54 10 0042422323231414252553533325252525535353535345455322534225252553
54 11 0053432553535342231414232314145353535353535353452553164531154200
54 12 0053431526435353532525535315533131312315535353151515151443313122
55  1 0043255315142542452553424242532514142525532553532525424242141414
55  2 0042535325151515144223535315531543434343432342424242421523000000
55  3 0015424225252515425353152342455345334242224242424225255353142525
55  4 0015144215151515535353222214531545423353535353535314141442532500
55  5 0042423142532553435353434242424242255353534342452525255353434242
55  6 0053431553334223255353533333333343314343422531254242535353534300
55  7 0042454543434343422525535345434533333342424342424545535353431515
55  8 0042434343535353532553534353225353154331333343252553333333332325
55  9 0025533315424242424253535353535322222242424545534323454553252500
55 10 0022252553535353151553255333535353535353534525252553531515151523
55 11 0023232343431553531542424214141415151553531423264242262642535300
55 12 0053141414232314255315264543234242532323231516152343264331151525
56  1 0015265315232253221523232323232315154315252525251523234245452215
56  2 0025534242434343531515152323422525531515232345535353252515530000
56  3 0015151515141515152342454542532525252542424225251523142214141443
56  4 0014535353151414532525255353535342255353232323454242424242424200
56  5 002525422232342535353535342535353535314535353534245452543535343
56  6 0053534545535353252543434343423353155353255331313131151553434223 00
56  7 0023232131313143151523232323232331151553425353422323234543434343
56  8 00153333151643223123424242422252553535353535353535353422553535343
56  9 0043424242534225424245424545332222435353535353431414424522255300
```

BEST DOCUMENT AVAILABLE

```
56 10 0053535353535322222253534325535353155322531414142222432553531515
56 11 0016255353152314145353151514434353142553252553534242255325162300
56 12 0015232323232342151415232323422323141525144343313131314242535323
57  1 0023254243151523422323232323232323232323422323232345454242452323
57  2 0023424242424343535315152325431514424242232323232525254325000000
57  3 0043251425141414142525151514434242255333334315151414331423232323
57  4 0025161523424245454242454545154542424223421414144253535314232300
57  5 0023232342424223234242232323144225252525255343434323141453431442
57  6 0042424242232323254342252525333316252515151553533325165353434300
57  7 0043433333333316332545424533254545454533334343535343432215151542
57  8 0042424545333315424243435353424242223333333151515234242425333325
57  9 0042452542255343434343422533454223422553434315235315155353531500
57 10 0016422342424523432516165333424242421553234545452243432325253343
57 11 0025252525334545232323252525254242252545454214425353255325255300
57 12 0025253325252525333454533333535314141414252525255315142525141553
58  1 0015231443252525331414232323255353152553254242252543252523232323
58  2 0042424223232323232323232314142323232323252523232325231442000000
58  3 0042254315453314141442424523162323232345535322531414141414142525
58  4 0025141423424223142323255325252553535322432323454545452323234200
58  5 0014145353535353535353142314535325434545452525424342422323232342
58  6 0042424242424242424325252533425333234242253333334343333333333300
58  7 0053165342424242534353434225333315534253533325535323232525333343
58  8 0043535353535353424353252525255353535353154253535353334322333333
58  9 0033455315161633224242434233531515333535353533325255353431514200
58 10 0025255343433333422222151522455353532525151545142225531522532553
58 11 0053535325252553531515151515454525535315152245424242252531231400
58 12 0053534542232323232323144223232323232323252525255353234315151515
59  1 0023235353531515151515152323151515152323232314141414142525424242
59  2 0025254543152342432343532345454525425353434315252525252553000000
59  3 0043251514145353531515151515151553531515153153141414235325535325
59  4 0025255315531515252553254243431514431414142323454253533333454500
59  5 0045454542251425255353311414142525252523151542454342234243434343
59  6 0025254353532525151522154242454245452323235353333315155333432200
59  7 0033535325334322223333535353535353532222435353534333434343435353
59  8 0043231515155333153342234543251445454553533333434342454353535353
59  9 0053435353535343232515152245425353141414314343254353434245252500
59 10 0033334223232323231414145353534316232323422525535342252543254353
59 11 0033144242535353333323234542454542252525535325534242422525532500
59 12 0053534215155353435353534325252515222514535353535315534325534242
60  1 0042424225255343455353535353535325424223232314232323422323252525
60  2 0053252525252525255353535325252545454522224245424223232323230000
60  3 0023232323231515152353531415532525255315232314421414151423231425
60  4 0053531515535342425353432525252353155353535343535353232323141400
60  5 0023421415232325533316252525251423232353252345252525142523315353
60  6 0053433323234243434353533333535353531543421422224542253325535300
60  7 0053535353535333424215152323232553535333424242424343435353533333
60  8 0033535333253333431515424242424353535353334533333345254553531553
60  9 0043252525155322434353252525434525532542424225252533534543234500
60 10 0033333325254353434253141414252525422322262525252525252553532525
60 11 0053531425535323424226141414145325252525535315151515224222532600
60 12 0026333314424225252525532553424242422323232525252526424242255314
61  1 0014252525255314141423232325252525422342424242454545142323232322
61  2 0053535353255353535353141414141414141414142314251543532525000000
61  3 0025531423232525232323252543155353532525232314141414141423232525
61  4 0053531443434253434533533343535325535353434245424545531514232300
61  5 0023234223424223262345532214144553532553535314535342425353534242
61  6 0042533353532525531525252553531515151553533143535353533342424200
61  7 0043535352531653535322433343533345535353334343454245454245424245
61  8 0043334525535353534245425315433253424545455353533333535325532553
61  9 0053535333452525534545252553535353534233252525252533234545535300
61 10 0053535353535342252515141515151514535345452553535353535353254315
61 11 0045451442534315535353532225434225535342535353154253262323422500
61 12 0025535315434215454545252525152515152323261415141515531543432325
62  1 0025162522151523234222152345224515232323232345432315231515151525
62  2 0053532342424242535353531423232323234545421542234242232323000000
62  3 0023422242454553534542231415531415155343151515232525142525422342
62  4 0045421425151522431553161515155343151525251553153333335343434300
62  5 0015151542422342454245422553434225334542333345333345452515151533
62  6 0033353435353533334542454532254343431515151543253353533333534200
62  7 0042234243424542424525255353425342424242532214424245424242424245
```

BEST DOCUMENT AVAILABLE

```
62  8 0045422553534345333315254242452342434325253333535333454542451643
62  9 004253534215144215331633335353535342232525252525225333353152500
62 10 0053331633334225251515151514142553333353533345424225532325232323
62 11 0023424242252325252525151523231442422525435353232525531553252500
62 12 0053532515155323232342252525252553145353252323452315232323232323
63  1 0023432515251543432323424222454545454242422342424242232323232323
63  2 0073151515252525251543232323231515422525252525252325252525000000
63  3 0025234253254242425345154253153314252553152233152245431515232323
```

TABLE A-1

ANNUAL 13 x 13 WIND FIELD TRANSITION MATRIX

Given Wind Field	Probability of Listed Wind Field Following Given Wind Field												
	14	15	16	22	23	25	26	31	33	42	43	45	53
14	0.423	0.061	0.002	0.017	0.113	0.084	0.000	0.004	0.004	0.088	0.050	0.010	0.143
15	0.089	0.389	0.021	0.048	0.119	0.037	0.012	0.002	0.015	0.062	0.056	0.029	0.121
16	0.015	0.104	0.104	0.060	0.060	0.060	0.000	0.030	0.149	0.060	0.060	0.090	0.209
22	0.063	0.089	0.025	0.165	0.044	0.063	0.013	0.019	0.057	0.089	0.114	0.101	0.158
23	0.095	0.036	0.001	0.014	0.550	0.061	0.009	0.006	0.000	0.121	0.026	0.050	0.031
25	0.024	0.046	0.008	0.012	0.028	0.444	0.003	0.004	0.036	0.053	0.042	0.020	0.280
26	0.082	0.020	0.000	0.041	0.122	0.020	0.245	0.000	0.020	0.204	0.041	0.122	0.082
31	0.030	0.075	0.015	0.030	0.075	0.030	0.015	0.343	0.030	0.060	0.149	0.015	0.134
33	0.026	0.044	0.018	0.015	0.029	0.050	0.003	0.000	0.355	0.085	0.109	0.076	0.191
42	0.026	0.013	0.002	0.011	0.081	0.101	0.008	0.003	0.014	0.448	0.066	0.120	0.106
43	0.029	0.083	0.020	0.020	0.058	0.065	0.003	0.015	0.041	0.133	0.333	0.049	0.150
45	0.007	0.021	0.012	0.028	0.036	0.104	0.009	0.009	0.062	0.194	0.083	0.308	0.126
53	0.046	0.072	0.007	0.020	0.016	0.068	0.004	0.008	0.060	0.047	0.077	0.019	0.557

TABLE A-2

WINTER 13 x 13 WIND FIELD TRANSITION MATRIX

Given Wind Field	Probability of Listed Wind Field Following Given Wind Field												
	14	15	16	22	23	25	26	31	33	42	43	45	53
14	0.462	0.066	0.003	0.020	0.114	0.100	0.000	0.003	0.003	0.080	0.034	0.006	0.111
15	0.104	0.404	0.010	0.055	0.153	0.039	0.020	0.003	0.003	0.042	0.042	0.033	0.091
16	0.043	0.087	0.043	0.087	0.130	0.087	0.000	0.043	0.087	0.087	0.043	0.130	0.130
22	0.076	0.109	0.011	0.152	0.065	0.076	0.011	0.011	0.033	0.098	0.076	0.087	0.196
23	0.101	0.033	0.002	0.014	0.597	0.054	0.008	0.002	0.000	0.101	0.021	0.041	0.025
25	0.025	0.054	0.008	0.015	0.033	0.464	0.004	0.002	0.019	0.050	0.040	0.019	0.268
26	0.108	0.027	0.000	0.054	0.108	0.027	0.270	0.000	0.027	0.135	0.054	0.135	0.054
31	0.045	0.091	0.000	0.045	0.136	0.045	0.045	0.318	0.000	0.091	0.045	0.000	0.136
33	0.091	0.030	0.015	0.030	0.030	0.061	0.000	0.000	0.273	0.136	0.091	0.076	0.167
42	0.038	0.016	0.000	0.021	0.088	0.147	0.008	0.003	0.000	0.413	0.043	0.088	0.134
43	0.024	0.130	0.024	0.006	0.112	0.142	0.012	0.018	0.018	0.077	0.225	0.036	0.178
45	0.018	0.030	0.012	0.036	0.054	0.138	0.012	0.006	0.030	0.186	0.054	0.299	0.126
53	0.069	0.087	0.006	0.023	0.019	0.087	0.008	0.005	0.029	0.045	0.044	0.019	0.561

TABLE A-3

SUMMER 13 x 13 WIND FIELD TRANSITION MATRIX

Given Wind Field	Probability of Listed Wind Field Following Given Wind Field												
	14	15	16	22	23	25	26	31	33	42	43	45	53
14	0.317	0.048	0.000	0.008	0.111	0.040	0.000	0.008	0.008	0.111	0.095	0.024	0.230
15	0.066	0.368	0.038	0.038	0.071	0.033	0.000	0.000	0.033	0.090	0.075	0.024	0.165
16	0.000	0.114	0.136	0.045	0.023	0.045	0.000	0.023	0.182	0.045	0.068	0.068	0.250
22	0.045	0.061	0.045	0.182	0.015	0.045	0.015	0.030	0.091	0.076	0.167	0.121	0.106
23	0.082	0.041	0.000	0.014	0.447	0.078	0.009	0.014	0.000	0.164	0.037	0.068	0.046
25	0.022	0.033	0.007	0.007	0.018	0.410	0.000	0.007	0.066	0.059	0.048	0.022	0.300
26	0.000	0.000	0.000	0.000	0.167	0.000	0.167	0.000	0.000	0.417	0.000	0.083	0.167
31	0.022	0.067	0.022	0.022	0.044	0.022	0.000	0.356	0.044	0.044	0.200	0.022	0.133
33	0.011	0.047	0.018	0.011	0.029	0.047	0.004	0.000	0.375	0.073	0.113	0.076	0.196
42	0.017	0.011	0.004	0.004	0.076	0.069	0.008	0.004	0.025	0.472	0.082	0.143	0.086
43	0.031	0.064	0.019	0.026	0.036	0.033	0.000	0.014	0.050	0.155	0.377	0.055	0.138
45	0.000	0.016	0.012	0.024	0.024	0.082	0.008	0.012	0.082	0.200	0.102	0.314	0.125
53	0.024	0.057	0.007	0.018	0.013	0.050	0.000	0.011	0.091	0.049	0.108	0.018	0.553

TABLE A-4

ANNUAL 5 x 5 WIND FIELD TRANSITION MARIX

Given Wind Field	Probability of Listed Wind Field Following Given Wind Field				
	1	2	3	4	5
1	0.476	0.212	0.024	0.151	0.137
2	0.111	0.530	0.029	0.174	0.157
3	0.093	0.107	0.359	0.261	0.180
4	0.069	0.178	0.041	0.587	0.125
5	0.125	0.105	0.069	0.142	0.560

APPENDIX B

The methodology used in calculating the probability, p, that a random sample of size s will have a value of p differing from the true value, Θ, by any given amount is developed in the following paragraphs. Suppose the hypothesis, "The probability of occurrence of the sequence 14, 14, 23 is 0.124 within a 95 percent confidence," is to be tested. These limits are calculated using the normal approximation to the binomial distribution. It is known that $Z = (sp - s\Theta)/[s\Theta(1-\Theta)]^{1/2}$ is approximately N(0,1) and that the two symmetrical values of Z (95 percent of the whole area of the normal distribution is included between these values) are ± 1.96. (The area of the tails beyond $Z = \pm 1.96$ is 0.05.) If Θ is the true value of the parameter, then the following inequality exists with a probability of 0.95:

$$-1.96 \leq \frac{sp - s\Theta}{[s\Theta(1-\Theta)]^{1/2}} \leq 1.96 \qquad (2.1)$$

Equation (2.1) can be written as:

$$(sp - s\Theta)^2 \leq (1.96)^2 \; s\Theta(1-\Theta) \qquad (2.2)$$

or

$$s(p-\Theta)^2 \leq 3.84\Theta(1-\Theta) \qquad (2.3)$$

Collecting the terms in Θ and Θ^2, Equation (2.3) can be written as:

$$\Theta^2(s + 3.84) - \Theta(2ps + 3.84) + sp^2 \leq 0 \qquad (2.4)$$

For this example, s = 202, p = 0.124:

$$\theta^2 (205.84) - \theta((2(0.124)202) + 3.84) + 202 (0.124)^2 = 0 \qquad (2.5)$$

$$205.84\theta^2 - 53.936\theta + 3.106 = 0 \qquad (2.6)$$

Using the quadratic equation:

$$r = \frac{(53.936 \pm \sqrt{(53.936)2 - 4(205.84)\ 3.106}}{2\ (205.84)} \qquad (2.7)$$

With 95 percent confidence, the true value of θ is calculated to be between 0.0854 and 0.262. This means that given the same sample size (202), the number of occurrences could have ranged between 17 and 53 with 95 percent confidence.

Based on the converted weather catalog, there are a total of 477 sequences beginning with 14 and of these there are 40 occurrences of the sequence 14, 25. Using the methodology presented in Equation (2.5), the following relation is obtained for estimating the range of occurrences of 14, 25 that might be expected within a 95 percent confidence interval.

$$\theta^2(477+3.84) - \theta(2(0.0838)477 + 3.84) + 477\ (0.0838)^2 \qquad (2.8)$$

This, in turn leads to the results

$$r_1 = 0.0621 \qquad r_2 = 0.1121 \qquad (2.9)$$

I.e., $29 \leq 40 \leq 53$ with 95 percent confidence.

A similar process is carried out for a second-order matrix. Taking a sample size of 29 corresponding to the sequence 14 25, and looking at the occurrence of the sequence 14 25 is such that x = 13

$$\Rightarrow p = 0.448$$

$$\theta^2(29 + 3.84) - \theta(2(0.448)\ 29 + 3.84) + 29\ (0.448)^2 = 0 \tag{2.10}$$

with the results

$4_1 = 0.2839 \qquad r_2 = 0.624$

Thus, given the sample size of 29, the number of occurrences of the sequence 14, 15, 15 could vary between 8 and 18 with 95 percent confidence, i.e., $8 \leq 13 \leq 18$.

FINAL REPORT--TASK II
EVALUATION OF CODAR DATA
LOWER COOK INLET, ALASKA

BERING SEA-GULF OF ALASKA PROJECT OFFICE
OUTER CONTINENTAL SHELF ENVIRONMENTAL
ASSESSMENT PROGRAM

JOB NO. 06797-014-88
October 31, 1980

Los Angeles, California

BEST DOCUMENT AVAILABLE

October 31, 1980

Outer Continental Shelf Environmental
Assessment Program
Bering Sea - Gulf of Alaska Project Office
Post Office Box 1808
Juneau, Alaska 99802

Attention: Herbert E. Bruce, Ph.D.
OCSEAP Project Manager

Gentlemen:

Final Report--Task II
Evaluation of CODAR Data
Lower Cook Inlet, Alaska
Bering Sea - Gulf of Alaska Project Office
Outer Continental Shelf Environmental
Assessment Program

We are pleased to submit our final report on an evaluation of CODAR data taken in Lower Cook Inlet, Alaska. This report has incorporated and responded to comments received from your Juneau staff, as well as the Wave Propagation Laboratory in Boulder, Colorado.

It has been a pleasure to work on this phase of our 1980 fiscal year contract with your Juneau staff. Please do not hesitate to contact us if you have any questions regarding the contents or findings of this study.

Very truly yours,

DAMES & MOORE
Marine Services Group

Roger S. Schlueter, Ph.D.
Managing Principal

Charles I. Rauw

Charles I. Rauw
Project Manager

RSS:CIR:sms

CONTENTS

Section Page

1.0 INTRODUCTION 385

1.1 BACKGROUND 385
1.2 PURPOSE 385
1.3 SCOPE 386
1.4 OBJECTIVES 386

2.0 EVALUATION OF CODAR DATA 388

2.1 CODAR SYSTEM DESCRIPTION 388
2.2 DATA AND ANALYSES 389

3.0 RESULTS AND CONCLUSIONS 394

3.1 SURFACE DRIFT COMPARISON 394
3.2 TRAJECTORY COMPARISON 395
3.3 CONCLUSIONS 397

REFERENCES 399

APPENDIX A: METEOROLOGICAL DATA 414

LIST OF FIGURES

1. Current Meter Array Location and Range of CODAR Mapping 401

2. 24 hour Mean Surface Current Vectors for July 1, 1978 402

3. 24 hour Mean Surface Current Vectors for July 2, 1978 403

4. 24 hour Mean Surface Current Vectors for July 3, 1978 404

5. 24 hour Mean Surface Current Vectors for July 4, 1978 405

6. 24 hour Mean Surface Current Vectors for July 5, 1978 406

7. 24 hour Mean Surface Current Vectors for July 6, 1978 407

8. 24 hour Mean Surface Current Vectors for July 7, 1978 408

9. Tidal Current Ellipses for M_2 Constituent 409

10. Tidal Current Ellipses for K_1 Constituent 410

11. Tidal Current Ellipses for O_1 Constituent 411

12. Comparison of C-2 Data with CODAR Data 412

13. Comparison of C-5 Data with CODAR Data 413

LIST OF TABLES

I. 24 Hour Mean Wind Drift Estimates 392

II. 24 Hour Mean Net Current Data 393

1.0 INTRODUCTION

1.1 BACKGROUND

This report describes a limited evaluation of CODAR data acquired in Lower Cook Inlet, Alaska during the period July 1-8, 1980.

This work was performed under Contract No. NA80RAC00075 between Dames & Moore and the National Oceanic and Atmospheric Administration. In addition to the study reported herein, other studies performed under Contract No. NA80RAC00075 include an oil spill trajectory analysis for Lower Cook Inlet and Shelikof Strait, a conceptual oil spill modeling study for Lower Cook Inlet and Shelikof Strait, and a wind transition matrix analysis. These studies have been submitted under separate cover to OCSEAP.

This study was supported by the Bureau of Land Management through interagency agreement with the National Oceanic and Atmospheric Administration, under which a multi-year program responding to needs of petroleum development of the Alaskan continental shelf is managed by the Outer Continental Shelf Environmental Assessment Program (OCSEAP) Office.

1.2 PURPOSE

This study was initiated by the Outer Continental Shelf Environmental Assessment Program (OCSEAP) on behalf of the Bureau of Land Management (BLM). This is one of a series of studies conducted by Dames & Moore to investigate the behavior of hypothetical oil spills within the Alaskan Outer Continental Shelf. One class of information that BLM has requested OCSEAP to consider is the identification and development of new monitoring techniques.

One of the more promising and newly emerging oceanographic monitoring technologies, with direct application to pollutant transport patterns and oil spill modeling, is the Coastal Ocean Dynamics Application Radar (CODAR). This technology permits mapping of surface currents over rather large geographical areas of water. The advantage of this technology over more conventional means of determining surface currents for studies of pollutant transport and oil spill modeling is obvious. This study presents a limited comparison of CODAR generated data to traditionally measured data and their subsequent application in predicting resultant surface drift.

1.3 SCOPE

This study was conducted in accordance with the scope of services for Task II detailed in the Dames & Moore proposal, "Oil Dispersion Analysis, Lower Cook Inlet and Shelikof Strait, Alaska," RFx41-436-2905, for National Oceanic and Atmospheric Administration, July 19, 1979, "Proposal Addendum, Oil Spill Dispersion Analysis," RFx41-436-2905, August 22, 1979, and "Proposal Addendum, Oil Spill Dispersion Analysis," RFx41-436-2905, October 14, 1979, subsequently amended in a letter dated February 4, 1980.

1.4 OBJECTIVES

The primary elements of the scope of services relating to the evaluation of CODAR data presented in the above documents are summarized below:

1. Process CODAR data taken in Lower Cook Inlet during the period July 1-8, 1978 between Augustine Island and Cape Douglas to yield digital data products and vector diagrams of net and tidal surface current components.

2. Compare CODAR data to other directly measured current data and to the seasonally averaged patterns developed in Task I (Dames & Moore, 1980); include a discussion of computer trajectories in light of the CODAR data.

The comparison of CODAR data to local current meter data was performed to provide an indication of the validity of deriving surface currents from Eulerian, submerged meter data. In addition, a qualitative discussion comparing trajectories calculated using the seasonal patterns and those that might have been calculated using CODAR data was to be provided. The above objectives have been met and are reported on in the following sections of this report.

2.0 EVALUATION OF CODAR DATA

2.1 CODAR SYSTEM DESCRIPTION

CODAR is the acronym for Coastal Ocean Dynamics Application Radar which is a method of surface-current measurement and mapping using a shore-based high frequency (HF) radar system. In early 1975, Dr. Donald Barrick of the Sea State Studies Branch of the Wave Propagation Laboratories (WPL) obtained initial funding from the joint NOAA/BLM Outer Continental Shelf Environmental Assessment Program (OCSEAP) to design the CODAR system. During the summer and fall of 1976 initial field tests of the system were carried out in the Miami-Ft. Lauderdale area. The feasibility and utility of the HF radar system for operational near real-time mapping of surface currents in remote coastal locations was demonstrated in subsequent field tests conducted during 1977 and 1978. One of those field tests was conducted in the Augustine Island-Cape Douglas area during late June and early July, 1978 (see Figure 1). It is data from this period of operation that is discussed here.

The operation of the HF radar system is based on the theories of sea scatter physics involving the backscatter from moving ocean waves, which in turn are being transported by an underlying current field. The wave and current motions are detected by radar as frequency displacements of the received echo from the transmitted signal ("Doppler" shifts). The surface current is determined from analysis of the spectrum reflected from the ocean surface. The details of the theory, development, and application of CODAR are presented in the following representative sample of references; Barrick and Peake (1967), Barrick and Lipu (1979), Barrick, et al., (1977), Evans (1978).

2.2 DATA AND ANALYSIS

Processed CODAR data was obtained from WPL for the period from July 1 through July 8, 1978 (Frisch, 1980). These data consisted of vector plots of 24 hour mean surface currents provided at approximate 12 hour intervals. Reproduction of the eight 24 hour mean surface current maps are provided in Figures 2 through 8. In addition to mean currents, tidal current ellipses were also calculated from the processed CODAR data for the M_2, O_1, and K_1 constituents. These ellispes are presented in Figures 9 through 11.

The CODAR data was taken during the same period of time that intense meteorological and oceanographical field programs were being conducted by the Pacific Marine Environmental Laboratories (PMEL) in Lower Cook Inlet. Concurrent wind and current meter data was obtained from Reynolds (1980) and Schumacher (1980) and forms the basis for this limited comparison study.

Figure 1 shows the location of five of the nearest operational current meter arrays deployed by PMEL during the same period of time. Data from each near surface meter was reduced to daily (24 hr) mean net currents and tidal current constituents based on 29 day analyses. For subsequent analyses, the net current data was assumed to be void of any wind drift component. This allowed the surface drift component to be estimated using an empirical relationship based on the surface wind velocity. Vectorially adding the current meter net velocity gave an overall net surface velocity which was then compared to the CODAR generated net surface velocity (which presumably contained both the wind drift and non-wind drift components of net surface flow).

The meteorological data used in this analysis was supplied by PMEL and is included as Appendix A. Although meteorological station coverage was good in this area of Lower Cook Inlet during July 1-8, 1978, data recovery was rather spotty. Thus, the derived wind fields are not as reliable as one would want for a comparison such as this. The following paragraph presents a general discussion of the wind patterns that existed during the period of CODAR measurements and was, in part, extracted from Reynolds (1980).

Just preceding July 1-8, 1978, the local wind flow was influenced by air moving from the Bering Sea and across Iliamna Gap. This situation created winds blowing up Shelikof Strait and from the west-northwest across Kamishak Bay (see Appendix A) and is very similar to wind field 5 presented in Dames & Moore (1980). On the first and second of July, the weather pattern changed suddenly and the geostrophic wind direction turned southwesterly with a pressure force directed approximately down Shelikof Strait. Winds in Lower Cook Inlet suddenly switched to an easterly direction down the pressure gradient within the limits of topographic constraint. In Shelikof Strait the winds also blew down the pressure gradient switching to a northeasterly direction. This latter flow pattern basically persisted throughout the duration of the CODAR measurements. Appendix A presents the flow field for this weather pattern which is very similar to wind field 2 presented in Dames & Moore (1980).

Meteorological station data obtained from PMEL consisted of wind speed and direction for stations located on Shuyak Island and near Iliamna Lake, and direction only for the station on Augustine Island. Unfortunately, Data Buoy EB 46007, which was located in the middle of Lower Cook Inlet, near the area of CODAR coverage, was not operational during this period of time. Since no data was available to provide direct wind speed over the area of interest, a simplified approach was used to estimate the wind speed based on the wind speeds measured at Shuyak Island and Iliamna Lake. That is, relationships were derived from the relative magnitudes of the wind vectors presented in wind fields 2 and 5 from Dames & Moore (1980). It is readily apparent that this approach can be considered only a rough approximation as many factors affecting the local wind speed have not been considered.

Although many theoretical and empirical relationships have been developed for describing the surface drift due to wind stress, the approach used in Dames & Moore (1980) will be adopted for this study. This approach assumes that the wind drift component is colinear in the direction of the wind and has a magnitude of 3.0 percent of the wind speed. These relationships were assumed for two reasons: first, to allow trajectory comparisons to be made consistent with the approach used in Dames & Moore (1980), and secondly, the data base available did not justify utilization of more sophisticated techniques. Table I presents 24 hour mean wind drift surface currents derived from the data and techniques described above. The component wind drift speeds are given for north-south and east-west directions. These components were added to the 24 hour mean net current components derived from the current meter data as an estimate of the overall net surface flow.

Table II presents the 24 hour mean net velocity components of speed and direction from the near surface current meter at each of the five arrays examined. The mean net velocity vectors of these five current meter locations were added to the daily mean wind drift vector from Table I to obtain a daily mean overall surface current vector. These were plotted on the CODAR surface current map corresponding to that particular day. These vectors are shown in Figures 2 through 8.

TABLE I

24 HOUR MEAN WIND DRIFT ESTIMATES

Da/Mo/Yr	Direction (° True)	Speed (cm/s)	Component Speeds North (cm/s)	Component Speeds East (cm/s)
29/06/78	280	31.5	-5.5	31.0
30/06/78	295	24.0	-10.1	21.8
01/07/78	140	18.0	13.8	-11.6
02/07/78	110	18.0	6.2	-16.9
03/07/78	100	30.0	5.2	-29.5
04/07/78	100	21.0	3.6	-20.7
05/07/78	110	21.0	7.2	-19.7
06/07/78	105	27.0	7.0	-26.1
07/07/78	115	18.0	7.6	-16.3

TABLE II

24 HOUR MEAN NET CURRENT DATA

Mooring	C-1B		C-2B		C-3B		C-4B		C-5B	
Lat.	59° 10.70'N		59° 13.50'N		59° 24.40'N		59° 16.70'N		59° 09.90'N	
Long.	153° 18.80'W		153° 07.70'W		152° 53.60'W		152° 54.90'W		152° 53.90'W	
Bottom Depth	40 m		62 m		64 m		83 m		135 m	
Meter	2504		3176		598		3294		2156	
Depth	18 m		18 m		25 m		19 m		27 m	
Date	Net Speed	Direction	Net Speed	Direction	Net Speed	Direction	Net Speed	Direction	Net Speed	Direction
(Da/Mo/Yr)	(cm/s)	(° True)	(cm/s)	(° True)	(cm/s)	(° True)	(cm/s)	(° True)	(cm/s)	(° True)
29/06/78	0.53	124	15.03	201	16.53	247	2.04	113	5.78	239
30/06/78	5.06	14	11.43	204	14.82	264	3.97	46	9.08	278
01/07/78	4.14	339	12.54	229	17.37	256	6.12	10	8.90	278
02/07/78	3.06	340	13.91	207	18.57	255	5.18	324	11.37	209
03/07/78	7.09	154	15.46	152	17.16	250	9.09	38	--	--
04/07/78	14.57	226	22.78	200	20.71	228	2.42	272	--	--
05/07/78	10.97	198	27.45	212	23.73	225	2.45	299	--	--
06/07/78	4.69	202	24.59	202	23.91	230	7.92	242	--	--
07/07/78	3.79	200	22.58	212	17.54	228	2.08	270	--	--
08/07/78	2.03	166	16.87	208	16.23	230	3.41	51	--	--

3.0 RESULTS AND CONCLUSIONS

3.1 SURFACE DRIFT COMPARISON

As shown in Figure 1, two of the current meter arrays, C-2B and C-5B, were located directly in the area of CODAR mapping coverage. Thus, it was possible to perform a direct comparison of speed and direction between the CODAR generated surface currents and the surface currents calculated at current meter locations, C-2B and C-5B. Figures 12 and 13 present these comparisons for current meter locations C-2B and C-5B, respectively.

Figure 12 shows a reasonable agreement in the direction of the surface current between the CODAR generated currents and those calculated at C-2B. The comparison of speed is not as good, but in general the data are the same magnitude and only show one day of radical departure, July 7th. The wind drift component is the dominant component when comparing the data presented in Tables I and II. Since the wind drift directional data was measured at Augustine Island, while the speed was estimated from data measured at Shuyak Island and Iliamna Lake, it is not surprising to find closer agreement between the directional data compared to the speed data.

Figure 13 shows a similar comparison for the location of current meter array C-5B. The near surface meter at C-5B produced only two overlapping days of data with the CODAR measurements. Thus, although the comparison is quite limited, close agreement was found between the CODAR and calculated surface currents.

Figures 2 through 8 show the calculated surface currents at the current meter locations plotted over the CODAR generated surface current maps. Although only two current meter locations overlap the area of CODAR coverage, the additional vectors at the other current meter locations help provide a general picture of the overall localized flow pattern from the current meter measured data. With the exception of the July 1st map (which was a transition period between weather patterns), the agreement in vector magnitudes and directions is remarkably good. This is especially true considering the manner in which the wind drift current component was calculated.

Both the CODAR generated surface currents and the surface currents calculated in a manner consistent with the approach used in Dames & Moore (1980) indicate the importance, if not major dominance, of the wind drift surface component over the net flow component. This is clearly evident in Figures 2 through 8 which cover a region where the net (non-wind drift) flow is relatively strong (compared to magnitudes of this component in other areas of Lower Cook Inlet) and has a dominant south and southwesterly flow.

Within the limits of available data, the treatment and calculation of the wind drift component is supportive of the approach taken in previous trajectory studies presented in Dames & Moore (1980, 1979, and 1976). The assumption of the wind drift current equal to 3.0 percent of the wind speed and colinear to the wind direction has not been refuted in this limited analysis. Based on the directional comparison presented in Figure 12 for the location of current meter C-2B, a deflection angle on the order of 15 to 20 degrees to the right of the wind vector would provide a general overall better fit of the data. However, this is a single point source conclusion and the effect on the overall flow pattern is difficult to evaluate with the limited data available.

3.2 TRAJECTORY COMPARISON

Trajectories calculated using the CODAR data for this period of time would be similar to trajectories calculated using wind field 2 and intensity factor 3 and the net and tidal fields as specified in Dames & Moore (1980). Typical values of the wind speed in the study area from wind field 2 and intensity factor 3 (Dames & Moore, 1980) range from 8 to 10 meters/sec. The direction of wind field 2 in this area is from 60 to 100 degrees (true). This would result in surface wind drift velocities calculated to be in the range of 25 to 30 cm/sec with the same directional characteristics.

The net current magnitudes in this vicinity for the summer net current pattern presented in Dames & Moore (1980) range from 5 to 30 cm/s, which is generally consistent with the measurements presented in Table II. The directions of the net currents used in Dames & Moore (1980) for this area of Lower Cook Inlet range from 100 to 220 degrees (true), which is also consistent with the direction of the stronger flows presented in Table II. (The weaker velocities have little influence on the resultant velocity vector magnitude or direction.)

The vectoral combination of the wind drift component with the net component of surface flow from the Dames & Moore (1980) fields would result in net trajectory movement with speeds ranging from 20 to 50 cm/s and directions ranging from 240 to 280 degrees (true). Similar ranges of speed and direction are observed for the majority of vectors of CODAR measured 24 hour mean surface currents presented on Figures 2 through 8. Thus, for this period of time, the general net movement of trajectories predicted by CODAR and the approach used in Dames & Moore (1980) would be very similar. The fluctuations caused by tidal excursions is difficult to quantitatively assess without actual application, but the following comments address some of the comparative aspects.

Although the tidal currents presented in Figures 9 through 11 are generally rotary in nature, the component in the direction of the minor axis is relatively small and would result in minor excursions in these directions. With the exception of a few boundary locations, the M2 constituent of the tidal current is shown in Figure 9 to be the primary tidal current constituent. The M2 tidal current constituent was assumed in Dames & Moore (1980 and 1979) to represent "average" tidal current conditions in Lower Cook Inlet and Shelikof Strait. Representative values in Dames & Moore (1980) for the M2 tidal constituent in this region of Lower Cook Inlet have magnitudes ranging from 40 to 60 cm/sec with ebb directions of 100 to 110 degrees (true) and flood directions of 270 to 290 degrees (true). The CODAR generated data have M2 tidal current constituents typically in the range of 30 to 50 cm/sec with ebb directions ranging from 90 to 140 degrees (true) and flood directions ranging from 290 to 320 degrees (true). The CODAR generated data naturally have a wider range of variability (due to the greater spatial resolution), but the typical values are not so different that they would result in radically different trajectories if this data set were utilized in such an analysis. It should also be recognized that the CODAR generated tidal current constituents were calculated based on a time series less than that necessary to provide accurate tidal constituent predictions.

3.3 CONCLUSIONS

It is concluded, based on a comparison of CODAR generated surface currents (24 hour means) with surface currents calculated from a measured daily mean net and daily mean wind drift current, that the approach used to calculated surface transport in Dames & Moore (1980, 1979, and 1976) is a valid and reasonably accurate approach (assuming the CODAR generated surface currents are taken as ground truth). There is some evidence to suggest a wind drift deflection angle of approximately 15-20 degrees to the right, but in general, overall flow patterns are reasonably well represented using a colinear wind-drift surface current direction. Tidal current constitutents calculated using the CODAR generated data reinforce and support the approach used in previous studies in which the M_2 tidal current constituent was found to be dominant and was assumed to reasonably represent "average" tidal current conditions.

The question of whether near surface current meter records (15 to 20 meters below the surface) can be used to represent net currents (minus wind drift component) could not be adequately resolved with the given data set. In general, the net currents were smaller than the calculated wind drift component and the vectoral sum was therefore dominated by the wind drift component. In other words, the vectoral sum would be little affected whether or not the net component was considered at all. In addition, the accuracy of the wind speed near Augustine Island is suspect given the rather crude methodology by which it was estimated.

References

Barrick, D.E., and R.J. Lipa, 1979. A compact transportable HF radar system for directional coastal wavefield measurements, in Ocean Wave Climate, M.D. Earle and A. Malahoff (Eds.), Plenum, New York.

Barrick, D.E., J.M. Headrick, R.W. Bogle, and D.D. Crombie, 1974. Sea back-scatter at HF: interpretation and utilization of the echo, Proc. IEEE, Vol., 62, pp. 673-680.

Barrick, D.E., 1972. First-order theory and analysis of MF/HF/VHF scatter from the Sea, IEEE Transactions on Antennas and Propagation, Vol. AP-20, pp. 2-10.

Barrick, D.E., and W.H. Peake, 1967. Scattering from surfaces with different roughness scales: analysis and interpretation, Battelle Research Report, BAT-197A-10-3, Columbus, Ohio.

Barrick, E.W., M.W. Evans, and B.L. Weber, 1977. Ocean surface currents mapped by radar, Science, 198: 138-144.

Evans, M.W., 1978. Surface current mapping radar: Theory and application, presented at Energy/Environment '78, a Symposium on Energy Development Transports.

Frisch, S., 1980. Personal communication, CODAR data for July 1, 1978 to July 8, 1978, Cape Douglas - Augustine Island, Alaska; 24 hr mean currents and tidal harmonic constituents (M_2, O_1, K_1), Wave Propagation Laboratory, NOAA.

Dames & Moore, 1980. Final Report--Task 1, Oil spill trajectory simulation, Lower Cook Inlet-Shelikof Strait, Alaska, for the Bering Sea-Gulf of Alaska Project Office, Outer Continental Shelf Environmental Assessment Program, Job number 06797-014-88.

_____, 1979. Final Draft, Oil spill trajectory analysis, Lower Cook Inlet, Alaska, Bering Sea-Gulf of Alaska Project Office, Outer Continental Shelf Environmental Assessment Program, Job number 06796-011-02.

_____, 1976. Report, Oil spill trajectory analysis, Lower Cook Inlet, Alaska. For NOAA, Job number 06797-003-20.

Reynolds, M., 1980. Personal communication, Meteorological data from Iliamna Lake, Shuyak Island, and Augustine Island for late June and July, 1978, Pacific Marine Environmental Laboratory, NOAA.

References (cont.)

Schumacher, J.D., 1980. Personal communication, Current dat summaries from near-surface current meters for C-1B C-2B, C-3B, C-4B, and C-5B arrays, Pacific Marin Environmental Laboratory, NOAA.

REVISIONS
BY ______ DATE ______

FILE ______

BY ______ DATE ______
CHECKED BY ______

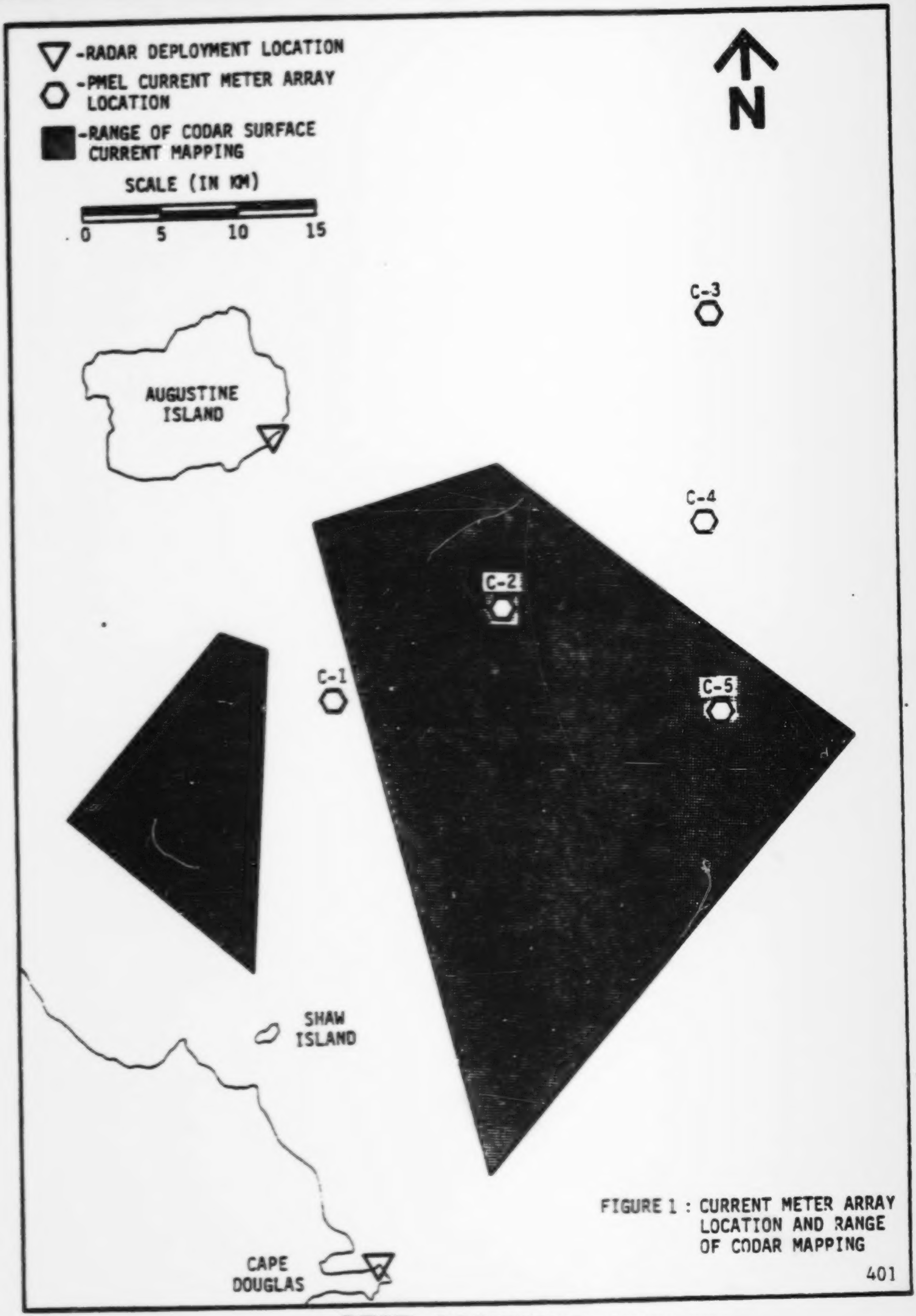
-RADAR DEPLOYMENT LOCATION
-PMEL CURRENT METER ARRAY LOCATION
-RANGE OF CODAR SURFACE CURRENT MAPPING
SCALE (IN KM)
0
5
10
15
N
C-3
AUGUSTINE ISLAND
C-4
C-2
C-1
C-5
SHAW ISLAND
CAPE DOUGLAS

FIGURE 1 : CURRENT METER ARRAY LOCATION AND RANGE OF CODAR MAPPING

BEST DOCUMENT AVAILABLE

REVISIONS BY ______ DATE ______

FILE ______

BY ______ DATE ______

CHECKED BY ______

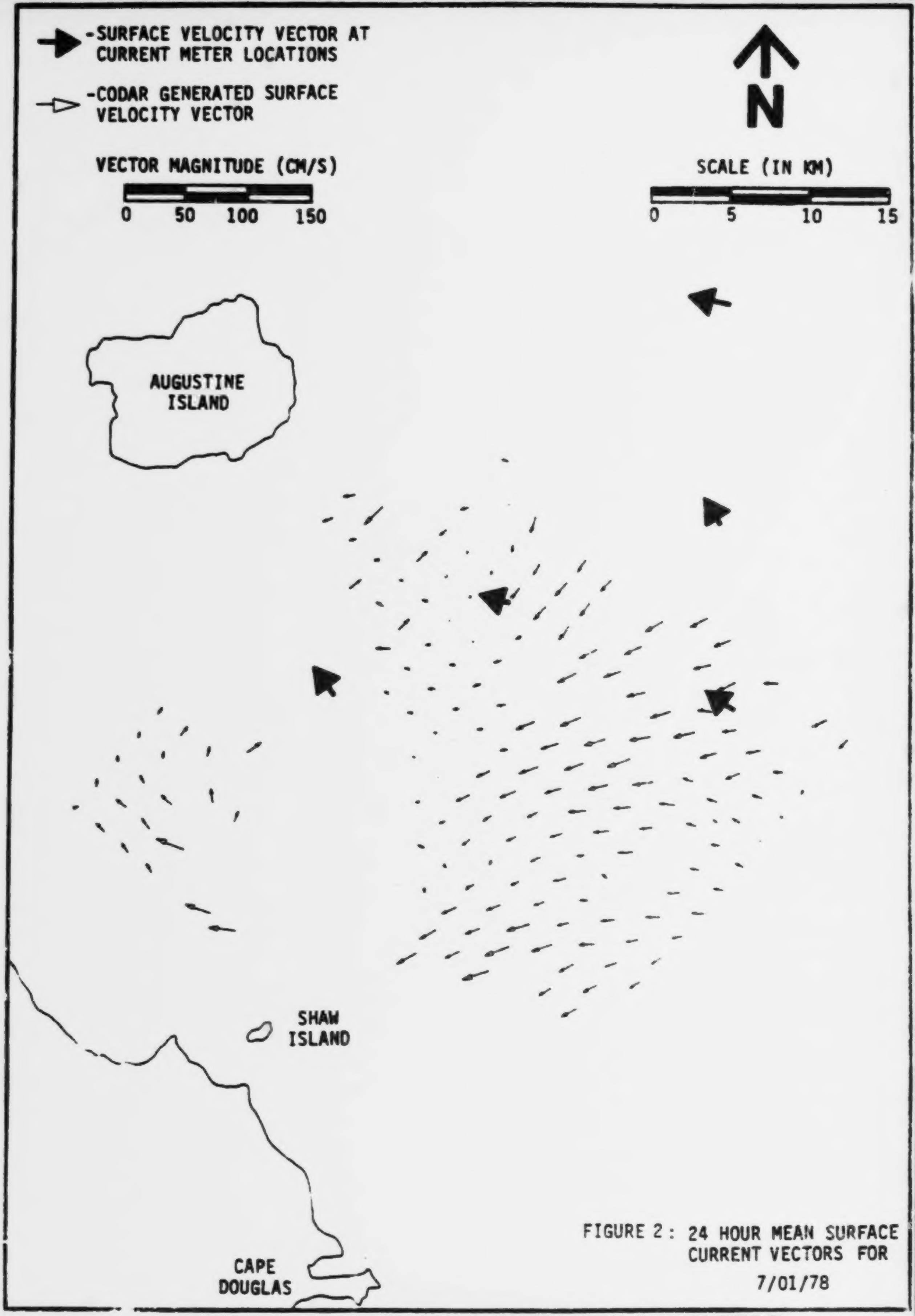
-SURFACE VELOCITY VECTOR AT CURRENT METER LOCATIONS
-CODAR GENERATED SURFACE VELOCITY VECTOR
VECTOR MAGNITUDE (CM/S)
0
50
100
150
N
SCALE (IN KM)
0
5
10
15
AUGUSTINE ISLAND
SHAW ISLAND
CAPE DOUGLAS

FIGURE 2: 24 HOUR MEAN SURFACE CURRENT VECTORS FOR 7/01/78

BEST DOCUMENT AVAILABLE

REVISIONS BY ________ DATE ________

FILE ________

BY ________ DATE ________

CHECKED BY ________

146.7 (REV. 6-61)

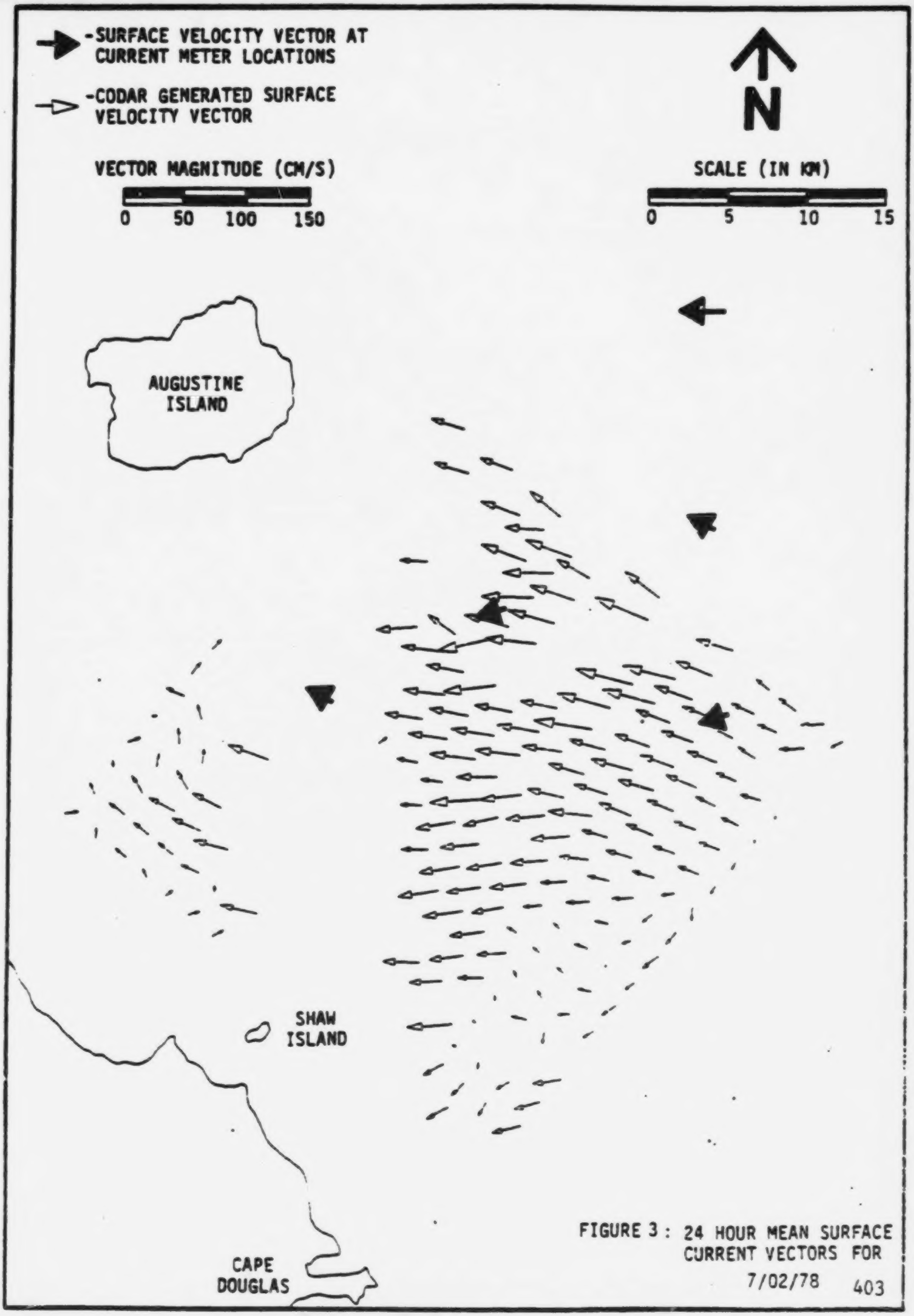
-SURFACE VELOCITY VECTOR AT CURRENT METER LOCATIONS
-CODAR GENERATED SURFACE VELOCITY VECTOR
N
VECTOR MAGNITUDE (CM/S)
0
50
100
150
SCALE (IN KM)
0
5
10
15
AUGUSTINE ISLAND
SHAW ISLAND
CAPE DOUGLAS

FIGURE 3 : 24 HOUR MEAN SURFACE CURRENT VECTORS FOR 7/02/78

BEST DOCUMENT AVAILABLE

REVISIONS BY ______ DATE ______

FILE ______

BY ______ DATE ______ CHECKED BY ______ DATE ______

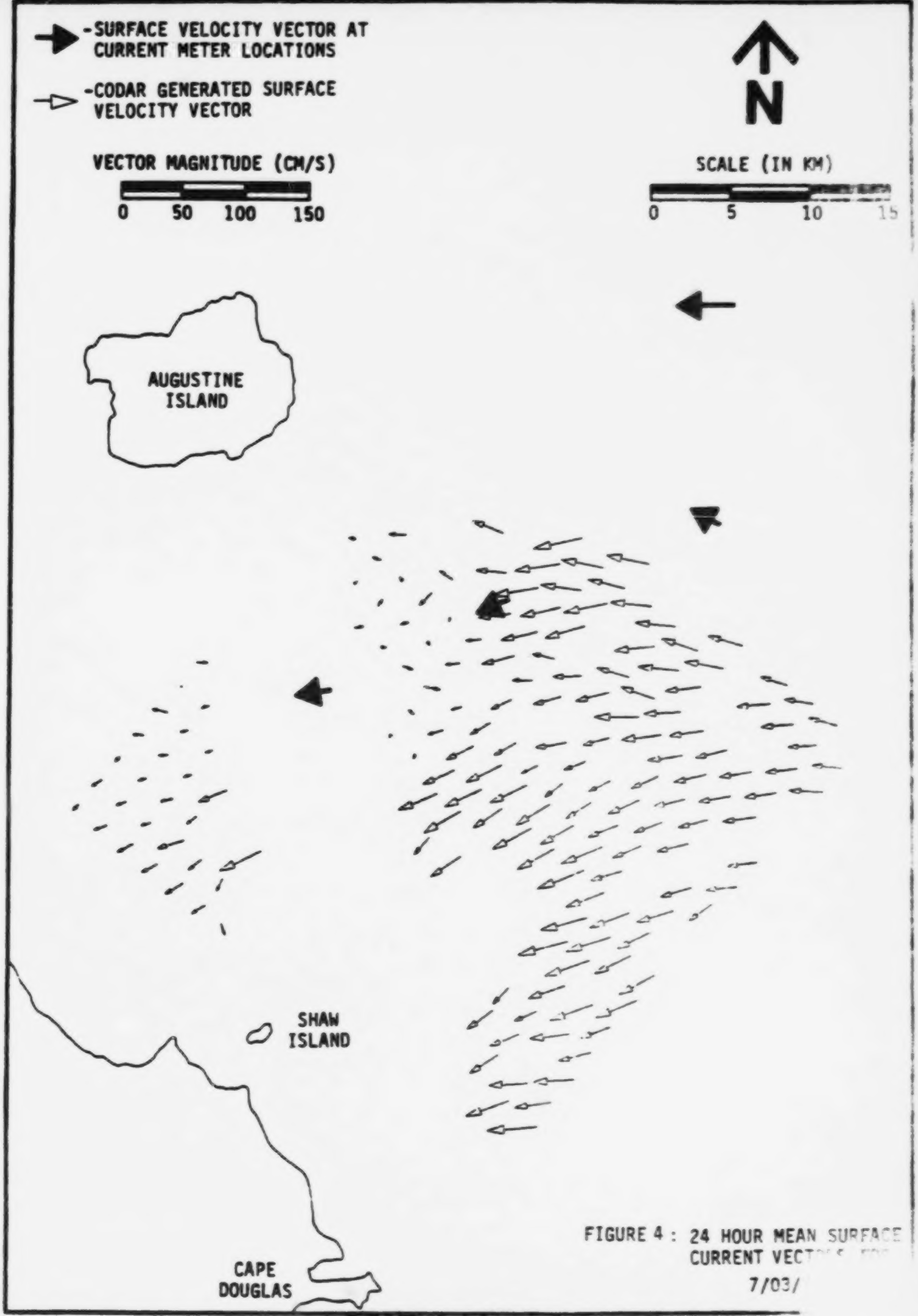

-SURFACE VELOCITY VECTOR AT CURRENT METER LOCATIONS
-CODAR GENERATED SURFACE VELOCITY VECTOR
N
VECTOR MAGNITUDE (CM/S)
0
50
100
150
SCALE (IN KM)
0
5
10
15
AUGUSTINE ISLAND
SHAW ISLAND
CAPE DOUGLAS

FIGURE 4 : 24 HOUR MEAN SURFACE CURRENT VECT

7/03/

BEST DOCUMENT AVAILABLE

REVISIONS
BY ______ DATE ______
FILE ______
BY ______ DATE ______
CHECKED BY ______

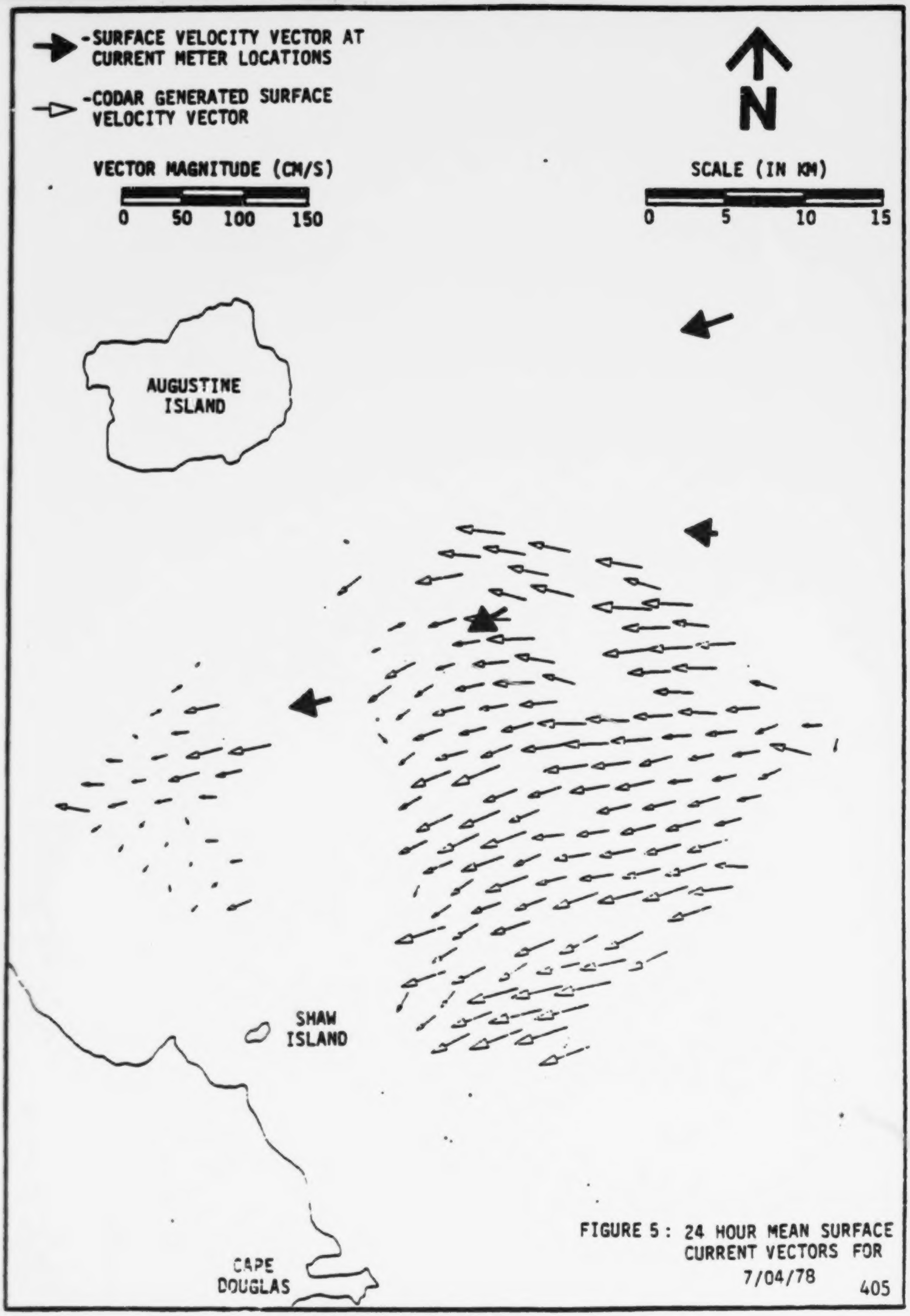
-SURFACE VELOCITY VECTOR AT CURRENT METER LOCATIONS
-CODAR GENERATED SURFACE VELOCITY VECTOR
N
VECTOR MAGNITUDE (CM/S)
0
50
100
150
SCALE (IN KM)
0
5
10
15
AUGUSTINE ISLAND
SHAW ISLAND
CAPE DOUGLAS

FIGURE 5 : 24 HOUR MEAN SURFACE CURRENT VECTORS FOR 7/04/78

REVISIONS
BY ________ DATE ________

FILE ________

BY ________ DATE ________
CHECKED BY ________

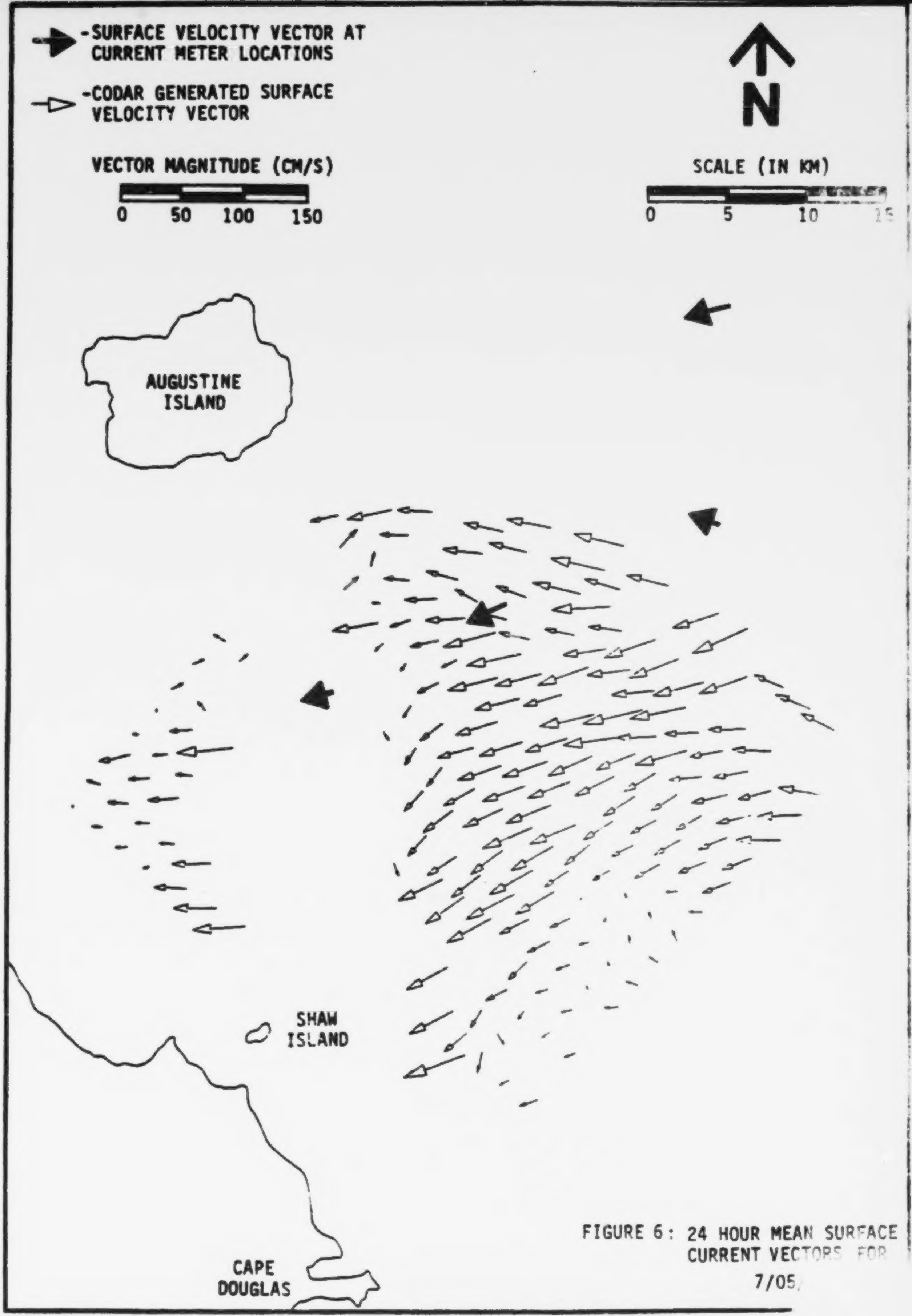

-SURFACE VELOCITY VECTOR AT CURRENT METER LOCATIONS
-CODAR GENERATED SURFACE VELOCITY VECTOR
VECTOR MAGNITUDE (CM/S)
0
50
100
150
N
SCALE (IN KM)
0
5
10
15
AUGUSTINE ISLAND
SHAW ISLAND
CAPE DOUGLAS

FIGURE 6: 24 HOUR MEAN SURFACE CURRENT VECTORS FOR 7/05

BEST DOCUMENT AVAILABLE

REVISIONS
BY ____ DATE ____

BY ____ DATE ____
CHECKED BY ____ FILE ____

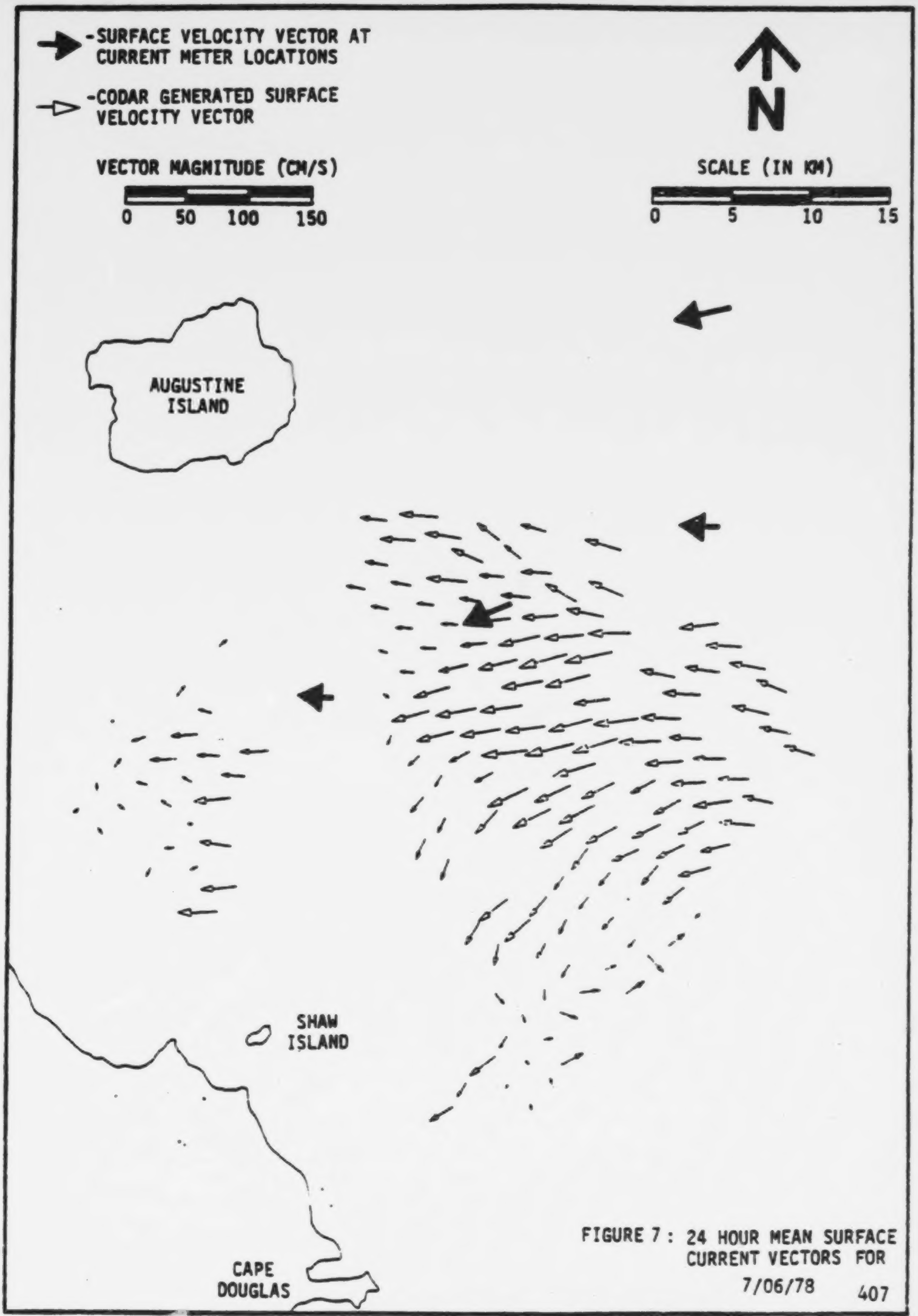
-SURFACE VELOCITY VECTOR AT CURRENT METER LOCATIONS
-CODAR GENERATED SURFACE VELOCITY VECTOR
N
VECTOR MAGNITUDE (CM/S)
0
50
100
150
SCALE (IN KM)
0
5
10
15
AUGUSTINE ISLAND
SHAW ISLAND
CAPE DOUGLAS

FIGURE 7: 24 HOUR MEAN SURFACE CURRENT VECTORS FOR 7/06/78

REVISIONS BY ______ DATE ______

FILE ______

BY ______ DATE ______
CHECKED BY ______

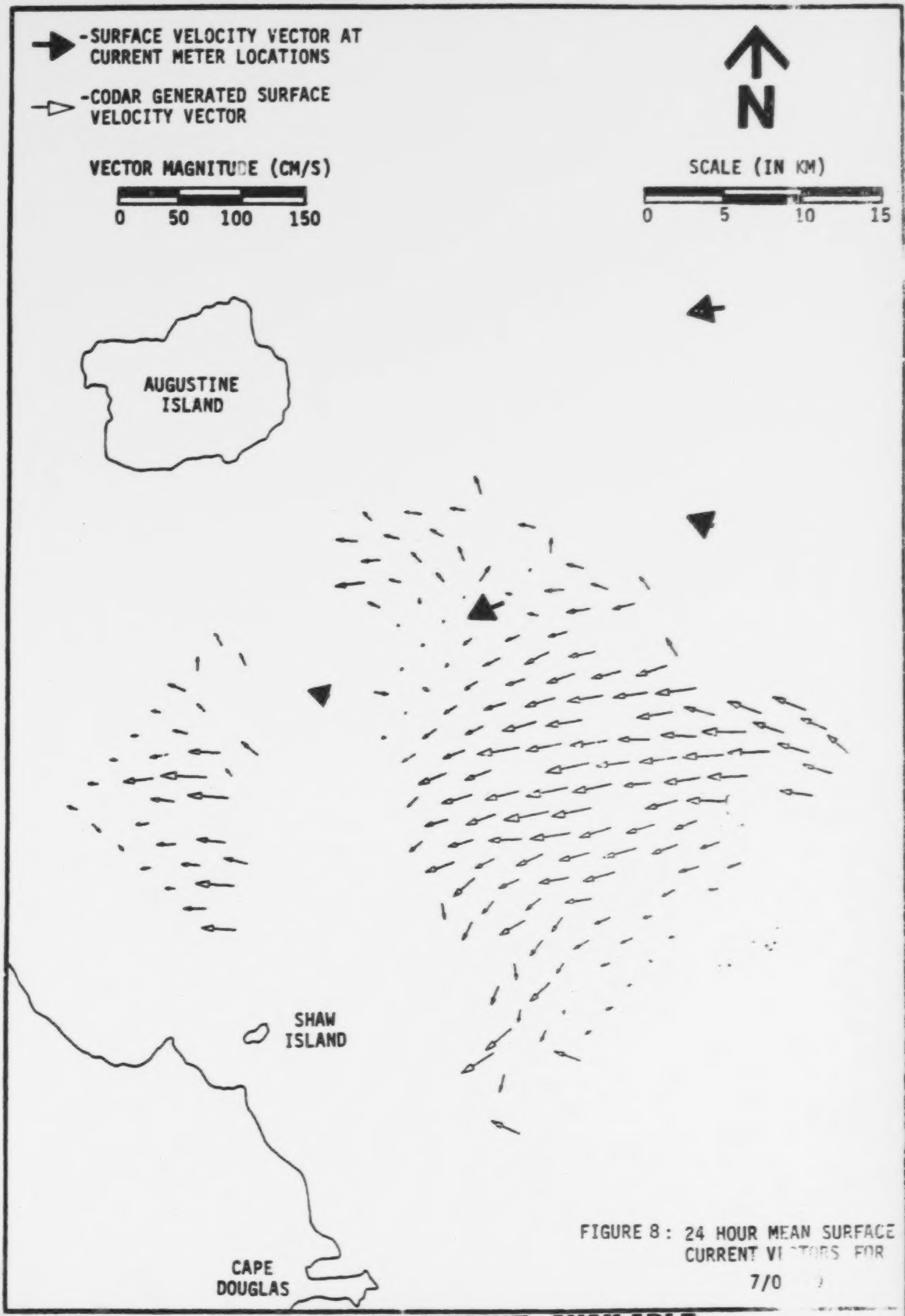
-SURFACE VELOCITY VECTOR AT CURRENT METER LOCATIONS
-CODAR GENERATED SURFACE VELOCITY VECTOR
VECTOR MAGNITUDE (CM/S)
0
50
100
150
N
SCALE (IN KM)
0
5
10
15
AUGUSTINE ISLAND
SHAW ISLAND
CAPE DOUGLAS

FIGURE 8: 24 HOUR MEAN SURFACE CURRENT VECTORS FOR 7/0

46.7 (REV. 6-61)

BEST DOCUMENT AVAILABLE

NOTE: TIDAL CURRENT VECTOR MEASURED FROM FROM CENTER OF ELLIPSE TO ANY POINT ON CURVE CORRESPONDING TO DESIRED TIDAL PHASE.

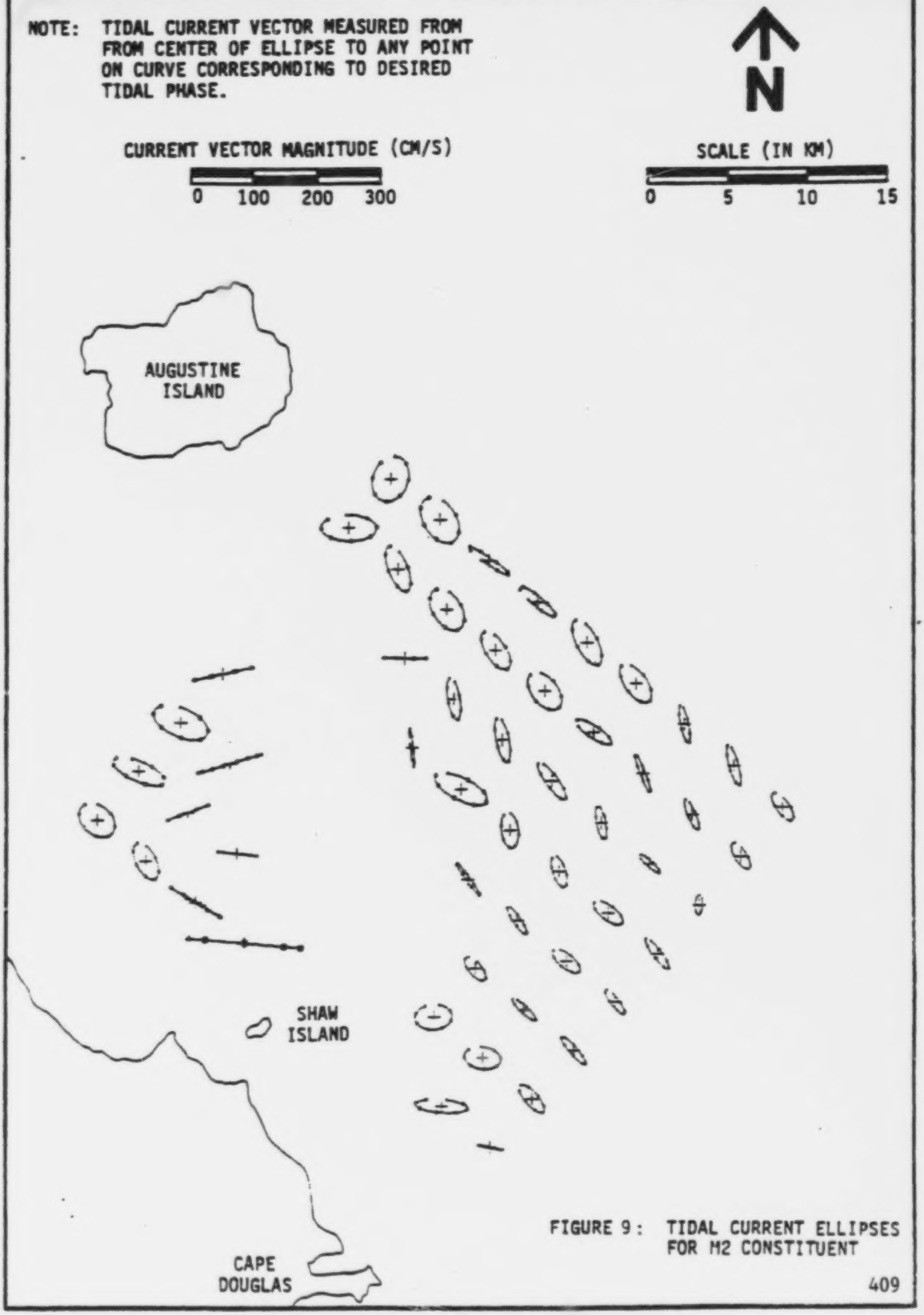
N
CURRENT VECTOR MAGNITUDE (CM/S)
0
100
200
300
SCALE (IN KM)
0
5
10
15
AUGUSTINE ISLAND
SHAW ISLAND
CAPE DOUGLAS

FIGURE 9: TIDAL CURRENT ELLIPSES FOR M2 CONSTITUENT

REVISIONS BY ______ DATE ______

FILE ______

BY ______ DATE ______

CHECKED BY ______

746./ (REV. 6-61)

BEST DOCUMENT AVAILABLE

REVISIONS
BY ______ DATE ______

FILE ______

BY ______ DATE ______
CHECKED BY ______

NOTE: TIDAL CURRENT VECTOR MEASURED FROM FROM CENTER OF ELLIPSE TO ANY POINT ON CURVE CORRESPONDING TO DESIRED TIDAL PHASE.

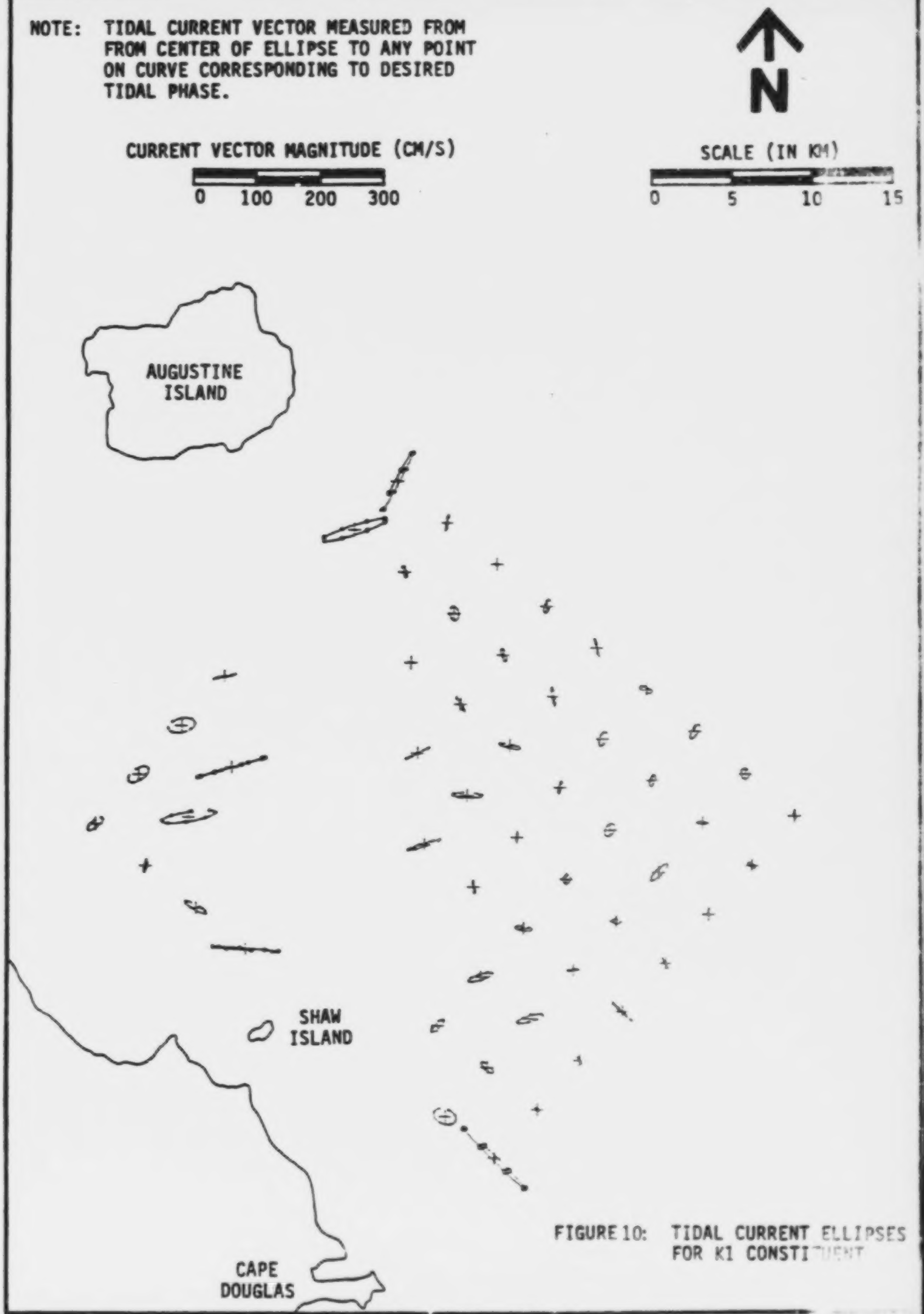
N
CURRENT VECTOR MAGNITUDE (CM/S)
0
100
200
300
SCALE (IN KM)
0
5
10
15
AUGUSTINE ISLAND
SHAW ISLAND
CAPE DOUGLAS

FIGURE 10: TIDAL CURRENT ELLIPSES FOR K1 CONSTITUENT

946.7 (REV. 6-61)

REVISIONS BY ______ DATE ______

FILE ______

BY ______ DATE ______
CHECKED BY ______

NOTE: TIDAL CURRENT VECTOR MEASURED FROM FROM CENTER OF ELLIPSE TO ANY POINT ON CURVE CORRESPONDING TO DESIRED TIDAL PHASE.

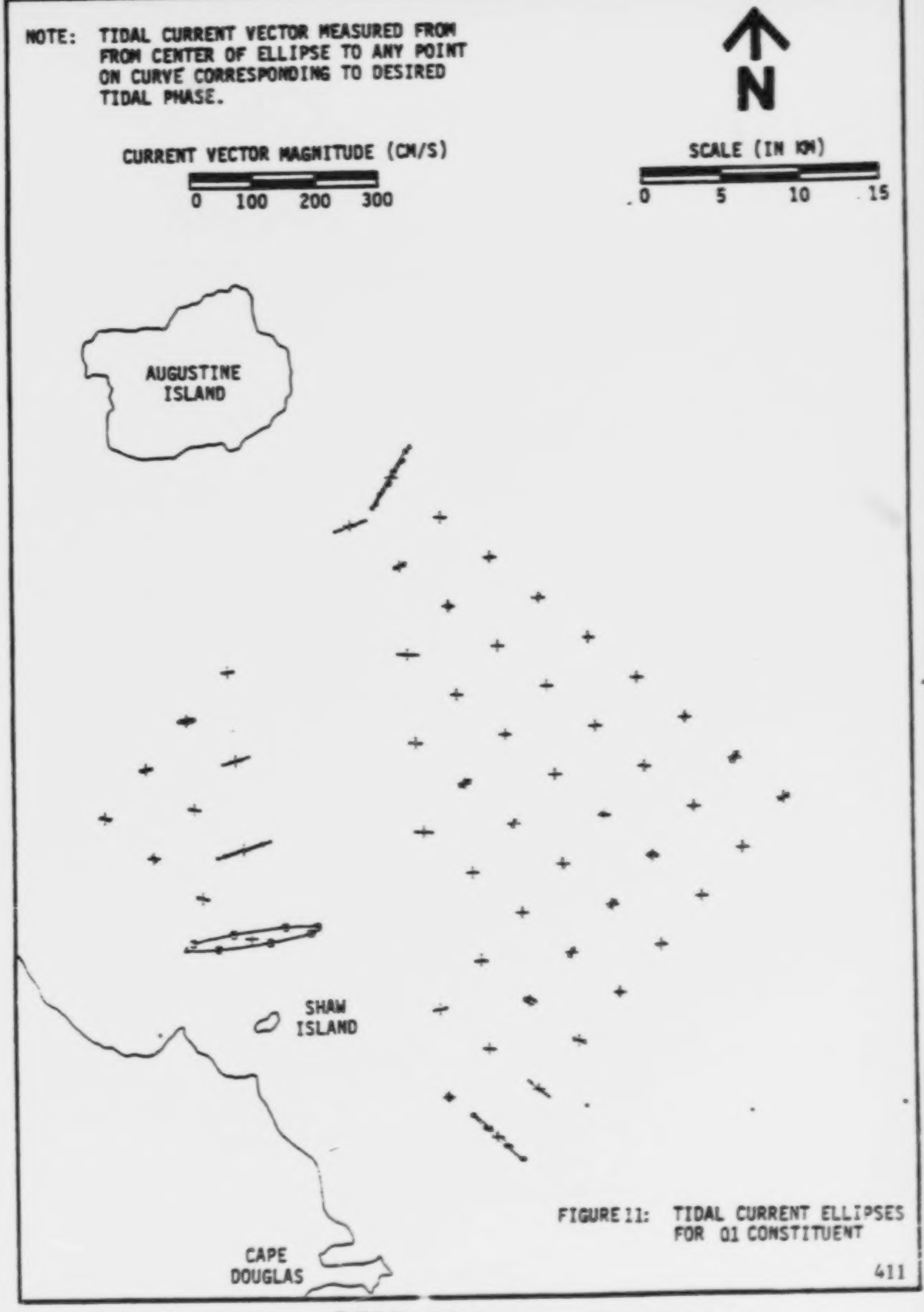
N
CURRENT VECTOR MAGNITUDE (CM/S)
0
100
200
300
SCALE (IN KM)
0
5
10
15
AUGUSTINE ISLAND
SHAW ISLAND
CAPE DOUGLAS

FIGURE 11: TIDAL CURRENT ELLIPSES FOR O1 CONSTITUENT

BEST DOCUMENT AVAILABLE

REVISIONS
BY ______ DATE ______
FILE ______
BY ______ DATE ______
CHECKED BY ______

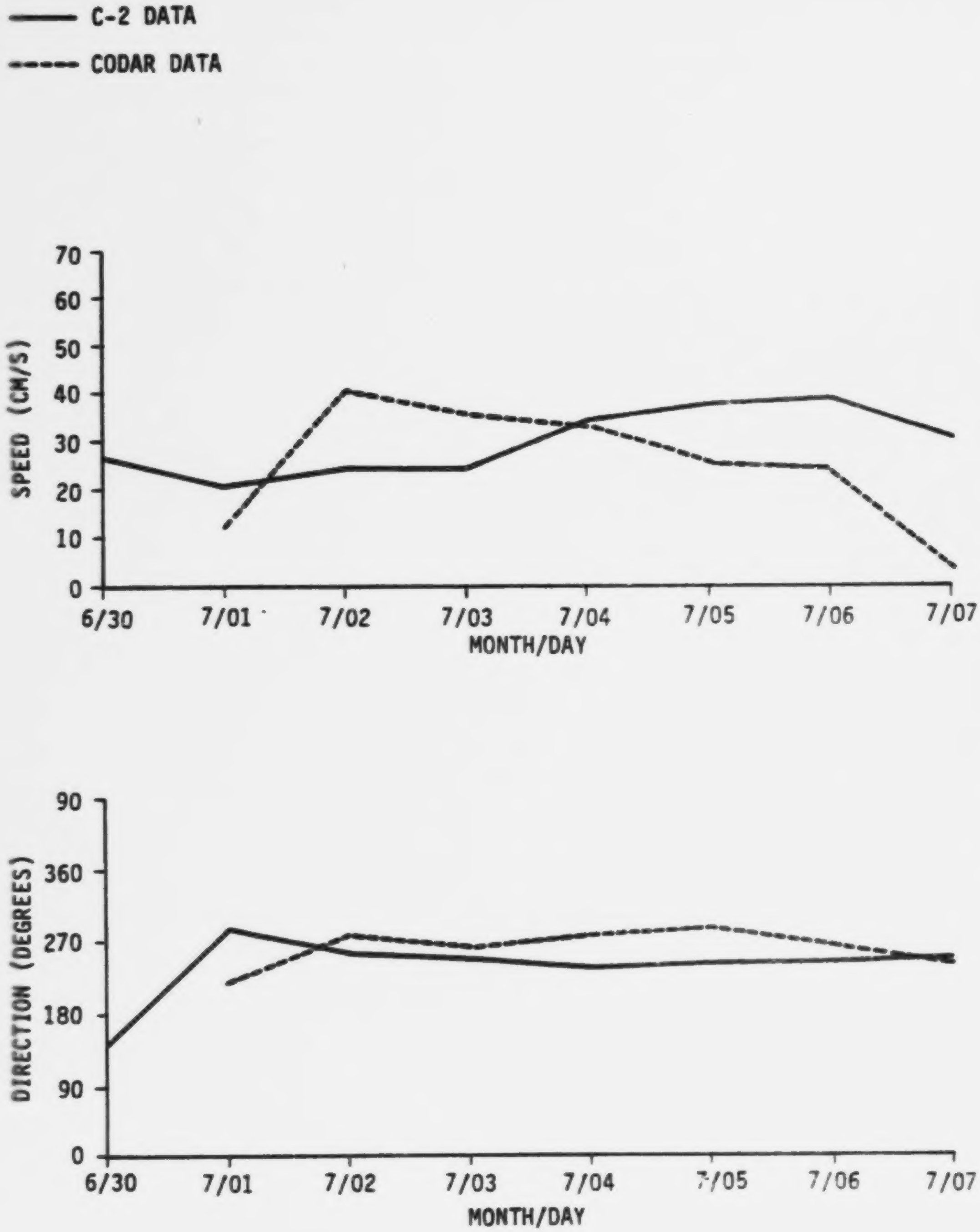

FIGURE 12: COMPARSON OF C-2 DATA WITH CODAR DATA

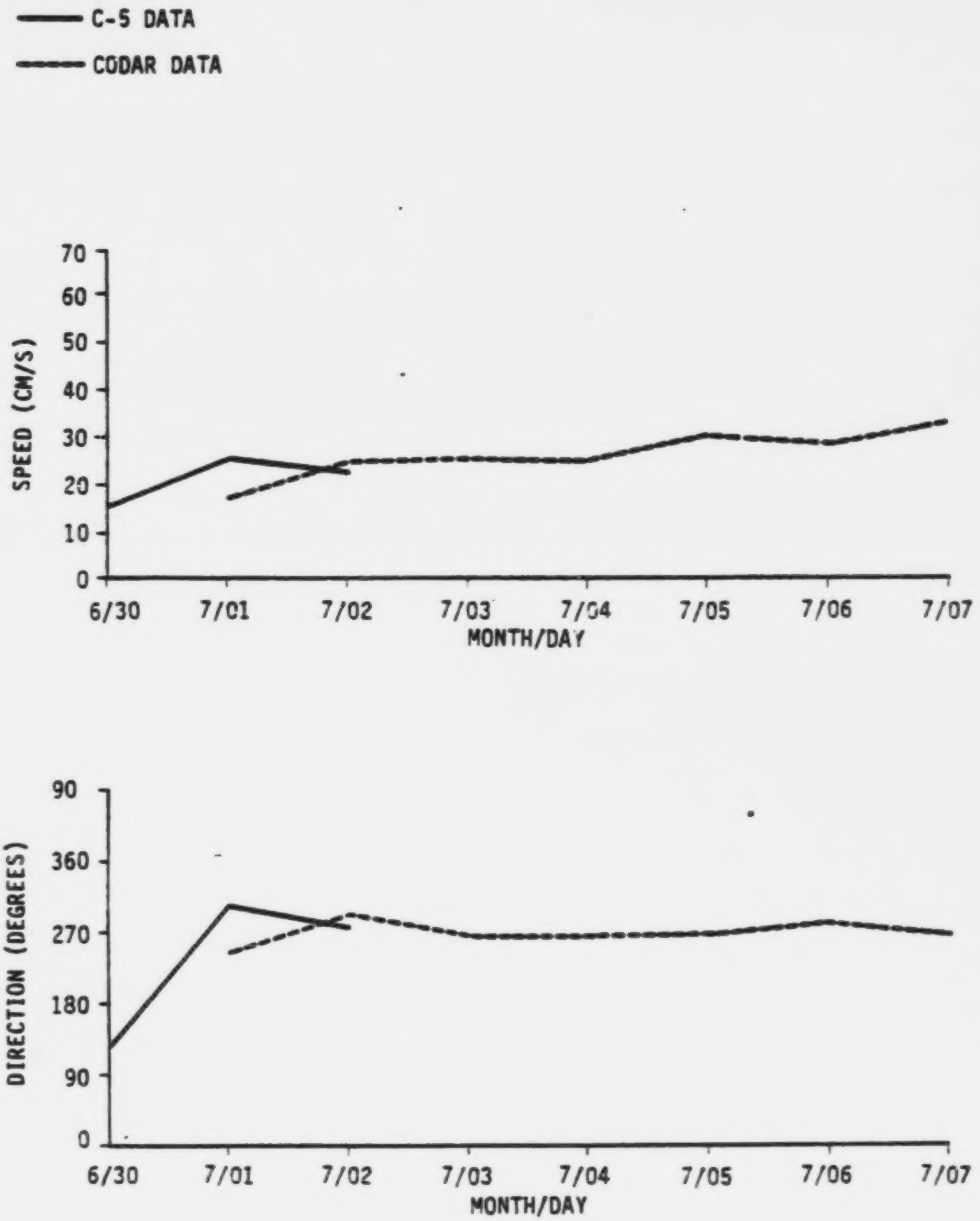

FIGURE 13: COMPARISON OF C-5 DATA WITH CODAR DATA

REVISIONS
BY ________ DATE ________

FILE ________

BY ________ DATE ________
CHECKED BY ________

946.7 (REV. 6-61)

BEST DOCUMENT AVAILABLE

Appendix A

Meteorological Data

BEST DOCUMENT AVAILABLE

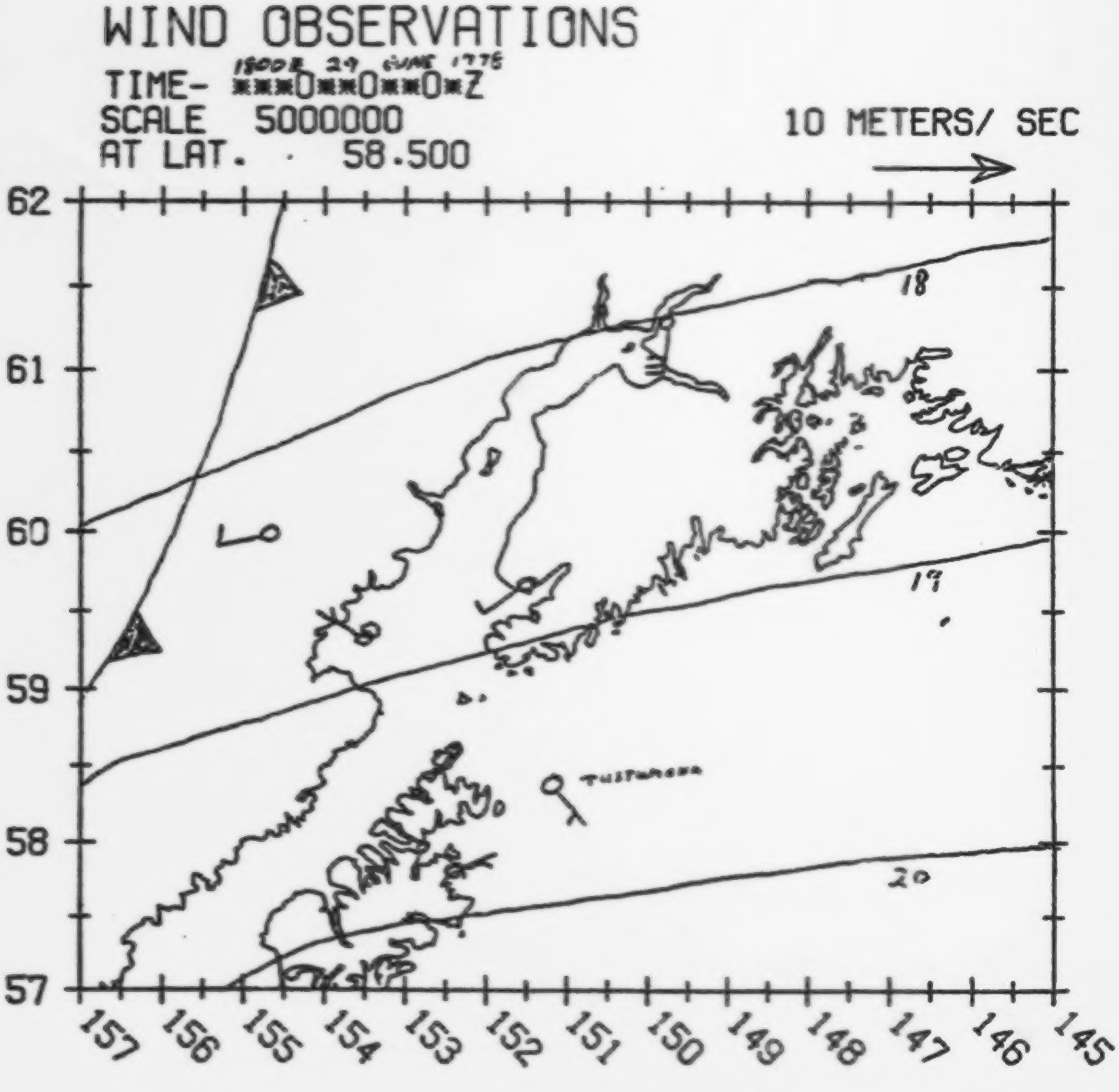
WIND OBSERVATIONS
1800Z 29 JUNE 1976
TIME- ***0**0***0*Z
SCALE 5000000
AT LAT. 58.500
10 METERS/ SEC
62
61
60
59
58
57
18
17
20
TUSTUMENA
157
156
155
154
153
152
151
150
149
148
147
146
145

BEST DOCUMENT AVAILABLE

WIND OBSERVATIONS

TIME- 12 noon 1 July 1975 ***0**0**0*Z
SCALE 5000000
AT LAT. 58.500

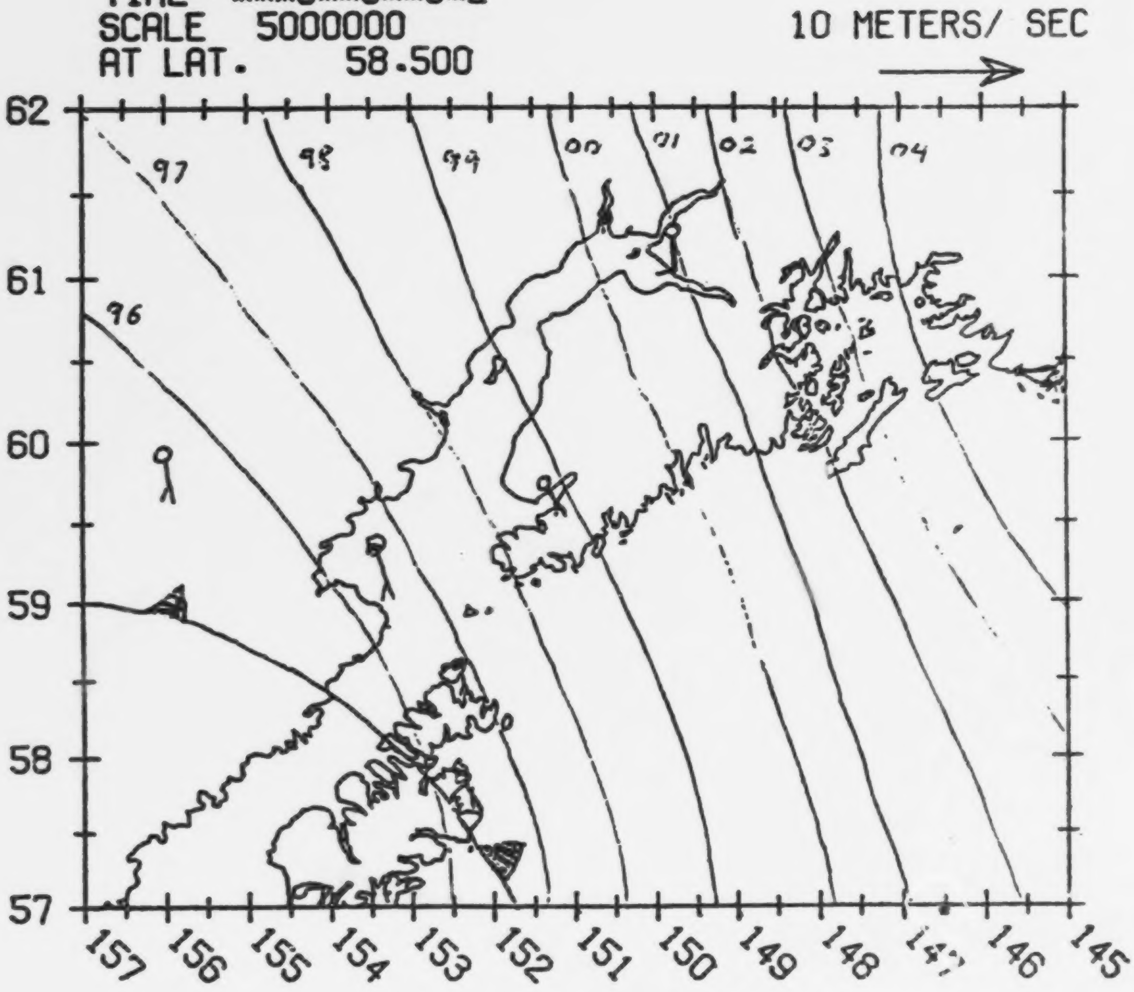
10 METERS/ SEC
62
61
60
59
58
57
157
156
155
154
153
152
151
150
149
148
147
146
145
96
97
98
99
00
01
02
03
04

BEST DOCUMENT AVAILABLE

WIND OBSERVATIONS

TIME- ***0**0**0*Z
1200Z 2 June 1979
SCALE 5000000
AT LAT. 58.500

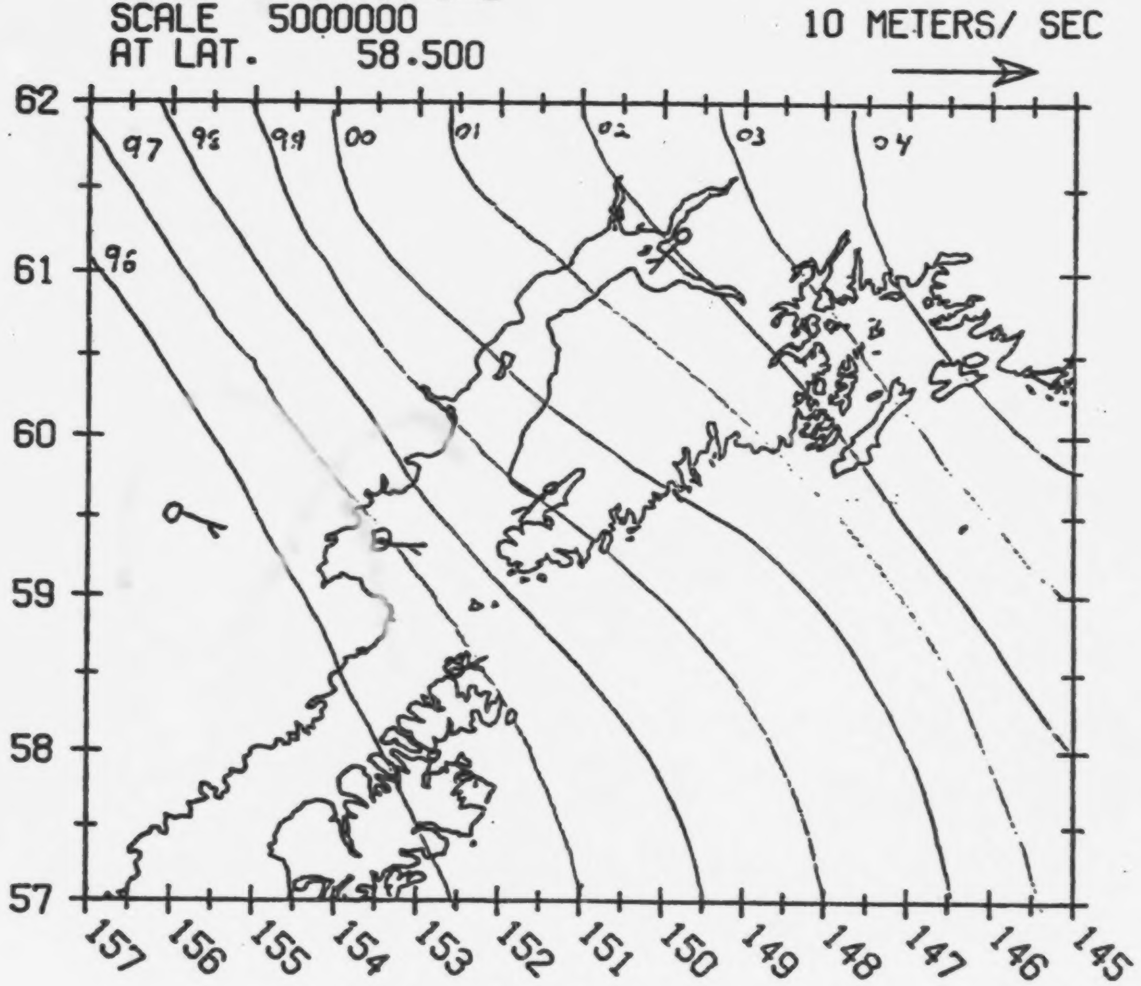

10 METERS/ SEC
97
98
99
00
01
02
03
04
96
62
61
60
59
58
57
157
156
155
154
153
152
151
150
149
148
147
146
145

Suggest Wind Pattern
29 JUNE 1979

BEST DOCUMENT AVAILABLE

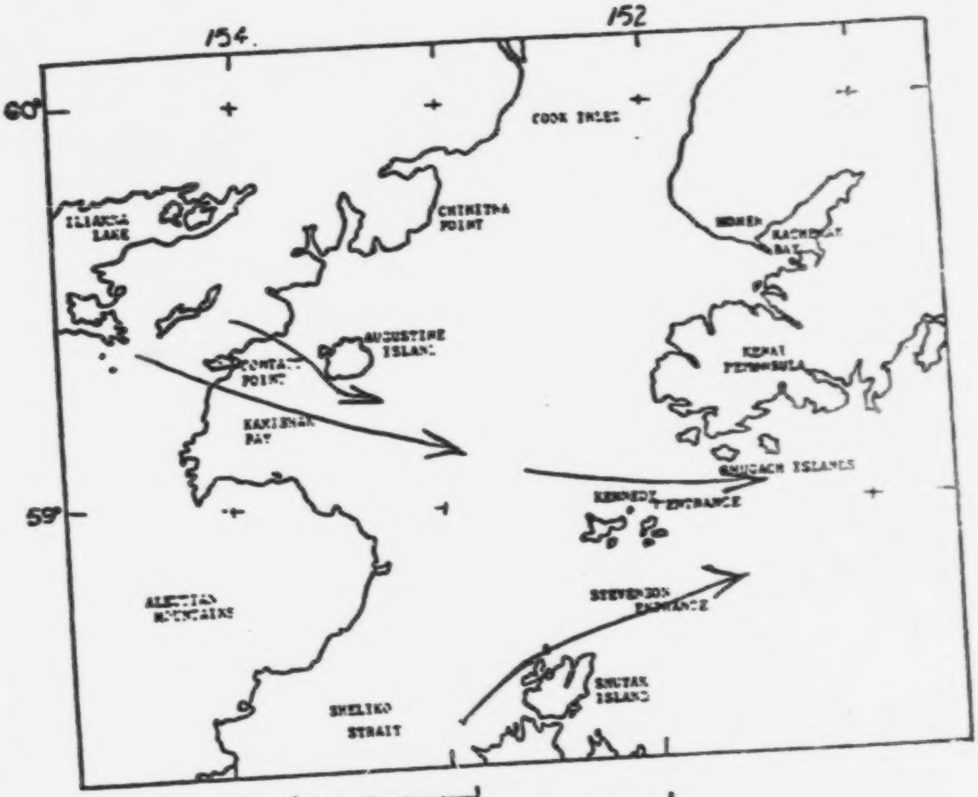
154
152
60°
59°
COOK INLET
ILIAMNA LAKE
CHINITNA POINT
HOMER
KACHEMAK BAY
AUGUSTINE ISLAND
CONTACT POINT
KENAI PENINSULA
KAMISHAK BAY
CHUGACH ISLANDS
KENNEDY ENTRANCE
ALEUTIAN MOUNTAINS
STEVENSON ENTRANCE
SHUYAK ISLAND
SHELIKOF STRAIT
0
50
100 km

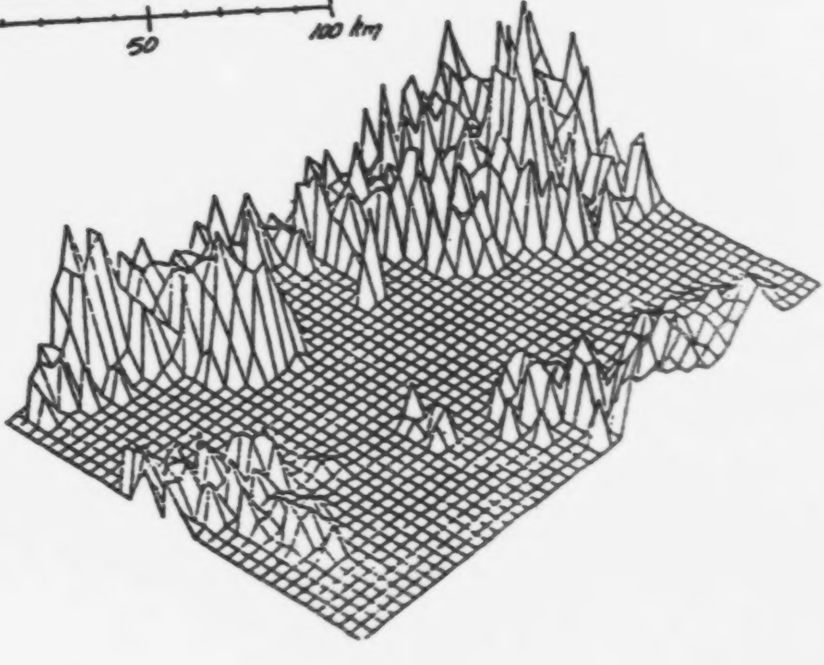

Suggest Wind Pattern
2 July 1979

BEST DOCUMENT AVAILABLE

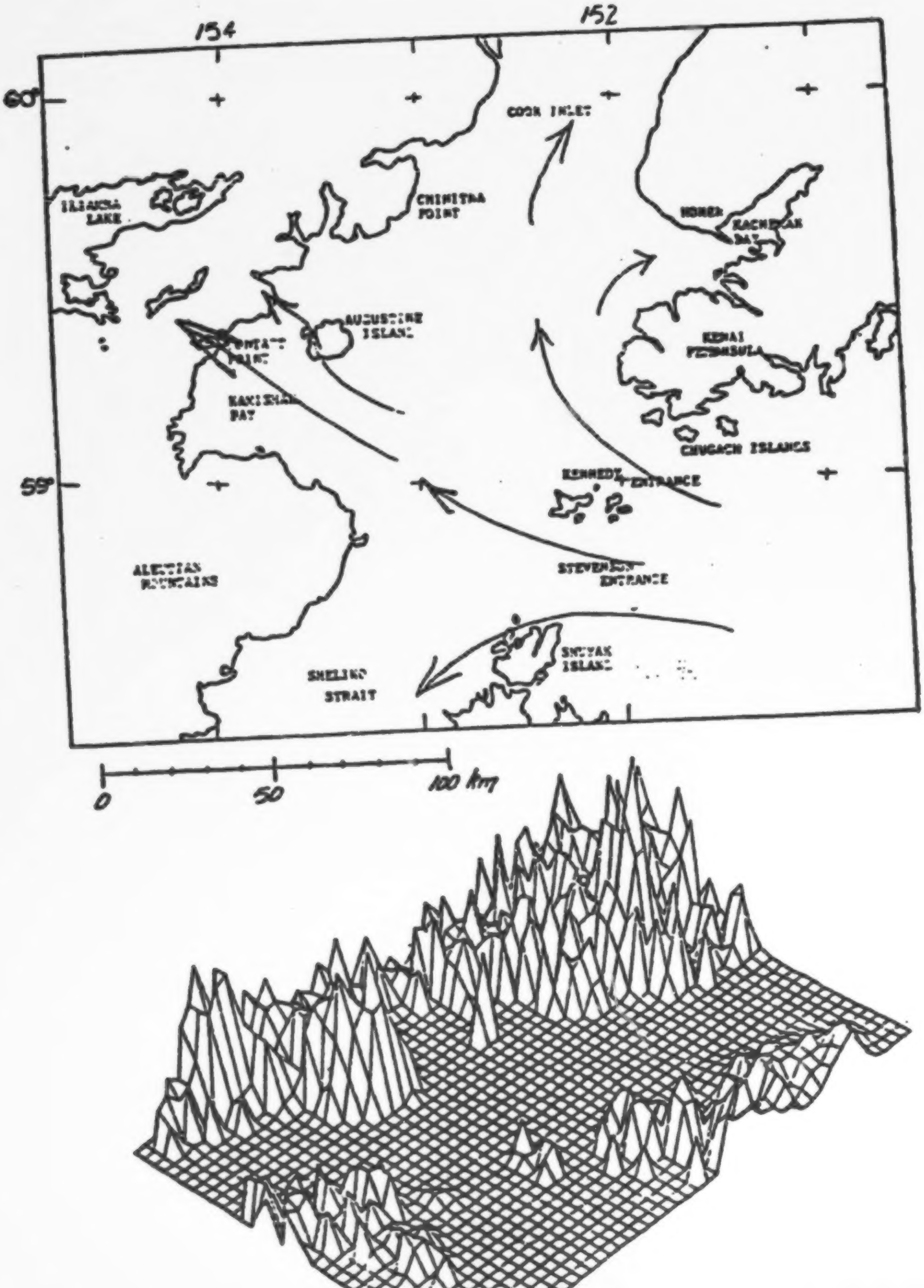
154
152
60°
59°
COOK INLET
ILIAMNA LAKE
CHINITNA POINT
HOMER
KACHEMAK BAY
AUGUSTINE ISLAND
CONTACT POINT
KAMISHAK BAY
KENAI PENINSULA
CHUGACH ISLANDS
KENNEDY ENTRANCE
STEVENSON ENTRANCE
ALEUTIAN MOUNTAINS
SHUYAK ISLAND
SHELIKOF STRAIT
0
50
100 km

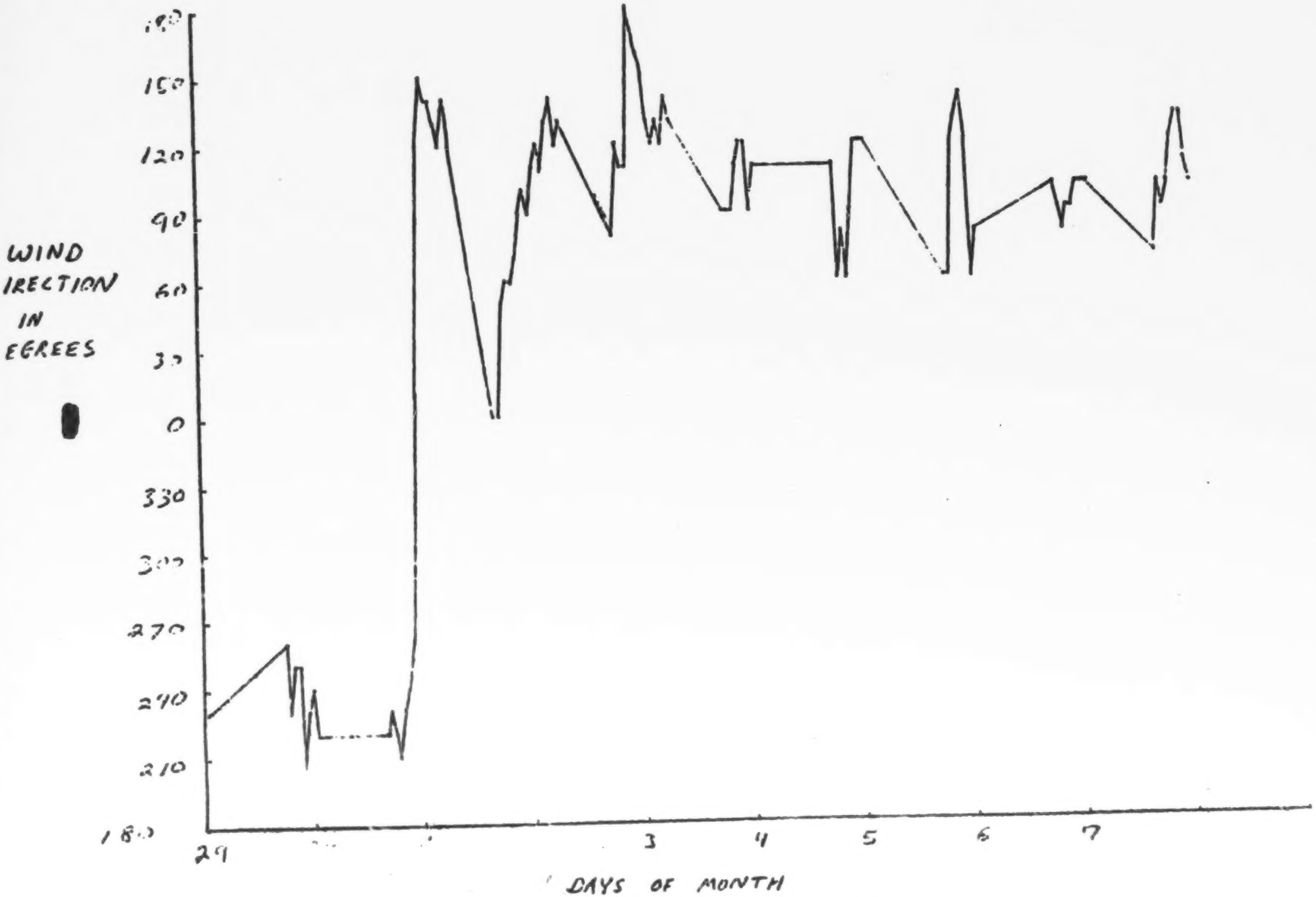

Iliamna

BEST DOCUMENT AVAILABLE

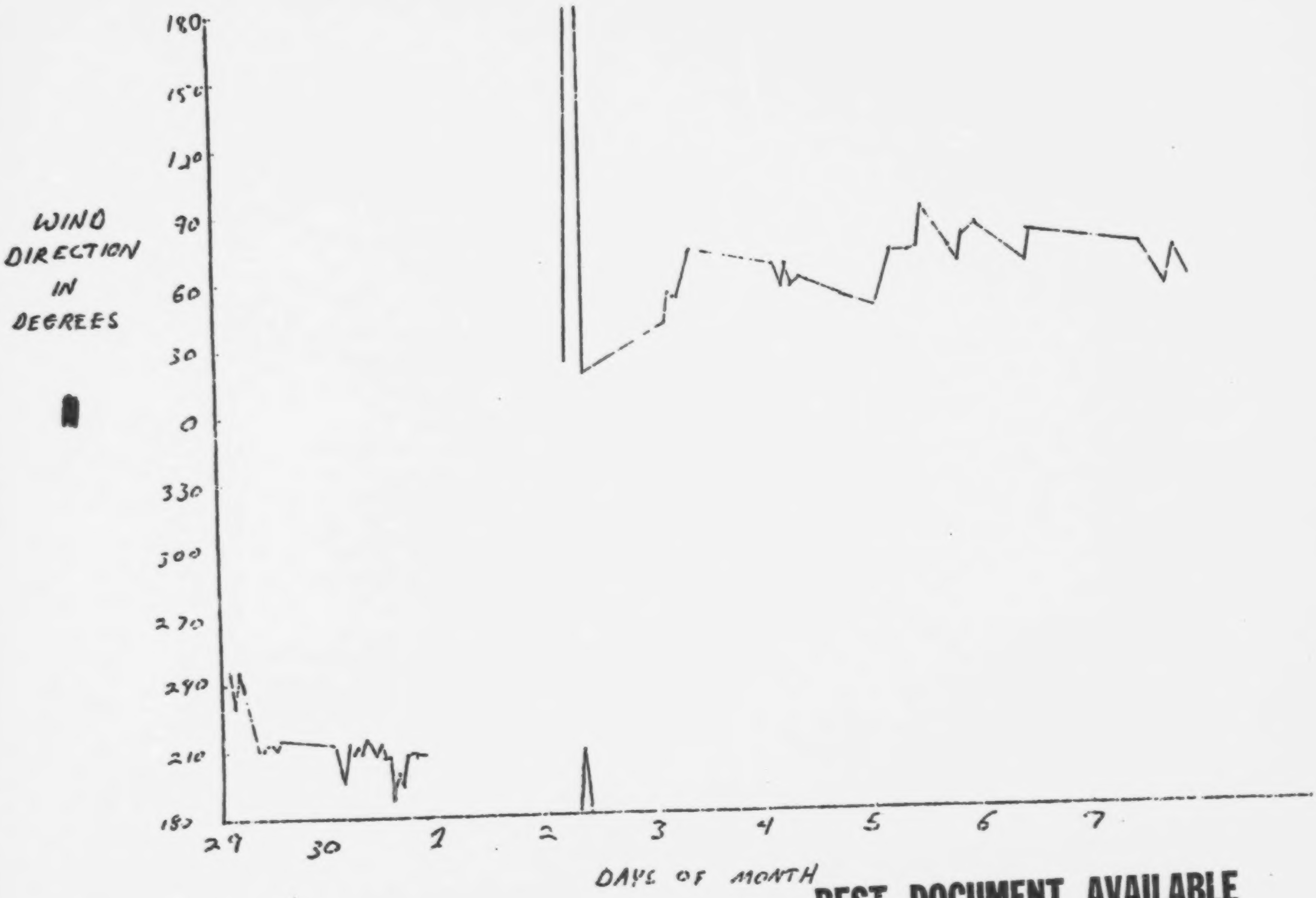

180
150
120
90
60
30
0
330
300
270
240
210
180
WIND DIRECTION IN DEGREES
29
30
1
2
3
4
5
6
7
DAYS OF MONTH

Shuyak

421

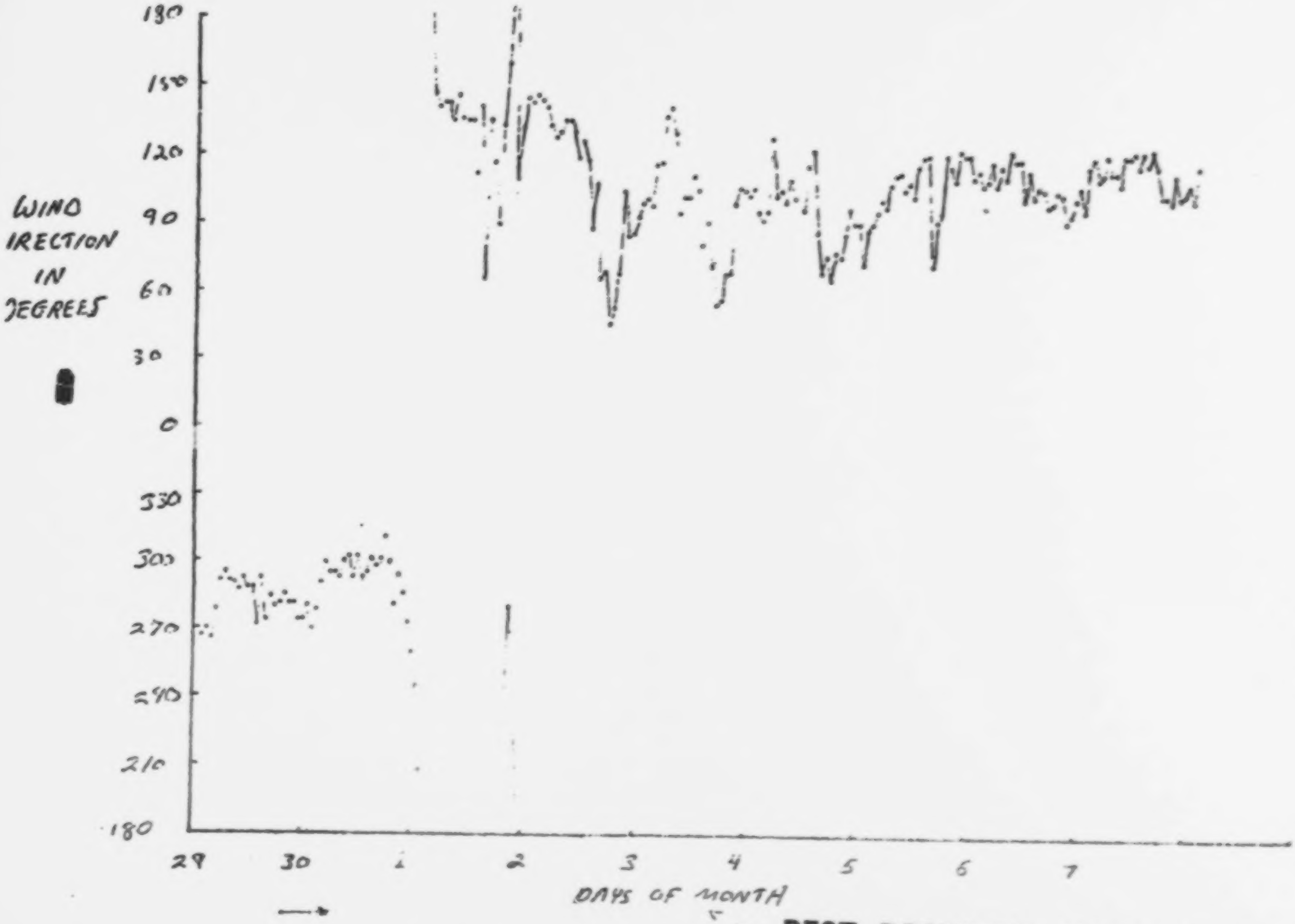

Augustine Island

BEST DOCUMENT AVAILABLE

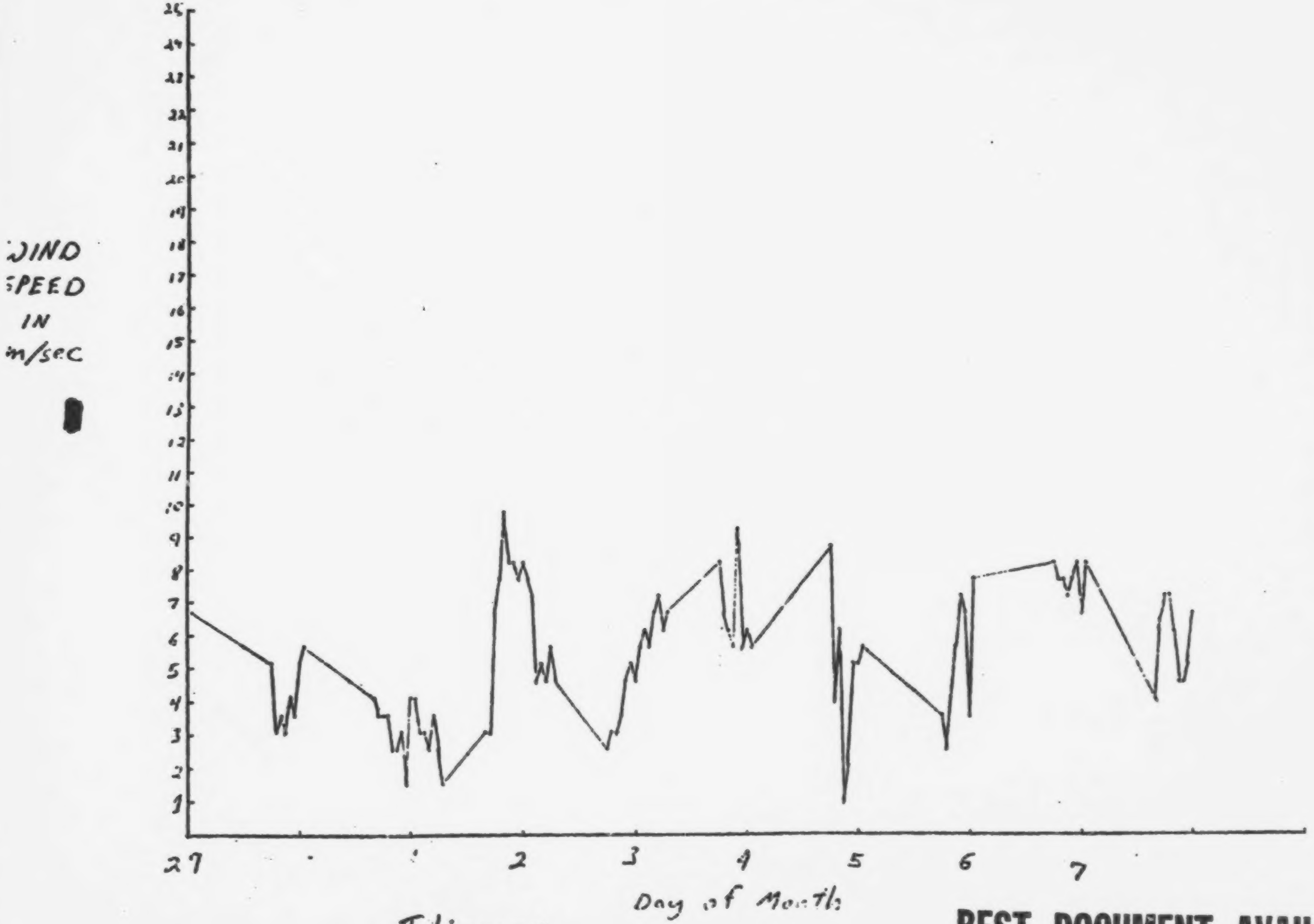
WIND
SPEED
IN
m/sec
25
24
23
22
21
20
19
18
17
16
15
14
13
12
11
10
9
8
7
6
5
4
3
2
1
27
1
2
3
4
5
6
7
Day of Month

Iliamna

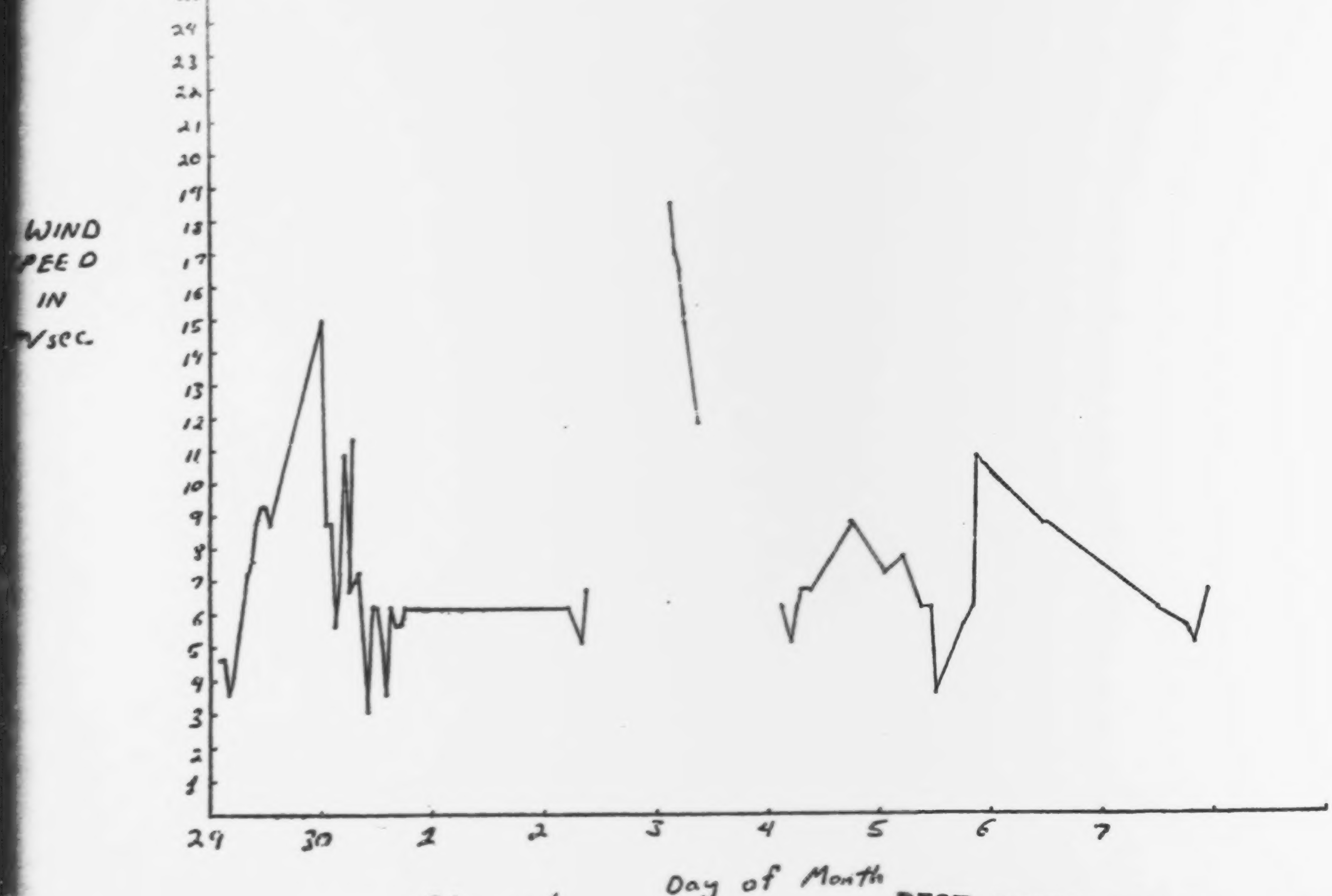
WIND
PEED
IN
/sec.
25
24
23
22
21
20
19
18
17
16
15
14
13
12
11
10
9
8
7
6
5
4
3
2
1
29
30
1
2
3
4
5
6
7
Day of Month

Shuyak

THE TRANSPORT AND BEHAVIOR OF OIL SPILLED IN AND UNDER SEA ICE

BLANK PAGE

Final Report
Research Unit 568
Contract 03-78-B01-62
Reporting Period: 1 May 1978-30 Sept. 1980

THE TRANSPORT AND BEHAVIOR OF OIL SPILLED IN AND UNDER SEA ICE

J. C. Cox, L. A. Schultz, R. P. Johnson
and R. A. Shelsby

ARCTEC, Incorporated
9104 Red Branch Road
Columbia, Maryland 21045

30 September 1980

7

TABLE OF CONTENTS

Page

PREFACE 429

LIST OF TABLES 430

LIST OF FIGURES 431

LIST OF VARIABLES 435

1. INTRODUCTION 440

2. SUMMARY 445

3. THEORETICAL FORMULATIONS 449

   3.1 Horizontal Transport of Oil Under Ice 449
   3.2 Vertical Migration of Oil Through Ice 457

4. SUMMARY OF EXPERIMENTAL PROGRAM AND PROCEDURES 460

   4.1 Selection of Test Oils 460
   4.2 Scaling Considerations 462
   4.3 Static Equilibrium Thickness of Oil Under Ice 463
   4.4 Oil Under Smooth Ice 463
   4.5 Oil Interaction with Small Ice Roughness Elements 467
   4.6 Oil Interaction with Large Ice Roughness Elements 468
   4.7 Flow Pattern in the Wake of Large Ice Roughness Elements . 470
   4.8 Oil in the Wake of Large Ice Roughness Elements 471
   4.9 Oil in Cavities 472

5. TEST RESULTS 475

   5.1 General Observations 475

      5.1.1 Static Equilibrium Thickness of Oil Under Ice . . . 475
      5.1.2 Oil Under Smooth Ice 475
      5.1.3 Oil Interaction with Small Ice Roughness Elements . 476
      5.1.4 Oil Interaction with Large Ice Roughness Elements . 476
      5.1.5 Oil Interaction with Porous Ice Roughness 477
      5.1.6 Behavior of Oil in Wakes 478
      5.1.7 Behavior of Oil in Cavities 478

   5.2 Summary of Quantitative Data 479

BEST DOCUMENT AVAILABLE

TABLE OF CONTENTS (Continued)

Page

6. ANALYSIS OF TEST RESULTS 496

6.1 Static Equilibrium Thickness 496
6.2 Oil Under Smooth Ice 496
6.3 Oil Interaction with Small Ice Roughness 504
6.4 Oil Interaction with Large Ice Roughness 508
6.5 Wake Trapping of Oil 513
6.6 Cavity Trapping of Oil 514
6.7 Discussion of Small and Large Roughness Results 522
6.8 Vertical Entrapment of Oil by First-Year Ice 524
6.9 Vertical Entrapment of Oil by Multi-Year Ice 526

7. APPLICATION OF RESULTS . . . . .

7.1 Calculational Procedure 528
7.2 Sample Calculations 533

7.2.1 Small Roughness Ice 533
7.2.2 Individual Large Roughness Element with Flushing Failure 534
7.2.3 Individual Large Roughness Element with Frontal and Wake Containment 535
7.2.4 Cavity Containment with Vortex and Shear Control . . . 537
7.2.5 Cavity Containment with Shear Control Only 538

8. RECOMMENDATIONS 540

9. REFERENCES 543

APPENDIX A - VERTICAL MIGRATION 545

APPENDIX B - STATIC EQUILIBRIUM SLICK THICKNESS 557

APPENDIX C - OIL INTERACTION WITH SMALL ROUGHNESS 560

APPENDIX D - OIL INTERACTION WITH LARGE ROUGHNESS 563

APPENDIX E - VELOCITY PROFILES 582

APPENDIX F - TEST EQUIPMENT 594

PREFACE

The assistance, cooperation, and support of Dr. Gunter Weller and Dr. William Stringer, the Technical Representatives for the Outer Continental Shelf Environmental Assessment Program, contributed substantially to the success of the program. In an experimental program such as this where new insight into governing physical phenomena is constantly being realized, it is often necessary to redirect portions of the program in order to keep the results in perspective. Their guidance and insight is gratefully acknowledged.

Significant contributions to the project were also made under subcontract by Dr. Timothy Kao of Catholic University and Dr. Seelye Martin of the University of Washington. Dr. Kao contributed much to the analysis of the horizontal transport and containment of oil, while Dr. Martin provided information on field and laboratory studies of the vertical migration of oil through sea ice. The coordinating efforts of Dr. Max Coon, Program Manager of Tasks 2 and 3 of the project, of Flow Research Co. are also gratefully acknowledged. His efforts continually insured that the results of this laboratory study would properly interface with other portions of the three task research effort.

Finally, the authors wish to recognize the talented staff members of ARCTEC, Incorporated who participated in this program. Mr. William Grosskopf led portions of the early laboratory tests and assisted in formulating some of the basic oil containment theory. In addition to Mr. Grosskopf, the test team consisted of L. Schnebelen, W. Devane, D. Tinkle, T. Worrell, S. Burrows, P. Dobson, D. Martin, A. Radzius, and S. Wallace. The entire project team is to be complimented on the excellence of their performance, especially under very difficult working conditions.

LIST OF TABLES

No. Title Page

4.1 Target Oil Properties 461

5.1 Pre-Test Oil Properties 480

5.2 Static Equilibrium Oil Thicknesses 481

5.3 Oil Under Smooth and Small Roughness Ice Test Results 483

5.4 Oil Interaction with Large Roughness Ice Test Results 484

5.5 Results of Wake Measurement Tests 485

5.6 Results of Cavity Tests 486

6.1 Nondimensional Data for Oil Under Smooth and Small Roughness Ice . . . .

6.2 Nondimensional Data for Oil Interaction with Large Roughness Ice . . . .

6.3 Analysis of Cavity Test Results 516

7.1 Summary of Equations for Calculating the Transport or Containment of Oil Beneath Ice in the Presence of a Current . . .

7.2 Definition of Terms for Equations for Calculating the Transport or Containment of Oil Beneath Ice in the Presence of a Current . . . .

E.1 Flume Velocity Profile Data 584

E.2 Velocity Profiles Measured Downstream of a 10 cm Deep Ice Roughness Element for a Current Velocity of 20.5 cm/sec 591

E.3 Velocity Profiles Measured Downstream of a 10 cm Deep Ice Roughness Element for a Current Velocity of 31 cm/sec 592

LIST OF FIGURES

No.	Title	Page
3.1	Sketch of an Oil Drop Beneath an Ice Sheet	450
3.2	Sketch of the Shape Taken by a Slick Confined Behind a Large Roughness Element or Obstruction	453
3.3	Sketch of Oil Leakage From Upstream of a Large Roughness Element to the Wake Region Behind the Element	456
3.4	Generalized Description of Oil Contained in an Ice Roughness Cavity Under the Influence of a Current	458
4.1	Section View of the Piston Injector	464
4.2	Sketch of Oil Injection Cylinder	466
4.3*	Photograph of Under-Ice Small Roughness Consisting of 1 cm Amplitude Recesses on 4 cm Spacing	
4.4	Schematic Representation of a Large Roughness Element	469
4.5*	Photograph Showing the Insertion of a Large Roughness Element in the Level Ice Sheet	
4.6	Sketches of Protruding and Recessed Cavities	474
5.1*	Photograph of Small Oil Droplets Moving Beneath an Ice Sheet with Small Roughness Elements by Bouncing from Element to Element	
5.2*	Photograph Showing the Onset of Headwave Instability for a Slick Contained Upstream of a Large Roughness Element	
5.3*	Photograph Showing Flushing Failure Initiating from the Headwave for a Slick Contained Upstream of a Triangular Large Roughness Element	
5.4*	Photograph of the Oil-Water Interface Shape for Oil Contained in a Cavity Showing the Offset or Thinner Slick Thickness Behind the Upstream Tip in Comparison to the Thicker Slick Farther Downstream	
5.5	Typical Transformation of an Oil/Water Interface With Changes of Free Stream Current for a Number 4 Oil Trapped in a Half Meter Cavity of 14 cm Depth	488

* These photographs have been deleted from this report since copies provided were not reproducible.

LIST OF FIGURES (Continued)

No.	Title	Page
5.6	Typical Transformation of an Oil/Water Interface with Changes of Free Stream Current for a Number 4 Oil Trapped in a Half Meter Cavity of 19 cm Depth	489
5.7	Typical Transformation of an Oil/Water Interface with Changes of Free Stream Current for a Number 4 Oil Trapped in a 1 Meter Cavity of 9 cm Depth	490
5.8	Typical Transformation of an Oil/Water Interface with Changes of Free Stream Current for a Number 4 Oil Trapped in a 2 Meter Cavity of 9 cm Depth	491
5.9	Typical Transformation of an Oil/Water Interface with Changes of Free Stream Current for a Number 4 Oil Trapped in a 1 Meter Recessed Cavity of 9 cm Depth	492
5.10	Typical Transformation of an Oil/Water Interface with Changes in Free Stream Current for a Number 5 Heavy Oil Trapped in a Half Meter Cavity of 15 cm Depth	493
5.11	Typical Transformation of an Oil/Water Interface with Changes in Free Stream Current for a Number 5 Heavy Oil Trapped in a 1 Meter Cavity of 9 cm Depth	494
5.12	Typical Transformation of an Oil/Water Interface with Changes in Free Stream Current for a Number 5 Heavy Oil Trapped in a 2 Meter Cavity of 11 cm Depth	495
6.1	Empirical Relationship Between Slick Thickness and Density Difference	497
6.2	Slick Speed vs Current Speed for No. 2 Fuel Oil Under Smooth Ice	498
6.3	Slick Speed vs Current Speed for No. 4 Oil Under Smooth Ice . .	499
6.4	Slick Speed vs Current Speed for No. 5L Oil Under Smooth Ice . .	500
6.5	Slick Speed vs Current Speed for No. 5H Oil Under Smooth Ice . .	501
6.6	Plot of Oil Slick Threshold Velocity vs Oil Viscosity for Oil Beneath Smooth Ice	502
6.7	Plot of Oil Slick Velocity vs Current Velocity for the Horizontal Transport of Oil Beneath Smooth Ice Cover	503

LIST OF FIGURES (Continued)

No. Title Page

6.8 Plot of Nondimensionalized Data for the Transport of Oil Beneath Smooth and Small Roughness Ice 505

6.9 Variation of Under-Ice Slick Threshold Velocity with Ice Surface Roughness 506

6.10 Projection of Friction Coefficient Amplification Factor as a Function of the Roughness Amplitude to Spacing Ratio 509

6.11 Relationship Between Failure Velocity and Water-Oil Density Difference for Containment of Oil Upstream of an Obstruction . . 510

6.12 Vortex Zone Offset vs Local Current Speed for Oil Trapped in a Cavity 515

6.13 Densimetric Froude Number Based on Offset Size vs Local Current Speed for Oil Trapped in a Cavity 518

6.14 Vortex Zone Length Versus Local Current Speed for Oil Trapped in a Cavity 520

6.15 Schematic Representation of the Shift in Oil-Water Interface Position within a Cavity as a Function of Increasing Current . . 525

7.1 Flow Chart of the Procedure for Calculating the Transport or Containment of Oil Beneath Ice in the Presence of a Current . 529

A.1 Brine Channel Patterns in Young and Multi-Year Sea Ice 546

A.2 Static Oil Rise in an Open Brine Channel 548

A.3 Equilibrium Oil Level in a Brine Channel Only Partially Extending to Datum Level 551

A.4 Equilibrium Oil Level in a Brine Channel Extending Through the Datum Level But Not to the Ice Surface 552

B.1 Sessile Drop of Oil Beneath an Ice Cover 558

D.1 Sketch of Frontal Trapping of an Oil Slick by a Large Roughness Element 564

D.2 Slick Thickness Ratio vs Free Stream Densimetric Froude Number for Large Roughness 566

LIST OF FIGURES (Continued)

No.	Title	Page
D.3	Sketch of the Viscous Region of a Contained Slick	569
D.4	Sketch Showing the Method of Approximating the Volume Per Unit Width of a Frontally Trapped Slick	573
D.5	Sketch of Oil Leakage from Upstream of a Large Roughness Element to the Wake Region Behind the Element	574
D.6	Velocity Measurements in the Wake of a Fence Taken from Rouse [24].	576
D.7	Variation of Wake Length with Roughness Height	577
D.8	Generalized Description of Oil Contained in an Ice Roughness Cavity Under the Influence of a Current	579
D.9	Schematic Representation of the Shift in Oil-Water Interface Position Within a Cavity as a Function of Increasing Current . .	581
E.1	Locations Where Velocity Profiles were Measured in the Flume . .	583
E.2	Velocity Profile at Position No. 1 with Flow Rate of 1100 gpm . .	585
E.3	Velocity Profile at Position No. 2 with Flow Rate of 1100 gpm . .	586
E.4	Velocity Profile at Position No. 3 with Flow Rate of 1100 gpm . .	587
E.5	Velocity Profile at Position No. 4 with Flow Rate of 1100 gpm . .	588
E.6	Velocity Profile at Posotion No. 5 with Flow Rate of 1100 gpm . .	589
E.7	Velocity Profile at Position No. 6 with Flow Rate of 1100 gpm . .	590
E.8	Plots of Velocity Profiles Measured Downstream of a 10 cm Deep Ice Roughness Element for a Current Velocity of 20.5 cm/sec . . .	593
E.9	Plots of Velocity Profiles Measured Downstream of a 10 cm Deep Ice Roughness Element for a Current Velocity of 31 cm/sec	593
F.1	Schematic Drawing of ARCTEC Ice Flume	595
F.2	ARCTEC Ice Flume Carriage Arrangement	597

LIST OF VARIABLES

a	characteristic drop thickness $=\sqrt{\frac{\sigma_{o/w}}{\Delta\rho_w g}}$	cm
A	empirical coefficient	--
A_{frontal}	frontal projected slick area	cm^2
A_{plan}	horizontal areal coverage of slick	cm^2
A_{total}	gross areal coverage	cm^2
A_{voids}	areal coverage of voids	cm^2
b	intercept of upper oil-smooth ice relation	cm/sec
B	empirical coefficient	--
C_D	roughness form drag coefficient	--
C_f	slick form drag coefficient	--
C_i	oil-smooth ice friction coefficient	--
C_s	interfacial shear coefficient	--
d	brine channel diameter	cm
d_{crit}	diameter where vertical oil migration ceases	cm
$d_{\text{inception}}$	diameter for initiating vertical oil migration	cm
D	water depth	cm
D_H	hydraulic diameter of flume $= \frac{4\text{ (area)}}{\text{wetted perimeter}}$	cm
f_s	interfacial friction factor	--
F_D	freestream densimetric Froude Number $\frac{U_w}{\sqrt{\Delta g D}}$	--
F_f	form drag force	gm-cm/sec^2
F_i	oil ice sliding friction force	gm-cm/sec^2
F_s	interfacial shear force	gm-cm/sec^2

F_δ	slick densimetric Froude Number $\frac{U_w}{\sqrt{\Delta g \delta}}$	--
F_{ε_1}	offset densimetric Froude Number $\frac{U_w}{\sqrt{\Delta g \varepsilon_1}}$	--
g	gravitational constant	gm/sec^2
h	pressure head	cm
k_{ice}	thermal conductivity of ice	gm-cal/°C sec-cm
K	friction amplification factor for rough ice	--
ℓ_1	ice draft	cm
ℓ_2	brine channel related dimension	cm
ℓ_3	brine channel related dimension	cm
L, $L(t)$	ice thickness	cm
m	slope of lower oil-smooth ice curve	--
n	porosity	--
N	number of brine channels	--
N'	number of brine channels per unit area	--
P	pressure	gm/cm-sec^2
$\overline{P}$	pressure change	gm/cm-sec^2
P'	incremental pressure	gm/cm-sec^2
P_B	buoyant pressure	gm/cm-sec^2
P_c	capillary pressure	gm/cm-sec^2
P_∞	pressure far upstream of slick	gm/cm-sec^2
q_{ice}	heat flux through ice	gm-cal/sec-cm^2
q_{water}	heat flux from water	gm-cal/sec-cm^2
Q	flow rate	cm^3/sec
r	sessile drop radius	cm
R	radius of curvature	cm
t	time	sec

T	time interval	sec
$\overline{u}_2$	vertical migration speed	cm/sec
$u_{1,2,3}$	velocity components	cm/sec
$u'_{1,2,3}$	turbulent velocity perturbations	cm/sec
U	under-ice velocity profile values	cm/sec
$U_\infty - u$	velocity defect in the wake	cm/sec
U_*	friction velocity $= \sqrt{\frac{\tau_o}{\rho_w}}$	cm/sec
U_{crit}	critical velocity for Kelvin-Helmholtz instability	cm/sec
U_{fail}	freestream velocity when containment failure occurs	cm/sec
U_s	slick speed	cm/sec
U_{th}	threshold current speed for slick movement	cm/sec
U_w	mean current speed	cm/sec
U_∞	freestream current outside the boundary layer	cm/sec
V	slick volume	cm^3
V'	slick volume per unit width	cm^3/cm
V_{total}	gross volume of ice including voids	cm^3
V_{voids}	volume of voids in ice	cm^3
w	slick width	cm
x	horizontal dimension	cm
X	slick length	cm
X_{shear}	length of the shear zone	cm
y	vertical dimension	cm

α	interfacial tension contact angle	--
β	empirical wake growth parameter	--
δ	slick thickness	cm
δ_{eq}	static equilibrium slick thickness	cm
δ_{head}	thickness of contained slick headwave	cm
δ_{neck}	thickness of contained slick neck	cm
$\delta_{stagnation}$	thickness of contained slick at point of flow reattachment	cm
δ_{tail}	thickness of contained slick tail	cm
Δ	relative density difference = $\frac{\rho_w - \rho_o}{\rho_w}$	--
ε_1	offset of the oil-water interface in the vortex zone	cm
ε_2	offset of the oil-water interface at the stagnation point	cm
ξ	wake length	cm
η	ice roughness height	cm
θ_m	melting temperature	°C
θ_o	ice surface temperature	°C
Θ	temperature difference = $\theta_m - \theta_o$	°C
ΘT	thawing degree time	°C-sec
ι	vortex cell length	cm
κ	von Karman's constant = 0.35	--
λ	ice roughness spacing	cm
Λ	heat of fusion	gm-cal/gm
μ_o	viscosity of oil	gm/cm-sec
ν	kinematic viscosity of water	cm^2/sec
ν_o	kinematic viscosity of oil	cm^2/sec
ρ_f	ice density after time interval T	gm/cm^3

ρ_i	initial ice density	gm/cm^3
ρ_{ice}	ice density	gm/cm^3
ρ_o	oil density	gm/cm^3
ρ_w	water density	gm/cm^3
$\sigma_{o/w}$	interfacial tension	gm/sec^2
τ_B	boundary shear stress	$gm/cm\text{-}sec^2$
τ_s	interfacial shear stress	$gm/cm\text{-}sec^2$
ϕ	interfacial angle	--
ψ	nondimensional slick thickness = $\frac{\delta}{D}$	--

1. INTRODUCTION

The continuing dependence of our nation on foreign sources of oil and gas, and the continuing undependability of these sources of supply, indicate that the petroleum reserves already found, and expected to be found, in the Alaskan offshore region will be developed in a timely manner. While the development of these petroleum reserves will proceed with an unprecedented concern for protection of the environment, the simple fact is that any petroleum industry activity related to exploration, development, production, or transportation of Alaskan oil and gas in areas where such activity has not occurred previously must necessarily increase the potential for accidental spills of oil in the region.

The Outer Continental Shelf Environmental Assessment Program (OCSEAP) is a comprehensive environmental study program associated with the proposed development of oil and gas on the outer continental shelf. The program is managed by the National Oceanic and Atmospheric Administration (NOAA) for the Bureau of Land Management (BLM). The OCSEAP studies are designed to provide an environmental information base to support management decisions associated with the identification and selection of lease sale areas. The program is organized into topical areas of contaminant baselines, sources, hazards, transport, reconnaissance, and effects.

The primary objective of the Alaskan OCSEAP is to provide the technical information required to support management decisions associated with the protection of the OCS marine environment from damage due to oil and gas exploration, development, and production activities in Alaska. The program is geared towards the development of providing meaningful data in a readily usable form and in a timely manner so that any required corrective action can be taken before serious or irreversable environmental damage can occur. A major portion of this effort is allocated to a description and characterization of the fate of oil spilled in and under sea ice within the Alaskan OCS lease areas. As part of this effort, NOAA issued a Request for Proposal (RFP) in December 1977 for a study entitled "The Transport and Behavior of Oil Spilled In and Under Sea Ice." In broad terms, this study was to be concerned with the containment potential and transport of oil by ice moving over the continental shelf, and the determination of the likely long-range trajectories of ice and spilled oil contained in the ice. The work of this project was formulated in the RFP in terms of three tasks as follows:

TASK 1 - To determine by field and laboratory experiments the physical processes by which spilled oil gets incorporated in and transported under sea ice.

TASK 2 - To determine by numerical modeling the ice velocity field and the deformation of sea ice on the continental shelves of both the Beaufort and Chukchi Seas so that oil spill trajectories and percent oil incorporation can be deduced for different ice conditions under mean climatological conditions and extreme events, including a major sea ice breakout from the Chukchi Sea to the Northern Bering Sea.

TASK 3 - To determine by combining the relevant information obtained under Tasks 1 and 2 as well as any other relevant information the sequence of events, likely trajectories, and destination points for oil in a number of hypothetical oil spill scenarios.

Contracts for this work were awarded by NOAA in June 1978, with the contract for Task 1 awarded to ARCTEC, Incorporated of Columbia, Maryland, and the contract for Tasks 2 and 3 awarded to Flow Research Company of Kent, Washington. These contracts were designated within the OCSEAP project structure as Research Units 568 and 567 respectively, and administered through the OCSEAP Arctic Project Office in Fairbanks, Alaska by Dr. Gunter Weller and Dr. William Stringer. This report is the final report on the work performed by ARCTEC, Incorporated under Task 1 of the program. In keeping with the original program plan, the results of this work on oil-ice interaction have been combined with the work of Task 2 consisting of a numerical model of ice dynamics, and the work of Task 3 consisting of the projection of likely trajectories and destination points, for specific offshore Alaskan oil spill scenarios. The work completed under Tasks 2 and 3 of the program have been separately reported by Flow Research Company.

The work of Task 1 of the program was further divided in the RFP into three subtasks as follows:

Subtask 1.1 - To determine how and at what rates oil moves upward through multi-year ice to the surface.

Subtask 1.2 - To determine how and at what rates oil gets incorporated into pressure ridges formed from ice of various thicknesses.

Subtask 1.3 - To determine how oil of different viscosities spreads and is moved by ocean currents under sea ice with different underside roughness characteristics.

The three subtasks were therefore basically concerned with the vertical migration of oil through ice, the interaction of oil with pressure ridges, and the horizontal transport of oil beneath ice cover. The RFP also raised a number of questions which hopefully would be answered by the work of this study as follows:

1. How does oil move through first-year and multi-year ice? Under what conditions will it reach the surface, and how long will it take to reach the surface?

2. How does oil get incorporated into pressure ridges, and how and when does it get released?

3. How much oil can be expected to be trapped within pressure ridges, in rafted ice, hummocks, leads, and surface relief in the bottom of the ice surface?

4. How does oil move horizontally under ice of different surface roughnesses through the action of ocean currents? How thick are the oil films likely to be under ice cover having a range of surface conditions?

5. What is the bulk transport of spilled oil by sea ice of different concentrations?

6. How does oil of different viscosities respond to these various vertical and horizontal dispersion processes?

The program was therefore initially formulated in terms of the interaction of spilled oil with various ice conditions and ice features including smooth ice, undulating ice, rough ice, broken ice fields, rafted ice, hummocks, unconsolidated pressure ridges, consolidated pressure ridges, leads, and ice edges. In performing the preliminary theoretical analysis of oil-ice interaction and in planning the laboratory test program in more detail, it quickly became apparent that the problems could be addressed in more generalized categories rather than in terms of specific ice conditions and ice features. The problems to be addressed in this study were then reorganized in terms of the interaction of spilled oil with smooth ice, with ice having small roughness characteristics, and with ice having large roughness characteristics. For the purposes of this study, small ice roughness was defined as roughness whose amplitude is less than the smooth ice equilibrium slick thickness of the oil. A large roughness element is therefore defined as an element of roughness whose amplitude is greater than the smooth ice equilibrium slick thickness of oil. The interaction of spilled oil with large roughness elements was then further categorized in terms of the interaction of spilled oil with a single element where the interest lies in the oil containment capability of the element in terms of its upstream barrier-type containment and its downstream wake region containment, and interaction with multiple large roughness elements which form a cavity having the potential to contain spilled oil. The smooth ice case, while unlikely to be a significant case in most field applications, was a necessary base case for this study. The analysis and interpretation of results for the small roughness and large roughness cases were built upon the analysis and interpretation of results obtained for the simpler smooth ice case.

One final introductory comment concerns the constraints imposed upon these studies of the interaction of spilled oil with ice in the presence of a current by the specific application to be addressed as specified in the RFP

BEST DOCUMENT AVAILABLE

and subsequent meetings with the project administrators. The source of the hypothetical spills for use in the development of spill scenarios was specified as the nearshore Beaufort Sea along the Prudhoe Bay meridian. The spill discharge area is therefore characterized in general terms as an area of relatively shallow water depths, typically less than 60 ft; relatively low currents, typically less than 30 cm/sec; and relatively continuous and well mannered ice conditions over the long term. In terms of the study of the interaction of spilled oil with ice, the shallow water release was interpreted to impose the requirement that the material being dealt with was indeed an oil, rather than an oil-water emulsion, or mousse, which could result from a deep water blowout. The limited currents meant that the upper limit of water current for testing in the laboratory was 30 cm/sec. The well behaved ice conditions and the relatively long time frame of the ice dynamics mathematical model meant that broken ice fields, leads, and ice edges were short-term phenomena, not capable of existing in the mathematical model, and therefore not studied in this program of oil-ice interaction. It was also assumed that any gas released with the oil would quickly, relative to the time frame of the mathematical model of ice dynamics, result in rupture of the ice cover, from which time the gas would be vented to the atmosphere as the oil continued to be released and spread beneath the ice surface. As a result, none of the oil-ice interaction situations investigated in this study included the presence of gas beneath the ice sheet.

As for the incorporation of oil-ice interaction into the mathematical model of ice dynamics to result in the projection of oil spill trajectories, the behavior of the spilled oil is analyzed in four distinct stages consisting of the initial spread of the oil, the incorporation of oil into the ice, the transport of oil with, or relative to, the ice, and the ultimate release of the oil from the ice. The oil-ice interaction problems can therefore be reduced in their simplest terms to a determination of whether oil spilled beneath ice in the presence of a current is contained by the ice and therefore transported with the ice, or whether it is transported by the current relative to the ice. The level of capability for quantitatively defining the behavior of spilled oil beneath ice in the presence of a current has been advanced substantially as a result of the work reported herein, however, this capability still remains far from complete. The emphasis throughout this program was placed on extending the results of the limited laboratory tests to the greatest extent possible through extrapolations based upon theoretical analysis. Approximations and estimates have been made where necessary to provide as complete an assembly of relationships describing the interaction of spilled oil with ice as is possible in a form readily allowing application of the results to both mathematical modeling and field spill situations. These assumptions and approximations were made by the authors with some degree of boldness, however the authors feel that such approximations and estimates would have to be made by someone in order to provide a complete statement of oil-ice interaction, and feel obliged to make the best assumptions and approximations possible based upon the insight into the behavior of spilled oil beneath ice gained during the course of this program. The alternative is to leave holes in the statement of oil-ice interaction which must be filled by each individual user to the best of his or her ability. All assumptions, approximations, and estimates made by the authors are, of course, identified as such.